

V/STOL TILT ROTOR AIRCRAFT STUDY MATHEMATICAL MODEL FOR A REAL TIME SIMULATION OF A TILT ROTOR AIRCRAFT (BOEING VERTOL MODEL 222)

VOLUME VIII

By: H. Rosenstein
M. A. McVeigh
P. A. Mollenkof

APRIL 1973

Distribution of this Report is provided in the
interest of information exchange. Responsibility
for the contents resides in the author or orga-
nization that prepared it.

Prepared Under Contract No. NAS2-6598 by

BOEING VERTOL COMPANY
A DIVISION OF THE BOEING COMPANY
P.O. BOX 16858
PHILADELPHIA, PENNSYLVANIA 19142

for

AMES RESEARCH CENTER
NATIONAL AERONAUTICS AND SPACE ADMINISTRATION

and

UNITED STATES ARMY AIR MOBILITY RESEARCH & DEVELOPMENT LABORATORY
AMES DIRECTORATE

NASA-CR-11460 V/STOL TILT ROTOR AIRCRAFT STUDY N73-31547
MATHEMATICAL MODEL FOR A REAL TIME SIMULATION
OF A TILT ROTOR AIRCRAFT BOEING VERTOL CO. PHILADELPHIA, PA.
570 P HC 30.50
CSCL OIC
63/02 18184

- Volume III -- Overall Research Aircraft Project Plan,
Schedules, and Estimated Cost, NASA
CR-114439
- Volume IV -- Wind Tunnel Investigation Plan for a
Full Scale Tilt Rotor Research Aircraft,
CR-114440
- Volume V -- Definition of Stowed Rotor Research
Aircraft, NASA CR-114598
- Volume VI -- Preliminary Design of a Composite Wing
for Tilt Rotor Aircraft, NASA CR-114599
- Volume VII -- Tilt Rotor Flight Control Program
Feedback Studies, NASA CR-114600
- Volume VIII -- Mathematical Model for a Real Time
Simulation of a Tilt Rotor Aircraft
(Boeing Vertol Model 222), NASA CR-114601
- Volume IX -- Piloted Simulator Evaluation of the
Boeing Vertol Model 222 Tilt Rotor
Aircraft, NASA CR-114602
- Volume X -- Performance and Stability Test of a
1/4.622 Froude Scaled Boeing Vertol
Model 222 Tilt Rotor Aircraft (Phase I),
NASA CR-114603

SUMMARY

This report documents the development of a real time mathematical model of a tilt rotor aircraft. This mathematical model is to be used in conjunction with the NASA Flight Simulator for Advanced Aircraft (FSAA) at Ames Research Center for evaluation of aircraft performance and handling qualities. In addition to developing the mathematical model, a parallel programming effort was conducted utilizing Boeing-Vertol's Hybrid Simulation Laboratory for the purpose of developing and evaluating model simplification.

The mathematical model is an eleven degree of freedom total force model. This model includes the basic six degree of freedom rigid body outer loop equations written about the instantaneous center of gravity with the inertial and aerodynamic terms included. The rotor is treated as a point source of forces and moments with appropriate response time lags and actuator dynamics. The wing has one vertical bending and one wing torsion degree of freedom. These structural degrees of freedom are treated on a "quasistatic" basis; i.e., the natural frequencies of vibration of the structure are much higher than the frequencies of the rigid body motion, and the coupling is in the aerodynamic terms. Each nacelle has an independent pitch degree of freedom about the wing pivot. The aerodynamics of the wing, tail, rotors, landing gear and fuselage are included. Wing and tail mutual interference effects and turbine engine performance and dynamic responses are represented.

The control system elements represented include pilot command (longitudinal and lateral stick, pedals, nacelle position and rate, power), three-axis stability augmentation systems (SAS), thrust management system (includes rotor constant speed governor) and a load alleviation system (LAS). The LAS system incorporates feedback to rotor cyclic and collective pitch for purposes of improving stability, blade load reduction, gust alleviation and increased damping of aeroelastic modes. Control system actuator dynamics are represented by appropriate second order systems.

The mathematical model was programmed on Boeing's hybrid computer. This program was real time and was used to evaluate model simplification and also to develop and optimize stability augmentation, control, and load alleviation systems.

The mathematical model was written to make it as flexible and as general as possible while still retaining the real time execution capability. This program is a valuable design tool for control system design, SAS optimization, and flying qualities evaluations and improvements. The model is capable of operating in all modes of V/STOL flight (forwards, backwards, and sideways) with no restrictions. This mathematical model represents the Model 222 tilt rotor configuration as proposed in Boeing's "Study of V/STOL Tilt Rotor Research Aircraft Program (Phase II)", dated January 1973.

TABLE OF CONTENTS

	<u>PAGE</u>
FOREWORD	iii
SUMMARY	v
LIST OF ILLUSTRATIONS	xi
NOMENCLATURE	xv
1.0 INTRODUCTION	1.0-1
2.0 GENERAL DESCRIPTION OF SIMULATION	2.0-1
3.0 SIGN CONVENTIONS	3.0-1
4.0 MODEL 222 TILT ROTOR AIRCRAFT DESCRIPTION	4.0-1
5.0 EQUATIONS OF MOTION	5.0-1
5.1 AXES SYSTEM	5.0-1
5.2 AIRCRAFT GROUND TRACK	5.0-3
5.3 FORCE EQUATIONS	5.0-4
5.4 MOMENT EQUATIONS	5.0-5
5.5 EQUATIONS OF MOTION FOR A MASS ELEMENT	5.0-5
5.6 EQUATIONS OF MOTION FOR NACELLES	5.0-10
5.7 DETERMINATION OF ROTOR GYROSCOPIC MOMENTS	5.0-13
6.0 AIRFRAME AERODYNAMICS	6.0-1
6.1 FUSELAGE	6.0-1
6.2 NACELLES	6.0-3
6.3 HORIZONTAL TAIL	6.0-4
6.4 VERTICAL TAIL	6.0-10
6.5 WING AERODYNAMICS	6.0-12
6.5.1 BASIC WING AERODYNAMICS	6.0-12
6.5.2 ROTOR SLIPSTREAM INTERFERENCE	6.10-13

TABLE OF CONTENTS

	<u>PAGE</u>
7.0 ROTOR AERODYNAMICS	7.0-1
7.1 FORMAT AND RANGE OF DATA	7.0-1
7.2 PROGRAMS USED TO COMPUTE ROTOR DATA	7.0-4
7.3 ROTOR SIGN CONVENTION	7.0-10
7.4 CURVE FIT FORMAT	7.0-10
7.5 EFFECT OF WING UPWASH ON ROTOR PERFORMANCE	7.0-12
7.6 ROTOR/ROTOR INTERFERENCE	7.0-12
7.7 ISOLATED ROTOR AERODYNAMICS	7.0-13
7.7.1 THRUST	7.0-13
7.7.2 POWER	7.0-14
7.7.3 NORMAL FORCE	7.0-14
7.7.4 SIDE FORCE	7.0-15
7.7.5 HUB PITCHING MOMENT	7.0-15
7.7.6 HUB YAWING MOMENT	7.0-16
7.8 CORRELATIONS OF ROTOR PREDICTION METHODS WITH TEST DATA	7.0-18
7.8.1 MODEL 213 FOUR BLADE HINGELESS ROTOR CORRELATION	7.0-18
7.8.2 CORRELATION WITH MODEL 222 26-FOOT DIAMETER ROTOR TEST IN NASA-AMES 40x80-FOOT TUNNEL	7.0-18
7.8.3 CORRELATION WITH MODEL 222 1/4.622 SCALE MODEL DATA	7.0-21
8.0 CONTROL SYSTEM DESCRIPTION	8.0-1
8.1 CONTROL AERODYNAMIC CONFIGURATION	8.0-1
8.2 LONGITUDINAL CONTROL	8.0-1
8.3 LATERAL CONTROL	8.0-3

TABLE OF CONTENTS

	<u>PAGE</u>
8.4 DIRECTIONAL CONTROL	8.0-5
8.5 THRUST/COLLECTIVE CONTROL	8.0-5
8.6 CONTROL FEEL	8.0-6
8.7 STABILITY AUGMENTATION SYSTEMS	8.0-7
8.8 LOAD ALLEVIATION SYSTEM (LAS)	8.0-8
8.9 THRUST MANAGEMENT SYSTEM	8.0-10
9.0 ENGINE REPRESENTATION	9.0-1
10.0 GROUND EFFECTS	10.0-1
11.0 AIRFRAME REPRESENTATION (PREPROCESSOR)	11.0-1
12.0 AEROELASTIC REPRESENTATION	12.0-1
13.0 CONCLUSIONS AND RECOMMENDATIONS	13.0-1
14.0 REFERENCES	14.0-1

APPENDICES

A. TREATMENT OF WING FLEXIBILITY	A-1
A.1 WING TWIST	A-1
A.2 WING VERTICAL BENDING	A-5
B. DERIVATION OF LANDING GEAR EQUATIONS	B-1
C. VELOCITY AND ACCELERATION TRANSFORMATION AND CENTER OF GRAVITY/INERTIA EQUATIONS	C-1
C.1 VELOCITY TRANSFORMATIONS	C-1
C.2 CENTER OF GRAVITY AND INERTIA EQUATIONS	C-5
C.3 PILOT STATION ACCELERATION-BODY AXES	C-8
C.4 AIRCRAFT INERTIAS	C-9

TABLE OF CONTENTS

	<u>PAGE</u>
D. CALCULATIONS OF SLIPSTREAM-IMMERSED WING AREAS	D-1
E. COMPUTER REPRESENTATION	E-1
F. MATHEMATICAL MODEL INPUT DATA	F-1
F.1 CONTROL SYSTEM INPUT DATA	F-11
F.2 ENGINE INPUT DATA	F-26
F.3 ROTOR AERODYNAMIC INPUT DATA	F-34
F.4 AIRFRAME AERODYNAMIC INPUT DATA	F-44
F.5 GEOMETRIC, WEIGHTS AND BALANCE DATA	F-50
F.6 SIMULATION INPUT DATA	F-53
G. IN-HOUSE HYBRID SIMULATION	G-1
G.1 SIMULATION ARCHITECTURE	G-3
G.2 TRIM LOOPS	G-160
G.3 SIMULATION PROGRAM OUTPUT	G-238
H. VALIDATION OF THE MODEL 222 SIMULATION AT AMES RESEARCH CENTER	H-1
H.1 VALIDATION PLAN AND CRITERIA	H-1
H.2 SIMULATION ACCEPTANCE	H-3
H.3 OPERATING INSTRUCTIONS AND LIMITATIONS	H-8

LIST OF ILLUSTRATIONS

<u>FIGURE NO.</u>	<u>TITLE</u>	<u>PAGE</u>
1.1	SUMMARY OF USES FOR PILOTED SIMULATION1.0-2
2.1	SALIENT FEATURES OF MATH MODEL2.0-5
4.1	MODEL 222 TILT ROTOR RESEARCH AIRCRAFT . .	.4.0-3
5.1	AXES SYSTEMS5.0-2
6.1	VARIATION OF HORIZONTAL TAIL DOWNWASH ANGLE WITH THRUST COEFFICIENT6.0-5
6.2	CORRELATION OF THEORY WITH TEST FOR PRE- DICTIONS OF SLIPSTREAM FORCES AND MOMENTS .	.6.0-20
7.1	ROTOR SIGN CONVENTIONS7.0-11
7.2	MODEL 213 1/9 SCALE CONVERSION MODEL - 85 FT/SEC DERIVATIVE VARIATION WITH RPM .	.7.0-19
7.3	26 FT. ROTOR TEST STAND IN NASA's 40'x80' TUNNEL7.0-20
7.4	CORRELATION OF 26 FT ROTOR TEST DATA WITH VARIOUS ROTOR DERIVATIVE PROGRAMS7.0-22
7.5	CORRELATION OF 26 FT ROTOR TEST DATA WITH VARIOUS ROTOR DERIVATIVE PROGRAMS - CYCLIC MOMENT DERIVATIVES7.0-23
7.6	CORRELATION OF 26 FT ROTOR TEST DATA WITH VARIOUS ROTOR DERIVATIVE PROGRAMS - CYCLIC FORCE DERIVATIVES7.0-24
7.7	ROTOR MOMENT AND AZIMUTH ANGLE DUE TO ANGLE OF ATTACK - CORRELATION WITH 26 FT ROTOR DATA7.0-25
7.8	COMPARISON OF CALCULATED AND TEST ROTOR HUB FORCE AND MOMENT DERIVATIVES FOR M222 1/4.622 SCALE MODEL (YAW SWEEP) $\Omega=386$ RPM :	.7.0-27
7.9	COMPARISON OF CALCULATED AND TEST ROTOR HUB FORCE AND MOMENT DERIVATIVES FOR M222 1/4.622 SCALE MODEL (PITCH SWEEP) $\Omega=386$ RPM	.7.0-28
10.1	EFFECT OF ROTOR HEIGHT ON THRUST AUGMENTATION RATIO	10.0-3

LIST OF ILLUSTRATIONS

<u>FIGURE NO.</u>	<u>TITLE</u>	<u>PAGE</u>
A.1	WING GEOMETRY FOR DERIVATION OF FLEXIBILITY .	A-3
A.2	WING BENDING FUNCTIONS	A-10
B.1	GEOMETRY OF LANDING GEAR	B-2
C.1	REFERENCE AXES SYSTEMS	C-2
D.1	GEOMETRY OF ROTOR SLIPSTREAM/WING PLANFORM INTERACTION	D-4
E.1	BLOCK DIAGRAM ELEMENT INDEX NUMBERS . . .	E-2
F.1	MASS PROPERTIES	F-7
F.2	C.G. LIMIT DIAGRAM	F-9
F.3	DIFFERENTIAL LONG. CYCLIC FOR YAW CONTROL VS NACELLE INCIDENCE	F-14
F.4	ROTOR ROLL CONTROL SCHEDULES IN TRANSITION .	F-15
F.5	LONGITUDINAL CYCLIC FOR PITCH CONTROL GAIN VS NACELLE INCIDENCE	F-16
F.6	LOAD ALLEVIATION SYSTEM GAIN SCHEDULE . . .	F-17
F.7	PROGRAMMED CYCLIC, ELEVATOR, AND FLAP DEFLECTION VS NACELLE INCIDENCE	F-18
F.8	ROLL CONTROL DEFLECTION VS STICK DEFLECTION .	F-19
F.9	SPOILER ACTUATOR LIMIT VS AIRSPEED	F-20
F.10	ASSUMED THROTTLE TRAVEL MODEL 222 SIMULATION BOTH ENGINES	F-21
F.11	ENGINE CHARACTERISTICS LYCOMING T53-L13 ENGINE	F-22
F.12	ENGINE CHARACTERISTICS LYCOMING T53-L13 ENGINE	F-23
F.13	THRUST MANAGEMENT SYSTEM-SCHEDULED PARAMETERS	F-24
F.14	THRUST MANAGEMENT SYSTEM - SCHEDULED PARAMETERS	F-25

LIST OF ILLUSTRATIONS

<u>FIGURE NO.</u>	<u>TITLE</u>	<u>PAGE</u>
F.15	TURBINE ENGINE PERFORMANCE - ENGINE CYCLE 1.78	F-30
F.16	TURBINE ENGINE PERFORMANCE - ENGINE CYCLE 1.78	F-31
F.17	TURBINE ENGINE PERFORMANCE - ENGINE CYCLE 1.78	F-32
F.18	TURBINE ENGINE PERFORMANCE - ENGINE CYCLE 1.78	F-33
F.19	COEFFICIENTS OF CURVE FIT EQUATIONS FOR THRUST COEFFICIENT	F-35
F.20	COEFFICIENTS OF CURVE FIT EQUATIONS FOR POWER COEFFICIENT	F-36
F.21	COEFFICIENTS OF CURVE FIT EQUATIONS FOR NORMAL FORCE COEFFICIENT	F-37
F.22	COEFFICIENTS OF CURVE FIT EQUATIONS FOR SIDE FORCE COEFFICIENT	F-38
F.23	COEFFICIENTS OF CURVE FIT EQUATIONS FOR PITCHING MOMENT COEFFICIENT	F-39
F.24	COEFFICIENTS OF CURVE FIT EQUATIONS FOR YAWING MOMENT COEFFICIENT	F-40
F.25	CURVE FIT COEFFICIENTS FOR $\frac{\partial C_{PM}}{\partial Q}$	F-41
F.26	CURVE FIT COEFFICIENTS FOR $\frac{\partial C_{YM}}{\partial R}$	F-42
F.27	CONSTANTS FOR CYCLIC PITCH EFFECTIVENESS IN ROTOR EQUATIONS	F-43
F.28	MODEL 222 DOWNWASH FUNCTIONS @ $C_T=0$, $i_w=+2.0^\circ$	F-47
F.29	VARIATION OF LIFT CURVE SLOPE WITH GROUND HEIGHT	F-48
F.30	ROTOR/ROTOR AND WING/ROTOR INTERFERENCE	F-49
F.31	MODEL 222 PILOT STATION REQUIREMENTS	F-54

LIST OF ILLUSTRATIONS

<u>FIGURE NO.</u>	<u>TITLE</u>	<u>PAGE</u>
F.32	MODEL 222 CONTROL FORCE GRADIENTS AND BREAKOUT FORCES	F-55
G.1	UTILIZATION OF THE HYBRID LABORATORY FOR THE MODEL 222 MATH MODEL	G-5
G.2	FOREGROUND OPTIONS	G-8
G.3	GHP PHASE OVERLAY STRUCTURE (DIGITAL CORE ALLOCATIONS)	G-10
G.4	CONTENTS OF REAL TIME TASK - FAST LOOP	G-11
G.5	CONTENTS OF REAL TIME TASK - SLOW LOOP	G-13
G.6	MODEL 222 SIMULATION DIGITAL LISTING	F-15
G.7	ANALOG SYMBOLS	G-161
G.8	ANALOG DIAGRAMS FOR MODEL 222 SIMULATION	G-162
G.9	ANALOG STATIC CHECK ROUTINE (DIGITAL)	G-194
G.10	TYPICAL MODEL 222 TRIM SHEET	G-239
G.11	DEFINITION OF TRIM SHEET PARAMETERS	G-241
G.12	TYPICAL TIME HISTORY RESPONSE TO A .25 INCH LONGITUDINAL STICK PULSE AT 150 KNOTS	G-243

LIST OF TABLES

<u>TABLE NO.</u>	<u>TITLE</u>	<u>PAGE</u>
7.1	RANGE OF ROTOR DATA	7.0-5
8.1	FLIGHT CONTROL MIXING	8.0-2
9.1	ENGINE CYCLE DATA FORMAT	9.0-2
12.1	WING UNCOUPLED FREQUENCIES (BLADES OFF) CRUISE CONFIGURATION	12.0-2

NOMENCLATURE

<u>Symbol</u>	<u>Definition</u>	<u>Units</u>
A	Rotor disc area (per rotor)	ft ²
AR	Aspect ratio	N.D.
A _{D(u+5v)}	Coefficients of curve fit equation for wing drag coefficient as a function of angle of attack and surface deflection	--
A _{NF(u+4v)}	Coefficients of curve fit equation for normal force coefficient with zero cyclic pitch	--
A _{P(u+4v)}	Coefficients of curve fit equation for rotor power coefficient with zero cyclic pitch	--
A _{PM(u+4v)}	Coefficients of curve fit equation for rotor pitching moment coefficient with zero cyclic pitch	--
A _{SF(u+4v)}	Coefficients of curve fit equation for rotor side force coefficient with zero cyclic pitch	--
A _{T(u+4v)}	Coefficients of curve fit equation for rotor thrust coefficient with zero cyclic pitch	--
A _{YM(u+4v)}	Coefficients of curve fit equation for rotor yawing coefficient with zero cyclic pitch	--
A _{lc}	Lateral cyclic angle in rotor wind axes	deg
A' _{lc}	Lateral cyclic angle in swashplate axes	deg
A'' _{lc}	Lateral cyclic angle in swashplate axes resolved through swashplate phase angle	deg
\bar{a}	Speed of sound or acceleration	ft/sec or ft/sec ²
a	Acceleration	ft/sec ²
(a _g /a)	Ratio of lift curve slope in ground effect to lift curve slope out of ground effect	ND

NOMENCLATURE

<u>Symbol</u>	<u>Definition</u>	<u>Units</u>
B_G	Percent brake pedal deflection	N.D.
B.L.	Aircraft butt line	inches
B_{lc}	Longitudinal cyclic angle in rotor wind axes	deg
B'_{lc}	Longitudinal cyclic angle in swashplate axes	deg
B''_{lc}	Longitudinal cyclic angle in swashplate axes resolved through swashplate phase angle	deg
b	Span of lifting surface (wing, tail, etc.)	feet
C	Chord	ft.
C_D	Drag coefficient = $\frac{D}{qS}$	ND
C_{D_o}	Drag coefficient at zero lift	ND
ΔC_D	Drag coefficient increment	ND
C_{DS}	Drag coefficient referred to rotor slipstream dynamic pressure = $D/q_s S$	ND
C_L	Lift coefficient = L/qS	ND
C_{L_o}	Average lift coefficient	ND
ΔC_L	Lift coefficient increment	ND
C_{L_s}	Lift coefficient referred to rotor slipstream dynamic pressure = $L/q_s S$	ND
C_{L_α}	Lift curve slope	1/rad
C_{L_δ}	Lift increment due to flap deflection	1/deg
C_L	Rolling moment coefficient = $L/q bS$	ND
C_{L_s}	Rolling moment coefficient referred to rotor slipstream dynamic pressure = $L/q_s bS$	ND

NOMENCLATURE

<u>Symbol</u>	<u>Definition</u>	<u>Units</u>
C_M	Pitching moment coefficient = M/qSC	ND
C_{M_0}	Wing pitching moment coefficient as a function of flap deflection; pitching moment coefficient of fuselage or nacelles at zero angle of attack	ND
ΔC_M	Pitching moment coefficient increment	ND
C_{M_s}	Pitching moment coefficient referred to rotor slipstream dynamic pressure = $M/q_s SC$	
C_{M_δ}	Change in wing/body pitching moment coefficient as a function of flaperon deflection	ND
C_N	Yawing moment coefficient = N/qSb	ND
C_{N_0}	Yawing moment coefficient of fuselage or nacelles at zero angle of attack	ND
C_{n_s}	Yawing moment coefficient referred to rotor slipstream dynamic pressure = $N/q_s Sb$	ND
C_{NF}	Rotor normal force coefficient = $NF/\rho\pi\Omega^2 R^4$	ND
C_{NF_0}	Rotor normal force coefficient with zero cyclic pitch	ND
C_p	Rotor power coefficient = $\frac{550RHP}{\rho\pi\Omega^3 R^5}$	ND
C_{p_0}	Rotor power coefficient with zero cyclic pitch	ND
C_{PM}	Rotor hub pitching moment coefficient = $PM/\rho\pi\Omega^2 R^5$	ND
C_{PM_0}	Rotor hub pitching moment coefficient with zero cyclic pitch	ND
C_{SF}	Rotor side force coefficient = $SF/\rho\pi\Omega^2 R^4$	ND

NOMENCLATURE

<u>Symbol</u>	<u>Definition</u>	<u>Units</u>
C_{SF_0}	Rotor side force coefficient with zero cyclic pitch	ND
C_T	Rotor thrust coefficient = $T/\rho\pi\Omega^2R^4$	ND
C_{T_0}	Rotor thrust coefficient with zero cyclic pitch	ND
C_{T_s}	Rotor thrust coefficient referred to rotor slipstream dynamic pressure = T/q_sA	ND
C_Y	Side force coefficient = Y/qS	ND
C_{YM}	Rotor yawing moment coefficient $\eta/\rho\pi\Omega^2R^5$	ND
C_{YM_0}	Rotor yawing moment coefficient with zero cyclic pitch	ND
C_{Y_α}	Lift curve slope of vertical tail	1/rad
C_0	Coefficient of equation that defines pitching moment coefficient as a function of flap deflection	ND
C_1	Coefficient of equation that defines pitching moment coefficient as a function of flap deflection	1/rad
C_2	Coefficient of equation that defines pitching moment coefficient as a function of flap deflection	1/rad ²
D	Rotor diameter	ft.
(D/T)	Aircraft download to thrust ratio	ND
$D_{NF_{1 \rightarrow 4}}$	Coefficients in the equation for the change in normal force coefficient with lateral cyclic angle	1/deg
$D_{PM_{1 \rightarrow 7}}$	Coefficients in the equation for the change in hub pitching moment coefficient with lateral cyclic angle	1/deg
$D_{SF_{1 \rightarrow 4}}$	Coefficients in the equation for the change in side force coefficient with lateral cyclic angle	1/deg

NOMENCLATURE

<u>Symbol</u>	<u>Definition</u>	<u>Units</u>
D_{ST_n}	Damping coefficients of the landing gear oleo struts	lb/ft/sec
$D_{YM_{1 \rightarrow 7}}$	Coefficients in the equation for the change in hub yawing moment coefficient with lateral cyclic angle	1/deg
dC_{NF}/dA_{1c}	Change in normal force coefficient with lateral cyclic angle	1/deg
dC_{NF}/dB_{1c}	Change in normal force coefficient with longitudinal cyclic angle	1/deg
dC_{PM}/dA_{1c}	Change in hub pitching moment coefficient with lateral cyclic angle	1/deg
dC_{PM}/dB_{1c}	Change in hub pitching moment coefficient with longitudinal cyclic angle	1/deg
dC_{PM}/dQ	Change in hub pitching moment coefficient with pitch rate	1/rad/sec
dC_{SF}/dA_{1c}	Change in side force coefficient with lateral cyclic angle	1/deg
dC_{SF}/dB_{1c}	Change in side force coefficient with longitudinal cyclic angle	1/deg
dC_{YM}/dA_{1c}	Change in hub yawing moment coefficient with lateral cyclic angle	1/deg
dC_{YM}/dB_{1c}	Change in hub yawing moment coefficient with longitudinal cyclic angle	1/deg
dC_{YM}/dR	Change in hub yawing moment coefficient with yaw rate	1/rad/sec
dC_M / dC_L	Change in wing pitching moment with lift coefficient	ND
$d\sigma/d\beta$	Change in fuselage sidewash angle with sideslip angle	ND
EI	Product of modulus of elasticity and moment of inertia	lb-in ²
EI_O	Product of modulus of elasticity and moment of inertia at wing root	lb-in ²

NOMENCLATURE

<u>Symbol</u>	<u>Definition</u>	<u>Units</u>
$E_{NF_{1 \rightarrow 4}}$	Coefficients in the equation for the change in normal force coefficient with longitudinal cyclic angle	1/deg
$E_{PM_{1 \rightarrow 7}}$	Coefficients in the equation for the change in hub pitching moment coefficient with longitudinal cyclic angle	1/deg
$E_{SF_{1 \rightarrow 4}}$	Coefficients in the equation for the change in side force coefficient with longitudinal cyclic angle	1/deg
$E_{YM_{1 \rightarrow 7}}$	Coefficients in the equation for the change in hub yawing moment coefficient with longitudinal cyclic angle	1/deg
e	Oswald efficiency of wing or tail	ND
F	Generalized force or force on nacelle	lb
FPR	Lateral-directional SAS function	--
FR1	Lateral-directional SAS function	--
$F\phi$	Lateral-directional SAS function	--
$F\phi 1$	Lateral-directional SAS function	--
$F\phi 2$	Lateral-directional SAS function	--
$F\psi 1$	Lateral-directional SAS function	--
$F\psi 2$	Lateral-directional SAS function	--
F_a	Aerodynamic force on nacelle	lb
F_{qzn}	Landing gear oleo strut vertical force	lb
F_{sn}	Landing gear oleo strut lateral force	lb
F_x	Longitudinal generalized force	lb
F_y	Lateral generalized force	lb
F_z	Vertical generalized force	lb
$F_{\mu n}$	Landing gear oleo strut longitudinal force	lb

NOMENCLATURE

<u>Symbol</u>	<u>Definition</u>	<u>Units</u>
f_{e_u}	Leading edge umbrella drag	ft ²
f_{NF}	Multiplier on rotor normal force	ND
f_p	Multiplier on rotor power	ND
f_{PM}	Multiplier on rotor hub pitching moment	ND
f_Q	Multiplier on rotor torque	ND
f_{SF}	Multiplier on rotor side force	ND
f_T	Multiplier on rotor thrust	ND
f_{YM}	Multiplier on rotor hub yawing moment	ND
G	Generalized moment	ft-lb
GEF	Ground effect factor = $\left[1 - \frac{(\Delta \epsilon)_g}{\epsilon}\right]$	ND
G_{A1_α}	Load alleviation system gain - change in lateral cyclic with angle of attack	deg/deg
G_{A1_β}	Load alleviation system gain - change in lateral cyclic with angle of sideslip	deg/deg
G_{B1_α}	Load alleviation system gain - change in longitudinal cyclic with angle of attack	deg/deg
G_{G1}	Governor gain	deg/sec/rad/sec
G_{G2}	Governor gain	deg/sec/rad/sec
G_{G3}	Governor gain	deg/sec/deg
G_p	Lateral directional SAS gain	inches/rad/sec
G_{pr1}	Lateral directional SAS gain	inches/rad/sec
$G_{p\delta_s}$	Lateral directional SAS gain	inches/inch
G_q	Longitudinal SAS gain	deg/rad/sec
G_r	Lateral directional SAS gain	inches/rad/sec

NOMENCLATURE

<u>Symbol</u>	<u>Definition</u>	<u>Units</u>
G_{r2}	Lateral directonal SAS gain	inches/rad/sec
$G_{r\delta r}$	Lateral directional SAS gain	inches/rad/sec
$G_{\beta p}$	Lateral directional SAS gain	inches/rad
$G_{\beta r}$	Lateral directional SAS gain	inches/rad
$G_{\beta\delta r}$	Lateral directional SAS gain	inches/inch
$G_{\delta B1}$	Longitudinal SAS gain	deg/inch
$G_{\delta B2}$	Longitudinal SAS gain	deg/inch
$G_{\delta TH}$	Governor throttle gain	deg/inch
G_{θ}	Longitudinal SAS gain	deg/rad/sec
G_{ϕ}	Lateral-directional SAS gain	inches/rad/sec
G_{ψ}	Lateral directional SAS gain	inch/inch
$G_{\psi\delta r}$	Lateral directional SAS gain	inch/inch
g	Gravitational constant	ft/sec ²
H	Height	ft
HP	Horsepower	--
$H_{PM(u+4v)}$	Coefficients in the equation for the change in hub pitching moment with pitch rate	--
$H'_{w'FUEL}$	Horizontal distance between wing mass element center of gravity and fuel center of gravity	ft
$H'_{w'NF}$	Horizontal distance between wing mass element center of gravity and fixed nacelle center of gravity	ft
$H'_{w'w}$	Horizontal distance between wing mass element center of gravity and fixed nacelle center of gravity	ft

NOMENCLATURE

<u>Symbol</u>	<u>Definition</u>	<u>Units</u>
h	Height or angular momentum	ft or lb-ft-sec
h_{CG}^N	Angular momentum of nacelle about aircraft center of gravity	lb-ft-sec
h_F	Distance from wing pivot plane to fuselage mass element center of gravity	ft
h_p	Height of pivot above wing chord line or angular momentum of nacelle about the pivot	
h_T	Landing gear oleo strut deflection during ground contact	ft
h_w	Distance from wing pivot plane to wing mass element center of gravity	ft
h_O	Angular momentum of an element of mass about its own center of gravity	lb-ft-sec
h_1	Wing vertical bending deflection	ft
h/D	Rotor hub height to rotor diameter ratio	ND
h_θ	Distance from aircraft center of gravity bottom of right main gear following a positive pitch rotation	ft
h_ϕ	Distance from aircraft center of gravity to bottom of right main gear following a positive roll	ft
I	Mass moment of inertia	slug-ft ²
I_{xx}	Vehicle mass roll moment of inertia about center of gravity	slug-ft ²
I_{xx_O}	Mass roll moment of inertia of aircraft components about their own center of gravity	slug-ft ²
$I_{xx}^{(F)}$	Mass roll moment of inertia of fuselage mass element about its center of gravity	slug-ft ²

NOMENCLATURE

<u>Symbol</u>	<u>Definition</u>	<u>Units</u>
$I_{xx}^{(W)}$	Mass roll moment of inertia of wing mass element about its center of gravity	slug-ft ²
I'_{xx}	Mass roll moment of inertia of the tilting portion of <u>each</u> nacelle about its center of gravity	slug-ft ²
I_{YY}	Vehicle mass pitch moment of inertia about center of gravity	slug-ft ²
I_{YY_0}	Mass pitch moment of inertia of aircraft components about their own center of gravity	slug-ft ²
$I_{YY}^{(F)}$	Mass pitch moment of inertia of fuselage mass element about its center of gravity	slug-ft ²
$I_{YY}^{(W)}$	Mass pitch moment of inertia of wing mass element about its center of gravity	slug-ft ²
I'_{YY}	Mass pitch moment of inertia of the tilting portion of <u>each</u> nacelle about its center of gravity	slug-ft ²
I_{xz}	Vehicle mass product of inertia about center of gravity	slug-ft ²
I_{xz_0}	Mass product of inertia of aircraft components about their own center of gravity	slug-ft ²
$I_{xz}^{(F)}$	Mass product of inertia of fuselage mass element about its center of gravity	slug-ft ²
$I_{xz}^{(W)}$	Mass product of inertia of wing mass element about its center of gravity	slug-ft ²
I'_{xz}	Mass product of inertia of the tilting portion of <u>each</u> nacelle about its center of gravity	slug-ft ²

NOMENCLATURE

<u>Symbol</u>	<u>Definition</u>	<u>Units</u>
I_{zz}	Vehicle mass yaw moment of inertia about center of gravity	slug-ft ²
I_{zz0}	Mass yaw moment of inertia of aircraft components about their own center of gravity	slug-ft ²
$I_{zz}^{(F)}$	Mass yaw moment of inertia of fuselage mass element about its center of gravity	slug-ft ²
$I_{zz}^{(W)}$	Mass yaw moment of inertia of wing mass element about its center of gravity	slug-ft ²
I'_{zz}	Mass yaw moment of inertia of the tilting portion of <u>each</u> nacelle about its center of gravity	slug-ft ²
i	Incidence angle	deg or rad
\hat{i}	Unit vector in i direction	--
J_{xx}	Dummy inertia = $(I_{zz} - I_{yy})$	slug-ft ²
$J_{YM(u+4v)}$	Coefficients of curve fit equation for rotor hub moment with hub yaw rate	--
J_{yy}	Dummy inertia = $(I_{xx} - I_{zz})$	slug-ft ²
J_{zz}	Dummy inertia = $(I_{yy} - I_{xx})$	slug-ft ²
\hat{j}	Unit vector in j direction	--
K'_A	Wing slipstream correction factor	ND
$\frac{K_{D1}}{T} \rightarrow \frac{K_{D4}}{T}$	Coefficients of curve fit equation for wing download as a function of rotor height/diameter ratio	ND
$\frac{K_{M1}}{T} \rightarrow \frac{K_{M4}}{T}$	Coefficients of curve fit equation for wing pitching moment as a function of rotor height/diameter ratio	ND
$K_{\mathcal{L}}$	Multiplier on slipstream rolling moment coefficient	ND
K_{γ}	Multiplier on slipstream yawing moment coefficient	ND

NOMENCLATURE

<u>Symbol</u>	<u>Definition</u>	<u>Units</u>
$K_{ST\eta}$	Landing gear spring constants	lb/ft
$K_{WI} \rightarrow K_{W10}$	Coefficients for wing bending equations	--
K_{δ_B}	Multiplier on longitudinal cyclic pitch available from longitudinal stick	inch/inch
K_{δ_e}	Ratio between longitudinal stick motion and elevator deflection	deg/inch
K_{δ_R}	Multiplier on longitudinal cyclic pitch available from pedal displacement	inch/inch
$K_{\delta_{RUD}}$	Ratio between pedal and rudder deflection	deg/inch
K_{δ_s}	Multiplier on longitudinal cyclic pitch and differential collective available from lateral stick	inch/inch
$K_{\delta's}$	Provision for lateral cyclic pitch on lateral stick	deg/deg
K_{θ}	Wing stiffness	ft-lb/rad
K_O	Coefficient of fuselage drag coefficient equation to account for drag due to sideslip	1/rad ³
K_1	Coefficient of fuselage drag coefficient equation	1/rad ²
K_2	Coefficient of fuselage drag coefficient equation	1/rad
K_3	Coefficient of fuselage lift coefficient equation	1/rad
K_4	Coefficient of fuselage lift coefficient equation	1/rad ²
K_5	Coefficient of fuselage pitching moment coefficient equation	1/rad

NOMENCLATURE

<u>Symbol</u>	<u>Definition</u>	<u>Units</u>
K ₆	Coefficient of fuselage pitching moment coefficient equation	1/rad ²
K ₇	Coefficient of fuselage side force coefficient equation	1/rad
K ₈	Coefficient of fuselage side force coefficient equation	1/rad
K ₉	Coefficient of fuselage yawing moment coefficient equation	1/rad
K ₁₀	Coefficient of fuselage yawing moment coefficient equation	1/rad ²
K ₂₀	Wing/body interference effects on C _{Lβ}	1/rad
K ₂₁	Wing planform effects on C _{Lβ}	1/rad
K ₂₂	Wing planform and lift effects on C _{ηβ}	1/rad
K ₃₀	Coefficient of nacelle drag coefficient equation	1/rad
K ₃₁	Coefficient of nacelle drag coefficient equation	1/rad ²
K ₃₂	Coefficient of nacelle lift coefficient equation	1/rad
K ₃₄	Coefficient of nacelle pitching moment coefficient equation	1/rad
K ₃₅	Coefficient of nacelle pitching moment coefficient equation	1/rad ²
K ₃₆	Coefficient of nacelle side force coefficient equation	1/rad
K ₃₇	Coefficient of nacelle side force coefficient equation	1/rad ²
K ₃₈	Coefficient of nacelle yawing moment coefficient equation	1/rad
K ₃₉	Coefficient of nacelle yawing moment coefficient equation	1/rad ²

NOMENCLATURE

<u>Symbol</u>	<u>Definition</u>	<u>Units</u>
K_{40}	Coefficient of nacelle yawing moment coefficient equation	1/rad
K_{41}	Coefficient of nacelle yawing moment coefficient equation	1/rad ²
K_{42}	Coefficient of fuselage lift coefficient equation	ND
\hat{k}	Unit vector in k direction	--
L	Rolling moment or nacelle shaft length	ft-lb ,ft
L	Rolling Moment	ft-lb
l	Distance from nacelle pivot to nacelle center of gravity	ft
l'	Horizontal distance from nacelle pivot to noted aircraft component center of gravity position - positive forward from pivot	ft
l_{AC}	Horizontal distance from horizontal tail quarter chord to wing aerodynamic center	ft
l_F	Horizontal distance from pivot to center of gravity of fuselage mass element	ft
l_0	Wing root lift/foot	lb/ft :
l_{PA}	Horizontal distance from pivot to center of gravity of pilots station - positive forward from pivot	ft
l_w	Horizontal distance from pivot to wing mass element center of gravity	
M	Pitching moment	ft-lb
m	Pitching moment	ft-lb
M/T	Pitching moment/rotor thrust	ft-lb/lb
m	Aircraft total mass	slugs

NOMENCLATURE

<u>Symbol</u>	<u>Definition</u>	<u>Units</u>
\dot{m}_f	Mass of fuselage mass element	slugs
\dot{m}_N	Mass of one nacelle	slugs
\dot{m}_w	Mass of wing mass element	slugs
N	Yawing moment	ft-lb
η	Yawing moment	ft-lb
NF	Rotor normal force	lb
N_I	Engine gas generator speed	rev/min
N_1 IND	Engine gas generator indicator	--
N_I^*	Engine gas generator speed at sea level standard, static conditions	rev/min
N_{10} IND	Referred engine gas generator speed indicator	--
N_{II}	Engine power turbine speed	
N_{II}^*	Engine power turbine speed at sea level standard static conditions	
P	Body axes roll rate	rad/sec
PC	Horizontal distance from wing leading edge to pivot location	ft.
p_N	Nacelle axes roll rate	rad/sec
p_R	Nacelle wind axes roll rate	rad/sec
p	Body axes roll rate	rad/sec
Q	Body axes pitch rate or rotor torque	rad/sec or lb-ft
Q_{IND}	Torque indicator	ND
Q_{MAX}	Maximum engine torque available	lb-ft
Q_N	Nacelle axes pitch rate	rad/sec
Q_R	Nacelle wind axes pitch rate	rad/sec

NOMENCLATURE

<u>Symbol</u>	<u>Definition</u>	<u>Units</u>
Q^*	Engine torque at sea level standard static condition	lb-ft
q	Body axes pitch rate or freestream dynamic pressure	rad/sec or lb/ft ²
q_s	Dynamic pressure based on rotor slipstream = $(q + T/A)$	lb/ft ²
R	Body axes yaw rate or rotor resultant force or rotor radius	rad/sec or lb or ft
RHP	Rotor horsepower	--
R^N	Nacelle axes yaw rate	rad/sec
R^R	Nacelle wind axes yaw rate	rad/sec
r	Body axes yaw rate	rad/sec
\underline{r}	Radius vector	--
r_n	Landing gear tire radius	ft.
S	Surface area	ft ²
SF	Rotor side force	lb
SHP	Shaft horsepower	--
SHP*	Engine shaft horsepower at sea level standard static conditions	
T	Rotor thrust	lb
TEA	Engine referred turbine inlet temperature	degrees
(T_{IGE}/T_{OGE})	Ratio of the rotor thrust in ground effect to the thrust out of ground effect	--
$T_1 \rightarrow T_3$	Coefficients of curve fit equations for rotor/rotor interference	ND
t	Time	sec

NOMENCLATURE

<u>Symbol</u>	<u>Definition</u>	<u>Units</u>
u	Body axes longitudinal component of velocity at aircraft center of gravity or rotor hub, wing, horizontal and vertical tail velocities referred to rotor shaft and local surface chord axes respectively.	ft/sec
u'	Body axes longitudinal component of velocity at rotor hub and wing aerodynamic center	ft/sec
u _{PA}	Body axes longitudinal component of velocity at pilots station	ft/sec
V	Total velocity	ft/sec
V _t	Rotor tip speed	ft/sec
V'	Resultant flow through rotor disc	ft/sec
V _*	Non-dimensional rotor forward velocity	N.D.
<u>V</u>	Total Velocity Vector	—
v	Body axes lateral component of velocity at aircraft center of gravity or rotor hub wing, horizontal and vertical tail velocities referred to rotor shaft and local surface chord axes respectively	ft/sec
v'	Body axes lateral component of velocity at rotor hub and wing aerodynamic center	ft/sec
v _i	Rotor induced velocity	ft/sec
v _{PA}	Body axes lateral component of velocity at pilots station.	ft/sec
v _*	Non-dimensional rotor induced velocity	N.D.
W.L.	Fuselage water line position	inches
W'	Weight of aircraft components	lb.
WDTIND	Fuel flow indicator	—
w	Body axes vertical component of velocity at aircraft center of gravity or rotor	ft/sec

NOMENCLATURE

<u>Symbol</u>	<u>Definition</u>	<u>Units</u>
	hub, wing, horizontal and vertical tail velocities referred to rotor shaft and local surface chord axes respectively	
w'	Body axes vertical component of velocity at rotor hub and wing aerodynamic center	ft/sec
w_{PA}	Body axes vertical component of velocity at pilots station.	
$x_{\text{subscript}}$	Longitudinal distance, measured positive forward from nacelle pivot along body axes	ft.
$\Delta x_{\text{subscript}}$	Longitudinal force, measured positive forward along body axes	lb.
x_{aero}	Total longitudinal aerodynamic force at center of gravity measured positive forward along body axes.	lb.
$x_{\text{subscript}}^{\text{sprscript}}$	Longitudinal force, measured positive forward along body axes.	lb.
\dot{x}_{North}	Longitudinal ground track velocity	ft/sec
$y_{\text{subscript}}$	Lateral distance, measured positive along right wing along body axes	ft.
$\Delta y_{\text{subscript}}$	Lateral force, measured positive along right wing in body axes	lb.
y_{aero}	Total lateral aerodynamic force at center of gravity measured positive along right wing in body axes	lb.
$y_{\text{subscript}}^{\text{sprscript}}$	Lateral force, measured positive along right wing in body axes	lb.
\dot{y}_{East}	Lateral ground track velocity	ft/sec
$z_{\text{subscript}}$	Vertical distance, measured positive down nacelle pivot along body axes	ft.
$\Delta z_{\text{subscript}}$	Vertical force, measured positive down along body axes	lb.
z_{aero}	Total vertical aerodynamic force at center	lb.

NOMENCLATURE

<u>Symbol</u>	<u>Definition</u>	<u>Units</u>
	of gravity, measured positive down along body axes.	
$z^{\text{sprscript}}_{\text{subscript}}$	Vertical force, measured positive down along body axes	lb.
\dot{z}_{down}	Vertical ground track velocity	ft/sec
z	Vertical distance from nacelle pivot to center of gravity of aircraft component, positive down from nacelle pivot along body axes.	ft.
α	Angle of attack	rad
β	Angle of sideslip	rad
$\Delta'_{w' \text{fuel}}$	Vertical distance between wing fuel center of gravity and wing mass element center of gravity	ft.
$\Delta'_{w' \text{NF}}$	Vertical distance between fixed nacelle center of gravity and wing mass element center of gravity.	ft.
$\Delta'_{w' w}$	Vertical distance between wing center of gravity and wing mass element center of gravity.	ft.
δ	Control element (surface or stick) angular or linear displacement	deg. or in.
δ'_{C}	Vertical distance between cargo center of gravity and fuselage mass element center of gravity	ft.
δ'_{CR}	Vertical distance between crew center of gravity and fuselage mass element center of gravity	ft.
$\delta'_{\text{F'}}$	Vertical distance between fuselage center of gravity and fuselage mass element center of gravity.	ft.
δ'_{HT}	Vertical distance between horizontal tail center of gravity and fuselage mass element center of gravity	ft.

<u>Symbol</u>	<u>NOMENCLATURE</u>	<u>UNITS</u>
	<u>Definition</u>	
δ'_{VT}	Vertical distance between vertical tail center of gravity and fuselage mass element center of gravity	ft.
ϵ	Wing or rotor downwash angle	rad
ϵ_0	Wing downwash angle at zero wing angle of attach	rad
ϵ_{iLR}	Rotor/rotor interference angle, left rotor on right rotor	rad
ϵ_{iRL}	Rotor/rotor interference angle, right rotor on left rotor	rad
ϵ_w	Wing on rotor interference	rad
ζ	Rotor sideslip angle or damping ratio	rad or N.D.
$\zeta_{w1} \rightarrow \zeta_{w4}$	Wing damping ratio	N.D.
$H'_{w'fuel}$	Horizontal distance between wing fuel center of gravity and wing mass element center of gravity	ft.
$H'_{w'NF}$	Horizontal distance between fixed nacelle center of gravity and wing mass element center of gravity	ft.
$H'_{w'w}$	Horizontal distance between wing center of gravity and wing mass element center of gravity	ft.
η'_c	Horizontal distance between cargo center of gravity and fuselage mass element center of gravity	ft.
η'_{CR}	Horizontal distance between crew center of gravity and fuselage mass element center of gravity	ft.
η'_F	Horizontal distance between fuselage center of gravity and fuselage mass	ft

<u>Symbol</u>	<u>NOMENCLATURE</u> <u>Definition</u>	<u>Units</u>
	element center of gravity	
η_{HT}	Horizontal tail efficiency	N.D.
η'_{HT}	Horizontal distance between horizontal tail center of gravity and fuselage mass element center of gravity.	lb.
η_{VT}	Vertical tail efficiency factor	N.D.
η'_{VT}	Horizontal distance between vertical tail center of gravity and fuselage mass element center of gravity	ft.
η_{TR}	Transmission efficiency	N.D.
θ	Aircraft pitch or Euler angle or temperature ratio	rad or N.D.
θ_t	Wing twist angle	rad
$\theta_{0.75}$	Rotor collective pitch angle at three quarter radius	deg.
λ	Angle between the rotor shaft and a line drawn through the nacelle center of gravity from the pivot.	rad
μ	Rotor advance ratio = $V/\Omega R$	N.D.
μ_s	Tire sliding coefficient of friction when sliding sideways (for concrete)	N.D.
μ_0	Tire rolling coefficient of friction (for concrete)	N.D.
μ_1	Coefficient of rolling friction for brakes	N.D.
$\xi_{R1} \rightarrow \xi_{R4}$	Terms of wing immersed area calculation	—
π	3.14159	—
ρ	Ambient air density	slug/ft ³
σ	Fuselage sidewash angle	rad

<u>Symbol</u>	<u>NOMENCLATURE</u>	<u>Units</u>
	<u>Definition</u>	
σ_h	Ambient density ratio	N.D.
τ	Angle between freestream velocity and rotor resultant force	rad
τ_D	Engine response time constant	sec.
τ_E	Engine response time constant	sec.
τ_{HT}	Horizontal tail effectiveness	rad/rad
τ_{LAS}	Load alleviation system time constant	sec
τ_{VT}	Vertical tail effectiveness	rad/rad
τ_P	Lateral directional SAS time constant	sec
τ_r	Lateral directional SAS time constant	sec
τ_ϕ	Lateral directional SAS time constant	sec
$\tau_{\phi\delta_s}$	Lateral directional SAS time constant	sec
τ_ψ	Lateral directional SAS time constant	sec
$\tau_{\psi\delta_r}$	Lateral directional SAS time constant	sec
τ_1	Rotor thrust response time constant	sec
τ_2	Rotor thrust response time constant	sec
ϕ	Aircraft roll angle or Euler angle	rad
ϕ_P	Rotor swashplate phase angle	rad
$\phi_1 \rightarrow \phi_5$	Functions in wing vertical bending equations	—
χ	Rotor wake skew angle	rad
ψ	Aircraft yaw angle or Euler angle	rad
Ω	Rotor or engine rotational speed	rad/sec
$\underline{\Omega}$	Rotational speed vector	rad/sec
ω	Natural frequency	rad/sec
$\omega_{w1} \rightarrow \omega_{w3}$	Wing natural frequency	rad/sec

Subscripts

A	Available
AC	Aerodynamic center
ACT	Actuator
AERO	Aerodynamic force
a	Aileron
B	Longitudinal stick
c	Cargo
CG	Center of gravity
CR	Crew
C/4	Quarter chord
DUM	Dummy variable
E	Engine
EFF	Effective
e	Elevator or effective
F	Fuselage
FAC	Fuselage aerodynamic center
FUEL	Fuel in wing
FUEL _{CG}	Fuel center of gravity
FUS	Fuselage
F'	Fuselage less landing gear
f	Flap
GLAS	Load alleviation system
GYRO	Gyroscopic
g	Ground or gust
HL	Left rotor hub

Subscripts

HR	Right rotor hub
HT	Horizontal tail
HTCG	Horizontal tail center of gravity
IGE	In ground effect
i	Immersed
L	Left wing or rotor
LAS	Load alleviation system
LE	Left engine
LG	Landing gear
L-L	Rotor lead-lag
LN	Left nacelle
LR	Left rotor
LRH	Left rotor hub
LT	Left wing tip
LW	Left wing
LW _o	Left wing referred to freestream
MAX	Maximum
N	Nacelle or natural frequency
NF	Fixed portion of nacelle
NFCG	Fixed portion of nacelle center of gravity
NL	Left nacelle
NR	Right nacelle
NT	Tilting portion of nacelle
n	Landing gear index, n=1 left gear, n=2 right gear, n=3 nose gear

Subscripts

OGE	Out of ground effect
P	Power, nacelle pivot, or rotor polar moment of inertia
POWER	Power
PA	Pilot station
R	Right wing, rotor or rudder pedal
RE	Right engine
REQ	Required
RIGID	Rigid
RN	Right nacelle
RR	Right rotor
RRH	Right rotor hub
RT	Right wing tip
RUD	Rudder
RW	Right wing
RW_o	Right wing referred to freestream
S	Rotor shaft, side, or lateral stick
SP	Spoiler
STALL	Stall
T	Tail, total or wing tip
TH	Throttle
VT	Vertical tail
VTG	Vertical tail center of gravity
W	Wing
WAC	Wing aerodynamic center
WCG	Wing center of gravity

Subscripts

x	Along the lonitudinal body axes, positive forward
y	Along the lateral body axes, positive out right wing
z	Along the vertical body axes, positive down
—	Denotes a vector quantity

Superscripts

(c)	Referes to cargo or payload weight
(CR)	Refers to aircraft crew weight
F	Fuselage
F'	Fuselage less landing gear
HT	Horizontal tail
(HT)	Refers to horizontal tail weight component
IGE	In ground effect
LW	Left wing
N	Nacelle
NL	Left wing tip at pivot
NR	Right wing tip at pivot
(p)	Roll axes
(q)	Pitch axes
RW	Right wing
(r)	Yaw axes
T	Total of horizontal and vertical tail
VT	Vertical tail
(VT)	Referes to vertical tail weight component
W	Wing

Superscripts

(W'_{FUEL})	Refers to wing fuel weight
(W'_f)	Refers to fuselage weight component
(W'_{NF})	Refers to weight of fixed portion of nacelle
(W'_w)	Refers to wing weight component
•	First derivative with respect to time; represents velocity
••	Second derivative with respect to time; represents acceleration
"	Denotes an interim calculation or coefficient in local wind axes
'''	Denotes an interim calculation
-	Denotes average value
*	Denotes interim calculation or calculation in freestream wind axes
'	Denotes an interim calculation
+	Denotes an interim calculation
^	Denotes an interim calculation
	Absolute values

NOTES

1. Some symbols not defined in this section, but used in this report, are defined in the section of the report they are used.
2. Alternate definitions, where applicable, for each symbol are given. Select the appropriate definition for each particular section
3. All distances are measured with respect to the nacelle pivot. Distances are positive forward, down and to the right of the pivot. Forces are positive forward, down, and to the right.
4. Δ or δ preceding a symbol generally denotes an incremental change.

1.0 INTRODUCTION

Piloted simulation is a useful and important tool in the design, development and test of new flight vehicles. Figure 1.1 shows a summary of some of these uses as they could be applied to the Model 222 tilt rotor aircraft.

As part of Contract NAS2-6598 Boeing Vertol developed a complex mathematical model of the Model 222 tilt rotor, intended primarily for use with the NASA Flight Simulator for Advanced Aircraft (FSAA) at Ames Research Center. The purpose of this report is to document the development of that mathematical model and to substantiate the methods which were uniquely developed for this purpose.

- Evaluation of Tilt Rotor Handling Qualities
 - Stability and Control
 - Control System Optimization
 - Evaluation of Man-in-the-Loop System Compatibility
 - Evaluation of Malfunction Effects
- Evaluation of Tilt Rotor Performance
 - Maneuver Capability
 - VTOL and STOL Takeoff and Landing Capability
- As a Tool to Evaluate Configuration Changes
 - Changes in Cockpit Layout
 - Changes in Tail Size
 - Changes in Geometry
 - Changes in SAS Configuration
 - Changes in Elastic Characteristics
- As a Flight Test Support Tool
 - Development of Emergency Techniques
 - Familiarization of Flight Crews with Aircraft Characteristics Prior to Flight
 - Correlation Studies
 - Exploration of Flight-Discovered Phenomena

Figure No. 1.1. Summary of Uses for Piloted Simulation

2.0 GENERAL DESCRIPTION OF SIMULATION

The objective of this program was to develop a real time simulation program for a tilt rotor aircraft to be used at the NASA-Ames simulation facility in conjunction with the Flight Simulator for Advanced Aircraft (FSAA) for evaluation of tilt rotor aircraft performance and handling characteristics throughout the flight envelope and identifying problem areas within the envelope.

The mathematical model developed under this contract includes the basic 6 degree of rigid body freedom outer loop equations written about the instantaneous center of gravity with all inertial and aerodynamic coupling terms included. Euler angles are used to properly orient the aircraft in space.

Rotor forces and moments are input to the equations from curve-fit data. The rotor data bank applies to the Boeing Model 222 tilt rotor. Calculation of the rotor forces and moments on-line for real time simulation is not practical because of the complexity of the programs required to represent the lag-flap coupling effects of the soft-in-plane hingless rotor. Analytical studies show that the lag-flap coupling has a large effect upon the phasing of the hub forces and moments of the rotor thereby altering the direct rotor effects on aircraft stability significantly. The rotor rotational degree of freedom is included to represent the effects of rotor inertia which are included in the representation of the thrust management system.

The effects of rotor-on-wing, wing-on-rotor, and rotor-on-horizontal tail are included in this program. The effects of rotor-on-wing are represented by calculation of the slipstream angle of attack of the portions of the aircraft operating in the rotor slipstream by momentum methods and resolving the associated forces and moments to body axes. Correlation with test data are shown in Section 6.5.2 to verify these interference effects. The effects of the rotor slipstream on the horizontal tail downwash are also calculated by momentum methods. The angle through which the flow through the rotor is turned is assumed to represent the change in tail downwash. Provisions are made to incorporate the upwash effects of the wing on the rotor. Lifting line theory should be used to compute these effects.

The effects on lateral/directional parameters caused by rotor wake skew on the wing are included by computing the change in immersed wing area during sideways flight and sideslips.

Structural dynamics effects included consist of the first mode wing vertical bending and the first wing torsion mode. These wing structural modes have been included on a "quasistatic" basis; i.e. the natural frequencies of vibration of the structure are much higher than the frequencies of the rigid body motion, and the coupling is in the aerodynamic terms.

The aerodynamics of the fuselage, empennage, nacelles, wings and rotors are included in detail. The aerodynamics of the

wing and rotors are written separately for the left and right sides. The effects of the wing leading edge umbrellas are included, with provisions for the direct effects of wing down-load and pitching moment with the umbrellas open in slow flight. Ground effects are considered on the rotors, wing and horizontal tail. The effects of Mach number on the airplane are treated by application of the Prandtl-Glauert rule. The effects of Mach number on the rotor data have been included in the curve fit equations.

The control system elements represented include pilot command, three axis stability augmentation systems, a load alleviation system (LAS) and a thrust management system. Control system actuator dynamics are represented by appropriate first order and second order lags. The systems are assumed to be "tight" in that thresholds, biases and hysteresis loops are neglected.

Turbine engine performance with appropriate dynamic responses are included. Engine power is computed for the range of flight condition necessary to cover the flight envelope. A relatively simple engine dynamic response model modulates the power output in response to pilot control of throttle position.

Landing gear is represented by a spring-damper system without complex calculation of oleo strut response.

The effects of rotor tilt angle on the aircraft center of gravity and inertia are included. Forces and moments resulting from

acceleration of the nacelles during tilting maneuvers are calculated in the program.

An airframe representation/preprocessor calculation is included that enables the user to input the location of major structural elements of the aircraft in terms of water line, butt line and station line location. All lengths and inertias required by the equation are then calculated. This feature enables the user to quickly change the location of major elements to assess their impact on vehicle response. The rest of the input data required has been kept to a minimum to augment the programs' usefulness. Provisions have been included to provide a very flexible design tool which enables the astute user to perform a wide variety of studies. Figure 2.1 summarizes the salient features of the mathematical model described in this document. It should be emphasized that this model has full flight envelope capability.

- Full Flight Envelope Capability with Total Force Representation
- 6 Rigid Body Degrees of Freedom
- Independent Nacelle Pitch Degree of Freedom
- 2 Elastic Degrees of Freedom
- 1 Rotor Rotational Degree of Freedom
- Includes the Aerodynamics of:
 - Rotors
 - Wings
 - Rotor/Wing & Wing/Rotor Interference
 - Fuselage
 - Landing Gear
 - Tail Surfaces
 - Engines
- Control System Elements:
 - Pilot Command
 - SAS
 - Load Alleviation System (LAS)
 - Thrust and Power Management System
- Aeroelastic Representation
 - Wing Vertical Bending
 - Wing Torsion

Figure 2.1. Salient Features of Math Model

3.0 SIGN CONVENTIONS

Standard aircraft sign conventions have been used throughout this report. Sign conventions are as follows:

Positive X axis forward

Positive Y axis outward along the right wing.

Positive Z axis downward perpendicular to the XY plane.

Lift is positive along the negative Z axis.

Pitching moment is positive nose-up about the Y axis.

Sideforce is positive outward in the direction of the positive Y axis.

Yawing moment is positive nose-right.

Rolling moment is positive right wing down.

Positive elevator deflection is trailing edge down

Positive rudder deflection is rudder-trailing-edge-left.

Positive aileron deflection is right-flaperon-trailing-edge-down.

Positive spoiler deflection is left-hand-spoiler-deflected-upward.

Positive deflection of the pilot's stick and rudder pedals yields positive aircraft pitch, roll, and yaw moments from negative control deflections.

Rotor sign conventions are illustrated in Section 7.0

Special sign convention used in the derivations are noted in the appropriate section.

4.0 MODEL 222 TILT ROTOR AIRCRAFT DESCRIPTION

The Boeing Model 222 Tilt Rotor Research Aircraft, shown in Figure 4.1 uses two 26-foot diameter soft in-plane hingeless rotors of the same design that has already been demonstrated in the NASA/Ames 40 by 80-foot tunnel. The soft in-plane rotor is mechanically simple and provides excellent flying qualities characteristics as well as freedom from aeroelastic problems. It is service proven on the FAA certified BO-105 helicopter. For transition, the rotors tilt from hover position (rotor disk horizontal) to cruise position (rotor disk vertical). Intermediate nacelle positions provide optimum performance capability for climb, descent and for STOL operations.

The Model 222 is powered by two modified Lycoming T53-L-13B turboshaft engines mounted in fixed (nontilting) nacelles at each wing tip. The rotors are interconnected by a cross shaft for single engine operation. The engine power available yields excellent single engine and temperature-altitude performance.

Fuselage and empennage are production (MU-2J) components, modified to accept the Model 222 wing and two production (OV-10) ejection seats. The retractable tricycle landing gear is also the existing MU-2J gear modified to provide increased energy absorption.

Collective and cyclic pitch of the rotors, together with nacelle tilt, provide high control power in hover. In the cruise mode, control is by conventional airplane elevators,

rudder, flaperons and spoilers. Leading-edge "umbrella" flaps and large deflection trailing-edge flaps reduce download and ground effect turbulences in hover. Operation of flaps, umbrellas and elevator as well as phasing out of the rotor controls is mechanically programmed with nacelle tilt to relieve pilot workload.

A limited-authority stability augmentation system includes feedback from angle-of-attack, yaw angle, and dynamic pressure. In cruise flight it feeds back two axes of cyclic pitch to the rotor control. This provides increased static stability and reduces blade loads to increase fatigue margins. The feedback system is not required for either stability or structural integrity. This system permits easy variation of the stability characteristics of the aircraft.



Figure No. 4.1. Model 222 Tilt Rotor Research Aircraft

5.0 EQUATIONS OF MOTION

This section presents the derivation of the airframe equations of motion and the simplifications that were made in order to obtain the final equations as presented in Appendix E. The treatment accounts for all six rigid-body degrees-of-freedom including the effects of the tilting nacelles and rotors. The principal features of the derivation are:

- Assumption of X-Z plane of symmetry
- The basic equations are derived about the instantaneous center of gravity of the aircraft since the center of gravity is strongly dependent on nacelle incidence.
- Rotor and engine gyroscopic terms are included
- The wing elastic degrees of freedom do not couple inertially. The coupling occurs through the aerodynamic terms in the equations as discussed in Section 12.
- Wing aeroelastic effects are not included in the center of gravity calculations.

5.1 AXES SYSTEM

A set of right-handed orthogonal axes OXYZ is placed at the center of mass of the aircraft and is fixed in the aircraft such that OX lies in the lateral plane of symmetry and is positive forward parallel to the fuselage water line zero. The remaining axes are placed as shown in Figure 5.1.

The orientation of the aircraft is defined with respect to a

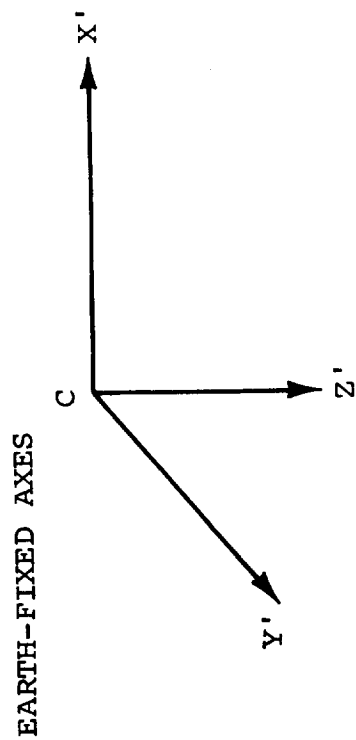
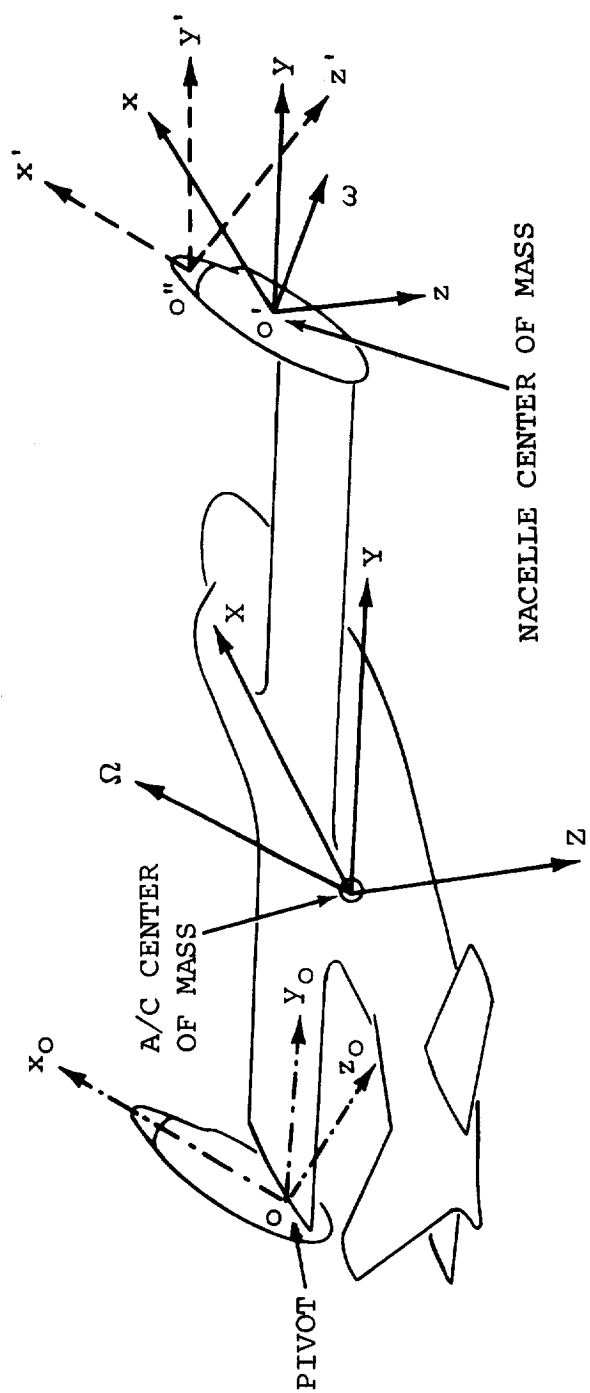


Figure 5.1. Axes Systems

set of earth-fixed axes $C X'Y'Z'$. With the axes $OXYZ$ initially parallel to $C X'Y'Z'$, the aircraft is yawed to the right about O through an angle ψ , then pitched up about OZ through the angle θ and finally rolled right about OX through the angle ϕ .

If \underline{V} and $\underline{\Omega}$ are the aircraft velocity and angular velocity vectors relative to the earth-fixed axes, the projections of these vectors on the moving axes are U , V , and W , for the components along OX , OY and OZ , and P , Q and R for the angular velocity components.

Thus

$$\underline{V} = U\hat{i} + V\hat{j} + W\hat{k} \quad (5.1)$$

$$\underline{\Omega} = P\hat{i} + Q\hat{j} + R\hat{k} \quad (5.2)$$

where the unit vectors \hat{i} , \hat{j} and \hat{k} lie along OX , OY and OZ .

5.2 AIRCRAFT GROUND TRACK

The components of \underline{V} relative to the earth-fixed axes are obtained in terms of U , V , W and ψ, θ, ϕ as, (See Reference 10),

$$\begin{aligned} \frac{dX'}{dt} = & U \cos \theta \cos \psi + V(\sin \phi \sin \theta \cos \psi - \cos \phi \sin \psi) \\ & + W (\cos \phi \sin \theta \cos \psi + \sin \theta \sin \psi) \end{aligned}$$

$$\begin{aligned} \frac{dY'}{dt} = & U \cos \theta \sin \psi + V(\sin \phi \sin \theta \sin \psi + \cos \phi \cos \psi) \\ & + W (\cos \phi \sin \theta \sin \psi - \sin \phi \cos \psi) \end{aligned} \quad (5.3)$$

$$\frac{dZ'}{dt} = -U \sin \theta + V \sin \phi \cos \theta + W \cos \phi \cos \theta$$

Integration of these equations gives the aircraft ground track.

A further relationship may be obtained between the rate of

change of the Euler angles (ψ, θ, ϕ) and the components of the angular velocity in the moving axes system, viz,

$$\begin{aligned}\dot{\psi} &= (R \cos \phi + Q \sin \phi) \sec \theta \\ \dot{\theta} &= Q \cos \phi - R \sin \phi \\ \dot{\phi} &= P + \dot{\psi} \sin \theta\end{aligned}\tag{5.4}$$

5.3 FORCE EQUATION

The total external force, \underline{F} , acting at the aircraft center of mass is given by

$$\underline{F} = \frac{d}{dt} (m \underline{V}) = m \left[\frac{\delta \underline{V}}{\delta t} + \underline{\Omega} \times \underline{V} \right]\tag{5.5}$$

where m is the mass of the aircraft and $\frac{\delta \underline{V}}{\delta t}$ is the rate of change of \underline{V} with respect to the moving reference frame OXYZ i.e.

$$\frac{\delta \underline{V}}{\delta t} = U \hat{i} + V \hat{j} + W \hat{k}\tag{5.6}$$

If \underline{F} has components F_x , F_y and F_z along the respective axes then

$$\underline{F} = F_x \hat{i} + F_y \hat{j} + F_z \hat{k} = m \left\{ U \hat{i} + V \hat{j} + W \hat{k} + \begin{vmatrix} \hat{i} & \hat{j} & \hat{k} \\ P & Q & R \\ U & V & W \end{vmatrix} \right\}$$

thus

$$\begin{aligned}F_x &= m (\dot{U} + QW - RV) \\ F_y &= m (\dot{V} + RU - PW) \\ F_z &= m (\dot{W} + PV - QU)\end{aligned}\tag{5.7}$$

The forces F_x , F_y and F_z are given by

$$\begin{aligned}
F_x &= X_{AERO} - mg \sin \theta \\
F_y &= Y_{AERO} + mg \sin \phi \cos \theta \\
F_z &= Z_{AERO} + mg \cos \phi \cos \theta
\end{aligned}
\tag{5.8}$$

where X_{AERO} , etc., are the components of the total aerodynamic force acting at the aircraft center of mass.

Substituting equations (5.8) in equations (5.7), the following equations are obtained for the aircraft accelerations,

$$\begin{aligned}
\dot{U} &= \frac{X_{AERO}}{m} - g \sin \theta - QW + RV \\
\dot{V} &= \frac{Y_{AERO}}{m} + g \cos \theta \sin \phi - RU + PW \\
\dot{W} &= \frac{Z_{AERO}}{m} + g \cos \theta \cos \phi + QU - PV
\end{aligned}
\tag{5.9}$$

5.4 MOMENT EQUATION

The derivation of the equations for the total moment acting about the aircraft center of mass is complicated by the fact that the center of mass changes position due to the tilting nacelles. Thus the centers of gravity of the principal aircraft component masses of the wings (m_w), fuselage (including tails) (m_f), and nacelles (m_N), move with respect to the reference axes OXYZ placed at the instantaneous overall center of gravity of the aircraft. The equation of motion for such a mass element will first be obtained and the total moment found by adding the contributions of all the elements.

5.5 EQUATION OF MOTION FOR A MASS ELEMENT

With reference to Figure (5.1) $O'xyz$ is a right-handed set of axes placed at the center of gravity of the representative mass. The axes are parallel to the set OXYZ. The mass, m ,

rotates about its own center of gravity with angular velocity $\underline{\omega}$ which, in general, differs from $\underline{\Omega}$ the angular velocity of the aircraft. If \underline{r} is the radius vector from O to O' then the velocity of the center of mass of the element is

$$\underline{V} = \frac{\delta \underline{r}}{\delta t} + \underline{\Omega} \times \underline{r} \quad (5.10)$$

The angular momentum of this mass about O is

$$\underline{h} = m (\underline{r} \times \underline{V}) + \underline{h}_0 \quad (5.11)$$

where \underline{h}_0 is the angular momentum of m about its own center of mass and is given by

$$\underline{h}_0 = \bar{I} \underline{\omega} \quad (5.12)$$

where

$$\bar{I} = \begin{bmatrix} I_{xx} & -I_{xy} & -I_{xz} \\ -I_{yx} & I_{yy} & -I_{yz} \\ -I_{zx} & -I_{zy} & I_{zz} \end{bmatrix} \quad (5.13)$$

and I_{xx} , etc., are the moments and products of inertia of the mass about O'xyz.

The total moment, \underline{G} , about the aircraft center of mass is given by

$$\underline{G} = \frac{d\underline{h}}{dt} = \frac{\delta \underline{h}}{\delta t} + \underline{\Omega} \times \underline{h} \quad (5.14)$$

Using equations (5.10), (5.11) and (5.12) in (5.14) the moment becomes

$$\begin{aligned} \underline{G} = m \left[\frac{\delta \underline{r}}{\delta t} \times \left(\frac{\delta \underline{r}}{\delta t} + \underline{\Omega} \times \underline{r} \right) + \underline{r} \times \frac{\delta}{\delta t} \left(\frac{\delta \underline{r}}{\delta t} + \underline{\Omega} \times \underline{r} \right) \right] + \frac{\delta}{\delta t} (\bar{I} \underline{\omega}) \\ + m \underline{\Omega} \times \left[\underline{r} \times \left(\frac{\delta \underline{r}}{\delta t} + \underline{\Omega} \times \underline{r} \right) \right] + \underline{\Omega} \times (\bar{I} \underline{\omega}) \end{aligned} \quad (5.15)$$

which reduces to

$$\underline{G} = 2m\underline{\Omega} \left(\underline{r} \cdot \frac{\delta \underline{r}}{\delta t} \right) + m \underline{r} \times \frac{\delta^2 \underline{r}}{\delta t^2} + m \frac{\delta \underline{\Omega}}{\delta t} (\underline{r} \cdot \underline{r}) - m \underline{r} \left(\underline{r} \cdot \frac{\delta \underline{\Omega}}{\delta t} \right) \quad (5.16)$$

$$- 2m \frac{\delta \underline{r}}{\delta t} (\underline{\Omega} \cdot \underline{r}) - m (\underline{r} \cdot \underline{\Omega}) (\underline{\Omega} \times \underline{r}) + I \frac{\delta \underline{\omega}}{\delta t} + \underline{\Omega} \times (\bar{I} \underline{\omega})$$

The only masses that possess angular velocities different from that of the aircraft are the nacelles, which are free to pitch about O' with angular rate $\dot{i} = \frac{di_N}{dt}$. Thus $\underline{\omega}$ may be written generally as

$$\underline{\omega} = P \hat{i} + (Q + \dot{i}_N) \hat{j} + R \hat{k} \quad (5.17)$$

Now, with $\underline{r} = X \hat{i} + Y \hat{j} + Z \hat{k}$, where X, Y, and Z are the instantaneous coordinates of the individual mass center relative to the aircraft mass center, the various terms of equation (5.16) are, in component form,

$$\underline{r} \cdot \frac{\delta \underline{r}}{\delta t} = \dot{X}X + \dot{Y}Y + \dot{Z}Z$$

$$\underline{r} \times \frac{\delta^2 \underline{r}}{\delta t^2} = (YZ - ZY) \hat{i} - (XZ - ZX) \hat{j} + (XY - YX) \hat{k}$$

$$\frac{\delta \underline{\Omega}}{\delta t} (\underline{r} \cdot \underline{r}) = (X^2 + Y^2 + Z^2) (\dot{P} \hat{i} + \dot{Q} \hat{j} + \dot{R} \hat{k})$$

$$\underline{r} \cdot \frac{\delta \underline{\Omega}}{\delta t} = X \dot{P} + Y \dot{Q} + Z \dot{R}$$

$$\underline{\Omega} \cdot \underline{r} = XP + YQ + ZR$$

$$(\underline{r} \cdot \underline{\Omega}) (\underline{\Omega} \times \underline{r}) = (XP + YQ + ZR) \left[(QZ - RY) \hat{i} - (PZ - RX) \hat{j} + (PY - XQ) \hat{k} \right]$$

$$\bar{I} \frac{\delta \underline{\omega}}{\delta t} = (I_{xx} \dot{P} - I_{xz} R) \hat{i} + I_{yy} (\dot{Q} + \dot{i}_N) \hat{j} + (I_{zz} \dot{R} - I_{xz} P) \hat{k}$$

$$\underline{\Omega} \times (\bar{I} \underline{\omega}) = (QR I_{zz} - QP I_{xz} - RQ I_{yy} - R \dot{i}_N I_{yy}) \hat{i}$$

$$- (PR I_{zz} - P^2 I_{xz} - PR I_{xx} + R^2 I_{xz}) \hat{j}$$

$$+ (QR I_{xz} + PQ I_{yy} + P \dot{i}_N I_{yy} - PQ I_{xx}) \hat{k}$$

where, in the last two terms, the products of inertia I_{xy} and I_{yz} are zero from symmetry considerations.

Substituting the above relations into equation (5.16) and noting that \dot{Y} and \ddot{Y} are always zero (no lateral motion of the individual masses) the following expressions are obtained for the components of the moment $\underline{G} = \Delta L \hat{i} + \Delta M \hat{j} + \Delta N \hat{k}$:

$$\begin{aligned} \Delta L = & \dot{P} [I_{xx} + m(Y^2 + Z^2)] - (\dot{R} + PQ) [I_{xz} + m XZ] \\ & + RQ [I_{zz} - I_{yy} + m(Y^2 - Z^2)] + m YZ (R^2 - Q^2) - I_{yy} R \dot{i}_N \\ & + m (Y\ddot{Z} - 2\dot{X}YR - 2\dot{X}ZR + 2Z\dot{Z}P - XY (\dot{Q} - PR)) \\ \Delta M = & \dot{Q} [I_{yy} + m(X^2 + Z^2)] - (R^2 - P^2) [I_{xz} + m XZ] \\ & + PR [I_{xx} - I_{zz} + m(Z^2 - X^2)] + I_{yy} \dot{i}_N \\ & + m [\ddot{X}Z - X\ddot{Z} + 2Q(Z\dot{Z} + X\dot{X}) - XY (\dot{P} + RQ) + YZ (PQ - \dot{R})] \end{aligned} \quad (5.19)$$

$$\begin{aligned} \Delta N = & \dot{R} [I_{zz} + m(X^2 + Y^2)] - (\dot{P} - RQ) [I_{xz} + m XZ] \\ & + PQ [I_{yy} - I_{xx} + m(X^2 - Y^2)] + I_{yy} P \dot{i}_N \\ & + m [2X\dot{X}R - Y\ddot{X} - 2XZP - 2Y\dot{Z}Q - YZ (\dot{Q} + PR) + XY (Q^2 - P^2)] \end{aligned} \quad (5.20)$$

Summing the rolling moment equation:

$$\begin{aligned} L = & I_{xx} \dot{P} - I_{xz} (\dot{R} + PQ) + (I_{zz} - I_{yy}) RQ \\ & + m_N (R^2 - Q^2) (Z_{NR} - Z_{NL}) Y_N + m_N \left\{ Y_N (\ddot{Z}_{NR} - \ddot{Z}_{NL}) \right. \\ & - 2Q (\dot{X}_{NR} - \dot{X}_{NL}) Y_N - 2R (\dot{X}_{NR} Z_{NR} + \dot{X}_{NL} Z_{NL}) + 2P (\dot{Z}_{NR} Z_{NR} + \\ & \left. \dot{Z}_{NL} Z_{NL}) - (\dot{Q} - PR) (X_{NR} - X_{NL}) Y_N \right\} + 2m_f Z_f (P\dot{Z}_f - \\ & R\dot{X}_f) + 2m_w Z_w (P\dot{Z}_w - R\dot{X}_w) - R I_{yy}^N (\dot{i}_{NL} + \dot{i}_{NR}) \end{aligned} \quad (5.21)$$

where I_{xx} , I_{xz} , I_{zz} and I_{yy} are the inertias of the aircraft about its center of gravity, and the subscripts f, w, NL and NR stand for fuselage, wing, left nacelle and right nacelle. The remaining symbols are defined in the List of Symbols. Similar expressions are obtained for the pitching moment and yawing

moment. In the interests of brevity the remainder of the discussion will be limited to equation (5.21).

Evaluation of the terms of the rolling moment equation indicate that this equation may be simplified considerably without a significant change in accuracy. For example, terms containing $(\dot{x}_{NR} - \dot{x}_{NL})$ may be dropped because \dot{x}_{NR} is normally identical to \dot{x}_{NL} , i.e. the nacelles are raised or lowered together at the same rate. Equation (5.21) may thus be written

$$L = I_{XX}\dot{P} - I_{XZ}(\dot{R} + P\dot{Q}) + (I_{ZZ} - I_{YY})R\dot{Q} + m_N Y_N (\ddot{x}_{NR} - \ddot{z}_{NL}) \quad (5.22)$$

where the last term has been retained in consideration of the high differential nacelle accelerations encountered during hover maneuvers.

From the relationships presented in Appendix C the last term of equation (5.22) may be rewritten as

$$\begin{aligned} & -\lambda m_N Y_N [\ddot{i}_{NR} \cos(i_{NR} - \lambda) + \dot{i}_{NL}^2 \sin(i_{NL} - \lambda) \\ & \quad - \dot{i}_{NR}^2 \sin(i_{NR} - \lambda) - \ddot{i}_{NL} \cos(i_{NL} - \lambda)] \end{aligned} \quad (5.23)$$

which may be approximated to

$$-\lambda m_N Y_N [\ddot{i}_{NR} \cos(i_{NR} - \lambda) - \ddot{i}_{NL} \cos(i_{NL} - \lambda)] \quad (5.24)$$

since the nacelle rates appear as squared terms.

Similar treatment of the pitching moment and yawing moment equations results in the following final form of the moment equations.

$$\begin{aligned}
L_{AERO} &= I_{XX} \dot{P} - I_{XZ} (\dot{R} + PQ) + (I_{ZZ} - I_{YY}) RQ \\
&\quad - \ell m_N Y_N [\ddot{i}_{NR} \cos(i_{NR} - \lambda) - \ddot{i}_{NL} \cos(i_{NL} - \lambda)] \\
M_{AERO} &= I_{YY} \dot{Q} - I_{XZ} (R^2 - P^2) + (I_{XX} - I_{ZZ}) PR \\
&\quad + \ddot{i}_{NR} \left\{ I_{YY_0}^N + \ell m_N [X_R \cos(i_{NR} - \lambda) - Z_R \sin(i_{NR} - \lambda)] \right\} \\
&\quad + \ddot{i}_{NL} \left\{ I_{YY_0}^N + \ell m_N [X_L \cos(i_{NL} - \lambda) - Z_L \sin(i_{NL} - \lambda)] \right\} \quad (5.25) \\
N_{AERO} &= I_{ZZ} \dot{R} - I_{XZ} (\dot{P} - RQ) + (I_{YY} - I_{XX}) PQ \\
&\quad + \ell m_N Y_N [\ddot{i}_{NR} \sin(i_{NR} - \lambda) - \ddot{i}_{NL} \sin(i_{NL} - \lambda)]
\end{aligned}$$

where the moments L_{AERO} , M_{AERO} and N_{AERO} represent the sum of the aerodynamic moments and rotor/engine gyroscopic moments about the aircraft center of mass. $I_{YY_0}^N$ is the nacelle pitch inertia referred to the nacelle-fixed axes system described in Appendix C. Equations for the aircraft inertias are also presented in that Appendix.

5.6 EQUATIONS OF MOTION FOR NACELLES

The equation of motion for a nacelle is required in order to obtain the moment exerted by the nacelle on the wing tip at the pivot. This moment is then used in the equations for wing twist.

The angular momentum of a nacelle about its pivot point is given by

$$\begin{aligned}
\underline{h}_p &= (\underline{r} - \underline{r}_p) \times m_N \underline{V} + \underline{h}_{oN} \\
&= m_n (\underline{r} \times \underline{V}) + \underline{h}_o - m_n \underline{r}_p \times \underline{V} \quad (5.26)
\end{aligned}$$

where \underline{r} is the radius vector from aircraft c.g. to nacelle c.g.
 \underline{V} is the velocity of the nacelle c.g.

\underline{h}_{ON} is the angular momentum of the nacelle about its own c.g.

m_N is the nacelle mass

and \underline{r}_p is the radius vector from aircraft c.g. to nacelle pivot

The term $m_N (\underline{r}_p \times \underline{V}) + \underline{h}_{ON}$ is the angular momentum of the nacelle about the aircraft c.g. ($= \underline{h}_{CG}^N$)

$$\text{i.e. } \underline{h}_p = \underline{h}_{CG}^N - m_N (\underline{r}_p \times \underline{V})$$

The moment about the pivot is

$$G_p = \frac{d\underline{h}_p}{dt} = \frac{d\underline{h}_N}{dt} - m_N \frac{d}{dt} (\underline{r}_p \times \underline{V}) = \underline{G}_{CG}^N - \underline{\Delta G} \quad (5.27)$$

Since the quantity \underline{G}_{CG}^N has already been obtained (equations (5.18), (5.19) and (5.20)), only the remaining term needs to be evaluated.

$$\begin{aligned} \underline{\Delta G} &= m_N \frac{d}{dt} (\underline{r}_p \times \underline{V}) = m_N \left\{ \frac{\delta \underline{r}_p}{\delta t} \times \underline{V} + \underline{r}_p \times \frac{\delta \underline{V}}{\delta t} + \underline{\Omega} (\underline{r}_p \times \underline{V}) \right\} \\ &= m_N \left\{ \frac{\delta \underline{r}_p}{\delta t} \times \left(\frac{\delta \underline{r}}{\delta t} + \underline{\Omega} \times \underline{r} \right) + \underline{r}_p \times \frac{\delta}{\delta t} \left(\frac{\delta \underline{r}}{\delta t} + \underline{\Omega} \times \underline{r} \right) \right. \\ &\quad \left. + \underline{\Omega} \times \left[\underline{r}_p \times \left(\frac{\delta \underline{r}}{\delta t} + \underline{\Omega} \times \underline{r} \right) \right] \right\} \quad (5.28) \end{aligned}$$

Expansion of these terms results in the following expression

$$\begin{aligned} \underline{\Delta G} &= m_N \left\{ \frac{\delta \underline{r}_p}{\delta t} \times \frac{\delta \underline{r}}{\delta t} + \underline{\Omega} \left(\underline{r}_p \cdot \frac{\delta \underline{r}_p}{\delta t} \right) - \underline{r}_p \left(\frac{\delta \underline{r}_p}{\delta t} \cdot \underline{\Omega} \right) + \underline{r}_p \times \frac{\delta^2 \underline{r}}{\delta t^2} + \frac{\delta \underline{\Omega}}{\delta t} (\underline{r}_p \cdot \underline{r}_p) \right. \\ &\quad - \underline{r}_p \left(\underline{r}_p \cdot \frac{\delta \underline{\Omega}}{\delta t} \right) + \underline{\Omega} \left(\frac{\delta \underline{r}}{\delta t} \cdot \underline{r}_p \right) - 2 \frac{\delta \underline{r}}{\delta t} (\underline{r}_p \cdot \underline{\Omega}) \\ &\quad \left. + \underline{r}_p \left(\frac{\delta \underline{r}}{\delta t} \cdot \underline{\Omega} \right) - (\underline{r}_p \cdot \underline{\Omega}) (\underline{\Omega} \times \underline{r}) \right\} \end{aligned}$$

We require only the \hat{j} component of this vector in order to obtain the nacelle pivot pitching moment.

The components of the vectors \underline{r}_p , \underline{r} and $\underline{\Omega}$ are

$$\begin{aligned}\underline{r}_p &= x_p \hat{i} + y_N \hat{j} + z_p \hat{k} = -x_{CG} \hat{i} + y_N \hat{j} - z_{CG} \hat{k} \\ \underline{r} &= x_N \hat{i} + y_N \hat{j} + z_N \hat{k} \\ \underline{\Omega} &= P \hat{i} + Q \hat{j} + R \hat{k}\end{aligned}$$

Noting that the \hat{j} components of $\frac{\delta \underline{r}_p}{\delta t}$, $\frac{\delta \underline{r}}{\delta t}$ are zero (since y_N is a constant), the above expression yields

$$\Delta M = m_N \left\{ \ddot{x}_N z_{CG} - \ddot{z}_N x_{CG} + \dot{z}_{CG} \dot{x}_N + \dot{z}_N \dot{x}_{CG} + PQ y_N z_N - RQ x_N y_N \right\} \quad (5.30)$$

Combining this equation with Equation (5.19) and using the transformations given in Appendix C, the final equation for the right-hand nacelle pivot actuator pitching moment becomes, after some simplification,

$$\begin{aligned}M_{NR} = & -I_{NR} \left[I_{YY_0}^N + \ell^2 m_N \left(1 - \frac{m_N}{m} \right) - \ell^2 m_N \left(1 - \frac{m_N}{m} \right) \dot{Q} - PR \cos 2(i_{NR} - \lambda) \right. \\ & \left. + (R^2 - P^2) \sin(i_{NR} - \lambda) \cos(i_{NR} - \lambda) \right] - (R^2 - P^2) I_{zz_0}^N \sin i_{NR} \cos i_{NR} \\ & - I_{YY_0} \dot{Q} + \ell \frac{m_N}{m} \left[x_{AERO} \sin(i_{NR} - \lambda) + z_{AERO} \cos(i_{NR} - \lambda) \right] \\ & - \ell m_N y_N \left\{ (\dot{R} - PQ) \sin(i_{NR} - \lambda) - (\dot{P} + RQ) \cos(i_{NR} - \lambda) \right\} \\ & + M_{NRAERO}\end{aligned} \quad (5.31)$$

where M_{NRAERO} includes the moment resulting from nacelle aerodynamic loads and the rotor gyroscopic moments. The terms x_{AERO} and z_{AERO} are, respectively, the total aircraft aerodynamic X and Z forces.

The corresponding equation for the left nacelle actuator moment is obtained by substituting $-y_N = y_N$ and changing the R subscript to L.

5.7 DETERMINATION OF ROTOR GYROSCOPIC MOMENTS

The gyroscopic moments are most readily obtained as follows. A set of axes $O''x'y'z'$ is taken at the rotor hub (rotor c.g.) parallel to the nacelle-fixed set of axes $Ox_0y_0z_0$. Associated with each axis are the corresponding unit vectors \hat{i}' , \hat{j}' and \hat{k}' . The angular velocity of the rotor with respect to these axes is the vector

$$\underline{\omega} = \Omega_R \hat{i}' \quad (5.32)$$

where Ω_R is the rotor rotational speed.

The angular momentum of the rotor with respect to its c.g. is

$$\underline{h}_O = \bar{I}_R \underline{\omega} \quad (5.33)$$

where \bar{I}_R is the inertia matrix

$$\begin{bmatrix} I_{R_x} & & \\ & I_{R_y} & \\ & & I_{R_z} \end{bmatrix}$$

the off-diagonal terms being zero since the axes $O''x'y'z'$ are principal axes of inertia of the rotor and hub.

In component form the angular momentum of the rotor is

$$\underline{h}_O = I_{R_y} \Omega_R \hat{j}' = I_R \Omega_R \hat{i}' \quad (5.34)$$

With respect to the inertial axes OXYZ, the components of \underline{h}_O are

$$\underline{h}_O = I_R \Omega_R \cos i_N \hat{i} - I_R \Omega_R \sin i_N \hat{k} \quad (5.35)$$

The hub moment is therefore given by

$$\underline{G}_{HUB} = \frac{d\underline{h}_O}{dt} = \frac{\delta \underline{h}_O}{\delta t} + \underline{\Omega} \times \underline{h}_O \quad (5.36)$$

$$\text{where } \underline{\Omega} = P \hat{i} + Q \hat{j} + R \hat{k} \quad (5.37)$$

Substitution of equations (5.35) and (5.37) into equation (5.36) results in the following equations for the rotor gyroscopic moments.

$$L_{\text{gyro}} = I_R \dot{\Omega}_R \cos i_N - I_R \Omega_R (\dot{i}_N + Q) \sin i_N \quad (5.38)$$

$$M_{\text{gyro}} = I_R P \Omega_R \sin i_N + I_R R \Omega_R \cos i_N \quad (5.39)$$

$$N_{\text{gyro}} = -I_R \dot{\Omega}_R \sin i_N - I_R \Omega_R (\dot{i}_N + Q) \cos i_N \quad (5.40)$$

The above terms appear in the Computer Representation (Appendix E) as additions to the rotor aerodynamic forces and moments.

6.0 AIRFRAME AERODYNAMICS

This section presents the mathematical equations and representations of the aerodynamic data for the aircraft without rotors. The contribution of the rotors is described in Section 7. The overall airframe aerodynamics are obtained from the following components:

- (a) Fuselage
- (b) Wings
- (c) Horizontal Tail
- (d) Vertical Tail
- (e) Nacelles

The data and equations for each of the aerodynamic components are discussed below, together with the substantiating methods. The aerodynamic data are presented in local wind axes. Resolution to aircraft body axes is accomplished as described in the mathematical model (Appendix E). Where required, the equations have been written so as to be applicable over the entire range of angle of attack ± 180 degrees.

6.1 FUSELAGE

The aerodynamic lift, drag and pitching moment coefficients of the fuselage were estimated using the methods of Reference 1. The forces and moments are referred to the point on the fuselage corresponding to the wing quarter chord position. This reference point was selected in order to minimize the number of force and moment transfer equations in the mathematical

model. Wing-to-body carryover effects have been included in fuselage loads.

The equations for the fuselage forces and moments are:

$$\text{Lift:} \quad C_{L_F} = K_{42} + K_3 \sin \alpha_F \cos \alpha_F + K_4 \sin \alpha_F \cos \alpha_F | \sin \alpha_F \cos \alpha_F |$$

$$\text{Drag:} \quad C_{D_F} = C_{D_{O_F}} (1 + K_O |\beta_F|^3) + K_2 (\sin \alpha_F \cos \alpha_F)^2 + K_1 | \sin \alpha_F \cos \alpha_F | + \Delta C_{D_{LG}}$$

$$\text{Side Force:} \quad C_{Y_F} = K_7 \sin \beta_F \cos \beta_F + K_8 \sin \beta_F \cos \beta_F | \sin \beta_F \cos \beta_F |$$

$$\text{Pitching Moment:} \quad C_{M_F} = C_{M_{O_F}} + K_5 \sin \alpha_F \cos \alpha_F + K_6 \sin \alpha_F \cos \alpha_F | \sin \alpha_F \cos \alpha_F | + \Delta C_{M_{LG}}$$

$$\text{Yawing Moment:} \quad C_{N_F} = C_{N_{O_F}} + K_9 \sin \beta_F \cos \beta_F + K_{10} \sin \beta_F \cos \beta_F | \sin \beta_F \cos \beta_F |$$

$$\text{Rolling Moment:} \quad C_{\ell_F} = 0$$

$$\text{where } \alpha_F = \tan^{-1} \left(\frac{W}{U} \right), \quad C_{L_F} = \frac{L_F}{\frac{1}{2} \rho V_{FUS}^2 S_W} \quad \text{etc.}$$

$$\beta_F = \tan^{-1} \left[\frac{V}{\sqrt{U^2 + W^2}} \right], \quad C_{M_F} = \frac{M_F}{\frac{1}{2} \rho V_{FUS}^2 S_W C_W} \quad \text{etc.}$$

and $\Delta C_{D_{LG}}$, $\Delta C_{M_{LG}}$, are the landing gear contributions to fuselage drag and pitching moment coefficients, when the landing gear is extended.

The fuselage forces and moments are then resolved into body axes at the aircraft C.G.

6.2 NACELLES

The forces and moments acting on the nacelles were estimated using the cross-flow methods of Reference 12. For convenience the resulting forces and moments are referred to the rotor hub, so that they may be added directly to the rotor forces and moments. The following equations are for the forces and moments on two nacelles:

$$C_{L_N} = K_{32} \sin \alpha_N \cos \alpha_N$$

$$C_{D_N} = C_{D_{O_N}} + K_{30} |\alpha_N| + K_{31} \alpha_N^2$$

$$C_{M_N} = C_{M_{O_N}} + K_{34} \sin \alpha_N \cos \alpha_N + K_{35} \sin \alpha_N \cos \alpha_N |\sin \alpha_N \cos \alpha_N|$$

$$C_{Y_N} = K_{36} \sin \beta_N \cos \beta_N + K_{37} \sin \beta_N \cos \beta_N |\sin \beta_N \cos \beta_N|$$

$$C_{N_N} = C_{N_{O_N}} + K_{38} \sin \beta_N \cos \beta_N + K_{39} \sin \beta_N \cos \beta_N |\sin \beta_N \cos \beta_N|$$

$$C_{x_N} = 0$$

The nacelle forces and moments in nacelle axes are:

$$\Delta X'_N = q_N S_W [-C_{D_N} \cos \alpha_N + C_{L_N} \sin \alpha_N - C_{Y_N} \sin \beta_N \cos \alpha_N]^{1/2}$$

$$\Delta Y'_N = q_N S_W [C_{Y_N} \cos \beta_N - C_{D_N} \sin \beta_N]^{1/2}$$

$$\Delta Z'_N = q_N S_W [-C_{L_N} \cos \alpha_N - C_{D_N} \cos \beta_N \sin \alpha_N - C_{Y_N} \sin \beta_N \sin \alpha_N]^{1/2}$$

$$\Delta x'_N = q_N S_W b_W \left[-\left(\frac{C_W}{b_W}\right) C_{M_N} \sin \beta_N \cos \alpha_N - C_{N_N} \sin \alpha_N \right]^{1/2}$$

$$\Delta M'_N = q_N S_W C_W [C_{M_N} \cos \beta_N]^{1/2}$$

$$\Delta N'_N = q_N S_W b_W [C_{N_N} \cos \alpha_N - \left(\frac{C_W}{b_W}\right) C_{M_N} \sin \beta_N \cos \alpha_N]^{1/2}$$

6.3 HORIZONTAL TAIL

Aerodynamics of the horizontal tail were obtained using the methods of Reference 1 in combination with test data. The horizontal tail includes a plain elevator.

The angle of attack of the horizontal tail, including interference effects, for zero elevator deflection, is

$$\alpha_{HT} = \tan^{-1} \left[\frac{w_{HT}}{u_{HT}} \right] - \epsilon + i_{HT}$$

where ϵ is the total downwash at the tail due to wing, rotor and ground effects and i_{HT} is the tail incidence angle.

The effect of elevator deflection on the effective tail angle of attack is introduced through the elevator effectiveness parameter, τ_{HT} , which is a function of the elevator and horizontal tail areas. Thus the effective horizontal tail angle of attack is

$$\alpha_{eHT} = \alpha_{HT} + \tau_{HT} \delta_e$$

where δ_e is the elevator deflection.

The tail downwash angle, ϵ , depends on wing angle of attack and on rotor slipstream deflection. At a given rotor angle of attack, the slipstream deflection is a function of rotor thrust coefficient, C_{TS} , where the coefficient is based on the slipstream dynamic pressure. Figure 6.1 presents data on downwash angles measured during tests on a tilt rotor wind tunnel model (Reference 7). As can be seen, the downwash at low values of thrust coefficient is the same as the value of the power-off wing

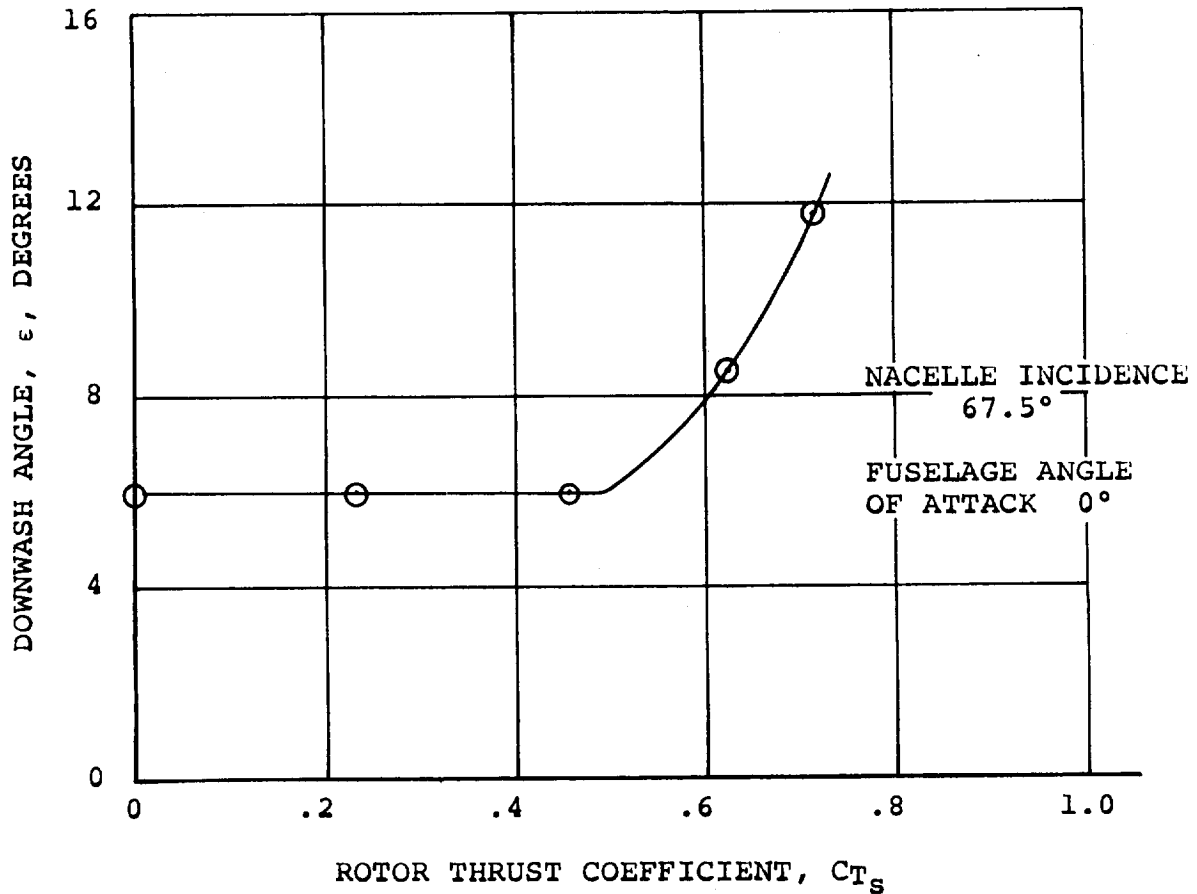


Figure 6.1. Variation of Horizontal Tail Downwash Angle with Thrust Coefficient

downwash ($C_{TS}=0$). Above values of C_{TS} in the neighborhood of $C_{TS}=0.5$ the downwash increases with increasing thrust coefficient. The values in the increasing portion of ϵ vs C_{TS} were found to correspond approximately to the slipstream deflection angle ϵ_p . Therefore, the approach adopted in the mathematical

model was to test if the rotor slipstream downwash ($\bar{\epsilon}_p$) exceeded the wing downwash and, if so, to use the computed slipstream downwash value as the tail downwash angle. Otherwise the wing downwash value was used. Thus if

$$\bar{\epsilon}_p \geq \epsilon_0 + \frac{d\epsilon}{d\alpha} (\bar{\alpha}_w - l_{AC} \frac{\dot{W}}{U^2})$$

$$\text{then } \epsilon = \frac{\bar{\epsilon}_p (1-GEF)}{\sqrt{1-M^2}}$$

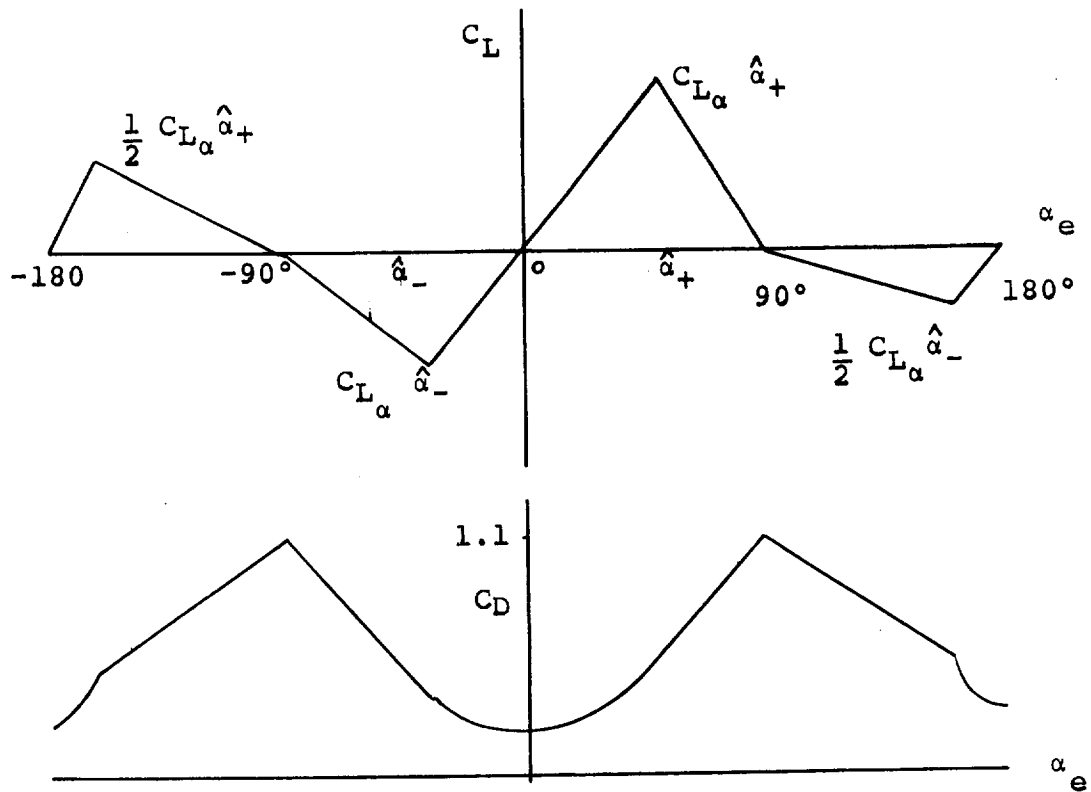
otherwise

$$\epsilon = \left[\epsilon_0 + \frac{d\epsilon}{d\alpha} (\bar{\alpha}_w - l_{AC} \frac{\dot{W}}{U^2}) \right] \frac{(1-GEF)}{\sqrt{1-M^2}}$$

In these expressions ϵ_0 is the wing downwash angle at zero wing angle-of-attack, $\frac{d\epsilon}{d\alpha}$ is the downwash derivative, l_{AC} is the distance from the wing to the tail aerodynamic centers, and $l_{AC} \frac{\dot{W}}{U^2}$ is the familiar downwash lag term. In general, the quantities ϵ_0 and $\frac{d\epsilon}{d\alpha}$ depend on the average of the left and right flaperon deflections. The effect of differential deflection of aileron/spoiler in producing an asymmetrical downwash field at the horizontal tail was not included because of the small contribution this makes to total aircraft rolling moment.

The term (1-GEF) in the above equations is the ground effect factor. This quantity was obtained from Reference 10 and is a function of the wing span and height of the horizontal tail above the ground. This factor, when multiplied by the downwash which would be found out of ground effect, yields the downwash in ground effect. Ground effect is discussed in more detail in Section 10.

The lift and drag forces acting on the horizontal tail are required over the complete range of angle of attack -180° to $+180^\circ$, since the tilt rotor can fly backwards. The following sketch shows the schematic variation of lift and drag coefficients over this range plotted as a function of the effective horizontal tail angle of attack, α_{eHT} .



The angle of attack for C_{LHTMAX} is denoted by $\hat{\alpha}_{HT+}$ and is the value of the effective angle of attack at the stall less 2 degrees i.e.

$$\hat{\alpha}_{HT+} = (\alpha_{HTSTALL} - 2^\circ) + \tau_{HT} \delta_e$$

Similarly the angle of attack for stall at negative angles of attack is

$$\hat{\alpha}_{HT-} = -(\alpha_{HTSTALL} - 2^\circ) + \tau_{HT} \delta_e$$

The slope of the lift curve within this range of positive and negative angles of attack is given by

$$C_{L_\alpha} = \frac{C_{L_{\alpha HT}} \left(\frac{a_g}{a} \right)}{\sqrt{1-M^2}}$$

where a_g/a is the ratio of tail lift-curve slopes in and out of ground effect, and $\sqrt{1-M^2}$ is the Prandtl-Glauert correction factor for the effect of Mach number on lift-curve slope.

Within this region on the lift curve the value of lift coefficient is given by $C_{L_{HT}} = C_{L_\alpha} \alpha_{eHT}$ and the corresponding drag coefficient by

$$C_{D_{HT}} = C_{D_{OHT}} + \frac{2C_{L_{HT}}^2}{\pi AR_{HT}}$$

After stall angle of attack is passed the lift is assumed to fall linearly to zero at $\alpha_e = \pm 90^\circ$.

In these regions the lift is given by

$$C_{L_\alpha} = C_{L_\alpha} \frac{\hat{\alpha}_\pm \frac{(+90 - \alpha_{eHT})}{(+90 - \hat{\alpha}_{HT\pm})}}{1}$$

where the appropriate signs are taken depending on the sign of α_{eHT} .

The corresponding drag is obtained by assuming a linear variation of drag from the value at $C_{L_{MAX}}$ to a value of $C_D = 1.1$ (flat plate normal to stream) at $\alpha_{eHT} = 90^\circ$. Thus

$$C_{L_{HT} \text{ STALL}} = C_{L_{\alpha}} \hat{\alpha}_{HT+}$$

$$C_{D_{HT} \text{ STALL}} = C_{D_{OHT}} + \frac{2C_{L_{HT} \text{ STALL}}^2}{\pi AR_{HT}}$$

and

$$C_{D_{HT}} = C_{D_{HT} \text{ STALL}} + \frac{(\alpha_{e_{HT}} - \hat{\alpha}_{HT+})(1.1 - C_{D_{HT} \text{ STALL}})}{(+90 - \hat{\alpha}_{HT+})}$$

If the effective angle of attack of the horizontal tail exceeds $+90^\circ$ the tail will point trailing-edge first into the relative wind. Under this condition early stalling is precipitated because of the sharp "leading edge" and blunt "trailing edge". In order to represent this, it was assumed that the attainable $C_{L_{MAX}}$ of the tail under these conditions is half that occurring in normal flight.

$$\text{Thus if } 90^\circ < \alpha_{e_{HT}} \leq (180 - \frac{1}{2} \hat{\alpha}_{HT-})$$

$$\text{or } (-180 + \frac{1}{2} \hat{\alpha}_{HT+}) \leq \alpha_{e_{HT}} < -90^\circ$$

then

$$C_{L_{HT}} = .5C_{L_{\alpha}} \hat{\alpha}_{HT-} \frac{(\alpha_{e_{HT}} - 90^\circ)}{(90^\circ - \frac{1}{2} \hat{\alpha}_{HT-})}$$

$$\text{or } C_{L_{HT}} = .5C_{L_{\alpha}} \hat{\alpha}_{HT+} \frac{(\alpha_{e_{HT}} + 90^\circ)}{(-90^\circ + \frac{1}{2} \hat{\alpha}_{HT+})}$$

The corresponding drag coefficients are:

$$\text{for } 90^\circ < \alpha_{e_{HT}} \leq (180 - \frac{1}{2} \hat{\alpha}_{HT-});$$

$$C_{L_{HT} \text{ STALL}} = 0.5 C_{L_{\alpha}} \hat{\alpha}_{HT-}$$

$$C_{D_{HT} \text{ STALL}} = \frac{2C_{L_{HT} \text{ STALL}}^2}{\pi AR_{HT}} + C_{D_{OHT}}$$

which gives $C_{D_{HT}} = C_{D_{HT_{STALL}}} + \frac{(\alpha_{e_{HT}} + 0.5 \hat{\alpha}_{HT_{-}} - 180^\circ)(1.1 - C_{D_{HT_{STALL}}})}{(0.5 \hat{\alpha}_{HT_{-}} - 90^\circ)}$

and for $(-180 + \frac{1}{2} \hat{\alpha}_{HT_{+}}) \leq \alpha_{e_{HT}} < -90^\circ$;

$$C_{L_{HT_{STALL}}} = 0.5 C_{L_\alpha} \hat{\alpha}_{HT_{+}}$$

$$C_{D_{HT_{STALL}}} = \frac{2C_{L_{HT_{STALL}}}^2}{\pi AR_{HT}} + C_{D_{O_{HT}}}$$

which gives $C_{D_{HT}} = C_{D_{HT_{STALL}}} - \frac{(\alpha_{e_{HT}} + 180^\circ - .5 \hat{\alpha}_{HT_{+}})(1.1 - C_{D_{HT_{STALL}}})}{(.5 \hat{\alpha}_{HT_{+}} - 90^\circ)}$

In the range $(180 - .5 \hat{\alpha}_{HT_{-}}) \leq \alpha_{e_{HT}} \leq 180^\circ$ when the tail has unstalled

$$C_{L_{HT}} = C_{L_\alpha} (\alpha_{e_{HT}} - 180^\circ)$$

$$C_{D_{HT}} = C_{D_{O_{HT}}} + \frac{2C_{L_{HT}}^2}{\pi AR_{HT}}$$

and similarly for the range $-180^\circ \leq \alpha_{e_{HT}} < (-180 + .5 \hat{\alpha}_{HT_{+}})$

$$C_{L_{HT}} = C_{L_\alpha} (\alpha_{e_{HT}} + 180^\circ)$$

$$C_{D_{HT}} = C_{D_{O_{HT}}} + \frac{2C_{L_{HT}}^2}{\pi AR_{HT}}$$

The above equations define the variation of tail lift and drag over the entire range of angle of attack. The tail pitching moment is not computed since it makes only a small contribution to the total aircraft pitching moment.

6.4 VERTICAL TAIL

The aerodynamic forces and moments acting on the vertical tail were estimated using the methods of Reference 1. The angle of attack of the vertical tail is given by

$$\alpha_{VT} = - \tan^{-1} \left[\frac{v_{VT}}{\sqrt{u_{VT}^2 + w_{VT}^2}} \right] + \beta_F \left(\frac{d\sigma}{d\beta} \right)$$

where u_{VT} , v_{VT} and w_{VT} are the components of velocity at the vertical tail aerodynamic center as given in Appendix C. The term $\beta_F \left(\frac{d\sigma}{d\beta} \right)$ is the sidewash correction for the presence of the fuselage.

As in the treatment of the horizontal tail, the effect of rudder deflection is obtained using a rudder effectiveness parameter τ_{VT} . Thus the effective angle of attack of the vertical tail when the rudder is deflected is

$$\alpha_{eVT} = \alpha_{VT} + \tau_{VT} \delta_{RUD}$$

The treatment of the vertical tail aerodynamics through the complete angle of attack range -180° to $+180^\circ$ then follows the same lines as that for the horizontal tail aerodynamics previously described.

The vertical tail forces and moments in body axes are then obtained from:

$$\begin{aligned} X_{AERO}^{VT} &= \bar{q} S_{VT} \eta_{VT} \left[-C_{D_{VT}} \cos(\beta_{VT} - \sigma) \cos(\alpha_{HT} - i_{HT}) \right. \\ &\quad \left. - C_{Y_{VT}} \sin(\beta_{VT} - \sigma) \cos(\alpha_{HT} - i_{HT}) \right] \\ Y_{AERO}^{VT} &= \bar{q} S_{VT} \eta_{VT} \left[C_{Y_{VT}} \cos(\beta_{VT} - \sigma) - C_{D_{VT}} \sin(\beta_{VT} - \sigma) \right] \\ Z_{AERO}^{VT} &= \bar{q} S_{VT} \eta_{VT} \left[-C_{D_{VT}} \cos(\beta_{VT} - \sigma) \sin(\alpha_{HT} - i_{HT}) - C_{Y_{VT}} \sin(\beta_{VT} - \sigma) \right. \\ &\quad \left. \sin(\alpha_{HT} - i_{HT}) \right] \end{aligned}$$

$$M_{AERO}^{VT} = Z_{AERO}^{VT} (X_{CG} - X_{VT}) + X_{AERO}^{VT} (Z_{VT} - Z_{CG})$$

$$N_{AERO}^{VT} = -Y_{AERO}^{VT} (X_{CG} - X_{VT})$$

$$L_{AERO}^{VT} = -Y_{AERO}^{VT} (Z_{VT} - Z_{CG})$$

6.5 WING AERODYNAMICS

The treatment of the wing aerodynamics is the most complex of all the components. Because wing flexibility must be represented, each wing panel required a separate treatment. The approach adopted for simulation purposes was first to obtain the aerodynamic forces and moments on the complete wing considered as rigid and uninfluenced by slipstream interference effects. With this data as a basis the effects of elastic deflection were introduced as an increment in the effective angle of attack of each wing panel and the rotor slipstream interference was then calculated. This approach is described in detail below.

6.5.1 BASIC WING AERODYNAMICS

The basic wing lift, drag and pitching moment coefficients for the wing in the presence of the fuselage rotors-off, were calculated using the methods of Reference 1. This data is applicable to low speed flight. Corrections for Mach number effects are introduced through the Prandtl-Glauert factor $\sqrt{1-M^2}$. Beyond stall angle of attack, the lift, drag and pitching moment curves are extended linearly to $\pm 90^\circ$.

angle of attack in order to provide a representation of wing behavior at low transition speeds when wing angles of attack approach 90° . The data was calculated for the complete range of flaperon settings.

The complete wing basic lift, drag and pitching moment data also applies to each individual wing panel provided the data is obtained at the appropriate panel angle of attack. This approximation is acceptable if the angles of attack of each wing panel are not substantially different. This condition is normally fulfilled.

In addition to the above data, the effects of spoiler deflection on panel lift, drag and pitching moment are required. These were estimated using the data of Reference 1. As can be seen from the equations presented in Appendix E the spoiler effectiveness is strongly dependent upon flaperon deflection, a result of the spoilers being slot-lip spoilers.

6.5.2 ROTOR SLIPSTREAM INTERFERENCE

Before the basic wing aerodynamic data can be utilized in the calculation of the wing forces, the effects of the rotor slipstream must be calculated. The calculation procedure presented here has been developed and used at Boeing for some years, and gives acceptable agreement with wind tunnel test data on a wide variety of both tilt rotor and tilt wing configurations.

The method uses momentum theory to obtain the direction and

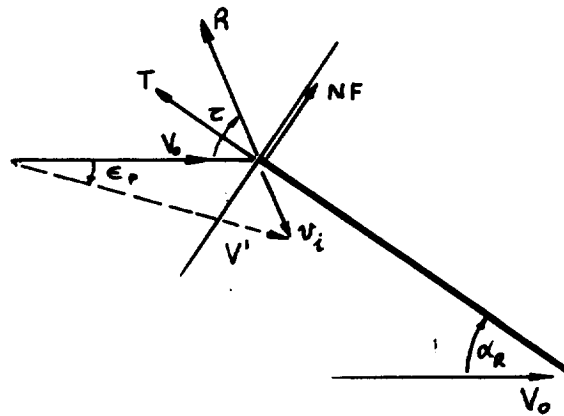
1

speed of the rotor slipstream in the neighborhood of the wing. From this the effective angle of attack of that part of the wing that is immersed in the slipstream is calculated. The lift, drag and pitching moment on the wing are then calculated for this angle of attack as if the entire wing were immersed. The area of the wing immersed in the slipstream is now computed and, using the ratio of the immersed to total wing area, the forces acting on the immersed portion are approximated.

At the angle of attack of the wing outside the slipstream, the wing forces and moments are obtained from the basic wing data as if no slipstream effects were present. These forces are then scaled by the ratio of unimmersed to total wing areas to obtain approximately the forces acting on the unimmersed wing. The sum of the approximations to immersed and unimmersed wing forces is now formed. This sum is then multiplied by a correction factor to obtain the final forces.

This correction factor is obtained from a consideration of the mass flows associated with the rotor-wing combination. In the following outline of the method only one rotor is considered.

From the following sketch, which shows the forces acting on the rotor, the inclination of



the resultant force on the rotor to the freestream direction is given by

$$\tau_R = \alpha_R + \tan^{-1} \left(\frac{NF}{T} \right)$$

The resultant force on the rotor is

$$R = \sqrt{T^2 + NF^2 + SF^2}$$

where T, NF and SF are the thrust, normal force and sideforce, respectively.

The mass flow through the disc is

$$m = \rho A V'$$

where A is the disc area and V' is obtained from the induced velocity triangle at the disc plane.

$$V' = \sqrt{(V_0 + v_i \cos \tau)^2 + (v_i \sin \tau)^2}$$

The resultant force on the rotor is related to the mass flow by (Glauert's assumption)

$$R = 2m v_i = 2\rho A V' v_i$$

From these equations the following quartic equation is obtained for the induced velocity at the disc.

$$v_*^4 + 2V_* v_*^3 \cos \tau + v_*^2 V_*^2 = 1$$

where the nondimensional notations

$$v_* = \frac{v_i}{\sqrt{\frac{R}{2\rho A}}} \quad V_* = \frac{V_o}{\sqrt{\frac{R}{2\rho A}}}$$

have been introduced.

This equation is then solved for v_* and the direction of the slipstream just behind the rotor disc is calculated from

$$\epsilon_p = \tan^{-1} \left[\frac{v_* \sin \tau}{v_* \cos \tau + V_*} \right]$$

The rotor thrust coefficient CT_s is defined as

$$CT_s = \frac{T}{(q + \frac{T}{A})A}$$

NOTE: Because the rotor diameter to wingchord is large the slipstream is considered to be uncontracted in the vicinity of the wing.

with $T = R \cos (\tau - \alpha_R)$

and $q = \frac{1}{2} \rho V^2 = \frac{1}{4} V_*^2 R$

then $CT_s = \frac{\cos (\tau - \alpha_R)}{\cos (\tau - \alpha_R) + \frac{V_*^2}{4}}$

The aspect ratio of the slipstream-immersed wing area is given by

$$AR_i = \frac{S_i}{c^2}$$

where S_i is the immersed area calculated by the method described in Appendix D, and c is the wing chord.

The lift on the wing, if the slipstream were absent, is obtained by calculating the effective angle of attack of the wing outside the slipstream from

$$\alpha_o = \sin^{-1} \left[\frac{w_w}{\sqrt{u_w^2 + w_w^2}} \right] + \theta_t$$

where w_w , u_w are the velocities at the wing aerodynamic center and θ_t is the elastic twist at the point. The lift coefficient (C_L^*) for this angle of attack is obtained from the aerodynamic data for the appropriate flaperon/spoiler deflection.

Similarly the lift (C_L'') and drag (C_D'') coefficients of the wing in the slipstream (assuming wing is completely immersed) are obtained from the aerodynamic data at the angle of attack

$$\alpha_s = \alpha_o - \epsilon$$

The total lift coefficient of the wing with slipstream is therefore

$$C_{L_s} = K'_A \left[\frac{S_i}{S} (C_L'' \cos \epsilon - C_D'' \sin \epsilon) + C_L^* (1 - C_{T_s}) (1 - \frac{S_i}{S}) \right]$$

where

$$C_{L_s} = \frac{L}{q_s S_w}$$

in which q_s is the nominal slipstream dynamic pressure, defined

$$\text{by } q_s = q + \frac{T}{A}$$

The factor K'_A is a correction factor to account for the fact that the lift-sharing between the immersed and unimmersed portions

of the wing is not simply proportional to the respective areas.

From considerations of the mass flows associated with the wing-rotor combination the factor K'_A was obtained in the form

$$K'_A = \frac{V_* + \frac{C_{L_{\alpha i}}}{C_{L_{\alpha}}} v_*}{V_* + v_*}$$

where, from wing theory,

$$\frac{C_{L_{\alpha i}}}{C_{L_{\alpha}}} = \frac{1}{1 + \frac{C_{L_{\alpha}}}{\pi} \left[\frac{1}{AR_i} - \frac{1}{AR} \right]}$$

The drag and pitching moments for the wing with slipstream are obtained similarly and are given by:

$$C_{D_S} = K'_A \left\{ \frac{S_i}{S} (C''_L \sin \epsilon + C''_D \cos \epsilon) + C^*_D (1 - C_{TS}) \left(1 - \frac{S_i}{S}\right) \right\}$$

$$C_{M_S} = K'_A \left\{ \frac{S_i}{S} C''_M + C^*_M (1 - C_{TS}) \left(1 - \frac{S_i}{S}\right) \right\}$$

The rolling moment and yawing moment coefficients for the wing are given by

$$C_{\ell_S} = (K_{20} + K_{21} \bar{C}_L) (1 - \bar{C}_{TS}) \beta_F + \bar{Y}_{AC} \left(\frac{1 - C_{TS}}{2b_W} \right) (C^*_{L_{LW}} - C^*_{L_{RW}}) + \Delta C_{\ell_S \text{ POWER}}$$

$$C_{\eta_S} = K_{22} \bar{C}_L^2 (1 - C_{TS}) \beta_F + \bar{Y}_{AC} \left(\frac{1 - C_{TS}}{2b_W} \right) (C^*_{D_{RW}} - C^*_{D_{LW}}) + \Delta C_{\eta_S \text{ POWER}}$$

where the increment in rolling moment due to power is

$$\Delta C_{\ell_S \text{ POWER}} = \frac{1}{4} \left\{ [C_{L_{S_{LW}}} - (1 - \bar{C}_{TS}) C^*_{L_{LW}}] \left[1 - \frac{1}{2} \left(\frac{S_i}{S} \right)_{LW} \right] - [C_{L_{S_{RW}}} - (1 - \bar{C}_{TS}) C^*_{L_{RW}}] \left[1 - \frac{1}{2} \left(\frac{S_i}{S} \right)_{RW} \right] \right\}$$

and the increment in yawing moment is

$$\Delta C_{\eta_{S_{POWER}}} = \frac{1}{4} \left\{ \left[C_{D_{S_{RW}}} - (1 - \bar{C}_{T_S}) C_{D_{RW}}^* \right] \left[1 - \frac{1}{2} \left(\frac{S_i}{S} \right)_{RW} \right] \right. \\ \left. - \left[C_{D_{S_{LW}}} - (1 - \bar{C}_{T_S}) C_{D_{LW}}^* \right] \left[1 - \frac{1}{2} \left(\frac{S_i}{S} \right)_{LW} \right] \right\}$$

Figure 6.2 shows a correlation between the wing-in-slipstream method described above and experimental results for the Boeing Model 160 tilt rotor aircraft. As may be seen the simple treatment gives acceptable predictions of wing forces and moments.

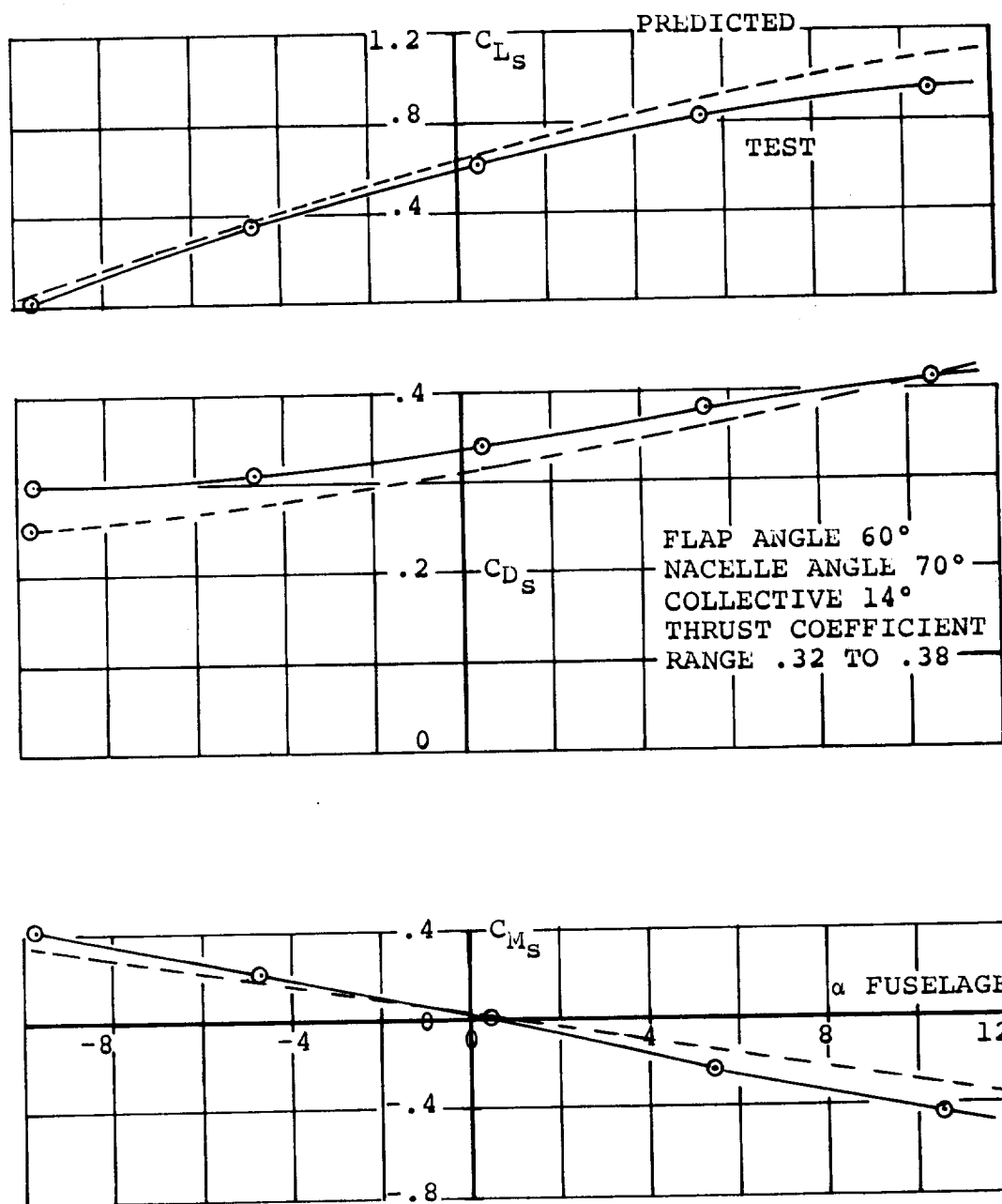


Figure 6.2. Correlation of Theory with Test for Predictions of Slipstream Forces and Moments

7.0 ROTOR AERODYNAMICS

The rotor aerodynamics as used in the mathematical model are described in this section. Also presented are the methods used to compute the rotor aerodynamics, a discussion on wing upwash as it effects the rotor, and a description of the technique used to account for rotor on rotor interference in skewed flight. In addition, correlation of the methods described in this section with test data for soft-in-plane hingeless rotors are presented. Calculation of the Model 222 rotor forces and moments was not practicable because of the complexity and size of the programs required to represent the lag-flap coupling effects of the rotor. In this mathematical model, the rotor forces and moments are input from a series of curve plot fit equations. These equations were generated by computing rotor data using the computer programs discussed in Section 7.2, and then a least squares curve fit program was used to obtain the curve fit equations. The rotor forces and moments used in the mathematical model include the six basic forces and moments (thrust, power, normal force, side force, pitching moment, yawing moment), hub pitching and yawing moments due to aircraft pitch and yaw rate, and changes to the six basic forces and moments due to cyclic pitch application.

7.1 FORMAT AND RANGE OF DATA

Rotor forces and moments are functions of thirteen variables. In order to reduce the size of the data bank, these variables were combined and non-dimensionalized. Each rotor force and

moment can be written as:

$$F = f(V, V_t, \theta_{0.75} \text{ or } T, \alpha, \beta, P, Q, R, A_1, B_1, P_N^R, Q_N^R, R_N^R) \quad (7-1)$$

where

V	= Forward speed
V_t	= Rotor tip speed
$\theta_{0.75}$	= Collective pitch at the .75 radius
T	= Rotor thrust
α	= Rotor angle of attack
β	= Rotor sideslip angle
P	= Body axis roll rate
Q	= Body axis pitch rate
R	= Body axis yaw rate
A_1	= Longitudinal cyclic pitch
B_1	= Lateral cyclic pitch
P_N^R	= Rotor wind axis roll rate
Q_N^R	= Rotor wind axis pitch rate
R_N^R	= Rotor wind axis yaw rate

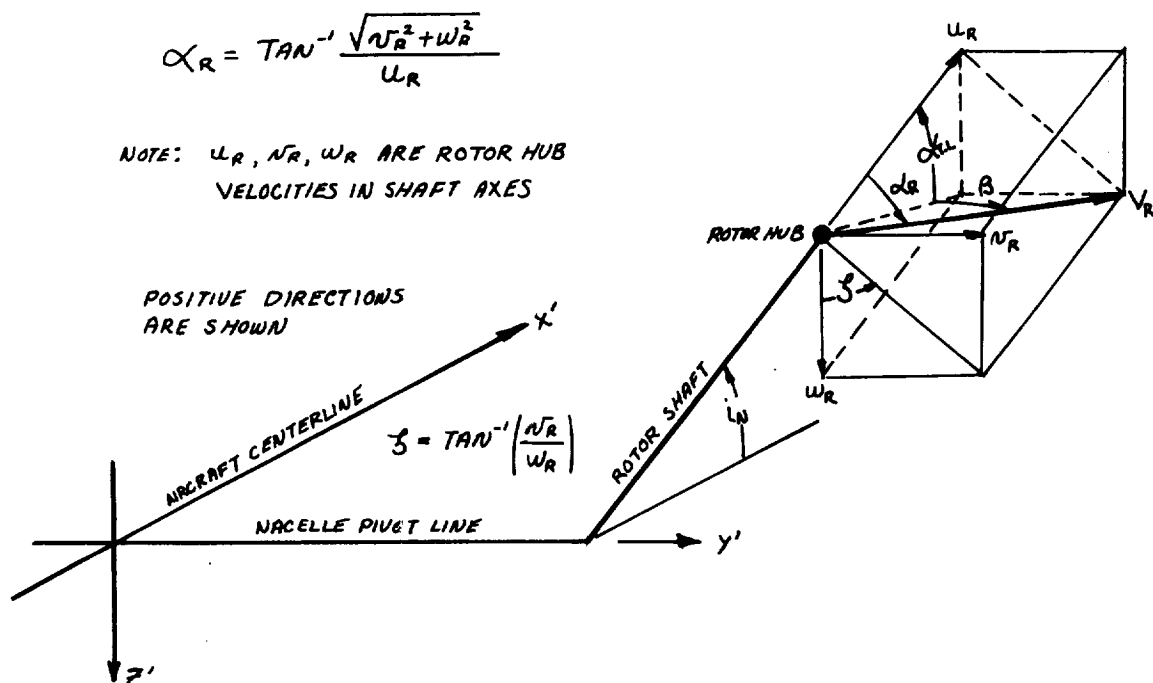
Forward speed and tip speed were combined to form rotor advance ratio and collective pitch or thrust were retained. Rotor angles of attack and sideslip and body axis roll, pitch and yaw rates were combined into a resultant angle of attack. Longitudinal and lateral cyclic pitch angles are retained. By combining the thirteen variables in this manner, Equation 7-1 can be expressed as:

$$F = f(\mu, \theta_{.75} \text{ or } C_T, \alpha_R) + [\Delta F = f(A_1, B_1)] + [\Delta F = f(P_N^R, Q_N^R, R_N^R)] \quad (7-2)$$

where μ = rotor advance ratio

α_R = rotor resultant angle of attack

By using this functional relationship, basic rotor forces and moments can be written as functions of three variables plus increments due to cyclic pitch control application and wind axis pitch roll and yaw rates at the rotor hub. This is the format used in the mathematical model. In addition, the rotor forces and moments are non-dimensionalized by dividing forces by $(\rho \pi R^2 V_t^2)$, moments by $(\rho \pi R^2 V_t^2 R)$, and power by $(\rho \pi R^2 V_t^3)$.



The above sketch shows a rotor under condition of combined angle of attack ($\alpha_{T.L.}$) and sideslip (β). The resultant angle of attack (α_R) is the angle between the " u_R " component of velocity at the rotor hub and the total velocity (V_R) at the hub. The velocity components that define this resultant angle are the rotor hub velocities resolved to shaft axes and

derived in Appendix C. They include body axes pitch, roll and yaw rates. Other functional relationships that define the rotor resultant angle of attack are shown in Appendix D. Also shown on the sketch is the rotor sideslip angle (ζ). This angle represents the inclination of the plane containing the resultant velocity. Rotor wind axis forces and moments are defined relative to this plane. Since the resultant angle is defined from 0 through 180° the inclination of the rotor sideslip angle (ζ) determines the signs of the rotor forces and moments when they are resolved back to body axes.

After the functional format for the rotor data was established, the ranges of the variables were established. Discrete speeds and rotor rpm conditions were selected. A range of rotor resolved angles of attack and thrust levels were selected at each combination. These conditions were carefully selected to cover the total operating envelope of the Model 222. The ranges of the rotor data are shown in Table 7.1.

7.2 PROGRAMS USED TO COMPUTE ROTOR DATA

Rotor data used in the mathematical model were predicted from Boeing-developed computer programs. Hover and cruise performance (thrust-power) were obtained from a propeller performance analysis computer program (B-92). This analysis establishes a radial distribution of induced velocity based on a prescribed wake contraction schedule to calculate rotor induced and total power coefficients at specified thrust or

TABLE 7.1 RANGE OF ROTOR DATA

Total Velocity (V) ~ KTS	Rotor Speed (rpm)	Resultant Angle of Attack Range (α_R) ~ deg	Rotor Thrust (T) ~ Lb
0	551	0 \rightarrow 180°	500 \rightarrow 7000
45	551	0 \rightarrow 180°	500 \rightarrow 7000
60	551	0 \rightarrow 180°	2000 \rightarrow 6500
90	551	0 \rightarrow 180°	2000 \rightarrow 6500
120	400	0 \rightarrow 45°	500 \rightarrow 2600
142	386	0 \rightarrow 20°	-700 \rightarrow 3500
160	386	0 \rightarrow 20°	-500 \rightarrow 4750
200	386	0 \rightarrow 20°	-500 \rightarrow 6000
240	386	0 \rightarrow 20°	0 \rightarrow 3700
280	386	0 \rightarrow 20°	0 \rightarrow 3800
320	386	0 \rightarrow 20°	0 \rightarrow 4800
360	386	0 \rightarrow 20°	0 \rightarrow 3500

thrust coefficients. The radial airload distribution is also defined. A detailed description of this program is given in Reference 4.

Transition performance data, in-plane forces and moments and cyclic pitch effectiveness throughout the flight envelope were estimated using computer program D88 (Reference 5).

The D-88 computer program is an aeroelastic analysis for the study of aerodynamic, dynamic, and structural characteristics of current and advanced rotor and prop/rotor concepts. Airloads are calculated considering the effects of section geometry, compressibility and non-uniform inflow. An iterative process between the airloads and coupled flap-pitch dynamic response establishes blade accelerations which in turn are used to compute hub loads and rotor aerodynamic performance.

The rotor analysis is based on the idealization of a continuous, elastic, non-uniform beam into one composed of lumped discrete masses connected by weightless elastic sections. Associated with each mass is a flat rigid airfoil segment, with the mass center located at the midpoint. The aerodynamic loads generated by each segment are assumed to act at the mass center.

The effects of non-uniform inflow are included by considering a discontinuous constant circulation along part of the rotor blade, of sufficient strength to maintain the desired thrust. A vortex is assumed to trail from the inboard and outboard

circulation discontinuities, of equal and opposite strength. By summing the effects of all the vortices on a given blade around the azimuth the non-uniform induced flow for each blade at every dynamic bay is determined. Total velocity at each point in the blade is computed by vector addition of the velocity components.

The local angle of attack of each blade element is then computed at every blade station for specified azimuth angles and the aerodynamic coefficients (C_L , C_D , C_M) are looked up from tables of coefficients as a function of Mach number. From these coefficients the airloads are computed. The vertical, tangential and pitching aerodynamic loads are then harmonically analyzed into 10 harmonics and act as the forcing functions for each blade section.

To obtain a thrust match, an iteration process is performed on the airloads until a steady collective pitch angle is obtained which corresponds to the desired thrust. To perform the dynamic analysis, the lumped mass and elastic bay elements of the idealized rotor blade are transformed into a sequence of transfer matrix products, by means of the Associated Matrix Method. This method replaces each blade element by an equivalent "transfer matrix" that transfers the dynamic system variables, shear, moment, deflection and slope, inboard across the element. Therefore, multiplying the system variables outboard of the element by the transfer matrix gives the variables

inboard of the element. The whole mass, elastic blade idealization is then reduced to a sequence of transfer matrix products.

In-plane elastic rotor derivatives (both static and rate) in axial flow were calculated using computer program C-41 (Reference 2).

Dynamic derivatives for a rotor system are defined taking account of the modal behavior of the blades in two general flap-lag modes. These derivatives are given as matrix arrays of the partial derivatives of rotor forces with respect to unit amounts of elementary linear and angular motions of the hub and unit displacements in the blade modes. These effects are separated into inertial, damping and gyroscopic, and stiffness effects. Thus an element m_{ij} in the inertia derivative matrix is $\partial F_i / \partial g_j$, i.e., the force in the i direction due to unit acceleration in the j direction, all other quantities being held constant.

Similarly element d_{ij} of the damping derivative matrix will represent $\partial F_i / \partial g_j$ which might for appropriate (ij) be the aggregate gyroscopic and aerodynamic pitching moment due to unit velocity of yaw.

Similarly the elements of the stiffness derivative matrix represent such quantities as the normal force due to unit amount of shaft angle of attack, and generalized forces in the blade freedoms due to unit displacements in each of the other freedoms.

The matrices are of order 15 x 15 maximum. The first 6 rows and columns refer to forces in the vertical, lateral and axial directions and moments in the yaw pitch and roll directions due to unit acceleration, rates and displacements in each of the directions. These are the only numbers present if the rotor blades are assumed rigid. Three additional rows and columns are added for each blade mode considered. A limit of two blade modes is currently applied. The final three rows are for cyclic and collective pitch.

These derivative matrices provide a ready means for evaluating the contribution of the rotor to the coefficients of the aircraft dynamic equations. This program also provides the in-plane elastic rotor derivatives.

Elastic rotor rate derivatives in transition were estimated using computer program C-49 (Reference 3). This program evaluates hub force and moment derivatives for shaft angles varying from cruise to hover conditions. Dynamic derivatives suitable for transient analysis are computed. The dynamic derivatives are the partial differentials of hub forces and moments with respect to hub positions rates and accelerations and include inertial and gyroscopic effects as well as aerodynamic effects. For the static derivatives a constant shaft angle to the relative wind is assumed and the resulting blade motion computed. The effects of blade aerodynamic and inertia and gyroscopic forces are combined to give the hub derivatives

due to constant shaft angle and constant rate of change of shaft angle.

The output rotor forces and moments of these programs are in rotor wind axis.

7.3 ROTOR SIGN CONVENTION

The rotor sign conventions as used in this mathematical model are shown in Figure 7.1 . Positive directions of all rotor forces, moments and cyclic pitch angles are noted.

7.4 CURVE FIT FORMAT

The rotor data generated for the Model 222 mathematical model was curve fit at each advance ratio. A curve fit which is third order in angle of attack and second order in thrust coefficient or collective pitch was found to yield the most accurate results. The curve fits have the following general form.

$$C_F = \sum_{v=0}^2 \sum_{u=0}^3 \left[A_{(u+4v)} \alpha^u C_T^v \right]$$

The double summation is expanded starting with the inner quantity i.e. set v and expand u from 0 to 3. Repeat until the summations are satisfied. The expansion of the generalized form is

$$\begin{aligned} C_F = & A_0 + A_1 \alpha + A_2 \alpha^2 + A_3 \alpha^3 \\ & + (A_4 + A_5 \alpha + A_6 \alpha^2 + A_7 \alpha^3) C_T \\ & + (A_8 + A_9 \alpha + A_{10} \alpha^2 + A_{11} \alpha^3) C_T^2 \end{aligned}$$

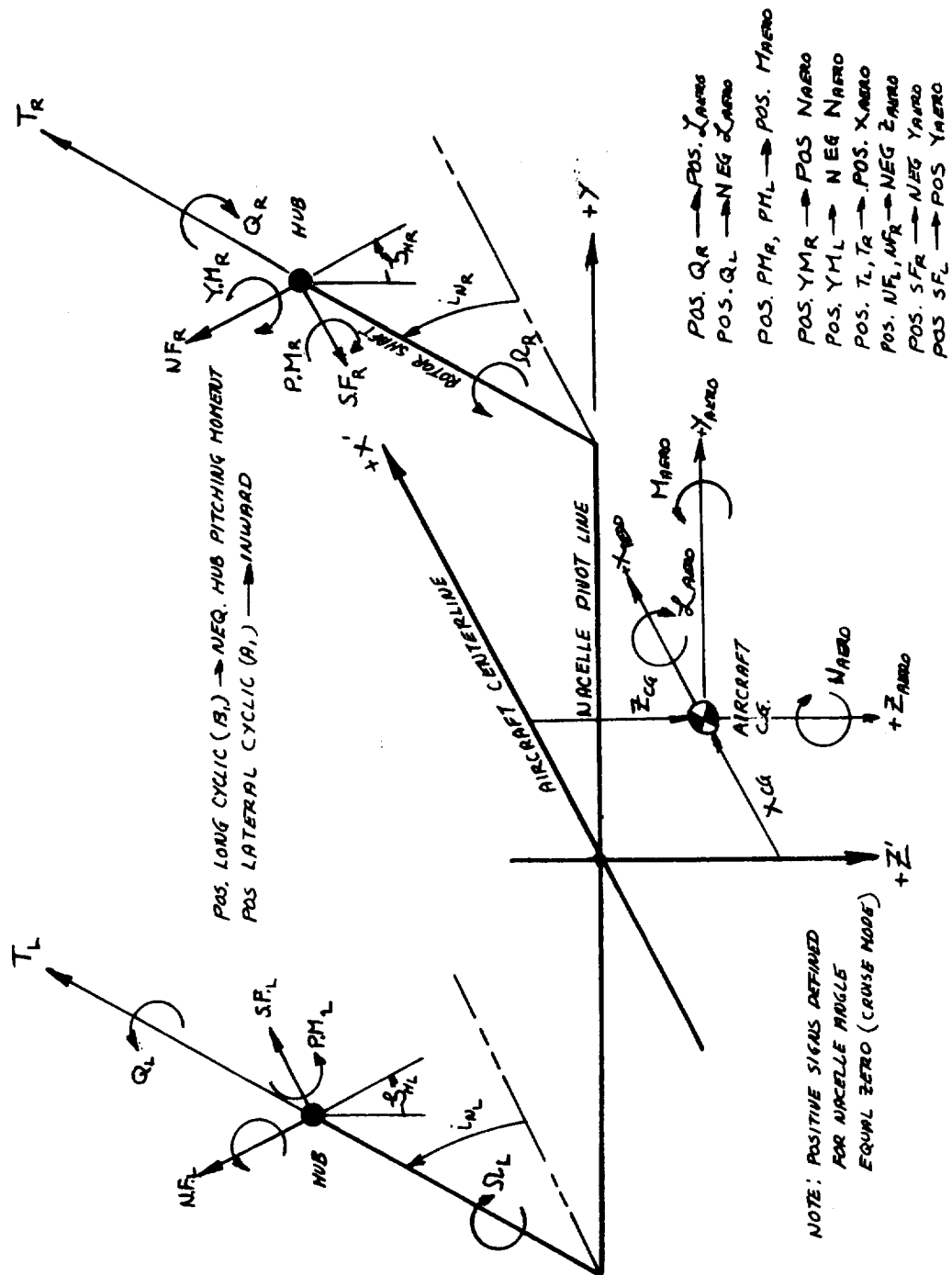


Figure 7.1. Rotor Sign Conventions

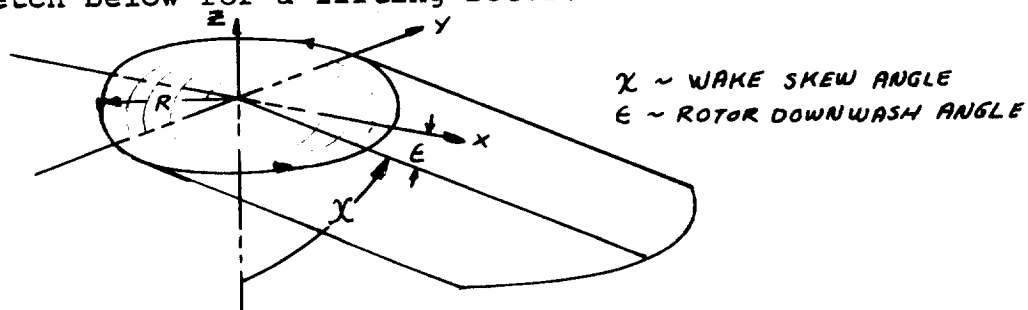
All of the rotor forces and moments are curve fit in this format. The coefficients of the equation were obtained from a least squares fit of the computed rotor data. The criteria used to determine the final coefficients was to have not more than a 5% difference between the curve fit equations and the computed rotor data at the nominal aircraft trim condition. In general this criteria was met.

7.5 EFFECT OF WING UPWASH ON ROTOR PERFORMANCE

The rotor operates in the upwash field associated with the lifting wing. Thus, the rotor behaves as if it were operating at an increased angle of attack. The effective upwash angles were calculated using lifting line theory. In the mathematical model the upwash angles are input in the form of a table of upwash angles as a function of wing lift coefficient, and nacelle incidence angle.

7.6 ROTOR/ROTOR INTERFERENCE

In order to obtain the correct lateral stick gradient when flying sideways or at large sideslip angles, a calculation for rotor-on-rotor interference is included in the mathematical model. In Reference 11, the wake skew angle is defined as in the sketch below for a lifting rotor.



Also presented in this reference are contour charts of the normal component of induced velocity near a rotor with a triangular disc loading for six different skew angles in the range from 0° to 90°. For the Model 222 geometry, a curve of normal induced velocity/average induced velocity as a function of skew angle was obtained. For the case of the Model 222 flying sideways, the downwind rotor is assumed to be operating at a lower angle of attack than the upwind rotor, and will therefore generate different forces and moments. The downwash angle is calculated from the normal component of induced velocity. The rotor/rotor interference is washed out as a function of nacelle angle and sideslip angle such that there is no interference in the high transition speed and cruise modes. The equations derived are shown in Appendix E , under the rotor/rotor interference section.

7.7 ISOLATED ROTOR AERODYNAMICS

The equations utilized to represent the isolated rotor aerodynamics are presented below. These equations are then resolved into body axis forces and moments to be used in the equation of motion.

7.7.1 Thrust (1)

$$C_{T_R}^I = [C_{T_{ORR}} \cos A_{1CR} \cos B_{1CR}]$$

$$\text{where } C_{T_{ORR}} = \sum_{v=0}^2 \sum_{u=0}^3 [A_T(u+4v) \alpha_{RR}^u \theta_{RR}^v 0.75]$$

(1) In the equations that follow, subscript RR denotes right rotor. The left rotor is identical provided due regard is paid to sign convention and azimuth reference.

$A_T(u+4v)$ = function of $\mu \left(\mu = \frac{V}{V_t} \right)$ and is obtained from Appendix F

A_{1C_R} = Lateral cyclic pitch

B_{1C_R} = Longitudinal cyclic pitch

$\theta_{0.75}$ = Blade pitch angle at 75% blade radius

$$\alpha_{RR} = \tan^{-1} \left\{ \frac{\sqrt{V_{RR}^2 + (W_{RR} + u_{RR} \epsilon_{wRR})^2}}{u_{RR}} \right\} + \epsilon_{iLR}$$

u_{RR}, V_{RR}, W_{RR} = rotor shaft axis velocity components

ϵ_{wRR} = Wing upwash angle

ϵ_{iLR} = Rotor/rotor interference angle

The effect of close proximity to the ground is accounted for by use of the following relationships

$$C_{T_{RR}} = C'_{T_{RR}} \left(\frac{T_{IGE}}{T_{OGE}} \right)_{RR}$$

where $\left(\frac{T_{IGE}}{T_{OGE}} \right)$ is defined in Section 10 under the discussion of ground effect.

7.7.2 Power

$$C_{P_{RR}} = C_{P_{ORR}} = \sum_{v=0}^2 \sum_{u=0}^3 \left[A_p(u+4v) \alpha_{RR}^u C_{T_{RR}}^{1v} \right]$$

where: $A_p(u+4v)$ may be obtained from Appendix F as a function of μ_{RR}

7.7.3 Normal Force

$$C_{NF_{RR}} = C_{NF_{ORR}} + \frac{dC_{NF_{RR}}}{dA_{1C_R}} A_{1C_R} + \frac{dC_{NF_{RR}}}{dB_{1C_R}} B_{1C_R}$$

$$\text{where: } C_{NF_{ORR}} = \sum_{v=0}^2 \sum_{u=0}^3 \left[A_{NF}(u+4v) \alpha_{RR}^u C_{T_{RR}}^{1v} \right]$$

$A_{NF}(u+4v)$ = Function of μ_{RR} and may be obtained from Appendix F.

$$\frac{dC_{NFRR}}{dA_{1CR}} = D_{NF1} C_{T_{RR}} + D_{NF2} \mu_{RR}^2 + D_{NF3} \mu_{RR} + D_{NF4}$$

$$\frac{dC_{NFRR}}{dB_{1CR}} = E_{NF1} C_{T_{RR}} + E_{NF2} \mu_{RR}^2 + E_{NF3} \mu_{RR} + E_{NF4}$$

The coefficients in the above 2 equations may be obtained from Appendix F.

7.7.4 Side Force

$$C_{SFRR} = C_{SF_{ORR}} + \frac{dC_{SFRR}}{dA_{1CR}} A_{1CR} + \frac{dC_{SFRR}}{dB_{1CR}} B_{1CR}$$

$$\text{where: } C_{SF_{ORR}} = \sum_{v=0}^2 \sum_{u=0}^3 \left[A_{SF}(u+4v) \alpha_{RR}^u C_{T_{RR}}^v \right]$$

$A_{SF}(u+4v)$ = function of μ_{RR} and may be obtained from Appendix F.

$$\frac{dC_{SFRR}}{dA_{1CR}} = D_{SF1} C_{T_{RR}} + D_{SF2} \mu_{RR}^2 + D_{SF3} \mu_{RR} + D_{SF4}$$

$$\frac{dC_{SFRR}}{dB_{1CR}} = E_{SF1} C_{T_{RR}} + E_{SF2} \mu_{RR}^2 + E_{SF3} \mu_{RR} + E_{SF4}$$

The coefficients in the above 2 equations may be obtained from Appendix F.

7.7.5 Hub Pitching Moment

$$C_{PMRR} = C_{PM_{ORR}} + \frac{dC_{PMRR}}{dA_{1CR}} A_{1CR} + \frac{dC_{PMRR}}{dB_{1CR}} B_{1CR} + \frac{dC_{PMRR}}{dQ} Q_{NR}^R$$

$$\text{where: } C_{PM_{ORR}} = \sum_{v=0}^2 \sum_{u=0}^3 \left[A_{PM}(u+4v) \alpha_{RR}^u C_{T_{RR}}^v \right]$$

$A_{PM}(u+4v)$ = function of μ_{RR} and may be obtained from Appendix F.

$$\frac{dC_{PM_{RR}}}{dQ} = \sum_{v=0}^2 \sum_{u=0}^3 \left[H_{PM}(u+4v) \alpha_{RR}^u C_{T_{RR}}^{i_v} \right]$$

$H_{PM}(u+4v)$ = function of μ_{RR} and may be obtained from Appendix F

$$Q_{NR}^R = Q_{NR}^N \cos \zeta_{HR} + R_{NR}^N \sin \zeta_{HR}$$

$$Q_{NR}^N = Q + i_{NR}$$

$$R_{NR}^N = -R \cos i_{NR} - P \sin i_{NR}$$

ζ_{HR} = right rotor sideslip angle

i_{NR} = right nacelle velocity

i_{NR} = right nacelle angle

$$\begin{aligned} \frac{dC_{PM_{RR}}}{dA_{1C_R}} &= D_{PM_1} C_{T_{RR}} + D_{PM_2} \mu_{RR}^2 + D_{PM_3} \mu_{RR} + D_{PM_4} (\mu_{RR} \leq .35) \\ &= D_{PM_1} C_{T_{RR}} + D_{PM_5} \mu_{RR}^2 + D_{PM_6} \mu_{RR} + D_{PM_7} (\mu_{RR} > .35) \end{aligned}$$

$$\begin{aligned} \frac{dC_{PM_{RR}}}{dB_{1C_R}} &= E_{PM_1} C_{T_{RR}} + E_{PM_2} \mu_{RR}^2 + E_{PM_3} \mu_{RR} + E_{PM_4} (\mu_{RR} \leq .35) \\ &= E_{PM_1} C_{T_{RR}} + E_{PM_5} \mu_{RR}^2 + E_{PM_6} \mu_{RR} + E_{PM_7} (\mu_{RR} > .35) \end{aligned}$$

Values for the coefficients in the above 2 sets of equations may be found in Appendix F.

7.7.6 Hub Yawing Moment

$$C_{YM_{RR}} = C_{YM_{ORR}} + \frac{dC_{YM_{RR}}}{dA_{1C_R}} A_{1C_R} + \frac{dC_{YM_{RR}}}{dB_{1C_R}} B_{1C_R} + \frac{dC_{YM_{RR}}}{dR} R_{NR}^R$$

$$\text{where: } C_{YM_{ORR}} = \sum_{v=0}^2 \sum_{u=0}^3 \left[A_{YM}(u+4v) \alpha_{RR}^u C_{T_{RR}}^{i_v} \right]$$

$A_{YM}(u+4v)$ is a function of μ_{RR} and may be obtained from Appendix F.

$$\frac{dC_{YM_{RR}}}{dR} = \sum_{v=0}^2 \sum_{u=0}^3 \left[J_{YM}(u+4v) \alpha_{RR}^u C_{T_{RR}}^v \right]$$

$J_{YM}(u+4v)$ is a function of μ_{RR} and may be obtained from Appendix F.

$$R_{NR}^R = R_{NR}^N \cos \zeta_{HR} - Q_{NR}^N \sin \zeta_{HR}$$

$$R_{NR}^N = -R \cos i_{NR} - P \sin i_{NR}$$

$$Q_{NR}^N = Q + i_{NR}$$

ζ_{HR} = Right rotor sideslip angle

i_{NR} = Right nacelle velocity

i_{NR} = Right nacelle angle

$$\begin{aligned} \frac{dC_{YM_{RR}}}{dA_1 C_R} &= D_{YM1} C_{T_{RR}} + D_{YM2} \mu_{RR}^2 + D_{YM3} \mu_{RR} + D_{YM4} (\mu_{RR} \leq .35) \\ &= D_{YM1} C_T + D_{YM5} \mu_{RR}^2 + D_{YM6} \mu_{RR} + D_{YM7} (\mu_{RR} > .35) \end{aligned}$$

$$\begin{aligned} \frac{dC_{YM_{RR}}}{dB_1 C_R} &= E_{YM1} C_T + E_{YM2} \mu_{RR}^2 + E_{YM3} \mu_{RR} + E_{YM4} (\mu_{RR} \leq .35) \\ &= E_{YM1} C_{T_{RR}} + E_{YM5} \mu_{RR}^2 + E_{YM6} \mu_{RR} + E_{EM7} (\mu_{RR} > .35) \end{aligned}$$

Values for the coefficients in the above 2 sets of equations may be found in Appendix F.

Notes: (1) Application of rotor equations for left rotor follow similar format with subscript "RR" changed to "LR".

(2) When solving equations with double summations for values of μ not given in tables, solve equations for the two values of μ closest to the value desired and then interpolate linearly for exact value of μ .

7.8 CORRELATIONS OF ROTOR PREDICTION METHODS WITH TEST DATA

This section presents the results of correlation studies that were conducted to verify the adequacy of the rotor prediction methods used for the Model 222 tilt rotor. In general, prediction of trends is excellent with quite good agreement in absolute magnitudes.

7.8.1 Model 213 Four Blade Hingeless Rotor Correlation

Figure 7.2 presents correlation with rotor derivatives measured on a 1/9 scale dynamically similar model of a tilt/stowed rotor conversion model. In this test the rotor hub forces and moments were carefully measured over a range of RPM in which the lead-lag modal frequency progressed from less than 1 per rev at 900 RPM to values significantly greater than 1 per rev as the rotor was feathered. The measured values confirm the predicted behavior trend and the quantitative correlation is also excellent.

7.8.2 Correlation with Model 222 26-Foot Diameter Rotor

Test in NASA-Ames 40 x 80-Foot Tunnel

Figure 7.3 shows the schematic of the windmilling test stand and its instrumentation. Test data were obtained from strain gages mounted on the outer portion of the wing as shown, and calibrated to measure normal force, pitching moment and yawing moment. Comparison with test data was made by calculating the moments about the wing strain gage locations using forces and moments predicted by the C-41 program. The results of this

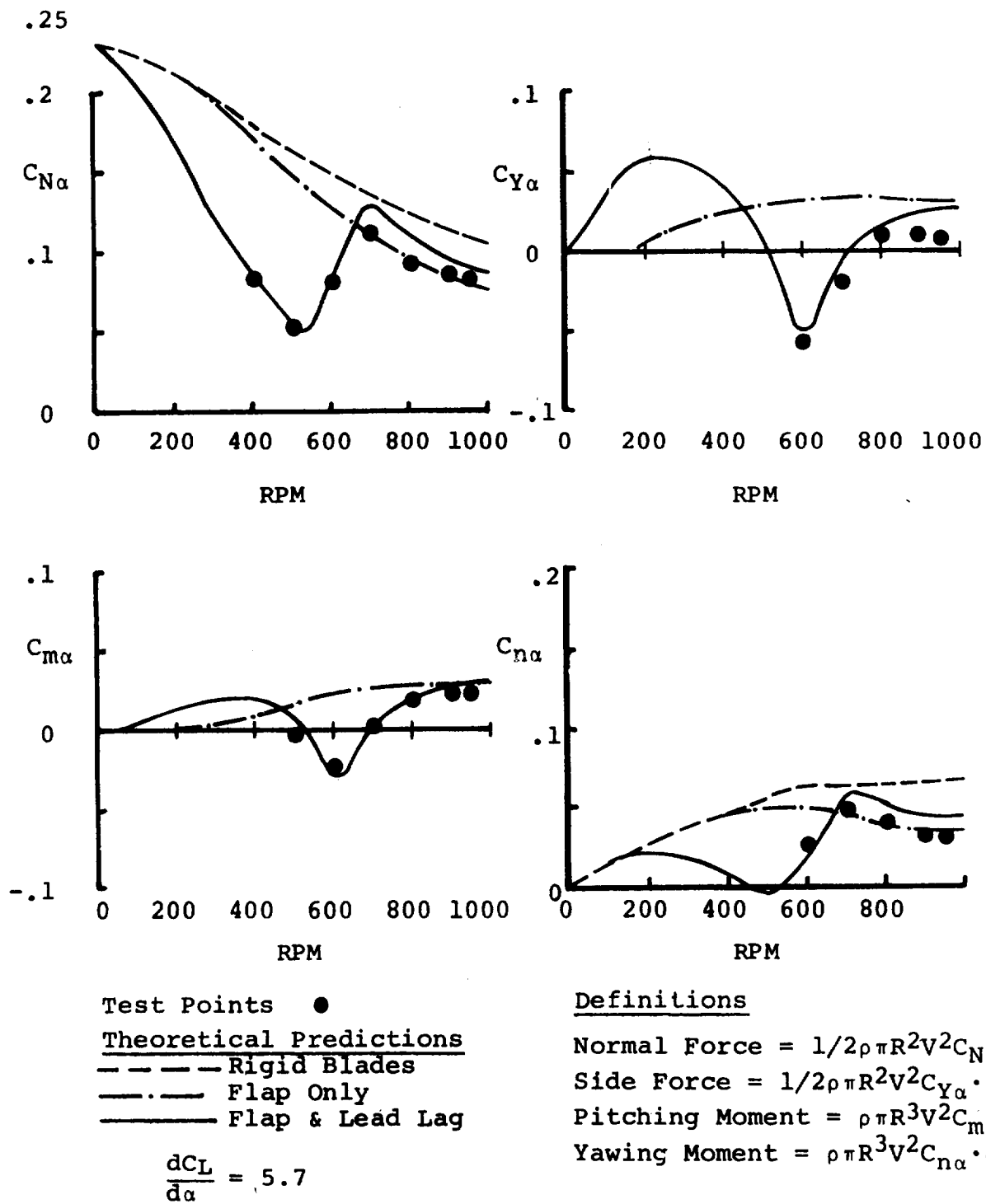


Figure 7.2. Model 213 1/9 Scale Conversion Model – 85 Ft/Sec Derivative Variation with RPM

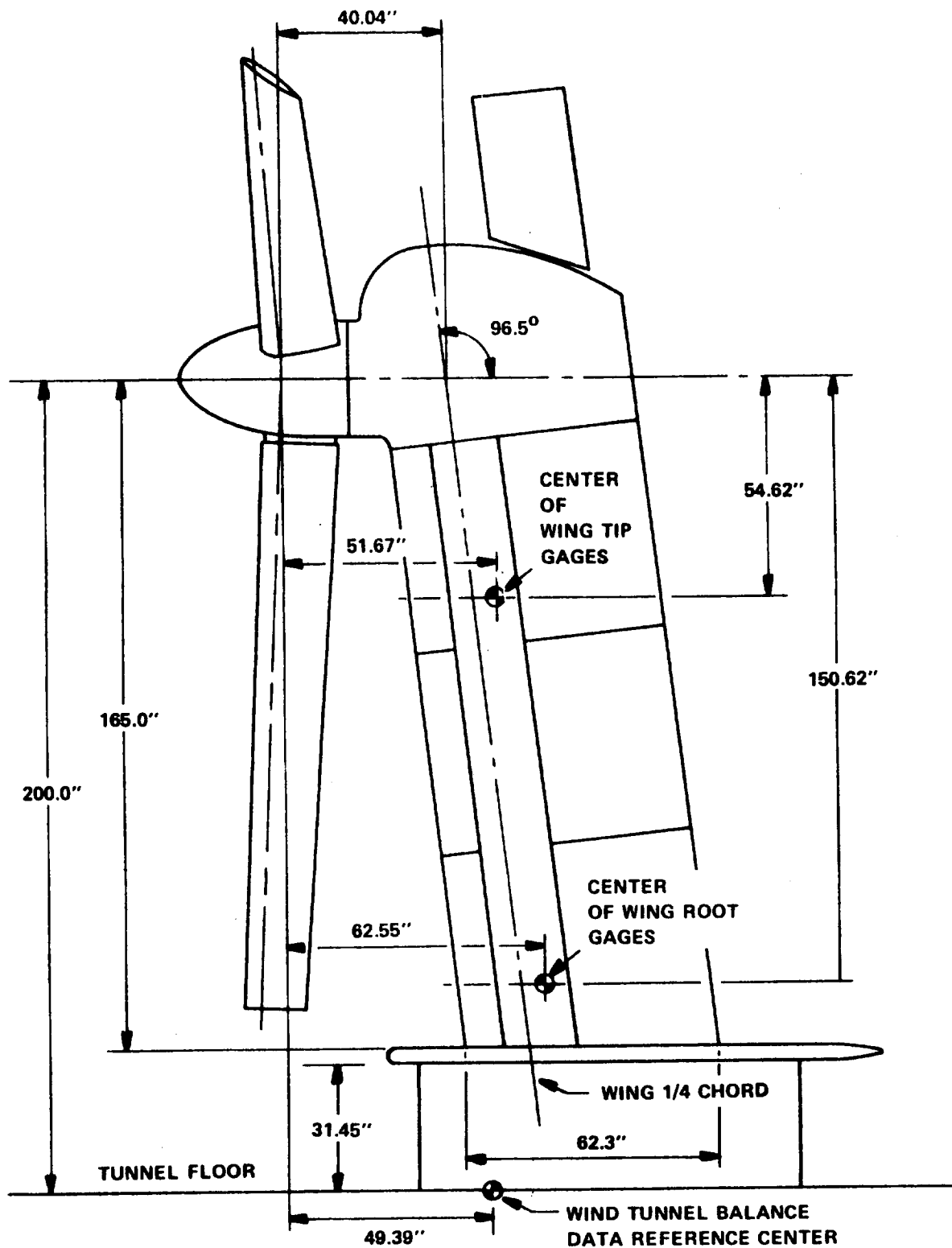


Figure 7.3. 26 Ft. Rotor Test Stand in NASA's 40' x 80' Tunnel

comparison for alpha derivatives are given in Figure 7.4 and for cyclic pitch derivatives in Figures 7.5 and 7.6 .

The analysis did not attempt to account for force and moment contributions from nacelle and wing aerodynamic interference. Nevertheless, quite good correlation is observed. These plots also show the values of derivatives predicted by several other programs. These include D-88 program which accounts for compressible non-linear downwash and L-22 which uses linear airfoil theory and uncoupled flap-lag freedoms. C-49 accounts for unsteady aerodynamics while C-41 uses a linear representation. C-41 and C-49 use a modal representation of blade freedoms (2 coupled flap-lag modes) while D-88 and L-22 make use of a finite element discrete mass representation.

The rotor derivative data was also compared with C-41 using a total unresolved moment approach. Total moments about the center of the wing tip gages and the reference azimuth position (orientation of the moment vector in the rotor disc plane) were calculated from the C-41 hub forces and moments and compared with test results (Figure 7.7). The interesting conclusion which is not apparent from the resolved forces and moments is that the total moment is predicted well but there are slight differences in the reference azimuth position.

7.8.3 Correlation with Model 222 1/4.622 Scale Model Data

The subject model is a dynamically similar version of the M222. The test data presented in Figures 7.8 and 7.9 were taken

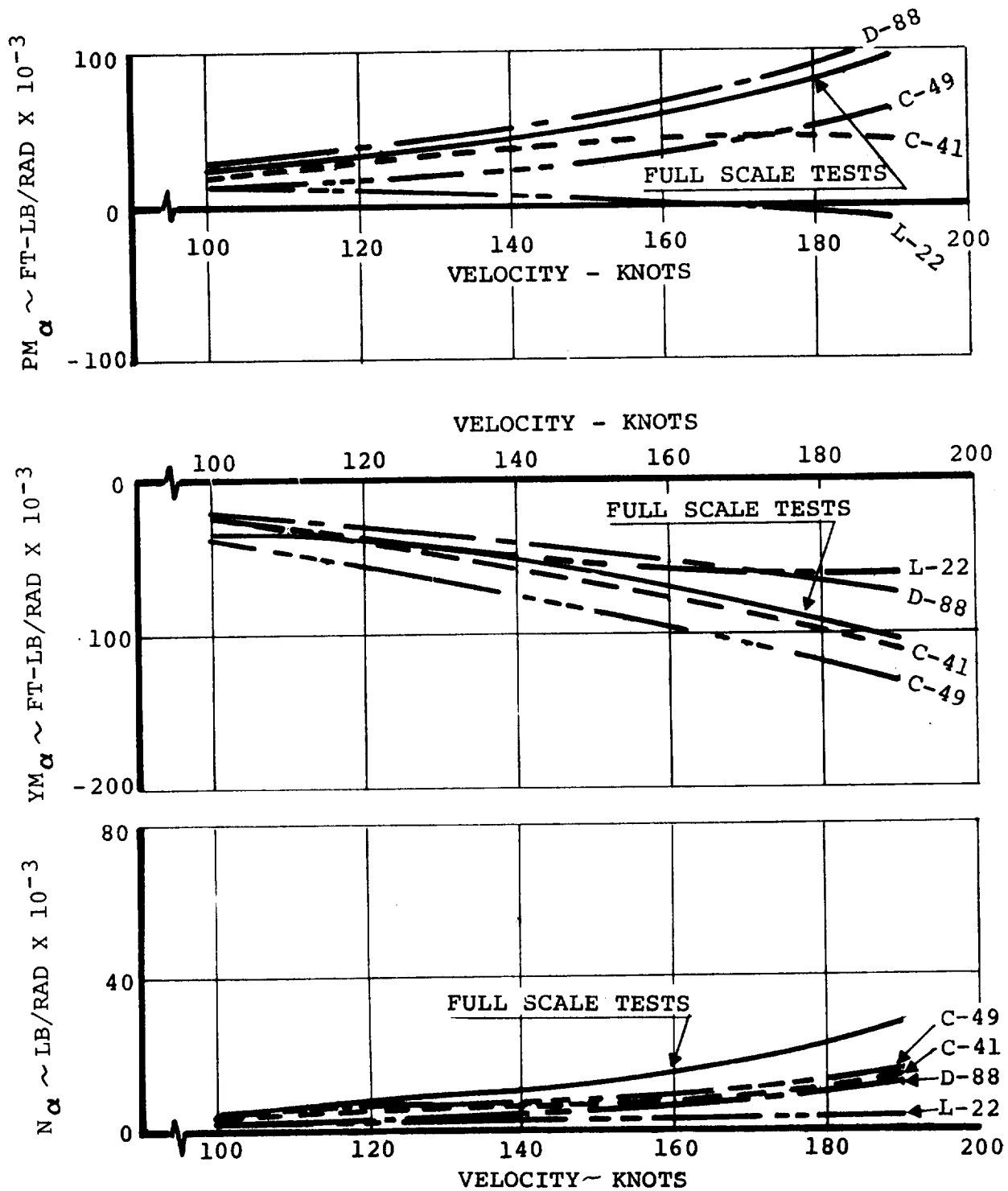


Figure 7.4. Correlation of 26 Ft Rotor Test Data with Various Rotor Derivative Programs

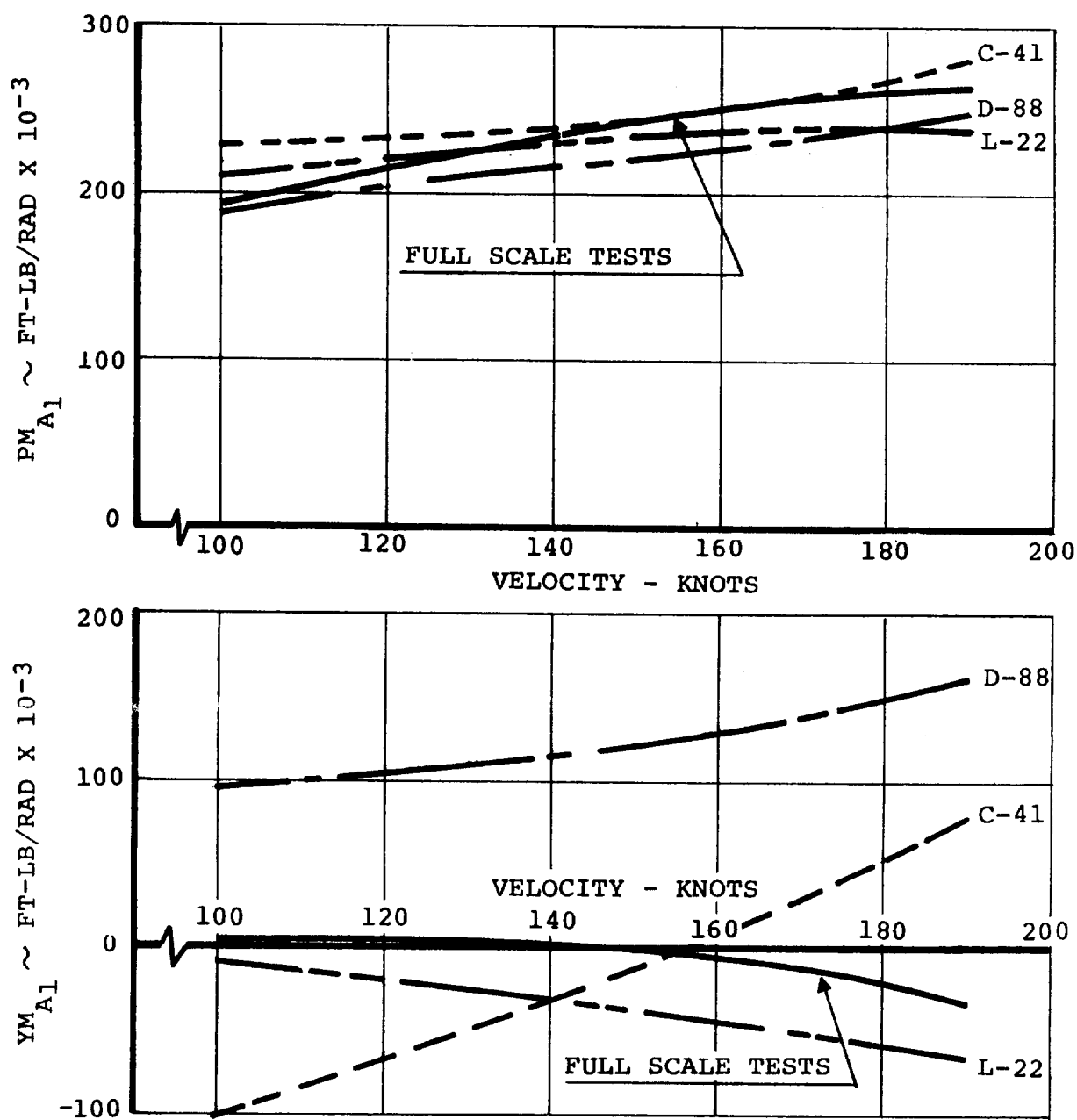


Figure 7.5. Correlation of 26 Ft Rotor Test Data with Various Rotor Derivative Programs – Cyclic Moment Derivatives

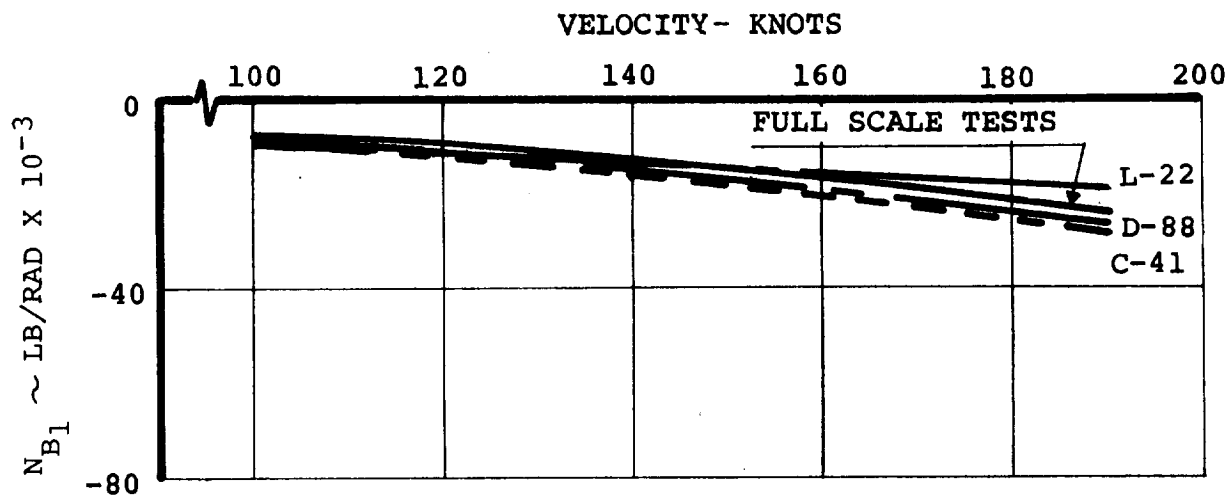
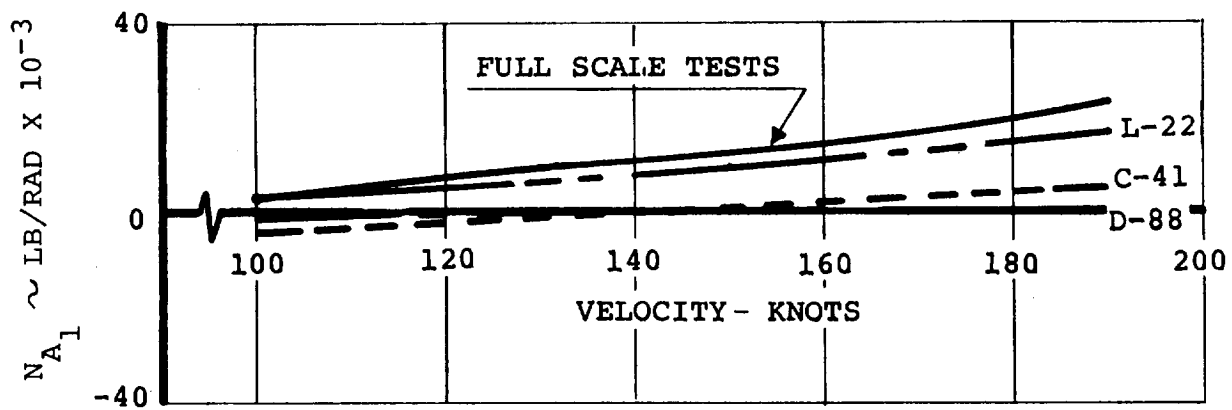


Figure 7.6. Correlation of 26 Ft Rotor Test Data with Various Rotor Derivative Programs — Cyclic Force Derivatives

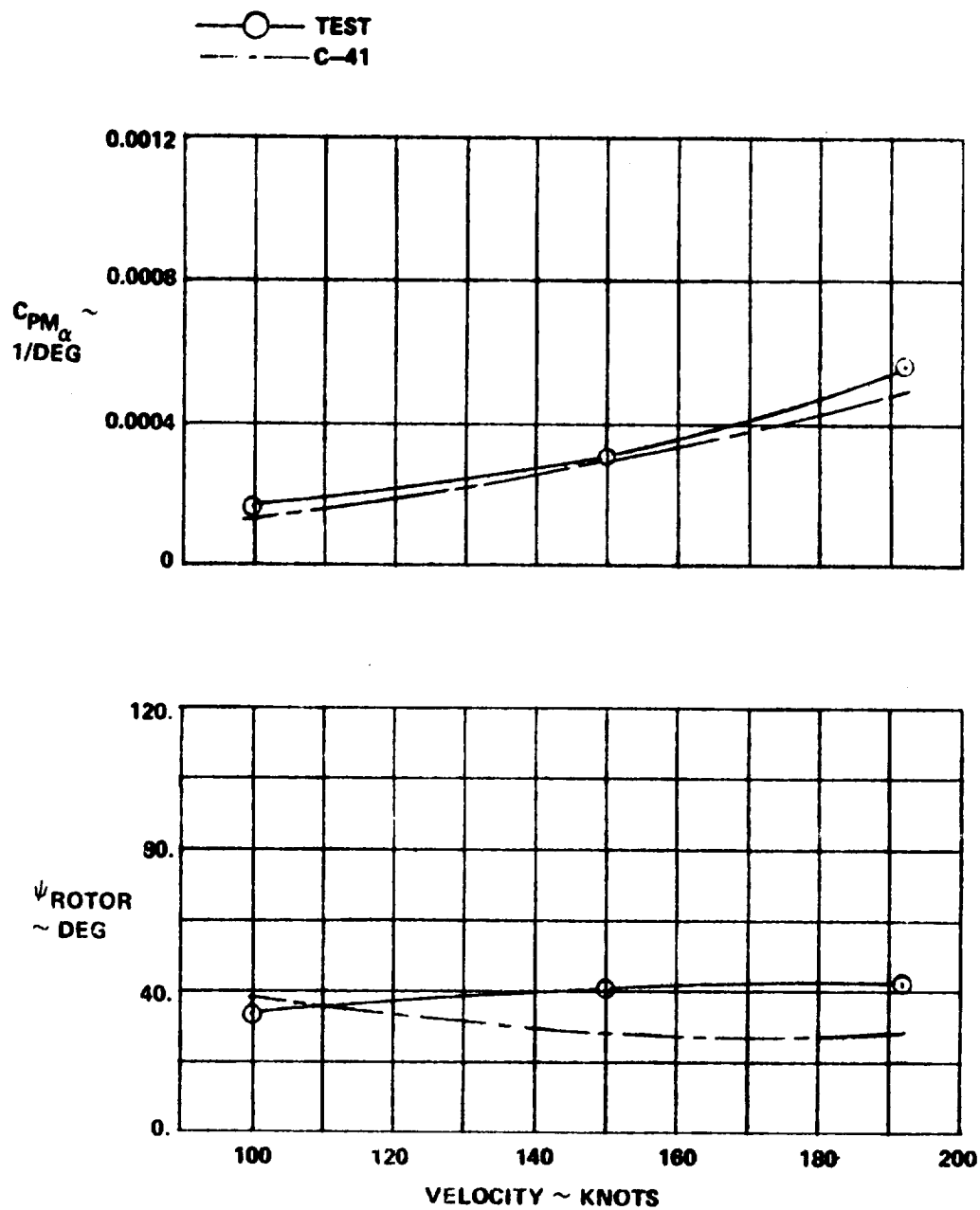


Figure 7.7. Rotor Moment and Azimuth Angle Due to Angle of Attack — Correlation with 26 Ft Rotor Data

with the model mounted on a pedestal in the tunnel. The rotors were given angles of attack to the free stream by pitching the complete model with zero sideslip angle and yawing the model at zero angle of attack. The yawing data contains minimal wing induced flow effects and comparison with the pitch data indicates the importance of induced flow on the rotor forces and moments. Forces and moments were computed for the isolated rotor and it is seen from Figure 7.8 that correlation with test data is excellent when wing induced effects are small; in Figure 7.9 wing effects introduce perceptible shifts which increase with dynamic pressure.

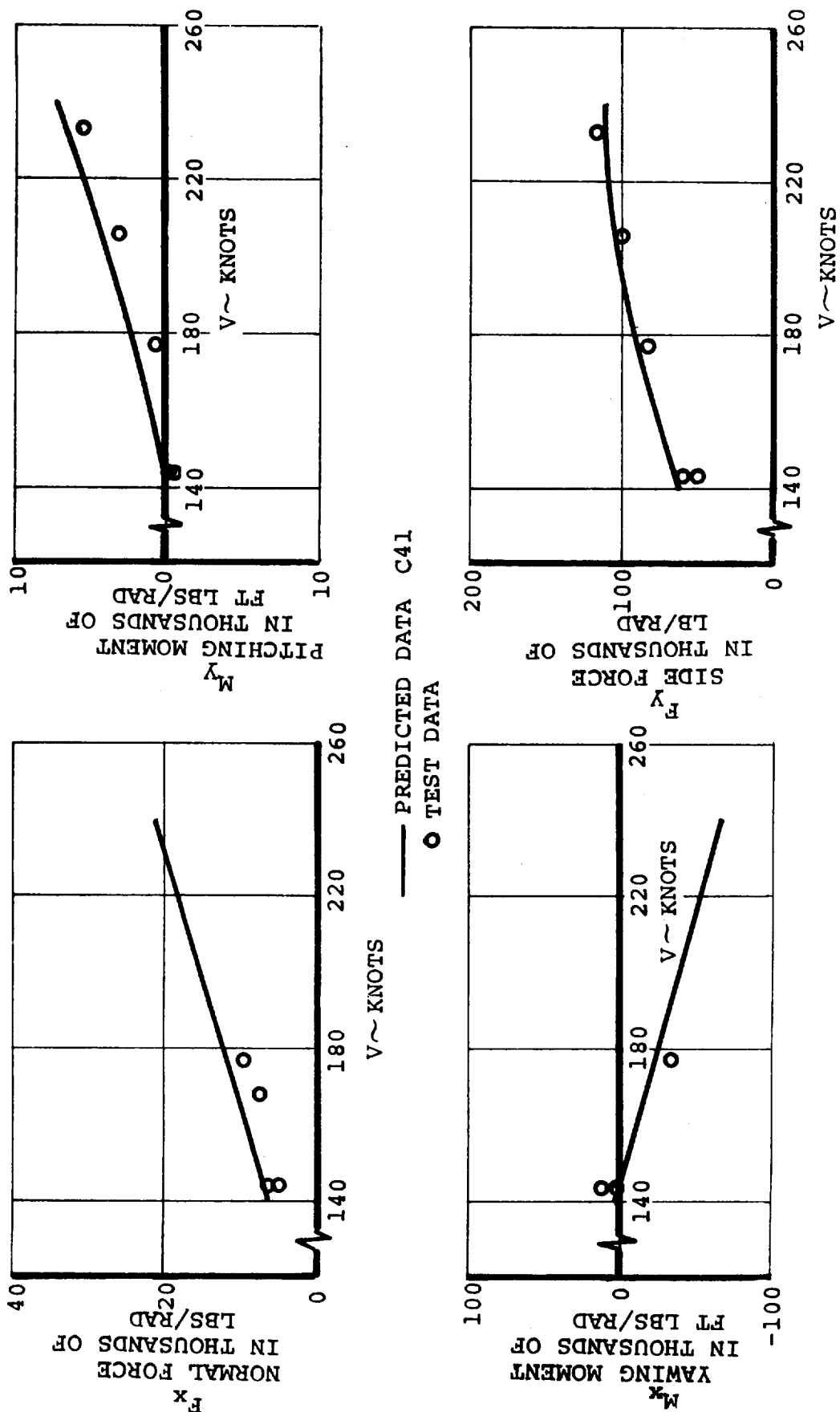


Figure 7.8. Comparison of Calculated and Test Rotor Hub Force and Moment Derivatives for M222
 1/4.622 Scale Model (Yaw Sweep) $\Omega = 386$ RPM

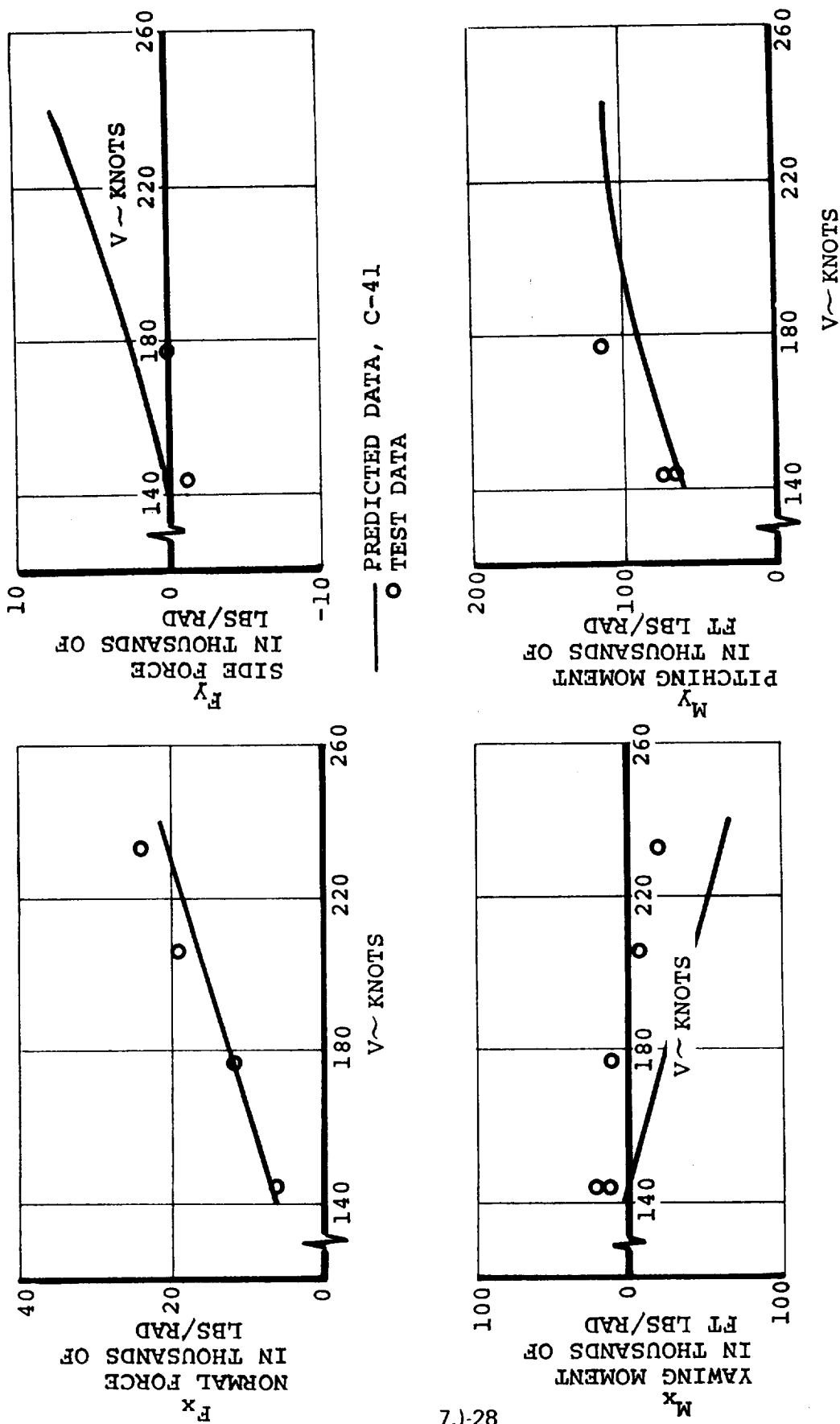


Figure 7.9. Comparison of Calculated and Test Rotor Hub Force and Moment Derivatives for M222
 1/4.622 Scale Model (Pitch Sweep) $\Omega = 386$ RPM

8.0 CONTROL SYSTEM DESCRIPTION

This section describes the control system, stability augmentation systems, load alleviation system and thrust management system utilized in the mathematical model. A more complete description is given in Reference 8. .

8.1 CONTROL AERODYNAMIC CONFIGURATION

Control of the Model 222 aircraft is accomplished by utilization of longitudinal cyclic, differential longitudinal cyclic, collective and differential collective pitch, and differential nacelle tilt control in conjunction with the airplane control surfaces. The airplane control surfaces consist of conventional elevator and rudder and a flaperon and spoiler arrangement. The primary controls in each axis for each regime of flight are shown in Table 8.1.

The rotor controls provide a major portion of the control capability from hover through the low transition speed range, but airplane surface controls are operative in all regimes of flight, including hover. The rotor controls are phased out during transition as nacelle incidence decreases, speed increases, and the surface controls become more effective.

8.2 LONGITUDINAL CONTROL

Longitudinal control in hover is provided by longitudinal cyclic pitch. This is phased out through transition as the elevator becomes more effective. The elevator provides longitudinal control in the cruise mode.

TABLE 8.1 FLIGHT CONTROL MIXING

FLIGHT MODE	PRIMARY CONTROLS
<u>Helicopter (Hover)</u>	
Pitch	Longitudinal Cyclic
Roll	Differential Collective
Yaw	Differential Longitudinal Cyclic and Differential Nacelle Tilt
Height Control	Collective/Engine Power
<u>Transition</u>	
Pitch	Longitudinal Cyclic and Elevator
Roll	Differential Collective, Differential Longitudinal Cyclic, Differential Nacelle Tilt, Aileron and Spoiler
Yaw	Differential Longitudinal Cyclic, Differential Nacelle Tilt, and Rudder
<u>Airplane</u>	
Pitch	Elevator
Roll	Aileron and Spoiler
Yaw	Rudder

8.3 LATERAL CONTROL

Lateral control in hover is provided by differential collective pitch, together with differential engine fuel flow (power). The differential engine power is provided to ensure maintaining roll control in the event of a cross shaft failure. It also serves to minimize the cross shaft torque. In transition, differential collective and differential cyclic are scheduled as a function of nacelle tilt.

When differential cyclic pitch is commanded the nacelles are also actuated to tilt differentially, thereby increasing the thrust vectoring effect of the cyclic pitch. Differential deflection of the nacelles is ± 1.55 degrees per degree of cyclic plus approximately ± 0.20 degrees of differential nacelle tilt due to elasticity of wing and nacelles. This results in a large increase in control power as compared to the control power available from cyclic alone. The control power requirements may, therefore, be met with modest amounts of cyclic control resulting in low blade stresses and long rotor fatigue life. Collective pitch is also scheduled with nacelle tilt so that when the nacelles are tilted differentially, pitch is increased on the rotor whose disc is tilted down, and decreased on the rotor which is tilted up. This maintains the thrust approximately equal on the two rotors, ensuring that thrust vectoring rather than differential thrust is achieved by the differential cyclic pitch and differential nacelle tilt.

The wing has full span flaps and spoilers mounted on the trailing edge. The flaps are single slotted of 30 percent chord with a fixed hinge point 14.6 percent below the wing chord line. The flaps act as flaperons for roll control and deflect downward only by a maximum of 20 degrees from the nominal flap setting. Maximum incremental lift from the flaps is attained at approximately 35 degrees deflection and the maximum rolling moment occurs at the same time, so the flaperon deflection for roll control is limited to a maximum total flap deflection of 35 degrees. If, for example, the flaps are symmetrically deflected 30 degrees, only 5 degrees additional deflection is utilized for roll control. Full span spoilers of 12.7 percent chord are located forward of the flaps and hinged to the rear spar. The spoilers are "slot-lipped", i.e., they open up the slot forward of the flap with the flaps extended resulting in a large increase in roll control as compared to the control power with flaps closed. Maximum deflection of the spoilers for roll control is 45 degrees from the closed position.

Maximum spoiler rolling moment coefficient is also attained with flaps deflected approximately 35 degrees. Spoiler effectiveness with the flaps retracted is approximately one-third that attainable with the flaps extended. Spoiler rolling moment is further reduced at high speed by limiting the spoiler actuator force capability, thereby restricting the spoiler extension at speeds above 175 knots.

The spoilers and flaps are also used in conjunction with download alleviation devices referred to as umbrellas mounted on the leading edge of the wing for download relief in the hover and low-speed ranges. The umbrellas are 18.6 percent chord on the upper and lower wing surfaces. Maximum deflections of the surfaces for download alleviation are: flaps 70 degrees, spoilers 110 degrees from closed, and umbrellas aft-edge-of-the-upper surface up to 20 degrees from vertical and aft-edge-of-lower-surface down to 10 degrees from vertical. The umbrellas and spoilers retract at 50 knots automatically.

8.4 DIRECTIONAL CONTROL

Directional control in hover is provided by differential longitudinal cyclic pitch, which, as discussed above under lateral control, also actuates differential nacelle tilt to amplify the thrust vectoring effect of the cyclic pitch.

In transition, the differential cyclic and its associated nacelle tilt are phased out as the rudder becomes more effective. This results in near zero initial roll acceleration in response to a yaw input.

8.5 THRUST/COLLECTIVE CONTROL

In hover, forward motion of the thrust/collective lever mechanically commands both increased collective pitch and increased power. The governor provides a fine adjustment to the collective pitch to maintain rpm. Over travel of the pilot's lever, beyond the normal max power position, provides a collective

pitch landing flare capability. The over travel is entered by going through a "gate", which shuts down the rotor governor and leaves the pilot's lever directly connected to collective pitch, just like a helicopter collective pitch lever.

The collective pitch is also scheduled through transition as a function of nacelle incidence, minimizing the adjustment needed from the governor and also providing the pitch variation with differential nacelle tilt required for roll and yaw control.

In cruise the mechanical interconnection of the thrust/collective lever with collective pitch is phased out completely so that a pure power demand system with governed pitch, like a conventional fixed wing airplane, is provided. The control system block diagrams are shown in Appendix E.

8.6 CONTROL FEEL

Control force gradient variation with dynamic pressure prevents excessive sensitivity of control at high speed. In the model 222, the force gradients of the primary controls (longitudinal and lateral stick, and pedals) are varied linearly with dynamic pressure. The rudder and elevator deflections vary linearly with pilot's rudder pedal and longitudinal stick travel. Aileron deflection is programmed linearly and spoiler deflection nonlinearly with lateral stick deflection, to provide near-linear rolling moment effectiveness to near cruise speed. As mentioned earlier, spoiler deflection is limited at high speed by limiting the actuator capacity. The control force breakout forces and gradients are shown in Appendix F.

8.7 STABILITY AUGMENTATION SYSTEMS

Stability augmentation systems are provided to enhance aircraft flying qualities. The system consists of longitudinal, lateral and direction SAS. The longitudinal stability augmentation system incorporates a pitch rate feedback and a longitudinal stick pickoff. In addition, a lagged pitch rate signal is incorporated to provide some degree of attitude stabilization without the autopilot. (An autopilot is not represented in this simulation.) These signals are shaped and put through an authority limit. The longitudinal SAS commands longitudinal cyclic pitch to provide the required damping in hover and transition. It is not required in the cruise mode and is phased out at 175 knots. The block diagram of the longitudinal SAS is given in Appendix E.

The lateral stability augmentation system is operative in all flight modes. It consists of roll rate feedback for increased damping in roll, lagged roll rate feedback to provide roll attitude stability, and a lateral stick pickoff. In addition a sideslip feedback is incorporated to decrease the strong dihedral effect. These feedback loops are shaped and phased to yield good aircraft dynamic characteristics. A lateral SAS authority limit is incorporated in the circuit. The output of the lateral stability augmentation system is input to the control system in terms of equivalent lateral stick, since the drive actuator is in series with, and commands the same control as, the pilots lateral stick control linkage. The

lateral SAS never opposes the pilots' command. The block diagram of this system is shown in Appendix E.

A directional stability augmentation system is provided and operates in all flight regimes. The yaw channel consists of yaw rate feedback for increased directional damping in hover and low speed flight modes, lagged yaw rate feedback to provide yaw attitude stability, and a rudder pedal pickoff for quickening. Directional damping provided by the rotors is quite high in the higher transition and cruise speed ranges. No additional yaw rate damping is therefore needed in cruise. A feedback is provided to modify the effective yawing moment due to roll rate which exists in the basic unaugmented aircraft configuration in the cruise speed range. The feedback gains, and the relative phasing of these gains have been optimized to provide good directional dynamic response. A directional SAS authority limit is incorporated. The SAS command is input to the control system in terms of equivalent inches of rudder pedal. The block diagram for the directional stability augmentation system is shown in Appendix E.

The stability augmentation systems used for the simulation are not set up to investigate individual component failures. Modifications are required in order to do malfunction type studies with this simulation.

8.8 LOAD ALLEVIATION SYSTEM (LAS)

Propeller type aircraft experience significant blade loads during exposure to skewed flow due to steady state or transient conditions (climb, sideslip, gusts, etc). The tilt rotor configuration can have similar problems. However, since cyclic pitch is a basic part of the tilt rotor control system it provides the means to significantly reduce the sensitivities to these effects. It also can be used to reduce the destabilizing moments which come from the rotors and thus improve static stability.

An automatic load alleviation system is provided and operates via the swashplate to reduce both transient and steady state hub forces and moments and the destabilizing moments at the nacelle pivot. It is not a required system for the Model 222, but will significantly enhance the static stability and the fatigue margins of the aircraft.

The overall objectives to be achieved through the use of cyclic feedback control are:

- Reduce rotor hub forces and moments for both steady state operation and gust encounter
- Improve flying qualities of the aircraft by using the cyclic control system to reduce pilot workload and improve short period response by reducing destabilizing forces and moments of the rotors

- Reduce aircraft structural loads resulting from gust turbulence
- Improve ride qualities by damping the response to gust turbulence

The load alleviation system, as mechanized in this simulation consists of angle of attack, angle of sideslip, and dynamic pressure sensors which drive through appropriate gains and filters to reduce the longitudinal and lateral moments at the nacelle pivot. The lateral cyclic pitch used for load alleviation is authority limited and drives separate actuators in each hub. The longitudinal cyclic pitch is summed in with the longitudinal SAS. The block diagram for this system as mechanized is shown in Appendix . This system is operative from low transition speed (approx. 50 knots) through dive speed and reduces the pivot moments from 50% in the 150 to 200 knot range to 100% in all other modes of flight.

8.9 THRUST MANAGEMENT SYSTEM

The thrust and power management system for a tilt rotor aircraft must be compatible with both the helicopter and airplane configurations. Thrust control for the hover task, rpm control, gust response (especially in the cruise flight regime), and effect on aircraft flying qualities must all be considered. Classically, helicopters have used collective pitch demand to control thrust and fuel governing to control rpm while fixed-wing aircraft have used fuel flow demand to control thrust and

collective pitch governing to control rpm. Each system has its advantages. For a tilt rotor aircraft it is desirable from a practical viewpoint to have one type of governing for both the helicopter and fixed-wing flight regimes. Collective pitch governing was chosen for Model 222 for several reasons:

- It is more readily adapted to the hover flight regime than the fuel governor is to cruise
- It has better gust response characteristics
- It is fast acting and has high accuracy
- Thrust response to pilot control can be easily shaped with feed forward loops
- It has been demonstrated successfully in hover, transition and cruise in the CL-84 aircraft

With collective pitch governing there are two areas in the thrust management system to be considered: (1) style of the collective pitch governor; and (2) the feed forward loops for shaping pilot thrust control. The block diagram for this system as mechanized in this simulation is shown in Appendix E.

Several different governor configurations were considered for The M222 in order to determine the governor system best suited to meet the following objectives: (1) 0.3 percent steady state error in 2.5 to 3 seconds; (2) 2 percent rpm overshoot; and (3), satisfactory effect on aircraft flying qualities in the

all-operational mode (i.e., all aircraft components operational and performing as designed) and various failure modes. A single governor reference which used the rpm signal from each rotor and averaged them was chosen as the configuration that best satisfied the design criteria. To achieve the required accuracy and transient response goals, integral as well as proportional feedback of rpm was necessary in both the hover and cruise regimes. Governor gain is scheduled with nacelle incidence to maintain a near optimum level of governing throughout the flight envelope. Gains are varied linearly as the rotor rpm is changed from 551 in hover to 386 in cruise. The second requirement of the governor system is shaping the rotor thrust output for a pilot throttle input. Considerations in determining the proper shaping include:

- (1) throttle sensitivity;
- (2) time constant to reach 63% of steady-state thrust; and
- (3) allowable thrust overshoot

Variable pilot's control sensitivity is employed to give the optimum sensitivity in the hover power range yet maintain full power control within a reasonable throttle throw (8 inches). Shaping of the pilot command with collective quickening is done to improve the thrust time constant and thrust response transient shaping so that the pilot may perform the precision hover task with a minimum of difficulty. In the cruise regime, shaping of the thrust output is unnecessary and is phased out during transition.

The thrust/collective pitch control system is designed in such a manner that, during hover, when the pilot moves his control, he commands both a change in engine fuel setting and, mechanically, a change in collective setting. The governor then operates with a time lag to trim the collective to the value required to maintain rpm. The mechanical collective change feature is washed out as a function of nacelle incidence so that when nacelle incidence is decreased to zero, the pilot commands only engine fuel. In addition, the reference setting schedule for collective has been established to maintain equal thrust output from both rotors during application of differential nacelle tilt.

As was mentioned previously, additional details on the Model 222 control system may be obtained from Reference 8.

9.0 ENGINE REPRESENTATION

This section describes the engine performance and dynamic model representation that is used in the mathematical model. The basic engine cycle performance data consists of tabulated values of four variables: power, fuel flow, gas generator shaft rpm, and power turbine shaft rpm. These parameters are a function of Mach number and turbine inlet temperature. All data are in referred, normalized format as shown in Table 9.1. Because of the normalized, referred format, all data are valid for any ambient conditions. The effects on engine performance of operating at non-optimum power turbine speed are included in this model. The referred format also facilitates including engine thermodynamic and mechanical limits. Limitations on engine cycle operation may be input on any combination of the following: fuel flow, torque, gas generator speed, gas generator referred rpm or output shaft speed. A detailed description of this routine is in Reference 9. The flow charts which describe this routine mathematically are shown in Appendix E.

A simplified dynamic model of the Lycoming T53-L-13 engine was formulated for use in the tilt rotor mathematical model. This model was coupled to the output of the engine performance program described above. The model consists basically of 2 first order lags in series with variable time constants and gains. The output of the model is rate limited to reflect actual engine performance. This simplified model gives satisfactory

results for both large and small power transients. The block diagram for this system is shown as part of the thrust management system block diagram shown in Appendix E.

TABLE 9.1 ENGINE CYCLE DATA FORMAT

VARIABLE	SYMBOL	REFERRED, NORMALIZED FORM
Thrust	F_N	$F_N / \delta F_N^*$
Power	SHP	$SHP / \delta \sqrt{\theta} SHP^*$
Gas Generator rpm	N_I	$N_I / \sqrt{\theta} N_I^*$
Power Turbine rpm	N_{II}	$N_{II} / \sqrt{\theta} N_{II}^*$
Fuel Flow	W_F	$W_F / \delta \sqrt{\theta} F_N^*$
		$W_F / \delta \sqrt{\theta} SHP^*$
Turbine Inlet Temperature	T	T / θ
Where:	<p>* = Max. Power Setting, Static, Sea Level, Standard Day</p> <p>θ = Ambient Temperature ($^{\circ}R$) Divided by 518.69$^{\circ}R$</p> <p>δ = Ambient Pressure (psia) Divided by 14.696 psia</p>	

10.0 GROUND EFFECTS

The effects of operating near the ground on the rotors and airframe are included in this model. The presence of the ground on the airframe imposes a boundary condition which inhibits the downward flow of air normally associated with the lifting action of the wing and tail. The reduced downwash has three main effects;

- A reduction in the downwash angle at the tail
- An increase in the wing lift curve slope
- An increase in the tail lift curve slope

These have been accounted for by the methods given in Reference 10 Appendix B-7. The data given in the reference for the change in wing and tail lift curve slope has been used directly. The equation specified for the change in downwash angle at the tail due to ground proximity was modified for convenience. The equation as stated is:

$$\frac{(\Delta \epsilon)_g}{\epsilon} = \frac{b_1^2 + 4(h-H)^2}{b_1^2 + 4(h+H)^2}$$

where $(\Delta \epsilon)_g$ = the change in tail downwash angle due to ground proximity

ϵ = the downwash remote from ground

h = the height of the tail root quarter chord point above the ground

H = the height of the wing root quarter chord point above the ground

b_1 = a function of wing lift and wing flap geometry

For this mathematical model, the b_1 in the above equation was taken to be equal to the wing span, b_w . This results in a small error in the change in horizontal tail downwash. It is, however, sufficiently accurate for this simulation.

Ground effects on the rotor are difficult to predict analytically, especially in forward flight. Wind tunnel test data for the Model 160 powered model, Reference 6 was plotted as a thrust ratio versus effective rotor height/diameter ratio, for two rotor advance ratios. This data, shown in Figure 10.1 was curve fit and linearly interpolated for advance ratio. The resulting equation is as follows: - (for the right rotor. The left rotor is identical except for subscripts)

$$\left(\frac{T_{IGE}}{T_{OGE}} \right)_{RR} = \left[\left(\frac{h}{D} \right)_{EFF}^2 (.1741 - .6216 \mu_{RR}) + \left(\frac{h}{D} \right)_{EFF} (1.4779 \mu_{RR} - .4143) + 1.2479 - .8806 \mu_{RR} \right]$$

$$\text{where } \left(\frac{h}{D} \right)_{EFF} = \frac{2R[|\sin(\theta + i_{NR}) \cos \phi| + .0174]}{h_{RR}}$$

$$h_{RR} = -Z_{DOWN} + (L_S \cos i_{NR} - X_{CG}) \sin \theta$$

$$+ [(L_S \sin i_{NR} + Z_{CG}) \cos \phi - Y_N \sin \phi] \cos \theta$$

= Rotor hub height above the ground

L_S = Distance from the nacelle pivot to the rotor hub

X_{CG} = Longitudinal distance from the pivot to the CG

Z_{CG} = Vertical distance from the pivot to the CG

θ = Aircraft pitch attitude

ϕ = Aircraft roll attitude

i_{NR} = Right rotor nacelle angle

Y_N = Wing semispan

$$\left(\frac{T_{IGE}}{T_{OGE}}\right) = \left[\left(\frac{h}{D}\right)_{EFF}^2 (.1741 - .6216\mu) + \left(\frac{h}{D}\right)_{EFF} (1.4779\mu - .4143) + 1.2479 - .8806\mu\right]$$

NOTE: If $\mu > 0.283$; $\left(\frac{T_{IGE}}{T_{OGE}}\right) = 1.0$
 or
 If $\left(\frac{h}{D}\right)_{EFF} > 1.3$; $\left(\frac{T_{IGE}}{T_{OGE}}\right) = 1.0$

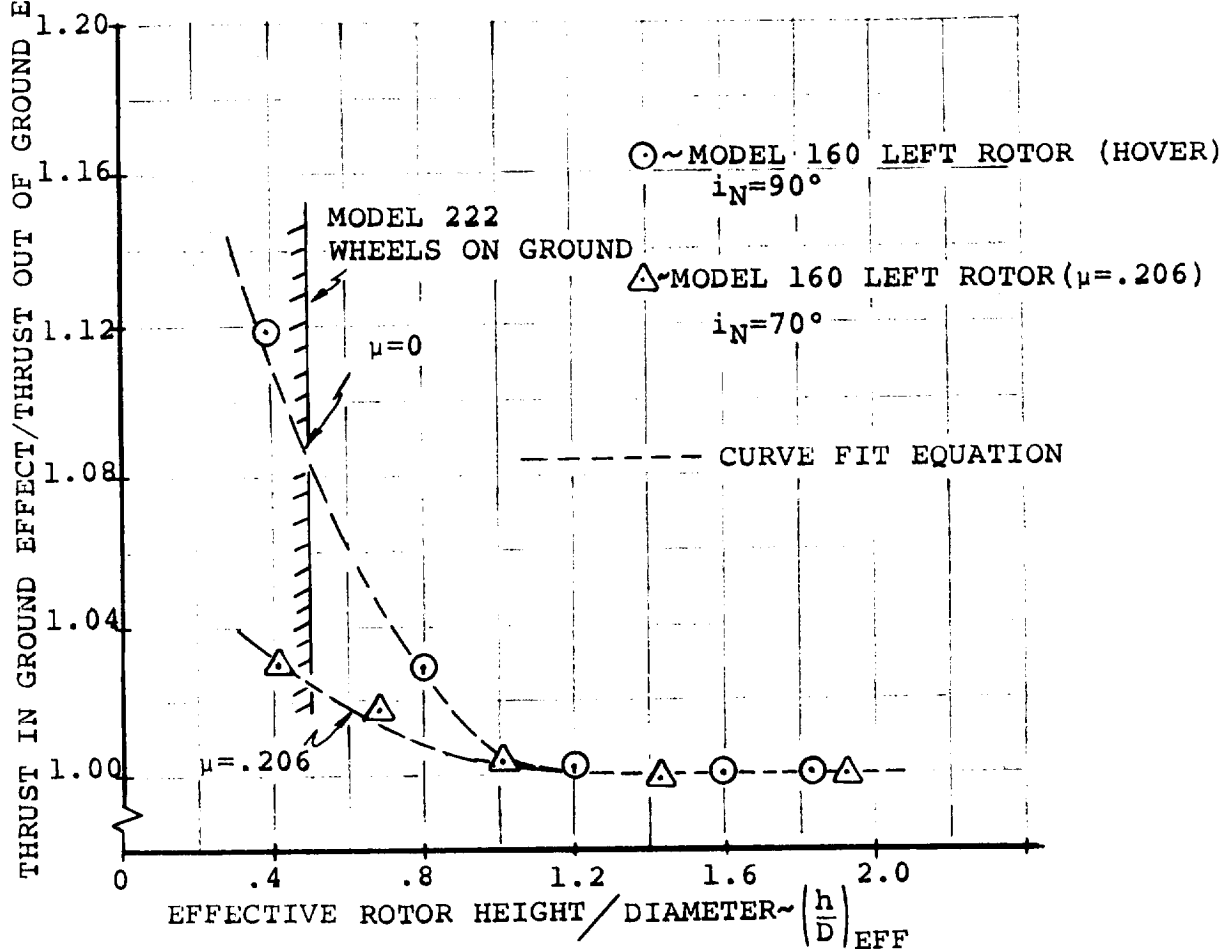


Figure 10.1. Effect of Rotor Height on Thrust Augmentation Ratio

The equation for the effective rotor height to diameter ratio $(h/D)_{EFF}$ was derived by dividing the rotor hub height by $[\sin(\theta+i_N)\cos \phi]$. This yields the rotor height along the shaft. For the cruise condition the hub height is infinite, $(h/D)_{EFF}$ is infinite and the augmentation ratio due to ground effect is unity. Some special conditions which must be observed when using these equations are noted in Figure 10.1.

11.0 AIRFRAME REPRESENTATION (PREPROCESSOR)

An airframe representation/preprocessor calculation is included in the mathematical model that enables the user to input the location of major structural elements of the aircraft in terms of water line, butt line and station line location. All lengths, center of gravity distances and inertias used in the equations are then calculated. This feature enables the user to quickly change the location of major structural elements to assess their impact on vehicle response.

In the derivation of the basic equations of motion, the aircraft was divided into three principal mass elements. The fuselage mass element (m_f), the wing mass element (m_W) and the tilting nacelle mass element (m_N). The components of the three mass elements are shown below and are available from a standard mass properties buildup of the Model 222.

- fuselage mass element (m_f)
 - { Fuselage and contents
 - { Horizontal tail and contents
 - { Vertical tail and contents
 - { Crew and trapped liquids
 - { Cargo
- wing mass element (m_W)
 - { Wing and contents
 - { Fuel carried in wing
 - { Fixed nacelles and/or engines
- tilting nacelle mass element (m_N)
 - { Tilting nacelle (including rotors)

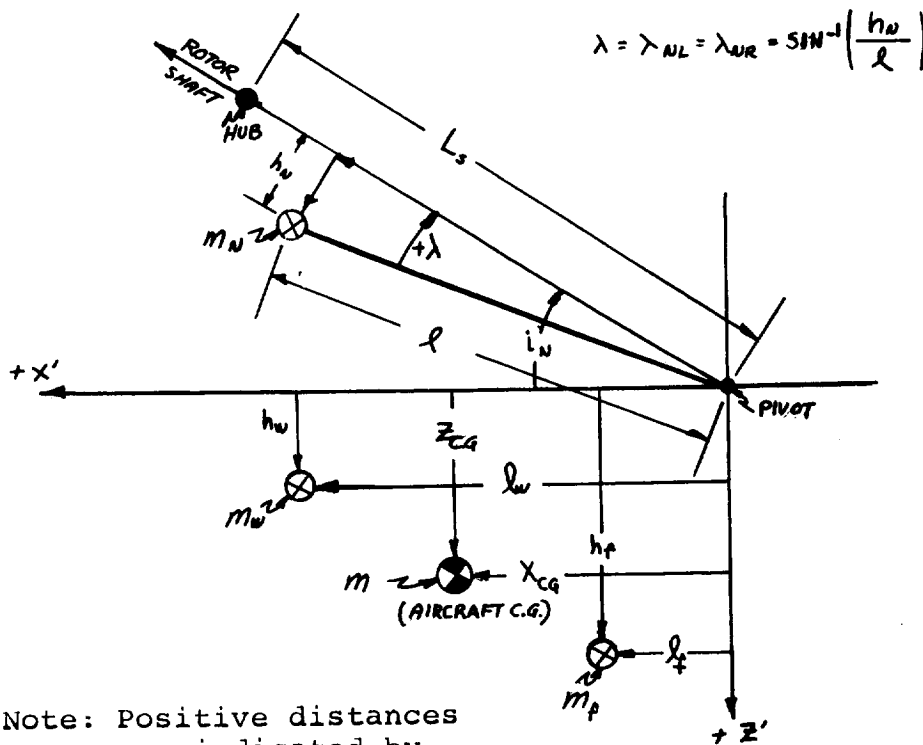
These three mass elements along with their respective distances from the nacelle pivot to the center of each mass element are used to compute the aircraft center of gravity distances with

respect to the nacelle pivot. The equations for these center of gravity distances, derived in Appendix C, and including the effects of nacelle tilt are:

$$x_{CG} = \frac{m_f \ell_f + m_w \ell_w}{m} + \ell \left(\frac{m_N}{m} \right) \left[\cos(i_{NL} - \lambda) + \cos(i_{NR} - \lambda) \right]$$

$$z_{CG} = \frac{m_f h_f + m_w h_w}{m} - \ell \left(\frac{m_N}{m} \right) \left[\sin(i_{NL} - \lambda) + \sin(i_{NR} - \lambda) \right]$$

The masses and distances used in these equations are defined on the sketch below.



Note: Positive distances are indicated by the direction of the arrows

The quantities required to compute m_f , l_f , m_w , l_w , m , l , m_N , λ , h_f , h_w are available from an aircraft three-view drawing and a standard mass properties buildup. The quantities l and λ (defined in the sketch) are easily obtainable from a drawing. The mass quantities (m , m_N , m_f , m_w) are computed from a mass properties buildup by adding up the components of each mass element as described in the previous paragraph. The lengths l_f , l_w , h_f and h_w are computed by summing the weight moments of the components of each mass element about the nacelle pivot. The equations for these operations have been derived and are presented in Appendix E under the preprocessor equations. The input data to these equations include the weight of each component, and its location in terms of water line, fuselage station line, and butt line.

When the center of gravity distance of each mass element has been determined, the component and total aircraft mass moments of inertia can be computed. The equations for the total aircraft mass moments of inertia are presented in Appendix C. The moments of inertia of each mass element are computed by application of the parallel axis theorem. The moments of inertia of each component about its own center of gravity must be known. The parallel axis theorem states:

$$I_{xx} = \sum_{i=1}^N \left[I_{xx_{O_i}} + m_i (y_i^2 + z_i^2) \right]$$

$$I_{YY} = \sum_{i=1}^N \left[I_{YY_{O_i}} + m_i (z_i^2 + x_i^2) \right]$$

$$I_{ZZ} = \sum_{i=1}^N \left[I_{ZZ_{O_i}} + m_i (x_i^2 + y_i^2) \right]$$

$$I_{XZ} = \sum_{i=1}^N \left[I_{XZ_{O_i}} + m_i (x_i z_i) \right]$$

where N represents the number of component masses.

These equations have been expanded to compute the moments of inertia of each mass element and are shown in Appendix E under the preprocessor section. The only additional input data required are the inertias of each component about their own centers of gravity. These are readily available from the mass properties buildup of the Model 222.

Other lengths required for the mathematical model are computed in this section. The input data for these computations are in terms of the water line, butt line and fuselage station line locations of the elements in question.

12.0 AERO-ELASTIC REPRESENTATION

Two aero-elastic degrees of freedom are included in the tilt rotor mathematical model. These are first mode wing vertical bending and first mode wing torsion. The stability and control characteristics of flexible airplanes may be significantly influenced by distortions of the structure under transient loading conditions. When the separation in frequency between the elastic degrees of freedom and the rigid body motions is not large, then significant aerodynamic and inertial coupling can occur between the two. Many of the important effects of elastic distortion, however, can be accounted for simply by modifying the aerodynamic equations. The assumption is made that the changes in aerodynamic loading take place so slowly that the structure is at all times in static equilibrium. This is equivalent to assuming that the natural frequencies of vibration of the structure are much higher than the frequencies of the rigid body motions. Thus a change in load produces a proportional change in the shape of the airplane, which in turn influences the load. This is known as the method of "quasistatic" deflections where all the coupling occurs in the aerodynamic equations.

The wing uncoupled natural frequencies were investigated to determine which method would be used. Table 12.1 shows the

TABLE 12.1 WING UNCOUPLED FREQUENCIES (BLADES OFF)
CRUISE CONFIGURATION

<u>Symmetric Mode</u>	<u>Frequency</u>
Vertical Bending	3.6 cps
Chordwise Bending	5.4 cps
Torsion	6.1 cps
<u>Antisymmetric Mode</u>	<u>Frequency</u>
Vertical Bending	11.2 cps
Chordwise Bending	9.1 cps
Torsion	5.7 cps

Model 222 wing uncoupled frequencies for the cruise condition for both the symmetric and anti-symmetric modes. As can be noted in the table, the lowest vertical bending frequency is 3.6 cps and the lowest wing torsional frequency is 5.7 cps. The rigid body short period mode varies from approximately 0.40 cps to 1.35 cps. Since the rigid body short period modes are separated from the elastic modes by a substantial margin, the method of "quasistatic" deflection is used to represent the wing bending and torsion modes, with the only coupling in the aerodynamic terms (through angle of attack). The wing twists and bends instantaneously when subjected to an applied load. The assumptions made in deriving the wing bending and torsion relationships are as follows:

- No coupling between bending and torsion modes
- Wings are cantilevered from the fuselage
- Elliptical loading assumed for the rigid untwisted wing
- Aerodynamic loads act at the wing quarter chord
- Wing elastic axis coincident with cross shaft
- Wing center of mass assumed to lie on the elastic axis
- First wing torsional mode assumed linear from tip to root

In the mathematical model, wing twist at the tip is calculated using the following equation:

$$K_{\theta_t} \theta_t = M_{ACT} - I_E \Omega_E R + q \frac{c_w^2 b_w}{C_w} C_{m_0} + q C_w^2 \left(\frac{dC_{m_c}/4}{dC_l} + \frac{x_{WAC}}{C_w} \left(\frac{C_{L_\alpha}^2 b_w}{6\pi} \right) \right) (4\theta_t + 3\pi \alpha_{RIGID})$$

where: K_{θ_t} = Wing torsional spring constant

θ_t = Wing twist angle in degrees

M_{ACT} = Nacelle actuator pitching moment

I_E = Engine inertia

Ω_E = Engine speed

R = Body yaw rate

q = Dynamic pressure

c_w = Wing reference chord

b_w = Wing reference span

C_{m_0} = Wing zero lift pitching moment coefficient

$\frac{dC_{m_c}/4}{dC_l}$ = Wing pitching moment slope with lift coefficient

C_{L_α} = Wing lift curve slope

α_{RIGID} = Wing angle of attack without twist

Assuming a linear mode shape from the wing tip to the root and a cantilevered wing (zero twist at root), the wing twist at the aerodynamic center location of the wing is obtained by linear interpolation. The wing twist represents the change in angle of attack of the wing tip and aerodynamic center and are used in the aerodynamic equations.

Wing vertical bending deflection is also treated on a "quasi-static" basis. The form of the equation used in the mathematical model for the wing tip deflection is as follows:

$$h_1 = K_{W1} Z_{AERO}^N + K_{W2} Z_{AERO}^W - K_{W3} L_{AERO}^N - K_{W4} \bar{a}_T - K_{W5} \bar{a}_{WAC}$$

where: h_1 = Wing tip deflection

Z_{AERO}^W = Wing lift

Z_{AERO}^N = Total wing lift

L_{AERO}^N = Nacelle rolling moment

\bar{a}_T = Vertical acceleration of the nacelle

\bar{a}_{WAC} = Vertical acceleration of the wing aerodynamic center

$K_{W1} \rightarrow K_{W5}$ = Constants for Model 222 wing

The form of the equation for the wing deflection at the aerodynamic center is written similarly:

$$h_{1_{WAC}} = K_{W6} Z_{AERO}^N + K_{W7} Z_{AERO}^W - K_{W8} L_{AERO}^N - K_{W9} \bar{a}_T - K_{W10} \bar{a}_{WAC}$$

The symbols represent the same quantities as the tip deflections except the quantities K_{W6} to K_{W10} are different from K_1 to K_5 .

These equations are derived in Appendix A. Since the wings are assumed cantilevered, these equations may be written for

the left and right sides. The equations as used in the mathematical model are written in Appendix E.

The wing tip and aerodynamic center vertical bending velocities are computed by dividing the change in vertical bending deflection by the simulation time frame. The vertical bending deflections and velocities are then added to the velocity components at the wing tip and aerodynamic center. These velocity components are then used in the calculation of the aerodynamic angle of attack.

In addition to the aerodynamic coupling via angle of attack, as discussed above, the wing tip vertical forces and moments act as the driving functions to a set of second order equations that are forced at the wing vertical bending frequency. This results in giving the pilot a "seat of the pants" feel for the vibratory aspects of the wing vertical bending mode. The equations were written in this manner to see if the pilot could induce a P.I.O. (pilot induced oscillation) during the piloted simulations due to wing vertical bending.

13.0 CONCLUSIONS AND RECOMMENDATIONS

1. Formulation of an eleven degree of freedom tilt rotor mathematical model and setting up an in-house hybrid simulation program using this model have been successfully completed.
2. The simulation model has been successfully checked out and validated at the Ames Research Center.
3. The in-house simulation model is "real time" and executes in 40 milliseconds. The Ames simulation is also real time with a 50 millisecond time frame. This increased time is due to the all digital nature of the Ames simulation.
4. It is desirable to shorten the frame time of the simulation. This may be accomplished by streamlining the following elements of the mathematical model:
 - Slipstream aerodynamics
 - Input aerodynamic data in body axes rather than wind axes to eliminate axes transforms
5. The simulation could be improved by incorporating advances in methodology in such areas as:
 - Rotor Representation - Formulate a simplified analytical model to adequately represent the dynamics and aerodynamics of soft-in-plane hingeless

rotors for all flight regimes. This would avoid the necessity for complex time-consuming table look ups of rotor data.

- Slipstream Aerodynamics - Simplify the analytical representation based on wind tunnel test data.
- Interference Effects - Improve the prediction of the tail downwash environment at low transition speeds.

14.0 REFERENCES

1. USAF Stability and Control DATCOM, Air Force Flight Dynamics Laboratory, October 1960, (Revised September 1970).
2. Reed, T. J., "User Report" Prop/Rotor Dynamic Derivative Program C41 J.N.", Boeing Document D210-10116-1, Vertol Division, The Boeing Company, Philadelphia, Pa., June 1970.
3. Amos, A. K.; Miao, W., "Program C-49: Rotor Stability Derivatives", Boeing Interoffice Memorandum, 8-7453-1-2483, Vertol Division, The Boeing Company, Philadelphia, Pa., July 1971.
4. Davenport, F. J., "Analysis of Propeller and Rotor Performance in Static and Axial Flight by an Explicit Vortex Influence Technique", Boeing Document R-372, Boeing Company, Vertol Division, Philadelphia, Pa., February 1965.
5. Tarzanin, F. and Thomas, E., "Aeroelastic Rotor Analysis", Boeing Document D8-0614, Boeing Company, Vertol Division, Philadelphia, Pa., May 1967.
6. Magee, J. P., et al, "Test Program II, Wind Tunnel Test of a Powered Tilt Rotor Performance Model, Volume VI, Results and Analysis", Boeing Document D213-10000-6, Boeing Company, Vertol Division, Philadelphia, Pa., August 1970.
7. Smith, M. C., "University of Maryland Wind Tunnel Test 489, Force, Moment and Downwash Measurements on a Rigid Rotor

and Semispan Wing", (4 volumes), Boeing Document D8-1062-1, The Boeing Company, Vertol Division, Philadelphia, Pa., March 1968.

8. "Study of V/STOL Tilt Rotor Research Aircraft Program (Phase I)", Volumes II and III, Prepared under contract NAS2-7259 for NASA, Ames Research Center, Boeing Vertol Company, Philadelphia, Pa., January 1973.
9. Schoen, A. H., "User's Manual for VASCOMP II, The V/STOL Aircraft Sizing and Performance Computer Program", Boeing Document D8-0375, Volume VI, Boeing Company, Vertol Division, Philadelphia, Pa., March 1968.
10. Etkin, Bernard, "Dynamics of Flight", John Wiley and Sons, Inc., 1959.
11. Heyson, Harry H. and Katzoff, S.; "Induced Velocities Near a Lifting Rotor with Non-uniform Disk Loading", NACA Report 1319, December 7, 1956.
12. Allen, H.J. and Perkins, E.W., "A Study of Effects of Viscosity on Flow Over Slender Inclined Bodies of Revolution", NACA TR 1048, 1951.

APPENDIX A - TREATMENT OF WING FLEXIBILITY

As described in Section 12 the large separation which exists between the natural frequencies of vibration of the wing structure and the aircraft rigid body motions, enables the elastic deformations of the wing structure to be calculated on a quasi-static basis.

In the simple treatment presented below, the bending and torsion modes are considered to be uncoupled. The wing is treated as a cantilever with a built-in root end. The wing is free to twist about the elastic axis which is assumed to coincide with the nacelle pivot line. The center of mass of each chordwise strip is also taken to lie on the pivot line. The unloaded wing has neither geometric nor aerodynamic twist.

WING TWIST

Spanwise twisting of the wing takes place under the action of the nacelle aerodynamic and inertial moments, the wing lift distribution, and the spanwise distribution of aerodynamic pitching moment. The nacelle aerodynamic moments consist of rotor hub loads, transferred to the pivot, together with the aerodynamic loads on the nacelle itself. Nacelle inertial moments include the gyroscopic effects of the rotor drive system.

With reference to Figure A.1 , M_N is the moment supplied or absorbed by the nacelle tilt actuator. If K_θ is the wing stiffness as seen by the wing tip, then

$$M_N = K_\theta \theta_T \quad (A-1)$$

The total moment about the elastic axis due to wing aerodynamics, nacelle loads and engine gyroscopic torque is

$$T = \int_0^{b/2} m \, dy + M_N + M_{\text{gyro}} \quad (A-2)$$

The aerodynamic moment about the elastic axis at any station y is given by

$$m = m_{c/4} + \ell x \quad (A-3)$$

where ℓ is the section lift and x is the distance from the quarter chord to the elastic axis. In terms of the section aerodynamic coefficients,

$$m(y) = \frac{1}{2} \rho V^2 c^2 C_{m_{c/4}} + \frac{1}{2} \rho V^2 c^2 C_\ell \frac{x}{c} \quad (A-4)$$

The section lift coefficient, C_ℓ , is given by

$$\begin{aligned} C_\ell &= k \frac{dC_\ell}{d\alpha} (\alpha - \alpha_o) \sqrt{1 - \left(\frac{2y}{b}\right)^2} \\ &= k a_o (\alpha_R - \epsilon_p - \alpha_o + \theta_t(y)) \sqrt{1 - \left(\frac{2y}{b}\right)^2} \end{aligned} \quad (A-5)$$

where α_R is the wing root section angle of attack
 ϵ_p is the rotor induced downwash, assumed constant spanwise
 α_o is the section zero-lift angle
 θ_t is the structural twist at station y

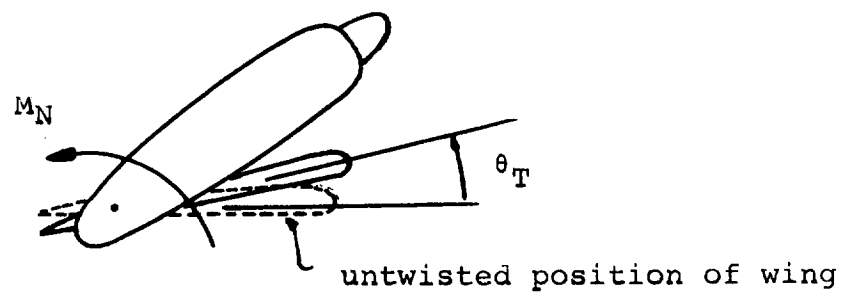
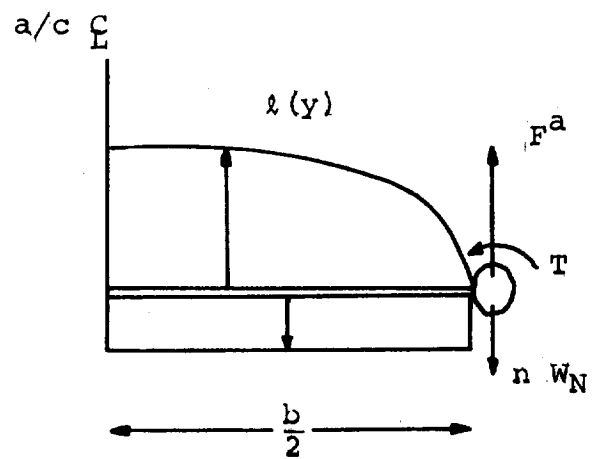


Figure A.1. Wing Geometry for Derivation of Flexibility

The factor $k\sqrt{1-\left(\frac{2y}{b}\right)^2}$ is introduced so that, for the untwisted wing, the lift distribution is elliptical. The value of k is obtained from the rigid wing elliptical loading as

$$k = \frac{4}{\pi} \frac{C_{L\alpha}}{a_0} \quad (A-6)$$

Thus the equation for C_ℓ becomes, with $\alpha_{RIGID} = \alpha_R - \epsilon \bar{p} \alpha_0$,

$$C_\ell = \frac{4}{\pi} C_{L\alpha} \left[\alpha_{RIGID} \sqrt{1-\left(\frac{2y}{b}\right)^2} + \theta_t \sqrt{1-\left(\frac{2y}{b}\right)^2} \right] \quad (A-7)$$

In equation (A-4) we can write, for low angles of attack,

$$C_{mC/4} = C_{mO} + \frac{dC_{mC/4}}{dC_\ell} C_\ell \quad (A-8)$$

and therefore

$$m(y) = \frac{1}{2} \rho V^2 c^2 \left\{ C_{mO} + \left(\frac{dC_{mC/4}}{dC_\ell} + \frac{x}{c} \right) C_\ell \right\} \quad (A-9)$$

The equation for the total wing twisting moment, equation (A-2), can now be written as,

$$T = M_{actuator} + M_{GYRO} + \frac{1}{4} \rho V^2 c^2 C_{mO} b + \frac{1}{2} \rho V^2 c^2 \left(\frac{dC_{mC/4}}{dC_\ell} + \frac{x}{c} \right) \int_0^{b/2} C_\ell dy \quad (A-10)$$

Using equation (A-7), assuming a linear structural twist from root to tip and performing the indicated integrations, the equation for total wing twisting moment becomes

$$T = K_\theta \theta_T = M_{actuator} + M_{gyro} + \frac{1}{4} \rho V^2 b c^2 C_{mO} + \frac{1}{2} \rho V^2 c^2 \left(\frac{dC_{mC/4}}{dC_\ell} + \frac{x}{c} \right) \times \frac{C_{L\alpha} b}{6\pi} \left(3\pi \alpha_{RIGID} + 4\theta_T \right) \quad (A-11)$$

The equation for the actuator moment is given in the equations of motion, Section 5.0.

Rearranging, and writing $q = q_s (1 - C_{T_s}) = \frac{1}{2} \rho V^2$

$$\theta_T = \frac{M_N + M_{gyro} + \frac{1}{2} q_s (1 - C_{T_s}) c_w^2 \left[6\pi \alpha_{rigid} \left(\frac{dC_m}{dC_L} + \frac{x}{c} \right) + b_w C_{m_O} \right]}{K_\theta - \frac{2}{3\pi} q_s b_w c_w^2 C_{L_\alpha} (1 - C_{T_s}) \left(\frac{dC_m}{dC_L} + \frac{x}{c} \right)} \quad (A-12)$$

where C_{m_O} , the zero-lift wing section pitching moment coefficient, is a function of flap deflection:

$$C_{m_O} = C_1 + C_2 \delta_f + C_3 \delta_f^2 \quad (A-13)$$

Knowing the tip value of twist, the twist at any other spanwise station is obtained by assuming a linear variation of twist from zero at the root to the tip value.

WING VERTICAL BENDING

The spanwise bending moment at any spanwise station y , on the wing is the sum of the bending moments due to wing aerodynamic lift, wing weight, nacelle lift, nacelle weight and net torque on the nacelle. The expressions for each contribution to the bending moments are derived below.

• Bending moment due to wing loading.

Assuming an elliptical distribution of lift the bending moment is given by

$$\begin{aligned} M^a(y_1) &= \int_{y_1}^{b/2} \ell(y) (y - y_1) dy \\ &= \frac{\ell_O b^2}{4} \int_{y_1}^{b/2} \sqrt{1 - \left(\frac{2y}{b}\right)^2} \left(\frac{2y}{b} - \frac{2y_1}{b} \right) d\left(\frac{2y}{b}\right) \end{aligned} \quad (A-14)$$

where ℓ_0 is the lift per unit length at the wing root. Introducing the spanwise variable $\theta = \cos^{-1}\left(\frac{2y}{b}\right)$ making the required substitutions and integrating, the bending moment at any point y is:

$$M^a(y) = \frac{\ell_0 b^2}{4} \left[\frac{1}{2} (\sin \theta - \theta \cos \theta) - \frac{1}{6} \sin^3 \theta \right] \quad (A-15)$$

- Bending due to nacelle net vertical load.

The net vertical force on nacelle is

$$F = F^a - nW_N$$

where F^a is the aerodynamic force and nW_N is the inertial load on the nacelle. The bending moment due to nacelle force is

$$M^N(y) = \frac{Fb}{2} (1 - \cos \theta) \quad (A-16)$$

- Bending due to wing weight.

Assuming a uniform distribution of wing weight

$$M^W(y_1) = -n \int_{y_1}^{b/2} w(y) (y - y_1) dy$$

and $w(y) = 2W/b$ where W is the weight of one wing panel

$$\therefore M^W(y_1) = \frac{2nW}{b} \int_{y_1}^{b/2} (y - y_1) dy \quad (A-17)$$

$$\text{i.e. } M^W(y) = - \frac{nWb}{2} (1 - \cos \theta - \frac{1}{2} \sin^2 \theta)$$

- Bending due to nacelle torque (rolling moment)

$$T(y) = \text{constant} = T \quad (A-18)$$

Total bending moment at station y is therefore

$$M(y) = M^a(y) + M^N(y) + M^W(y) + T \quad (A-19)$$

Assuming a linear variation of EI from root to tip given by

$$EI(y) = EI_0 \left[1 - a \left(\frac{2y}{b} \right) \right] = EI_0 (1 - a \cos \theta), \quad (A-20)$$

the curvature of the wing due to bending is

$$\begin{aligned} \frac{M(y)}{EI(y)} = \frac{d^2z}{dy^2} = & \frac{L_0 b^2}{8EI_0} \left[\frac{(\sin \theta - \theta \cos \theta) - \frac{1}{3} \sin^3 \theta}{1 - a \cos \theta} \right] + \frac{F_a b}{2EI_0} \left[\frac{1 - \cos \theta}{1 - a \cos \theta} \right] \\ & - \frac{nW_N b}{2EI_0} \left[\frac{1 - \cos \theta}{1 - a \cos \theta} \right] - \frac{nW_W b}{2EI_0} \left[\frac{1 - \cos \theta - \frac{1}{2} \sin^2 \theta}{1 - a \cos \theta} \right] \\ & + \frac{T}{EI_0} \left[\frac{1}{(1 - a \cos \theta)} \right] \end{aligned} \quad (A-21)$$

Double integration of this equation yields the following expression for the bending deflection of the wing at any point y on the span:-

$$\begin{aligned} z(y) = & \frac{Lb^3}{8\pi EI_0} \phi_1 + \frac{b^3 F_a}{8EI_0} \phi_2 - \frac{nW_N b^3}{8EI_0} \phi_3 \\ & - \frac{nW_W b^3}{8EI_0} \phi_4 + \frac{Tb^3}{4EI_0} \phi_5 \end{aligned} \quad (A-22)$$

$$\text{where } \phi_1 = \int_0^y \left\{ \int_0^y \frac{(\sin \theta - \theta \cos \theta) - \frac{1}{3} \sin^3 \theta}{1 - a \cos \theta} dy \right\} dy$$

$$\phi_2 = \phi_3 = \int_0^y \left\{ \int_0^y \frac{1 - \cos \theta}{1 - a \cos \theta} dy \right\} dy$$

$$\phi_4 = \int_0^y \left\{ \int_0^y \frac{1 - \cos \theta - \frac{1}{2} \sin^2 \theta}{1 - a \cos \theta} dy \right\} dy$$

$$\phi_5 = \int_0^y \left\{ \int_0^y \frac{dy}{1-a \cos \theta} \right\} dy$$

and where the wing lift (2 wing panels) $L = \pi \frac{\rho_0 b}{4}$. The function ϕ_1 through ϕ_5 were obtained numerically and are presented in Figure A.2 .

$$\text{Since } L = -2 z_{\text{AERO}}^W$$

$$F^a = - z_{\text{AERO}}^N$$

$$T = - L_{\text{AERO}}^N$$

$$nW_w = \frac{1}{2} m_w \frac{z_{\text{AERO}}}{m} = \frac{1}{2} m_w \bar{a}_{\text{WAC}}$$

$$nW_N = m_N \bar{a}_T$$

where m_w is the mass of two wing panels

m is the total aircraft mass

\bar{a}_{WAC} is the acceleration of the wing aerodynamic center

\bar{a}_T is the acceleration of the wing tip

and since the values of ϕ_1 through ϕ_5 are constant for any given station y on the wing we can write the final equation for wing bending in the form

$$h_1 = K_{W1} z_{\text{AERO}}^N + K_{W2} z_{\text{AERO}}^W - K_{W3} L_{\text{AERO}}^N - K_{W4} \bar{a}_T - K_{W5} \bar{a}_{\text{WAC}}$$

where $h_1 = -z$

$$K_{W1} = \frac{b^3 \phi_2}{8EI_0}$$

$$K_{W_2} = \frac{b^3 \phi_1}{4\pi EI_O}$$

$$K_{W_3} = \frac{b^3 \phi_5}{4EI_O}$$

$$K_{W_4} = \frac{m_N b^3 \phi_2}{8EI_O}$$

$$K_{W_5} = \frac{m_W b^3 \phi_4}{8EI_O}$$

This is the form given in the computer representation. The bending deflection at the aerodynamic center and at the wing tip are obtained using the values of $\phi_1 \rightarrow \phi_5$ appropriate to these stations.

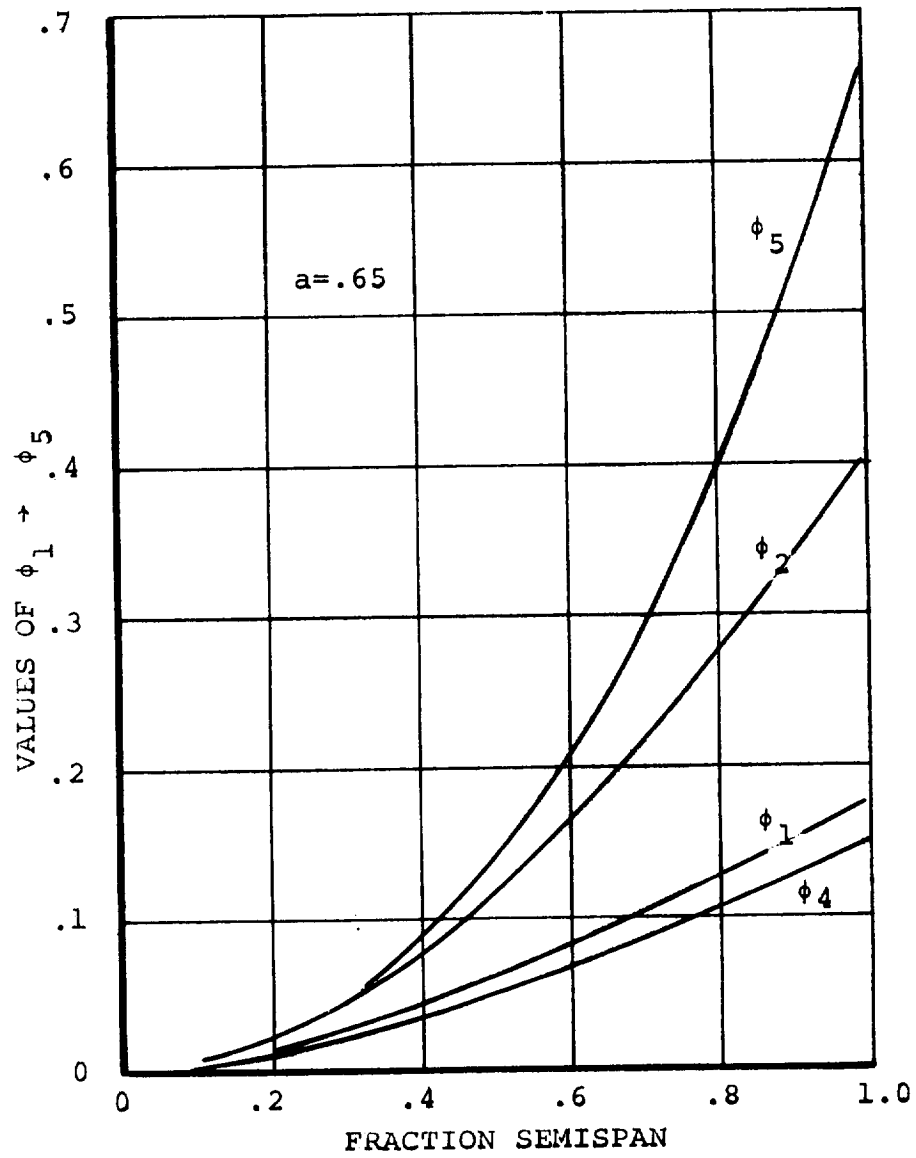


Figure A.2. Wing Bending Functions

APPENDIX B - DERIVATION OF LANDING GEAR EQUATIONS

Presented below are the equations for landing gear forces and moments arising from ground contact. The derivation accounts for brake and friction forces together with a simplified representation of the oleo dynamics. Nose wheel steering is not included.

With reference to Figure B-1 the distance from the center of gravity to the bottom of the right main wheel following a positive pitch rotation is

$$h_{\theta} = X \sin \theta - Z \cos \theta - r \quad (B-1)$$

where X and Z are the coordinates of the hub of the wheel relative to the C.G. and r is the tire radius. If the aircraft is now rolled right, through the angle ϕ , the bottom of the right gear moves through a distance

$$h_{\phi} = [Y \sin \phi + (Z+r)(\cos \phi - 1)] \cos \theta \quad (B-2)$$

The height of the bottom of the wheel above the ground is therefore

$$h = H_{CG} + h_{\theta} - h_{\phi} \quad (B-3)$$

and the oleo deflection during ground contact is given by

$$h_T = \frac{H_{CG} + h_{\theta} - h_{\phi}}{\cos \phi \cos \theta} \quad (B-4)$$

By differentiation of equation B-4 and making small angle assumptions regarding the aircraft pitch and roll angles during touchdown, the rate of change of oleo strut deflection is

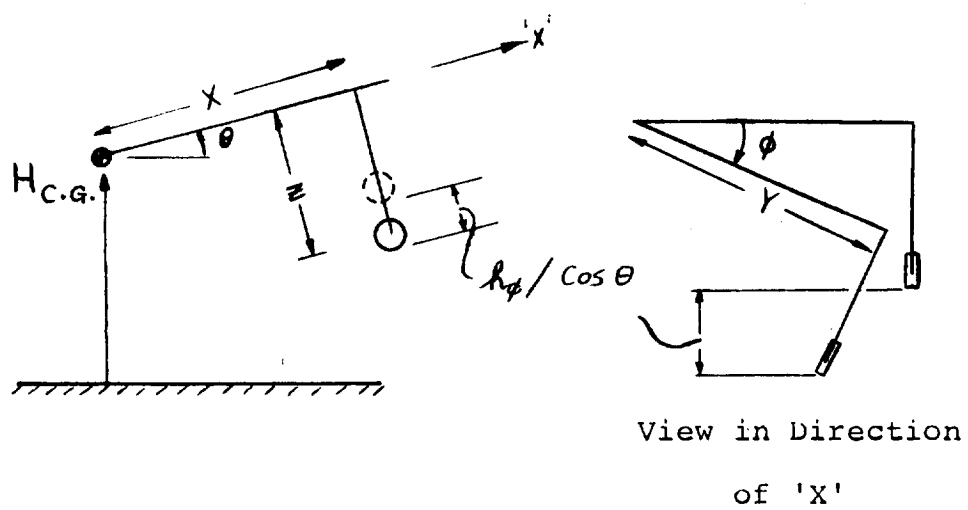


Figure B.1. Geometry of Landing Gear

obtained as

$$\dot{h}_T = \frac{\dot{H}_{CG}}{\cos \phi \cos \theta} + XQ - YP \quad (B-5)$$

Assuming that the oleo response is that of a second order system, the equation of motion for the landing gear is

$$F_G = K_{ST} h_T + D_{ST} \dot{h}_T \quad (B-6)$$

where K_{ST} and D_{ST} are the equivalent spring rates and damping for the oleo, and F_G is the force on the landing gear strut.

Tire Friction and Side Force

The friction force acting on each tire during ground contact is resolved into a force F_μ along the line of intersection of the plane of the wheel and the ground plane, positive forward, and a side force F_ν at right angles to F_μ lying in the ground plane and positive to starboard. The friction force F_s is assumed to be proportional to oleo force and the amount of braking exerted by the pilot. The side force is proportional to the oleo force.

The components of tire friction are:

$$F_\mu = (\mu_0 + \mu_1 B_G) F_{GZ} \frac{u}{|u|} \quad (B-7)$$

$$F_s = \mu_s F_{GZ} \frac{v}{|v|} \quad (B-8)$$

where μ_s , μ_1 and μ_0 are the coefficients for rolling friction, brake friction and sliding friction. B_G is expressed as a percentage of full brake pedal deflection. The signs of the forward and sideways velocity are introduced to properly orient the tire forces.

The force and moment contributions of each landing gear to the aircraft total forces and moments are, assuming small angles;

$$\Delta X_n = F_{\mu_n} - F_{GZ_n} \theta \quad (B-9)$$

$$\Delta Y_n = F_{s_n} + F_{GZ_n} \phi \quad (B-10)$$

$$\Delta Z_n = F_{\mu_n} \theta - F_{s_n} \phi + F_{GZ_n} \quad (B-11)$$

$$\Delta M_n = -\Delta Z_n X_n + \Delta X_n (Z_n + r_n + h_{T_n}) \quad (B-12)$$

$$\Delta L_n = \Delta Z_n Y_n - \Delta Y_n (Z_n + r_n + h_T) \quad (B-13)$$

$$\Delta N_n = -\Delta X_n Y_n + X_n \Delta Y_n \quad (B-14)$$

where $n=1,2$ and 3 denote the left main gear, right main gear and nose gear, respectively.

The total contribution of the landing gear forces to the forces and moments at the center of gravity of the aircraft are:

$$\Delta X_{LG} = \sum_{n=1}^3 \Delta X_n$$

$$\Delta Y_{LG} = \sum_{n=1}^3 \Delta Y_n$$

$$\Delta Z_{LG} = \sum_{n=1}^3 \Delta Z_n$$

$$\Delta L_{LG} = \sum_{n=1}^3 \Delta L_n$$

$$\Delta M_{LG} = \sum_{n=1}^3 \Delta M_n$$

$$\Delta N_{LG} = \sum_{n=1}^3 \Delta N_n$$

APPENDIX C - VELOCITY AND ACCELERATION TRANSFORMATIONS AND
CENTER OF GRAVITY/INERTIA EQUATIONS

C.1 Velocity Transformations

The calculation of aerodynamic forces on wings, fuselage, nacelles and tail surfaces requires that the angle of attack and relative wind velocity at these surfaces be known. These velocities are obtained most conveniently in terms of the velocity of the pivot reference point.

With reference to Figure C.1 , the velocity of a general point in the aircraft relative to the airplane center of gravity is

$$\underline{V} = \frac{\delta \underline{r}}{\delta t} + \underline{\Omega} \times \underline{r} \quad (C-1)$$

where \underline{r} is the radius vector from the c.g. to the point and $\underline{\Omega}$ is the angular velocity of the aircraft. Thus, expanding equation C-1, the velocity of the pivot relative to the c.g. is

$$\begin{aligned} u'_p &= \dot{X}_p + QZ_p - Y_p R \\ v'_p &= \dot{Y}_p - PZ_p + X_p R \\ w'_p &= \dot{Z}_p + PY_p - QX_p \end{aligned} \quad (C-2)$$

where X_p , Y_p and Z_p are the distances of the pivot from the c.g., measured positively forward, to the right and downwards, respectively. If we measure all distances from the pivot location then $X_p = -X_{CG}$, $Y_p = -Y_{CG} = 0$, $Z_p = -Z_{CG}$ and the velocity of the pivot relative to inertial space can be written,

$$\begin{aligned} u_p &= U + u'_p = U - \dot{X}_{CG} - QZ_{CG} \\ v_p &= V + v'_p = V + PZ_{CG} - X_{CG} R \\ w_p &= W + w'_p = W + QX_{CG} - \dot{Z}_{CG} \end{aligned} \quad (C-3)$$

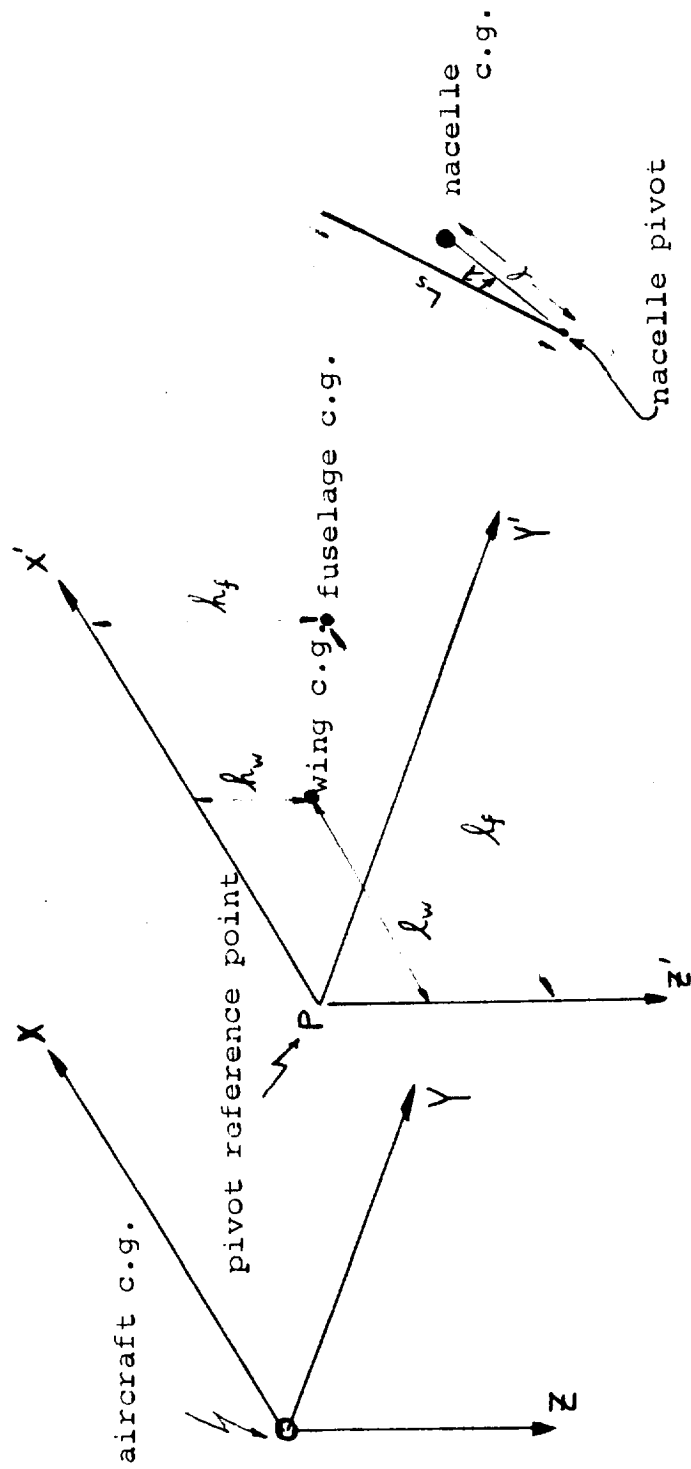


Figure C.1. Reference Axes Systems

where U, V and W are the components of the velocity of the airplane center of gravity.

The velocity of a point in the aircraft relative to the pivot is

$$\begin{aligned}u &= \dot{X} + QZ - YR \\v &= \dot{Y} + RX - PZ \\w &= \dot{Z} + PY - QX\end{aligned}\tag{C-4}$$

where X, Y, and Z are measured from the pivot to the point. By adding equations (C-3) and (C-4) the velocities of the following components are obtained relative to inertial space. The indicated distances are measured relative to the pivot.

Velocity of Horizontal Tail Aerodynamic Center

$$\begin{aligned}u_{HT} &= u_P + Z_{HT}Q \\v_{HT} &= v_P + X_{HT}R - Z_{HT}P \\w_{HT} &= w_P - X_{HT}Q\end{aligned}\tag{C-5}$$

Velocity of Vertical Tail Aerodynamic Center

$$\begin{aligned}u_{VT} &= u_P + Z_{VT}Q \\v_{VT} &= u_P + X_{VT}R - Z_{VT}P \\w_{VT} &= w_P + X_{VT}Q\end{aligned}\tag{C-6}$$

Velocity of Left Wing Aerodynamic Center - Body Axes

$$\begin{aligned}u'_{LW} &= u_P + Q (Z_{WAC} + h_{1LWAC}) + Y_{WAC}R \\v'_{LW} &= u_P + X_{WAC}R - P (Z_{WAC} + h_{1LWAC}) \\w'_{LW} &= w_P - Y_{WAC}P - X_{WAC}Q + \dot{h}_{1LWAC}\end{aligned}\tag{C-7}$$

where h_{1LWAC} is the elastic deflection of the left wing aerodynamic center. The equations for the right wing are obtained by substituting

$$Y_{RWAC} = -Y_{LWAC}$$

$$\text{and } h_{1RWAC} = h_{1LWAC}$$

Velocity of Left Wing Aerodynamic Center-Chord Axes

In order to compute wing angle-of-attack the velocity components are required relative to the wing chord line. If the wing chord makes an angle i_w with the body centerline then

$$\begin{aligned} u_{LW} &= u'_{LW} \cos i_w - w'_{LW} \sin i_w \\ v_{LW} &= v'_{LW} \\ w_{LW} &= w'_{LW} \cos i_w + u'_{LW} \sin i_w \end{aligned} \tag{C-8}$$

The equations for the right wing are obtained by changing the subscript.

Velocity of Left Rotor Hub - Body Axes

$$\begin{aligned} u'_{RL} &= u_P + RY_N - L_S (\dot{i}_{NL} + Q) \sin i_{NL} + Qh_{1L} \\ v'_{RL} &= v_P + L_S (R \cos i_{NL} + P \sin i_{NL}) - Ph_{1L} \\ w'_{RL} &= w_P - PY_N - L_S (\dot{i}_{NL} + Q) \cos i_{NL} + \dot{h}_{1L} \end{aligned} \tag{C-9}$$

where L_S is the distance from the rotor pivot point to the rotor hub and h_{1L} is the deflection of the wing tip. The equations for the right hub are obtained by changing subscripts and substituting $Y_N = -Y_N$.

Velocity of Left Rotor Hub - Shaft Axes

Since the rotor aerodynamic forces and moments are functions of the shaft angle of attack and sideslip, the velocity components are required relative to shaft axes.

$$\begin{aligned}u_{RL} &= u'_{RL} \cos i_{NL} - w'_{RL} \sin i_{NL} \\v_{RL} &= v'_{RL} \\w_{RL} &= w'_{RL} \sin i_{NL} + u'_{RL} \cos i_{NL}\end{aligned}\tag{C-10}$$

The corresponding equations for the right hub are obtained by changing the subscript.

C.2 Center of Gravity and Inertia Equations

Equations are required that express the overall aircraft center of gravity position and inertias in terms of the centers of gravity and inertias of the individual mass components. In order to do this a fixed reference point is chosen in the aircraft defined by the intersection of the line joining the nacelle pivots and the vertical plane of symmetry of the aircraft, see Figure C.1. A set of axes $PXPYPZP$ is taken at this pivot reference point, parallel to the axes $OXYZ$ at the aircraft center of gravity. If the location of the aircraft center of gravity with respect to the pivot reference axes is $(x'_{CG}, y'_{CG}, z'_{CG})$ and if (l_f, h_f) and (l_w, h_w) are the x and z coordinates of the fuselage and wing masses measured from the pivot, then the following relationships are obtained between the centers of mass of the components and the aircraft center of gravity.

Fuselage CG Relative to Aircraft CG

$$x_f = \ell_f - x'_{CG} \quad (C-11)$$

$$x_f = h_f - z_{CG}$$

Wing CG Relative to Aircraft CG

$$x_w = \ell_w - x'_{CG} \quad (C-12)$$

$$z_w = h_w - z'_{CG}$$

Nacelle CG Relative to Aircraft CG

$$x_{NR} = \ell \cos (i_{NR} - \lambda) - x'_{CG}$$

$$x_{NL} = \ell \cos (i_{NL} - \lambda) - x'_{CG} \quad (C-13)$$

$$z_{NR} = \ell \sin (i_{NR} - \lambda) - z'_{CG}$$

$$z_{NL} = \ell \sin (i_{NL} - \lambda) - z'_{CG}$$

where ℓ is the distance from the nacelle pivot point to the nacelle c.g., and λ is the angular depression of the nacelle center of mass below the nacelle pivot, when the nacelle is in the down position, see Figure C.1.

Aircraft Center of Gravity Position

By taking moments about the pivot, the aircraft center of gravity is given by

$$\dot{x}_{CG} = \frac{m_f \ell_f + m_w \ell_w}{m} + \ell \left(\frac{m_N}{m} \right) \left[\cos(i_{NL}-\lambda) + \cos(i_{NR}-\lambda) \right] \quad (C-14)$$

$$\dot{z}_{CG} = \frac{m_f h_f + m_w h_w}{m} - \ell \left(\frac{m_N}{m} \right) \left[\sin(i_{NL}-\lambda) + \sin(i_{NR}-\lambda) \right]$$

The equations of motion (Section 5) require the first and second time derivatives of the center of gravity position. They are as follows:

Center of Gravity Velocity Relative to Pivot Point

$$\dot{x}_{CG} = -\ell \left(\frac{m_N}{m} \right) \left[i_{NR} \sin(i_{NR}-\lambda) + i_{NL} \sin(i_{NL}-\lambda) \right] \quad (C-15)$$

$$\dot{z}_{CG} = -\ell \left(\frac{m_N}{m} \right) \left[i_{NR} \cos(i_{NR}-\lambda) + i_{NL} \cos(i_{NL}-\lambda) \right]$$

Center of Gravity Acceleration Relative to Pivot Point

$$\ddot{x}_{CG} = -\ell \left(\frac{m_N}{m} \right) \left[\ddot{i}_{NR} \sin(i_{NR}-\lambda) + \ddot{i}_{NL} \sin(i_{NL}-\lambda) + \dot{i}_{NL}^2 \cos(i_{NL}-\lambda) + \dot{i}_{NR}^2 \cos(i_{NR}-\lambda) \right] \quad (C-16)$$

$$\ddot{z}_{CG} = -\ell \left(\frac{m_N}{m} \right) \left[\ddot{i}_{NR} \cos(i_{NR}-\lambda) + \ddot{i}_{NL} \cos(i_{NL}-\lambda) - \dot{i}_{NL}^2 \sin(i_{NL}-\lambda) - \dot{i}_{NR}^2 \sin(i_{NR}-\lambda) \right]$$

Pilot Station Velocities - Body Axes

The velocities at the pilot's station are required in order to drive the visual display. From equations (C-3) and (C-4) the components of velocity of the pilot's station in body axes are:

$$u_{PA} = u_P + QZ_{PA} - RY_{PA}$$

$$v_{PA} = v_P + R\ell_{PA} - PZ_{PA}$$

$$w_{PA} = w_P + PY_{PA} - Q\ell_{PA}$$

C-3 Pilot Station Acceleration - Body Axes

The pilot station acceleration is also required to drive the visual display. These accelerations are derived here.

The velocity at the pilot's station is

$$\underline{V}_{PA} = \underline{V}_{CG} + \underline{\Omega} \times \underline{r}_{PA} + \frac{\delta \underline{r}_{PA}}{\delta t}$$

where \underline{r}_{PA} is the vector from the aircraft CG to the pilot's station and $\frac{\delta \underline{r}_{PA}}{\delta t}$ is the rate of change of the pilot's station with respect to the aircraft CG.

The pilot's station acceleration is

$$\begin{aligned} \underline{a}_{PA} &= \frac{d\underline{V}_{PA}}{dt} = \frac{d\underline{V}_{CG}}{dt} + \frac{d}{dt} (\underline{\Omega} \times \underline{r}_{PA}) + \frac{d}{dt} \left(\frac{\delta \underline{r}_{PA}}{\delta t} \right) \\ &= \underline{a}_{CG} + \frac{\delta}{\delta t} (\underline{\Omega} \times \underline{r}_{PA}) + \underline{\Omega} \times (\underline{\Omega} \times \underline{r}_{PA}) + \frac{\delta^2 \underline{r}_{PA}}{\delta t^2} + \underline{\Omega} \times \frac{\delta \underline{r}_{PA}}{\delta t} \\ &= \underline{a}_{CG} + \frac{\delta \underline{\Omega}}{\delta t} \times \underline{r}_{PA} + 2\underline{\Omega} \times \frac{\delta \underline{r}_{PA}}{\delta t} + \underline{\Omega} (\underline{r}_{PA} \cdot \underline{\Omega}) - \Omega^2 \underline{r}_{PA} + \frac{\delta^2 \underline{r}_{PA}}{\delta t^2} \end{aligned}$$

$$\text{with } \underline{\Omega} = P\hat{i} + Q\hat{j} + R\hat{k}$$

$$\frac{\delta \underline{\Omega}}{\delta t} = \dot{P}\hat{i} + \dot{Q}\hat{j} + \dot{R}\hat{k}$$

$$\underline{r}_{PA} = (x_{PA} - x_{CG})\hat{i} + (y_{PA} - y_{CG})\hat{j} + (z_{PA} - z_{CG})\hat{k}$$

$$\frac{\delta \underline{r}_{PA}}{\delta t} = (\dot{x}_{PA} - \dot{x}_{CG})\hat{i} + (\dot{y}_{PA} - \dot{y}_{CG})\hat{j} + (\dot{z}_{PA} - \dot{z}_{CG})\hat{k}$$

and noting that Y_{CG} and the time derivatives of X_{PA} , Y_{PA} , Z_{PA} are always zero, the above equation yields the pilot's station accelerations as: -

$$a_{x_{PA}} = \frac{X_{AERO}}{m} + (\dot{Q} + PR)(Z_{PA} - Z_{CG}) + (Q^2 + R^2)(X_{CG} - l_{PA}) \\ + Y_{PA}(PQ - \dot{R}) - 2Q\dot{Z}_{CG} - \ddot{X}_{CG}$$

$$a_{y_{PA}} = \frac{Y_{AERO}}{m} + (\dot{P} - QR)(Z_{CG} - Z_{PA}) + (\dot{R} + PQ)(l_{PA} - X_{CG}) \\ - Y_{PA}(R^2 + P^2) + 2(P\dot{Z}_{CG} - R\dot{X}_{CG})$$

$$a_{z_{PA}} = \frac{Z_{AERO}}{m} + (\dot{Q} - PR)(X_{CG} - l_{PA}) + (P^2 + Q^2)(Z_{CG} - Z_{PA}) \\ + Y_{PA}(\dot{P} + QR) + 2Q\dot{X}_{CG} - \ddot{Z}_{CG}$$

where $a_{x_{CG}} = \frac{Z_{AERO}}{m}$ etc.

$X_{PA} = l_{PA}$, the distance from the pivot to the pilot's station

C.4 Aircraft Inertias

The aircraft roll inertia about the aircraft center of gravity is, from the parallel axis theorem,

$$I_{xx} = I_{xx}^f + I_{xx}^w + I_{xx}^{NL} + I_{xx}^{NR} + m_f Z_f^2 + m_w Z_w^2 + 2m_N Y_N^2 + m_N Z_{NL}^2 + m_N Z_{NR}^2 \quad (C-17)$$

where I_{xx}^f , etc., are the inertias of the various components about their individual centers of gravity.

In the case of the nacelles the inertias I_{xx}^{NL} , I_{xx}^{NR} are dependent on the nacelle tilt angle, i_N . These inertias are related to the inertias of the nacelle with respect to a set of nacelle-fixed axes $O''xyz$ placed as shown in Figure 5.1. The relationships are

$$I_{xx}^N = I_{xxO}^N + (I_{zzO}^N - I_{xxO}^N) \sin^2 i_N - I_{xzO} \sin 2i_N$$

$$I_{yy}^N = I_{yyO}^N \quad (C-18)$$

$$I_{zz}^N = I_{zzO}^N + (I_{xxO}^N - I_{zzO}^N) \sin^2 i_N + I_{xzO} \sin 2i_N$$

$$I_{xz}^N = I_{xzO}^N \cos 2i_N + \frac{1}{2} (I_{xxO}^N - I_{zzO}^N) \sin 2i_N$$

Using equations (C-18) together with (C-13), (C-11) and (C-12), in equation (C-17), the roll inertia becomes

$$\begin{aligned} I_{xx} = & I_{xx}^f + I_{xx}^w + 2I_{xxO}^N + (I_{zzO}^N - I_{xxO}^N) (\sin^2 i_{NL} + \sin^2 i_{NR}) \\ & - I_{xzO}^N (\sin 2i_{NL} + \sin 2i_{NR}) + 2 m_N Y_N^2 + m_f h_f z_f \\ & + m_w h_w z_w - m_f z_f z'_{CG} - m_w z_w z'_{CG} \\ & - m_N z_{NL} z'_{CG} - m_N z_{NR} z'_{CG} \\ & - 2m_N \left[z_{NR} \sin(i_{NR} - \lambda) + z_{NL} \sin(i_{NL} - \lambda) \right] \end{aligned}$$

$$\begin{aligned}
&= I_{xx}^f + I_{xx}^w + 2I_{xx_0}^N + (I_{zz_0}^N - I_{xx_0}^N) (\sin^2 i_{NL} + \sin^2 i_{NR}) \\
&\quad - I_{xz_0}^N (\sin 2i_{NL} + \sin 2i_{NR}) + 2m_N Y_N^2 + m_f h_f Z_f \\
&\quad + m_w h_w Z_w - \ell m_N \left[Z_{NR} \sin (i_{NR} - \lambda) + Z_{NL} \sin (i_{NL} - \lambda) \right]
\end{aligned}$$

since the terms containing Z_{CG} sum to zero.

Similarly

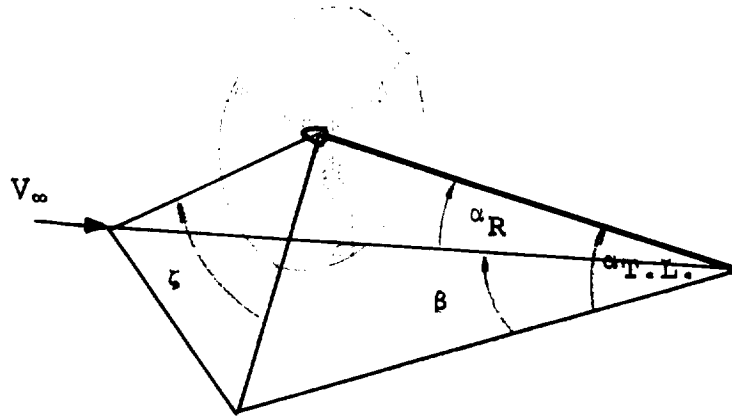
$$\begin{aligned}
I_{xz} &= I_{xz}^f + I_{xz}^w + I_{xz}^N (\cos 2i_{NL} + \cos 2i_{NR}) \\
&\quad + \frac{1}{2} (I_{xx_0}^N - I_{zz_0}^N) (\sin 2i_{NL} + \sin 2i_{NR}) + m_f \ell_f Z_f \\
&\quad + m_w Z_w \ell_w + \ell m_N \left[Z_{NR} \cos (i_{NR} - \lambda) + Z_{NL} \cos (i_{NL} - \lambda) \right]
\end{aligned}$$

$$\begin{aligned}
(I_{zz} - I_{yy}) &= I_{zz}^f - I_{yy}^f + I_{zz}^w - I_{yy}^w + 2(I_{zz_0}^N - I_{yy_0}^N) \\
&\quad + (I_{xx_0}^N - I_{zz_0}^N) (\sin^2 i_{NL} + \sin^2 i_{NR}) + I_{xz_0}^N (\sin 2i_{NL} + \sin 2i_{NR}) \\
&\quad - (m_f h_f Z_f + m_w h_w Z_w) + m_N \ell \left[Z_{NL} \sin (i_{NL} - \lambda) \right. \\
&\quad \left. + Z_{NR} \sin (i_{NR} - \lambda) \right] + 2m_N Y_N^2
\end{aligned}$$

Similar expressions are obtained for I_{yy} and I_{zz} and these are presented in Appendix E.

APPENDIX D - CALCULATION OF SLIPSTREAM-IMMERSED WING AREAS

The wing areas washed by the rotor slipstreams are required in the calculation of wing lift and drag. These immersed areas depend on rotor shaft inclination, wing angle of attack and sideslip, and rotor thrust. The equations presented in Appendix E for the immersed areas S_{iL} and S_{iR} were obtained as follows.



The above sketch shows a rotor under conditions of combined angle of attack ($\alpha_{T.L.}$) and sideslip (β). The resultant angle of attack of the shaft is given by

$$\alpha_R = \cos^{-1} (\cos \alpha_{T.L.} \cos \beta) \quad (D-1)$$

If the rotor shaft is inclined to the fuselage centerline at angle i_N and the fuselage is at angle of attack α_f then

$$\alpha_{T.L.} = \alpha_f + i_N \quad (D-2)$$

The rotor "sideslip" angle, ζ , is defined by

$$\zeta = \tan^{-1} \left[\frac{\tan \beta}{\sin \alpha_{T.L.}} \right] \quad (D-3)$$

and is the angle shown in the sketch.

Figure D.1 presents four views of the geometry of rotor slipstream/wing planform interaction.

Figure D.1[a] is a view of the plane taken through the rotor shaft parallel to the aircraft vertical plane of symmetry. The line PT is the wing chord, the distances PC and h_p are the horizontal and vertical coordinates of the pivot measured from the wing leading edge, and l is the spinner-to-pivot shaft length.

Figure D.1[b] is a view taken normal to the rotor disc plane. In this view, the traces of the slipstream on planes taken through the wing leading and trailing edges parallel to the disc plane appear as circles. This assumes that the slipstream is a sheared circular cylinder.

Figure D.1[c] is a section taken in the plane containing the rotor shaft and the freestream velocity vector V_∞ . The angle ϵ is the deflection of the slipstream relative to the freestream direction. Planes are taken through the wing leading and trailing edges parallel to the rotor disc. These intersect the rotor shaftline at the points O and T, and intersect the slipstream centerline at the points O' and O". These points enable the slipstream traces shown in (b) to be constructed.

Figure (D.1[d]) is a view taken perpendicular to the wing surface showing the areas washed by the slipstream. For convenience this view combines the immersed areas of both left and right wings. In general, the imprint of the slipstream on the wing will be bounded in the chordwise direction by curved lines; however, the approximation is made that these lines are straight.

The immersed area of the right wing panel is (assuming that the tip is immersed),

$$\begin{aligned} S_{i_R} &= \frac{1}{2}(PM + TN)c \\ &= \frac{1}{2}(PR + RM + TS + SN)c \end{aligned} \quad (D-4)$$

$$\text{From Figure D.1[b]} \quad PR = OO' \sin \zeta \quad (D-5)$$

$$\text{From Figure D.1[c]} \quad OO' = (\ell - OD) \tan (\alpha_R - \epsilon) \quad (D-6)$$

$$\text{From Figure D.1[a]} \quad OD = PC \cos (i_N - i_W) - h_p \sin (i_N - i_W) \quad (D-7)$$

$$\text{From Figure D.1[b]} \quad RM = R'M' = \sqrt{\frac{D_S^2}{4} - O'R'^2} \quad (D-8)$$

$$\text{From Figure D.1[b]} \quad O'R' = OO' \cos \zeta + OP \quad (D-9)$$

$$\text{From Figure D.1[a]} \quad OP = PC \sin (i_N - i_W) + h_p \cos (i_N - i_W) \quad (D-10)$$

These equations define the leading edge intersection PM. If RM is zero or negative, the slipstream does not intersect the leading edge and the wing is considered to be unaffected by the slipstream.

For the trailing edge intersection, TN:

$$TS = OO'' \sin \zeta \quad (D-11)$$

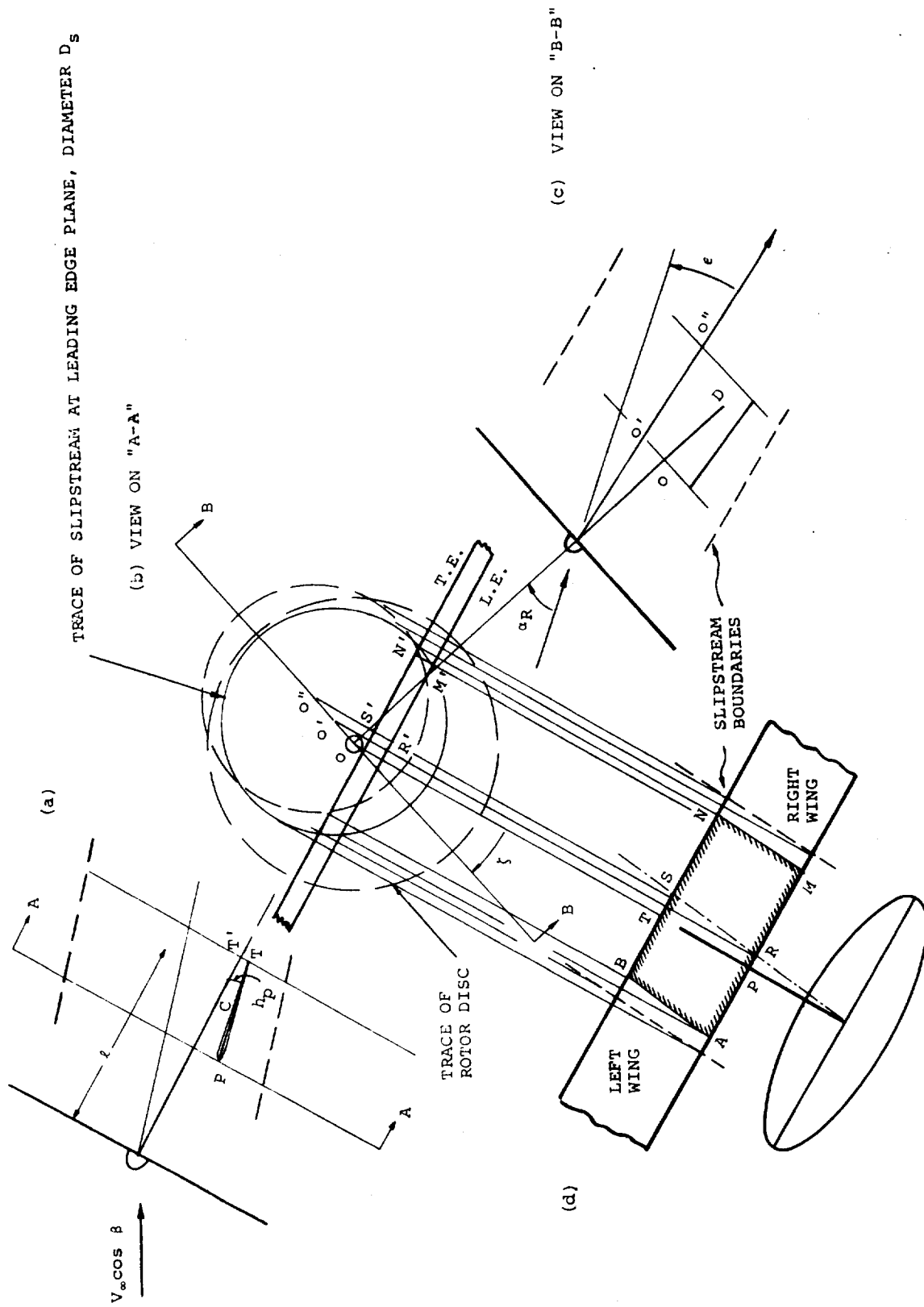


Figure D.1. Geometry of Rotor Slipstream/Wing Platform Interaction

$$OO'' = (\ell + c \cos (i_N - i_W) - OD) \tan (\alpha_R - \epsilon) \quad (D-12)$$

$$SN = S'N' = \frac{D_S^2}{4} - O''S'^2 \quad (D-13)$$

$$O''S' = OO'' \cos \zeta + TT' \quad (D-14)$$

$$TT' = OP - c \sin (i_N - i_W) \quad (D-15)$$

If we write

$$\xi_1 = PR, \xi_2 = RM, \xi_3 = TS, \text{ and } \xi_4 = SN$$

then, using the above equations,

$$\xi_1 = [\ell - PC \cos (i_N - i_W) + h_p \sin (i_N - i_W)] \tan (\alpha_R - \epsilon) \sin \zeta \quad (D-16)$$

and

$$\xi_2 = \sqrt{\frac{D_S^2}{4} - \{[\ell - PC \cos (i_N - i_W) + h_p \sin (i_N - i_W)] \tan (\alpha_R - \epsilon) \cos \zeta + PC \sin (i_N - i_W) + h_p \cos (i_N - i_W)\}^2} \quad (D-17)$$

The corresponding equations for ξ_3 and ξ_4 are obtained by replacing PC in (D-16) and (D-17) with (PC-c)

Thus the immersed area of the right wing panel is given

$$\text{by } S_{i_R} = \frac{1}{2} c (\xi_1 + \xi_2 + \xi_3 + \xi_4) \quad (D-18)$$

From the symmetry of Figure D.1(d), $SN=BS$ and $RM=AR$. The total immersed area of both wing panels is

$$S_{i_T} = \frac{1}{2} c (AM + BN) = \frac{1}{2} c (2\xi_2 + 2\xi_4) = c(\xi_2 + \xi_4) \quad (D-19)$$

and therefore the immersed area of the left wing is obtained from

$$S_{i_L} = S_{i_T} - S_{i_R} \quad (D-20)$$

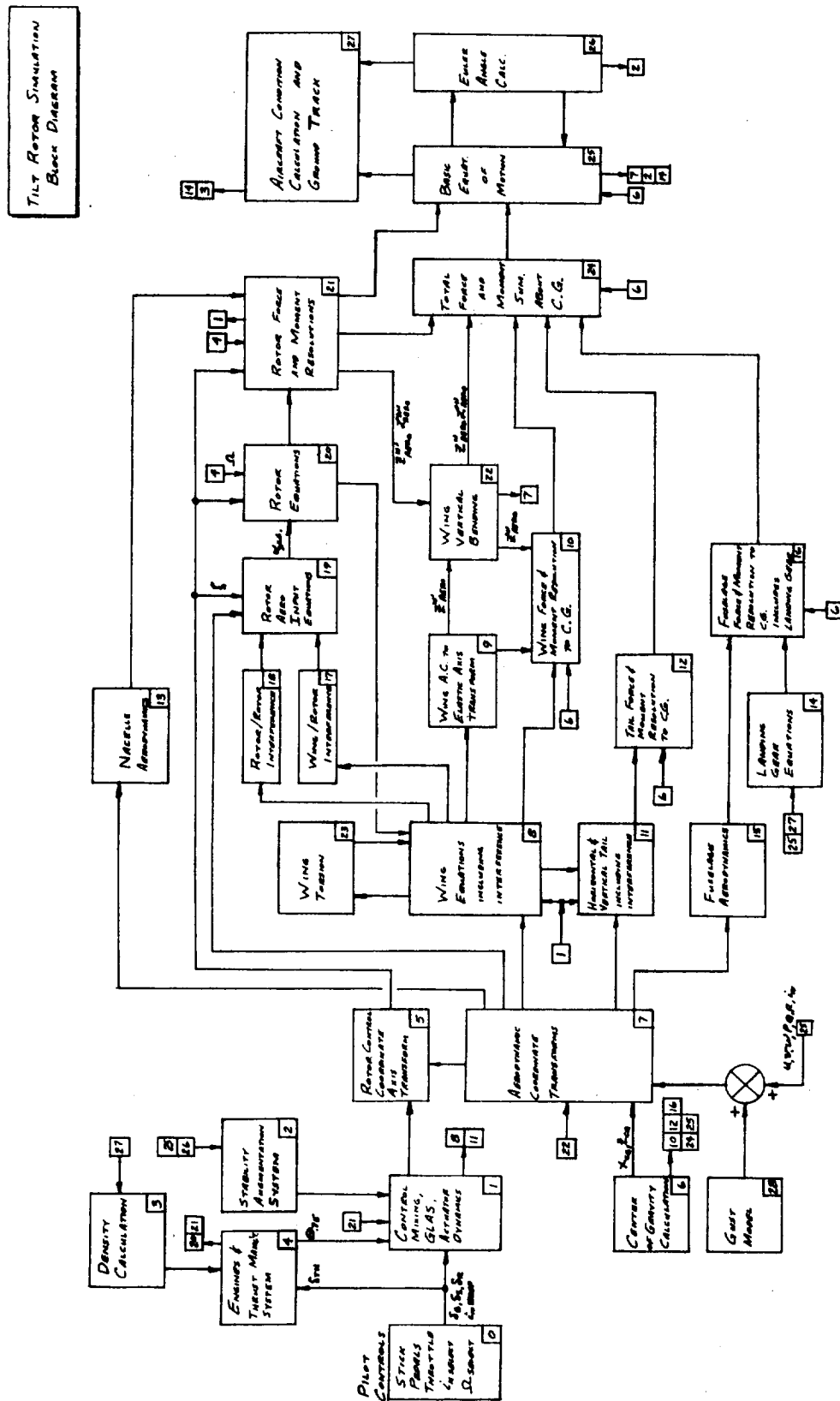
The above equations correspond to those presented in Appendix E for calculating immersed wing area.

APPENDIX E COMPUTER REPRESENTATION

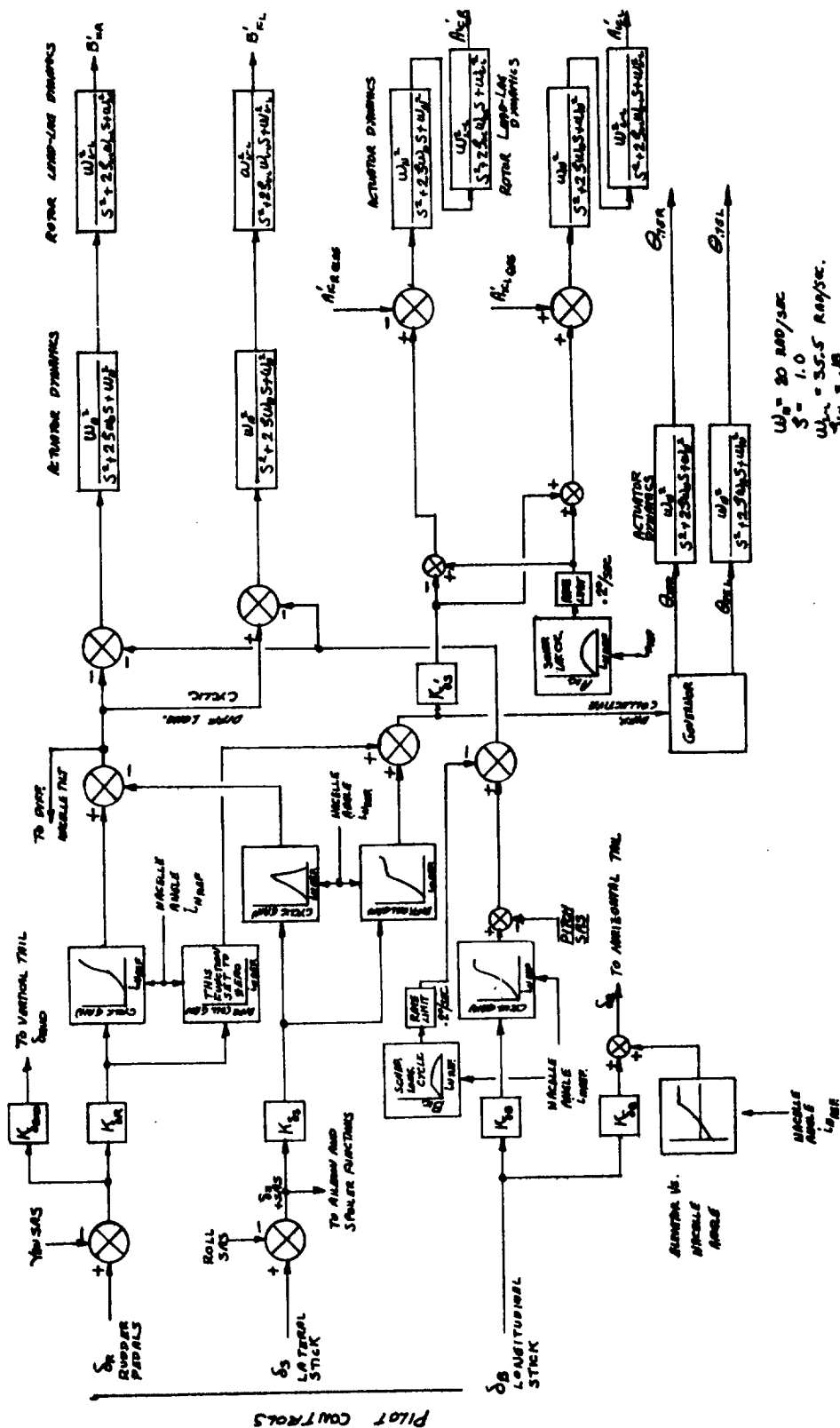
The equations derived in previous sections of this report have been collected and written in a format to facilitate computer programming. The complete set of equations which define the Model 222 simulation mathematical model are contained in this section. The computer block diagram for the simulation is also included. Each element of this block diagram contains an index number. Figure E.1 lists the index number, the name of the element, and its page number in this appendix. In addition the input and output, where appropriate, to each element are identified by their index numbers.

INDEX NUMBER	BLOCK DIAGRAM ELEMENT NAMES	PAGE NUMBER
1.	Control Mixing, Load Alleviation System and Actuator Dynamics	E-4
2.	Stability Augmentation System	E-7
3.	Density Calculation	E-9
4.	Engines and Thrust Management System	E-10
5.	Rotor Control Coordinate Axis Transforms	E-14
6.	Center of Gravity Calculation	E-15
7.	Aerodynamic Coordinate Transforms	E-16
8.	Wing Equations (Including Interference)	E-19
9.	Wing A.C. to Elastic Axis Transform	E-33
10.	Wing Force and Moment Resolution to Center of Gravity	E-34
11.	Horizontal and Vertical Tail Aerodynamics (Including Interference)	E-35
12.	Tail Force and Moment Resolution to Center of Gravity	E-43
13.	Nacelle Aerodynamics	E-44
14.	Landing Gear Equations	E-46
15.	Fuselage Aerodynamics	E-49
16.	Fuselage Force and Moment Resolution to Center of Gravity (Includes Landing Gear)	E-50
17.	Wing/Rotor Interference	E-51
18.	Rotor/Rotor Interference	E-52
19.	Rotor Aero Input Equations	E-53
20.	Rotor Equations	E-54
21.	Rotor Force and Moment Resolution	E-61
22.	Wing Vertical Bending	E-64
23.	Wing Torsion	E-66
24.	Total Force and Moment Summation About Center of Gravity	E-67
25.	Basic Equations of Motion	E-68
26.	Euler Angle Calculation	E-77
27.	Aircraft Condition Calculation and Ground Track	E-78
28.	Gust Model	E-80
29.	Preliminary Calculation (Preprocess)	E-81
30.	Trim Loops	E-87

Figure E.1. Block Diagram Element Index Numbers

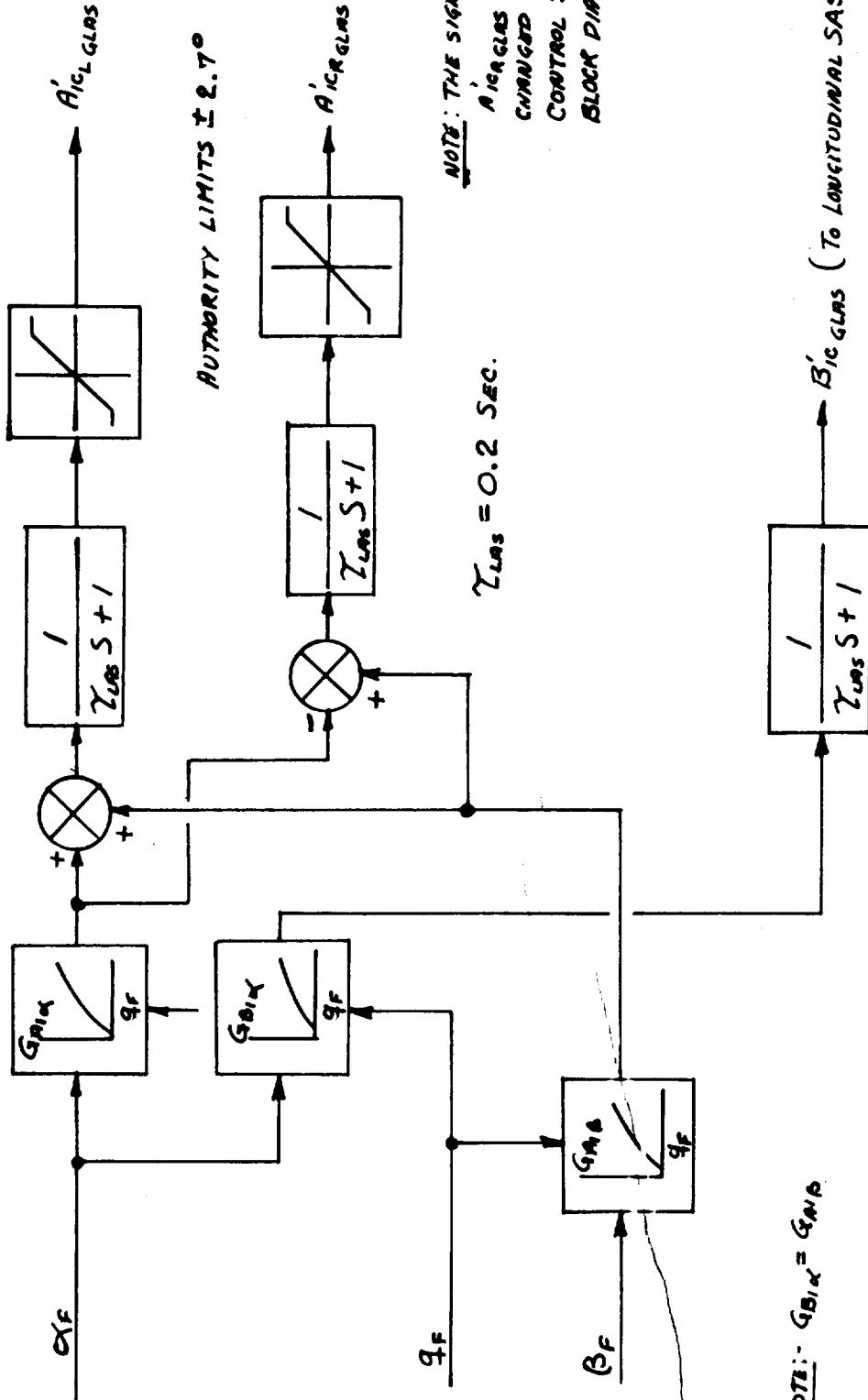


PRELIMINARY CONTROL SYSTEM BLOCK DIAGRAM



MODEL 222 LOAD ALLEVIATION SYSTEM (LAS)

(FOR PIVOT MOMENTS - SINGLE COMMON LONG. ACTUATOR)



NOTE:- $G_{B1 \alpha} = G_{M1 \beta}$

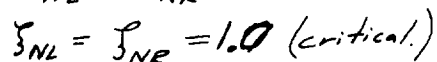
Governing Equations

$$A'_{ic LAS} = G_{M1 \alpha} \alpha + G_{M1 \beta} \beta$$

$$A'_{ic LAS} = G_{M1 \alpha} \alpha - G_{M1 \beta} \beta$$

$$B'_{ic LAS} = G_{M1 \alpha} \alpha$$

NACELLE, FLAP, FLAPERON, & SPOILER CONTROLS



LATERAL-DIRECTIONAL SAS

$$G_{\psi\delta_r} = \frac{G_{\psi}(M_G)_{\delta_r}}{G_r} = 1.183\%$$

$$G_{\psi\delta_r} = .5''/\text{deg}$$

$$G_{\psi} = 7.5''/\text{deg}$$

$$T_{\psi\delta_r} = 1.0 \text{ SEC}$$

$$T_{\psi} = 10 \text{ SEC}$$

$$G_{\psi} = 10''/\text{deg}$$

$$G_{\psi} = 0$$

$$T_{\psi} = 2 \text{ SEC}$$

$$G_{\psi r} = 3.64''/\text{deg}$$

$$G_{\psi r} = 0.5$$

$$G_{\psi r} = .5''/\text{deg}$$

$$G_{\psi} = 5''/\text{deg}/\text{SEC}$$

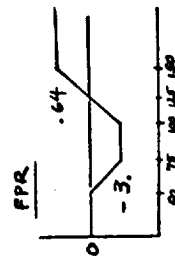
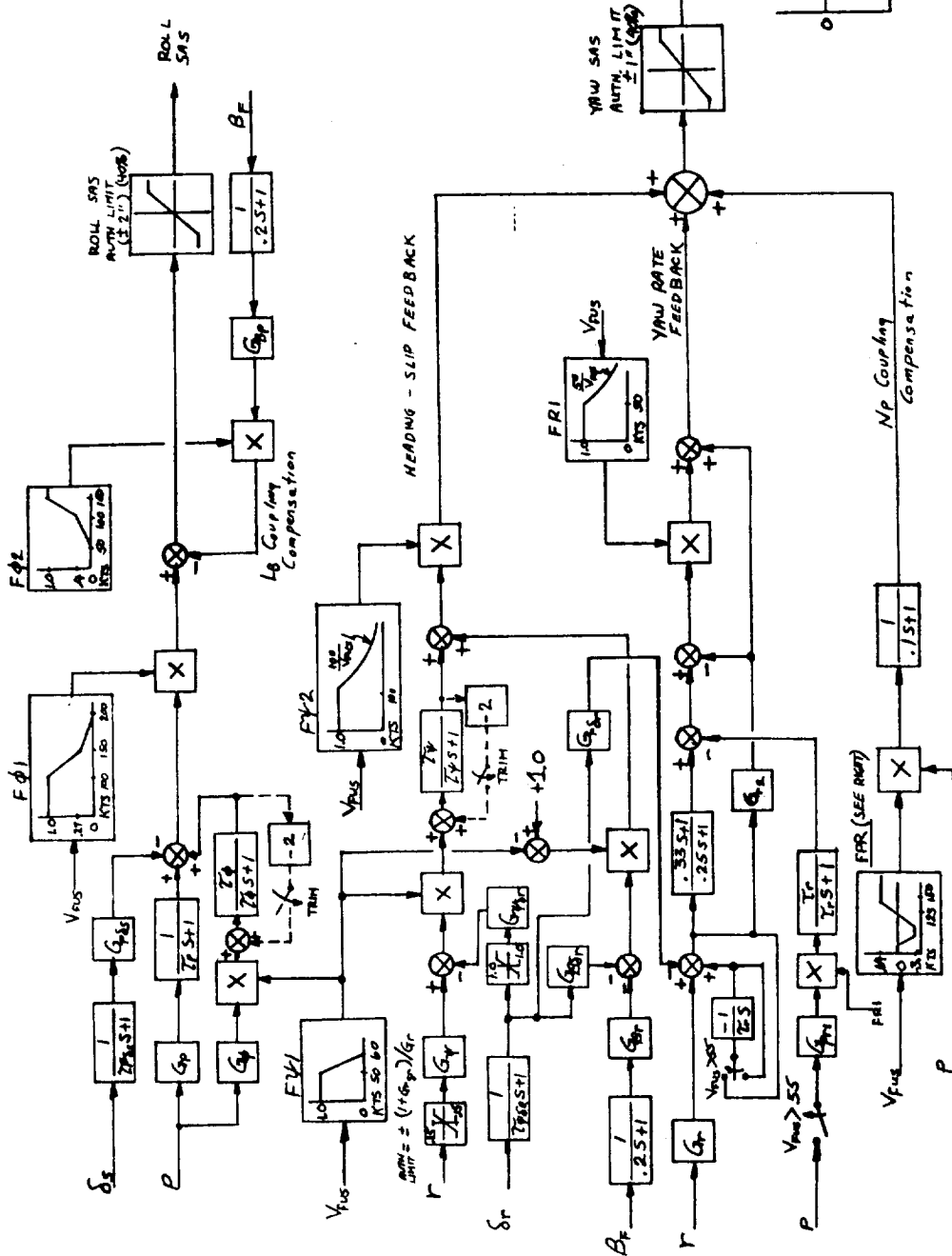
$$G_{\psi} = 5''/\text{deg}/\text{SEC}$$

$$T_{\psi\delta_r} = .1 \text{ SEC}$$

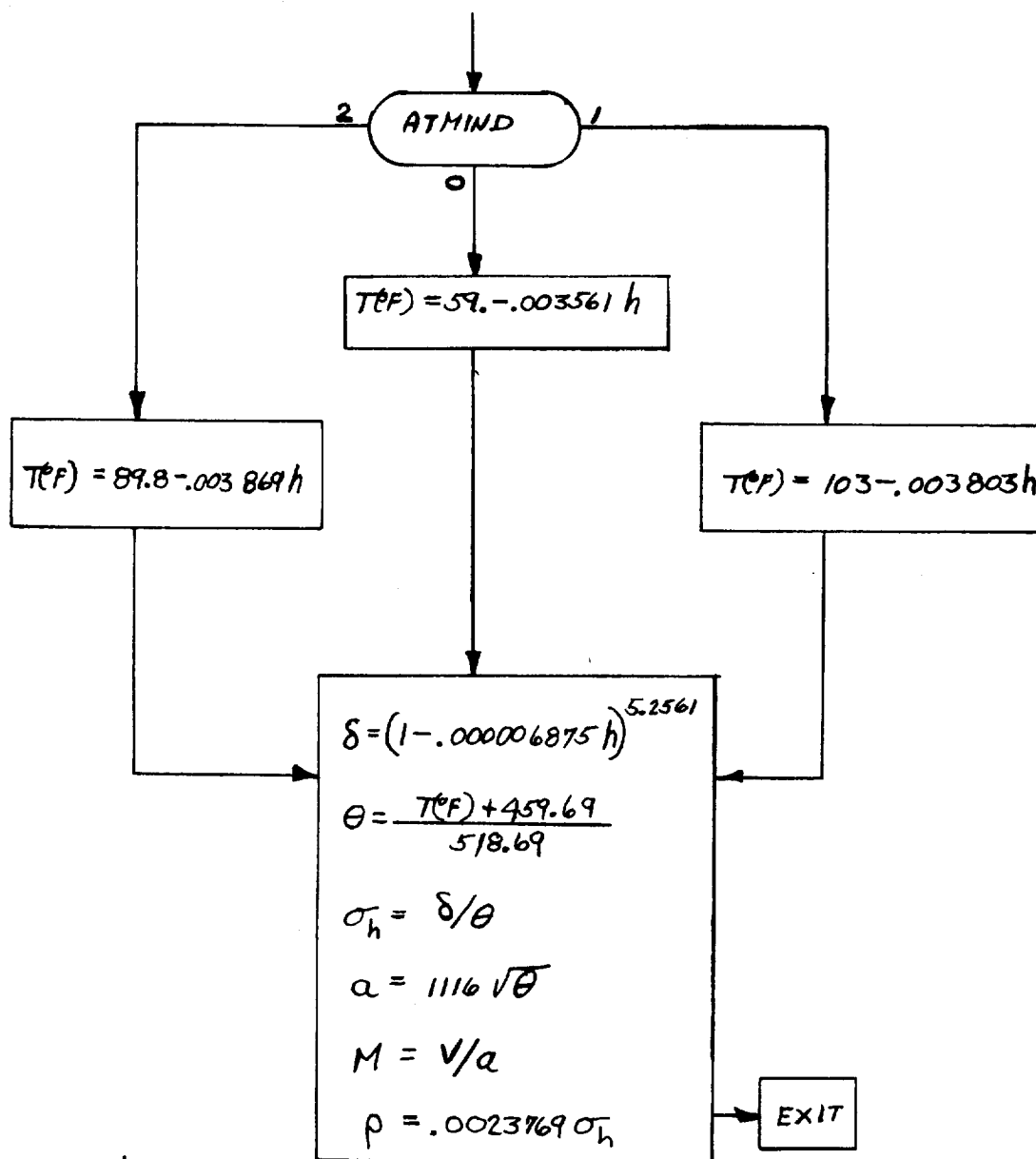
$$T_{\psi} = .1 \text{ SEC}$$

$$T_{\psi} = 5 \text{ SEC}$$

$$G_{\psi r} = 10''/\text{deg}$$



DENSITY CALCULATIONS



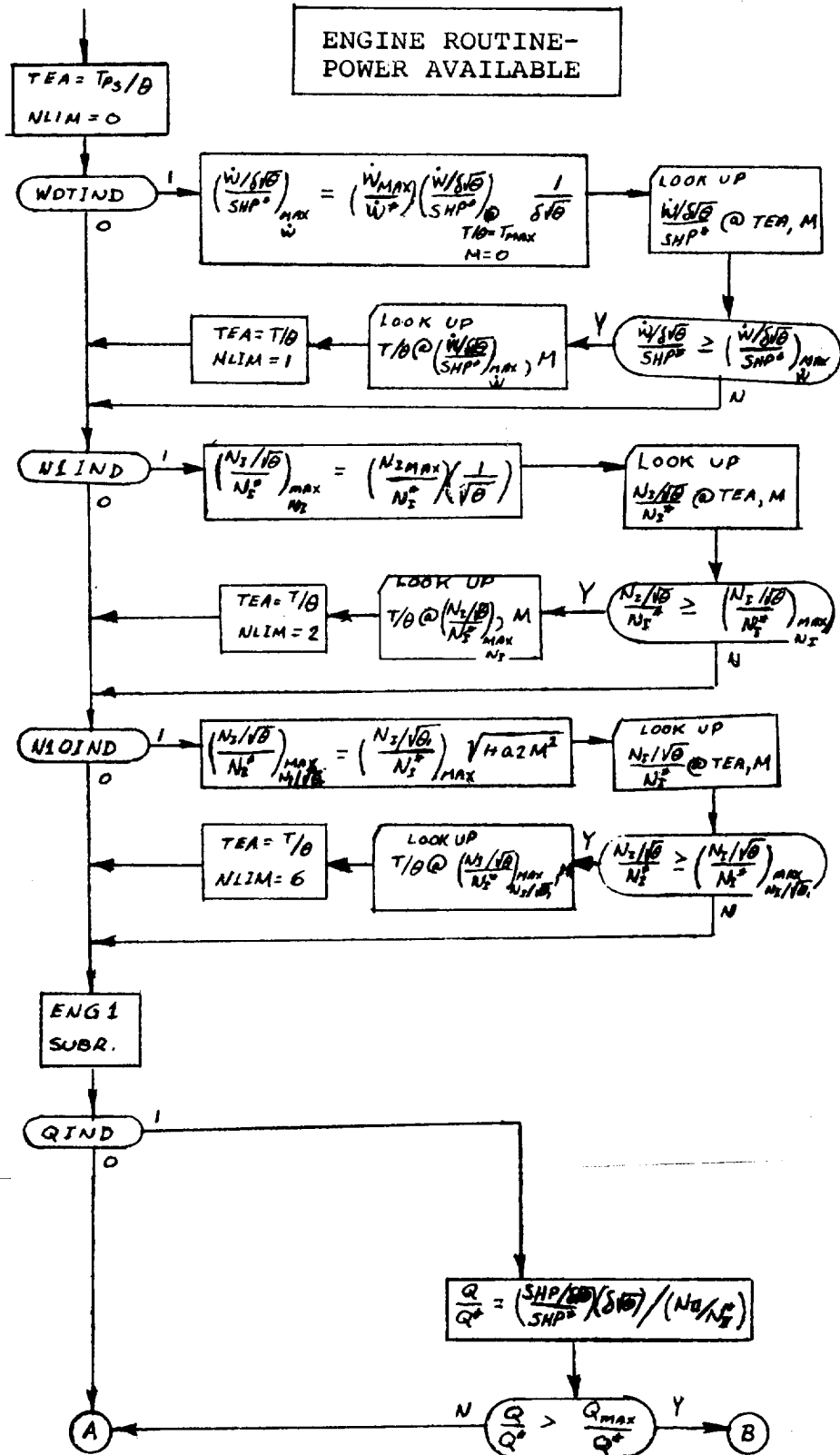
INPUT: h

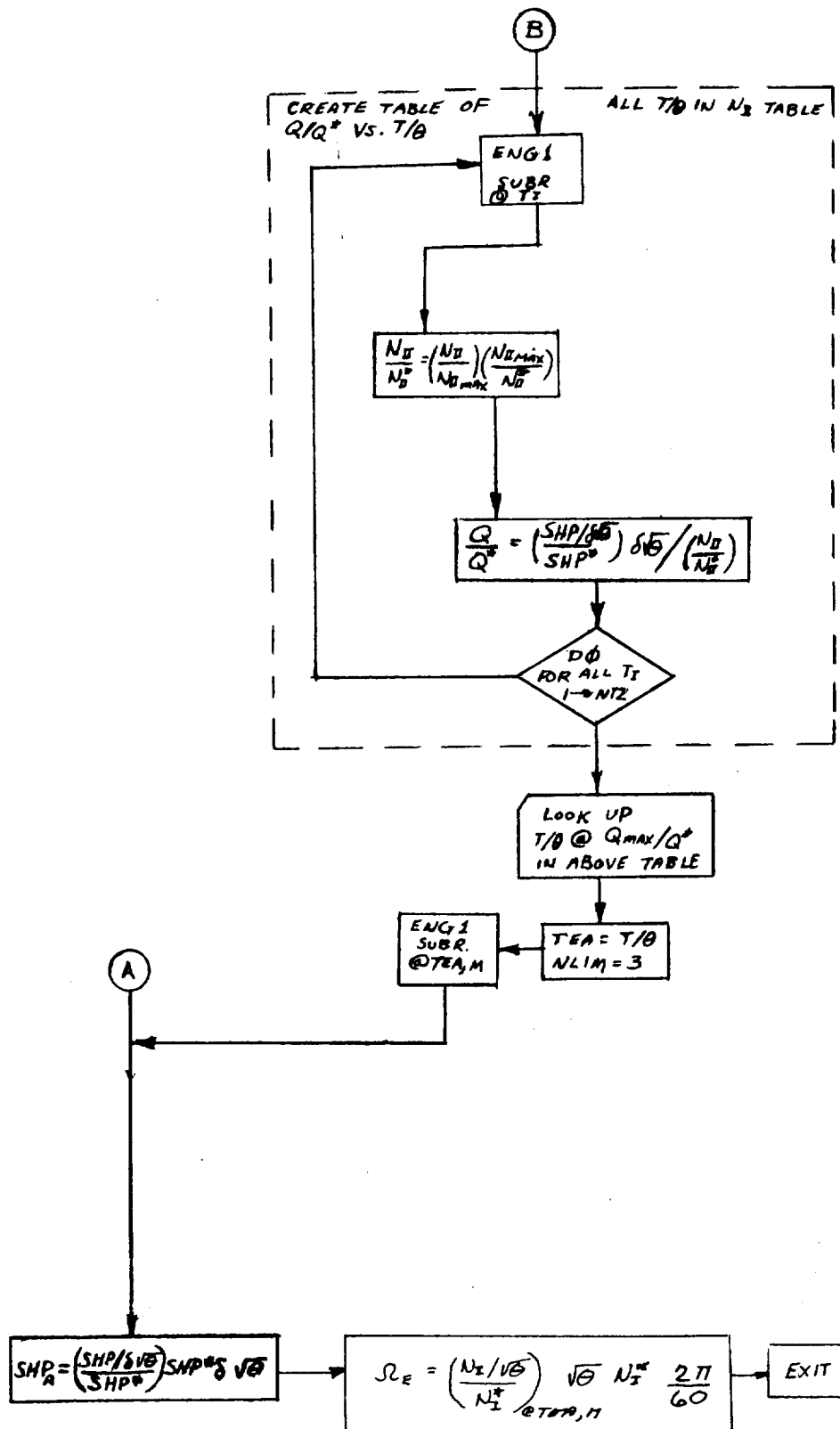
ATMIND: 0 ~ STD ATMOS

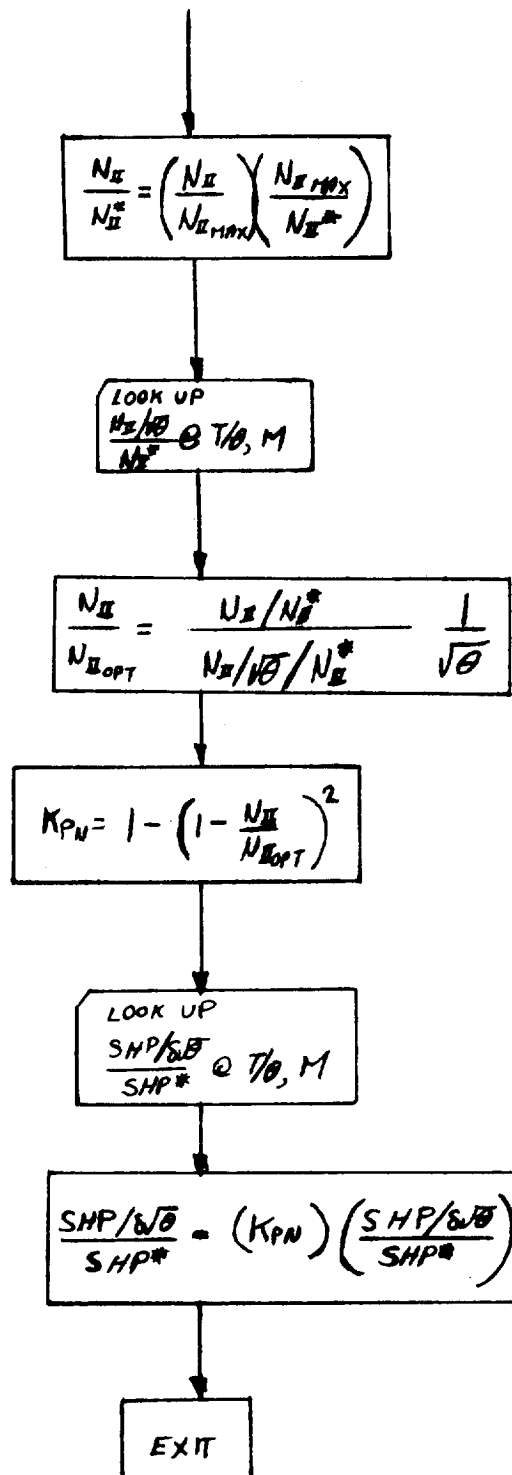
1 ~ HOT ATMOS

2 ~ TROPICAL ATMOS

OUTPUT: $\delta, \theta, \sigma_h, a, M, \rho$







ENG 1 SUBROUTINE, FLOW CHART

[illegible]

ROTOR CONTROL COORDINATE AXIS TRANSFORM

LEFT

$$A_{1CL}'' = A_{1CL}' \cos \phi_p + B_{1CL}' \sin \phi_p$$

$$B_{1CL}'' = -A_{1CL}' \sin \phi_p + B_{1CL}' \cos \phi_p$$

$$A_{1CL} = A_{1CL}'' \cos \zeta_{HL} - B_{1CL}'' \sin \zeta_{HL}$$

$$B_{1CL} = A_{1CL}'' \sin \zeta_{HL} + B_{1CL}'' \cos \zeta_{HL}$$

RIGHT

$$A_{1CR}'' = A_{1CR}' \cos \phi_p + B_{1CR}' \sin \phi_p$$

$$B_{1CR}'' = -A_{1CR}' \sin \phi_p + B_{1CR}' \cos \phi_p$$

$$A_{1CR} = +A_{1CR}'' \cos \zeta_{HR} + B_{1CR}'' \sin \zeta_{HR}$$

$$B_{1CR} = -A_{1CR}'' \sin \zeta_{HR} + B_{1CR}'' \cos \zeta_{HR}$$

ROTOR SIDESLIP ANGLE

$$\zeta_{HR} = \tan^{-1} \frac{v_{RR}}{w_{RR} + \epsilon_{wRR} u_{RR}}$$

$$\zeta_{HL} = \tan^{-1} \frac{v_{RL}}{w_{RL} + \epsilon_{wRL} u_{RL}}$$

FORM THE SIN & COS OF ζ_{HR} & ζ_{HL}

NOTE: ϕ_p IS THE CONTROL PHASE ANGLE. ϕ_p IS POSITIVE

FOR THE CONTROL AXIS MOVED OPPOSITE TO ROTOR ROTATION.

CENTER OF GRAVITY CALCULATION

C.G. LOCATION w.r.t. PIVOT

$$X_{CG} = \frac{m_f l_f + m_w l_w}{m} + l \left(\frac{m_N}{m} \right) [\cos(i_{NL} - \lambda) + \cos(i_{NR} - \lambda)]$$

$$Z_{CG} = \frac{m_f h_f + m_w h_w}{m} - l \left(\frac{m_N}{m} \right) [\sin(i_{NL} - \lambda) + \sin(i_{NR} - \lambda)]$$

C.G. VELOCITY w.r.t. PIVOT

$$\dot{X}_{CG} = -l \frac{m_N}{m} [\dot{i}_{NL} \sin(i_{NL} - \lambda) + \dot{i}_{NR} \sin(i_{NR} - \lambda)]$$

$$\dot{Z}_{CG} = -l \frac{m_N}{m} [\dot{i}_{NL} \cos(i_{NL} - \lambda) + \dot{i}_{NR} \cos(i_{NR} - \lambda)]$$

C.G. ACCELERATION w.r.t. PIVOT

$$\ddot{X}_{CG} = -l \frac{m_N}{m} [\ddot{i}_{NL} \sin(i_{NL} - \lambda) + \dot{i}_{NL}^2 \cos(i_{NL} - \lambda) + \ddot{i}_{NR} \sin(i_{NR} - \lambda) + \dot{i}_{NR}^2 \cos(i_{NR} - \lambda)]$$

$$\ddot{Z}_{CG} = -l \frac{m_N}{m} [\ddot{i}_{NL} \cos(i_{NL} - \lambda) - \dot{i}_{NL}^2 \sin(i_{NL} - \lambda) + \ddot{i}_{NR} \cos(i_{NR} - \lambda) - \dot{i}_{NR}^2 \sin(i_{NR} - \lambda)]$$

FUSELAGE PIVOT VELOCITY

$$U_P = U - Z_{CG} \dot{\gamma} - \dot{X}_{CG}$$

$$V_P = V + Z_{CG} p - X_{CG} r$$

$$W_P = W + X_{CG} \dot{\gamma} - \dot{Z}_{CG}$$

AERO DYNAMIC COORDINATE TRANSFORM

LEFT WING A.C. VELOCITY - BODY AXES

$$U'_{LW} = U_P + Z_{WAC} q + Y_{WAC} r + q h_{LWAC}$$

$$V'_{LW} = V_P + X_{WAC} r - Z_{WAC} P - P h_{LWAC}$$

$$W'_{LW} = W_P - Y_{WAC} P - X_{WAC} q + \dot{h}_{LWAC}$$

RIGHT WING A.C. VELOCITY - BODY AXES

$$U'_{RW} = U_P + Z_{WAC} q - Y_{WAC} r + q h_{RWAC}$$

$$V'_{RW} = V_P + X_{WAC} r - Z_{WAC} P - P h_{RWAC}$$

$$W'_{RW} = W_P + Y_{WAC} P - X_{WAC} q + \dot{h}_{RWAC}$$

LEFT ROTOR HUB VELOCITY - BODY AXES

$$U'_{RL} = U_P + r Y_N - L_S \sin i_{NL} (\dot{i}_{NL} + q) + q h_{IL}$$

$$V'_{RL} = V_P + L_S (r \cos i_{NL} + p \sin i_{NL}) - p h_{IL}$$

$$W'_{RL} = W_P - p Y_N - L_S (\dot{i}_{NL} + q) \cos i_{NL} + \dot{h}_{IL}$$

RIGHT ROTOR HUB VELOCITY - BODY AXES

$$U'_{RR} = U_P - r Y_N - L_S \sin i_{NR} (\dot{i}_{NR} + q) + q h_{IR}$$

$$V'_{RR} = V_P + L_S (r \cos i_{NR} + p \sin i_{NR}) - p h_{IR}$$

$$W'_{RR} = W_P + p Y_N - L_S (\dot{i}_{NR} + q) \cos i_{NR} + \dot{h}_{IR}$$

AERODYNAMIC COORDINATE TRANSFORM (CONT'D.)

LEFT ROTOR HUB VELOCITY - SHAFT AXES

$$U_{RL} = U'_{RL} \cos i_{NL} - W'_{RL} \sin i_{NL}$$

$$V_{RL} = V'_{RL}$$

$$W_{RL} = U'_{RL} \sin i_{NL} + W'_{RL} \cos i_{NL}$$

RIGHT ROTOR HUB VELOCITY - SHAFT AXES

$$U_{RR} = U'_{RR} \cos i_{NR} - W'_{RR} \sin i_{NR}$$

$$V_{RR} = V'_{RR}$$

$$W_{RR} = U'_{RR} \sin i_{NR} + W'_{RR} \cos i_{NR}$$

LEFT WING A.C. VELOCITY - CHORD AXES

$$U_{LW} = U'_{LW} \cos i_w - W'_{LW} \sin i_w$$

$$V_{LW} = V'_{LW}$$

$$W_{LW} = U'_{LW} \sin i_w + W'_{LW} \cos i_w$$

RIGHT WING A.C. VELOCITY - CHORD AXES

$$U_{RW} = U'_{RW} \cos i_w - W'_{RW} \sin i_w$$

$$V_{RW} = V'_{RW}$$

$$W_{RW} = U'_{RW} \sin i_w + W'_{RW} \cos i_w$$

AERODYNAMIC COORDINATE TRANSFORM (Cont'd)

HORIZONTAL STABILIZER A.C. VELOCITY

$$U_{HT} = U_P + Z_{HT} q$$

$$V_{HT} = V_P + X_{HT} r - Z_{HT} p$$

$$W_{HT} = W_P - X_{HT} q$$

VERTICAL FIN A.C. VELOCITY

$$U_{VT} = U_P + Z_{VT} q$$

$$V_{VT} = V_P + X_{VT} r - Z_{VT} p$$

$$W_{VT} = W_P - X_{VT} q$$

WING EQUATIONS

$$\tau_{RR} = \alpha_{RR} + \tan^{-1} \left(\frac{N.F_R}{T_R} \right)$$

$$R_{RR} = \sqrt{T_R^2 + N.F_R^2 + S.F_R^2}$$

$$V_{*R} = \frac{V_{RR}}{\sqrt{\frac{|R_{RR}| + 10}{2\rho A}}}$$

$$V_{*R}^4 + 2 V_{*R}^3 \cos \tau_{RR} + V_{*R}^2 V_{*R}^2 = 1 \quad (\text{solve for } V_{*R})$$

$$\epsilon_{PRR} = \tan^{-1} \frac{V_{*R} \sin \tau_{RR}}{V_{*R} + V_{*R} \cos \tau_{RR}}$$

$$C_{TSRR} = \frac{\cos(\tau_{RR} - \alpha_{RR})}{\cos(\tau_{RR} - \alpha_{RR}) + \frac{V_{*R}^2}{4}}$$

$$\tau_{LR} = \alpha_{LR} + \tan^{-1} \left(\frac{N.F_L}{T_L} \right)$$

$$R_{LR} = \sqrt{T_L^2 + N.F_L^2 + S.F_L^2}$$

$$V_{*L} = \frac{V_{LR}}{\sqrt{\frac{|R_{LR}| + 10}{2\rho A}}}$$

$$V_{*L}^4 + 2 V_{*L}^3 \cos \tau_{LR} + V_{*L}^2 V_{*L}^2 = 1 \quad (\text{solve for } V_{*L})$$

$$\epsilon_{PLR} = \tan^{-1} \frac{V_{*L} \sin \tau_{LR}}{V_{*L} + V_{*L} \cos \tau_{LR}}$$

$$C_{TSLR} = \frac{\cos(\tau_{LR} - \alpha_{LR})}{\cos(\tau_{LR} - \alpha_{LR}) + \frac{V_{*L}^2}{4}}$$

WING EQUATIONS (Cont'd.)

$$\bar{\xi} = (\xi_{HR} + \xi_{HE}) \cdot 0.5$$

$$\bar{\alpha}_R = (\alpha_{RR} + \alpha_{LR}) \cdot 0.5$$

$$\bar{e}_p = (e_{PRR} + e_{PLR}) \cdot 0.5$$

$$\bar{C}_{TS} = (C_{TSRR} + C_{TSLR}) \cdot 0.5$$

} Used in Tail Aerodynamics

$$\bar{i}_N = (i_{NL} + i_{NR}) \cdot 0.5$$

$$C_{LW} = \frac{(C_{LSRW} + C_{LSLW})}{(1 - \bar{C}_{TS})} \cdot 0.5$$

} Used in Wing/Rotor Interfer.

$$\xi_{R1} = [L_s - PC \cos(\bar{i}_N - i_w) + h_p \sin(\bar{i}_N - i_w)] \tan(\bar{\alpha}_R - \bar{e}_p) \sin \bar{\xi}$$

$$\xi_{R2} = \sqrt{\frac{D^2}{4} - \left\{ [L_s - PC \cos(\bar{i}_N - i_w) + h_p \sin(\bar{i}_N - i_w)] \tan(\bar{\alpha}_R - \bar{e}_p) \cos \bar{\xi} + PC \sin(\bar{i}_N - i_w) + h_p \cos(\bar{i}_N - i_w) \right\}^2}$$

IF: $\xi_{R2} = 0$ OR Imaginary, $S_{iRW} = 0$ and $S_{iLW} = 0$,
also $\left(\frac{C_{Lwi}}{C_{L\alpha}}\right)_{RW} = 0$ and $\left(\frac{C_{Lwi}}{C_{L\alpha}}\right)_{LW} = 0.0$

FORM ξ_{R3} BY REPLACING PC IN ξ_{R1} EQUATION
WITH $(PC - C_w)$

FORM ξ_{R4} BY REPLACING PC IN ξ_{R2} EQUATION
WITH $(PC - C_w)$

IF: $\xi_{R4} = 0$ OR Imaginary; $S_{iRW} = 0$ and $S_{iLW} = 0$,
also $\left(\frac{C_{Lwi}}{C_{L\alpha}}\right)_{RW} = 0.0$ and $\left(\frac{C_{Lwi}}{C_{L\alpha}}\right)_{LW} = 0.0$

IF: UMBRELLAS OPEN; SET $C_{LW} = 0.0$

UMBRELLA LOGIC:

IF: $i_{NREF} < F_{iN}$ OR $q_F > 8.479 \frac{lb/ft^2}{ft^2}$
SET UMBRELLAS CLOSED (Hysteresis $F_{iN} \pm 1^\circ$; $q_F \pm 0.1 \frac{lb}{ft^2}$)

WING EQUATIONS (CONT'D)

$$S_{iRW} = \frac{C_W}{2} [\xi_{R1} + \xi_{R2} + \xi_{R3} + \xi_{R4}]$$

$$\left(\frac{S_i}{S}\right)_{RW} = 2 \left(\frac{S_{iR}}{S_W}\right)$$

$$S_{iT} = C_W [\xi_{R2} + \xi_{R4}]$$

$$S_{iLW} = S_{iT} - S_{iR}$$

$$\left(\frac{S_i}{S}\right)_{LW} = 2 \left(\frac{S_{iL}}{S_W}\right)$$

$$(R_i)_{LW} = \left(\frac{S_{iL}}{C_W^2}\right)$$

$$(R_i)_{RW} = \left(\frac{S_{iR}}{C_W^2}\right)$$

$$R_W = \frac{S_W}{C_W^2} \text{ (PRELIMINARY)}$$

$$\left(\frac{C_{L\alpha i}}{C_{L\alpha}}\right)_{LW} = \frac{1}{1 + \frac{C_{L\alpha W}}{\pi} \left[\frac{1}{(R_i)_{LW}} - \frac{1}{R_W} \right]}$$

$$\left(\frac{C_{L\alpha i}}{C_{L\alpha}}\right)_{RW} = \frac{1}{1 + \frac{C_{L\alpha}}{\pi} \left[\frac{1}{(R_i)_{RW}} - \frac{1}{R_W} \right]}$$

$$K'_{AL} = \frac{V_{\phi L} + \left(\frac{C_{L\alpha i}}{C_{L\alpha}}\right)_{LW} N_{\phi L}}{V_{\phi L} + N_{\phi L}}$$

$$K'_{AR} = \frac{V_{\phi R} + \left(\frac{C_{L\alpha i}}{C_{L\alpha}}\right)_{RW} N_{\phi R}}{V_{\phi R} + N_{\phi R}}$$

WING EQUATIONS (CONTINUED)

$$\bar{q}_s = \left[\frac{1}{2} \rho (u^2 + v^2 + w^2) + \frac{(T_L + T_R) \cdot S}{A} \right]$$

$$q_{s_{RW}} = \left[\frac{1}{2} \rho (u_{RW}^2 + v_{RW}^2 + w_{RW}^2) + \frac{T_R}{A} \right]$$

$$q_{s_{LW}} = \left[\frac{1}{2} \rho (u_{LW}^2 + v_{LW}^2 + w_{LW}^2) + \frac{T_L}{A} \right]$$

WING EQUATIONS (Cont'd.)

WING ANGLE OF ATTACK AND SIDESLIP

$$\alpha_{LWO} = \sin^{-1} \left[\frac{W_{LW}}{\sqrt{U_{LW}^2 + W_{LW}^2}} \right] + \theta_{ELWAC}$$

$$\alpha_{RWO} = \sin^{-1} \left[\frac{W_{RW}}{\sqrt{U_{RW}^2 + W_{RW}^2}} \right] + \theta_{ERWAC}$$

$$\beta_{LWO} = \sin^{-1} \left[\frac{V_{LW}}{\sqrt{U_{LW}^2 + V_{LW}^2 + W_{LW}^2}} \right]$$

$$\beta_{RWO} = \sin^{-1} \left[\frac{V_{RW}}{\sqrt{U_{RW}^2 + V_{RW}^2 + W_{RW}^2}} \right]$$

$$\alpha_{LWSSO} = \alpha_{LWO} - E_{PLR}$$

$$\alpha_{RWSSO} = \alpha_{RWO} - E_{PRR}$$

$$\bar{\alpha}_W = (\alpha_{LWO} + \alpha_{RWO}) \cdot 0.5$$

$$\alpha_{LWrigid} = \sin^{-1} \left[\frac{W_{LW}}{\sqrt{U_{LW}^2 + W_{LW}^2}} \right] - E_{PLR}$$

$$\alpha_{RWrigid} = \sin^{-1} \left[\frac{W_{RW}}{\sqrt{U_{RW}^2 + W_{RW}^2}} \right] - E_{PRR}$$

$$\alpha'_{LWO} = \alpha_{LWO} - i_W - \theta_{ELWAC}$$

$$\alpha'_{RWO} = \alpha_{RWO} - i_W - \theta_{ERWAC}$$

NOTE: IF α_{LWSSO} OR $\alpha_{RWSSO} \geq \alpha_{MAX}$; PRINT OUT STALL WARNING

WING EQUATIONS (CONT'D)

CALCULATION OF INCREMENTAL LIFT, DRAG AND MOMENT COEFFICIENTS

CALCULATE:

$$C_{L_{LW0}} = C_L @ \alpha = \alpha_{LWSS0}, \quad \delta = \delta_{a_{LW}} + \delta_f, \quad \delta_{SP} = \delta_{SP_L}$$

$$C_{L_{RW0}} = C_L @ \alpha = \alpha_{RWSS0}, \quad \delta = \delta_{a_{RW}} + \delta_f, \quad \delta_{SP} = \delta_{SP_R}$$

$$C_{L_{LW0}}^* = C_L @ \alpha = \alpha_{LW0}, \quad \delta = \delta_{a_{LW}} + \delta_f, \quad \delta_{SP} = \delta_{SP_L}$$

$$C_{L_{RW0}}^* = C_L @ \alpha = \alpha_{RW0}, \quad \delta = \delta_{a_{RW}} + \delta_f, \quad \delta_{SP} = \delta_{SP_R}$$

$$C_{L_0} = C_L @ \alpha_F + i_w, \quad \delta = \delta_f$$

CALCULATE:

$$\begin{aligned} \alpha_{N.L.}^+ &= 14.6^\circ - 0.12 \delta & (0^\circ \leq \delta \leq 40^\circ) \\ &= 9.8^\circ & (\delta > 40^\circ) \\ \alpha_{N.L.}^- &= -16.7^\circ - .1138\delta & (0^\circ \leq \delta \leq 40^\circ) \\ &= -21.25^\circ & (\delta > 40^\circ) \end{aligned}$$

IF: $\alpha_{N.L.}^- \leq \alpha \leq \alpha_{N.L.}^+$

$$C_L = 0.134 + C_{L_{W0}} \alpha + \Delta C_{L_\delta} + F \Delta C_{L_{SP}}$$

WHERE:

$$\begin{aligned} \Delta C_{L_\delta} &= .0269 \delta & (0^\circ \leq \delta \leq 22.22906^\circ) \\ &= -2.437137 + .20607 \delta - .003128 \delta^2 & (22.22906^\circ < \delta \leq 29.786^\circ) \\ &= .442100 + .0263 \delta - .000338 \delta^2 & (\delta > 29.786^\circ) \end{aligned}$$

$$\begin{aligned} \Delta C_{L_{SP}} &= -.01132 \delta_{SP} & (0^\circ \leq \delta_{SP} \leq 30^\circ) \\ &= .076 - .018666 \delta_{SP} + .00016 \delta_{SP}^2 & (\delta_{SP} > 30^\circ) \end{aligned}$$

$$\begin{aligned} F &= 1.003412 + .011163 \delta + .002168 \delta^2 & (0^\circ \leq \delta \leq 20.1665^\circ) \\ F &= -.756323 + .185684 \delta - .002159 \delta^2 & (\delta > 20.1665^\circ) \end{aligned}$$

WING EQUATIONS (CONT'D)

IF: $\alpha_{N.L}^+ < \alpha \leq \alpha_{N.L}^+ + 8.534^\circ$

CALCULATE: $C_{L'N.L} = 0.134 + C_{L\alpha_w} \alpha_{N.L}^+ + \Delta C_{L_S} + F \Delta C_{L_{SP}}$

$$\alpha_{DUM} = \alpha - \alpha_{N.L}^+ + 14.6^\circ$$

$$\Delta C_{L_{N.L}} = -0.00547619 \alpha_{DUM}^2 + 0.18254762 \alpha_{DUM} - 1.421571513$$

$$C_L = C_{L'N.L} + \Delta C_{L_{N.L}} \quad \text{AND PRINT STALL WARNING}$$

IF: $(\alpha_{N.L}^+ + 8.534^\circ) < \alpha < 90^\circ$

CALCULATE: $C_{L'N.L} = 0.134 + C_{L\alpha_w} \alpha_{N.L}^+ + \Delta C_{L_S} + F \Delta C_{L_{SP}}$

$$C_L = \frac{C_{L'N.L} (90^\circ - \alpha)}{90^\circ - (\alpha_{N.L}^+ + 8.534^\circ)} \quad \text{AND PRINT STALL WARNING.}$$

IF: $(\alpha_{N.L}^- - 8.534^\circ) \leq \alpha < \alpha_{N.L}^-$

CALCULATE:

$$C_{L'N.L} = 0.134 + C_{L\alpha_w} \alpha_{N.L}^- + \Delta C_{L_S} + F \Delta C_{L_{SP}}$$

$$\alpha_{DUM} = \alpha_{N.L}^- - \alpha + 14.6^\circ$$

$$\Delta C_{L_{N.L}} = -0.00547619 \alpha_{DUM}^2 + 0.18254762 \alpha_{DUM} - 1.421571513$$

$$C_L = C_{L'N.L} - \Delta C_{L_{N.L}} \quad \text{AND PRINT STALL WARNING}$$

IF: $-90^\circ \leq \alpha < (\alpha_{N.L}^- - 8.534^\circ)$

CALCULATE:

$$C_{L'N.L} = 0.134 + C_{L\alpha_w} \alpha_{N.L}^- + \Delta C_{L_S} + F \Delta C_{L_{SP}}$$

$$C_L = \frac{C_{L'N.L} (90^\circ + \alpha)}{90^\circ + \alpha_{N.L}^- - 8.534^\circ} \quad \text{AND PRINT STALL WARNING}$$

NOTE: - α , α_{DUM} , δ , $\delta_{u.w}$, $\delta_{a.m}$, δ_f , $\alpha_{N.L}^-$, $\alpha_{N.L}^+$, δ_{SPL} , δ_{SPR} , IN DEGREES; $C_{L\alpha_w} \sim \text{"/DEGREES}$

WING EQUATIONS (CONT'D)

CALCULATE:-

$$C_{D_{LW}} = C_D @ \alpha = \alpha_{LWSSO}, \quad \delta = \delta_f + \delta_{aLW}, \quad \delta_{SP} = \delta_{SP_L}$$

$$C_{D_{RW}} = C_D @ \alpha = \alpha_{RWSSO}, \quad \delta = \delta_f + \delta_{aRW}, \quad \delta_{SP} = \delta_{SP_R}$$

$$C_{D_{LW}}^* = C_D @ \alpha = \alpha_{LW0}, \quad \delta = \delta_f + \delta_{aLW}, \quad \delta_{SP} = \delta_{SP_L}$$

$$C_{D_{RW}}^* = C_D @ \alpha = \alpha_{RW0}, \quad \delta = \delta_f + \delta_{aRW}, \quad \delta_{SP} = \delta_{SP_R}$$

AS FOLLOWS:

IF:- $-20^\circ \leq \alpha \leq 20^\circ$

CALCULATE: $C_D = .00059250 \alpha^2 + .002109993 \alpha + .01765$
 $+ \sum_{n=0}^4 \sum_{u=0}^4 [A_D(u+5n) \delta^u \alpha^n] + \Delta C_{D_{SP}}$

WHERE: $\Delta C_{D_{SP}} = -.000098784 \delta_{SP} + .000009622 \delta_{SP}^2$

IF: $20^\circ < \alpha \leq 90^\circ$, $\alpha_{DUM} = 20^\circ$

CALCULATE: $C_D^+ = 0.31105749 + \sum_{n=0}^4 \sum_{u=0}^4 [A_D(u+5n) \delta^u \alpha_{DUM}^n] + \Delta C_{D_{SP}}$

$$C_D = C_D^+ + \frac{(1 - C_D^+)}{70^\circ} (\alpha - 20^\circ)$$

IF: $-90^\circ \leq \alpha < -20^\circ$, $\alpha_{DUM} = -20^\circ$

CALCULATE: $C_D^- = 0.19124389 + \sum_{n=0}^4 \sum_{u=0}^4 [A_D(u+5n) \delta^u \alpha_{DUM}^n] + \Delta C_{D_{SP}}$

$$C_D = C_D^- - \frac{(1 - C_D^-)}{70^\circ} (\alpha + 20^\circ)$$

NOTE: $\alpha, \alpha_{DUM}, \delta, \delta_{aRW}, \delta_{aLW}, \delta_{SP_R}, \delta_{SP_L}$ IN DEGREES

WING EQUATIONS (CONT'D)

CALCULATE:

$$C_{MLW} = C_M @ \alpha = \alpha_{LWSSO}, \quad \delta = \delta_f + \delta_{aLW}$$

$$C_{MAW} = C_M @ \alpha = \alpha_{RWSSO}, \quad \delta = \delta_f + \delta_{aRW}$$

$$C_{MLW}^* = C_M @ \alpha = \alpha_{LW0}, \quad \delta = \delta_f + \delta_{aLW}$$

$$C_{MAW}^* = C_M @ \alpha = \alpha_{RW0}, \quad \delta = \delta_f + \delta_{aRW}$$

AS FOLLOWS:

IF:- $-20^\circ \leq \alpha \leq 20^\circ$

CALCULATE:- $C_M' = -.030117 - .0003162 \alpha$

$$\Delta C_{Ms} = .0000778 \delta^2 - .010033 \delta \quad (0^\circ \leq \delta \leq 45^\circ)$$

$$\Delta C_{Ms} = .0000322 \delta^2 - .0049045 \delta - .1384272 \quad (\delta > 45^\circ)$$

$$C_M = C_M' + \Delta C_{Ms}$$

IF: $\alpha > 20^\circ$

CALCULATE: $C_M' = -.036441 + \Delta C_{Ms}$

$$C_M = C_M' \frac{(90^\circ - \alpha)}{70^\circ}$$

IF $\alpha < -20^\circ$

CALCULATE $C_M' = -.023793 + \Delta C_{Ms}$

$$C_M = C_M' \frac{(90^\circ + \alpha)}{70^\circ}$$

NOTE: $\alpha, \alpha_{LW}, \delta, \delta_{aRW}, \delta_{aLW}, \delta_{aP}, \delta_{aR}$ IN DEGREES

WING EQUATIONS (CONT'D)

CALCULATE :-

$$C_{LW}''' = C_{LW0} \quad ; \quad C_{DLW}''' = C_{DLW0} \quad ; \quad C_{MLW}'' = C_{MLW0}$$

$$C_{LRW}''' = C_{LRW0} \quad ; \quad C_{DRW}'' = C_{DRW0} \quad ; \quad C_{MRW}'' = C_{MRW0}$$

$$C_{LWMAX}'' = C_{LMAX} + \Delta C_{LS} + \Delta C_{LSP}$$

$$C_{LRWMAX}'' = C_{LMAX} + \Delta C_{LS} + \Delta C_{LSP}$$

$$C_{LRW}^{*'} = C_{LRW0}^{*'} \quad ; \quad C_{DRW}^{*'} = C_{DRW0}^{*'} \quad ; \quad C_{MRW}^{*'} = C_{MRW0}^{*'}$$

$$C_{LW}^{*'} = C_{LW0}^{*'} \quad ; \quad C_{DLW}^{*'} = C_{DLW0}^{*'} \quad ; \quad C_{MLW}^{*'} = C_{MLW0}^{*'}$$

$$C_{LWMAX}^{*'} = C_{LWMAX}''$$

$$C_{LRWMAX}^{*'} = C_{LRWMAX}''$$

$$\overline{C_L} = \frac{C_{L0} \left(\frac{a_g}{a} \right)_w}{\sqrt{1-M^2}}$$

$$C_{LW}''^{IGE} = C_{LW}''' \frac{\left(\frac{a_g}{a} \right)_w}{\sqrt{1-M^2}} \quad ; \quad C_{LRW}''^{IGE} = C_{LRW}''' \frac{\left(\frac{a_g}{a} \right)_w}{\sqrt{1-M^2}} \quad ;$$

$$C_{LW}^{*'}^{IGE} = C_{LW}^{*'} \frac{\left(\frac{a_g}{a} \right)_w}{\sqrt{1-M^2}} \quad ; \quad C_{LRW}^{*'}^{IGE} = C_{LRW}^{*'} \frac{\left(\frac{a_g}{a} \right)_w}{\sqrt{1-M^2}}$$

WING EQUATIONS (CONT'D)

$$\Delta C_{DLW}^{IGE} = K_{99} \frac{(C_{LLW}^{IGE} - C_{LLW}''')^2}{\pi AR_w}; \Delta C_{DRW}^{IGE} = K_{99} \frac{(C_{LRW}^{IGE} - C_{LRW}''')^2}{\pi AR_w};$$

$$\Delta C_{DLW}^{IGE*} = K_{99} \frac{(C_{LLW}^{IGE*} - C_{LLW}^{*1})^2}{\pi AR_w}; \Delta C_{DRW}^{IGE*} = K_{99} \frac{(C_{LRW}^{IGE*} - C_{LRW}^{*1})^2}{\pi AR_w}$$

$$\text{IF: } C_{LLW}^{IGE} \geq C_{LLW}^{IGEMAX}; \text{ SET } \Delta C_{DLW}^{IGE} = 0.0 \text{ \& } C_{LLW}^{IGE} = C_{LLW}^{IGEMAX}$$

$$\text{IF: } C_{LRW}^{IGE} \geq C_{LRW}^{IGEMAX}; \text{ SET } \Delta C_{DRW}^{IGE} = 0.0 \text{ \& } C_{LRW}^{IGE} = C_{LRW}^{IGEMAX}$$

$$\text{IF: } C_{LLW}^{IGE*} \geq C_{LLW}^{IGEMAX*}; \text{ SET } \Delta C_{DLW}^{IGE*} = 0.0 \text{ \& } C_{LLW}^{IGE*} = C_{LLW}^{IGEMAX*}$$

$$\text{IF: } C_{LRW}^{IGE*} \geq C_{LRW}^{IGEMAX*}; \text{ SET } \Delta C_{DRW}^{IGE*} = 0.0 \text{ \& } C_{LRW}^{IGE*} = C_{LRW}^{IGEMAX*}$$

$$\text{IF: } (a_2/a) > 1.0; \text{ SET } K_{99} = -1.0$$

$$(a_2/a) \leq 1.0; \text{ SET } K_{99} = +1.0$$

CALCULATE

$$C_{LLW}'' = C_{LLW}^{IGE}$$

$$C_{DLW}'' = C_{DLW}''' + \Delta C_{DLW}^{IGE}$$

$$C_{LRW}'' = C_{LRW}^{IGE}$$

$$C_{DRW}'' = C_{DRW}''' + \Delta C_{DRW}^{IGE}$$

$$C_{LLW}^{*} = C_{LLW}^{IGE*}$$

$$C_{DLW}^{*} = C_{DLW}^{*1} + \Delta C_{DLW}^{IGE*}$$

$$C_{LRW}^{*} = C_{LRW}^{IGE*}$$

$$C_{DRW}^{*} = C_{DRW}^{*1} + \Delta C_{DRW}^{IGE*}$$

WING EQUATIONS (cont'd.)

$$C_{LSLW} = K'_L \left\{ \left(\frac{S_i}{S}_{LW} \right) (C''_{LLW} \cos E_{PLR} - C''_{DLW} \sin E_{PLR}) + C^*_{LLW} (1 - C_{TSLR}) \left[1 - \left(\frac{S_i}{S} \right)_{LW} \right] \right\}$$

$$C_{LSRW} = K'_R \left\{ \left(\frac{S_i}{S}_{RW} \right) (C''_{LRW} \cos E_{PRR} - C''_{DRW} \sin E_{PRR}) + C^*_{LRW} (1 - C_{TSRR}) \left[1 - \left(\frac{S_i}{S} \right)_{RW} \right] \right\}$$

$$C_{DSLW} = K'_L \left\{ \left(\frac{S_i}{S}_{LW} \right) (C''_{LLW} \sin E_{PLR} + C''_{DLW} \cos E_{PLR}) + C^*_{DLW} (1 - C_{TSLR}) \left[1 - \left(\frac{S_i}{S} \right)_{LW} \right] \right\}$$

$$C_{DSRW} = K'_R \left\{ \left(\frac{S_i}{S}_{RW} \right) (C''_{LRW} \sin E_{PRR} + C''_{DRW} \cos E_{PRR}) + C^*_{DRW} (1 - C_{TSRR}) \left[1 - \left(\frac{S_i}{S} \right)_{RW} \right] \right\}$$

$$C_{MSLW} = K'_L \left\{ \left(\frac{S_i}{S}_{LW} \right) (C''_{MLW}) + C^*_{MLW} (1 - C_{TSLR}) \left[1 - \left(\frac{S_i}{S} \right)_{LW} \right] \right\}$$

$$C_{MSRW} = K'_R \left\{ \left(\frac{S_i}{S}_{RW} \right) (C''_{MRW}) + C^*_{MRW} (1 - C_{TSRR}) \left[1 - \left(\frac{S_i}{S} \right)_{RW} \right] \right\}$$

WING EQUATIONS (cont'd.)

$$\Delta C_{LSPower} = \frac{1}{4} \left\{ [C_{LSLW} - (1 - \bar{C}_{TS}) C_{LLW}^*] \left[1 - \frac{1}{2} \left(\frac{S_i}{S} \right)_{LW} \right] - [C_{LSRW} - (1 - \bar{C}_{TS}) C_{LRW}^*] \left[1 - \frac{1}{2} \left(\frac{S_i}{S} \right)_{RW} \right] \right\}$$

$$\Delta C_{NSPower} = \frac{1}{4} \left\{ [C_{DSRW} - (1 - \bar{C}_{TS}) C_{DRW}^*] \left[1 - \frac{1}{2} \left(\frac{S_i}{S} \right)_{RW} \right] - [C_{DSLW} - (1 - \bar{C}_{TS}) C_{DLW}^*] \left[1 - \frac{1}{2} \left(\frac{S_i}{S} \right)_{LW} \right] \right\}$$

$$C_{ZSW} = (K_{20} + K_{21} \bar{C}_L)(1 - \bar{C}_{TS}) \beta_f + \left(\frac{1 - \bar{C}_{TS}}{2b_w} \right) (K_2) (C_{LLW}^* - C_{LRW}^*) \bar{Y}_{AC}$$

$$+ \Delta C_{ZSPower}$$

$$C_{NSW} = (K_{22} \bar{C}_L^2)(1 - \bar{C}_{TS}) \beta_f + \left(\frac{1 - \bar{C}_{TS}}{2b_w} \right) (K_2) \left\{ (C_{DRW}^* - C_{DLW}^*) - [C_{LRW}^* \sin(\alpha_{RW0} - i_w) + C_{LLW}^* \sin(i_w - \alpha_{LW0})] \right\} \bar{Y}_{AC}$$

$$+ \Delta C_{NSPower}$$

WING EQUATIONS

SPECIAL CONDITIONS (FOR UMBRELLAS OPEN)

IF : UMBRELLAS CLOSED; GO THROUGH WING EQUATIONS

IF : UMBRELLAS OPEN ; CALCULATE THE WING FORCES AND MOMENTS AS FOLLOWS:

$$X_{AERO}^{LW} = f_{e_u} q_{SLW} (1 - C_{TSLR}) \left[\frac{-U_{LW}}{|U_{LW}| + 1} \right]$$

$$X_{AERO}^{RW} = f_{e_u} q_{SRW} (1 - C_{TSRR}) \left[\frac{-U_{RW}}{|U_{RW}| + 1} \right]$$

$$Y_{AERO}^{LW} = 0.0$$

$$Y_{AERO}^{RW} = 0.0$$

$$\left. \begin{aligned} Z_{AERO}^{LW} &= T_L \left(\frac{D}{T} \right)_L \\ Z_{AERO}^{RW} &= T_R \left(\frac{D}{T} \right)_R \end{aligned} \right\} \text{GO TO WING BENDING}$$

$$M_{AERO}^{LW} = -X_{\frac{C}{Z}} Z_{AERO}^{LW} + \left(\frac{M}{T} \right)_L T_L \left\{ Z_{AERO}^{LW} \text{ \& } Z_{AERO}^{RW} \text{ FROM} \right.$$

$$M_{AERO}^{RW} = -X_{\frac{C}{Z}} Z_{AERO}^{RW} + \left(\frac{M}{T} \right)_R T_R \left. \right\} \text{WING BENDING}$$

$$Z_{AERO}^W = \left(\frac{b_w}{Z} \right) \left\{ Z_{AERO}^{RW} \left[1 - \left(\frac{S_i}{S} \right)_{RW} \right] - Z_{AERO}^{LW} \left[1 - \left(\frac{S_i}{S} \right)_{LW} \right] \right\}$$

$$M_{AERO}^W = 0.0$$

$$\underline{\text{IF}}: \left[\frac{h}{D} \right]_{EFF_{LR}} \leq 1.3 ; \left(\frac{D}{T} \right)_L = K_{D1} \left[\frac{h}{D} \right]_{EFF_{LR}}^2 + K_{D2} \left[\frac{h}{D} \right]_{EFF_{LR}} + K_{D3} ;$$

$$\& \left(\frac{M}{T} \right)_L = K_{M1} \left[\frac{h}{D} \right]_{EFF_{LR}}^2 + K_{M2} \left[\frac{h}{D} \right]_{EFF_{LR}} + K_{M3}$$

$$\underline{\text{IF}}: \left[\frac{h}{D} \right]_{EFF_{LR}} > 1.3 ; \left(\frac{D}{T} \right)_L = K_{D4} ; \& \left(\frac{M}{T} \right)_L = K_{M4}$$

$$\underline{\text{IF}}: \left[\frac{h}{D} \right]_{EFF_{RR}} \leq 1.3 ; \left(\frac{D}{T} \right)_R = K_{D1} \left[\frac{h}{D} \right]_{EFF_{RR}}^2 + K_{D2} \left[\frac{h}{D} \right]_{EFF_{RR}} + K_{D3}$$

$$\& \left(\frac{M}{T} \right)_R = K_{M1} \left[\frac{h}{D} \right]_{EFF_{RR}}^2 + K_{M2} \left[\frac{h}{D} \right]_{EFF_{RR}} + K_{M3}$$

$$\underline{\text{IF}}: \left[\frac{h}{D} \right]_{EFF_{RR}} > 1.3 ; \left(\frac{D}{T} \right)_R = K_{D4} ; \& \left(\frac{M}{T} \right)_R = K_{M4}$$

WING A.C. TO ELASTIC AXIS TRANSFORM

PITCHING MOMENT

$$M_{AERO}^{RW} = C_{MSRW} q_{SRW} \frac{S_W}{Z} C_W - X_{WAC} Z_{AERO}^{RW} + Z_{WAC} X_{AERO}^{RW}$$

$$M_{AERO}^{LW} = C_{MSLW} q_{SLW} \frac{S_W}{Z} C_W - X_{WAC} Z_{AERO}^{LW} + Z_{WAC} X_{AERO}^{LW}$$

VERTICAL FORCES

$$Z_{AERO}^{RW'} = [-C_{LSRW} - C_{DSRW} \alpha'_{RWO}] q_{SRW} \frac{S_W}{Z}$$

$$Z_{AERO}^{LW'} = [-C_{LSLW} - C_{DSLW} \alpha'_{LWO}] q_{SLW} \frac{S_W}{Z}$$

NOTE: $Z_{AERO}^{RW'}$ & $Z_{AERO}^{LW'}$ ARE USED IN VERTICAL BENDING EQ.'S

WING FORCE & MOMENT RESOLUTION - BODY AXES @ C.G.

$$X_{AERO}^{LW} = [-C_{DSLW} + C_{LSLW} \alpha'_{LWO}] q_{SLW} \frac{S_w}{2}$$

$$X_{AERO}^{RW} = [-C_{DSRW} + C_{LSRW} \alpha'_{RWO}] q_{SRW} \frac{S_w}{2}$$

$$Y_{AERO}^{LW} = [-C_{DSLW} \beta_{LWO}] q_{SLW} \frac{S_w}{2}$$

$$Y_{AERO}^{RW} = [-C_{DSRW} \beta_{RWO}] q_{SRW} \frac{S_w}{2}$$

$$\left. \begin{array}{l} Z_{AERO}^{LW} \\ Z_{AERO}^{RW} \end{array} \right\} \text{FROM VERTICAL BENDING}$$

$$L_{AERO}^W = C_{Lsw} \bar{q}_s S_w b_w$$

$$M_{AERO}^W = M_{AERO}^{LW} + M_{AERO}^{RW} + X_{CG} (Z_{AERO}^{LW} + Z_{AERO}^{RW}) - Z_{CG} (X_{AERO}^{LW} + X_{AERO}^{RW})$$

$$N_{AERO}^W = C_{Nsw} \bar{q}_s S_w b_w$$

NOTE: OBSERVE WING EQUATION SPECIAL CONDITIONS

HORIZONTAL AND VERTICAL TAIL AERODYNAMICS

WING AND TAIL ALTITUDE ~ GROUND EFFECT

$$h_{wc/4} = -Z_{down} + (X_{wac} - X_{cg}) \sin \theta + (Z_{cg} - Z_{wac}) \cos \theta$$

$$h_{tc/4} = -Z_{down} + (X_{ht} - X_{cg}) \sin \theta + (Z_{cg} - Z_{ht}) \cos \theta$$

HORIZONTAL TAIL ANGLE OF ATTACK

$$l_{ac} = X_{wac} - X_{ht} \quad (\text{PRELIMINARY})$$

$$GEF = \left[b_w^2 + 4(h_{tc/4} - h_{wc/4})^2 \right] / \left[b_w^2 + 4(h_{tc/4} + h_{wc/4})^2 \right]$$

$$\underline{\text{IF:}} \quad \frac{\bar{E}_p (1-GEF)}{\sqrt{1-M^2}} \geq \left[E_0 + \frac{dE}{d\alpha} (\alpha_w - l_{ac} \frac{\dot{w}}{u^2}) \right] \frac{(1-GEF)}{\sqrt{1-M^2}}$$

$$E = \frac{\bar{E}_p (1-GEF)}{\sqrt{1-M^2}}$$

$$\underline{\text{IF:}} \quad \frac{\bar{E}_p (1-GEF)}{\sqrt{1-M^2}} < \left[E_0 + \frac{dE}{d\alpha} (\alpha_w - l_{ac} \frac{\dot{w}}{u^2}) \right] \frac{(1-GEF)}{\sqrt{1-M^2}}$$

$$E = \left[E_0 + \frac{dE}{d\alpha} (\alpha_w - l_{ac} \frac{\dot{w}}{u^2}) \right] \frac{(1-GEF)}{\sqrt{1-M^2}}$$

USE FOR
RESOLUTION
OF
FORCES

$$\alpha_{HT} = \tan^{-1} \left[\frac{W_{HT}}{U_{HT}} \right] - E + i_{HT}; \quad \text{NOTE: IF } U < 0 \quad \alpha_{HT} = \tan^{-1} \left[\frac{W_{HT}}{U_{HT}} \right] + i_{HT}$$

$$\text{WHERE } E_0 = f(\delta_L + \delta_R) \cdot 5 \quad \text{AND} \quad \frac{dE}{d\alpha} = f(\delta_L + \delta_R) \cdot 5$$

$$\underline{\text{IF:}} \quad |\alpha_{HT}| > 180^\circ;$$

$$\alpha_{HT} = -(\text{SIGN } \alpha_{HT}) 360^\circ + \alpha_{HT}$$

USE ONLY IN EQ. FOR FORCE AND
MOMENT COEFF.

HORIZONTAL AND VERTICAL TAIL AERODYNAMICS (CONT'D)

HORIZONTAL TAIL LIFT AND DRAG

$$\alpha_{eHT} = \alpha_{HT} + I_{HT} \delta_e$$

$$\hat{\alpha}_{HT+} = (\alpha_{HTSTALL} - 2^\circ) + I_{HT} \delta_e$$

$$\hat{\alpha}_{HT-} = -(\alpha_{HTSTALL} - 2^\circ) + I_{HT} \delta_e$$

$$C_{L\alpha} = C_{L\alpha_{HT}} \left(\frac{a_q}{a_{HT}} \right) / \sqrt{1-M^2}$$

$$\text{WHERE } \left(\frac{a_q}{a} \right)_{HT} = f(h_{TC/a}); \quad I_{HT} = f(s_e/s_T)$$

IF:- $\hat{\alpha}_{HT-} \leq \alpha_{eHT} \leq \hat{\alpha}_{HT+}$

$$C_{LHT} = C_{L\alpha} \alpha_{eHT}$$

$$C_{DHT} = C_{D0HT} + \frac{2C_{LHT}^2}{\pi R_{HT}}$$

IF:- $\hat{\alpha}_{HT+} < \alpha_{eHT} \leq 90^\circ$

$$C_{LHT} = C_{L\alpha} \hat{\alpha}_{HT+} \left[\frac{90^\circ - \alpha_{eHT}}{90^\circ - \hat{\alpha}_{HT+}} \right]$$

$$C_{LHTSTALL} = C_{L\alpha} \hat{\alpha}_{HT+}$$

$$C_{DHTSTALL} = C_{D0HT} + \frac{2C_{LHTSTALL}^2}{\pi R_{HT}}$$

$$C_{DHT} = C_{DHTSTALL} + \frac{(\alpha_{eHT} - \hat{\alpha}_{HT+})(1.1 - C_{DHTSTALL})}{90^\circ - \hat{\alpha}_{HT+}}$$

HORIZONTAL AND VERTICAL TAIL AERODYNAMICS (CONT'D)

HORIZONTAL TAIL LIFT AND DRAG (CONT'D)

IF:- $90^\circ < \alpha_{\text{HT}} < (180^\circ - .5 \hat{\alpha}_{\text{HT-}})$

$$C_{LHT} = .5 C_{L\alpha} \hat{\alpha}_{\text{HT-}} \frac{(\alpha_{\text{HT}} - 90^\circ)}{(90^\circ - .5 \hat{\alpha}_{\text{HT-}})}$$

$$C_{LHT\text{STALL}} = .5 C_{L\alpha} \hat{\alpha}_{\text{HT-}}$$

$$C_{DHT\text{STALL}} = \frac{2 C_{LHT\text{STALL}}^2}{\pi R_{\text{HT}}} + C_{D_{\text{OHT}}}$$

$$C_{DHT} = C_{DHT\text{STALL}} + \frac{(\alpha_{\text{HT}} + .5 \hat{\alpha}_{\text{HT-}} - 180^\circ)(1.1 - C_{DHT\text{STALL}})}{(.5 \hat{\alpha}_{\text{HT-}} - 90^\circ)}$$

IF:- $(180^\circ - .5 \hat{\alpha}_{\text{HT-}}) \leq \alpha_{\text{HT}} \leq 180^\circ$

$$C_{LHT} = C_{L\alpha} (\alpha_{\text{HT}} - 180^\circ)$$

$$C_{DHT} = C_{D_{\text{OHT}}} + \frac{2 C_{LHT}^2}{\pi R_{\text{HT}}}$$

IF:- $-90^\circ \leq \alpha_{\text{HT}} < \hat{\alpha}_{\text{HT-}}$

$$C_{LHT} = C_{L\alpha} \hat{\alpha}_{\text{HT-}} \frac{(-90^\circ - \alpha_{\text{HT}})}{(-90^\circ - \hat{\alpha}_{\text{HT-}})}$$

$$C_{LHT\text{STALL}} = C_{L\alpha} \hat{\alpha}_{\text{HT-}}$$

$$C_{DHT\text{STALL}} = C_{D_{\text{OHT}}} + \frac{2 C_{LHT\text{STALL}}^2}{\pi R_{\text{HT}}}$$

$$C_{DHT} = C_{DHT\text{STALL}} + \frac{(\alpha_{\text{HT}} - \hat{\alpha}_{\text{HT-}})(1.1 - C_{DHT\text{STALL}})}{(-90^\circ - \hat{\alpha}_{\text{HT-}})}$$

HORIZONTAL AND VERTICAL TAIL AERODYNAMICS (CONT'D)

HORIZONTAL TAIL LIFT AND DRAG (CONT'D)

IF:- $(-180^\circ + .5\hat{\alpha}_{HT}) < \alpha_{HT} < -90^\circ$

$$C_{LHT} = .5 C_{L\alpha} \hat{\alpha}_{HT} \frac{(\alpha_{HT} + 90^\circ)}{(-90^\circ + .5\hat{\alpha}_{HT})}$$

$$C_{LHTSTALL} = .5 C_{L\alpha} \hat{\alpha}_{HT}$$

$$C_{DHTSTALL} = C_{DHT} + \frac{2 C_{LHTSTALL}^2}{\pi R_{HT}}$$

$$C_{DHT} = C_{DHTSTALL} - \frac{(\alpha_{HT} + 180^\circ - .5\hat{\alpha}_{HT})(1.1 - C_{DHTSTALL})}{(.5\hat{\alpha}_{HT} - 90^\circ)}$$

IF:- $-180^\circ \leq \alpha_{HT} < (-180^\circ + .5\hat{\alpha}_{HT})$

$$C_{LHT} = C_{L\alpha} (\alpha_{HT} + 180^\circ)$$

$$C_{DHT} = C_{DHT} + \frac{2 C_{LHT}^2}{\pi R_{HT}}$$

HORIZONTAL AND VERTICAL TAIL AERODYNAMICS (CONT'D)

VERTICAL TAIL AERODYNAMICS

VERTICAL TAIL ANGLE OF ATTACK AND SIDESLIP

$$\beta_{VT} = \tan^{-1} \frac{v_{VT}}{\sqrt{u_{VT}^2 + w_{VT}^2}}$$

$$\alpha_{VT} = -\beta_{VT} + \beta_f \left(\frac{d\sigma}{d\beta} \right) \quad \left\{ \begin{array}{l} \text{NOTE: THIS VALUE OF } \alpha_{VT} \text{ IS USED IN RESOLUTION} \\ \text{OF FORCES AND MOMENTS} \end{array} \right\}$$

$$\text{IF: } |\alpha_{VT}| > 180^\circ; \alpha_{VT} = \alpha_{VT} - (\text{SIGN } \alpha_{VT} \times 360^\circ) \quad \left\{ \begin{array}{l} \text{NOTE: THIS VALUE OF } \alpha_{VT} \text{ ONLY USED} \\ \text{IN CALC. OF FORCE AND} \\ \text{MOMENT COEFFICIENTS} \end{array} \right\}$$

$$\alpha_{eVT} = (\alpha_{VT} + i_{VT} \delta_{rud})$$

$$\hat{\alpha}_{VT+} = (\alpha_{VT_{stall}} - 2^\circ) + i_{VT} \delta_{rud}$$

$$\hat{\alpha}_{VT-} = -(\alpha_{VT_{stall}} - 2^\circ) + i_{VT} \delta_{rud}$$

$$C_{Y\alpha} = C_{Y\alpha_{VT}} / \sqrt{1-M^2}$$

TAIL DYNAMIC PRESSURE AND SIDESLASH

$$\bar{q} = \frac{\rho}{2} (u^2 + v^2 + w^2)$$

$$\sigma = \frac{d\sigma}{d\beta} \beta_f$$

VERTICAL TAIL LIFT AND DRAG

$$\text{IF: } \hat{\alpha}_{VT-} \leq \alpha_{eVT} \leq \hat{\alpha}_{VT+}$$

$$C_{YVT} = C_{Y\alpha} \alpha_{eVT}$$

$$C_{DVT} = C_{D_{OUT}} + \frac{2 C_{YVT}^2}{\pi A_{VT}}$$

HORIZONTAL AND VERTICAL TAIL AERODYNAMICS (CONT'D)

VERTICAL TAIL LIFT AND DRAG (CONT'D)

IF:- $\hat{\alpha}_{VT+} < \alpha_{EVT} < 90^\circ$

$$C_{YVT} = C_{Y\alpha} \hat{\alpha}_{VT+} \left[\frac{90^\circ - \alpha_{EVT}}{90^\circ - \hat{\alpha}_{VT+}} \right]$$

$$C_{YVTSTALL} = C_{Y\alpha} \hat{\alpha}_{VT+}$$

$$C_{DVTSTALL} = C_{D0VT} + \frac{2 C_{YVTSTALL}^2}{\pi R_{VT}}$$

$$C_{DVT} = C_{DVTSTALL} + \frac{(\alpha_{EVT} - \hat{\alpha}_{VT+}) \times 1.1 - C_{DVTSTALL}}{90^\circ - \hat{\alpha}_{VT+}}$$

IF:- $90^\circ < \alpha_{EVT} \leq (180^\circ - .5 \hat{\alpha}_{VT-})$

$$C_{YVT} = .5 C_{Y\alpha} \hat{\alpha}_{VT-} \left(\frac{\alpha_{EVT} - 90^\circ}{90^\circ - .5 \hat{\alpha}_{VT-}} \right)$$

$$C_{YVTSTALL} = .5 C_{Y\alpha} \hat{\alpha}_{VT-}$$

$$C_{DVTSTALL} = C_{D0VT} + \frac{2 C_{YVTSTALL}^2}{\pi R_{VT}}$$

$$C_{DVT} = C_{DVTSTALL} + \frac{(\alpha_{EVT} + .5 \hat{\alpha}_{VT-} - 180^\circ) \times 1.1 - C_{DVTSTALL}}{(.5 \hat{\alpha}_{VT-} - 90^\circ)}$$

IF:- $(180^\circ - .5 \hat{\alpha}_{VT-}) \leq \alpha_{EVT} \leq 180^\circ$

$$C_{YVT} = C_{Y\alpha} (\alpha_{EVT} - 180^\circ)$$

$$C_{DVT} = C_{D0VT} + \frac{2 C_{YVT}^2}{\pi R_{VT}}$$

HORIZONTAL AND VERTICAL TAIL AERODYNAMICS (CONT'D)

VERTICAL TAIL LIFT AND DRAG (CONT'D)

IF:- $-90^\circ \leq \alpha_{eVT} < \hat{\alpha}_{VT-}$

$$C_{YVT} = C_{Y\alpha} \hat{\alpha}_{VT-} \frac{(-90^\circ - \alpha_{eVT})}{(-90^\circ - \hat{\alpha}_{VT-})}$$

$$C_{YVT\text{STALL}} = C_{Y\alpha} \hat{\alpha}_{VT-}$$

$$C_{DVT\text{STALL}} = C_{D0VT} + \frac{2 C_{YVT\text{STALL}}^2}{\pi R_{VT}}$$

$$C_{DVT} = C_{DVT\text{STALL}} + \frac{(\alpha_{eVT} - \hat{\alpha}_{VT-})(1.1 - C_{DVT\text{STALL}})}{(-90^\circ - \hat{\alpha}_{VT-})}$$

IF:- $(-180^\circ + .5 \hat{\alpha}_{VT+}) < \alpha_{eVT} < -90^\circ$

$$C_{YVT} = .5 C_{Y\alpha} \hat{\alpha}_{VT+} \frac{(\alpha_{eVT} + 90^\circ)}{(-90^\circ + .5 \hat{\alpha}_{VT+})}$$

$$C_{YVT\text{STALL}} = .5 C_{Y\alpha} \hat{\alpha}_{VT+}$$

$$C_{DVT\text{STALL}} = C_{D0VT} + \frac{2 C_{YVT\text{STALL}}^2}{\pi R_{VT}}$$

$$C_{DVT} = C_{DVT\text{STALL}} - \frac{(\alpha_{eVT} + 180^\circ - .5 \hat{\alpha}_{VT+})(1.1 - C_{DVT\text{STALL}})}{(.5 \hat{\alpha}_{VT+} - 90^\circ)}$$

IF:- $-180^\circ \leq \alpha_{eVT} < (-180^\circ + .5 \hat{\alpha}_{VT+})$

$$C_{YVT} = C_{Y\alpha} (\alpha_{eVT} + 180^\circ)$$

$$C_{DVT} = C_{D0VT} + \frac{2 C_{YVT}^2}{\pi R_{VT}}$$

HORIZONTAL AND VERTICAL TAIL AERODYNAMICS (CONT'D)

TAIL EQUATIONS LOGIC

HORIZONTAL TAIL

1. IF $hw_{CH} > 100 \text{ FT.}$, SET $GEF = 0.0$
2. IF THE UMBRELLAS OPEN; SET $\epsilon = \frac{\bar{G}_P (1 - GEP)}{\sqrt{1 - M^2}}$
3. IF $\alpha_{ENT} > \hat{\alpha}_{HT+}$ PRINT STALL WARNING.
4. IF $\alpha_{ENT} < \hat{\alpha}_{HT-}$ PRINT STALL WARNING

VERTICAL TAIL

1. IF $\alpha_{VT} > \hat{\alpha}_{VT+}$ PRINT STALL WARNING
2. IF $\alpha_{VT} < \hat{\alpha}_{VT-}$ PRINT STALL WARNING

TAIL FORCE AND MOMENT RESOLUTION TO C.G.

HORIZONTAL TAIL

NOTE: - IF UMBRELLAS OPEN AND $M > 0$; SET $\eta_{HT} = 0.5 \eta_{NT}$

$$X_{AERO}^{HT} = [-C_{DHT} \cos(\alpha_{HT} - i_{HT}) \cos(\beta_{VT} - \sigma) + C_{LHT} \sin(\alpha_{HT} - i_{HT})] \bar{q} S_{HT} \eta_{HT}$$

$$Y_{AERO}^{HT} = [-C_{DHT} \sin(\beta_{VT} - \sigma)] \bar{q} S_{HT} \eta_{HT}$$

$$Z_{AERO}^{HT} = [-C_{LHT} \cos(\alpha_{HT} - i_{HT}) - C_{DHT} \cos(\beta_{VT} - \sigma) \sin(\alpha_{HT} - i_{HT})] \bar{q} S_{HT} \eta_{HT}$$

$$\mathcal{L}_{AERO}^{HT} = -Y_{AERO}^{HT} (Z_{HT} - Z_{CG})$$

$$M_{AERO}^{HT} = Z_{AERO}^{HT} (X_{CG} - X_{HT}) + X_{AERO}^{HT} (Z_{HT} - Z_{CG})$$

$$\eta_{AERO}^{HT} = -Y_{AERO}^{HT} (X_{CG} - X_{HT})$$

VERTICAL TAIL

$$X_{AERO}^{VT} = [-C_{DVT} \cos(\beta_{VT} - \sigma) \cos(\alpha_{HT} - i_{HT}) - C_{YVT} \sin(\beta_{VT} - \sigma) \cos(\alpha_{HT} - i_{HT})] \bar{q} S_{VT} \eta_{VT}$$

$$Y_{AERO}^{VT} = [C_{YVT} \cos(\beta_{VT} - \sigma) - C_{DVT} \sin(\beta_{VT} - \sigma)] \bar{q} S_{VT} \eta_{VT}$$

$$Z_{AERO}^{VT} = [-C_{DVT} \cos(\beta_{VT} - \sigma) \sin(\alpha_{HT} - i_{HT}) - C_{YVT} \sin(\beta_{VT} - \sigma) \sin(\alpha_{HT} - i_{HT})] \bar{q} S_{VT} \eta_{VT}$$

$$\mathcal{L}_{AERO}^{VT} = -Y_{AERO}^{VT} (Z_{VT} - Z_{CG})$$

$$M_{AERO}^{VT} = Z_{AERO}^{VT} (X_{CG} - X_{VT}) + X_{AERO}^{VT} (Z_{VT} - Z_{CG})$$

$$\eta_{AERO}^{VT} = -Y_{AERO}^{VT} (X_{CG} - X_{VT})$$

TOTAL TAIL CONTRIBUTION

$$X_{AERO}^T = X_{AERO}^{VT} + X_{AERO}^{HT} ; Z_{AERO}^T = Z_{AERO}^{VT} + Z_{AERO}^{HT} \quad M_{AERO}^T = M_{AERO}^{VT} + M_{AERO}^{HT}$$

$$Y_{AERO}^T = Y_{AERO}^{VT} + Y_{AERO}^{HT} ; \mathcal{L}_{AERO}^T = \mathcal{L}_{AERO}^{VT} + \mathcal{L}_{AERO}^{HT} \quad \eta_{AERO}^T = \eta_{AERO}^{VT} + \eta_{AERO}^{HT}$$

NACELLE AERODYNAMICS

NACELLE ANGLE OF ATTACK AND SIDESLIP

$$\alpha_{RN} = \tan^{-1} \frac{W_{RR}}{U_{RR}}$$

$$; q_{RN} = \frac{1}{2} \rho V_{RR}^2$$

$$\alpha_{LN} = \tan^{-1} \frac{W_{RL}}{U_{RL}}$$

$$; q_{LN} = \frac{1}{2} \rho V_{LR}^2$$

$$\beta_{RN} = \tan^{-1} \frac{V_{RR}}{\sqrt{U_{RR}^2 + W_{RR}^2}}$$

$$\beta_{LN} = \tan^{-1} \frac{V_{RL}}{\sqrt{U_{RL}^2 + W_{RL}^2}}$$

NACELLE WIND AXIS FORCE & MOMENT COEF.'S

$$\left. \begin{aligned} C_{DRN} &= C_{DORN} + K_{30} |\alpha_{RN}| + K_{31} |\alpha_{RN}|^2 \\ C_{DLN} &= C_{DOLN} + K_{30} |\alpha_{LN}| + K_{31} |\alpha_{LN}|^2 \end{aligned} \right\} \begin{array}{l} \text{NOTE: CHECK RANGE} \\ \text{OF } \alpha_{RN} \text{ \& } \alpha_{LN} \text{ TO} \\ \text{DETERMINE VALUES FOR} \\ \text{CONSTANTS.} \end{array}$$

$$\text{WHERE: } C_{DORN} = C_{DON}$$

$$C_{DOLN} = C_{DON}$$

$$C_{LRN} = K_{32} \sin \alpha_{RN} \cos \alpha_{RN}$$

$$C_{LLN} = K_{32} \sin \alpha_{LN} \cos \alpha_{LN}$$

$$C_{MNRN} = C_{MON} + K_{34} \sin \alpha_{RN} \cos \alpha_{RN} + K_{35} (\sin \alpha_{RN} \cos \alpha_{RN}) |\sin \alpha_{RN} \cos \alpha_{RN}|$$

$$C_{MLN} = C_{MON} + K_{34} \sin \alpha_{LN} \cos \alpha_{LN} + K_{35} (\sin \alpha_{LN} \cos \alpha_{LN}) |\sin \alpha_{LN} \cos \alpha_{LN}|$$

SPECIAL CONDITIONS

1. IF: $V_{RR}^2 \leq 1 (\text{ft/sec})^2$; RIGHT NACELLE AERO $\equiv 0.0$ & HOLD VALUE OF α_{RN} & β_{RN}
2. IF: $V_{LR}^2 \leq 1 (\text{ft/sec})^2$; LEFT NACELLE AERO $\equiv 0.0$ & HOLD VALUE OF α_{LN} & β_{LN}

NACELLE AERODYNAMICS (Cont'd.)

$$C_{YRN} = K_{36} \sin \beta_{RN} \cos \beta_{RN} + K_{37} (\sin \beta_{RN} \cos \beta_{RN}) |\sin \beta_{RN} \cos \beta_{RN}|$$

$$C_{YLN} = K'_{36} \sin \beta_{LN} \cos \beta_{LN} + K'_{37} (\sin \beta_{LN} \cos \beta_{LN}) |\sin \beta_{LN} \cos \beta_{LN}|$$

$$C_{NRN} = C_{NORN} + K_{38} \sin \beta_{RN} \cos \beta_{RN} + K_{39} (\sin \beta_{RN} \cos \beta_{RN}) |\sin \beta_{RN} \cos \beta_{RN}|$$

$$C_{NLN} = C_{NOLN} + K'_{38} \sin \beta_{LN} \cos \beta_{LN} + K'_{39} (\sin \beta_{LN} \cos \beta_{LN}) |\sin \beta_{LN} \cos \beta_{LN}|$$

$$C_{XRN} = C_{ZLN} \equiv 0.0$$

NACELLE FORCES & MOMENTS - NACELLE AXES

RIGHT

$$\Delta X'_{RN} = q_{RN} S_w \left[-C_{DRN} \cos \alpha_{RN} + C_{LRN} \sin \alpha_{RN} - C_{YRN} \sin \beta_{RN} \cos \alpha_{RN} \right] \frac{1}{2}$$

$$\Delta Y'_{RN} = q_{RN} S_w \left[C_{YRN} \cos \beta_{RN} - C_{DRN} \sin \beta_{RN} \right] \frac{1}{2}$$

$$\Delta Z'_{RN} = q_{RN} S_w \left[-C_{LRN} \cos \alpha_{RN} - C_{DRN} \cos \beta_{RN} \sin \alpha_{RN} - C_{YRN} \sin \beta_{RN} \sin \alpha_{RN} \right] \frac{1}{2}$$

$$\Delta L'_{RN} = q_{RN} S_w b_w \left[-\left(\frac{C_w}{b_w}\right) C_{MRN} \sin \beta_{RN} \cos \alpha_{RN} - C_{NRN} \sin \alpha_{RN} \right] \frac{1}{2}$$

$$\Delta M'_{RN} = q_{RN} S_w C_w \left[C_{MRN} \cos \beta_{RN} \right] \frac{1}{2}$$

$$\Delta N'_{RN} = q_{RN} S_w b_w \left[C_{NRN} \cos \alpha_{RN} - \left(\frac{C_w}{b_w}\right) C_{MRN} \sin \beta_{RN} \cos \alpha_{RN} \right] \frac{1}{2}$$

LEFT

$$\Delta X'_{LN} = q_{LN} S_w \left[-C_{DLN} \cos \alpha_{LN} + C_{LLN} \sin \alpha_{LN} - C_{YLN} \sin \beta_{LN} \cos \alpha_{LN} \right] \frac{1}{2}$$

$$\Delta Y'_{LN} = q_{LN} S_w \left[C_{YLN} \cos \beta_{LN} - C_{DLN} \sin \beta_{LN} \right] \frac{1}{2}$$

$$\Delta Z'_{LN} = q_{LN} S_w \left[-C_{LLN} \cos \alpha_{LN} - C_{DLN} \cos \beta_{LN} \sin \alpha_{LN} - C_{YLN} \sin \beta_{LN} \sin \alpha_{LN} \right] \frac{1}{2}$$

$$\Delta L'_{LN} = q_{LN} S_w b_w \left[-\left(\frac{C_w}{b_w}\right) C_{MLN} \sin \beta_{LN} \cos \alpha_{LN} - C_{NLN} \sin \alpha_{LN} \right] \frac{1}{2}$$

$$\Delta M'_{LN} = q_{LN} S_w C_w \left[C_{MLN} \cos \beta_{LN} \right] \frac{1}{2}$$

$$\Delta N'_{LN} = q_{LN} S_w b_w \left[C_{NLN} \cos \alpha_{LN} - \left(\frac{C_w}{b_w}\right) C_{MLN} \sin \beta_{LN} \cos \alpha_{LN} \right] \frac{1}{2}$$

LANDING GEAR EQUATIONS

PERFORM THE FOLLOWING CALCULATIONS FOR EACH OF THREE LANDING GEAR i.e. $n = 1, 2, 3$.

LANDING GEAR-A/C LOCATION

$$X_n = -X_{CG} + X_{Gn}$$

$$Y_n = Y_{Gn}$$

$$Z_n = -Z_{CG} + Z_{Gn}$$

$n=1$ LEFT MAIN GEAR

$n=2$ RIGHT MAIN GEAR

$n=3$ NOSE GEAR

Strut Deflection

$$h_{Gn} = X_n \sin \theta - Z_n \cos \theta - r_n$$

$$h_{Gpn} = [Y_n \sin \phi + (Z_n + r_n)(\cos \phi - 1)] \cos \theta$$

$$h_{Tn} = (-Z_{down} + h_{Gn} - h_{Gpn}) / (\cos \phi \cos \theta)$$

Rate of Strut Deflection

$$\dot{h}_{Tn} = -\dot{Z}_{down} \left(\frac{1}{\cos \phi \cos \theta} \right) + X_n q - Y_n p$$

Vertical force

$$F_{Gzn} = K_{STn} h_{Tn} + D_{STn} \dot{h}_{Tn}$$

NOTE: COMPUTE F_{Gzn} ONLY IF $h_{Tn} < 0$;

IF $h_{Tn} > 0$; $F_{Gzn} = 0.0$

REMAINING CALCULATIONS MAY BE SET
TO ZERO.

LANDING GEAR EQUATIONS (cont'd.)

Longitudinal force:

$$F_{Ln} = + (\mu_0 + \mu_1 B_{Ln}) F_{Gzn} \frac{+u}{|u|}$$

i.e. IF $u > 0$ F_{Ln} is negative
IF $u < 0$ F_{Ln} is positive
IF $u = 0$ $F_{Ln} \equiv 0.0$

NOTE: B_{Ln} is percent brake pedal deflection

Side force:

$$F_{Sn} = \mu_s F_{Gzn} \frac{+v}{|v|}$$

i.e. IF $v > 0$ F_{Sn} is negative
IF $v < 0$ F_{Sn} is positive
IF $v = 0$ $F_{Sn} = 0.0$

FORCE & MOMENT CONTRIBUTION OF EACH GEAR

$$\Delta X_n = F_{Ln} - F_{Gzn} \theta$$

$$\Delta Y_n = F_{Sn} + F_{Gzn} \phi$$

$$\Delta Z_n = F_{Ln} \theta - F_{Sn} \phi + F_{Gzn}$$

$$\Delta M_n = -\Delta Z_n X_n + \Delta X_n (Z_n + r_n + h_{Tn})$$

$$\Delta L_n = \Delta Z_n Y_n - \Delta Y_n (Z_n + r_n + h_{Tn})$$

$$\Delta N_n = -\Delta X_n Y_n + X_n \Delta Y_n$$

LANDING GEAR EQUATIONS (Cont'd.)

$$\Delta X_{LG} = \sum_1^3 \Delta X_n$$

$$\Delta Y_{LG} = \sum_1^3 \Delta Y_n$$

$$\Delta Z_{LG} = \sum_1^3 \Delta Z_n$$

$$\Delta \alpha_{LG} = \sum_1^3 \Delta \alpha_n$$

$$\Delta m_{LG} = \sum_1^3 \Delta m_n$$

$$\Delta n_{LG} = \sum_1^3 \Delta n_n$$

FUSELAGE AERODYNAMICS

FUSELAGE INPUT EQUATIONS

$$\alpha_F = \tan^{-1} \frac{W}{U}$$

$$\beta_F = \tan^{-1} \frac{V}{\sqrt{U^2 + W^2}}$$

$$\alpha'_F = \sin \alpha_F \cos \alpha_F$$

$$\beta'_F = \sin \beta_F \cos \beta_F$$

$$V_F = \sqrt{U^2 + V^2 + W^2}$$

$$q_F = \frac{1}{2} \rho V_F^2$$

(q) SAME AS TAIL DYNAMIC PRESSURE

$$V_{FUS} = V_F \sqrt{\sigma_h}$$

FUSELAGE WIND AXIS COEF'S

$$C_{DF} = C_{DOF} (1 + K_0 |\beta_F|^3) + K_2 \alpha_F^2 + K_1 |\alpha_F| + \Delta C_{DLG}$$

$$C_{LF} = K_3 \alpha'_F + K_4 \alpha'_F |\alpha'_F| + K_{42}$$

$$C_{YF} = K_7 \beta'_F + K_8 \beta'_F |\beta'_F|$$

$$C_{MF} = C_{MOF} + K_5 \alpha'_F + K_6 \alpha'_F |\alpha'_F| + \Delta C_{MLG}$$

$$C_{NF} = C_{NOF} + K_9 \beta'_F + K_{10} \beta'_F |\beta'_F|$$

NOTE: IF GEAR IS UP; $\Delta C_{DLG} \neq \Delta C_{MLG} = 0.0$

SPECIAL CONDITIONS

1. IF $V_F^2 \leq 1 \text{ (ft/sec)}^2$ FUSELAGE AERO = 0.0 \neq
HOLD VALUE OF $\alpha_F \neq \beta_F$

FUSELAGE FORCES & MOMENT ABOUT A/C C.G.

$$X_{AERO}^{F'} = [-C_{DF} \cos \alpha_F + C_{LF} \sin \alpha_F - C_{YF} \sin \beta_F \cos \alpha_F] q_F S_w$$

$$Y_{AERO}^{F'} = [C_{YF} \cos \beta_F - C_{DF} \sin \beta_F] q_F S_w$$

$$Z_{AERO}^{F'} = [-C_{LF} \cos \alpha_F - C_{DF} \cos \beta_F \sin \alpha_F - C_{YF} \sin \beta_F \sin \alpha_F] q_F S_w$$

$$\begin{aligned} \mathcal{L}_{AERO}^{F'} = & \left[-\left(\frac{C_w}{b_w}\right) C_{MF} \sin \beta_F \cos \alpha_F - C_{NF} \sin \alpha_F \right] q_F S_w b_w + \\ & + Y_{AERO}^{F'} [Z_{CG} - Z_{FAC}] \end{aligned}$$

$$\begin{aligned} \mathcal{M}_{AERO}^{F'} = & [C_{MF} \cos \beta_F] q_F S_w C_w + Z_{AERO}^{F'} [X_{CG} - X_{FAC}] \\ & - X_{AERO}^{F'} [Z_{CG} - Z_{FAC}] + \end{aligned}$$

$$\begin{aligned} \mathcal{N}_{AERO}^{F'} = & [C_{NF} \cos \alpha_F - \left(\frac{C_w}{b_w}\right) C_{MF} \sin \beta_F \sin \alpha_F] q_F S_w b_w \\ & - Y_{AERO}^{F'} [X_{CG} - X_{FAC}] + \end{aligned}$$

$$X_{AERO}^F = X_{AERO}^{F'} + \Delta X_{LG}$$

$$Y_{AERO}^F = Y_{AERO}^{F'} + \Delta Y_{LG}$$

$$Z_{AERO}^F = Z_{AERO}^{F'} + \Delta Z_{LG}$$

$$\mathcal{L}_{AERO}^F = \mathcal{L}_{AERO}^{F'} + \Delta \mathcal{L}_{LG}$$

$$\mathcal{M}_{AERO}^F = \mathcal{M}_{AERO}^{F'} + \Delta \mathcal{M}_{LG}$$

$$\mathcal{N}_{AERO}^F = \mathcal{N}_{AERO}^{F'} + \Delta \mathcal{N}_{LG}$$

WING ON ROTOR INTERFERENCE

AVERAGE NACELLE INCIDENCE

$$\bar{i}_N = 0.5 (i_{NL} + i_{NR})$$

AVERAGE LIFT COEF.

$$C_{LW} = 0.5 \frac{(C_{LSRW} + C_{LSLW})}{(1 - \bar{C}_{TS})}$$

LOOK-UP: E_{WRR} & E_{WRL} @ \bar{i}_N & C_{LW}

WING INTERFERENCE LOGIC

1. IF: UMBRELLAS OPEN, SET $C_{LW} = 0.0$ & $E = \frac{E_p(1 - GEP)}{\sqrt{1 - M^2}}$

ROTOR / ROTOR INTERFERENCE

POSITIVE SIDESLIP i.e., $v > 0.0$ (LOGIC REQUIRED)

$$\chi = 1.5708 - \epsilon_{PRR}$$

$$\left(\frac{\delta v_{RL}^*}{v_{RR}^*} \right) = T_1 + T_2(\chi) + T_3(\chi)^2$$

$$\delta v_{RL} = \left(\frac{\delta v_{RL}^*}{v_{RR}^*} \right) v_{RR} \sqrt{\frac{R_{RR}}{2\rho\pi R^2}}$$

$$\epsilon'_{iRL} = -\tan^{-1} \left[\frac{\delta v_{RL}}{v_{LR} + 1.0} \right]$$

$$\epsilon_{iRL} = (|\beta_F|)(.40528 i_{NL}) \epsilon'_{iRL}$$

$$\epsilon_{iLR} = 0.0$$

NEGATIVE SIDESLIP i.e. $v < 0.0$

$$\chi = 1.5708 - \epsilon_{PLR}$$

$$\left(\frac{\delta v_{LR}^*}{v_{LR}^*} \right) = T_1 + T_2(\chi) + T_3(\chi)^2$$

$$\delta v_{LR} = \left(\frac{\delta v_{LR}^*}{v_{RR}^*} \right) v_{NL} \sqrt{\frac{R_{LR}}{2\rho\pi R^2}}$$

$$\epsilon'_{iLR} = -\tan^{-1} \left[\frac{\delta v_{LR}}{v_{RR} + 1.0} \right]$$

$$\epsilon_{iLR} = (|\beta_F|)(.40528 i_{NR}) \epsilon'_{iLR}$$

$$\epsilon_{iRL} = 0.0$$

NOTE: $v_{RR} \neq v_{NL}$ FROM WING EQUATIONS.

ROTOR AERO INPUT EQUATIONS

RIGHT ROTOR

$$\alpha_{RR} = \tan^{-1} \left\{ \frac{\sqrt{V_{RR}^2 + (W_{RR} + U_{RR} \epsilon_{WRR})^2}}{U_{RR}} \right\} + \epsilon_{iLR}$$

$$V_{RR} = \sqrt{U_{RR}^2 + V_{RR}^2 + W_{RR}^2} \quad ; \quad \mu_{RR} = \frac{V_{RR}}{\Omega_R R}$$

LEFT ROTOR

$$\alpha_{LR} = \tan^{-1} \left\{ \frac{\sqrt{V_{RL}^2 + (W_{RL} + U_{RL} \epsilon_{WRL})^2}}{U_{RL}} \right\} + \epsilon_{iLR}$$

$$V_{LR} = \sqrt{U_{RL}^2 + V_{RL}^2 + W_{RL}^2} \quad ; \quad \mu_{LR} = \frac{V_{LR}}{\Omega_L R}$$

ROTOR ANGULAR RATE TRANSFORMS

RIGHT - NACELLE AXES

$$P_{NR}^N = -p \cos i_{NR} + r \sin i_{NR}$$

$$Q_{NR}^N = q + \dot{i}_{NR}$$

$$R_{NR}^N = -r \cos i_{NR} - p \sin i_{NR}$$

LEFT - NACELLE AXES

$$P_{NL}^N = p \cos i_{NL} - r \sin i_{NL}$$

$$Q_{NL}^N = q + \dot{i}_{NL}$$

$$R_{NL}^N = r \cos i_{NL} + p \sin i_{NL}$$

RIGHT WIND AXES

$$P_{NR}^R = P_{NR}^N$$

$$Q_{NR}^R = Q_{NR}^N \cos \beta_{HR} + R_{NR}^N \sin \beta_{HR}$$

$$R_{NR}^R = R_{NR}^N \cos \beta_{NR} - Q_{NR}^N \sin \beta_{NR}$$

LEFT WIND AXES

$$P_{NL}^R = P_{NL}^N$$

$$Q_{NL}^R = Q_{NL}^N \cos \beta_{HL} - R_{NL}^N \sin \beta_{HL}$$

$$R_{NL}^R = R_{NL}^N \cos \beta_{NL} + Q_{NL}^N \sin \beta_{NL}$$

NOTE: USE WIND AXIS RATES IN ROTOR ROUTINE

ROTOR EQUATIONS

RIGHT ROTOR

THRUST

$$C'_{TRR} = \left[\frac{Z_1 S + 1}{Z_2 S + 1} \right] \left[C_{TORR} \cos A_{IGR} \cos B_{IOR} \right]$$

WHERE:-

$$C_{TORR} = \sum_{N=0}^2 \sum_{U=0}^3 \left[A_{T(U+4N)} \propto_{RR}^U \theta_{GTSR}^N \right] \left. \begin{array}{l} \text{INTERPOLATE } C_{TORR} \\ \text{LINEARLY BETWEEN } \mu\text{'S} \end{array} \right\}$$

$$A_{T(U+4N)} = f(\mu_{RR})$$

GROUND EFFECT

$$h_{RR} = -Z_{DOWN} + (L_S \cos i_{NR} - X_{CG}) \sin \theta \\ + \left[(L_S \sin i_{NR} + Z_{CG}) \cos \phi - Y_N \sin \phi \right] \cos \theta$$

$$\left(\frac{h}{D} \right)_{EFF_{RR}} = \frac{h_{RR}}{2R \left[|\sin(\theta + i_{NR}) \cos \phi| + 0.0174 \right]}$$

$$\left(\frac{T_{IGE}}{T_{OGE}} \right)_{RR} = \left[\left(\frac{h}{D} \right)_{EFF_{RR}}^2 (.1741 - .6216 \mu_{RR}) \right. \\ \left. + \left(\frac{h}{D} \right)_{EFF_{RR}} (1.4779 \mu_{RR} - .4143) \right. \\ \left. + 1.2474 - .8806 \mu_{RR} \right]$$

$$C_{TRR} = C'_{TRR} \left(\frac{T_{IGE}}{T_{OGE}} \right)_{RR}$$

SPECIAL CONDITIONS: IF $\mu_{RR} \geq 0.203$; $\left(\frac{T_{IGE}}{T_{OGE}} \right)_{RR} = 1.0$

OR IF $\left(\frac{h}{D} \right)_{EFF_{RR}} \geq 1.3$; $\left(\frac{T_{IGE}}{T_{OGE}} \right)_{RR} = 1.0$

ROTOR EQUATIONS (CONTINUOUS)

POWER

$$C_{PRR} = C_{PORR}$$

WHERE:-

$$C_{PORR} = \sum_{N=0}^2 \sum_{u=0}^3 \left[A_P(u+4N) \alpha_{RR}^u C_{TRR}'^N \right] \left. \begin{array}{l} \text{INTERPOLATE } C_{PORR} \\ \text{LINEARLY BETWEEN } \mu\text{'s} \end{array} \right\}$$

$$A_P(u+4N) = f(\mu_{RR})$$

NORMAL FORCE

$$C_{NFRR} = C_{NFORR} + \frac{dC_{NFR}}{dA_{ICR}} A_{ICR} + \frac{dC_{NFR}}{dB_{ICR}} B_{ICR}$$

WHERE:-

$$C_{NFORR} = \sum_{N=0}^2 \sum_{u=0}^3 \left[A_{NF}(u+4N) \alpha_{RR}^u C_{TRR}'^N \right] \left. \begin{array}{l} \text{INTERPOLATE } C_{NFORR} \\ \text{LINEARLY BETWEEN} \\ \mu\text{'s} \end{array} \right\}$$

$$A_{NF}(u+4N) = f(\mu_{RR})$$

$$\frac{dC_{NFR}}{dA_{ICR}} = D_{NF1} C_{TRR} + D_{NF2} \mu_{RR}^2 + D_{NF3} \mu_{RR} + D_{NF4}$$

$$\frac{dC_{NFR}}{dB_{ICR}} = E_{NF1} C_{TRR} + E_{NF2} \mu_{RR}^2 + E_{NF3} \mu_{RR} + E_{NF4}$$

ROTOR EQUATIONS (CONTINUED)

SIDE FORCE

$$C_{SF_{RR}} = C_{SF_{ORR}} + \frac{dC_{SF_{RR}}}{dA_{ICR}} A_{ICR} + \frac{dC_{SF_{RR}}}{dB_{ICR}} B_{ICR}$$

WHERE:-

$$C_{SF_{ORR}} = \sum_{N=0}^2 \sum_{u=0}^3 \left[A_{SF}(u+4N) \alpha_{RR}^u C_{TRR}^{IN} \right] \left. \vphantom{\sum_{N=0}^2 \sum_{u=0}^3} \right\} \begin{array}{l} \text{INTERPOLATE } C_{SF_{ORR}} \\ \text{LINEARLY} \\ \text{BETWEEN } \mu\text{'S} \end{array}$$

$$A_{SF}(u+4N) = f(\mu_{RR})$$

$$\frac{dC_{SF_{RR}}}{dA_{ICR}} = D_{SF1} C_{TRR} + D_{SF2} \mu_{RR}^2 + D_{SF3} \mu_{RR} + D_{SF4}$$

$$\frac{dC_{SF_{RR}}}{dB_{ICR}} = E_{SF1} C_{TRR} + E_{SF2} \mu_{RR}^2 + E_{SF3} \mu_{RR} + E_{SF4}$$

ROTOR EQUATIONS (CONTINUED)

HUB PITCHING MOMENT

$$C_{PMRQ} = C_{PMORR} + \frac{dC_{PMORR}}{dA_{ICR}} A_{ICR} + \frac{dC_{PMORR}}{dB_{ICR}} B_{ICR} + \frac{dC_{PMORR}}{dQ} Q_{NR}^R$$

WHERE:-

$$C_{PMORR} = \sum_{N=0}^2 \sum_{u=0}^3 \left[A_{PM}(u+4\pi) \alpha_{RR}^u C_{TRR}'^N \right]$$

$$A_{PM}(u+4\pi) = f(\mu_{RR})$$

$$\frac{dC_{PMORR}}{dQ} = \sum_{N=0}^2 \sum_{u=0}^3 \left[H_{PM}(u+4\pi) \alpha_{RR}^u C_{TRR}'^N \right]$$

$$H_{PM}(u+4\pi) = f(\mu_{RR})$$

INTERPOLATE
C_{PMORR} AND
 $\frac{dC_{PMORR}}{dQ}$
LINEARLY
BETWEEN μ 'S

NOTE:-

FOR $\mu_{RR} \leq 0.35$

$$\frac{dC_{PMORR}}{dA_{ICR}} = D_{PM1} C_{TRR} + D_{PM2} \mu_{RR}^2 + D_{PM3} \mu_{RR} + D_{PM4}$$

FOR $\mu_{RR} > 0.35$, THE COEFFS. ABOVE CHANGE AS FOLLOWS

$$D_{PM2} \equiv D_{PM5}$$

$$D_{PM3} \equiv D_{PM6}$$

$$D_{PM4} \equiv D_{PM7}$$

ROTOR EQUATIONS (CONTINUED)

HUB PITCHING MOMENT (CONTINUED)

$$\frac{d C_{PMR}}{d B_{ICR}} = E_{PM1} C_{TRR} + E_{PM2} \mu_{RR}^2 + E_{PM3} \mu + E_{PM4}$$

NOTE:- USE THE ABOVE EQUATION FOR $\mu_{RR} \leq 0.35$

$$\text{FOR } \mu_{RR} > 0.35: \quad E_{PM2} \equiv E_{PM5}$$

$$E_{PM3} \equiv E_{PM6}$$

$$E_{PM4} \equiv E_{PM7}$$

HUB YAWING MOMENT

$$C_{YMRR} = C_{YMORR} + \frac{d C_{MRR}}{d A_{ICR}} A_{ICR} + \frac{d C_{MRR}}{d B_{ICR}} B_{ICR} + \frac{d C_{MRR}}{d R} R_{UR}^R$$

WHERE:-

$$\left. \begin{aligned} C_{YMORR} &= \sum_{N=0}^2 \sum_{u=0}^3 \left[A_{YM}(u+4N) \alpha_{RR}^u C'_{TRR} \right] \\ A_{YM}(u+4N) &= f(\mu_{RR}) \\ \frac{d C_{MRR}}{d R} &= \sum_{N=0}^2 \sum_{u=0}^3 \left[J_{YM}(u+4N) \alpha_{RR}^u C'_{TRR} \right] \\ J_{YM}(u+4N) &= f(\mu_{RR}) \end{aligned} \right\} \begin{array}{l} \text{INTERPOLATE} \\ C_{YMRR} \text{ AND } \frac{d C_{YMRR}}{d R} \\ \text{LINEARLY BETWEEN} \\ \mu's. \end{array}$$

ROTOR EQUATIONS (CONTINUED)

HUB YAWING MOMENT (CONTINUED)

FOR $\mu_{RR} \leq 0.35$

$$\frac{d C_{YMRR}}{d \mu_{RR}} = D_{YM1} C_{TRR} + D_{YM2} \mu_{RR}^2 + D_{YM3} \mu_{RR} + D_{YM4}$$

FOR $\mu_{RR} > 0.35$

$$D_{YM2} \equiv D_{YM5}$$

$$D_{YM3} \equiv D_{YM6}$$

$$D_{YM4} \equiv D_{YM7}$$

FOR $\mu_{RR} \leq 0.35$

$$\frac{d C_{YMRR}}{d \mu_{RR}} = E_{YM1} C_{TRR} + E_{YM2} \mu_{RR}^2 + E_{YM3} \mu_{RR} + E_{YM4}$$

FOR $\mu_{RR} > 0.35$

$$E_{YM2} \equiv E_{YM5}$$

$$E_{YM3} \equiv E_{YM6}$$

$$E_{YM4} \equiv E_{YM7}$$

ROTOR EQUATIONS (Cont'd)

ROTOR FORCE & MOMENT CALCULATION

$$T_R = f_{TR} C_{TRR} \rho \pi R^4 \Omega_R^2$$

$$N.F.R. = f_{NR} C_{NRR} \rho \pi R^4 \Omega_R^2$$

$$S.F.R. = f_{SR} C_{SRR} \rho \pi R^4 \Omega_R^2$$

$$M_R = f_{MR} C_{MRR} \rho \pi R^5 \Omega_R^2$$

$$N_R = f_{NR} C_{NRR} \rho \pi R^5 \Omega_R^2$$

$$Q_{REQ} = f_{QR} C_{QRR} \rho \pi R^5 \Omega_R^2$$

$$RHP_{RR} = f_{PR} C_{PRR} \rho \pi R^5 \Omega_R^3 / 550 \quad \text{OR} \quad RHP_{RR} = Q_{REQ} \left(\frac{\Omega_R}{550} \right)$$

LEFT ROTOR FOLLOWS SIMILAR FORMAT

WITH SUBSCRIPTS CHANGED.

THE LEFT ROTOR ALTITUDE EQUATION IS AS FOLLOWS:

$$h_{LR} = -Z_{DOWN} + (L_S \cos i_{NL} - X_{CG}) \sin \theta \\ + \left[(L_S \sin i_{NL} + Z_{CG}) \cos \phi + Y_N \sin \phi \right] \cos \theta$$

OR;

$$h_{LR} = h_{RR} + 2 Y_N \sin \phi \cos \theta$$

ROTOR FORCE & MOMENT RESOLUTION

HUB MOMENTS - NACELLE AXES

LEFT

$$L_{LRH} = -Q_{LREQ} - I_P \dot{\Omega}_L$$

$$M_{LRH} = M_L \cos \delta_{HL} - N_L \sin \delta_{HL} \\ - I_P \Omega_L (p \sin i_{NL} + r \cos i_{NL})$$

$$N_{LRH} = -N_L \cos \delta_{HL} - M_L \sin \delta_{HL} + I_P \Omega_L (\dot{i}_{NL} + q)$$

RIGHT

$$L_{RRH} = Q_{RREQ} + I_P \dot{\Omega}_R$$

$$M_{RRH} = M_R \cos \delta_{HR} + N_R \sin \delta_{HR} \\ + I_P \Omega_R (p \sin i_{NR} + r \cos i_{NR})$$

$$N_{RRH} = N_R \cos \delta_{HR} - M_R \sin \delta_{HR} - I_P \Omega_R (\dot{i}_{NR} + q)$$

NOTE: NACELLE AXES ARE RIGHT HANDED SYSTEMS

ROTOR FORCES & MOMENT RESOLUTION (Cont'd.)

LEFT TIP PIVOT - BODY AXES @ TIP (w/ NACELLE AERO)

$$X_{AERO}^{NL} = (T_L + \Delta X'_{LN}) \cos i_{NL} - \sin i_{NL} (N.F.L \cos \beta_{HL} + S.F.L \sin \beta_{HL} - \Delta Z'_{LN})$$

$$Y_{AERO}^{NL} = S.F.L \cos \beta_{HL} - N.F.L \sin \beta_{HL} + \Delta Y'_{LN}$$

$$Z_{AERO}^{NL} = -(T_L + \Delta X'_{LN}) \sin i_{NL} - \cos i_{NL} (N.F.L \cos \beta_{HL} + S.F.L \sin \beta_{HL} - \Delta Z'_{LN})$$

$$\mathcal{L}_{AERO}^{NL} = (\mathcal{L}_{LRH} + \Delta \mathcal{L}'_{LN}) \cos i_{NL} + \sin i_{NL} (\mathcal{M}_{LRH} + \Delta \mathcal{M}'_{LN} + L_S Y_{AERO}^{NL})$$

$$\mathcal{M}_{AERO}^{NL} = \mathcal{M}_{LRH} + \Delta \mathcal{M}'_{LN} + N.F.L L_S \cos \beta_{HL} + S.F.L L_S \sin \beta_{HL} - L_S \Delta Z'_{LN} - I_E \Omega_{EL} r$$

$$\mathcal{N}_{AERO}^{NL} = \cos i_{NL} (\mathcal{M}_{LRH} + \Delta \mathcal{M}'_{LN} + L_S Y_{AERO}^{NL}) - \sin i_{NL} (\mathcal{L}_{LRH} + \Delta \mathcal{L}'_{LN}) + I_E \Omega_{EL} q$$

NACELLE EQUATION INPUT - LEFT

$$\mathcal{M}_{NLAERO} = \mathcal{M}_{LRH} + \Delta \mathcal{M}'_{LN} + (N.F.L \cos \beta_{HL} + S.F.L \sin \beta_{HL} - \Delta Z'_{LN}) L_S$$

GLAS INPUTS - LEFT

$$\mathcal{M}_{NLAERO}^{GLAS} = \mathcal{M}_{LRH} + L_S (N.F.L \cos \beta_{HL} + S.F.L \sin \beta_{HL})$$

$$\mathcal{N}_{NLAERO}^{GLAS} = \mathcal{M}_{LRH} + L_S (S.F.L \cos \beta_{HL} - N.F.L \sin \beta_{HL})$$

ROTOR FORCE & MOMENT RESOLUTION (Cont'd.)

RIGHT TIP PIVOT - BODY AXES @ TIP (w/ NACELLE AERO)

$$X_{AERO}^{NR} = (T_R + \Delta X'_{RN}) \cos i_{NR} + \sin i_{NR} (-N.F.R \cos \zeta_{HR} + S.F.R \sin \zeta_{HR} + \Delta Z'_{RN})$$

$$Y_{AERO}^{NR} = -S.F.R \cos \zeta_{HR} - N.F.R \sin \zeta_{HR} + \Delta Y'_{RN}$$

$$Z_{AERO}^{NR} = -(T_R + \Delta X'_{RN}) \sin i_{NR} + \cos i_{NR} (-N.F.R \cos \zeta_{HR} + S.F.R \sin \zeta_{HR} + \Delta Z'_{RN})$$

$$\mathcal{L}_{AERO}^{NR} = (\mathcal{L}_{RRH} + \Delta \mathcal{L}'_{RN}) \cos i_{NR} + \sin i_{NR} (M_{RRH} + L_S Y_{AERO}^{NR} + \Delta M'_{RN})$$

$$M_{AERO}^{NR} = M_{RRH} + \Delta M'_{RN} + N.F.R L_S \cos \zeta_{HR} - S.F.R L_S \sin \zeta_{HR} - L_S \Delta Z'_{RN} - I_E \Omega_{ER} r$$

$$N_{AERO}^{NR} = \cos i_{NR} (M_{RRH} + \Delta M'_{RN} + L_S Y_{AERO}^{NR}) - \sin i_{NR} (\mathcal{L}_{RRH} + \Delta \mathcal{L}'_{RN}) + I_E \Omega_{ER} q$$

NACELLE EQUATION INPUT - RIGHT

$$M_{NRAERO} = M_{RRH} + \Delta M'_{RN} + (N.F.R \cos \zeta_{HR} - S.F.R \sin \zeta_{HR} - \Delta Z'_{NR}) L_S$$

GLAS INPUTS - RIGHT

$$M_{NRAERO}^{GLAS} = M_{RRH} + L_S (N.F.R \cos \zeta_{HR} - S.F.R \sin \zeta_{HR})$$

$$N_{NRAERO}^{GLAS} = M_{RRH} - L_S (S.F.R \cos \zeta_{HR} + N.F.R \sin \zeta_{HR})$$

WING VERTICAL BENDING

RIGHT WING TIP DEFLECTION

$$\bar{a}_{RT} = \frac{Z_{AERO}}{m} + Y_N \dot{p}$$

$$\bar{a}_{RWAC} = \frac{Z_{AERO}}{m} + Y_{WAC} \dot{p}$$

$$h_{IR} = K_{W1} Z_{AERO}^{NR'} + K_{W2} Z_{AERO}^{RW'} + K_{W3} L_{AERO}^{NR'} - K_{W4} \bar{a}_{RT} - K_{W5} \bar{a}_{RWAC}$$

$$\dot{h}_{IR} = \Delta h_{IR} / \Delta t$$

WHERE: Δh_{IR} IS THE DIFFERENCE OF h_{IR} BETWEEN TIME FRAMES
AND Δt IS THE TIME FRAME

RIGHT WING A.C. DEFLECTION

$$h_{IRWAC} = K_{W6} Z_{AERO}^{NR'} + K_{W7} Z_{AERO}^{RW'} + K_{W8} L_{AERO}^{NR'} - K_{W9} \bar{a}_{RT} - K_{W10} \bar{a}_{RWAC}$$

$$\dot{h}_{IRWAC} = \Delta h_{IRWAC} / \Delta t$$

WHERE: Δh_{IRWAC} IS THE DIFFERENCE OF h_{IRWAC} BETWEEN TIME
FRAMES AND Δt IS THE TIME FRAME.

FORCE AND MOMENT EFFECTS

$$\ddot{Z}_{AERO}^{NR} = -Z \sum_{W1} W_{W1} \ddot{Z}_{AERO}^{NR} - W_{W1}^2 Z_{AERO}^{NR} + W_{W1}^2 Z_{AERO}^{NR'}$$

$$\ddot{Z}_{AERO}^{RW} = -Z \sum_{W2} W_{W2} \ddot{Z}_{AERO}^{RW} - W_{W2}^2 Z_{AERO}^{RW} + W_{W2}^2 Z_{AERO}^{RW'}$$

$$\ddot{L}_{AERO}^{NR} = -Z \sum_{W3} W_{W3} \ddot{L}_{AERO}^{NR} - W_{W3}^2 L_{AERO}^{NR} + W_{W3}^2 L_{AERO}^{NR'}$$

$$\text{FORM } Z_{AERO}^{NR}, Z_{AERO}^{RW}, L_{AERO}^{NR}$$

WING VERTICAL BENDING (Cont'd.)

LEFT WING TIP DEFLECTION

$$\bar{a}_{LT} = \frac{Z_{AERO}}{m} - Y_N \dot{p}$$

$$\bar{a}_{LWAC} = \frac{Z_{AERO}}{m} - Y_{WAC} \dot{p}$$

$$h_{iL} = K_{W1} Z_{AERO}^{NL'} + K_{W2} Z_{AERO}^{LW'} - K_{W3} L_{AERO}^{NL'} - K_{W4} \bar{a}_{LT} - K_{W5} \bar{a}_{LWAC}$$

$$\dot{h}_{iL} = \Delta h_{iL} / \Delta t$$

WHERE: Δh_{iL} IS THE DIFFERENCE OF h_{iL} BETWEEN TIME FRAMES
AND Δt IS THE TIME FRAME

LEFT WING A.C. DEFLECTION

$$h_{iLWAC} = K_{W6} Z_{AERO}^{NL'} + K_{W7} Z_{AERO}^{LW'} - K_{W8} L_{AERO}^{NL'} - K_{W9} \bar{a}_{LT} - K_{W10} \bar{a}_{LWAC}$$

$$\dot{h}_{iLWAC} = \Delta h_{iLWAC} / \Delta t$$

WHERE: Δh_{iLWAC} IS THE DIFFERENCE OF h_{iLWAC} BETWEEN TIME
FRAMES AND Δt IS THE TIME FRAME

FORCE AND MOMENT EFFECTS

$$\ddot{Z}_{AERO}^{NL} = -Z \sum_{W1} W_{W1} \dot{Z}_{AERO}^{NL} - W_{W1}^2 Z_{AERO}^{NL} + W_{W1}^2 Z_{AERO}^{NL'}$$

$$\ddot{Z}_{AERO}^{LW} = -Z \sum_{W2} W_{W2} \dot{Z}_{AERO}^{LW} - W_{W2}^2 Z_{AERO}^{LW} + W_{W2}^2 Z_{AERO}^{LW'}$$

$$\ddot{L}_{AERO}^{NL} = -Z \sum_{W3} W_{W3} \dot{L}_{AERO}^{NL} - W_{W3}^2 L_{AERO}^{NL} + W_{W3}^2 L_{AERO}^{NL'}$$

FORM Z_{AERO}^{NL} , Z_{AERO}^{LW} , & L_{AERO}^{NL}

WING TORSION

LEFT WING TWIST @ TIP

$$\begin{aligned}
 K_{\theta} \theta_{ELW} = & M_{NACT} - I_E \Omega_{ELW} \\
 & + q_{SLW} \frac{c_w^2 b_w}{2} C_{M0} (1 - C_{TSR}) \\
 & + (1 - C_{TSR}) q_{SLW} c_w^2 \left(\frac{dC_{MWL/4}}{dC_L} + \frac{X_{WAC}}{c_w} \right) \left(\frac{C_L b_w}{6\pi} \right) \left(4\theta_{ELW} + 3\pi \alpha_{RWrigid} \right)
 \end{aligned}$$

RIGHT WING TWIST @ TIP

$$\begin{aligned}
 K_{\theta} \theta_{ERW} = & M_{NACT} - I_E \Omega_{ERW} \\
 & + q_{SRW} \frac{c_w^2 b_w}{2} C_{M0} (1 - C_{TSR}) \\
 & + (1 - C_{TSR}) q_{SRW} c_w^2 \left(\frac{dC_{MWL/4}}{dC_L} + \frac{X_{WAC}}{c_w} \right) \left(\frac{C_L b_w}{6\pi} \right) \left(4\theta_{ERW} + 3\pi \alpha_{RWrigid} \right)
 \end{aligned}$$

WHERE: $C_{M0} = C_1 + C_2 \delta_F + C_3 \delta_F^2$

$$\theta_{ELWAC} = \frac{Y_{WAC}}{Y_N} \theta_{ELW}$$

$$\theta_{ERWAC} = \frac{Y_{WAC}}{Y_N} \theta_{ERW}$$

NOTE: IF UMBRELLAS ARE OPEN ; SET TERMS CONTAINING

$q_s (1 - C_{TS})$ EQUAL TO ZERO

TOTAL FORCE AND MOMENT SUMMATION ABOUT C.G.

$$X_{AERO} = X_{AERO}^{NL} + X_{AERO}^{NR} + X_{AERO}^F + X_{AERO}^{LW} + X_{AERO}^{RW} + X_{AERO}^T$$

$$Y_{AERO} = Y_{AERO}^{NL} + Y_{AERO}^{NR} + Y_{AERO}^F + Y_{AERO}^{LW} + Y_{AERO}^{RW} + Y_{AERO}^T$$

$$Z_{AERO} = Z_{AERO}^{NL} + Z_{AERO}^{NR} + Z_{AERO}^F + Z_{AERO}^{LW} + Z_{AERO}^{RW} + Z_{AERO}^T$$

$$\begin{aligned} L_{AERO} = & L_{AERO}^{NL} + L_{AERO}^{NR} + L_{AERO}^F + L_{AERO}^W + L_{AERO}^T \\ & + Y_N (Z_{AERO}^{NR} - Z_{AERO}^{NL}) + Z_{CG} (Y_{AERO}^{NL} + Y_{AERO}^{NR}) \end{aligned}$$

$$\begin{aligned} M_{AERO} = & M_{AERO}^{NL} + M_{AERO}^{NR} + M_{AERO}^F + M_{AERO}^W + M_{AERO}^T \\ & + X_{CG} (Z_{AERO}^{NL} + Z_{AERO}^{NR}) - Z_{CG} (X_{AERO}^{NL} + X_{AERO}^{NR}) \end{aligned}$$

$$\begin{aligned} N_{AERO} = & N_{AERO}^{NL} + N_{AERO}^{NR} + N_{AERO}^F + N_{AERO}^W + N_{AERO}^T \\ & + Y_N (X_{AERO}^{NL} - X_{AERO}^{NR}) - X_{CG} (Y_{AERO}^{NL} + Y_{AERO}^{NR}) \end{aligned}$$

NOMENCLATURE

- $l_f, h_f \sim$ FUSELAGE MASS CENTER W.R.T. PIVOT FUSE. CENTER, AXES.
 $l_w, h_w \sim$ WING " " " " " "
 $l \sim$ NACELLE PIVOT TO NACELLE C.G. DISTANCE
 $\lambda \sim$ ANGLE BETWEEN NACELLE SHAFT AXIS AND ITS C.G. TO PIVOT AXIS.
 $m_f \sim$ MASS OF FUSELAGE
 $m_w \sim$ MASS OF BOTH WINGS
 $m_N \sim$ MASS OF ONE NACELLE
 $\dot{\gamma}_N \sim$ NACELLE SHAFT TO FUSELAGE X-AXIS ANGLE
 $I_{xx}^{(f)}, I_{yy}^{(f)}, I_{zz}^{(f)}, I_{xz}^{(f)} \sim$ FUSELAGE INERTIAS ABOUT ITS C.G.
 $I_{xx}^{(w)}, I_{yy}^{(w)}, I_{zz}^{(w)}, I_{xz}^{(w)} \sim$ WING INERTIAS ABOUT THEIR C.G.
 $I'_{xx}, I'_{yy}, I'_{zz}, I'_{xz} \sim$ MOMENTS OF INERTIA OF ONE NACELLE ABOUT ITS C.G.
 $p, q, r \sim$ FUSELAGE BODY AXIS ANGULAR RATES
 $u, v, w \sim$ FUSELAGE BODY AXIS LINEAR RATES
 $I_p \sim$ ROTOR POLAR MOMENT OF INERTIA
 $\Omega \sim$ ROTOR SPEED, ANGULAR
 $X_{\text{AERO}}; Y_{\text{AERO}}; Z_{\text{AERO}} \sim$ TOTAL AERODYNAMIC FORCES IN THE BODY AXIS.

SUBSCRIPTS

- $R \sim$ RIGHT
 $L \sim$ LEFT
 $w \sim$ WING
 $f \sim$ FUSELAGE

BASIC EQUATIONS OF MOTION

PRELIMINARY CALCULATIONS

FUSELAGE C.G. w.r.t. A/C C.G.

$$X_f = l_f - X_{CG}$$

$$Z_f = h_f - Z_{CG}$$

WING C.G. w.r.t. A/C C.G.

$$X_w = l_w - X_{CG}$$

$$Z_w = h_w - Z_{CG}$$

NACELLE C.G.'s w.r.t. A/C C.G.

$$X_R = l \cos(i_{NR} - \lambda) - X_{CG}$$

$$Z_R = -l \sin(i_{NR} - \lambda) - Z_{CG}$$

$$X_L = l \cos(i_{NL} - \lambda) - X_{CG}$$

$$Z_L = -l \sin(i_{NL} - \lambda) - Z_{CG}$$

PRELIMINARY CALCULATIONS

INERTIA TERMS

$$\sum_k I_{ij}^{(k)} = I_{ij}^{(f)} + I_{ij}^{(w)} + 2I'_{ij}$$

$$\begin{aligned} I_{xx} = & \sum_k I_{xx}^{(k)} + (I'_{zz} - I'_{xx})(\sin^2 i_{NR} + \sin^2 i_{NL}) \\ & - I'_{xz}(\sin 2i_{NR} + \sin 2i_{NL}) + 2m_N Y_N^2 \\ & + m_f h_f Z_f + m_w h_w Z_w + \\ & - \rho m_N [Z_R \sin(i_{NR} - \lambda) + Z_L \sin(i_{NL} - \lambda)] \end{aligned}$$

$$\begin{aligned} J_{xx} = & \sum_k (I_{zz}^{(k)} - I_{yy}^{(k)}) + (I'_{xx} - I'_{zz})(\sin^2 i_{NR} + \sin^2 i_{NL}) \\ & + I'_{xz}(\sin 2i_{NR} + \sin 2i_{NL}) + 2m_N Y_N^2 \\ & - (m_f h_f Z_f + m_w h_w Z_w) \\ & + \rho m_N [Z_R \sin(i_{NR} - \lambda) + Z_L \sin(i_{NL} - \lambda)] \end{aligned}$$

$$\begin{aligned} I_{xz}^{(p)} = & I_{xz}^{(f)} + I_{xz}^{(w)} + \frac{1}{2}(I'_{xx} - I'_{zz})(\sin 2i_{NR} + \sin 2i_{NL}) \\ & + I'_{xz}(\cos 2i_{NR} + \cos 2i_{NL}) + (m_f l_f Z_f + m_w l_w Z_w) \\ & + m_N \rho [Z_R \cos(i_{NR} - \lambda) + Z_L \cos(i_{NL} - \lambda)] \end{aligned}$$

INERTIA TERMS

$$I_{yy} = \sum_k I_{yy}^{(k)} + m_f (l_f x_f + h_f z_f) + m_w (l_w x_w + h_w z_w) \\ + m_N l [X_R \cos(i_{NR} - \lambda) - Z_R \sin(i_{NR} - \lambda)] \\ + m_N l [X_L \cos(i_{NL} - \lambda) - Z_L \sin(i_{NL} - \lambda)]$$

$$J_{yy} = (I_{xx}^{(f)} - I_{zz}^{(f)}) + (I_{xx}^{(w)} - I_{zz}^{(w)}) + \dots \\ + (I'_{xx} - I'_{zz}) (\cos 2i_{NR} + \cos 2i_{NL}) \\ - 2I'_{xz} (\sin 2i_{NR} + \sin 2i_{NL}) + m_f (-l_f x_f + h_f z_f) \\ + m_w (-l_w x_w + h_w z_w) \\ - m_N l [X_R \cos(i_{NR} - \lambda) + Z_R \sin(i_{NR} - \lambda) + X_L \cos(i_{NL} - \lambda) \\ + Z_L \sin(i_{NL} - \lambda)]$$

$$I_{xz}^{(g)} = I_{xz}^{(f)} + I_{xz}^{(w)} + \frac{1}{2} (I'_{xx} - I'_{zz}) (\sin 2i_{NR} + \sin 2i_{NL}) \\ + I'_{xz} (\cos 2i_{NR} + \cos 2i_{NL}) \\ - m_N l [X_R \sin(i_{NR} - \lambda) + X_L \sin(i_{NL} - \lambda)] \\ + m_f h_f x_f + m_w h_w x_w$$

INERTIA TERMS

$$\begin{aligned}
 I_{zz} = & \sum_k I_{zz}^{(k)} + (I'_{xx} - I'_{zz})(\sin^2 i_{NR} + \sin^2 i_{NL}) \\
 & + I'_{xz} (\sin 2i_{NR} + \sin 2i_{NL}) + 2m_N Y_N^2 \\
 & + m_f l_f X_f + m_w l_w X_w \\
 & + m_N l [X_R \cos(i_{NR} - \lambda) + X_L \cos(i_{NL} - \lambda)]
 \end{aligned}$$

$$\begin{aligned}
 J_{zz} = & \sum_k (I_{yy}^{(k)} - I_{xx}^{(k)}) + (I'_{xx} - I'_{zz})(\sin^2 i_{NR} + \sin^2 i_{NL}) \\
 & + I'_{xz} (\sin 2i_{NR} + \sin 2i_{NL}) - 2m_N Y_N^2 \\
 & + m_f l_f X_f + m_w l_w X_w \\
 & + m_N l [X_R \cos(i_{NR} - \lambda) + X_L \cos(i_{NL} - \lambda)]
 \end{aligned}$$

$$\begin{aligned}
 I_{xz}^{(r)} = & I_{xz}^{(f)} + I_{xz}^{(w)} + \frac{1}{2}(I'_{xx} - I'_{zz})(\sin 2i_{NR} + \sin 2i_{NL}) \\
 & + I'_{xz} (\cos 2i_{NR} + \cos 2i_{NL}) + m_f l_f X_f + m_w l_w X_w \\
 & - l m_N [X_R \sin(i_{NR} - \lambda) + X_L \sin(i_{NL} - \lambda)]
 \end{aligned}$$

BASIC EQUATIONS - FINAL SIMPLIFICATION

ROLL EQUATION

$$\begin{aligned} I_{xx} \dot{p} = & -J_{xx} r q + I_{xz}^{(p)} (\dot{r} + p q) \\ & + I_{mN} Y_N \{ \ddot{i}_{NR} \cos(i_{NR} - \lambda) - \ddot{i}_{NL} \cos(i_{NL} - \lambda) \} \\ & + L_{AERO} \end{aligned}$$

PITCH EQUATION

$$\begin{aligned} I_{yy} \dot{q} = & -J_{yy} p r - I_{xz}^{(q)} (p^2 - r^2) \\ & - \ddot{i}_{NR} \{ I'_{yy} + I_{mN} [-Z_R \sin(i_{NR} - \lambda) + X_R \cos(i_{NR} - \lambda)] \} \\ & - \ddot{i}_{NL} \{ I'_{yy} + I_{mN} [-Z_L \sin(i_{NL} - \lambda) + X_L \cos(i_{NL} - \lambda)] \} \\ & + M_{AERO} \end{aligned}$$

YAW EQUATION

$$\begin{aligned} I_{zz} \dot{r} = & -J_{zz} p q - (r q - \dot{p}) I_{xz}^{(r)} \\ & - I_{mN} Y_N \{ \ddot{i}_{NR} \sin(i_{NR} - \lambda) - \ddot{i}_{NL} \sin(i_{NL} - \lambda) \} \\ & + N_{AERO} \end{aligned}$$

BASIC EQUATIONS

RIGHT NACELLE ACTUATOR PITCHING MOMENT EQUATION

$$\begin{aligned} M_{NRACT} = & -\ddot{i}_{NR} \left[I'_{yy} + l^2 m_N \left(1 - \frac{m_N}{m} \right) \right] \\ & - l^2 m_N \left(1 - \frac{m_N}{m} \right) \left[-pr \cos 2(i_{NR} - \lambda) + \dot{q} \right. \\ & \quad \left. + (r^2 - p^2) \sin(i_{NR} - \lambda) \cos(i_{NR} - \lambda) \right] \\ & - (r^2 - p^2) \left[I'_{zz} \sin i_{NR} \cos i_{NR} \right] - I'_{yy} \dot{q} \\ & + l \frac{m_N}{m} \left[X_{AERO} \sin(i_{NR} - \lambda) + Z_{AERO} \cos(i_{NR} - \lambda) \right] \\ & - l m_N Y_N \left\{ (\dot{r} - pq) \left[\sin(i_{NR} - \lambda) \right] \right. \\ & \quad \left. - (\dot{p} + rq) \left[\cos(i_{NR} - \lambda) \right] \right\} \\ & + M_{NRAERO} \end{aligned}$$

Note: The above equation must be calculated
for wing torsion calculation only

BASIC EQUATIONS

LEFT NACELLE ACTUATOR PITCHING MOMENT EQUATION

$$\begin{aligned} M_{NLACT} = & - \ddot{i}_{NL} \left[I'_{yy} + l^2 m_N \left(1 - \frac{m_N}{m} \right) \right] \\ & - l^2 m_N \left(1 - \frac{m_N}{m} \right) \left[-pr \cos 2(i_{NL} - \lambda) + \dot{p} \right. \\ & \quad \left. + (r^2 - p^2) \sin(i_{NL} - \lambda) \cos(i_{NL} - \lambda) \right] \\ & - (r^2 - p^2) \left[I'_{zz} \sin i_{NL} \cos i_{NL} \right] - I'_{yy} \dot{p} \\ & + l \frac{m_N}{m} \left[X_{Aero} \sin(i_{NL} - \lambda) + Z_{Aero} \cos(i_{NL} - \lambda) \right] \\ & + l m_N Y_N \left\{ (\dot{r} - pq) [\sin(i_{NL} - \lambda)] \right. \\ & \quad \left. - (\dot{p} + rq) [\cos(i_{NL} - \lambda)] \right\} \\ & + M_{NLAERO} \end{aligned}$$

NOTE: The above equation must be calculated for wing torsion calculation only.

AIRCRAFT CONDITION CALCULATIONS
LINEAR EQUATIONS OF MOTION (ψ, θ, ϕ -EULER SYSTEM)

$$\dot{u} = \frac{X_{AERO}}{m} - g \sin \theta - \dot{\phi} w + r v$$

$$\dot{v} = \frac{Y_{AERO}}{m} + g \cos \theta \sin \phi - r u + p w$$

$$\dot{w} = \frac{Z_{AERO}}{m} + g \cos \theta \cos \phi + \dot{\phi} u - p v$$

EULER ANGLE CALCULATION - ψ, θ, ϕ SYSTEM

$$\dot{\psi} = (r \cos \phi + z \sin \phi) / \cos \theta$$

$$\dot{\theta} = z \cos \phi - r \sin \phi$$

$$\dot{\phi} = \rho + \dot{\psi} \sin \theta$$

AIRCRAFT CONDITION CALCULATIONS

GROUND TRACK

NORTHWARD VELOCITY

$$\begin{aligned}\dot{X}_{\text{NORTH}} = & U \cos \Theta \cos \psi + V (\sin \phi \sin \Theta \cos \psi \\ & - \cos \phi \sin \psi) \\ & + W (\cos \phi \sin \Theta \cos \psi + \sin \phi \sin \psi)\end{aligned}$$

EASTWARD VELOCITY

$$\begin{aligned}\dot{Y}_{\text{EAST}} = & U \cos \Theta \sin \psi + V (\sin \phi \sin \Theta \sin \psi + \cos \phi \cos \psi) \\ & + W (\cos \phi \sin \Theta \sin \psi - \sin \phi \cos \psi)\end{aligned}$$

DOWNWARD VELOCITY

$$\dot{Z}_{\text{DOWN}} = -U \sin \Theta + V \sin \phi \cos \Theta + W \cos \phi \cos \Theta$$

AIRCRAFT CONDITION CALCULATIONS (CONTINUED)

PILOT STATION ACCELERATIONS (BODY AXES)

$$\begin{aligned} a_{xPA} = & \frac{\dot{X}_{AERO}}{m} + (\dot{q} + pr)(Z_{PA} - Z_{CG}) \\ & + (\dot{q}^2 + r^2)(X_{CG} - l_{PA}) + Y_{PA}(\dot{p}\dot{q} - \dot{r}) \\ & - 2\dot{q}\dot{Z}_{CG} - \ddot{X}_{CG} \end{aligned}$$

$$\begin{aligned} a_{yPA} = & \frac{\dot{Y}_{AERO}}{m} + (\dot{p} - qr)(Z_{CG} - Z_{PA}) + (\dot{r} + pq)(l_{PA} - X_{CG}) \\ & - Y_{PA}(\dot{r}^2 + \dot{p}^2) + 2(\dot{p}\dot{Z}_{CG} - \dot{r}\dot{X}_{CG}) \end{aligned}$$

$$\begin{aligned} a_{zPA} = & \frac{\dot{Z}_{AERO}}{m} + (\dot{q} - pr)(X_{CG} - l_{PA}) + (\dot{p}^2 + \dot{q}^2)(Z_{CG} - Z_{PA}) \\ & + Y_{PA}(\dot{p} + qr) + 2\dot{q}\dot{X}_{CG} - \ddot{Z}_{CG} \end{aligned}$$

PILOT STATION VELOCITIES (BODY AXES)

$$U_{PA} = U_P + qZ_{PA} - rY_{PA}$$

$$V_{PA} = V_P + r l_{PA} - pZ_{PA}$$

$$W_{PA} = W_P + pY_{PA} - q l_{PA}$$

GUST MODEL

The Gust Model to be used with the simulation will consist of:

NASA-AMES program number NAPS-80.

The output of this program is in the form of gust components that will be added to the inertial components of the basic equations of motion. In practice, the following equations will be used in formulating the input to the aerodynamic coordinate transforms etc.,.

$$\begin{aligned}U &= U' + U_g & P &= P' + P_g \\V &= V' + V_g & Q &= Q' + Q_g \\W &= W' + W_g & R &= R' + R_g\end{aligned}$$

The primed terms above are derived from the basic equations.

Alterations to nomenclature in the Vertol equations has been resisted at this time for the sake of simplicity.

PRELIMINARY CALCULATIONS (PREPROCESS)
CENTER OF GRAVITY CALCULATIONS

$$m = \frac{1}{32.174} \left[W'_f + W'_{NT} + W'_{HT} + W'_{VT} + W'_w + W'_{NF} + W'_{CR} + W'_{FUEL} + W'_c \right]$$

$$m_N = \frac{1}{32.174} \left(\frac{W'_{NT}}{2} \right)$$

$$m_f = \frac{1}{32.174} \left[W'_f + W'_{HT} + W'_{VT} + W'_{CR} + W'_c \right]$$

$$m_w = \frac{1}{32.174} \left[W'_w + W'_{FUEL} + W'_{NF} \right]$$

$$l'_f = \left[(FS)_p - (FS)_{f'} \right] \frac{1}{12}$$

$$l'_{NT} = \left[(FS)_p - (FS)_{NTCG} \right] \frac{1}{12}$$

$$l'_{VT} = \left[(FS)_p - (FS)_{VTCG} \right] \frac{1}{12}$$

$$l'_{PA} = \left[(FS)_p - (FS)_{PA} \right] \frac{1}{12}$$

$$l'_c = \left[(FS)_p - (FS)_c \right] \frac{1}{12}$$

$$l_f = \frac{1}{m_f(32.174)} \left[W'_f l'_f + W'_{NT} l'_{NT} + W'_{VT} l'_{VT} + W'_{CR} l'_{PA} + W'_c l'_c \right]$$

$$l'_w = \left[(FS)_p - (FS)_w \right] \frac{1}{12}$$

$$l'_{FUEL} = \left[(FS)_p - (FS)_{FUEL} \right] \frac{1}{12}$$

$$l'_{NF} = \left[(FS)_p - (FS)_{NF} \right] \frac{1}{12}$$

$$l_w = \frac{1}{m_w(32.174)} \left[W'_w l'_w + W'_{FUEL} l'_{FUEL} + W'_{NF} l'_{NF} \right]$$

PRELIMINARY CALCULATIONS (CONT'D.)

$$z'_f = \left[(WL)_P - (WL)_{f'} \right] \frac{1}{12}$$

$$z'_{HT} = \left[(WL)_P - (WL)_{HTCG} \right] \frac{1}{12}$$

$$z'_{VT} = \left[(WL)_P - (WL)_{VTCG} \right] \frac{1}{12}$$

$$z'_{PA} = \left[(WL)_P - (WL)_{PA} \right] \frac{1}{12}$$

$$z'_c = \left[(WL)_P - (WL)_c \right] \frac{1}{12}$$

$$h_f = \frac{1}{(32.174) m_f} \left[w'_f z'_f + w'_{HT} z'_{HT} + w'_{VT} z'_{VT} + w'_{CR} z'_{PA} + w'_c z'_c \right]$$

$$z'_w = \left[(WL)_P - (WL)_w \right] \frac{1}{12}$$

$$z'_{FUEL} = \left[(WL)_P - (WL)_{FUEL} \right] \frac{1}{12}$$

$$z'_{NF} = \left[(WL)_P - (WL)_{NF} \right] \frac{1}{12}$$

$$h_w = \frac{1}{(32.174) m_w} \left[w'_w z'_w + w'_{FUEL} z'_{FUEL} + w'_{NF} z'_{NF} \right]$$

$$X_{WAC} = \left[(FS)_P - (FS)_{WAC} \right] \frac{1}{12}$$

$$Y_{WAC} = \left[(BL)_{WAC} \right] \frac{1}{12}$$

$$Z_{WAC} = \left[(WL)_P - (WL)_{WAC} \right] \frac{1}{12}$$

$$Y_N = \left[(BL)_N \right] \frac{1}{12}$$

8.

PRELIMINARY CALCULATIONS (CONT'D.)

$$X_{HT} = \left[(FS)_P - (FS)_{HT} \right] \frac{1}{12}$$

$$Z_{HT} = \left[(WL)_P - (WL)_{HT} \right] \frac{1}{12}$$

$$X_{VT} = \left[(FS)_P - (FS)_{VT} \right] \frac{1}{12}$$

$$Z_{VT} = \left[(WL)_P - (WL)_{VT} \right] \frac{1}{12}$$

$$A = 3.14159 R^2$$

$$\bar{Y}_{WAC} = \left[(\bar{BL})_{WAC} \right] \frac{1}{12}$$

$$X_{G2} = X_{G1} = \left[(FS)_P - (FS)_{G2} \right] \frac{1}{12}$$

$$Z_{G2} = Z_{G1} = \left[(WL)_P - (WL)_{G2} \right] \frac{1}{12}$$

$$Y_{G2} = \left[(BL)_{G2} \right] \frac{1}{12}$$

$$Y_{G1} = -Y_{G2}$$

$$Y_{G3} = 0.$$

$$Y_{PA} = \left[(BL)_{PA} \right] \frac{1}{12} \quad ; \quad \text{POSITIVE FOR PILOT IN RIGHT SEAT}$$

$$X_{FAC} = \left[(FS)_P - (FS)_{FAC} \right] \frac{1}{12}$$

$$Z_{FAC} = \left[(WL)_P - (WL)_{FAC} \right] \frac{1}{12}$$

57.

PRELIMINARY CALCULATIONS (CONT'D)

$$X_{CH} = [(FS)_P - (FS)_{CH}] \frac{1}{12}$$

$$Z_{G3} = [(WL)_P - (WL)_{G3}] \frac{1}{12}$$

$$X_{G3} = [(FS)_P - (FS)_{G3}] \frac{1}{12}$$

$$Y_{NF} = [(BL)_{NF CG}] \frac{1}{12}$$

$$Y_{HT} = [(BL)_{HT CG}] \frac{1}{12}$$

$$Y_w = [(BL)_{w CG}] \frac{1}{12}$$

$$Y_{FUEL} = [(BL)_{FUEL CG}] \frac{1}{12}$$

INERTIA CALCULATIONS

$$\eta'_{f'} = l_f - l'_{f'}$$

$$\delta'_{f'} = h_f - z'_{f'}$$

$$\eta'_{HT} = l_f - l'_{HT}$$

$$\delta'_{HT} = h_f - z'_{HT}$$

$$\eta'_{VT} = l_f - l'_{VT}$$

$$\delta'_{VT} = h_f - z'_{VT}$$

$$\eta'_{CA} = l_f - l_{PA}$$

$$\delta'_{CA} = h_f - z_{PA}$$

PRELIMINARY CALCULATIONS (CONT'D)

$$\eta'_c = l_f - l'_c$$

$$\delta'_c = h_f - z'_o$$

$$\begin{aligned} I_{yy}^{(p)} = & I_{yy_o}^{(w_p)} + I_{yy_o}^{(HT)} + I_{yy_o}^{(VT)} + I_{yy_o}^{(CR)} + I_{yy_o}^{(c)} + \frac{W'_f}{32.174} (\eta'^2_{f'} + \delta'^2_{f'}) \\ & + \frac{W'_{HT}}{32.174} (\eta'^2_{HT} + \delta'^2_{HT}) + \frac{W'_{VT}}{32.174} (\eta'^2_{VT} + \delta'^2_{VT}) \\ & + \frac{W'_{CR}}{32.174} (\eta'^2_{CR} + \delta'^2_{CR}) + \frac{W'_c}{32.174} (\eta'^2_c + \delta'^2_c) \end{aligned}$$

$$\begin{aligned} I_{xx}^{(p)} = & I_{xx_o}^{(w_p)} + I_{xx_o}^{(HT)} + I_{xx_o}^{(VT)} + I_{xx_o}^{(CR)} + I_{xx_o}^{(c)} + \frac{W'_f}{32.174} \delta'^2_{f'} + \frac{W'_{HT}}{32.174} (\delta'^2_{HT} + Y'^2_{HT}) \\ & + \frac{W'_{VT}}{32.174} \delta'^2_{VT} + \frac{W'_{CR}}{32.174} \delta'^2_{CR} + \frac{W'_c}{32.174} \delta'^2_c \end{aligned}$$

$$\begin{aligned} I_{zz}^{(p)} = & I_{zz_o}^{(w_p)} + I_{zz_o}^{(HT)} + I_{zz_o}^{(VT)} + I_{zz_o}^{(CR)} + I_{zz_o}^{(c)} + \frac{W'_f}{32.174} \eta'^2_{f'} + \frac{W'_{HT}}{32.174} (\eta'^2_{HT} + Y'^2_{HT}) \\ & + \frac{W'_{VT}}{32.174} \eta'^2_{VT} + \frac{W'_{CR}}{32.174} \eta'^2_{CR} + \frac{W'_c}{32.174} \eta'^2_c \end{aligned}$$

$$\begin{aligned} I_{xz}^{(p)} = & I_{xz_o}^{(w_p)} + I_{xz_o}^{(HT)} + I_{xz_o}^{(VT)} + I_{xz_o}^{(CR)} + I_{xz_o}^{(c)} + \frac{W'_f}{32.174} \eta'_{f'} \delta'_{f'} \\ & + \frac{W'_{HT}}{32.174} \eta'_{HT} \delta'_{HT} + \frac{W'_{VT}}{32.174} \eta'_{VT} \delta'_{VT} + \frac{W'_{CR}}{32.174} \eta'_{CR} \delta'_{CR} \\ & + \frac{W'_c}{32.174} \eta'_c \delta'_c \end{aligned}$$

$$H'_{w'w} = l_w - l'_w$$

$$\Delta'_{w'w} = h_w - z'_w$$

$$H'_{w'FUEL} = l_w - l'_{FUEL}$$

$$\Delta'_{w'FUEL} = h_w - z'_{FUEL}$$

PRELIMINARY CALCULATIONS (CONT'D)

$$H'_{w'NF} = l_w - l'_{NF}$$

$$\Delta'_{w'NF} = h_w - z'_{NF}$$

$$I_{yy}^{(w)} = I_{yy_0}^{(w'_w)} + I_{yy_0}^{(w'_{FUEL})} + I_{yy_0}^{(w'_{NF})} + \frac{W'_w}{32.174} (H'^2_{w'_w} + \Delta'^2_{w'_w})$$

$$+ \frac{W'_{FUEL}}{32.174} (H'^2_{w'_{FUEL}} + \Delta'^2_{w'_{FUEL}}) + \frac{W'_{NF}}{32.174} (H'^2_{w'_{NF}} + \Delta'^2_{w'_{NF}})$$

$$I_{xx}^{(w)} = I_{xx_0}^{(w'_w)} + I_{xx_0}^{(w'_{FUEL})} + I_{xx_0}^{(w'_{NF})} + \frac{W'_w}{32.174} (\Delta'^2_{w'_w} + Y_w^2)$$

$$+ \frac{W'_{FUEL}}{32.174} (\Delta'^2_{w'_{FUEL}} + Y_{FUEL}^2) + \frac{W'_{NF}}{32.174} (\Delta'^2_{w'_{NF}} + Y_{NF}^2)$$

$$I_{zz}^{(w)} = I_{zz_0}^{(w'_w)} + I_{zz_0}^{(w'_{FUEL})} + I_{zz_0}^{(w'_{NF})} + \frac{W'_w}{32.174} (H'^2_{w'_w} + Y_w^2)$$

$$+ \frac{W'_{FUEL}}{32.174} (H'^2_{w'_{FUEL}} + Y_{FUEL}^2) + \frac{W'_{NF}}{32.174} (H'^2_{w'_{NF}} + Y_{NF}^2)$$

$$I_{xz}^{(w)} = I_{xz_0}^{(w'_w)} + I_{xz_0}^{(w'_{FUEL})} + I_{xz_0}^{(w'_{NF})} + \frac{W'_w}{32.174} H'_{w'_w} \Delta'_{w'_w}$$

$$+ \frac{W'_{FUEL}}{32.174} H'_{w'_{FUEL}} \Delta'_{w'_{FUEL}} + \frac{W'_{NF}}{32.174} H'_{w'_{NF}} \Delta'_{w'_{NF}}$$

MATH MODEL TRIM LOOPS - STEADY FLIGHT

INITIALIZE $u, v, \theta, h, \Omega, P, q, r$ AT DESIRED FLIGHT CONDITION.

CLOSE THE FOLLOWING TRIM FEEDBACK LOOPS TO TRIM MATH MODEL FOR FLIGHT.

$$i_{NREF} = K_{T1} \int \dot{u} dt + K_{T2} \dot{u}$$

$$\phi = -K_{T3} \int \dot{v} dt - K_{T4} \dot{v}$$

$$w = K_{T5} \int \dot{w} dt + K_{T6} \dot{w}$$

$$\delta_S = -K_{T7} \int \dot{p} dt - K_{T8} \dot{p}$$

$$\delta_R = -K_{T9} \int \dot{r} dt - K_{T10} \dot{r}$$

$$\delta_B = -K_{T11} \int \dot{q} dt - K_{T12} \dot{q}$$

$$i_{NR} = K_{T13} \iint \ddot{i}_{NR} dt dt + K_{T14} \int \ddot{i}_{NR} dt$$

$$i_{NL} = K_{T13} \iint \ddot{i}_{NL} dt dt + K_{T14} \int \ddot{i}_{NL} dt$$

$$\delta_{TH} = K_{T15} \int \dot{z}_{DOWN} dt + K_{T16} \dot{z}_{DOWN}$$

- NOTE:
- 1.) HOLD INTEGRATED VALUE WHEN GOING TO FLIGHT.
 - 2.) START SECOND TRIM FROM FIRST TRIM VALUES.
 - 3.) DETERMINE K'S EXPERIMENTALLY TO MINIMIZE TRIM TIME.
 - 4.) TRIM WITH ALL ACTUATOR DYNAMICS, SAS, AND GOVERNOR IN OPERATING CONDITION TO INSURE PROPER COCKPIT CONTROL AND COLLECTIVE POSITIONS.

$$5) \dot{z}_{DOWN} = \dot{z}_{DOWN} - \dot{z}_{DOWN}^{TRIM}; \text{ set } \dot{z}_{DOWN}^{TRIM} \text{ at desired R/C}$$

8

MATH MODEL TRIM LOOP OPTIONS

1.) When specifying i_{NREF} , form:

$$\theta = K_{TI} \int \dot{u} dt + K_{TID} \dot{u}$$

Note: This option will be commonly used in cruise flight when the nacelles are down and locked.

APPENDIX F MATHEMATICAL MODEL INPUT DATA

Presented in this section is the input data for the mathematical model. A general description of the Model 222 tilt rotor was given in Section 4.0. Model 222 dimensional data and control surface deflections and travels are given on the following pages. Weight, balance and moment of inertia data for five nominal design operating conditions are defined in Figure F.1 . Center of gravity envelopes for the condition of nacelle incidence zero (cruise configuration) and nacelle incidence 90 degrees (hover configuration) are illustrated in Figure F.2. The mathematical model input data are given in Section F.1 to F.5 and are referenced by page number to the equations presented in Appendix E.

MODEL 222 DIMENSIONAL DATA

WING

AREA (THEO.)	200 FT ²
ASPECT RATIO	5.61
SPAN (BETWEEN ROTOR \bar{C})	33.42 FT
TAPER RATIO	1.00
CHORDS:	
ROOT	71.8 IN
TIP	71.8 IN
MEAN AERODYNAMIC	71.8 IN
SWEEPBACK	0 DEGREES
DIHEDRAL	0 DEGREES
INCIDENCE	
ROOT	2.0 DEGREES
TIP	2.0 DEGREES
AIRFOIL SECTION	
ROOT	NACA 63 ₄ 221 (MODIFIED)
TIP	NACA 63 ₄ 221 (MODIFIED)

FUSELAGE

LENGTH	38.83 FT
DEPTH (NOT INCLUDING SPONSONS)	5.45 FT
WIDTH (NOT INCLUDING SPONSONS)	5.45 FT
WETTED AREA (INCLUDING SPONSONS)	582 FT ²

MODEL 222 DIMENSIONAL DATA (Continued)

NACELLES

ENGINE

LENGTH	5.58 FT
DEPTH	2.37 FT
WIDTH	2.37 FT
WETTED AREA (PER NACELLE)	21 FT ²

TILTING

LENGTH	3.70 FT
DEPTH	3.35 FT
WIDTH	2.37 FT
WETTED AREA (PER NACELLE)	22 FT ²

HORIZONTAL TAIL

AREA (EXPOSED)	46.3 FT ²
AREA (THEO)	58.3 FT ²
SPAN	15.75 FT
ASPECT RATIO	4.26
TAPER RATIO	.379
DISTANCE $(\bar{c}/4)_W$ to $(\bar{c}/4)_{HT}$	20.29 FT
CHORDS	
ROOT	66.0 IN
TIP	25.0 IN
MEAN AERODYNAMIC	48.0 IN
SWEEPBACK AT 0 PERCENT CHORD	14° 51'
DIHEDRAL	0 DEGREES

MODEL 222 DIMENSIONAL DATA (Continued)

INCIDENCE

ROOT 0 DEGREES

TIP 0 DEGREES

AIRFOIL SECTION

ROOT NACA 64A010 (MODIFIED)

TIP NACA 64A010 (MODIFIED)

VERTICAL TAIL

AREA (EXPOSED, EXCLUDES DORSAL) 35.5 FT²

AREA (REFERENCE) 43.3 FT²

SPAN (REFERENCE) 8.14 FT

ASPECT RATIO 1.53

TAPER RATIO .303

DISTANCE $(\bar{c}/4)_W$ to $(\bar{c}/4)_{VT}$ 18.88 FT

CHORDS (REFERENCE)

ROOT 8.17 FT

TIP 2.48 FT

MEAN AERODYNAMIC 5.83 FT

SWEEPBACK AT 0 PERCENT CHORD 46° 28'

AIRFOIL SECTION NACA 64A008

CONTROL SURFACES

FLAPERON

AREA (AFT OF HINGE) 52.5 FT

SPAN (LENGTH EACH SIDE) 151.56 IN

CHORD (% OF WING CHORD) 30

SWEEPBACK OF HINGE LINE 0°

SPOILERS

AREA 19.15 FT²

CONTROL SURFACE DEFLECTIONS AND CONTROL TRAVELS

Control Surface Deflections (Positive deflection is trailing edge down unless indicated otherwise)

Elevator	+20° (Pilot Stick Command-Deflection From Scheduled Elevator Position)
Flaperon (Flap Mode)	+70°, -0°
(Aileron Mode)	+20°, -0° (Flaperon Used for Roll Control to a Maximum of 35° Combined Flap + Aileron Mode Deflection)
Rudder	+20°
Spoiler (Roll Control)	45° (T.E. Up)
(Max. Download Alleviation in Hover)	110° (T.E. Up)
Umbrella Upper Surface	Aft Edge 20° From Vertical
Lower Surface	Aft Edge 10° From Vertical

Rotor Control Authorities

Longitudinal Cyclic	+2.5° for Pitch Trim Plus Maneuver +2.7° for Combined SAS + Load Alleviation
Differential Longitudinal Cyclic	+4.5° Maximum for Roll Command (Function of Nacelle Incidence)
Maximum Longitudinal Cyclic for Combined Inputs	±7°
Collective Pitch	0° to 56.5° (at .75R)
Differential Collective	+3.0° Maximum for Yaw Command & +4.8° for Maximum Roll Command (Function of Nacelle Incidence)
Lateral Cyclic	+2.7° for Rotor Load Alleviation

Nacelle Deflection Authorities

Nacelle Tilt	0° to 105°
Differential Nacelle Tilt	1.55° Per Degree Differential Longitudinal Cyclic

Pilot Control Movements

Stick - Longitudinal	+6 Inches
- Lateral	+5 Inches
Rudder Pedals	+2.5 Inches

MASS PROPERTIES

(WEIGHT, BALANCE AND MOMENTS OF INERTIA)

SUB-GROUPS	WEIGHT	NACELLE BALANCE			HORIZONTAL INERTIA - SLUG FT ²			NACELLE BALANCE			VERTICAL INERTIA - SLUG FT ²		
		X (F.S.)	Y (W.S.)	Z (W.L.)	IXX (ROLL)	IYY (PITCH)	IZZ (YAW)	X (F.S.)	Y (W.S.)	Z (W.L.)	IXX (ROLL)	IYY (PITCH)	IZZ (YAW)
* FUSELAGE & CONTENTS	3696	149.7	-9.0		903	6058	6152						
* HORIZONTAL TAIL	130	419.4	27.7	13.4	23	15	38						
* VERTICAL TAIL	96	406.7	63.8		15	22	7						
* WING & CONTENTS	1695	182.2	107.4	40.3	1266	200	1346						
* NACELLE & CONTENTS	(4267)	160.0	(210.1)	(42.4)	(224)	(1393)	(1507)						
FIXED TILTING	1475 2792	202.7 137.5	227.8 200.7	43.1 42.0	43 45	115 386	61 369	176.4	200.7	84.3	389	388	45
OPER. WEIGHT EMPTY	9884	165.8	22.6		48674	12256	57263	176.8		34.6	50751	13308	56238
* OBSERVER	200	150.0	1.0		6	7	4						
* FUEL	1280	178.6	109.0	37.0	380	32	416						
* INSTRU. & RES	1157	178.6		.5	110	275	300						
* OTHER	1020	171.5		.5	110	250	225						
BASIC DESIGN GROSS WEIGHT	13541	168.3	20.1		52843	13191	61576	176.3		28.8	55176	14482	50533
* OBSERVER	200	150.0	1.0		6	7	4						
* FUEL	1375	178.6	109.0	37.0	380	32	416						
* INSTRU. & RES	1157	178.6		.5	110	275	300						
* OTHER	1020	171.5		.5	110	250	225						
* BALLAST	1864	171.5		.5	120	350	375						
ALTERNATE GROSS WEIGHT	15500	168.8	17.9		53308	13697	62254	175.7		25.5	55781	15120	61204
* FUEL	1280	178.6	109.0	37.0	380	32	416						
* INSTRU. & RES	1157	178.6		.5	110	275	300						
TYPICAL FLIGHT TAKE-OFF WEIGHT	12321	168.3	22.0		52573	12787	61359	177.1		31.6	54826	13971	60290
* FUEL	759	178.6	109.0	33.0	187	12	195						
* INSTRU. & RES	1157	178.6		.5	110	275	300						
MEAN OPERATING GROSS WEIGHT	11800	167.9	21.1		51053	12717	59743	177.1		31.1	53291	13856	58673

NOTE: * ROTOR BLADE INERTIAS (I₀) ARE NOT INCLUDED IN THE ABOVE VALUES. THE ROTOR BLADE WEIGHT IS ASSUMED TO BE ACTING AT THE HUB \bar{g} .

* ROTOR BLADE WEIGHT (COMPLETE AS REMOVED FROM HUB), BALANCE AND INERTIAS (I₀) ARE AS FOLLOWS:

BLADE WEIGHT 124 LBS., SPAN BALANCE 54.9" FROM HUB \bar{g} , CHORD BALANCE FROM LEADING EDGE OF BLADE 4.7", INERTIAS (SLUG FT² AROUND BLADE C.G.) I_{XX} = 52, I_{YY} = 2, I_{ZZ} = 55.

Figure F.1. Mass Properties

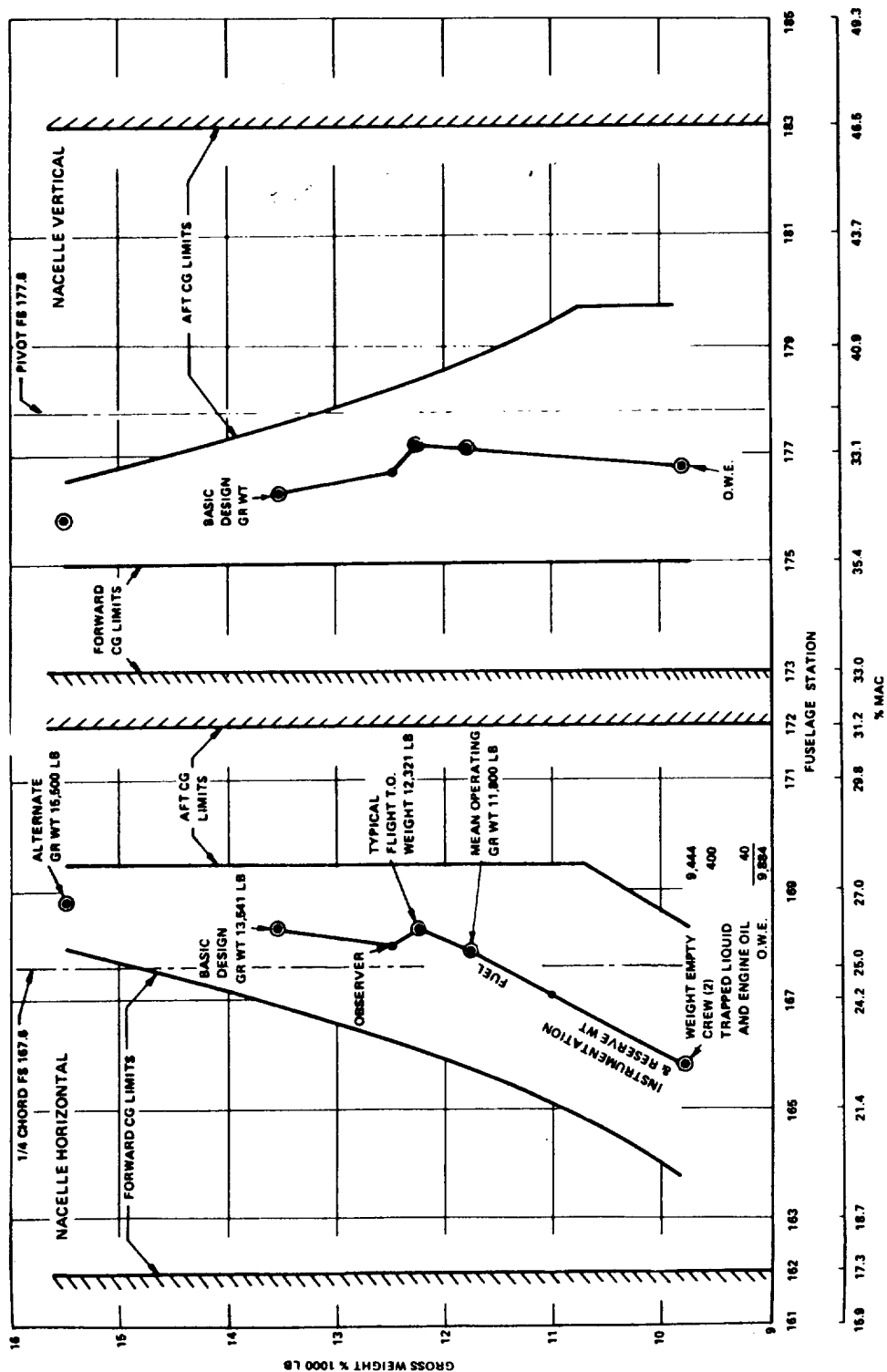


Figure F.2. C.G. Limit Diagram

F-9/-10

F.1 CONTROL SYSTEM INPUT DATA

The input data for the control system, SAS, thrust management, and load alleviation system are in this section, and are referenced by page number to the equations presented in Appendix E. Figures F.3 to F.14 present the scheduled function.

F.1.1 Control System Input Data ⁽¹⁾

Control Mixing (Page E.4)

$$K_{\delta RUD} = -8 \text{ deg/inch}$$

$$K_{\delta R} = 1.0$$

$$K_{\delta S} = 1.0$$

$$K_{\delta B} = 1.0$$

$$K_{\delta e} = -3.33 \text{ deg/inch}$$

$$K_{\delta' S} = 0$$

Actuator Dynamics

$$\omega_N = 20 \text{ rad/sec}$$

$$\zeta = 1.0$$

Lead-lag Dynamics

$$\omega_{L-L} = 35.5 \text{ rad/sec}$$

$$\zeta = .18$$

Scheduled Functions - Refer to Graphs

a) Scheduled Longitudinal Cyclic vs Nacelle Incidence

(1) Gains and time constants not shown on these pages are noted on the block diagrams.

- b) Cyclic Gain vs Nacelle Incidence (Pedals)
- c) Differential Collective Gain vs Nacelle Incidence (Pedals)
- d) Differential Collective Gain vs Nacelle Incidence (Lateral Stick)
- e) Longitudinal Cyclic Gain vs Nacelle Incidence (Long. Stick)
- f) Lateral Cyclic Gain vs Nacelle Incidence
- g) Elevator Deflection vs Nacelle Incidence
- h) Scheduled Lateral Cyclic vs Nacelle Incidence

Load Alleviation System (LAS) (Page E.5)

$$\tau_{LAS} = 0.2 \text{ sec.}$$

LAS Functions

$G_{B_{1\alpha}}$, $G_{A_{1\beta}}$, $G_{A_{1\alpha}}$ vs Dynamic Pressure

Nacelle and Airplane Controls (Page E.6)

Nacelle Actuator Dynamics

$$\omega_{NR} = \omega_{NL} = 10 \text{ rad/sec}$$

$$\zeta_{NL} = \zeta_{NR} = 1.0$$

Scheduled Functions

- a) Scheduled Flap Angle vs Nacelle Incidence
- b) Flaperon vs Lateral Stick
- c) Spoiler Deflection vs Lateral Stick
- d) Spoiler Actuator Limit

Stability Augmentation System (Page E.7 and E.8)

Gains, time constants and scheduled functions noted on block diagrams.

Roll SAS Authority Limit = ± 2 inches
Yaw SAS Authority Limit = ± 1 inch
Pitch SAS Authority Limit = $\pm 2.7^\circ$

Thrust Management System (Page E.13)

$$(N_{II}/N_{II\text{MAX}})_{\text{REF}} = .8865$$

$$\Omega_{\text{REF}} = 57.6923 \text{ rad/sec}$$

$$\eta_{\text{TR}} = 1.0$$

$$I_P = 564 \text{ slug-ft}^2$$

$$\dot{G}_1 = 2.5 \text{ deg/sec / rad/sec}$$

$$G_2 = 2.66 \text{ deg/rad/sec}$$

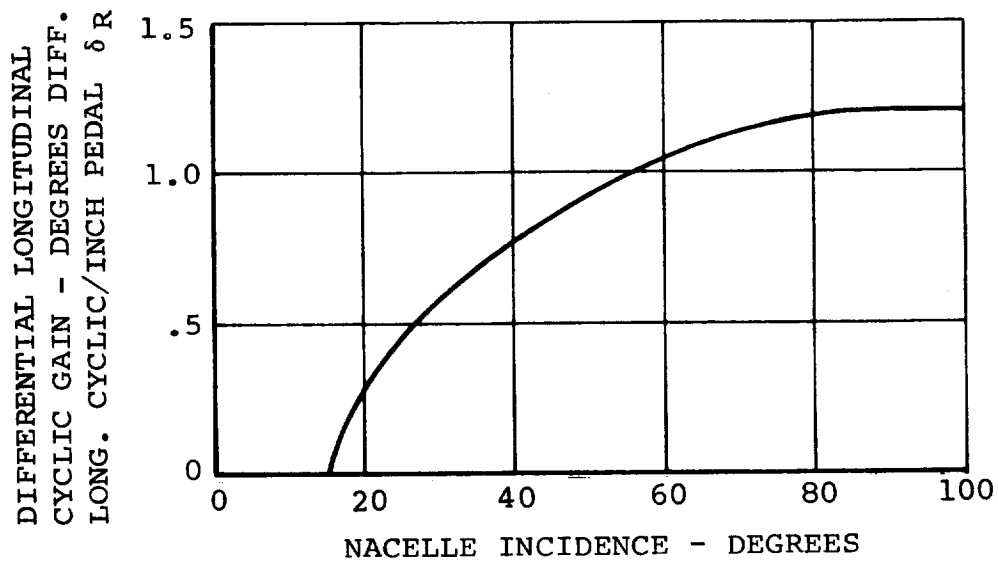
$$G_3 = .05 \text{ deg/sec/deg}$$

Scheduled Functions

- a) Turbine Inlet Temperature vs Throttle Position
- b) τ_D vs (ΔHP)
- c) $\tau_e \delta / \sqrt{\theta}$ vs SHP
- d) Output Gain Ratio vs Power Output
- e) Governor Gain Schedule
- f) RPM Select Schedule
- g) Throttle Collective Gain Schedule
- h) Incremental Collective Schedule
- i) Variable Authority Limit

Rotor Control Coordinate Axis Transforms (Page E.14)

$$\phi_P = -12 \text{ degrees}$$



NOTE: DIFFERENTIAL NACELLE TILT IS 1.55 DEGREES PER NACELLE PER DEGREE OF DIFF. CYCLIC

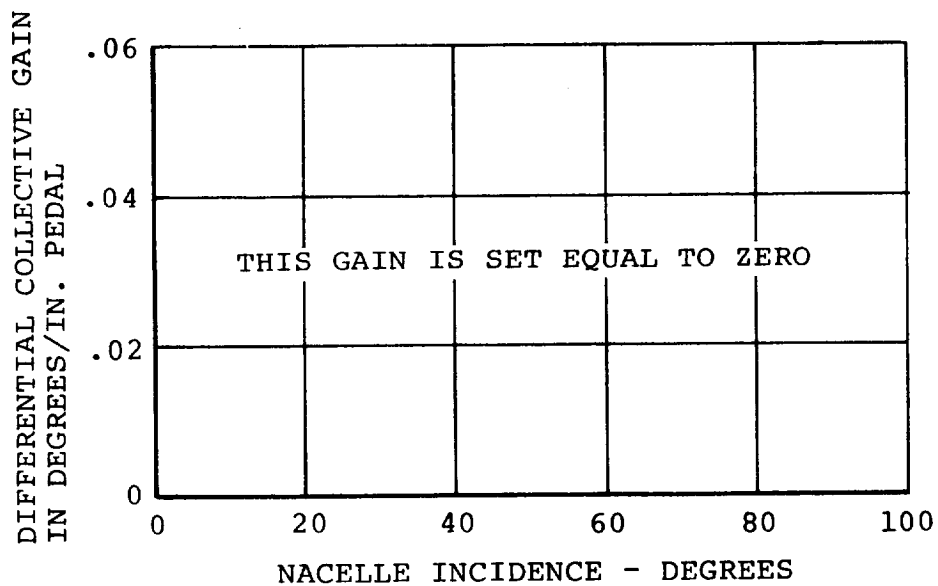
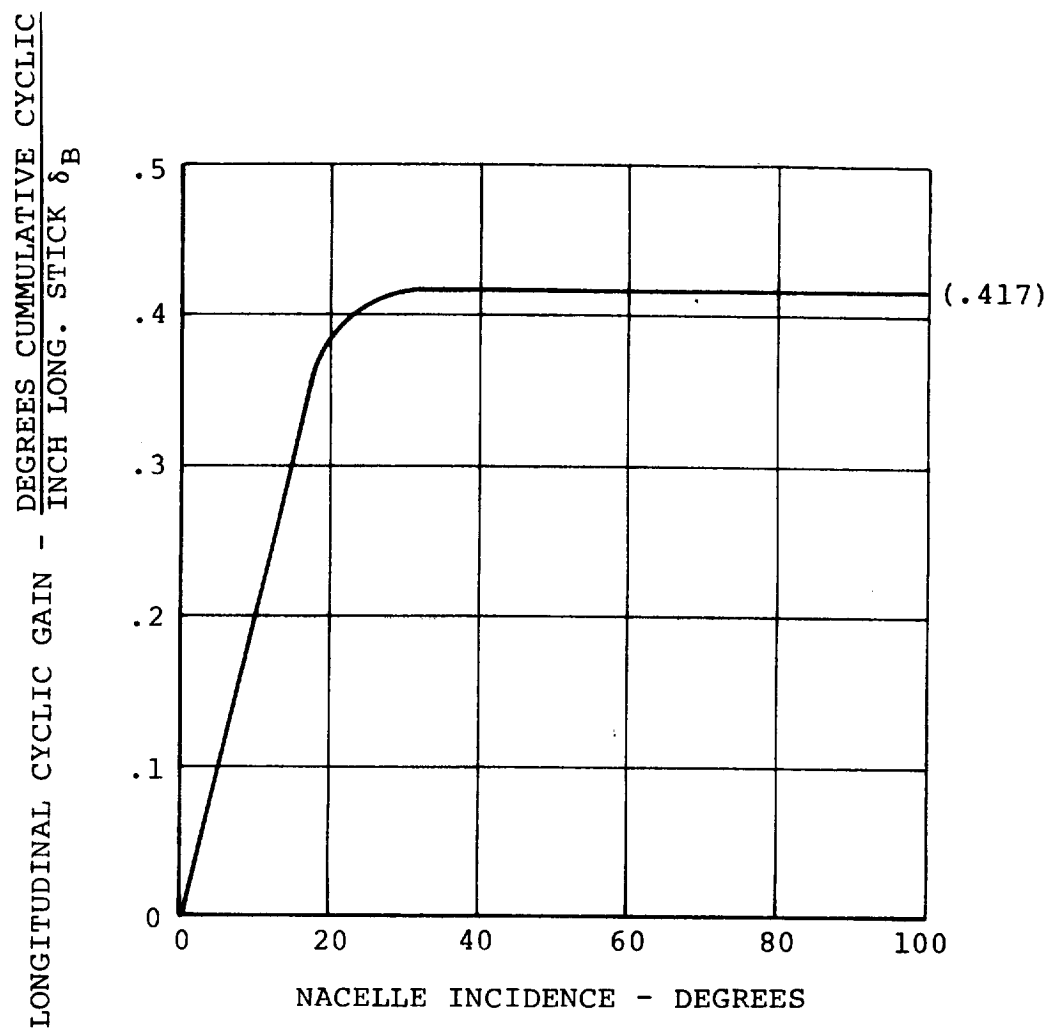


Figure F.3. Differential Long. Cyclic for Yaw Control vs Nacelle Incidence



NOTE: ELEVATOR DEFLECT 3.3333 DEGREES
PER INCH OF LONGITUDINAL STICK

MAXIMUM LONG. STICK TRAVEL IS ± 6 INCHES

Figure F.5. Longitudinal Cyclic for Pitch Control Gain vs Nacelle Incidence

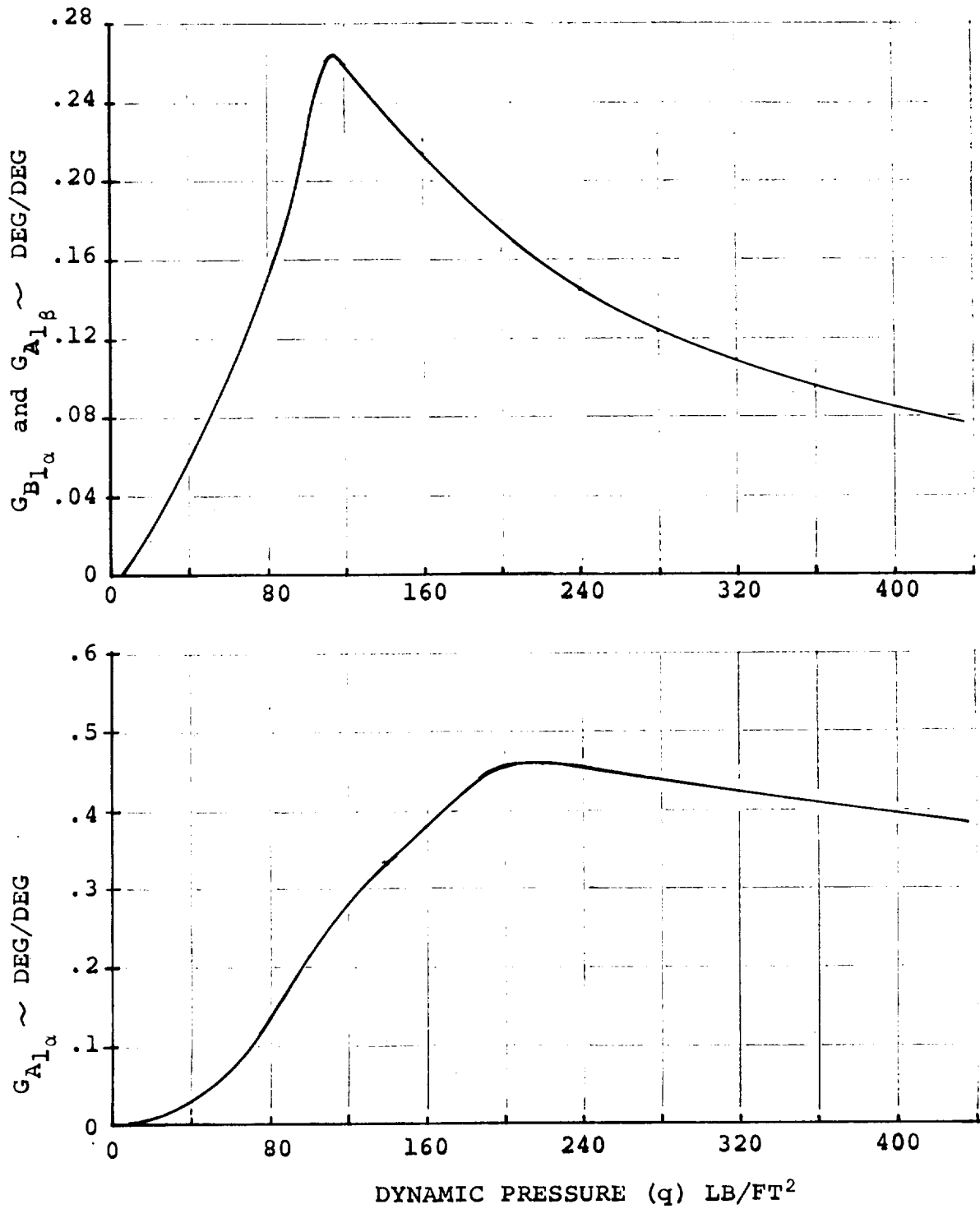


Figure F.6. Load Alleviation System Gain Schedule.

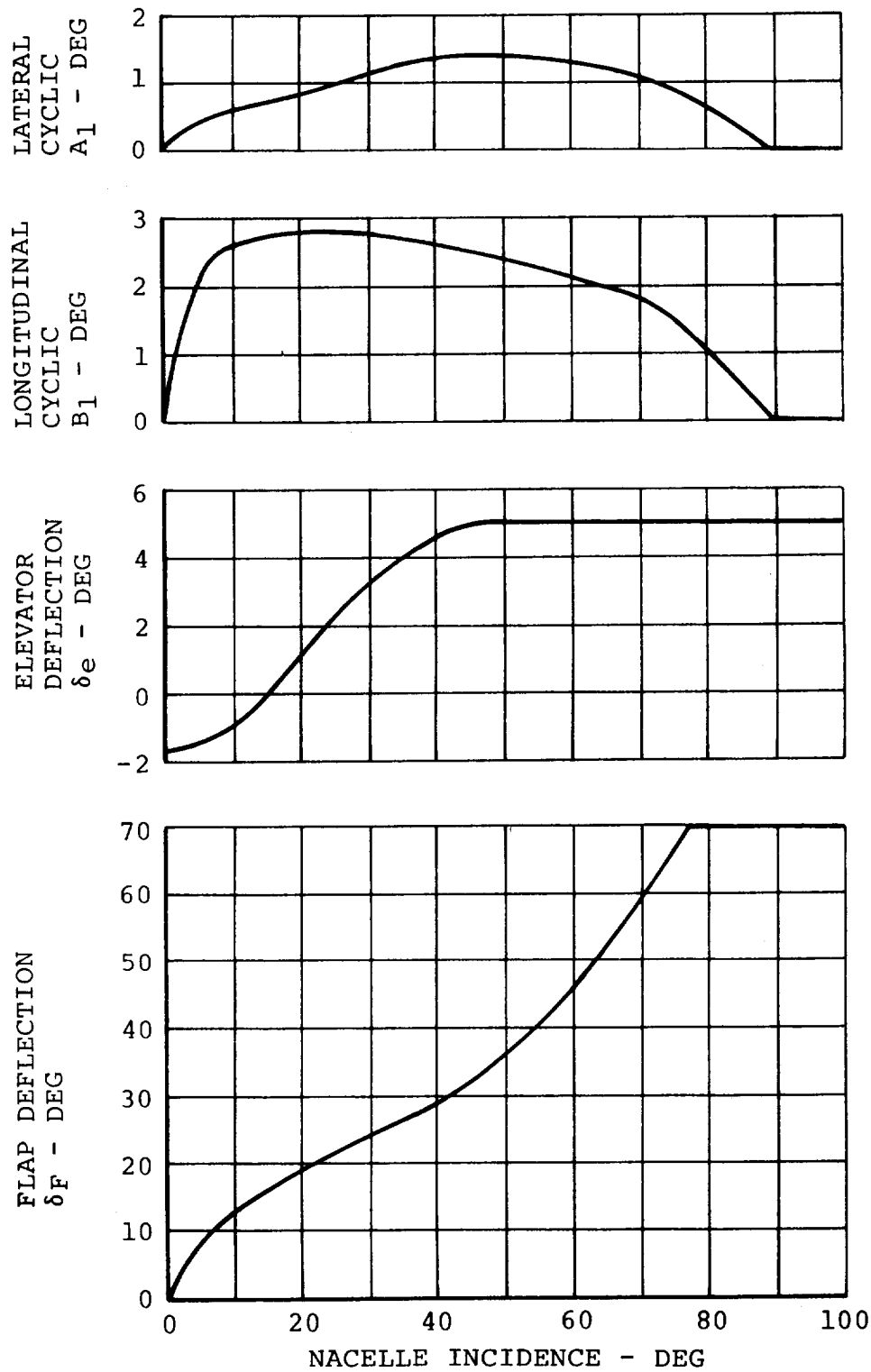
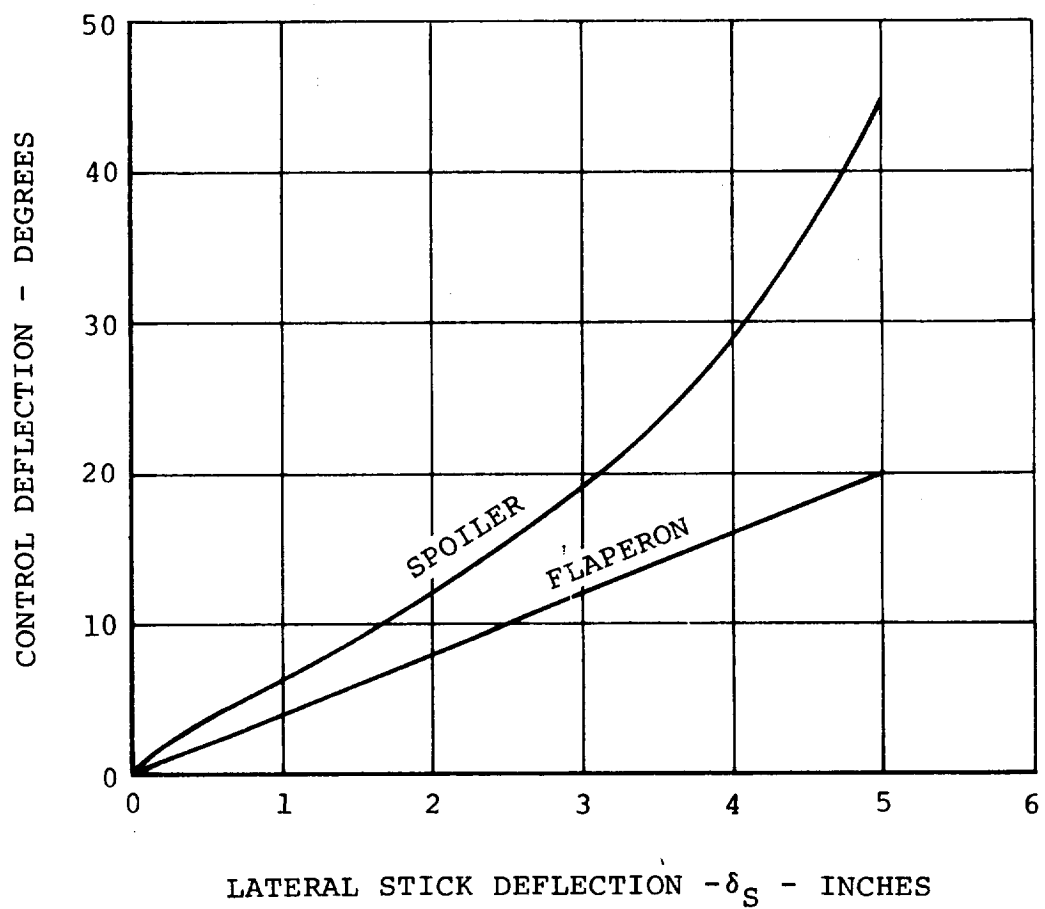


Figure F.7. Programmed Cyclic, Elevator, and Flap Deflection vs Nacelle Incidence



MAXIMUM LATERAL STICK TRAVEL IS \pm 5 INCHES

Figure F.8. Roll Control Deflection vs Stick Deflection

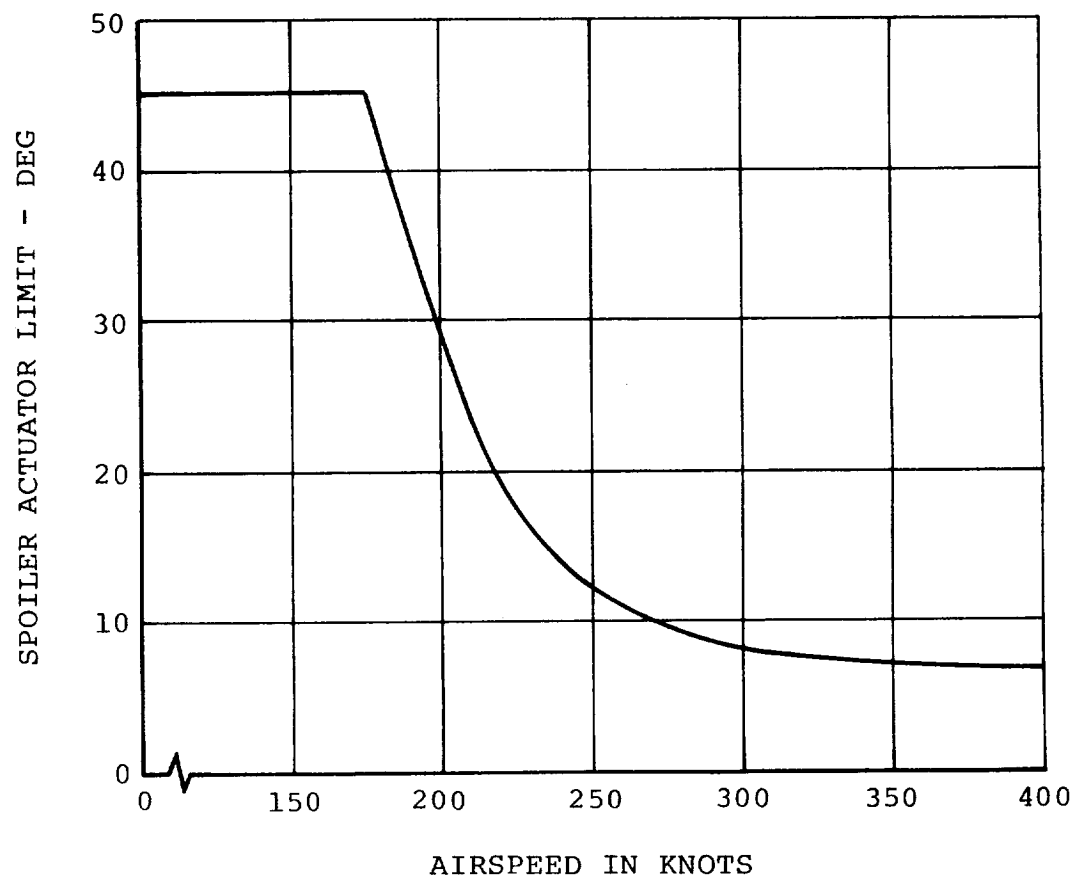


Figure F.9. Spoiler Actuator Limit vs Airspeed

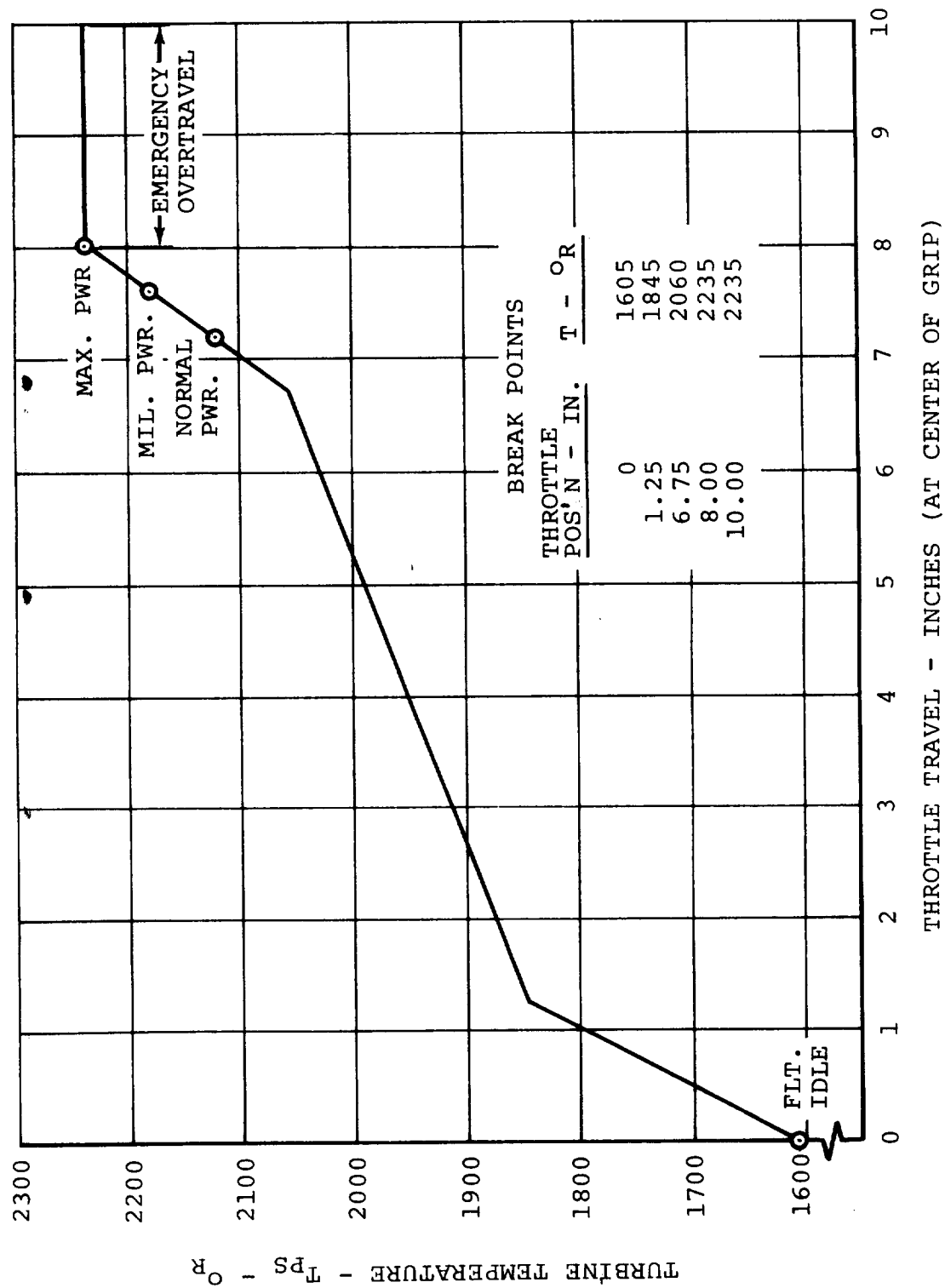


Figure F.10. Assumed Throttle Travel Model 222 Simulation Both Engines

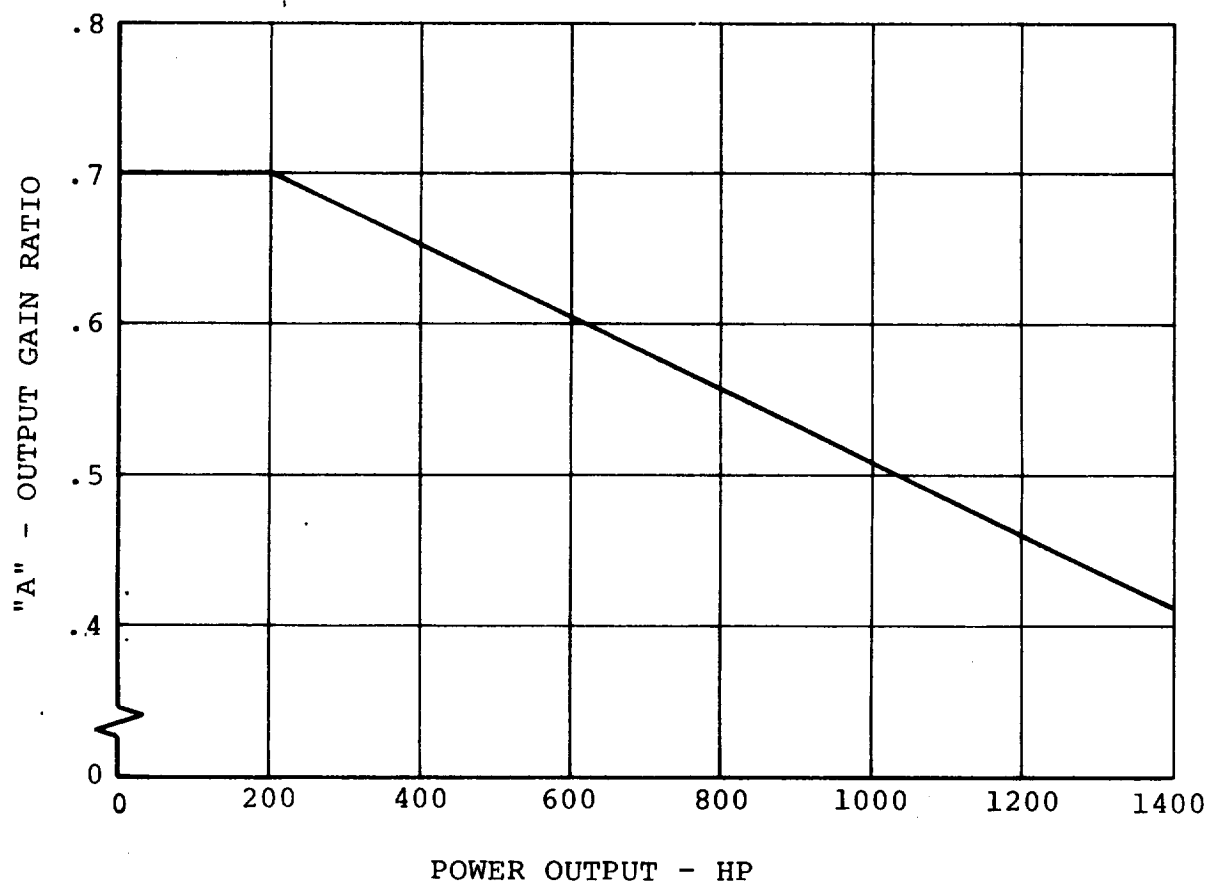


Figure F.12. Engine Characteristics Lycoming T53-L13 Engine

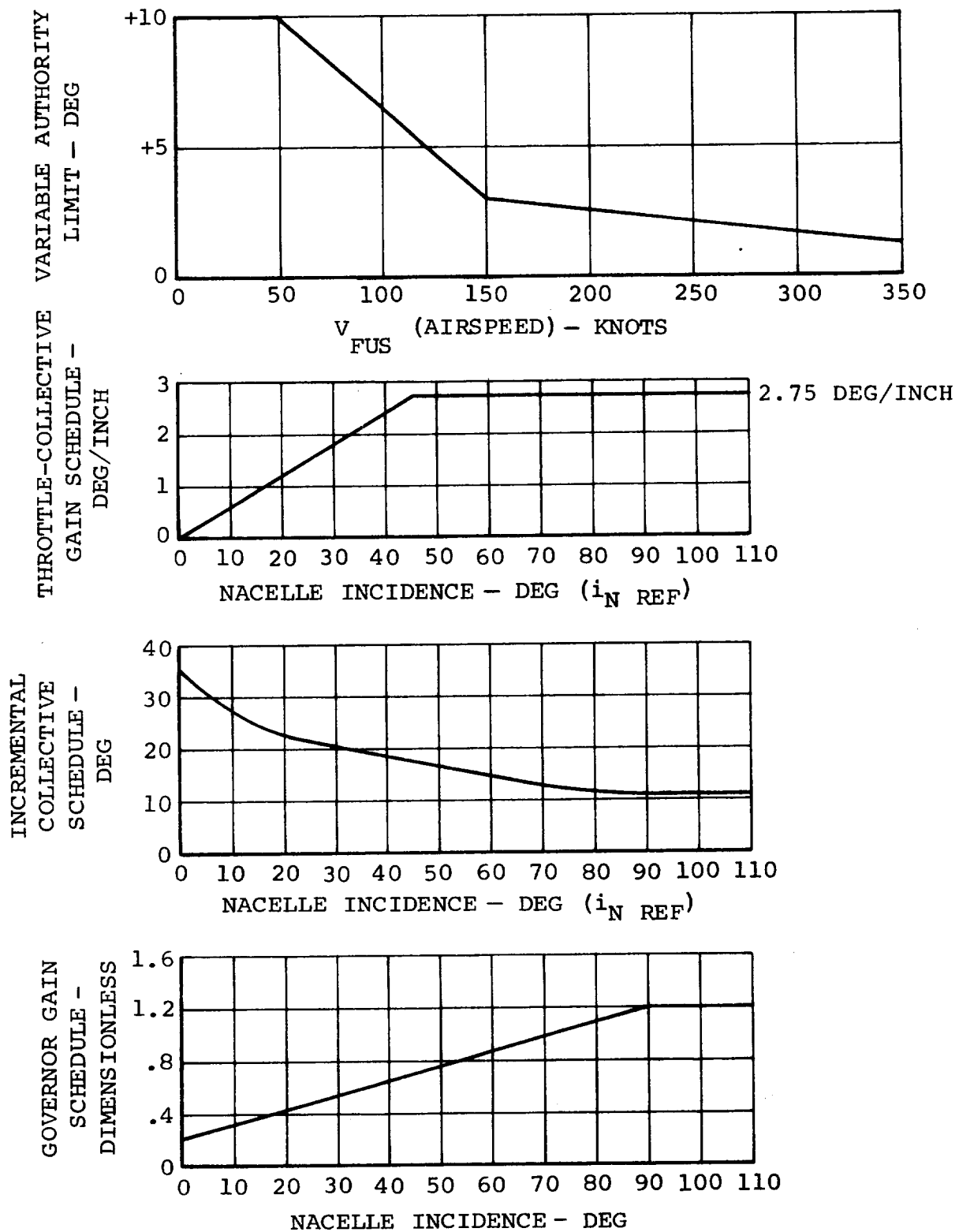


Figure F.13. Thrust Management System-Scheduled Parameters

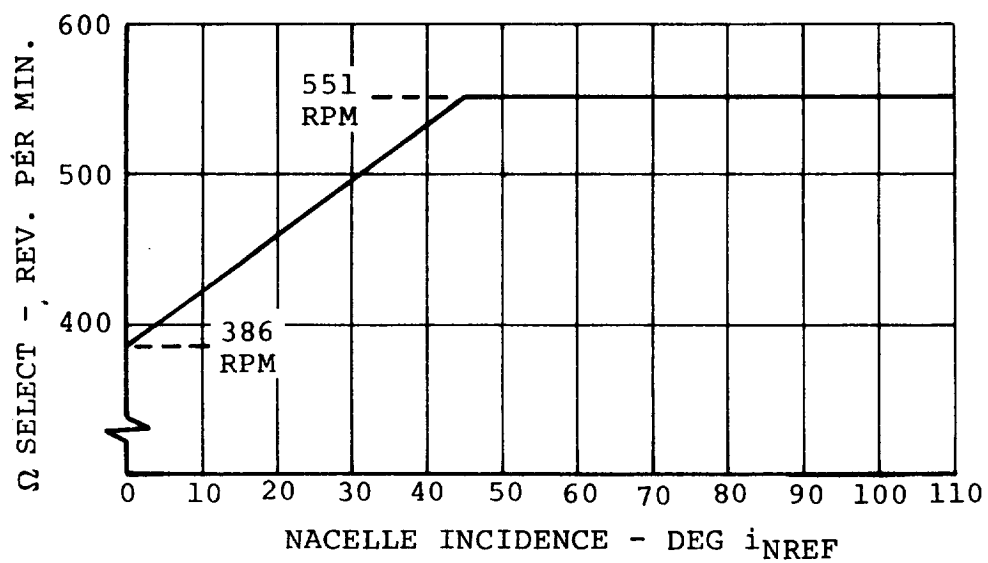


Figure F.14. Thrust Management System-Scheduled Parameters

F.2 ENGINE INPUT DATA

The input data for the engine performance subroutine is given in this section, and are referenced by page number to the equation presented in Appendix E. Plotted data are shown in Figures F.15 to F.18.

F.2.1 Turbine Engine Performance Input Data

Engine Performance Data (Pages E.10, E.11 and E.12)

$$\text{SHP}^* = 1550$$

$$\text{WDTIND} = 1.0$$

$$\text{N1IND} = 1.0$$

$$\text{N10IND} = 0$$

$$\text{QIND} = 1.0$$

$$\dot{w}_{\text{MAX}}/\dot{w}^* = 1.11$$

$$\text{N}_{\text{IMAX}}/\text{N}_{\text{I}}^* = 1.04$$

$$(\text{N}_{\text{I}}/\sqrt{\theta_1}/\text{N}_{\text{I}}^*)_{\text{MAX}} = 0$$

$$\text{Q}_{\text{MAX}}/\text{Q}^* = 1.446$$

$$\text{N}_{\text{IIMAX}}/\text{N}_{\text{II}}^* = 1.128$$

$$\text{N}_{\text{I}}^* = 25425 \text{ RPM}$$

$$(\text{N}_{\text{II}}/\text{N}_{\text{IIMAX}})_{\text{REF}} = .8865$$

$$\Omega_{\text{REF}} = 57.6923$$

Tabular Engine Cycle Input Data

- a) Values of Referred Horsepower
- b) Values of Referred Fuel Flow
- c) Values of Referred Gas Generator Speed
- d) Values of Referred Power Turbine Speed

1. VALUES OF REFERRED HORSEPOWER $\text{SHP}/\delta\sqrt{\theta}/\text{SHP}^*$

MACH NO.	T/ θ =1600	T/ θ =1800	T/ θ =2000	T/ θ =2200	T/ θ =2400	T/ θ =2600	T/ θ =2800
0	.035	.330	.630	.920	1.200	1.340	1.400
.2	.075	.375	.670	.960	1.245	1.390	1.450
.4	.125	.425	.720	1.010	1.295	1.440	1.500
.6	.180	.480	.775	1.065	1.350	1.495	1.550
.8	.240	.534	.835	1.125	1.410	1.550	1.600

2. VALUES OF REFERRED FUEL FLOW $W/\delta\sqrt{\theta}/\text{SHP}^*$

MACH NO.	T/ θ =1600	T/ θ =1800	T/ θ =2000	T/ θ =2200	T/ θ =2400	T/ θ =2600	T/ θ =2800
0	.150	.278	.407	.535	.662	.750	.802
.2	.150	.278	.407	.535	.662	.750	.802
.4	.150	.278	.407	.535	.662	.750	.802
.6	.150	.278	.407	.535	.662	.750	.802
.8	.150	.278	.407	.535	.662	.750	.802

3. VALUES OF REFERRED GAS GENERATOR SPEED $N_I/\sqrt{\theta}/N_I^*$

MACH NO.	T/ θ =1600	T/ θ =1800	T/ θ =2000	T/ θ =2200	T/ θ =2400	T/ θ =2600	T/ θ =2800
0	.722	.840	.925	.990	1.045	1.097	1.150
.2	.735	.846	.927	.992	1.048	1.100	1.154
.4	.748	.853	.933	.997	1.052	1.105	1.158
.6	.766	.860	.939	1.004	1.059	1.111	1.162
.8	.789	.871	.950	1.015	1.068	1.119	1.170

4. VALUES OF REFERRED POWER TURBINE SPEED $N_{II}/\sqrt{\theta}/N_{II}^*$

MACH NO.	T/ θ =1600	T/ θ =1800	T/ θ =2000	T/ θ =2200	T/ θ =2400	T/ θ =2600	T/ θ =2800
0	.445	.685	.856	.983	1.084	1.178	1.264
.2	.461	.699	.880	.997	1.088	1.169	1.246
.4	.500	.734	.908	1.009	1.089	1.158	1.224
.6	.557	.789	.940	1.023	1.086	1.145	1.197
.8	.640	.858	.973	1.029	1.076	1.123	1.161

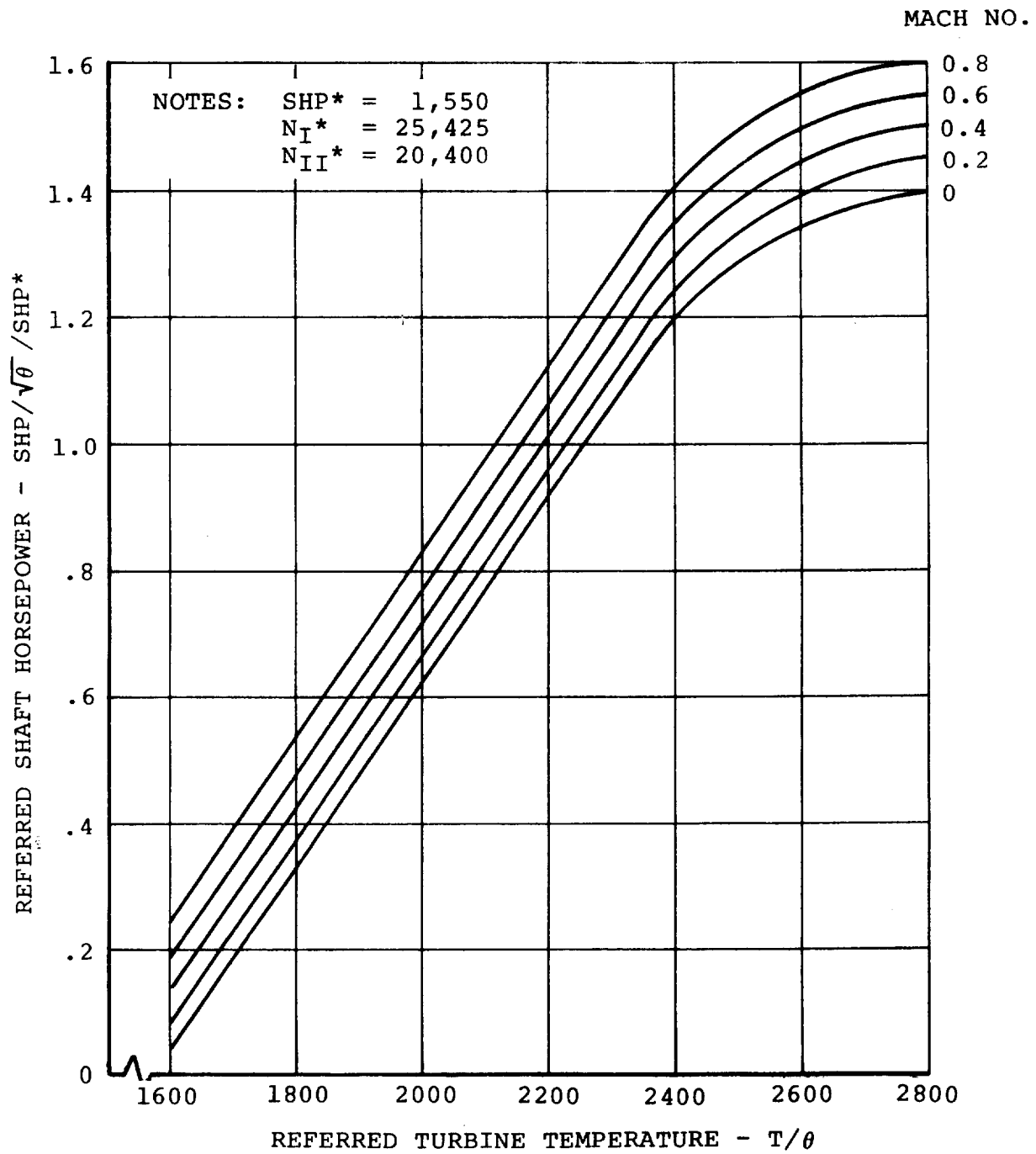


Figure F.15. Turbine Engine Performance - Engine Cycle 1.78

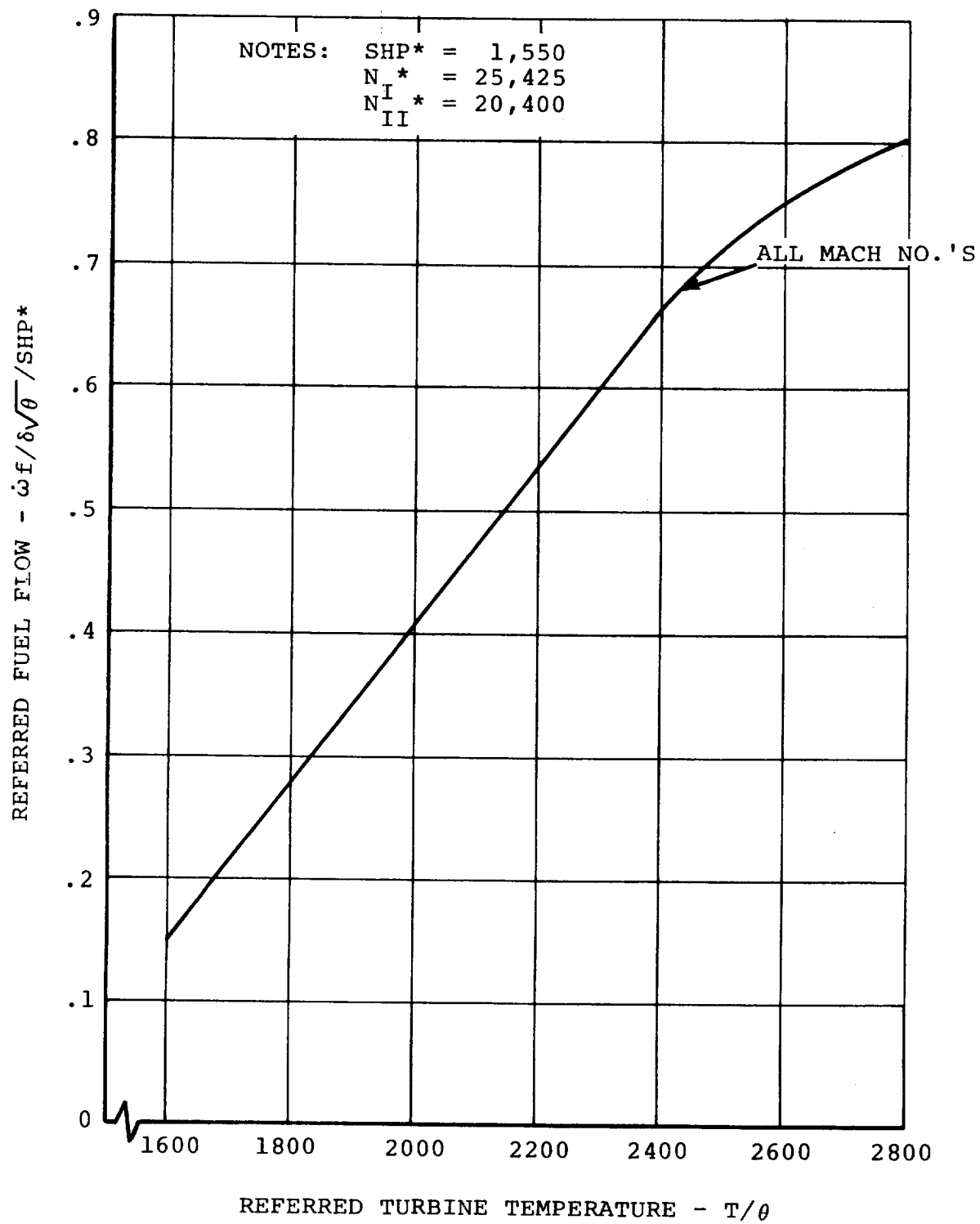


Figure F.16. Turbine Engine Performance - Engine Cycle 1.78

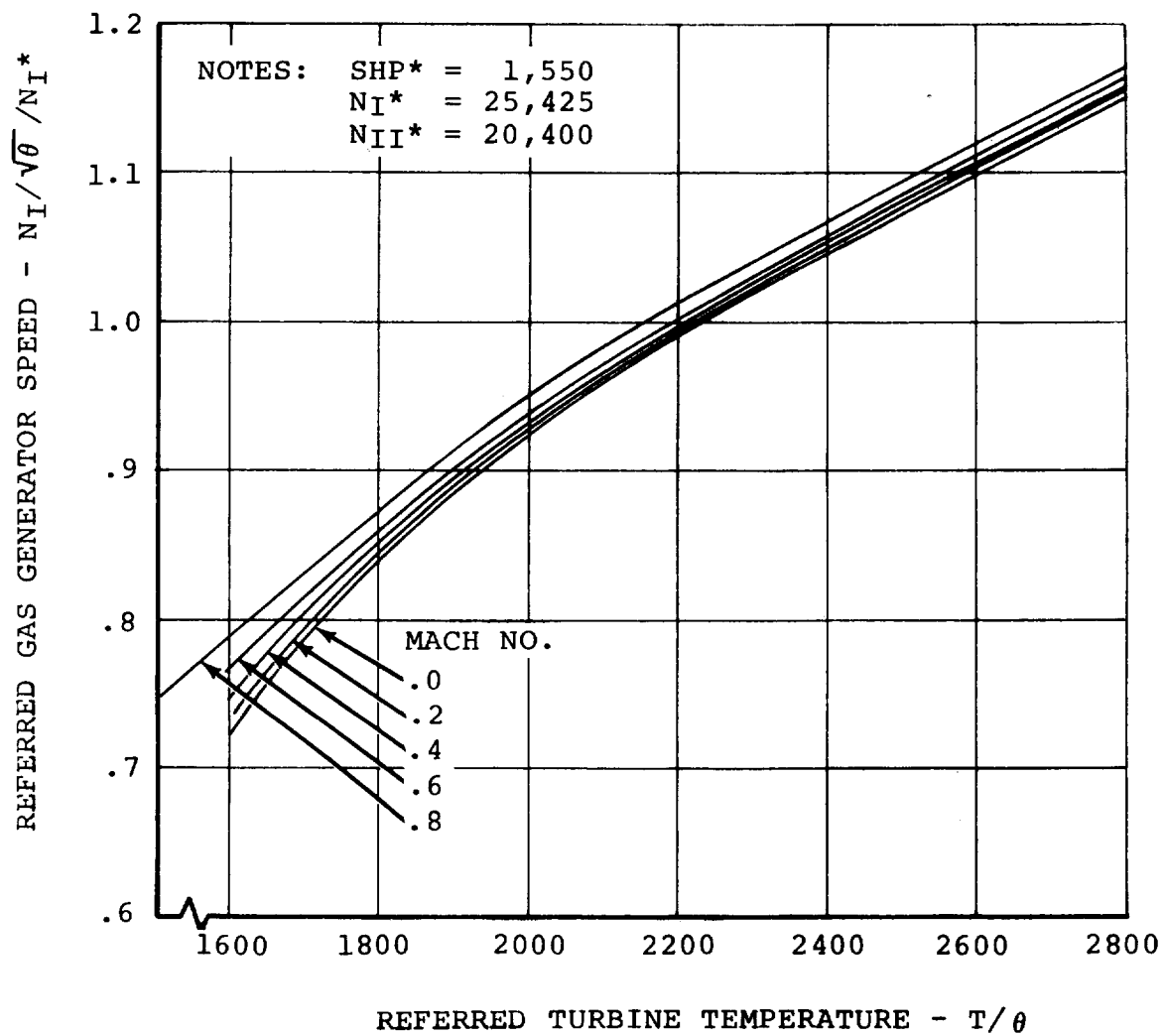


Figure F.17. Turbine Engine Performance - Engine Cycle 1.78

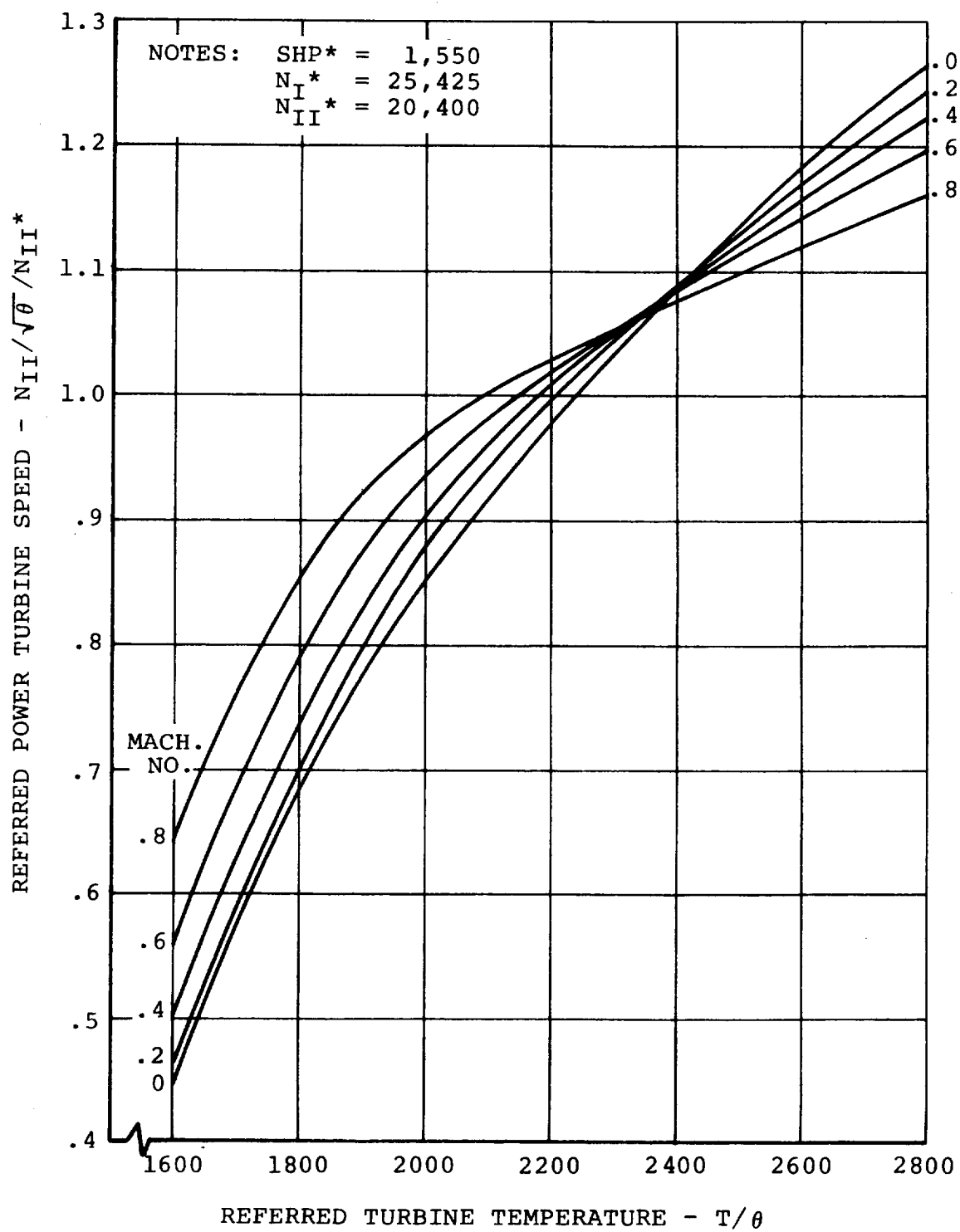


Figure F.18. Turbine Engine Performance - Engine Cycle 1.78

F.3 ROTOR AERODYNAMIC INPUT DATA

The input data for the rotor aerodynamics are given in this section, and are referenced by page number to the equations presented in Appendix E. Tabulated coefficients of the curve fit equations are shown in Figures F.19 to F.27.

F.3.1 Rotor Aerodynamic Input Data

Rotor Thrust (Page E.54)

$$\tau_1 = .10$$

$$\tau_2 = .10$$

$$R = 13 \text{ Ft.}$$

Rotor Force and Moment Calculations (Page E.60)

$$f_{TR} = f_{TL} = 1.0$$

$$f_{NFR} = f_{NFL} = 1.0$$

$$f_{SFR} = f_{SFL} = 1.0$$

$$f_{PMR} = f_{PML} = 1.0$$

$$f_{YMR} = f_{YML} = 1.0$$

$$f_{QR} = f_{QL} = 1.0$$

$$f_{PR} = f_{PL} = 1.0$$

μ	0	.1014	.1351	.2027	.3723	.4565	.6432	.8038	1.125
A_{T0}	.131167x10 ⁻²	-.539532x10 ⁻²	-.203368x10 ⁻¹	-.427861x10 ⁻¹	-.470950x10 ⁻¹	-.439534x10 ⁻¹	-.522445x10 ⁻¹	-.708703x10 ⁻¹	-.878713x10 ⁻¹
A_{T1}	0	-.119838x10 ⁻³	.841758x10 ⁻⁴	.481855x10 ⁻³	.266417x10 ⁻³	0	0	0	0
A_{T2}	0	.26831x10 ⁻⁵	.260200x10 ⁻⁵	.399507x10 ⁻⁶	-.596957x10 ⁻⁵	0	0	0	0
A_{T3}	0	-.904463x10 ⁻⁸	-.127543x10 ⁻⁷	-.681927x10 ⁻⁸	.36307x10 ⁻⁷	0	0	0	0
A_{T4}	.747733x10 ⁻³	.784148x10 ⁻³	.254258x10 ⁻²	.250025x10 ⁻²	.186317x10 ⁻²	.108914x10 ⁻²	.408704x10 ⁻³	.766317x10 ⁻³	.704819x10 ⁻³
A_{T5}	0	.8905x10	-.387201x10	-.220100x10	-.270408x10 ⁻⁴	0	0	0	0
A_{T6}	0	-.699401x10 ⁻⁷	.413387x10 ⁻⁶	.151901x10 ⁻⁶	-.510959x10 ⁻⁶	0	0	0	0
A_{T7}	0	.156844x10 ⁻⁹	-.151355x10 ⁻⁸	-.407612x10 ⁻⁹	.306610x10 ⁻⁷	0	0	0	0
A_{T8}	.120357x10 ⁻⁴	.996174x10 ⁻⁵	-.926255x10 ⁻⁴	-.825240x10 ⁻⁵	-.307987x10 ⁻⁵	.100012x10 ⁻⁴	.214303x10 ⁻⁴	.163128x10 ⁻⁴	.161866x10 ⁻⁴
A_{T9}	0	-.592706x10 ⁻⁸	.371573x10 ⁻⁵	.215847x10 ⁻⁶	-.1111356x10 ⁻⁶	0	0	0	0
A_{T10}	0	-.10436x10 ⁻⁸	-.449157x10 ⁻⁷	-.725582x10 ⁻⁹	.769226x10 ⁻⁷	0	0	0	0
A_{T11}	0	.388825x10 ⁻¹¹	.168184x10 ⁻⁹	-.196520x10 ⁻¹¹	.167159x10 ⁻⁸	0	0	0	0

NOTE: α and $\theta 0.75$ must be in degrees when these coefficients are used in the thrust equation.

Figure F. 19. Coefficients of Curve Fit Equations for Thrust Coefficient

$\mu \rightarrow$	0	.1014	.1351	.2027	.3723	.4565	.6432	.8038	1.125
Ap0	.118188x10 ⁻³	.117752x10 ⁻³	.575597x10 ⁻³	.204675x10 ⁻³	.283014x10 ⁻³	.362823x10 ⁻³	.511711x10 ⁻³	.539983x10 ⁻³	.12581x10 ⁻²
Ap1	0	.262107x10 ⁻⁵	-.835529x10 ⁻⁵	-.551959x10 ⁻⁵	-.952757x10 ⁻⁵	0	0	0	0
Ap2	0	.379347x10 ⁻⁷	.973647x10 ⁻⁷	.145048x10 ⁻⁶	-.615163x10 ⁻⁷	0	0	0	0
Ap3	0	-.147777x10 ⁻⁹	-.180303x10 ⁻⁹	-.391787x10 ⁻⁹	.131638x10 ⁻⁸	0	0	0	0
Ap4	.223227x10 ⁻¹	.143376x10 ⁰	.143289x10 ⁰	.304517x10 ⁰	.383465x10 ⁰	.466013x10 ⁰	.662959x10 ⁰	.854989x10 ⁰	.114909x10 ⁻¹
Ap5	0	-.263395x10 ⁻²	-.391803x10 ⁻²	-.56844x10 ⁻²	-.278572x10 ⁻²	0	0	0	0
Ap6	0	.115613x10 ⁻⁴	.421318x10 ⁻⁴	.336549x10 ⁻⁴	.129237x10 ⁻⁴	0	0	0	0
Ap7	0	-.239424x10 ⁻⁷	-.174886x10 ⁻⁶	-.109523x10 ⁻⁶	-.595181x10 ⁻⁶	0	0	0	0
Ap8	.601436x10 ¹	.153503x10 ¹	-.759331x10 ⁰	-.718612x10 ¹	-.297074x10 ⁻¹	.186185x10 ⁻¹	-.810072x10 ⁻¹	.960492x10 ⁻³	.631924x10 ⁰
Ap9	0	.212258x10 ⁰	.443411x10 ⁰	.50642x10 ⁰	-.477549x10 ⁻²	0	0	0	0
Ap10	0	-.297147x10 ⁻²	-.703113x10 ⁻²	-.624918x10 ⁻²	.327815x10 ⁻³	0	0	0	0
Ap11	0	.985059x10 ⁻⁵	.27991x10 ⁻⁴	.221158x10 ⁻⁴	-.543824x10 ⁻⁵	0	0	0	0

NOTE: α must be in degrees when these coefficients are used in the power equation.

Figure F.20. Coefficients of Curve Fit Equations for Power Coefficient

	$\mu=0$	$\mu=.1014$	$\mu=.1351$	$\mu=.2027$	$\mu=.3723$	$\mu=.4565$
ANF0	0	-.154857x10 ⁻⁵	.204691x10 ⁻⁵	.450018x10 ⁻⁴	-.982094x10 ⁻⁴	.179585x10 ⁻⁶
ANF1	0	.467546x10 ⁻⁵	.942028x10 ⁻⁵	.211604x10 ⁻⁴	.19641x10 ⁻³	.323623x10 ⁻³
ANF2	0	-.285003x10 ⁻⁷	-.100977x10 ⁻⁶	-.251209x10 ⁻⁶	-.639116x10 ⁻⁵	.684873x10 ⁻⁶
ANF3	0	.128888x10 ⁻¹⁰	.270048x10 ⁻⁹	.746916x10 ⁻⁹	.657985x10 ⁻⁷	-.249423x10 ⁻⁷
ANF4	0	-.102821x10 ⁻³	.224724x10 ⁻³	.929207x10 ⁻³	-.157595x10 ⁻²	-.809587x10 ⁻⁴
ANF5	0	.749984x10 ⁻³	.125801x10 ⁻²	.178593x10 ⁻²	.24356x10 ⁻²	.572817x10 ⁻²
ANF6	0	-.945697x10 ⁻⁵	-.132674x10 ⁻⁴	-.217638x10 ⁻⁴	.234598x10 ⁻³	.109167x10 ⁻²
ANF7	0	.293263x10 ⁻⁷	.348545x10 ⁻⁷	.65423x10 ⁻⁷	-.470641x10 ⁻⁵	-.963463x10 ⁻⁴
ANF8	0	.109342x10 ⁰	.275072x10 ⁻¹	-.543699x10 ⁻¹	.443939x10 ⁻¹	.53212x10 ⁻²
ANF9	0	.943903x10 ⁻¹	.696523x10 ⁻¹	.18035x10 ⁰	-.138981x10 ⁻¹	.159926x10 ⁰
ANF10	0	-.109604x10 ⁻²	-.923809x10 ⁻³	-.232838x10 ⁻²	.632501x10 ⁻³	-.115516x10 ⁰
ANF11	0	.317682x10 ⁻⁵	.29846x10 ⁻⁵	.738683x10 ⁻⁵	-.814596x10 ⁻⁵	.994553x10 ⁻²

	$\mu=.5147$	$\mu=.6432$	$\mu=.772$	$\mu=.9008$	$\mu=1.03$	$\mu=1.158$
ANF0	.137987x10 ⁻⁵	.161374x10 ⁻⁵	.245107x10 ⁻⁵	-.132502x10 ⁻⁶	-.173383x10 ⁻⁵	.585875x10 ⁻⁵
ANF1	.439095x10 ⁻³	.760961x10 ⁻³	.109347x10 ⁻²	.140037x10 ⁻²	.170687x10 ⁻²	.199778x10 ⁻²
ANF2	.228487x10 ⁻⁵	.440349x10 ⁻⁶	.823616x10 ⁻⁶	-.191532x10 ⁻⁶	-.139327x10 ⁻⁵	-.209278x10 ⁻⁵
ANF3	-.762918x10 ⁻⁷	-.152524x10 ⁻⁷	-.545001x10 ⁻⁷	.257742x10 ⁻⁷	.512513x10 ⁻⁷	.76607x10 ⁻⁷
ANF4	-.792338x10 ⁻³	-.58501x10 ⁻³	-.578165x10 ⁻⁴	-.185878x10 ⁻³	.212865x10 ⁻²	-.228619x10 ⁻²
ANF5	.665352x10 ⁻²	.282596x10 ⁻²	-.625689x10 ⁻²	-.258884x10 ⁻²	-.513321x10 ⁻²	.123733x10 ⁻¹
ANF6	-.208908x10 ⁻³	.266667x10 ⁻³	.122656x10 ⁻²	.658596x10 ⁻³	.878786x10 ⁻³	-.583625x10 ⁻³
ANF7	.776787x10 ⁻⁵	-.517496x10 ⁻⁵	-.361453x10 ⁻⁴	-.249126x10 ⁻⁴	-.316126x10 ⁻⁴	.101001x10 ⁻⁴
ANF8	.324054x10 ⁻¹	.487661x10 ⁻¹	-.60177x10 ⁻¹	.804597x10 ⁻²	-.162981x10 ⁰	.466581x10 ⁻¹
ANF9	-.688518x10 ⁻¹	.113439x10 ⁰	.642961x10 ⁰	.208291x10 ⁻¹	.515108x10 ⁰	-.898786x10 ⁰
ANF10	.875982x10 ⁻²	-.243064x10 ⁻¹	-.967895x10 ⁻¹	-.520537x10 ⁻²	-.665886x10 ⁻¹	.324115x10 ⁻¹
ANF11	-.327294x10 ⁻³	.563958x10 ⁻³	.300992x10 ⁻²	.261473x10 ⁻³	.221409x10 ⁻²	-.439838x10 ⁻³

NOTE: α must be in degrees when these coefficients are used in the normal force equation.

Figure F.21. Coefficients of Curve Fit Equations for Normal Force Coefficient

	$\mu = 0$	$\mu = .1014$	$\mu = .1351$	$\mu = .2027$	$\mu = .3723$	$\mu = .4565$
A SF0	0	.291745x10 ⁻⁶	.115843x10 ⁻⁵	.564885x10 ⁻⁴	.610186x10 ⁻⁸	.237281x10 ⁻⁷
A SF1	0	-.12407x10 ⁻⁵	-.106448x10 ⁻⁵	.633856x10 ⁻⁶	.557813x10 ⁻⁴	.650575x10 ⁻⁵
A SF2	0	.113747x10 ⁻⁷	.671759x10 ⁻⁸	-.252897x10 ⁻⁷	-.598734x10 ⁻⁶	.769321x10 ⁻⁷
A SF3	0	-.245444x10 ⁻¹⁰	-.440653x10 ⁻¹¹	.119483x10 ⁻⁹	-.659238x10 ⁻⁸	-.349334x10 ⁻⁸
A SF4	0	.143202x10 ⁻³	.317272x10 ⁻³	.147537x10 ⁻²	-.842079x10 ⁻⁴	.117121x10 ⁻⁴
A SF5	0	-.830999x10 ⁻⁴	-.118232x10 ⁻³	-.544752x10 ⁻⁴	-.550991x10 ⁻⁴	-.300935x10 ⁻²
A SF6	0	.958551x10 ⁻⁷	.242609x10 ⁻⁶	-.267651x10 ⁻⁵	-.171925x10 ⁻⁴	-.563082x10 ⁻⁴
A SF7	0	.200043x10 ⁻⁸	.227584x10 ⁻⁸	.163762x10 ⁻⁷	.296356x10 ⁻⁶	.233296x10 ⁻⁵
A SF8	0	-.193731x10 ⁻²	-.509539x10 ⁻²	-.833551x10 ⁻¹	.686884x10 ⁻²	-.759009x10 ⁻³
A SF9	0	.407909x10 ⁻²	.722497x10 ⁻²	.315085x10 ⁻²	-.101352x10 ⁻¹	.111362x10 ⁻¹
A SF10	0	-.450147x10 ⁻⁴	-.916859x10 ⁻⁴	.612312x10 ⁻⁴	.130744x10 ⁻²	.411265x10 ⁻²
A SF11	0	.124524x10 ⁻⁶	.285967x10 ⁻⁶	-.428818x10 ⁻⁶	-.239885x10 ⁻⁴	-.168146x10 ⁻³

	$\mu = .5147$	$\mu = .6432$	$\mu = .772$	$\mu = .9008$	$\mu = 1.03$	$\mu = 1.158$
A SF0	.136092x10 ⁻⁵	.976607x10 ⁻⁶	-.97825x10 ⁻⁶	.786968x10 ⁻⁶	-.216019x10 ⁻⁵	-.253321x10 ⁻⁵
A SF1	-.23559x10 ⁻⁴	-.130694x10 ⁻³	-.316773x10 ⁻³	-.557452x10 ⁻³	-.809093x10 ⁻³	-.109376x10 ⁻²
A SF2	.127659x10 ⁻⁵	-.366955x10 ⁻⁶	-.859884x10 ⁻⁶	-.124574x10 ⁻⁶	-.856051x10 ⁻⁷	.385756x10 ⁻⁵
A SF3	-.572509x10 ⁻⁷	.121016x10 ⁻⁷	.301607x10 ⁻⁷	.115477x10 ⁻⁷	.178906x10 ⁻⁷	-.120107x10 ⁻⁶
A SF4	.119258x10 ⁻²	-.100898x10 ⁻³	.725157x10 ⁻³	.258719x10 ⁻⁴	.167271x10 ⁻³	.130762x10 ⁻²
A SF5	-.740273x10 ⁻²	-.367008x10 ⁻²	-.55614x10 ⁻²	-.320731x10 ⁻²	-.721592x10 ⁻²	.259621x10 ⁻³
A SF6	.104627x10 ⁻²	.662111x10 ⁻⁴	.25791x10 ⁻³	-.165071x10 ⁻³	.327913x10 ⁻³	-.372471x10 ⁻³
A SF7	-.487885x10 ⁻⁴	-.2585357x10 ⁻⁵	-.751767x10 ⁻⁵	.278601x10 ⁻⁶	-.134919x10 ⁻⁴	.126176x10 ⁻⁴
A SF8	-.177106x10 ⁰	.363417x10 ⁻²	-.600228x10 ⁻¹	-.274394x10 ⁻¹	.157176x10 ⁻¹	-.693893x10 ⁻¹
A SF9	.683888x10 ⁰	-.104633x10 ⁰	-.660259x10 ⁻¹	-.178098x10 ⁰	.175384x10 ⁰	-.835669x10 ⁻²
A SF10	-.161739x10 ⁰	-.180444x10 ⁻²	-.812251x10 ⁻²	.208395x10 ⁻¹	-.938934x10 ⁻²	.198682x10 ⁻¹
A SF11	.75356x10 ⁻²	.896371x10 ⁻⁴	.125335x10 ⁻³	-.295016x10 ⁻³	.401628x10 ⁻³	-.916932x10 ⁻³

NOTE: α must be in degrees when these coefficients are used in the side force equation.

Figure F.22. Coefficients of Curve Fit Equations for Side Force Coefficient

	$\mu=0$	$\mu=.1014$	$\mu=.1351$	$\mu=.2027$	$\mu=.3723$	$\mu=.4565$
A_{PM0}	0	.377218x10 ⁻⁵	.688095x10 ⁻⁵	-.79344x10 ⁻⁵	-.310285x10 ⁻⁶	-.884622x10 ⁻⁸
A_{PM1}	0	.539482x10 ⁻⁵	.125905x10 ⁻⁴	.316671x10 ⁻⁴	.820375x10 ⁻⁴	.141415x10 ⁻⁴
A_{PM2}	0	-.12652x10 ⁻⁶	-.252414x10 ⁻⁶	-.581828x10 ⁻⁶	-.27116x10 ⁻⁶	.345339x10 ⁻⁷
A_{PM3}	0	.537895x10 ⁻⁹	.101607x10 ⁻⁸	.226169x10 ⁻⁸	-.151223x10 ⁻⁷	-.105759x10 ⁻⁸
A_{PM4}	0	.172117x10 ⁻³	.562525x10 ⁻³	.201324x10 ⁻²	.193688x10 ⁻³	-.738879x10 ⁻⁵
A_{PM5}	0	.146772x10 ⁻²	.1652x10 ⁻²	.206142x10 ⁻²	.464123x10 ⁻²	-.159412x10 ⁻²
A_{PM6}	0	-.11507x10 ⁻⁴	-.121292x10 ⁻⁴	-.131115x10 ⁻⁴	-.229179x10 ⁻⁴	.508798x10 ⁻⁵
A_{PM7}	0	.185794x10 ⁻⁷	.164608x10 ⁻⁷	.913233x10 ⁻⁸	-.119169x10 ⁻⁶	-.10134x10 ⁻⁶
A_{PM8}	0	-.165488x10 ⁻¹	-.189205x10 ⁻¹	.766096x10 ⁻¹	-.133686x10 ⁻¹	.955878x10 ⁻³
A_{PM9}	0	.181983x10 ⁻²	.224173x10 ⁻³	-.692308x10 ⁻²	-.487350x10 ⁻²	.216812x10 ⁻¹
A_{PM10}	0	-.236138x10 ⁻⁴	.16657x10 ⁻⁶	.684175x10 ⁻⁴	.362062x10 ⁻³	-.13177x10 ⁻²
A_{PM11}	0	.796661x10 ⁻⁷	-.470343x10 ⁻⁸	-.176422x10 ⁻⁶	-.598035x10 ⁻⁵	.362472x10 ⁻⁴
$\mu=.5147$ $\mu=.6432$ $\mu=.772$ $\mu=.9008$ $\mu=1.03$ $\mu=1.158$						
A_{PM0}	-.163818x10 ⁻⁶	-.771885x10 ⁻⁶	-.248968x10 ⁻⁵	.145349x10 ⁻⁶	.168996x10 ⁻⁵	.274231x10 ⁻⁶
A_{PM1}	-.177418x10 ⁻⁵	-.922672x10 ⁻⁴	-.202383x10 ⁻³	-.308712x10 ⁻³	-.383796x10 ⁻³	-.470485x10 ⁻³
A_{PM2}	.356703x10 ⁻⁷	.111958x10 ⁻⁶	.704986x10 ⁻⁶	.536055x10 ⁻⁷	-.912361x10 ⁻⁷	.25489x10 ⁻⁶
A_{PM3}	-.137756x10 ⁻⁸	-.216285x10 ⁻⁹	-.328566x10 ⁻⁷	.53226x10 ⁻⁹	-.27077x10 ⁻⁹	-.640161x10 ⁻⁸
A_{PM4}	.401368x10 ⁻⁴	.225413x10 ⁻⁴	.778302x10 ⁻³	-.483831x10 ⁻³	-.497667x10 ⁻³	-.321648x10 ⁻³
A_{PM5}	-.240092x10 ⁻²	-.399324x10 ⁻²	-.641948x10 ⁻²	-.70195x10 ⁻²	-.100188x10 ⁻¹	-.687551x10 ⁻²
A_{PM6}	-.120839x10 ⁻⁴	-.665199x10 ⁻⁴	-.128724x10 ⁻³	-.119008x10 ⁻³	-.416504x10 ⁻⁴	-.344122x10 ⁻³
A_{PM7}	.387065x10 ⁻⁶	.204615x10 ⁻⁵	.638786x10 ⁻⁵	.396756x10 ⁻⁵	.168316x10 ⁻⁵	.12192x10 ⁻⁴
A_{PM8}	-.227747x10 ⁻²	.261322x10 ⁻¹	-.424198x10 ⁻¹	.428319x10 ⁻¹	.392666x10 ⁻¹	.256492x10 ⁻¹
A_{PM9}	-.751961x10 ⁻¹	-.183726x10 ⁰	.359543x10 ⁻¹	.143102x10 ⁻¹	.949637x10 ⁻¹	-.135728x10 ⁰
A_{PM10}	.10527x10 ⁻²	.210223x10 ⁻¹	-.33401x10 ⁻³	.856042x10 ⁻²	.12569x10 ⁻¹	.336543x10 ⁻¹
A_{PM11}	-.393332x10 ⁻⁴	-.726143x10 ⁻³	-.78287x10 ⁻⁴	-.33099x10 ⁻³	-.435573x10 ⁻³	-.115452x10 ⁻²

NOTE: α must be in degrees when these coefficients are used in the pitching moment equation.

Figure F.23. Coefficients of Curve Fit Equations for Pitching Moment Coefficient

	$\mu = 0$	$\mu = .1014$	$\mu = .1351$	$\mu = .2027$	$\mu = .3723$	$\mu = .4565$
A _{YM0}	0	.109092x10 ⁻⁵	.286933x10 ⁻⁷	-.110543x10 ⁻⁴	-.115949x10 ⁻⁴	.75428x10 ⁻⁶
A _{YM1}	0	.126647x10 ⁻⁴	.191392x10 ⁻⁴	.250948x10 ⁻⁴	.442163x10 ⁻⁴	.199993x10 ⁻³
A _{YM2}	0	-.148631x10 ⁻⁶	-.229016x10 ⁻⁶	-.220845x10 ⁻⁶	.979871x10 ⁻⁶	.672974x10 ⁻⁶
A _{YM3}	0	.435436x10 ⁻⁹	.68199x10 ⁻⁹	.154233x10 ⁻⁹	-.231738x10 ⁻⁷	-.198906x10 ⁻⁷
A _{YM4}	0	.216295x10 ⁻³	.61904x10 ⁻³	.303865x10 ⁻⁴	.76278x10 ⁻³	-.989016x10 ⁻⁴
A _{YM5}	0	.636091x10 ⁻⁴	.533431x10 ⁻⁴	.880677x10 ⁻³	.600766x10 ⁻²	.890334x10 ⁻²
A _{YM6}	0	.290233x10 ⁻⁵	.265736x10 ⁻⁵	-.16908x10 ⁻⁴	-.24055x10 ⁻³	.101251x10 ⁻⁴
A _{YM7}	0	-.182158x10 ⁻⁷	-.164399x10 ⁻⁷	.10332x10 ⁻⁶	.289645x10 ⁻⁵	-.239883x10 ⁻⁶
A _{YM8}	0	-.158447x10 ⁻¹	-.2112x10 ⁻¹	-.171322x10 ⁻¹	-.27995x10 ⁻¹	.646468x10 ⁻²
A _{YM9}	0	.147256x10 ⁻²	.323912x10 ⁻³	-.426356x10 ⁻²	.116529x10 ⁻¹	.486429x10 ⁻¹
A _{YM10}	0	-.178633x10 ⁻⁴	-.158877x10 ⁻⁵	.873694x10 ⁻⁴	-.78607x10 ⁻³	-.277348x10 ⁻²
A _{YM11}	0	.579483x10 ⁻⁷	.374405x10 ⁻⁸	-.533888x10 ⁻⁶	.133698x10 ⁻⁴	.407947x10 ⁻⁴

	$\mu = .5147$	$\mu = .6432$	$\mu = .772$	$\mu = .9008$	$\mu = 1.03$	$\mu = 1.158$
A _{YM0}	.811278x10 ⁻⁶	-.689819x10 ⁻⁶	-.140611x10 ⁻⁵	-.959155x10 ⁻⁶	.232776x10 ⁻⁵	.776742x10 ⁻⁶
A _{YM1}	.2549x10	.358353x10 ⁻³	.40651x10 ⁻³	.423457x10 ⁻³	.404494x10 ⁻³	.400109x10 ⁻³
A _{YM2}	.298133x10 ⁻⁶	-.483638x10 ⁻⁶	.711836x10 ⁻⁶	.366298x10 ⁻⁶	-.978679x10 ⁻⁶	.483519x10 ⁻⁶
A _{YM3}	-.7069x10 ⁻⁸	.165027x10 ⁻⁷	-.242848x10 ⁻⁷	-.201739x10 ⁻⁷	.384779x10 ⁻⁷	-.178582x10 ⁻⁷
A _{YM4}	-.138358x10 ⁻³	-.376316x10 ⁻³	-.111605x10 ⁻³	-.498142x10 ⁻³	-.859507x10 ⁻³	-.170495x10 ⁻³
A _{YM5}	.84517x10 ⁻²	.731418x10 ⁻²	.111654x10 ⁻¹	.700776x10 ⁻²	.495335x10 ⁻²	.937562x10 ⁻³
A _{YM6}	.511468x10 ⁻⁴	.25651x10 ⁻³	-.397326x10 ⁻³	-.179799x10 ⁻³	.475445x10 ⁻³	.428652x10 ⁻³
A _{YM7}	-.113402x10 ⁻⁵	-.882347x10 ⁻⁵	.127859x10 ⁻⁴	.100219x10 ⁻⁴	-.172489x10 ⁻⁴	-.224772x10 ⁻⁴
A _{YM8}	.135303x10 ⁻³	.322547x10 ⁻¹	.931734x10 ⁻²	.392748x10 ⁻¹	.62677x10 ⁻¹	.242592x10 ⁰
A _{YM9}	.664771x10 ⁻¹	.729796x10 ⁻¹	-.283071x10 ⁰	-.697861x10 ⁻¹	.101986x10 ⁰	.629868x10 ⁰
A _{YM10}	-.647118x10 ⁻²	-.170565x10 ⁻¹	.292923x10 ⁻¹	.166632x10 ⁻¹	-.284635x10 ⁻¹	-.600989x10 ⁻¹
A _{YM11}	.140141x10 ⁻³	.575827x10 ⁻³	-.960904x10 ⁻³	-.821801x10 ⁻³	.101423x10 ⁻²	.245749x10 ⁻²

NOTE: α must be in degrees when these coefficients are used in the yawing moment equation.

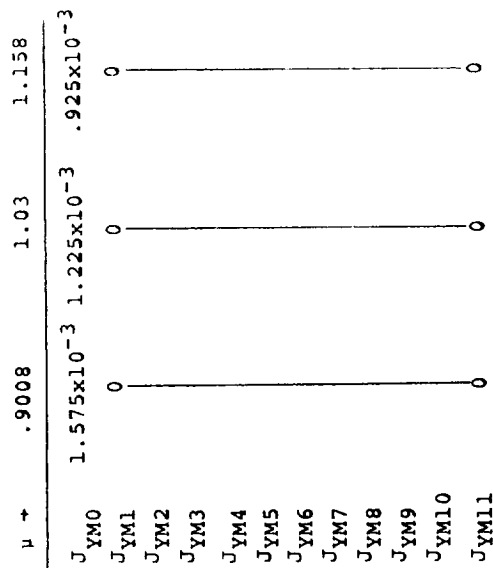
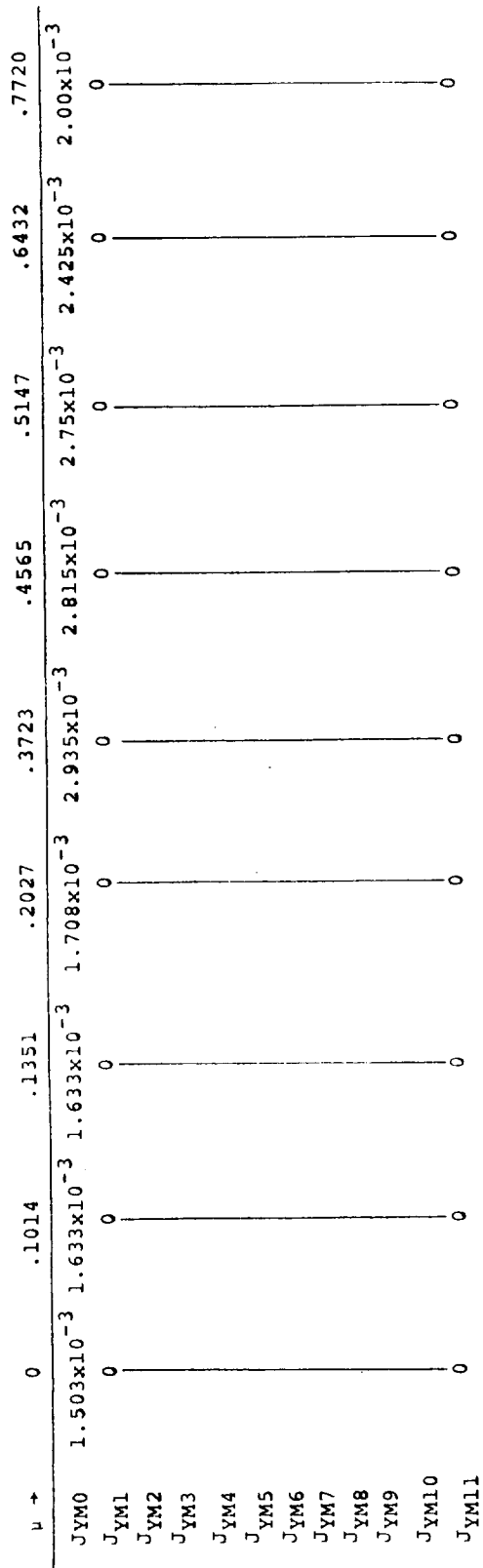
Figure F.24. Coefficients of Curve Fit Equations for Yawing Moment Coefficient

$\mu \rightarrow$	0	.1014	.1351	.2027	.3723	.4565	.5147	.6432	.7720
H _{PM0}	-1.503x10 ⁻³	-1.633x10 ⁻³	-1.633x10 ⁻³	-1.708x10 ⁻³	-2.935x10 ⁻³	-2.815x10 ⁻³	-2.75x10 ⁻³	-2.425x10 ⁻³	-2.00x10 ⁻³
H _{PM1}	0	0	0	0	0	0	0	0	0
H _{PM2}	0	0	0	0	0	0	0	0	0
H _{PM3}	0	0	0	0	0	0	0	0	0
H _{PM4}	0	0	0	0	0	0	0	0	0
H _{PM5}	0	0	0	0	0	0	0	0	0
H _{PM6}	0	0	0	0	0	0	0	0	0
H _{PM7}	0	0	0	0	0	0	0	0	0
H _{PM8}	0	0	0	0	0	0	0	0	0
H _{PM9}	0	0	0	0	0	0	0	0	0
H _{PM10}	0	0	0	0	0	0	0	0	0
H _{PM11}	0	0	0	0	0	0	0	0	0

$\mu \rightarrow$.9009	1.03	1.158
H _{PM0}	-1.575x10 ⁻³	-1.225x10 ⁻³	-0.925x10 ⁻³
H _{PM1}	0	0	0
H _{PM2}	0	0	0
H _{PM3}	0	0	0
H _{PM4}	0	0	0
H _{PM5}	0	0	0
H _{PM6}	0	0	0
H _{PM7}	0	0	0
H _{PM8}	0	0	0
H _{PM9}	0	0	0
H _{PM10}	0	0	0
H _{PM11}	0	0	0

NOTE: α must be in degrees when these coefficients are used in the pitching moment rate equation.

Figure F.25. Curve Fit Coefficients for $\alpha_{C_{PM}}^{\alpha_Q}$



NOTE: α must be in degrees when these equations are used in the hub yawing moment rate equation.

Figure F.26. Curve Fit Coefficients for $\frac{\alpha_C Y_M}{\alpha_R}$

$$\left. \begin{array}{l} \text{ENF}_1 = -.024 \\ \text{ENF}_2 = -.002703 \\ \text{ENF}_3 = -.000346 \\ \text{ENF}_4 = .00039 \end{array} \right\} \text{Coeff. of } \frac{dC_{NF}}{dB_{1C}} \sim \frac{1}{DEG}$$

$$\left. \begin{array}{l} \text{DNF}_1 = .006 \\ \text{DNF}_2 = -.0012318 \\ \text{DNF}_3 = .000033 \\ \text{DNF}_4 = -.0000268 \end{array} \right\} \text{Coeff. of } \frac{dC_{NF}}{dA_{1C}} \sim \frac{1}{DEG}$$

$$\left. \begin{array}{l} \text{ESF}_1 = .0025 \\ \text{ESF}_2 = .0011896 \\ \text{ESF}_3 = -.00001246 \\ \text{ESF}_4 = .00001669 \end{array} \right\} \text{Coeff. of } \frac{dC_{SF}}{dB_{1C}} \sim \frac{1}{DEG}$$

$$\left. \begin{array}{l} \text{DSF}_1 = .025 \\ \text{DSF}_2 = .0025356 \\ \text{DSF}_3 = -.0002264 \\ \text{DSF}_4 = -.000044 \end{array} \right\} \text{Coeff. of } \frac{dC_{SF}}{dA_{1C}} \sim \frac{1}{DEG}$$

$$\left. \begin{array}{l} \text{EPM}_1 = -.0025 \\ \text{EPM}_2 = -.0014304 \\ \text{EPM}_3 = .0003029 \\ \text{EPM}_4 = -.0002938 \\ \text{EPM}_5 = -.0001367 \\ \text{EPM}_6 = -.0004888 \\ \text{EPM}_7 = -.0001767 \end{array} \right\} \text{Coeff. of } \frac{dC_{PM}}{dB_{1C}} \sim \frac{1}{DEG}$$

$$\left. \begin{array}{l} \text{DPM}_1 = -.0015 \\ \text{DPM}_2 = .0010726 \\ \text{DPM}_3 = -.0001564 \\ \text{DPM}_4 = .0001762 \\ \text{DPM}_5 = +.0000966 \\ \text{DPM}_6 = .000571 \\ \text{DPM}_7 = .0000422 \end{array} \right\} \text{Coeff. of } \frac{dC_{PM}}{dA_{1C}} \sim \frac{1}{DEG}$$

$$\left. \begin{array}{l} \text{EYM}_1 = .0025 \\ \text{EYM}_2 = -.0013888 \\ \text{EYM}_3 = .000336 \\ \text{EYM}_4 = -.000187 \\ \text{EYM}_5 = -.0000723 \\ \text{EYM}_6 = -.0006354 \\ \text{EYM}_7 = -.0000098 \end{array} \right\} \text{Coeff of } \frac{dC_{YM}}{dB_{1C}} \sim \frac{1}{DEG}$$

$$\left. \begin{array}{l} \text{DYM}_1 = -.0025 \\ \text{DYM}_2 = -.0009883 \\ \text{DYM}_3 = .000089 \\ \text{DYM}_4 = -.0002866 \\ \text{DYM}_5 = -.0001503 \\ \text{DYM}_6 = -.0004564 \\ \text{DYM}_7 = -.0001993 \end{array} \right\} \text{Coeff of } \frac{dC_{YM}}{dA_{1C}} \sim \frac{1}{DEG}$$

Figure F.27. Constants for Cyclic Pitch Effectiveness in Rotor Equations

F.4 AIRFRAME AERODYNAMIC INPUT DATA

The input data for the airframe aerodynamic data are given in this section and are referenced by page number to the equations presented in Appendix E. Plotted aerodynamic data are presented in Figures F.28 to F.30 .

F.4.1 Input Data

<u>PAGE</u>		<u>PAGE</u>	
E.21	$C_{L_{\alpha W}} = 3.94 \text{ 1/rad}$	E.43	$\eta_{HT} = 1.0$
E.28	$C_{L_{MAX}} = 1.232$		$\eta_{VT} = 1.0$
E.31	$K_{20} = -.0975/\text{RAD}$ $K_{21} = -.0916/\text{RAD}$ $K_{22} = .015$ $K_{\alpha} = 1.0$ $K_{\eta} = 1.0$	E.44	$\alpha_N \leq .5236\text{RAD}/>.5236\text{RAD}$ $C_{DON} = .001821/- .016179$ $K_{30} = .04773/- .2034$ $K_{31} = .16086/- .071138$ $K_{32} = .1087$
E.32	$f_{eu} = 60 \text{ ft}^2$ $D/T = .05$ $K_{D1}/T = 0.0$ $K_{D2}/T = 0.0$ $K_{D3}/T = .05$ $K_{D4}/T = .05$ $K_{M1}/T = 0.0$ $K_{M2}/T = 0.0$ $K_{M3}/T = 0.0$ $K_{M4}/T = 0.0$		$C_{MON} = 0$ $K_{34} = 0$ $K_{35} = 0$ $K_{36} = -.1087$ $K_{37} = 0$ $K_{36} = -.1087$ $K_{37} = 0$ $C_{NON} = 0$ $K_{38} = 0$ $K_{39} = 0$ $K_{40} = 0$ $K_{41} = 0$
E.36	$\tau_{HT} = .52$ $\alpha_{HT\text{STALL}} = 16 \text{ DEG}$ $C_{L_{\alpha HT}} = .061 \text{ 1/DEG}$ $C_{D_{OHT}} = .0084202$	E.49	$C_{DOF} = .0075705$ $K_0 = 18$ $K_1 = -.03581$ $K_2 = .2561$ $\Delta C_{DLG} = .05$ $K_3 = .922/\text{RAD}$ $K_4 = 0$ $K_5 = .67709$ $K_6 = 0$ $K_7 = -.478$
E.39	$\frac{d\sigma}{d\beta} = -.025$ $\tau_{VT} = .55$ $\alpha_{VT\text{STALL}} = 20.0 \text{ DEG}$ $C_{x_{\alpha VT}} = .0546 \text{ 1/DEG}$ $C_{D_{OVT}} = .0078915$		

$$\begin{aligned}
 \text{E.49} \quad K_8 &= 0 \\
 K_9 &= -.131/\text{RAD} \\
 K_{10} &= 0 \\
 C_{\text{MOF}} &= .0001883 \\
 C_{\text{NOF}} &= 0 \\
 \Delta C_{\text{MLG}} &= 0 \\
 K_{42} &= .0537
 \end{aligned}$$

$$\begin{aligned}
 \text{E.52} \quad T_1 &= 0 \\
 T_2 &= -.04808 \\
 T_3 &= .3795
 \end{aligned}$$

$$\begin{aligned}
 \text{E.54} \quad \tau_1 &= .1 \\
 \tau_2 &= .1
 \end{aligned}$$

$$\text{E.60} \quad f_{\text{TR}} = f_{\text{NFR}} = f_{\text{SFR}} = f_{\text{PMR}} = f_{\text{YMR}} = f_{\text{QR}} = f_{\text{PR}} = 1.0$$

$$\begin{aligned}
 \text{E.66} \quad \frac{dC_{\text{Mwc}}/4}{dC_L} &= -.03215 \\
 C_1 &= -.065 \\
 C_2 &= -.0025 \text{ 1/DEG} \\
 C_3 &= 0.0 \text{ 1/DEG}^2 \\
 C_{L\alpha} &= 3.94/\text{RAD}
 \end{aligned}$$

Wing Aerodynamic Input Data

Coefficients of $\sum_{v=0}^4 \sum_{u=0}^4 [A_{D(u+5v)} \delta^u \alpha^v]$ (Page E.26)

A_{D0}	$= .582990 \times 10^{-3}$
A_{D1}	$= .126170 \times 10^{-2}$
A_{D2}	$= .391649 \times 10^{-4}$
A_{D3}	$= .110058 \times 10^{-5}$
A_{D4}	$= -.159415 \times 10^{-7}$
A_{D5}	$= .245484 \times 10^{-3}$
A_{D6}	$= .265950 \times 10^{-3}$
A_{D7}	$= .404673 \times 10^{-5}$
A_{D8}	$= -.152693 \times 10^{-6}$
A_{D9}	$= .102320 \times 10^{-8}$
A_{D10}	$= -.313543 \times 10^{-5}$
A_{D11}	$= .624554 \times 10^{-6}$
A_{D12}	$= .141804 \times 10^{-6}$
A_{D13}	$= -.821732 \times 10^{-8}$
A_{D14}	$= .119984 \times 10^{-9}$
A_{D15}	$= -.474069 \times 10^{-5}$
A_{D16}	$= .771740 \times 10^{-6}$
A_{D17}	$= -.800800 \times 10^{-7}$
A_{D18}	$= .208761 \times 10^{-8}$
A_{D19}	$= -.114899 \times 10^{-10}$
A_{D20}	$= .238184 \times 10^{-6}$
A_{D21}	$= .196213 \times 10^{-7}$
A_{D22}	$= -.204613 \times 10^{-8}$
A_{D23}	$= .133330 \times 10^{-10}$
A_{D24}	$= .492127 \times 10^{-13}$

NOTES: δ, α in degrees.

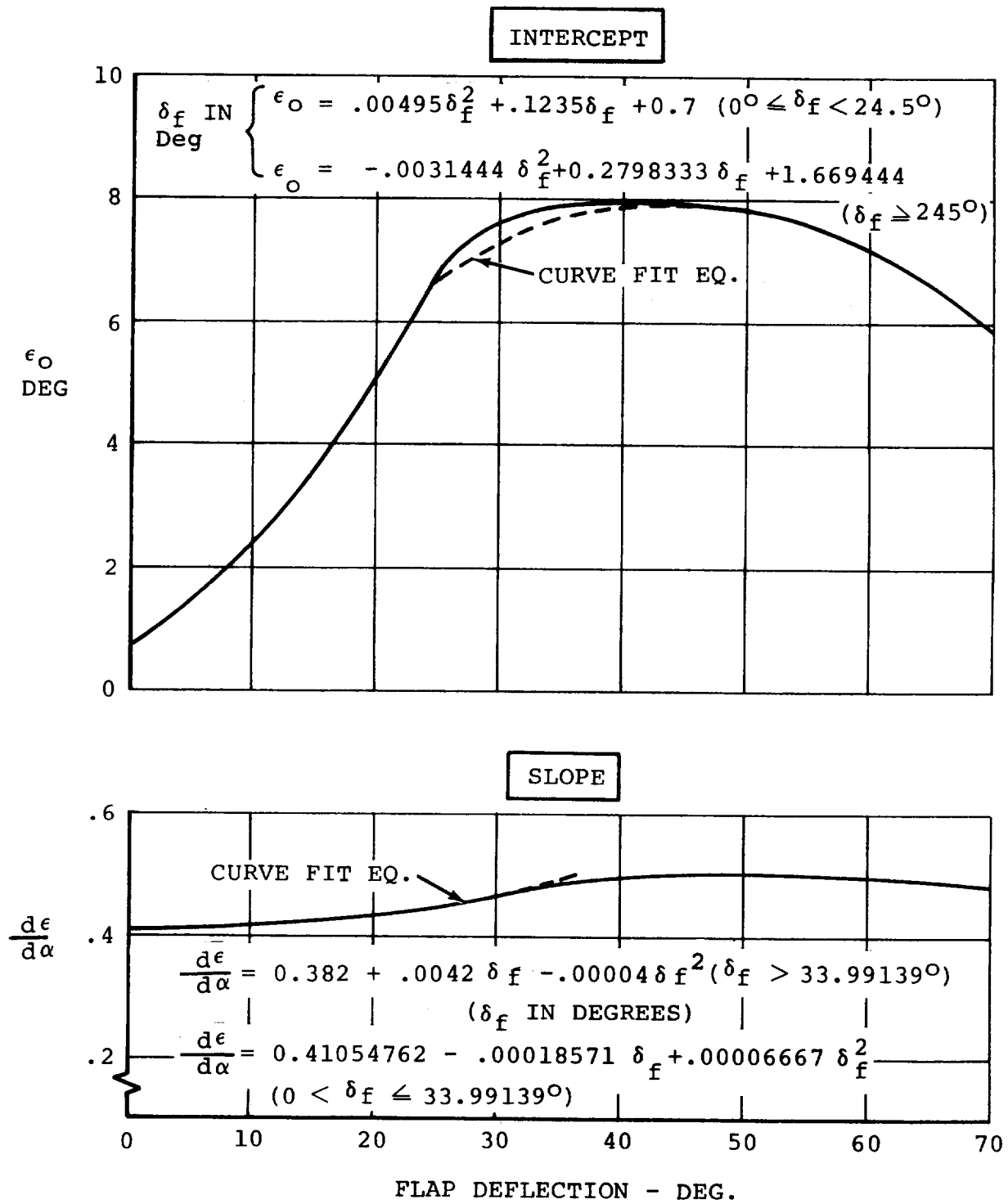


Figure F.28. Model 222 Downwash Functions @ $C_T = 0, i_w = +2.0^\circ$

REF: APPENDIX B-7 ETKIN

$$\left\{ \begin{array}{l} \text{FOR TAIL;} \\ \frac{a_g}{a} = 1.2103 - .038 h_T + .00184 h_T^2; h_T \leq 6.3219 \\ \frac{a_g}{a} = 1.1096 - .01284 h_T + .00038 h_T^2; h_T > 6.3219 \\ \frac{a_g}{a} = 1.00; h_{Tc/4} \geq 17. \end{array} \right.$$

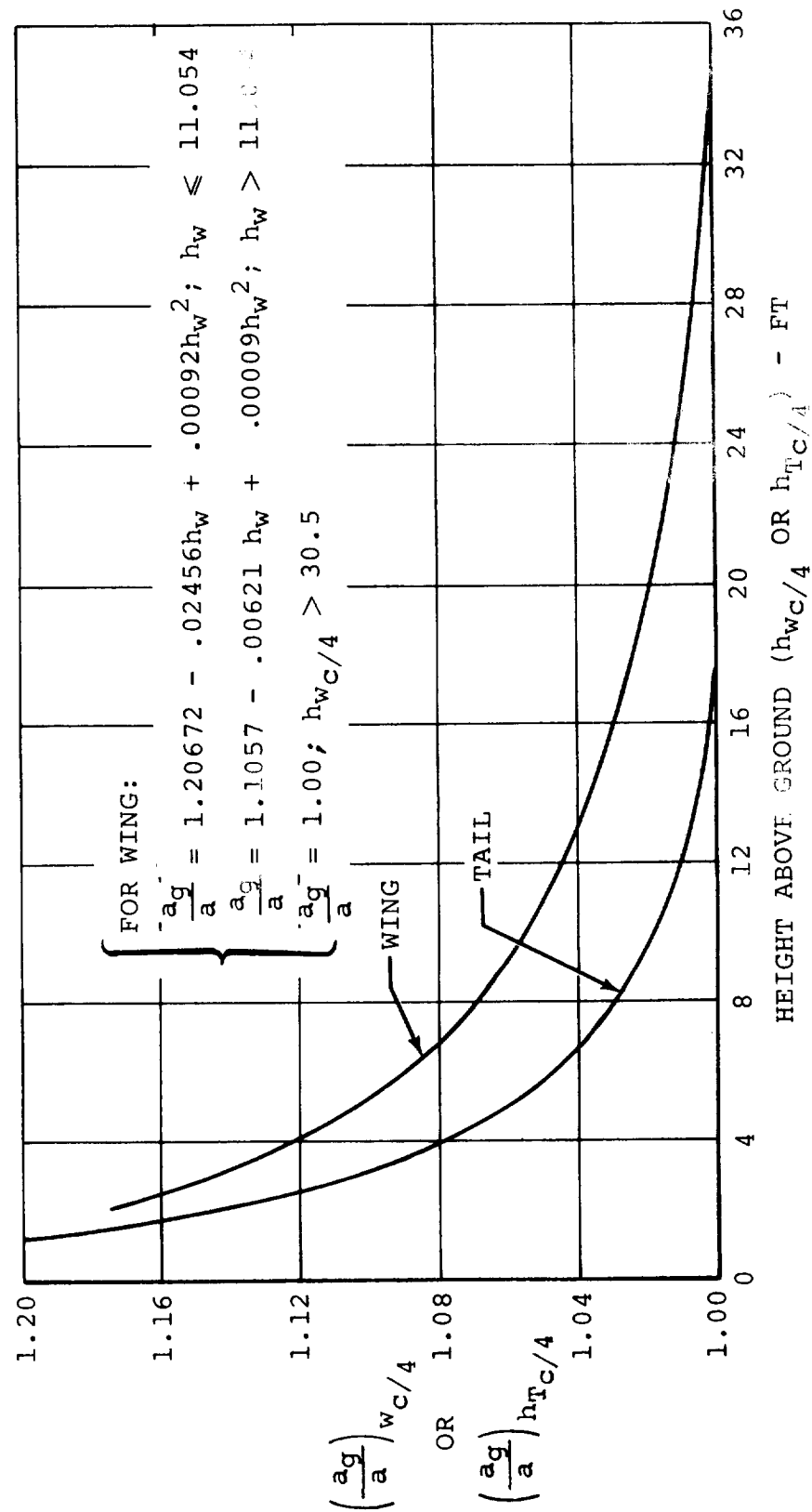
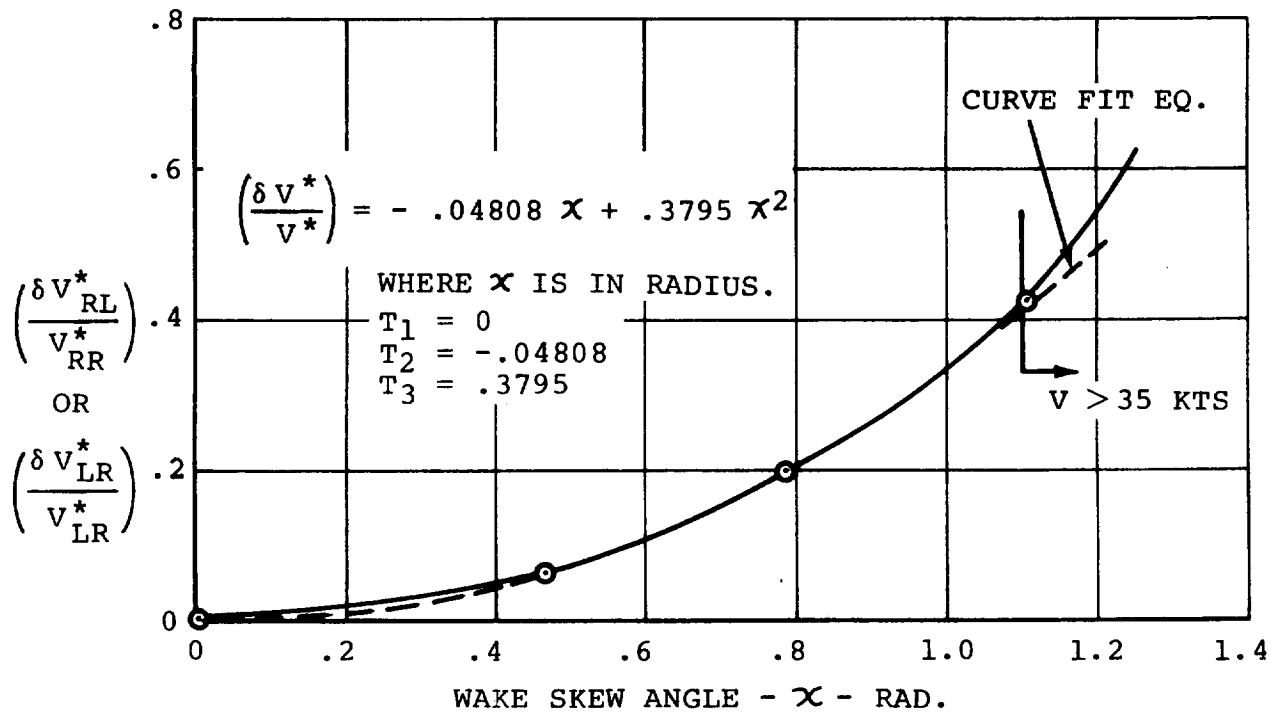


Figure F.29. Variation of Lift Curve Slope with Ground Height



ESTIMATED ROTOR/ROTOR INTERFERENCE PARAMETER

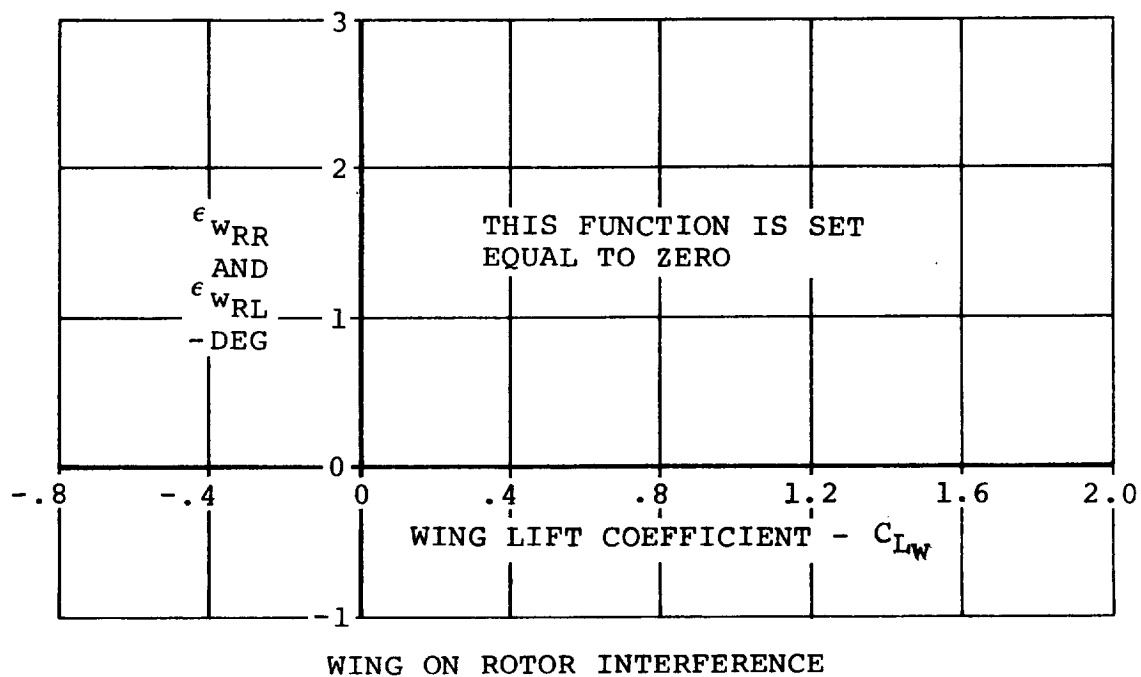


Figure F.30. Rotor/Rotor and Wing/Rotor Interference

F.5 GEOMETRIC, WEIGHTS AND BALANCE DATA

The input data for the Model 222 geometry, weights and balance are presented in this section, and are referenced in Appendix E. Input data for the preprocessor calculations are not presented, but are easily obtainable from an aircraft three-view drawing and the weights and balance data presented in this section. It should be emphasized that the lengths and inertias presented here were calculated using the preprocessor.

F.5.1 Input Data

<u>Page</u>		<u>Page</u>	
E.16	$X_{WAC} = .84 \text{ ft}$	E.23,E.17	$i_w = 2 \text{ DEG}$
	$Y_{WAC} = 8.333 \text{ ft}$	E.31	$b_w = 33.417 \text{ ft}$
	$Z_{WAC} = .4 \text{ ft}$		$\bar{Y} = 6.92 \text{ ft}$
	$L_S = 4.94 \text{ ft}$	E.32	$X_{C/2} = -.25 \text{ ft}$
	$Y_N = 16.666 \text{ ft}$	E.35	$i_{HT} = 0.0$
E.18	$X_{HT} = -19.45 \text{ ft}$	E.36	$AR_{HT} = 4.255$
	$Z_{HT} = 2.51 \text{ ft}$	E.39	$AR_{VT} = 1.768$
	$X_{VT} = -18.04 \text{ ft}$		$S_{HT} = 58.3 \text{ ft}^2$
	$Z_{VT} = -1.0226 \text{ ft}$		$S_{VT} = 43.3 \text{ ft}^2$
E.19	$A = 530929 \text{ ft}^2$	E.46	$Z_{G_1} = 7.08 \text{ ft}$
	$R = \text{ft}$		$Z_{G_2} = 7.08 \text{ ft}$
E.20	$PC = 2.36 \text{ ft}, F_{IN}=0^\circ$		$Z_{G_3} = 7.53 \text{ ft}$
	$h_p = .33 \text{ ft}$		$Y_{G_1} = -3.86 \text{ ft}$
	$c_w = 5.983 \text{ ft}$		$Y_{G_2} = 3.86 \text{ ft}$
	$S_w = 200 \text{ ft}^2$		$Y_{G_3} = 0$

Page

E.46

$$\begin{aligned} X_{G_1} &= -3.7 \text{ ft} \\ X_{G_2} &= -3.7 \text{ ft} \\ X_{G_3} &= 10.67 \\ r_1 &= 1.065 \text{ ft} \\ r_2 &= 1.065 \text{ ft} \\ r_3 &= .60 \text{ ft} \\ K_{ST_1} &= 3840 \text{ lb/ft} \\ K_{ST_2} &= 3840 \text{ lb/ft} \\ K_{ST_3} &= 3840 \text{ lb/ft} \\ D_{ST_1} &= 600 \text{ lb/ft/sec} \\ D_{ST_2} &= 600 \text{ lb/ft/sec} \\ D_{ST_3} &= 600 \text{ lb/ft/sec} \\ \mu_0 &= .03 \\ \mu_1 &= .005 \\ \mu_s &= .5 \end{aligned}$$

E.50

$$\begin{aligned} X_{FAC} &= .84 \text{ ft} \\ Z_{FAC} &= 3.66 \text{ ft} \end{aligned}$$

E.61

$$I_P = 564 \text{ slu-ft}^2$$

E.62

$$I_E = 1.47 \text{ slug-ft}^2$$

E.64

$$\begin{aligned} K_{W_1} &= .59678 \times 10^{-4} \\ K_{W_2} &= .1637 \times 10^{-4} \\ K_{W_3} &= .58356 \times 10^{-5} \\ K_{W_4} &= .2959 \times 10^{-2} \\ K_{W_5} &= .1656 \times 10^{-2} \end{aligned}$$

Page

E.64

$$\begin{aligned} \zeta_{W_1} &= .5 \\ \zeta_{W_2} &= .5 \\ \zeta_{W_3} &= .5 \\ \zeta_{W_4} &= .5 \\ \zeta_{W_5} &= .5 \\ K_{W_6} &= .1709 \times 10^{-4} \\ K_{W_7} &= .05768 \times 10^{-4} \\ K_{W_8} &= .1221 \times 10^{-5} \\ K_{W_9} &= .0847 \times 10^{-2} \\ K_{W_{10}} &= .0559 \times 10^{-2} \end{aligned}$$

$$\omega_{W1} = 19.92 \text{ rad/sec}$$

$$\omega_{W2} = 19.92 \text{ rad/sec}$$

$$\omega_{W3} = 19.92 \text{ rad/sec}$$

$$\omega_{W4} = 19.92 \text{ rad/sec}$$

E.66

$$K_{\theta t} = 0.98 \times 10^6 \text{ FT-LB/RAD}$$

$$\frac{X_{WAC}}{C_w} = .275$$

E.79

$$Y_{PA} = 0$$

$$l_{PA} = 6.75 \text{ ft}$$

$$Z_{PA} = 4.75 \text{ ft}$$

E.68 to

E.78 Equations of motion input constant (Weight = 12321 lb,
nominal CG)

$$m_W = 138.32 \text{ slugs}$$

$$m_N = 43.39 \text{ slugs}$$

$$m_f = 157.88$$

$$m = 382.98 \text{ (12321 LBS)}$$

$$I_{xx}^{(f)} = 789.3 \text{ slug-ft}^2$$

$$I_{yy}^{(f)} = 10845.6 \text{ slug-ft}^2$$

$$I_{zz}^{(f)} = 10707.4 \text{ slug-ft}^2$$

$$I_{xz}^{(f)} = 399.9 \text{ slug-ft}^2$$

$$I_{xx}^{(w)} = 23978.4 \text{ slug-ft}^2$$

$$I_{yy}^{(w)} = 664.8 \text{ slug-ft}^2$$

$$I_{zz}^{(w)} = 24513.6 \text{ slug-ft}^2$$

$$I_{xz}^{(w)} = 384.5 \text{ slug-ft}^2$$

$$I_{xx}' = 22.5 \text{ slug-ft}^2$$

$$I_{yy}' = 194.0 \text{ slug-ft}^2$$

$$I_{zz}' = 195.4 \text{ slug-ft}^2$$

$$I_{xz}' = -20.0 \text{ slug-ft}^2$$

$$l_f = .6917 \text{ ft}$$

$$h_f = 4.075 \text{ ft}$$

$$l_w = -.775 \text{ ft}$$

$$h_w = .30417$$

$$y_N = 16.666 \text{ ft}$$

$$l = 3.3624 \text{ ft}$$

$$\lambda = 2.841 \text{ DEG}$$

$$L_s = 4.94 \text{ ft}$$

F.6 SIMULATION INPUT DATA

This section presents the input data required to drive the Flight Simulator for Advanced Aircraft (FSAA). Figure F.31 shows the instrumentation requirements and Figure F.32 shows the Model 222 control force gradients and breakout forces.

CAB INSTRUMENTATION:

<u>Instrument</u>	<u>Range</u>
Vertical Situation Indicator	+90° Pitch and Roll
Horizontal Situation Indicator	+120° Heading
Airspeed	0 → 520 KIAS
Pressure Altimeter	0 → 10,000 Ft
Radar Altimeter	0 → 1000 Ft
Rate of Climb	+ 6000 FT/MIN
Turn and Bank	+ 3 Needle Widths
	+ 1 1/2 Ball Widths
"g" Meter	-1, +3 "g"
Nacelle Angle	0 → 120°
Clock	
Sideward Velocity	+ 40 Knots
Angle of Attack	+ 20°
Wing Flap Position	0 → 100°
Rotor Speed	0 → 125%
Engine Torque Meters (2)	0 → 125%

PRIMARY FLIGHT CONTROLS

Stick (+6° Long.; +5" Lateral)
Pedals (+2.5")
Power Lever (0→8" Normal; 0→10" Emergency)
Nacelle Position thumb Switch

MISCELLANEOUS EQUIPMENT AND FEATURES

Back Drives to Trim Stick and Pedals while in Initial Condition (I.C.)
Landing Gear Up - Down Switch with Indicator Light
SAS ON-OFF Switch
Detent Switches on Spring Cartridges (Pedals & Lateral Stick)
Magnetic Brake on Pedals, Long. and Lateral Controls
Long. and Lateral Beep Force Trim on Stick
Power Lever Null Meter
Toe Brakes
Specified Force Feel System

Figure F.31. Model 222 Pilot Station Requirements

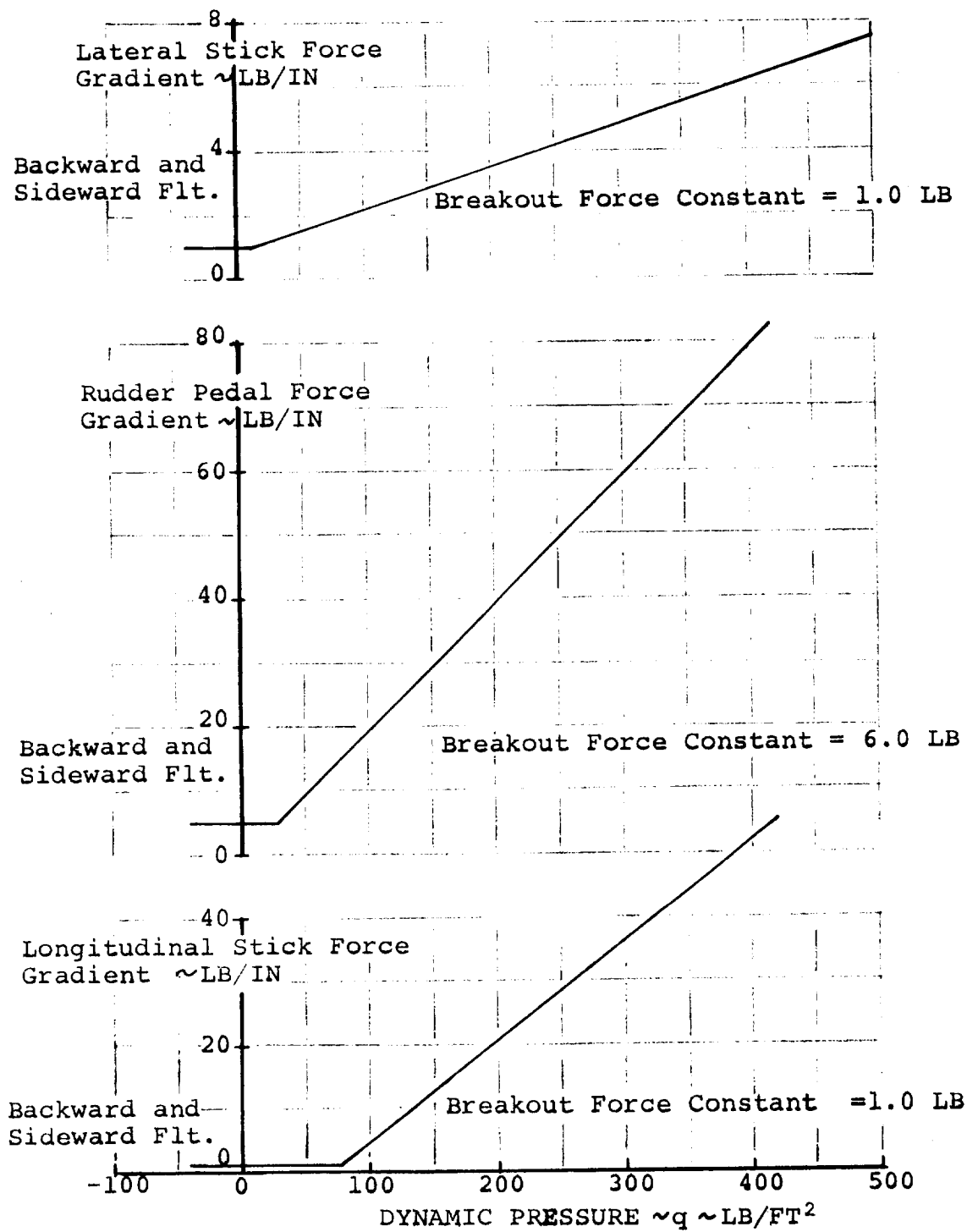


Figure F.32. Model 222 Control Force Gradients and Breakout Forces

APPENDIX G - IN-HOUSE HYBRID SIMULATION

The math model described in this report was mechanized in the Boeing Hybrid Simulation Laboratory for the purpose of developing and evaluating math model simplifications. This was accomplished in a parallel time frame to the NASA simulation, which also used the described math model.

The Hybrid Simulation Laboratory is a large scale hybrid computation complex. It is capable of providing simultaneous operation of several hybrid and analog simulations, depending on problem size. The complex is totally state of the art, with recent acquisition of two mini-computers for the purpose of multivariable function generation.

The Hybrid Simulation Laboratory complex is comprised of the following elements:

- Digital

- IBM 360/44 system

- 25600 byte core

- 32 priority interrupts

- 16 hi-speed floating point register

- 2 hi-speed, 1 low speed channels

- 2 - 800 B.P.I. tape transport

- 1 - 2311 disk system

- 2 - 2315 disk system

- 1 - hi-speed card read/punch

- 1 - hi-speed line printer

2 - alpha-meric scope/keyboard

1 - console typewriter

1 - ball printer

Basic Computer Arts Function Generation System (BOA)

1 - Interdata processor with 24000 byte core

1 - Interdata processor with 16000 byte core

2 - 16 channels analog to digital

2 - 16 channels digital to analog

2 - read only memory software systems

- Analog

4 - 3/4 expanded Applied Dynamics (AD-4)

771 amplifiers (all solid state)

4 resolver expansions

2 display consoles

10 ufd integrator system in 6 decades

1 - 1/8 expanded AD4 maintenance console

128 channels 100 KC analog to digital converters

128 channels digital to analog converters

1 applied dynamics 256

- Analog Output

4 - 8 channel Brush strip chart recorders

4 - 8 channel Varian Statos III strip chart recorders

4 - XY plotters

- Software System

Integrated disk resident state of the art system embracing
"real time" languages:

Assembly Language

Modified Fortran IV, Level G
and non-real time languages

Non-procedural block modeling, DSL/44

Fortran IV, Level G

Full utility system

Other special hybrid oriented programs

G.1 SIMULATION ARCHITECTURE

The tilt rotor simulation model utilized the entire hybrid facility. When tied to Boeing's Nudge Base Simulator, four consoles of Applied Dynamics from (AD-4's) analog, the Applied Dynamics 256 (AD-256) and two Simulator Laboratory analog computers were in use. In addition the IBM 360/44 digital computer and two Basic Computing Acts (BCA) function generators were utilized. Figure G.1 shows the utilization of the hybrid facility and also shows the location of the major elements of the tilt rotor mathematical model.

In programming the digital portion of the tilt rotor simulation, core size and execution time were of immediate concern. Along with the complex wing and rotor representations, there was a large number of functions which had to be handled in the digital computer with trade-offs considered on core used if functions were programmed as tables and execution time for digital table

look-up versus curve-fit equations. In most cases, curve-fit equations were used to program functions. A program was written to curve fit the various functions needed, and the equation programmed for the real time task.

The single largest difficulty was the rotor representation. To program the curve-fit equations for each of the eight functions, for both rotors, would take 30 milliseconds (timing estimates without rotor indicated only 10 milliseconds were available). To program as tables and look-up answers, would not only take too long, but use too much core. So the rotor data was put in the function generation mini-computers (BCA). To get the rotor data into format for the BCA, several steps had to be executed; 1) data points were input to the curve-fit program which punched out the coefficients of the curve-fit expansion, 2) these coefficients were input to a program that punched data in the correct format at the correct breakpoints to be input to 3) the BCA program which punched a deck of cards that are input to the function generator mini-computer.

Although the BCA enabled the programming of the rotor without using digital time or core, it did not have enough room to hold 8 functions x 2 rotors for the rotor 'maps' of the size required. To obviate this, the BCA was multiplexed, such that only one rotor's results would be calculated each BCA cycle, with the left and right rotor being alternated. In this case it took 8 milliseconds per BCA cycle, resulting in a total rotor update every 16 milliseconds.

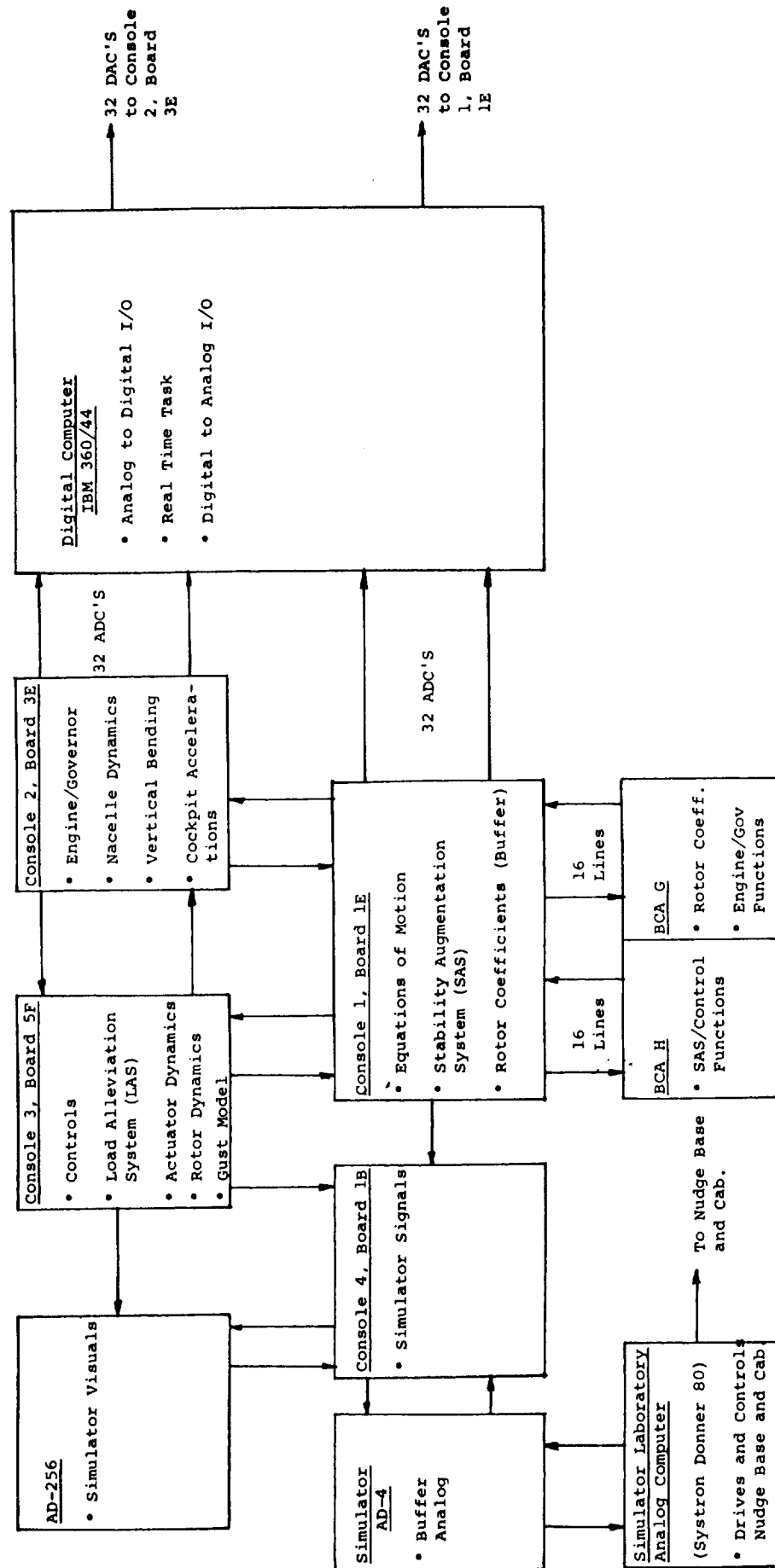


Figure G.1. Utilization of the Hybrid Laboratory for the Model 222 Math Model

As programming progressed, timing estimates showed the time frame would be a problem. The objective was a 40. millisecond (ms) time frame which results in 7 updates/cycle for the 3.5 cycle per second first mode vertical bending calculations. Due to the large number of angles and trigonometric functions, the complexity of the model and the real time requirement, every effort was made to reduce the time frame.

A parallel real time task method, where a 40 ms. time frame could be achieved, was selected. This method had two real time tasks, a 'Fast' real time task that was calculated every frame and a 'Slow' real time task that was executed every 3 frames. Thus, it was important to separate the equations to ensure only low frequency equations were placed in the slow loop. In order to minimize execution time, the system routines for taking the sine, cosine and square root, having unnecessary accuracy at the expense of time, were discarded and replaced by streamlined routines. Since there are a total of 21 sine-cosine pairs and 20 square-roots, the saving was substantial. The need for the time savings is emphasized by the fact that at present, using the parallel real time task, the total execution time is 38 ms. leaving 2 ms. for the foreground options, shown in Figure G.2 to be executed. The 40 ms. time frame objective has been achieved.

The digital portions of the simulation were programmed using the General Hybrid Program (GHP) structure, which utilizes a

- Direct control of the analog computer state and the interval timer (initial condition, hold, operate)
- Change aircraft trim conditions (airspeed, lateral speed, altitude, rate of climb, trim pitch attitude, trim nacelle angle)
- Control of line printer real-time printout
- Control of line printer trim printout
- Ability to change values of simulation flags (landing gear on/off ground effect on/off, vertical bending on/off, wing twist on/off)
- Ability to change real time phases (dual phase, total phase, plot phase; used to plot any digital function)

Figure G.2. Foreground Options

phase overlay scheme. The basic phase overlay structure is shown in Figure G.3. This figure also summarizes what is contained in each phase. Of most interest to this discussion are three phases; 1) the Preprocess phase, 2) the Run phase and 3) the Dual phase. The Preprocess phase loads the simulation data and sets up the analog computer by setting the potentiometers to the correct values and by reading out a test condition to ensure that no components are statically bad. Once the analogs are set up and checked, control is transferred by GHP to the run phase. This phase is in control while actually 'running' hybrid and executing the real time task. It is in the run phase that various options are provided, while the simulation is being used. These foreground options have been described in Figure G.2. The two line printer options, the line printer trim sheet and the line printer real time printout, are powerful tools allowing visibility into the simulation equations.

The Dual phase contains the two real time tasks, the fast (RTFAST) and the slow (RTSLOW). Figures G.4 and G.5 show what each real time task contains. The execution time of RTFAST is 32 ms. while that of RTSLOW is 18 ms. Since RTFAST is executed every 'frame' but RTSLOW only every 3 frames, the execution time is $32 + 18/3$ or 38 ms.

The digital listing for the simulation program is shown in Figure G.6. This listing contains the fast and slow real

<u>COMMON AREA</u> <ul style="list-style-type: none"> • CONSTANTS AND VARIABLES 			
<u>ROOT PHASE</u> <ul style="list-style-type: none"> • COMMON AREA FOR SUBROUTINES 			
<u>SET PHASE</u> <ul style="list-style-type: none"> • Specifies utilization of analog equipment i.e., no. of consoles no. of ADC's, no. of DAC's 	<u>PREPROCESS PHASE</u> <ul style="list-style-type: none"> • Loads Simulation Data • Sets initial conditions on analogs • Static checks analogs 		
		<u>SOLUTION PHASE</u> <ul style="list-style-type: none"> • Contains initial cond. used in run phase • Controls which phase below is loaded 	<u>POST PROCESS PHASE</u> <ul style="list-style-type: none"> • Tape Output Option
		<u>RUN PHASE</u> <ul style="list-style-type: none"> • Contains run option controls 	
		<u>DUAL PHASE</u> <ul style="list-style-type: none"> • Contains Real Time Task 	<u>PLOT PHASE</u> <ul style="list-style-type: none"> • Plots Output

Figure G.3. GHP Phase Overlay Structure (Digital Core Allocations)

1. ANALOG TO DIGITAL I/O
 - Reads analog ADC lines
 - Converts to floating point
2. ENTRY FOR STATIC CHECK OF FAST REAL TIME TASK
 - Used for test cases W/O I/O
3. ANGLE INITIALIZATION SECTION
 - $\sin, \cos i_{NL} \& i_{NR}$
 - $i_{NACELLE}$
 - $\sin, \cos i_{NL-\lambda}, i_{NR-\lambda}$ using trig
 - δ_{FLAP}^2
4. VELOCITY SECTION (VELOCITIES, VELOCITIES², FREESTREAM, DYN. PRESSURE, TRANSFORM.)
 - Fuselage (also $\alpha_{fus}, \beta_{fus}, \sin, \cos$)
 - Doors open/close logic-f(i_{NAC}, q_{FUSE})
 - Rotor Hub - body axes, shaft axes, free-stream
 - Wing A/C - body axes, chord axes, free-stream
 - Tail
5. ROTOR SECTION - LEFT AND RIGHT
 - $\alpha, \zeta, \sin, \cos$ of α and ζ
 - Rotor angular rate transform. p, q, R
 - $\Omega, V_{TIP}, \mu, \Omega^2, \mu^2$
 - Rotor control axes transform A_{1C}, B_{1C} WRT ϕ_p, ζ
 - Rotor EQS for CNF, CSF, CP, CYM
 - Forces and moments from coefficients $T, N.F., S.F., M, N, Q$
 - Hub moments - Nacelle axes
 - Resolution of forces & moments - body axes at tip
 - Summation with nacelle aero
 - Gust load alleviation system
6. WING SECTION - LEFT AND RIGHT
 - q_{LW}, q_{RW}, q_{WING}
 - Doors open/close check
 - If doors open
 - Calc. $X, Y, Z, L, M, N, AERO$
 - Leave wing section & Set $q's=0$
 - If doors closed
 - $\alpha, \beta, \alpha_{SSO}, \alpha_{RIG}, \bar{\alpha}$
 - Aileron, Spoiler, Flap contribution to lift, drag, moment; Call AILSP
 - Contribution due to totally washed wing; call CLCDCM
 - Contribution due to totally unwashed wing; call CLCDCM
 - \bar{C}_L ; Call CCF2
 - $\alpha, \sin \& \cos \alpha, \sin \& \cos \beta, \sin \& \cos \epsilon_p$
 - α, β check for stall
 - Aero Calc & resolution
 - Wing/rotor interference
7. TAIL SECTION
 - $\epsilon_{TAIL}, \epsilon_o$ if necessary; logic for doors open/closed
 - $\alpha_{HT}, \sin, \cos(\alpha_{HT}-i_{HT})$
 - 7 region C_{LHT}, C_{DHT} curve
 - $\beta_{VT}, \alpha_{VT}, \sigma, \sin, \cos(\beta_{VT}-\sigma)$
 - 7 Region C_{LVT}, C_{DVT} curve
 - If doors open; 1/2 efficiency of horizontal tail
 - Vertical tail Aero
 - Total tail Aero
8. EQUATION OF MOTION SECTION
 - Call gear subroutine
 - Total Fuse Aero
 - Calculate total aircraft Aero $X_{AERO}, Y_{AERO}, Z_{AERO}, L_{AERO}, M_{AERO}, N_{AERO}$
 - Break $Z_{AERO}, L_{AERO}, M_{AERO}$ into vertical bending/non-vertical bending parts
 - BOM coefficients
 - Vertical bending equations with flag
 - Torsion equation with flag
 - Fill DAC array (64)
9. DIGITAL TO ANALOG I/O
 - Convert DACS to integer
 - Write values

Figure G.5. Contents of Real Time Task - Slow Loop

1. ANALOG TO DIGITAL I/O
 - Reads discretes
 - Assigns flags to discretes
 - Check for trim sheet flag
 - Read 3rd console ADCS if required
2. ENTRY FOR STATIC CHECK OF SLOW REAL TIME TASK
 - Used for test cases w/o I/o
3. PRELIMINARY CALCULATIONS
 - $\sin^2 i_{NL}$, i_{NR} , \sin , $\cos 2i_{NR}$, $2i_{NL}$, h^2 , q_{FUSE}
 - XCG, ZCG
 - V_{NORTH} , V_{EAST} , ground track
4. AIR & ENGINE MODEL
 - δ , T^*F , ρ , a , M , $\sqrt{1-M^2}$
 - TEA, preliminary engine routine calculations
 - SHP, ΩE , ηQ ; call engine
5. FUSELAGE SECTION
 - C_{DF} , C_{LF} , C_{YF} , C_{MF} , C_{NF}
 - Aero calculation
6. GROUND EFFECT SECTION (WING & ROTOR)
 - $(a_g/a)_w$, K_{g9} , (T_{TGE}/T_{OGE}) , D/T , (M/T)
7. NACELLE SECTION LEFT & RIGHT
 - α_{NAC} , β_{NAC} , \sin & $\cos \alpha_{NAC}$, β_{NAC}
 - C_D , C_L , C_Y , C_M , C_N nacelle
 - Aero calculation
8. WING IMMERSSED AREA SECTION - LEFT & RIGHT
 - τ , V^* , Look-up v^* ,
 - $\bar{\epsilon}_p$, C_{TSR}
 - $\bar{\zeta}$, \bar{a}_R , $\bar{\epsilon}_p$, \bar{C}_{T_S} , $\sin \bar{\zeta} \cos \bar{\zeta}$, $\sin \bar{\zeta} \cos(\bar{I}_{NAC} - \bar{I}_w)$, $\tan(\bar{a}_R - \bar{\epsilon}_p)$
 - ζ_{R1} , ζ_{R2} , ζ_{R3} , ζ_{R4}
 - S_{iR} , S_{iL} , S_{iL}/S , S_{iR}/S , S_{iT} , AR_1 , CL_i , K_a
9. ROTOR/ROTOR INTERFERENCE
10. GROUND EFFECT - TAIL
 - $H_{wC/4}$, $H_{TC/4}$, $(a_q/a)_t$

Figure G.6. Model 222 Simulation Digital Listing

SUBROUTINE RTEAST

INDEX

300PLG	DCMIG	FTNPD	DOVT	FSO4ET	EFFMT	EFFVT	FIE	FINDEG	26 TO 34	
*EIP	FIXPR	FIXYM	FIXZF	FIXPR	FIXZM	FIYVF	FIYVF	FIYPR	35 TO 43	
*TIYM	FI2ZF	FI2PR	FI2YM	FMREF	PC	PI	PI	POTPRD	44 TO 52	
*DEPR	SRAPR	SC	SK7	SK9	SK1	SK2	SK3	SK3	53 TO 61	
*SK4	SK6	SK7	SK9	SK1	SK2	SK3	SK3	SK3	62 TO 70	
*SK22	CDNLC	SK310	SK32	CDNHI	SK34	SK35	SK36	SK36	71 TO 79	
*SK37	SK39	SK41	SK42	SK43	SK44	SK45	SK46	SK46	80 TO 88	
*SK46	SK47	SK48	SK49	SK50	SL	SLF	SLPA	SLM	89 TO 97	
*SM	SMF	SMN	SMW	SPAN	TAUHF	TAUVT	XFAC	XHT	98 TO 106	
*SMAC	XVT	YN	YPA	YMAC	ZFAC	ZHT	ZPA	ZMAC		
*ZVT	CLOAL	PHIPH	SK3PHI	ENZREF	XMC2	RT1	RT2	RT3		
*RKDIT	RKD2T	RKD3T	RKM1T	RKM2T	RKM3T	RKM4T	SK31HI			
*EEN	CLMAX	ALR8K	RKLSW	RKNSW	SQPRM	DEG20	DGTORD	HTVKT	133 TO 141	
*EIOV2	POTOG	ROTFS	SKFDS	ALNFBK	TAURTI	TAURT2				
COMMON/DACIO/	DAC1(32)	DAC2(32)								
COMMON/XLINTP/	AKY(15)	AME(21)	BKEY(15)	HMEM(2)	GKEY(13)	GHEM				
COMMON/XEJUP/	VSTAG(33)	TAIAG(9)	SVSTAG(33)	SOFAR(35)						
1	GAATAR(35)	GPATAR(35)	ALFTAB(35)							
1	COMMON/XCNTRL/	SKOLR	SKOLS	SKULR	SKOLE	SKOLRD	TH75LP	TH75LN		
2	TAUGLS	GLSLM	TAUGIC	STICM	CONTRBL(4)	GMA	ETAA			
3	SKDA	GTH	TAUTH	OMC	OMSLP	OML4	GOMG	SKDCOL	THOTLM	THOYLP
4	THOMN	SHPLM	STHGOV	OMR3	FIARD	TTNSLP	TTMSLN	GORI	G032	
5	TAURD	GOATTC	TAUR1	TAJ02	TAJTH	GLP	GLPSLP	GPOS	TAUPDS	
6	GP	TAUP	GBEFO	TAUHF	GP41	TAUJPHI	GPSIDR	GRETDR	GRDR	TAJDR
7	GPSI	TAURSI	GBETR	TAUPR	JPRI	TAUPRI	GR	TAJRI	TAJRC	TAUP3
8	PLM	DLBL	DLBL4	DLBLM	DLBL4					
9	TOMDLM	GULTM	SKW1	SHW2	SHW3	SKW4	SKW5			
10	SKW6	SKW7	SKW8	SKW9	SK413	GGUST	TAUGST	OMWR	ETAM3	GINRF
11	OMRE	ETAIPE	SKTHTM	SCI	SC2	DCMDCL	AINPLM	TAUR01	TAUR02	
12	TAUFE	TAUFR	DOVFLM	AL	ASLP	ALIM	TAUSHP	DELALM		
13	DLFLP									
14	COMMON/INTVR/									
15	1	AVEIN	CILAMR	COSINL	COSINR	COSPSI	C2INL	C2INR	DLFPSO	1 - 3
16	2	HSD	SILAML	SILAMP	SININL	SININR	SINPSI	SSQINL	SSQINR	10 - 18
17	3	SZINP								19
18	COMMON/VSUAR/									
19	1	VEAST	VNORT4	XCG	YDTGG	ZDS	ZDTGG			1 - 6
20	COMMON/VSUAR/									
21	1	AMAC4	AMAC5C	DEL	EMAXN1	EMAXN2	EMXWOT	ENDSTR	FSMACH	OMEGEL
22	2	OMECF	ONGVTC	OMVFSM	OMVSDTH	OMVTHDL	XDE	ROFQW2	SHPPRL	SHPPR
23	3	SMA	SD1MX	SD1HIC	SDMDTX	TDFEF	TEAL	TEAR	THODEL	THEIC
24	4	PCICL	PCICP							29 TO 29
25	COMMON/VELVAR/									
26	1	AMUL	AMULSQ	AMUP	AMJISQ	WPTL	CMJTL	CMJTR	OMEGAL	OMEGAR
27	2	AMSOL	AMSOR	AMT	AMJL	AMJLPR	AMJLWQ	AMJL	JRL	JURLR
28	3	IFLURL	UPR	URPR	URPRR	JRA	URPRR	JRWQ	USQ	UVT
29	4	VALFLM	VALFRM	VALFS	VALVCL	VALVNC	V3ETVT	VLM	VLMWQ	
30	5	VP	VRL	VRLPR	VRLVPL	VPR	VPRDR	VRRVR	VRR	VRR403
31	6	VWWSQ	VWQ	VVT01	VVT02	VVT03	VVT04	VVT05	VVT06	VVT07
32	7	VZFR	AMT	MLM	MLMDE	MLASQ	AP	MRL	MRLPR	MRLWRL
33	8	WRW	WRWPR	WRWSQ	WRP	WRPR	WRWRR	WQ	WVT	64 - 71
34	COMMON/FUSVAR/									
35	1	ALAP	ALAPRD	ALFSD	ALP4F	ANAPF	ANAREP	ANAREP	TEFAT	1 - 9
36	2	BETFSO	CRME	CRF	CLF	CMF	CNSF	COSALF	COSRTE	CVE
37	3	CLLG	DMLG	DMLG	DYLG	DZLG	JFSW	SBECAF	SRESAF	19 - 27

Figure G.6. (Continued)

SUBROUTINE RTFAST

2	FIZZ	FJXX	FJYY	FJZZ	JCVIXX,QWVIVY,QDVIZZ,PP	PQ		10 - 18
3	PO	QR	RO	TERMI	TERM2, TERM3, TERM4, TERM5, TERM6,			19 - 27
4	TERMP1, TERMQ1, TEKMB1, TERNM1, TRATTP	XAERO	XF	XFMELF,XL	XALCOS, XLSIN, XQ,			28 - 36
5	TOMTI, TRATTP	XAERO	XF	XFMELF,XL	XALCOS, XLSIN, XQ,			37 - 45
6	KPCOS, XRSIN, YAW	XWMH14,YAERO,ZAFRO,ZF	ZFMEHF,ZL					46 - 54
7	ZLCUS, ZLSIN, ZR	ZRCDS, ZRSIN, ZW	ZMMMH,P					55 - 63
8	R	U	V	W				
9	COMMON/TRMCN/	UTRIM,VTRIM,-TTRIM,HOTRIM,THTRIM,AITRIM,						
1	COMMON/XPAR3/	SCTRIM(113)						
1		CONSI, CONS2, CONS3, CONS4, CONS5, CONS6, CONS7,						1 TO 14
1		CONS8, CONS9, CONS10, CONS11, CONS12, CONS13, CONS14,						8 TO 14
2		CONS15, CONS16, CONS17, CONS18, CONS19, CONS20, CONS21,						15 TO 21
2		CONS22, CONS23, CONS24, CONS25, CONS26, CONS27, CONS28,						22 TO 28
3		CONS29, CONS30, CONS31, CONS32, CONS33, CONS34, CONS35,						29 TO 35
3		CONS36, CONS37, CONS38, CONS39, CONS40, CONS41, CONS42,						36 TO 42
4		CONS43, CONS44, CONS45, CONS46, CONS47, CONS48, CONS49,						43 TO 49
5		CONS50, CONS51, CONS52, CONS53, CONS54, CONS55, CONS56,						50 TO 56
6		CONS57, CONS58, CONS59, CONS60, CONS61, CONS62, CONS63,						57 TO 63
7		CONS64, CONS65, CONS66, CONS67, CONS68, CONS69, CONS70,						64 TO 70
8		DAPK1,DAPK2,DAPK3,DAPK4,DAPK5,DAPK6,DAPK7,						71 TO 77
9		DAPK8,DAPK9,DAPK10,DAPK11,DAPK12,DAPK13,DAPK14,						78 TO 84
0		DAPK15,DAPK16,DAPK17,DAPK18,DAPK19,DAPK20,DAPK21,						85 TO 91
*		SFTL,SFEVL,SFEFL,SFPM,L,SFYML,SFQL,SFPL,						
*		SFTI,SENER,SESPD,SFPMR,SFYMR,SFOR,SFPR						
E		CONS71,CONS72,CONS73,CONS74,CONS75,CONS76,CONS77						
E		-CONS78,CONS79,CONS80,CONS81						

30 31

G-18

TABLE OF PRE-COOKED COEFFICIENTS DEFINITION C

```

REGON = SLF*(1.-SMF/SM) - SLN*SMW/SM
RFEON = SLF*(1.-SMF/SM) - SHW*SMW/SM
RWFON = SMW*(1.-SMF/SM) - SLF*SMF/SM
RWGON = SMW*(1.-SMW/SM) - SHF*SMF/SM
RWKON = -(SMF*SLF + SMW*SLW)/SM
RWBON = -(SMF*SHF + SMW*SHW)/SM
RWBLCN = (SMF*SHF + 2.*SMW*Y1+YN
XXICON = SUM1XX + 2.*SMW*Y1+YN
YVICON = SUM1YY
YVICON = SUM1Z + 2.*SMN*Y1+YN
YVICON = FLXZF + FLXZW
YVICON = SUM1Z7 - SUM1YV + 2.*SMN*Y1+YN
YVICON = (FLXZF - FLZF)/ (FLXW-FLZW)
YVICON = (SUM1YV-SUM1XX) - 2.*SMN*Y1+YN
YVICON = SL*SMN/SM
YVICON = SL*(1.-SMN/SM)
YVICON = FLXPR - FLZPD
YVICON = SL*SMN
YVICON = SMF * SHF
YVICON = SMW * SHW
YVICON = SMF * SLF
YVICON = SMW * SLW
YVICON = SL*SMN+YN
YVICON = 1. / SM
YVICON = 9KLSM*YVAC/2./SPAN

```

Figure G.6. (Continued)

SUBROUTINE DTFAST

I N D E X

```

COEF12 = PI*SM*AV*YAC/2./SPAN
COEF13 = (PI*YDPR*SL*SM*SM*(1.-SM/SM))
COEF14 = APE*SPAN (S * R) * WING CHARACTERISTICS
COEF15 = CH / SPAN (C / R) * WING CHARACTERISTICS
COEF16 = S / 2
COEF17 = PI*OTRAD*OTRAC*OTRAD*OTRAD
COEF18 = COEF17 * OTTRAC
COEF19 = 1./PI*SM*PI*ARHT
COEF20 = 1./PI*SM*PI*ARHT
COEF21 = 1./PI*SM*PI*ARHT
COEF22 = 1./PI*SM*PI*ARHT
COEF23 = APE*SM*PI*ARHT
COEF24 = APE*SM*PI*ARHT
COEF25 = 1./PI*SM*PI*ARHT
COEF26 = COEF25 / 2.
COEF27 = 1./PI*SM*PI*ARHT
COEF28 = 1./PI*SM*PI*ARHT
COEF29 = PI*SM*PI*ARHT
COEF30 = 1./PI*SM*PI*ARHT
COEF31 = S * C / 2
COEF32 = S * C / 2
COEF33 = S * C / 2
COEF34 = YAC / V / X TH TWIST
COEF35 = S * C / 2
COEF36 = S * C / 2
COEF37 = S * C / 2
COEF38 = S * C / 2
COEF39 = S * C / 2
COEF40 = S * C / 2
COEF41 = S * C / 2
COEF42 = S * C / 2
COEF43 = S * C / 2
COEF44 = S * C / 2
COEF45 = S * C / 2
COEF46 = S * C / 2
COEF47 = S * C / 2
COEF48 = S * C / 2
COEF49 = S * C / 2
COEF50 = S * C / 2
COEF51 = S * C / 2
COEF52 = S * C / 2
COEF53 = S * C / 2
COEF54 = S * C / 2
COEF55 = S * C / 2
COEF56 = S * C / 2
COEF57 = S * C / 2
COEF58 = S * C / 2
COEF59 = S * C / 2
COEF60 = S * C / 2
COEF61 = S * C / 2
COEF62 = S * C / 2
COEF63 = S * C / 2
COEF64 = S * C / 2
COEF65 = S * C / 2
COEF66 = S * C / 2
COEF67 = S * C / 2
COEF68 = S * C / 2
COEF69 = S * C / 2
COEF70 = S * C / 2
COEF71 = S * C / 2
COEF72 = S * C / 2
COEF73 = S * C / 2
COEF74 = S * C / 2
COEF75 = S * C / 2
COEF76 = S * C / 2
COEF77 = S * C / 2
COEF78 = S * C / 2
COEF79 = S * C / 2
COEF80 = S * C / 2
COEF81 = S * C / 2
COEF82 = S * C / 2
COEF83 = S * C / 2
COEF84 = S * C / 2
COEF85 = S * C / 2
COEF86 = S * C / 2
COEF87 = S * C / 2
COEF88 = S * C / 2
COEF89 = S * C / 2
COEF90 = S * C / 2
COEF91 = S * C / 2
COEF92 = S * C / 2
COEF93 = S * C / 2
COEF94 = S * C / 2
COEF95 = S * C / 2
COEF96 = S * C / 2
COEF97 = S * C / 2
COEF98 = S * C / 2
COEF99 = S * C / 2
COEF100 = S * C / 2

```

Figure G.6. (Continued)

SUBROUTINE RTFAST

INDEX

```

52 V = VPRIME + VGUST
53 A = APRIME + AGUST
54 P = PPRIME + PGUST
55 Q = QPRIME + QGUST
56 R = RPRIME + RGUST
57 HSO = H*U
58 VSQ = V*V
59 HSO = H*W
60 VALF = FSORT(IUSQ+MSQ,WORK)
61 ALPHF = ATAN2(W,U)
62 RTAF = ATAN2(V,VALF)
63 VTOTAL = FSORT(IUSQ+VSQ+MSQ,WORK)
64 SOF = ROENV2*(IUSQ+VSQ+MSQ)
65 IF(SOF.GT.SQPRM) GO TO 13C
66 NCLOSE = 0
67 SQPRM = DHPKIR*CPK19
68 GO TO 14C
69 NCLOSE = 1
70 SQPRM = DHPK14-DHPK19
71 CONTINUE
72 GLAS SYSTEM
73 CALL LINTCKEY,GMEM,GMEM,I5TG,SOF,GATAB,GALF,GATAB,GALF,
74 1 ALFTAB,ALREF)
75 TAJDET = GRIALF
76 ALFGLS = ALPHF*ROTDG
77 RETGLS = RETAF*ROTDG
78 ATGLS = ALFGLS*GALF+RETGLS*GALBET
79 AICGS = RETGLS*GALBET-ALFGLS*GALALF
80 BICGS = ALFGLS*GALF
81 CUSELAG = PIVOT VELOCITY
82 JP = U - Q*ZCG - XDTG
83 VP = V + W*ZCG - YDTG
84 WP = W + Q*XCG - ZDTG
85
86 LEFT ROTOR HUB VELOCITY - BODY AXES
87 HJL = UP + P*VN - BL*SININL*(Q+AINDTL)*Q*HIL
88 VJLP = VP + BL*(P+COSINL+P*SININL) - P*HIL
89 WJLP = WP - P*VN - BL*(Q+AINDTL)*COSINL + HIDL
90
91 RIGHT ROTOR HUB VELOCITY - BODY AXES
92 HRP = UP - P*VN - BL*SININR*(Q+AINDR)*Q*HIR
93 VRP = VP + BL*(P+COSINR + P*SININR) - P*HIR
94 WRP = WP + P*VN - BL*(Q+AINDR)*COSINR + HIRDT
95
96 LEFT ROTOR HUB VELOCITY - SHAFT AXES
97 JPL = HJLP+COSINL - HJLP*SININL
98 VJLP = VJLP
99 WJLP = HJLP*SININL + WJLP*COSINL
100
101 RIGHT ROTOR HUB VELOCITY - SHAFT AXES
102 JRR = HRP+COSINR - WRP*SININR
103 VRR = VRR
104 WRR = WRR+COSINR + WRR*SININR

```

Figure G.6. (Continued)

```

101  LEFT STREAM VELOCITY
102  VELVL = VEL*VL
103  VALVSL = VEL*VSL
104  VALVSL = VEL*VSL
105  VALVSL = VEL*VSL
106  VALVSL = VEL*VSL
107  VALVSL = VEL*VSL
108  VALVSL = VEL*VSL
109  VALVSL = VEL*VSL
110  VALVSL = VEL*VSL
111  VALVSL = VEL*VSL
112  VALVSL = VEL*VSL
113  VALVSL = VEL*VSL
114  VALVSL = VEL*VSL
115  VALVSL = VEL*VSL
116  VALVSL = VEL*VSL
117  VALVSL = VEL*VSL
118  VALVSL = VEL*VSL
119  VALVSL = VEL*VSL
120  VALVSL = VEL*VSL
121  VALVSL = VEL*VSL
122  VALVSL = VEL*VSL
123  VALVSL = VEL*VSL
124  VALVSL = VEL*VSL
125  VALVSL = VEL*VSL
126  VALVSL = VEL*VSL
127  VALVSL = VEL*VSL
128  VALVSL = VEL*VSL
129  VALVSL = VEL*VSL
130  VALVSL = VEL*VSL
131  VALVSL = VEL*VSL

```

Figure G.6. (Continued)

SURROUTINE RTFAST

INDEX

```

196 CYMRIL = FYM1*CTL + FYM2*AMULSO + FYM3*AMUL + FYM4
197 CYMIL = DYMI*CTL + DYM2*AMULSO + DYM3*AMUL + DYM4
198
199 CONTINUE
200
201 CPMRIL = EPM1*CTL + EPM5*AMULSO + EPM6*AMUL + EPM7
202 CPMIL = DPM1*CTL + DPM5*AMULSO + DPM6*AMUL + DPM7
203
204 CYMRIL = FYM1*CTL + FYM5*AMULSO + FYM6*AMUL + FYM7
205 CYMIL = DYMI*CTL + DYM5*AMULSO + DYM6*AMUL + DYM7
206
207 CONTINUE
208
209 CNFL = CNFPL + CNFALL*ATCL + CNFRIL* BICL
210 CSFL = CSFPL + CSFALL*ATCL + CSFRIL* BICL
211 CPMFL = CPMPL + CPMALL*ATCL + CPMRIL *BICL
212 CYMFL = CYMPL + CYMALL*ATCL + CYMRIL *BICL
213
214
215
216
217
218
219
220
221
222
223
224
225
226
227
228
229
230
231
232
233
234
235
236
237
238
239
240
241

```

CALCULATIONS OF FORCES AND MOMENTS FROM COEFFICIENTS
 ROPIR4 = COEF19 * ROE
 ROPIR5 = COEF20 * ROE
 CTL = CTLDPM*TIGEL
 TL = CTL * FQPIR4 * OMSQL
 ENQML = CNFL * ROPIR4 * OMSQL
 ESTOEL = CSFL * ROPIR4 * OMSQL
 ANROTIL = CPMFL * ROPIR5 * OMSQL
 ANROTIL = CYMFL * ROPIR5 * OMSQL
 TORQL = CPI * ROPIR5 * OMSQL
 CTP = CTDRM*TIGER
 TR = CTR * ROPIR4 * OMSQR
 FNQMR = CNFR * ROPIR4 * OMSQR
 ESTDR = CSFR * ROPIR4 * OMSQR
 ANQDTR = CPMR * ROPIR5 * OMSQR
 ANQDTR = CYMR * ROPIR5 * OMSQR
 TORQR = CPP * ROPIR5 * OMSQR
 QMDTL = QMDOT
 QMDTR = QMDOT

HUB MOMENTS - NACELLE AXES
 FIPOML = FIP*OMEGAL
 FIPOM2 = FIP*OMEGAP
 TRMR1 = FIP*OMEGEL * R
 TRMR2 = FIP*OMEGER * R
 TRMR3 = ANROTIL*COSZHL-ANROTIL*SINZHL
 TRMR4 = -ANROTIL*COSZHL-ANROTIL*SINZHL
 TRMR5 = ANROTIL*COSZHR-ANROTIL*SINZHR
 TRMR6 = ANROTIL*COSZHR-ANROTIL*SINZHR
 LEFT
 ALLRH = -TORQL -FIP*QMDTL
 ALRPH = TRMR3-FIPOML*PNLH
 ANLRH = TRMR6+FIPOML*CNLH
 RIGHT
 ALRRH = TORQR + FIP*QMDTR
 ALRPH = TRMR5-FIPOMR*PNRH
 ANRRH = TRMR6-FIPOMR*CNRH

RTTO FORCE AND MOMENT RESOLUTION
 PRELIMINARY CALCULATIONS

Figure G.6. (Continued)

I N D E X

SUBROUTINE RTFAST

E +L

```

***** S Y N T A X E R R O R *****
270 SOWING = SQF + 0.5*DOVDSK*(T2 + TL)
271 SQLW = RDEOV2*(ULWSQ+VLWSQ+HLWSQ) + TL * DOVDSK
272 SQRW = RDEOV2*(URWSQ+VRWSQ+HRWSQ) + TR * DOVDSK
273 IF(NCLOSE.FQ.1) GO TO 420
274 FINPR = FINDEG-DBRK17
      EQUATIONS FOR DOORS OPEN
275 SGNULW = 1.0
276 IF(UL.LT.0.) SGNULW = -1.0
277 SGNURW = 1.0
278 IF(UR.LT.0.) SGNURW = -1.0
279 XAERLW = -SGNULW*FEU*SQLW*(1.-CTSLR)
280 XAFORW = -SGNURW*FEU*SQRW*(1.-CTSPR)
281 YAERLW = 0.
282 YAFORW = 0.
283 ZAERLW = DOVTL*TL
284 ZAFORW = DOVTR*TR
285 AMARLW = -XWC2*ZAERLW + AMOVL*TL
286 AMAPRW = -XWC2*ZAFORW + AMOVT*TR
287 ALAPRW = 0.5*SPAN*(ZAERRW*(1.-0.5*STRW)-7AERLW*(1.-0.5*SLWL))
288 ANARWS = 0.
      SET WING DYNAMIC PRESSURE = TO HARD 0.0 FOR THETA TWIST EQ
289 SOWING = 0.0
290 SOLW = 0.0
291 SQRW = 0.0
292 AVECLW = 0.0
293 GO TO 430
294 CONTINUE
      EQUATIONS FOR DOORS CLOSED
295 FINPR = FINDEG + DBRK17
      ANGLE OF ATTACK AND SIDESLIP
296 ALPHAW = ATAN2(MLN,ULW) + THTLAC
297 BETALW = ATAN2(VLM,VALFL4)
298 ALPHRW = ATAN2(PRW,UPW) + THTPAC
299 BETARW = ATAN2(VRW,VALFRW)
300 ALWSSO = ALPHAW - EPPLR
301 ADWSSO = ALPHRW - EPPRR
302 ALRGLW = ALWSSO - THTLAC
303 ALRGRW = ADWSSO - THTPAC

```

Figure G.6. (Continued)

LINE	TEXT	STATUS
304	AVEALM = 0.5*(ALPHM + ALP400)	C
305	CALCULATE LIFT AND DRAG INCREMENTS	C
306	FLAP , AILERON , SPOILER CONTRIBUTION	C
307	REVISED 11/29/72	C
308	CALL AILSP1 DELAIL , DELSP1, DCLLDA, DCOLDA, DCMLDA, DCLLSP, DCOLSP,	C
309	* DCMLSP1	C
310	CALL AILSP1 DELAIR , DELSP2, DCLRDA, DCLORDA, DCLRDA, DCLRSP, DCLDRSP,	C
311	* DCLRRSP1	C
312	CDICNTL= DCOLDA+DCOLSP	C
313	CMCNTL= DCMLDA+DCMLSP	C
314	CDICNTR= DCLORDA+DCLDRSP	C
315	CMCNTR= DCLRDA+DCLRRSP	C
316	CONTRIBUTION DUE TO TOTALLY DOWNWASHED WING (ALPHA - EPSILON)	C
317	CALL CLCOCMIALWSSD, DELAIL , DCLLDA, DCLLSP, CDCNTRL, CMCNTRL,	C
318	* CLLMSS, CLCMSS, CMLWSS, CLDUM, CODJW	C
319	CALL CLCOCMIALWSSD, DELAIR , DCLRDA, DCLRSP, CDCNTR, CMCNTR,	C
320	* CLRWSS, CORWSS, CRRWSS, CLDUM, CODJW	C
321	CALL CLCOCMIALPHLM, DELAIL , DCLLDA, DCLLSP, CDCNTRL, CMCNTRL,	C
322	* CLLMAD, CLLMAD, CMLWAD, CLLMWR, CLLMWR	C
323	CALL CLCOCMIALPHRM, DELAIR , DCLRDA, DCLRSP, CDCNTR, CMCNTR,	C
324	* CLRWAD, CORWAD, CRRWAD, CLRWPR, CRRWPR	C
325	CALL CLFLICELFLO, CLZERON	C
326	CALL CLFZIALPHF+ATNW, CLZERO, D.O, CLAVEI	C
327	ALLWPR= ALPHLM - AINW - THTLAC	C
328	ALRWPR= ALPHRM - AINW - THTRAC	C
329	SALLW= ALLWPR	C
330	CALLW= 1.0	C
331	SALRW= ALRWPR	C
332	CALRW= 1.0	C
333	SRETLW= RETALW	C
334	CRFTLW= 1.0	C
335	SRETRW= RETARW	C
336	CRFTRW= 1.0	C
337	IMAPN1(7)= .FALSE.	C
338	IMARN1(8)= .FALSE.	C
339	IMARN1(9)= .FALSE.	C
340	IMARN1(10)= .FALSE.	C

SURROUTINE RTFAST

Y N D F X

```

331 IF (ALWSSO.GT.DEG20) IMARNI( 7) = .TRUE.
332 IF (ARWSSO.GT.DEG20) IMARNI( 9) = .TRUE.
333 IF (ALPHLM.GT.DEG20) IMARNI( 9) = .TRUE.
334 IF (ALPHRM.GT.DEG20) IMARNI(10) = .TRUE.
335 CALL SINCOSIEPLR,SEPLW,CEPLW
336 CALL SINCOSIEPRR,SEPRW,CEPRW
C
337 TRMWG5 = (1.-CISLR)*(1.-SILW)
338 TRMWG6 = (1.-CISRR)*(1.-SIRW)
339 CLSLW = (SILW*(CLLWSS*CEPLW-COLWSS*SEPLW) + CLLWAO*TRMWG5)*
* RKALPR
340 CDSLW = (SILW*(CLLWSS*SEPLW+COLWSS*CEPLW) + COLWAO*TRMWG5)*
* RKALPP
341 CMSLW = (SILW*COLWSS + CMLWAO*TRMWG5)*BKALPR
C
342 CLSPW = (SIRW*(CLRWSS*CEPRW -CDRWSS*SEPRW) + CLRWAO*TRMWG6)*
* RKARPP
343 CDRPW = (SIRW*(CLRWSS*SEPRW +CDRWSS*CEPRW) + CDRWAO*TRMWG6)*
* RKARPP
344 CMSPW = (SIRW*CDRWSS + CRRWAO*TRMWG6)*RKARPR
C
345 COLSPW = .25*(1.-.5*SILW)*(CLSLW-CLLWAO*(1.-AVECTS))-(1.-.5*
* SIRW)*(CLSRW-CLRWAO*(1.-AVECTS))
346 DCNSPW = .25*(1.-.5*SIRW)*(CDSRW-CDRWAO*(1.-AVECTS))-(1.-.5*
* SILW)*(COLSW-COLWAO*(1.-AVECTS))
C
347 CLSM = (1.-AVECTS)*(9ETAF*(SK2*(CLAVE)+COEF11*(CLLWAO
* -CLRWAO)) + COLSPW
348 CMSW = (1.-AVECTS)*(9ETAF*(SK2*CLAVE+CLAVE+COEF12*(CDRWAO
* -CLRWAO- CLRWAO*(ALPHRM-ALPH )-CLLWAO*(AINW-ALPHLW ))) +DCNSPW
C
349 TRMWG7 = SOLW * COEF19
350 TRMWG9 = SORW * COEF19
C
351 ZAEPLW = -TRMWG7*(CLSLW*CALL4 +COSLW*CRETLW*SALLW )
352 XAEPLW = TRMWG7*(CLSLW*SALL4 -COSLW*CBETLW*CALLW )
353 YAEPLW = -TRMWG7*CDSLW * SAEPLW
354 AMAPLW = TRMWG7*CHORD *CMSLW * CRETLW
* -XWAC*ZAEPLW + ZWAC*XAEPLW
C
355 ZAEPRW = -TRMWG8*(CLSRW*CALRW +CDSRW*CBETRW*SALRW )
356 XAEPRW = TRMWG8*(CLSRW*SALRW -CDSRW*CBETRW*CALRW )
357 YAEPRW = -TRMWG8*CDSRW * SAEPRW
358 AAEPRW = TRMWG8*CHORD *CMSPW * CBETRW
* -XWAC*ZAEPRW + ZWAC*XAEPRW
C
359 AVECLW = .5*(CLSPW+CLSLW)/(1.-AVECTS)
43 CONTINUE
360 XAEOWG = XAEPLW + XAEPRW
361 YAEOWG = YAEPLW + YAEPRW
362 ZAEOWG = ZAEPLW + ZAEPRW
363 ALAPWG = CLSW * SCWING * COEF14
364

```

Figure G.6. (Continued)

•

[illegible]

1

Figure G.6. (Continued)

SUBROUTINE RTFAST

I N D E X

```

385 CONTINUE
386 EPTL1 = EPZERO+DEPDAL*(AVEALN- SLAC*WDOT/(U*U+C.C11))
387 IF(AVEPP.LT.EPTL1) GO TO 265
388 EPTAIL = AVEPP*(1.-GEF)*NOVFSM
389 GO TO 265
390
391 CONTINUE
392 EPTAIL = EPTL1*(1.-GEF)*NOVFSM
393 CONTINUE
394
395 IF(UPRIME.IE.C.) EPTAIL = C.
396 ALPHMT = ATAN2(WHT,WMT) -EPTAIL + ALHMT
397 IF(ALPHMT.GT.PI) ALPHMT=ALPHMT-2.*Pi
398 IF(ALPHMT.LT.-Pi) ALPHMT=ALPHMT+2.*Pi
399 CALL SINCOS(ALPHMT-ALHMT,SALHT,CALHMT)
400
401 ALHTP2 = TAHT*OFELV
402 ALHTE = ALHMT + ALHTP2
403 ALHTP = HTSTLL + ALHTP2
404 ALHTM = -HTSTLL + ALHTP2
405 CLAT = CLALHT*CLTOMP
406 TRMHT2 = 0.5 * ALHTP
407 TRMHT3 = 0.5 * ALHTM
408
409 IF(UPRIME.IE.C.) EPTAIL = C.
410 IF(ALHTE) 272,277,276
411 IF(ALHTE.GT.(-Pi +TRMHT2)) GO TO 272
412
413 REGION 7
414 CLHT = CLAT*(ALHTE+Pi)
415 CDHT = CDHT + CLHT*CLHT*COEF21
416 GO TO 288
417
418 IF(ALHTE.GT. -PIOV2) GO TO 274
419
420 REGION 6
421 CLHTST = CLAT*TRMHT2
422 CLHT = CLHTST*(ALHTE+PIOV2)/(1-PIOV2+TRMHT2)
423 CDHTST = CDHT + CLHTST*CLHTST*COEF21
424 CDHT = CDHTST*(1.1-CDHTST)*(ALHTE+Pi-TRMHT2)/(1-PIOV2 -PIOV2)
425 GO TO 288
426 IF(ALHTE.GT.ALHTM) GO TO 276
427
428 REGION 5
429 CLHTST = CLAT*ALHTM
430 CLHT = CLHTST*(PIOV2+ALHTE)/(PIOV2+ALHTM)
431 CDHTST = CDHT + CLHTST*CLHTST*COEF21
432 CDHT = CDHTST*(1.1-CDHTST)*(ALHTE-ALHTM)/(1-PIOV2 -ALHTM)
433 GO TO 288
434 IF(ALHTE.GT.ALHTP) GO TO 278
435
436 REGION 1
437 CLHT = CLAT*ALHTE
438 CDHT = CDHT + CLHT*CLHT*COEF21
439 IF(UPRIME.IE.C.) = .FALSE.
440 GO TO 288
441 IF(ALHTE.GT.PIOV2) GO TO 280
442
443 REGION 2
444 CLHTST = CLAT*ALHTP
445 CLHT = CLHTST*(PIOV2-ALHTE)/(PIOV2-ALHTP)
446

```

Figure G.6. (Continued)

```

4420 CONTST = CONTST + CLPTST*CLHTST*COEFF21
4421 CONT = CONTST + ((1.1-CONTST)/(ALHT-ALHTP1)/(PI*V2-ALHTP))
4422 GO TO 238
4423 IF (ALHT-ALHTP1) .LT. -4133) GO TO 242
4424 SECTION 3
4425 CLPTST = CLAT * TRMW2
4426 CLHT = CLPTST*(ALHT-PI*V2)/(PI*V2 - TRMW413)
4427 CONTST = CONTST + CLHTST*CLHTST*COEFF21
4428 CONT = CONTST + ((1.1-CONTST)*(ALHT-PI*TRMW413)/(TRMW413 - PI*V2) - PI*V2)
4429 GO TO 243
4430 SECTION 4
4431 CLHT = CLAT*(ALHT-PI)
4432 CONT = CONTST + CLPTST*CLHT*COEFF21
4433 CONTINUE
4434 VERTICAL TAIL AREA COORDINATE TRANSFORM
4435 IFMT = ATAN2(WT, VACTVT)
4436 ALDVTE = -ACTVT*DETA*DSHRET
4437 IF (CLPTST*CLHT,PI) ALDVTE = ALDVTE-2.*PI
4438 IF (CLPTST*V2,-PI) ALDVTE = ALDVTE+2.*PI
4439 SIGMA = DSHRET*DETA*E
4440 CALL SIGMA*SUBT-VT-SIGMA, SNETST, COEFFSG)
4441 ALVTP1 = TRMW * DELVTP
4442 ALVTE = ALDVTE + ALVTP1
4443 ALVTE = VTSLL + ALVTP1
4444 ALVTE = -VTSLL + ALVTP1
4445 CVAT = CVALVT + TRMW*E
4446 TRMW2 = 1.5 *ALVTP
4447 TRMW3 = 1.5 *ALVTE
4448
4449 IASPH111 = 1.0UE
4450 IF (ALVTE) 295,297,296
4451 IF (ALVTE,CT*(1-PI) + TRMW21) GO TO 292
4452 SECTION 5
4453 CVVT = CVATE*(ALVTE +PI)
4454 CONT = CONTST + CVVTE*CVVT + COEFF22
4455 GO TO 293
4456 IF (ALVTE,CT, -PI*V2) GO TO 296
4457 SECTION 6
4458 CVVTE = CVAT + TRMW2
4459 -CVVT = CVVTE + (ALVTE*PI*V2)/(1-PI*V2+TRMW21)
4460 CONTST = CONTST + CVVTE*CVVTE*COEFF23
4461 CONT = CONTST + ((1.1-CONTST)*(ALVTE*PI - PI*V2)/(TRMW21 - PI*V2) - PI*V2)
4462 GO TO 293
4463 IF (ALVTE,CT,ALVTE) GO TO 296
4464 SECTION 7
4465 CVVTE = CVAT + ALVTE
4466 CONTST = CONTST + CVVTE*CVVTE*COEFF24
4467 CONT = CONTST + ((1.1-CONTST)*(ALVTE-ALVTE*PI)/(1-PI*V2 - ALVTE)
4468 GO TO 293
4469 IF (ALVTE,CT,ALVTE) GO TO 296
4470 SECTION 8
4471 CVVTE = CVAT + ALVTE
4472 CONTST = CONTST + CVVTE*CVVTE*COEFF25
4473 CONT = CONTST + ((1.1-CONTST)*(ALVTE-ALVTE*PI)/(1-PI*V2 - ALVTE)
4474 GO TO 293
4475 IF (ALVTE,CT,ALVTE) GO TO 296
4476 SECTION 9
4477 CVVTE = CVAT + ALVTE
4478 CONTST = CONTST + CVVTE*CVVTE*COEFF26
4479 CONT = CONTST + ((1.1-CONTST)*(ALVTE-ALVTE*PI)/(1-PI*V2 - ALVTE)
4480 GO TO 293
4481 IF (ALVTE,CT,ALVTE) GO TO 296
4482 SECTION 10
4483 CVVTE = CVAT + ALVTE
4484 CONTST = CONTST + CVVTE*CVVTE*COEFF27
4485 CONT = CONTST + ((1.1-CONTST)*(ALVTE-ALVTE*PI)/(1-PI*V2 - ALVTE)
4486 GO TO 293
4487 IF (ALVTE,CT,ALVTE) GO TO 296
4488 SECTION 11
4489 CVVTE = CVAT + ALVTE
4490 CONTST = CONTST + CVVTE*CVVTE*COEFF28
4491 CONT = CONTST + ((1.1-CONTST)*(ALVTE-ALVTE*PI)/(1-PI*V2 - ALVTE)
4492 GO TO 293
4493 IF (ALVTE,CT,ALVTE) GO TO 296
4494 SECTION 12
4495 CVVTE = CVAT + ALVTE
4496 CONTST = CONTST + CVVTE*CVVTE*COEFF29
4497 CONT = CONTST + ((1.1-CONTST)*(ALVTE-ALVTE*PI)/(1-PI*V2 - ALVTE)
4498 GO TO 293
4499 IF (ALVTE,CT,ALVTE) GO TO 296
4500 SECTION 13
4501 CVVTE = CVAT + ALVTE
4502 CONTST = CONTST + CVVTE*CVVTE*COEFF30
4503 CONT = CONTST + ((1.1-CONTST)*(ALVTE-ALVTE*PI)/(1-PI*V2 - ALVTE)
4504 GO TO 293
4505 IF (ALVTE,CT,ALVTE) GO TO 296
4506 SECTION 14
4507 CVVTE = CVAT + ALVTE
4508 CONTST = CONTST + CVVTE*CVVTE*COEFF31
4509 CONT = CONTST + ((1.1-CONTST)*(ALVTE-ALVTE*PI)/(1-PI*V2 - ALVTE)
4510 GO TO 293
4511 IF (ALVTE,CT,ALVTE) GO TO 296
4512 SECTION 15
4513 CVVTE = CVAT + ALVTE
4514 CONTST = CONTST + CVVTE*CVVTE*COEFF32
4515 CONT = CONTST + ((1.1-CONTST)*(ALVTE-ALVTE*PI)/(1-PI*V2 - ALVTE)
4516 GO TO 293
4517 IF (ALVTE,CT,ALVTE) GO TO 296
4518 SECTION 16
4519 CVVTE = CVAT + ALVTE
4520 CONTST = CONTST + CVVTE*CVVTE*COEFF33
4521 CONT = CONTST + ((1.1-CONTST)*(ALVTE-ALVTE*PI)/(1-PI*V2 - ALVTE)
4522 GO TO 293
4523 IF (ALVTE,CT,ALVTE) GO TO 296
4524 SECTION 17
4525 CVVTE = CVAT + ALVTE
4526 CONTST = CONTST + CVVTE*CVVTE*COEFF34
4527 CONT = CONTST + ((1.1-CONTST)*(ALVTE-ALVTE*PI)/(1-PI*V2 - ALVTE)
4528 GO TO 293
4529 IF (ALVTE,CT,ALVTE) GO TO 296
4530 SECTION 18
4531 CVVTE = CVAT + ALVTE
4532 CONTST = CONTST + CVVTE*CVVTE*COEFF35
4533 CONT = CONTST + ((1.1-CONTST)*(ALVTE-ALVTE*PI)/(1-PI*V2 - ALVTE)
4534 GO TO 293
4535 IF (ALVTE,CT,ALVTE) GO TO 296
4536 SECTION 19
4537 CVVTE = CVAT + ALVTE
4538 CONTST = CONTST + CVVTE*CVVTE*COEFF36
4539 CONT = CONTST + ((1.1-CONTST)*(ALVTE-ALVTE*PI)/(1-PI*V2 - ALVTE)
4540 GO TO 293
4541 IF (ALVTE,CT,ALVTE) GO TO 296
4542 SECTION 20
4543 CVVTE = CVAT + ALVTE
4544 CONTST = CONTST + CVVTE*CVVTE*COEFF37
4545 CONT = CONTST + ((1.1-CONTST)*(ALVTE-ALVTE*PI)/(1-PI*V2 - ALVTE)
4546 GO TO 293
4547 IF (ALVTE,CT,ALVTE) GO TO 296
4548 SECTION 21
4549 CVVTE = CVAT + ALVTE
4550 CONTST = CONTST + CVVTE*CVVTE*COEFF38
4551 CONT = CONTST + ((1.1-CONTST)*(ALVTE-ALVTE*PI)/(1-PI*V2 - ALVTE)
4552 GO TO 293
4553 IF (ALVTE,CT,ALVTE) GO TO 296
4554 SECTION 22
4555 CVVTE = CVAT + ALVTE
4556 CONTST = CONTST + CVVTE*CVVTE*COEFF39
4557 CONT = CONTST + ((1.1-CONTST)*(ALVTE-ALVTE*PI)/(1-PI*V2 - ALVTE)
4558 GO TO 293
4559 IF (ALVTE,CT,ALVTE) GO TO 296
4560 SECTION 23
4561 CVVTE = CVAT + ALVTE
4562 CONTST = CONTST + CVVTE*CVVTE*COEFF40
4563 CONT = CONTST + ((1.1-CONTST)*(ALVTE-ALVTE*PI)/(1-PI*V2 - ALVTE)
4564 GO TO 293
4565 IF (ALVTE,CT,ALVTE) GO TO 296
4566 SECTION 24
4567 CVVTE = CVAT + ALVTE
4568 CONTST = CONTST + CVVTE*CVVTE*COEFF41
4569 CONT = CONTST + ((1.1-CONTST)*(ALVTE-ALVTE*PI)/(1-PI*V2 - ALVTE)
4570 GO TO 293
4571 IF (ALVTE,CT,ALVTE) GO TO 296
4572 SECTION 25
4573 CVVTE = CVAT + ALVTE
4574 CONTST = CONTST + CVVTE*CVVTE*COEFF42
4575 CONT = CONTST + ((1.1-CONTST)*(ALVTE-ALVTE*PI)/(1-PI*V2 - ALVTE)
4576 GO TO 293
4577 IF (ALVTE,CT,ALVTE) GO TO 296
4578 SECTION 26
4579 CVVTE = CVAT + ALVTE
4580 CONTST = CONTST + CVVTE*CVVTE*COEFF43
4581 CONT = CONTST + ((1.1-CONTST)*(ALVTE-ALVTE*PI)/(1-PI*V2 - ALVTE)
4582 GO TO 293
4583 IF (ALVTE,CT,ALVTE) GO TO 296
4584 SECTION 27
4585 CVVTE = CVAT + ALVTE
4586 CONTST = CONTST + CVVTE*CVVTE*COEFF44
4587 CONT = CONTST + ((1.1-CONTST)*(ALVTE-ALVTE*PI)/(1-PI*V2 - ALVTE)
4588 GO TO 293
4589 IF (ALVTE,CT,ALVTE) GO TO 296
4590 SECTION 28
4591 CVVTE = CVAT + ALVTE
4592 CONTST = CONTST + CVVTE*CVVTE*COEFF45
4593 CONT = CONTST + ((1.1-CONTST)*(ALVTE-ALVTE*PI)/(1-PI*V2 - ALVTE)
4594 GO TO 293
4595 IF (ALVTE,CT,ALVTE) GO TO 296
4596 SECTION 29
4597 CVVTE = CVAT + ALVTE
4598 CONTST = CONTST + CVVTE*CVVTE*COEFF46
4599 CONT = CONTST + ((1.1-CONTST)*(ALVTE-ALVTE*PI)/(1-PI*V2 - ALVTE)
4600 GO TO 293
4601 IF (ALVTE,CT,ALVTE) GO TO 296
4602 SECTION 30
4603 CVVTE = CVAT + ALVTE
4604 CONTST = CONTST + CVVTE*CVVTE*COEFF47
4605 CONT = CONTST + ((1.1-CONTST)*(ALVTE-ALVTE*PI)/(1-PI*V2 - ALVTE)
4606 GO TO 293
4607 IF (ALVTE,CT,ALVTE) GO TO 296
4608 SECTION 31
4609 CVVTE = CVAT + ALVTE
4610 CONTST = CONTST + CVVTE*CVVTE*COEFF48
4611 CONT = CONTST + ((1.1-CONTST)*(ALVTE-ALVTE*PI)/(1-PI*V2 - ALVTE)
4612 GO TO 293
4613 IF (ALVTE,CT,ALVTE) GO TO 296
4614 SECTION 32
4615 CVVTE = CVAT + ALVTE
4616 CONTST = CONTST + CVVTE*CVVTE*COEFF49
4617 CONT = CONTST + ((1.1-CONTST)*(ALVTE-ALVTE*PI)/(1-PI*V2 - ALVTE)
4618 GO TO 293
4619 IF (ALVTE,CT,ALVTE) GO TO 296
4620 SECTION 33
4621 CVVTE = CVAT + ALVTE
4622 CONTST = CONTST + CVVTE*CVVTE*COEFF50
4623 CONT = CONTST + ((1.1-CONTST)*(ALVTE-ALVTE*PI)/(1-PI*V2 - ALVTE)
4624 GO TO 293
4625 IF (ALVTE,CT,
```


SUBROUTINE RTEAST

I N D E X

```

538 * +YN*(XAERNL-XAERNR)-XCC*YAERNC
539 RQ = R*Q
540 PQ = P*Q
541 QR = R*R
542 PR = P*R
543 PP = P*P
544 RQ = R*Q
545 C POST EQUATION CROSS TERMS
546 TERMPI = -FJXX * RQ +FIXP* PQ
547 QDOT EQUATION CROSS TERMS
548 TERMQ1 = -FJYY * PR -FIXQ*(PP-RR)
549 RDOT EQUATION CROSS TERMS
550 TERMRI = -FJZZ * PQ -FIXR* RQ
551 C AINDDR EQUATION CROSS TERMS
552 TERMIR = COEF4*COEF2*( PR*(1.-2.*SILAMR*SILAMR)-(RR-PP)*SILAMR*
553 * CILAMR )
554 TERM2R = -(RR-PP)* F177PR*SINIR *COSINR +COEF1*(XAERQ*SILAMR
555 * + ZAFRQ*CILAMP )
556 TERM32 = COEF4*(PQ*SILAMR +RQ*CILAMR)
557 C
558 C AINDDL EQUATION CROSS TERMS
559 TERMIL = COEF4*COEF2*( PR*(1.-2.*SILAML*SILAML)-(RR-PP)*SILAML *
560 * CILAML )
561 TERM2L = -(RR-PP)* F177PR *SINIL *COSINL +COEF1*(XAERQ*SILAML
562 * + ZAFRQ*CILAML )
563 TERM3L = -COEF4*(PQ* SILAML + RQ*CILAML )
564 IF(INVR.EQ.1) GO TO 60
565 HIR = .
566 HINTP = .
567 HIL = .
568 HIDL = .
569 HWACR = .
570 HDTACR = .
571 HWACL = .
572 HDTACL = .
573 GO TO 70
574 C
575 C CONTINUE
576 TRMHIS= COEF10*ZAERO
577 HIR=SKW1*ZAERNP+SKW2*ZAEHP+SKW3*ALARNR-TRMHIS*(SKW4+SKW5)
578 HINTP= OVDTIM*(HIR-HIROL)
579 HIROL= HIR
580 HIL=SKW1*ZAERNL+SKW2*ZAFRLW+SKW3*ALARNL-TRMHIS*(SKW4+SKW5)
581 HIDL= OVDTIM*(HIL-HILOL)
582 HILOL= HIL
583 HWACR= SKW6*ZAERNR+SKW7*ZAFRRW+SKW9*ALARNP-TRMHIS*(SKW9+SKW10)
584 HDTACR= OVDTIM*(HWACR-HACRND)
585 HACROD= HWACR
586 HWACL= SKW4*ZAERNL+SKW7*ZAFRLW+SKW9*ALARNL-TRMHIS*(SKW9+SKW10)
587 HDTACL= OVDTIM*(HWACL-HACLOD)
588 HACLOD= HWACL
589 C
590 C TERMS FOR THETA TWIST EQUATION
591 CNDW= SCI + SC2*DELFLP
592 TRMTLL= SOLW*(1.-CTSLEP)

```

Figure G.6. (Continued)

SUBROUTINE RTFAST

I N D E X

```

622 C DAC1(11) = VTRIM
      WDOT EQUATION NON-WING BENDING TERMS
623 C DAC1(12) = ZARGG
      HTRIM DAC
624 C DAC1(13) = -HTRIM
      SORT(POE/ROEC)*VTOTAL FOR 9CA FUNCTIONS
625 C DAC1(14) = FSORT(ROE/ROEC)*U
      COEFFICIENT OF AINDDR IN THE QDOT EQUATION
626 C DAC1(15) = (FIVPR+COEF4*(XLCOS-ZLSINI))*DDVIY
      VTOTLR FOR MU CALC ON ANALOG
627 C DAC1(16) = VTOTLR
      COEFFICIENT OF AINDDL IN THE QDOT EQUATION
628 C DAC1(17) = (FIVPR+COEF4*(XLCOS-ZLSINI))*DDVIY
      LEFT ROTOR ALPHA FOR 9CA
629 C DAC1(18) = -ALPHLR
      THETA TRIM DAC
630 C DAC1(19) = HTRIM
      VTOTRR FOR MU CALC ON ANALOG
631 C DAC1(20) = VTOTRR
      AVERAGE ALPHA WING FOR SIMULATOR
632 C DAC1(21) = -AVEALW
      RIGHT ROTOR ALPHA TO USE IN 9CA
633 C DAC1(22) = -ALPHRR
      COEFFICIENT OF PDOT IN THE ROOT EQUATION
634 C DAC1(23) = FIXZR*DDVI7Z
      PNLR FOR MU CALC ON ANALOG
635 C DAC1(24) = PNLR
      COEFFICIENT OF AINDDR IN THE ROOT EQUATION
636 C DAC1(25) = SILAMR*DDVI7Z
      PNLR FOR MU CALC ON ANALOG
637 C DAC1(26) = PNLR
      COEFFICIENT OF AINDDL IN THE ROOT EQUATION
638 C DAC1(27) = SILAML*DDVI7Z
      VNORTH FOR SIMULATOR
639 C DAC1(28) = -VNORTH
      FUSELAGE DYNAMIC PRESSURE FOR SIMULATOR
640 C SGN5OF = 1.0
      (FUEL-T-0.1) SGN5OF = -1.0
641 C DAC1(29) = -SOF*SGN5OF
      YEAST FOR SIMULATOR
642 C DAC1(30) = -YEAST
      RFTA FUSE FOR CONTROL SYSTEM FEEDBACK
643 C DAC1(32) = -BETAF
      DAC2( 1) = -CILAMR
644 C DAC2(02) = HICGLS
      DAC2( 3) = COEFF3
645 C DAC2(04) = -AICLGS
      DAC2( 5) = SILAMP
      MOMENT ARM FOR CG ACCELERATION EQS FOR SIMULATOR
646 C DAC2( 6) = XCG-SLPA
      HDOT TRIM DAC
647 C DAC2(07) = HDOTTRIM
      AVAILABLE HORSEPOWER RIGHT ENGINE
648 C DAC2(08) = SHPPRR
      DAC2( 9) = CILAML
649 C
650 C
651 C
652 C
653 C

```

Figure G.6. (Continued)

SUBROUTINE RTFAST

I N D E X

```

461 CALL TPACK('RTFAST',2)
462 RETURN
463 DO 512 J=1,32
464 51) CALL DISAB(J-1)
465 52) IPAN= KPAN
466 RETURN
467 END

```

Figure G.6. (Continued)

... 20 1'14 57 FFAST

1
 2
 3
 4
 5

PSLW	1100																																																																																																																																																																																																																																																																																																																																																																																																																																																																																																																																																																																																																																																																																																																																																																																																																																																																																																																																																																																																																																																																																																																																																																																																																																																																																																																																																																																																																			
------	------	--	--	--	--	--	--	--	--	--	--	--	--	--	--	--	--	--	--	--	--	--	--	--	--	--	--	--	--	--	--	--	--	--	--	--	--	--	--	--	--	--	--	--	--	--	--	--	--	--	--	--	--	--	--	--	--	--	--	--	--	--	--	--	--	--	--	--	--	--	--	--	--	--	--	--	--	--	--	--	--	--	--	--	--	--	--	--	--	--	--	--	--	--	--	--	--	--	--	--	--	--	--	--	--	--	--	--	--	--	--	--	--	--	--	--	--	--	--	--	--	--	--	--	--	--	--	--	--	--	--	--	--	--	--	--	--	--	--	--	--	--	--	--	--	--	--	--	--	--	--	--	--	--	--	--	--	--	--	--	--	--	--	--	--	--	--	--	--	--	--	--	--	--	--	--	--	--	--	--	--	--	--	--	--	--	--	--	--	--	--	--	--	--	--	--	--	--	--	--	--	--	--	--	--	--	--	--	--	--	--	--	--	--	--	--	--	--	--	--	--	--	--	--	--	--	--	--	--	--	--	--	--	--	--	--	--	--	--	--	--	--	--	--	--	--	--	--	--	--	--	--	--	--	--	--	--	--	--	--	--	--	--	--	--	--	--	--	--	--	--	--	--	--	--	--	--	--	--	--	--	--	--	--	--	--	--	--	--	--	--	--	--	--	--	--	--	--	--	--	--	--	--	--	--	--	--	--	--	--	--	--	--	--	--	--	--	--	--	--	--	--	--	--	--	--	--	--	--	--	--	--	--	--	--	--	--	--	--	--	--	--	--	--	--	--	--	--	--	--	--	--	--	--	--	--	--	--	--	--	--	--	--	--	--	--	--	--	--	--	--	--	--	--	--	--	--	--	--	--	--	--	--	--	--	--	--	--	--	--	--	--	--	--	--	--	--	--	--	--	--	--	--	--	--	--	--	--	--	--	--	--	--	--	--	--	--	--	--	--	--	--	--	--	--	--	--	--	--	--	--	--	--	--	--	--	--	--	--	--	--	--	--	--	--	--	--	--	--	--	--	--	--	--	--	--	--	--	--	--	--	--	--	--	--	--	--	--	--	--	--	--	--	--	--	--	--	--	--	--	--	--	--	--	--	--	--	--	--	--	--	--	--	--	--	--	--	--	--	--	--	--	--	--	--	--	--	--	--	--	--	--	--	--	--	--	--	--	--	--	--	--	--	--	--	--	--	--	--	--	--	--	--	--	--	--	--	--	--	--	--	--	--	--	--	--	--	--	--	--	--	--	--	--	--	--	--	--	--	--	--	--	--	--	--	--	--	--	--	--	--	--	--	--	--	--	--	--	--	--	--	--	--	--	--	--	--	--	--	--	--	--	--	--	--	--	--	--	--	--	--	--	--	--	--	--	--	--	--	--	--	--	--	--	--	--	--	--	--	--	--	--	--	--	--	--	--	--	--	--	--	--	--	--	--	--	--	--	--	--	--	--	--	--	--	--	--	--	--	--	--	--	--	--	--	--	--	--	--	--	--	--	--	--	--	--	--	--	--	--	--	--	--	--	--	--	--	--	--	--	--	--	--	--	--	--	--	--	--	--	--	--	--	--	--	--	--	--	--	--	--	--	--	--	--	--	--	--	--	--	--	--	--	--	--	--	--	--	--	--	--	--	--	--	--	--	--	--	--	--	--	--	--	--	--	--	--	--	--	--	--	--	--	--	--	--	--	--	--	--	--	--	--	--	--	--	--	--	--	--	--	--	--	--	--	--	--	--	--	--	--	--	--	--	--	--	--	--	--	--	--	--	--	--	--	--	--	--	--	--	--	--	--	--	--	--	--	--	--	--	--	--	--	--	--	--	--	--	--	--	--	--	--	--	--	--	--	--	--	--	--	--	--	--	--	--	--	--	--	--	--	--	--	--	--	--	--	--	--	--	--	--	--	--	--	--	--	--	--	--	--	--	--	--	--	--	--	--	--	--	--	--	--	--	--	--	--	--	--	--	--	--	--	--	--	--	--	--	--	--	--	--	--	--	--	--	--	--	--	--	--	--	--	--	--	--	--	--	--	--	--	--	--	--	--	--	--	--	--	--	--	--	--	--	--	--	--	--	--	--	--	--	--	--	--	--	--	--	--	--	--	--	--	--	--	--	--	--	--	--	--	--	--	--	--	--	--	--	--	--	--	--	--	--	--	--	--	--	--	--	--	--	--	--	--	--	--	--	--	--	--	--	--	--	--	--	--	--	--	--	--	--	--	--	--	--	--	--	--	--	--	--	--	--	--	--	--	--	--	--	--	--	--	--	--	--	--	--	--	--	--	--	--	--	--	--	--	--	--	--	--	--	--	--	--	--	--	--	--	--	--	--	--	--	--	--	--	--	--	--	--	--	--	--	--	--	--	--	--	--	--	--	--	--	--	--	--	--	--	--	--	--	--	--	--	--	--	--	--	--	--	--	--	--	--	--	--	--	--	--	--	--	--	--	--	--	--	--	--	--	--	--	--	--	--	--	--	--	--	--	--	--	--	--	--	--	--	--	--	--	--	--	--	--	--	--	--	--	--	--	--	--	--	--	--	--	--	--	--	--	--	--	--	--	--	--	--	--	--	--	--	--	--	--	--	--	--	--	--	--	--	--	--	--	--	--	--	--	--	--	--	--	--	--	--	--	--	--	--	--	--	--	--	--	--	--	--	--	--	--	--	--	--	--	--	--	--	--	--	--	--	--	--	--	--	--	--	--	--	--	--	--	--	--	--	--	--	--	--	--	--	--	--	--	--	--	--	--	--	--	--	--	--	--	--	--	--	--	--	--	--	--	--	--	--	--	--	--	--	--	--	--	--	--	--	--	--	--	--	--	--	--	--	--	--	--	--	--	--	--	--	--	--	--	--	--	--	--	--	--	--	--	--	--	--	--	--	--	--	--	--	--	--	--	--	--	--	--	--	--	--	--	--	--	--	--	--	--	--	--	--	--	--	--	--	--	--	--	--	--	--	--	--	--	--	--	--	--	--	--	--	--	--	--	--	--	--	--	--	--	--	--	--	--	--	--	--	--	--	--	--	--	--	--	--	--	--	--	--	--	--	--	--	--	--	--	--	--	--	--	--	--	--	--

Figure G.6. (Continued)

I N D E X

CONS10	-	29C0
CONS11	-	29C0
CONS12	-	29C0
CONS13	-	29C0
CONS14	-	29C0
CONS15	-	29C0
CONS16	-	29C0
CONS17	-	29C0
CONS18	-	29C0
CONS19	-	29C0
CONS20	-	29C0
CONS21	-	29C0
CONS22	-	29C0
CONS23	-	29C0
CONS24	-	29C0
CONS25	-	29C0
CONS26	-	29C0
CONS27	-	29C0
CONS28	-	29C0
CONS29	-	29C0
CONS30	-	29C0
CONS31	-	29C0
CONS32	-	29C0
CONS33	-	29C0
CONS34	-	29C0
CONS35	-	29C0
CONS36	-	29C0
CONS37	-	29C0
CONS38	-	29C0
CONS39	-	29C0
CONS40	-	29C0
CONS41	-	29C0
CONS42	-	29C0
CONS43	-	29C0
CONS44	-	29C0
CONS45	-	29C0
CONS46	-	29C0
CONS47	-	29C0
CONS48	-	29C0
CONS49	-	29C0
CONS50	-	29C0
CONS51	-	29C0
CONS52	-	29C0
CONS53	-	29C0
CONS54	-	29C0
CONS55	-	29C0
CONS56	-	29C0
CONS57	-	29C0
CONS58	-	29C0
CONS59	-	29C0
CONS60	-	29C0

376
376
376

Figure G.6. (Continued)

510201)JTI'IF RTFAST

12345678910111213141516171819202122232425262728293031323334353637383940414243444546474849505152535455565758596061626364656667686970717273747576777879808182838485868788899091929394959697989910010110210310410510610710810911011111211311411511611711811912012112212312412512612712812913013113213313413513613713813914014114214314414514614714814915015115215315415515615715815916016116216316416516616716816917017117217317417517617717817918018118218318418518618718818919019119219319419519619719819920020120220320420520620720820921021121221321421521621721821922022122222322422522622722822923023123223323423523623723823924024124224324424524624724824925025125225325425525625725825926026126226326426526626726826927027127227327427527627727827928028128228328428528628728828929029129229329429529629729829930030130230330430530630730830931031131231331431531631731831932032132232332432532632732832933033133233333433533633733833934034134234334434534634734834935035135235335435535635735835936036136236336436536636736836937037137237337437537637737837938038138238338438538638738838939039139239339439539639739839940040140240340440540640740840941041141241341441541641741841942042142242342442542642742842943043143243343443543643743843944044144244344444544644744844945045145245345445545645745845946046146246346446546646746846947047147247347447547647747847948048148248348448548648748848949049149249349449549649749849950050150250350450550650750850951051151251351451551651751851952052152252352452552652752852953053153253353453553653753853954054154254354454554654754854955055155255355455555655755855956056156256356456556656756856957057157257357457557657757857958058158258358458558658758858959059159259359459559659759859960060160260360460560660760860961061161261361461561661761861962062162262362462562662762862963063163263363463563663763863964064164264364464564664764864965065165265365465565665765865966066166266366466566666766866967067167267367467567667767867968068168268368468568668768868969069169269369469569669769869970070170270370470570670770870971071171271371471571671771871972072172272372472572672772872973073173273373473573673773873974074174274374474574674774874975075175275375475575675775875976076176276376476576676776876977077177277377477577677777877978078178278378478578678778878979079179279379479579679779879980080180280380480580680780880981081181281381481581681781881982082182282382482582682782882983083183283383483583683783883984084184284384484584684784884985085185285385485585685785885986086186286386486586686786886987087187287387487587687787887988088188288388488588688788888989089189289389489589689789889990090190290390490590690790890991091191291391491591691791891992092192292392492592692792892993093193293393493593693793893994094194294394494594694794894995095195295395495595695795895996096196296396496596696796896997097197297397497597697797897998098198298398498598698798898999099199299399499599699799899910001001100210031004100510061007100810091010101110121013101410151016101710181019102010211022102310241025102610271028102910301031103210331034103510361037103810391040104110421043104410451046104710481049105010511052105310541055105610571058105910601061106210631064106510661067106810691070107110721073107410751076107710781079108010811082108310841085108610871088108910901091109210931094109510961097109810991100110111021103110411051106110711081109111011111112111311141115111611171118111911201121112211231124112511261127112811291130113111321133113411351136113711381139114011411142114311441145114611471148114911501151115211531154115511561157115811591160116111621163116411651166116711681169117011711172117311741175117611771178117911801181118211831184118511861187118811891190119111921193119411951196119711981199120012011202120312041205120612071208120912101211121212131214121512161217121812191220122112221223122412251226122712281229123012311232123312341235123612371238123912401241124212431244124512461247124812491250125112521253125412551256125712581259126012611262126312641265126612671268126912701271127212731274127512761277127812791280128112821283128412851286128712881289129012911292129312941295129612971298129913001

29C0	173	193			
29C1					
29C2					
29C3					
29C4	315AG	317			
29C5					
29C6	315AG	317			
29C7	316AG	319			
29C8					
29C9	315AG	311AG	313AG		
29CA	315AG	311AG	313AG		
29CB	316AG	314AG	314AG		
29CC	315AG	312AG	314AG		
29CD	316AG	317			
29CE					
29CF					
29CG					
29CH					
29CI					
29CJ					
29CK					
29CL					
29CM					
29CN					
29CO					
29CP					
29CQ					
29CR					
29CS					
29CT					
29CU					
29CV					
29CW					
29CX					
29CY					
29CZ					
29D0					
29D1					
29D2					
29D3					
29D4					
29D5					
29D6					
29D7					
29D8					
29D9					
29DA					
29DB					
29DC					
29DD					
29DE					
29DF					
29DG					
29DH					
29DI					
29DJ					
29DK					
29DL					
29DM					
29DN					
29DO					
29DP					
29DQ					
29DR					
29DS					
29DT					
29DU					
29DV					
29DW					
29DX					
29DY					
29DZ					
29E0					
29E1					
29E2					
29E3					
29E4					
29E5					
29E6					
29E7					
29E8					
29E9					
29EA					
29EB					
29EC					
29ED					
29EE					
29EF					
29EG					
29EH					
29EI					
29EJ					
29EK					
29EL					
29EM					
29EN					
29EO					
29EP					
29EQ					
29ER					
29ES					
29ET					
29EU					
29EV					
29EW					
29EX					
29EY					
29EZ					
29F0					
29F1					
29F2					
29F3					
29F4					
29F5					
29F6					
29F7					
29F8					
29F9					
29FA					
29FB					
29FC					
29FD					
29FE					
29FF					
29FG					
29FH					
29FI					
29FJ					
29FK					
29FL					
29FM					
29FN					
29FO					
29FP					
29FQ					
29FR					
29FS					
29FT					
29FU					
29FV					
29FW					
29FX					
29FY					
29FZ					
29G0					
29G1					
29G2					
29G3					
29G4					
29G5					
29G6					
29G7					
29G8					
29G9					
29GA					
29GB					
29GC					
29GD					
29GE					
29GF					
29GG					
29GH					
29GI					
29GJ					
29GK					
29GL					
29GM					
29GN					
29GO					
29GP					
29GQ					
29GR					
29GS					
29GT					
29GU					
29GV					
29GW					
29GX					
29GY					
29GZ					
29H0					
29H1					
29H2					
29H3					
29H4					
29H5					
29H6					
29H7					
29H8					
29H9					
29HA					
29HB					
29HC					
29HD					
29HE					
29HF					
29HG					
29HH					
29HI					
29HJ					
29HK					
29HL					
29HM					
29HN					
29HO					
29HP					
29HQ					
29HR					
29HS					
29HT					
29HU					
29HV					
29HW					
29HX					
29HY					
29HZ					
29I0					
29I1					
29I2					
29I3					
29I4					
29I5					
29I6					
29I7					
29I8					
29I9					
29IA					
29IB					
29IC					
29ID					
29IE					
29IF					
29IG					
29IH					
29II					
29IJ					
29IK					
29IL					
29IM					
29IN					
29IO					
29IP					
29IQ					
29IR					
29IS					
29IT					
29IU					
29IV					
29IW					
29IX					
29IY					
29IZ					
29J0					
29J1					
29J2					
29J3					
29J4					
29J5					
29J6					
29J7					
29J8					
29J9					
29JA					
29JB					
29JC					
29JD					
29JE					
29JF					
29JG					
29JH					
29JI					
29JJ					
29JK					
29JL					
29JM					
29JN					
29JO					
29JP					
29JQ					
29JR					
29JS					
29JT					
29JU					
29JV					
29JW					
29JX					
29JY					
29JZ					
29K0					
29K1					
29K2					
29K3					
29K4					
29K5					
29K6					
29K7					
29K8					
29K9					
29KA					
29KB					
29KC					
29KD					
29KE					
29KF					
29KG					
29KH					
29KI					
29KJ					
29KK					
29KL					
29KM					
29KN					
29KO					
29KP					
29KQ					
29KR					
29KS					
29KT					
29KU					
29KV					
29KW					
29KX					
29KY					
29KZ					
29L0					
29L1					
29L2					
29L3					
29L4					
29L5					
29L6					
29L7					
29L8					
29L9					
29LA					
29LB					
29LC					
29LD					
29LE					
29LF					
29LG					
29LH					
29LI					
29LJ					
29LK					
29LL					
29LM					
29LN					
29LO					
29LP					
29LQ					
29LR					
29LS					
29LT					
29LU					
29LV					
29LW					
29LX					
29LY					
29LZ					
29M0					
29M1					
29M2					
29M3					
29M4					
29M5					
29M6					
29M7					
29M8					
29M9					
29MA					
29MB					
29MC					
29MD					
29ME					
29MF					
29MG					
29MH					
29MI					

Figure G.6. (Continued)

SURROUTINE RTEAST

I V D F X

DLSL4	-	1500			
DNLG	-	2000	524		
DNLNC	-	2200	252		
DNPNC	-	2200	250		
DNF1	-	1000	170	190	
DNF2	-	1000	170	190	
DNF3	-	1000	170	190	
DNF4	-	1000	170	190	
DNLG	-	2000	525		
DNLNC	-	2200	250		
DNRNC	-	2200	258		
DDVT	-	1100			
DDVTL	-	2100	283		
DDVTR	-	2100	284		
DPM1	-	1000	175	181	201
DPM2	-	1000	175	195	
DPM3	-	1000	175	195	
DPM4	-	1000	175	195	
DPM5	-	1000	191	201	
DPM6	-	1000	191	201	
CP47	-	1000	181	201	
DRL4	-	1500			
DSDBET	-	1100	445		
DSF1	-	1000	172	192	
DSF2	-	1000	172	192	
DSF3	-	1000	172	192	
DSF4	-	1000	172	192	
DTIM	-	600			
DUM12	-	900			
DUM13	-	900			
DUM14	-	900			
DUM15	-	900			
DUM43	-	900			
DUM44	-	900			
CUM45	-	900			
DUM46	-	900			
DUM47	-	900			
DUM48	-	900			
DXLG	-	2000	520		
DXLNC	-	2200	247		
DXRNC	-	2200	256		
DYLG	-	2000	521		
CYLNC	-	2200	248		
DYM1	-	1000	177	183	203
DYM2	-	1000	177	197	
DYM3	-	1000	177	197	
DYM4	-	1000	177	197	
DYM5	-	1000	183	203	
CYM6	-	1000	183	203	
DYM7	-	1000	183	203	
DYRNC	-	2200	256		
DZLG	-	2000	522		
DZLNC	-	2200	243		
CZRNC	-	2200	244		
EFFHT	-	1100			

Figure G.6. (Continued)

SUPERROUTINE RTFAST

I N D E X

FILE	-	1100	229	230	254	252
FINDEG	-	1100	274	295		
FINPR	-	1100	274=	295=		
FIP	-	1100	227	228	235	238
FIP04L	-	2300	277=	236	237	
FIP04R	-	2300	228=	239	240	
FIXX	-	2700				
FIXXF	-	1100				
FIXXPR	-	1100				
FIXXM	-	1100				
FIXZF	-	1100				
FIXZP	-	2700	544	594		
FIXZPR	-	1100				
FIXZQ	-	2700	545			
FIXZR	-	2700	546	614		
FIXZM	-	1100				
FIYY	-	2700				
FIYVF	-	1100	606	608		
FIYVPR	-	1100				
FIYWM	-	1100				
FIZZ	-	2700				
FIZZF	-	1100	548	551		
FIZZPR	-	1100				
FIZZW	-	1100				
FJXX	-	2700	544			
FJYY	-	2700	545			
FJZZ	-	2700	546			
FLAGS	-	4*				
FN04L	-	2300	213=	241	245	
FN04R	-	2300	220=	242	246	
FSIOEL	-	2300	214=	241	245	
FSIDER	-	2300	221=	242	246	
FSWACH	-	1800				
THE VARIABLE- FSORT - IS USED BEFORE IT IS DEFINED						
FSORT	-	60	63	100	101	605
FUSVAR	-	20*				
GAATAB	-	1400	72AG			
GAIALF	-	72AG	76	77		
GAIBET	-	73=	76	77		
GBATAB	-	1400	72AG			
GBETDR	-	1500				
GBETP	-	1500				
GBETP	-	1500				
GRUTON	-	400				
GRIALF	-	72AG	73	78		
G0R1	-	1500				
G0R2	-	1500				
G0LTH	-	1500				
GEAR	-	518*				
GEF	-	2100	371	380	391	
GEFAP	-	21*				
GGUST	-	1500				
GICLY	-	1500				
GINRF	-	1500				
GKFY	-	1300	72AG			

Figure G.6. (Continued)

SUBROUTINE RTFAST

I N D E X

GLPSLP	-	1500	
GLPO	-	1500	
GLSLM	-	1500	
GMEW	-	1300	72AG
GOMG	-	1500	
GP	-	1500	
GPOS	-	1500	
GPHI	-	1500	
GPRI	-	1500	
GPSI	-	1500	
GPSIDP	-	1500	
GO	-	1500	
GR	-	1500	
GPR	-	1500	
GTH	-	1500	
GTHF	-	1500	
GTHGV	-	1500	
H	-	300	
THE VARIABLE= MACLOD -IS USED BEFORE IT IS DEFINED			
MACLOD	-	575	575=
THE VARIABLE= MACROD -IS USED BEFORE IT IS DEFINED			
MACROD	-	572	572=
MDT	-	700	
MDTACL	-	2500	561= 575=
MDTACR	-	2500	559= 572=
MDTRIM	-	2800	631
MGEFLR	-	2100	
MGEFRP	-	2100	
MLHJR	-	2100	
MOLD	-	600	
MOLD2	-	600	
MP	-	1100	
MRHJR	-	2100	
MSO	-	1600	
MTCA	-	2100	
MTRIM	-	2800	674
MTSTILL	-	800	472
MTVTKT	-	1100	
HWACL	-	2500	176 561= 574= 575 576
HWACR	-	2500	112 558= 571= 572 573
MWC4	-	2100	
MYBCON	-	5*	
MYBIN	-	7*	
MYOTL	-	2500	34 557= 560=
MYOTR	-	2500	37 555= 565=
MIL	-	2500	32 555= 568= 560 570
THE VARIABLE= MILOLD -IS USED BEFORE IT IS DEFINED			
MILOLD	-	569	570=
MIP	-	2500	34 558= 555= 556 567
THE VARIABLE= MIPOLD -IS USED BEFORE IT IS DEFINED			
MIPOLD	-	566	567=
IAP	-	400	
IC	-	600	
ICDOP	-	200	
ICIP	-	400	

* *

Figure G.6. (Continued)

SUBROUTINE RTFAST															PAGE 44
I N D E X															
P	-	27C0	54=	9C	93	94	95	87	107	108	113	114	129	139	
PC	-	141	145	147	539	541	542								
PCOL	-	11C0													
PCOR	-	18C0													
PGUST	-	18C0	449												
PHI	-	9C0	54												
PHIPH	-	11C0													
PI	-	11C0	396	397	408	439	416	435	439	441	446	447	459	460	
	-	467	496	490	492										
PILMSK	-	2C0													
PIOV2	-	11C0	412	414	416	420	422	429	431	433	437	439	463	465	
	-	467	471	473	480	482	484	488	490						
PNLN	-	23C0	139=	142	615										
PNLR	-	23C0	142=	151											
PNRN	-	23C0	145=	148											
PNRR	-	23C0	148=	152	617										
PP	-	27C0	542=	545	547	548	550	551							
PPRIME	-	9C0	31C0	54											
PQ	-	27C0	539=	544	546	549	552								
PR	-	27C0	541=	545	547	550									
PROJ	-	6C0													
PSI	-	9C0													
Q	-	27C0	55=	79	81	82	84	85	87	106	108	112	114	126	
	-	127	128	130	140	146	154	162	538	539	543				
QFSH	-	20C0													
QGUST	-	9C0	55												
QNLN	-	23C0	140=	143	144	237									
QNL	-	23C0	143=	646											
QNRN	-	23C0	146=	149	150	240									
QNR	-	23C0	149=	644											
QPRIME	-	9C0	55												
P	-	27C0	56=	80	82	93	85	86	106	107	112	113	129	139	
	-	141	145	147	229	230	538	540	541	543					
	-	11C0	74	75											
RTODG	-	24C0													
RESLR	-	24C0													
PESRR	-	24C0													
RETURN	-	662*	646*												
RGUST	-	9C0	56												
RLH	-	15C0													
RNLN	-	23C0	141=	143	144	236									
RNL	-	23C0	144=	648											
RNRN	-	23C0	147=	149	150	239									
RNR	-	23C0	150=	647											
RF	-	18C0	209	210	605										
RDEFV2	-	18C0	54	271	272										
ROED	-	3C0	605												
ROP1R4	-	23C0	212	214	213	214	219	220	221						
ROP1R5	-	23C0	212=	215	216	217	222	223	224	541					
ROTIPS	-	11C0	104	105											
ROT1RAD	-	11C0	155	156											
ROT1VAR	-	23*													
RP1TIME	-	9C0	56												
RQ	-	27C0	543=	546	544	546	549	552							
PR	-	27C0	540=	545	547	548	550	551							

Figure G.6. (Continued)

SK21	110	
SK22	110	
SK23	110	
SK24	110	
SK25	110	
SK26	110	
SK27	110	
SK28	110	
SK29	110	
SK30	110	
SK31	110	
SK32	110	
SK33	110	
SK34	110	
SK35	110	
SK36	110	
SK37	110	
SK38	110	
SK39	110	
SK40	110	
SK41	110	
SK42	110	
SK43	110	
SK44	110	
SK45	110	
SK46	110	
SK47	110	
SK48	110	
SK49	110	
SK50	110	
SK51	110	
SK52	110	
SK53	110	
SK54	110	
SK55	110	
SK56	110	
SK57	110	
SK58	110	
SK59	110	
SK60	110	
SK61	110	
SK62	110	
SK63	110	
SK64	110	
SK65	110	
SK66	110	
SK67	110	
SK68	110	
SK69	110	
SK70	110	
SK71	110	
SK72	110	
SK73	110	
SK74	110	
SK75	110	
SK76	110	
SK77	110	
SK78	110	
SK79	110	
SK80	110	
SK81	110	
SK82	110	
SK83	110	
SK84	110	
SK85	110	
SK86	110	
SK87	110	
SK88	110	
SK89	110	
SK90	110	
SK91	110	
SK92	110	
SK93	110	
SK94	110	
SK95	110	
SK96	110	
SK97	110	
SK98	110	
SK99	110	
SK100	110	

Figure G.6 (Continued)

T N D F X		SURROUTINE RTEFAST				
WRLWL	-	1900	25=	101		
WROL	-	1900	102=	104		
WROL	-	103=	105	137		
WPR	-	1900	93=	99		
WRRPR	-	1900	87=	91		
WRRWR	-	1900	99=	100		
WWR	-	1900	117=	124		
WWRPR	-	1900	114=	115		
WWSQ	-	1900	124=	125		
WWSQ	-	1900	59=	60		
WWT	-	1900	130=	131		
XAERF	-	2000	520=	526		
XAERLW	-	2400	279=	352=		
XAERNL	-	2300	263=	526		
XAERNL	-	2300	247=	263		
XAERNR	-	2300	255=	263		
XAERO	-	2700	526=	548		
XAERRW	-	2400	240=	356=		
XAERT	-	2600	510=	526		
XAERWG	-	2400	361=	365		
XAIO	-	9*				
XARFP	-	2000	520			
XARHT	-	2600	497=	501		
XARVT	-	2600	54=	510		
XCG	-	1700	30	365		
XCNTRL	-	15*				
XDTCG	-	1700	49=	70		
XF	-	2700				
XFAC	-	1100				
XFCON	-	800				
XFMLF	-	2700				
XFUNC	-	14*				
XHT	-	1100	107	501		
XL	-	2700				
XLCONS	-	2700	618			
XLINTP	-	13*				
XLSTN	-	2700				
XMAP	-	19*				
XPAR1	-	11*				
XPAR3	-	29*				
XR	-	2700				
XRCOS	-	2700	616			
XRLCON	-	900				
XRSIN	-	2700				
XVT	-	1100	129	130		
XW	-	2700				
XWAC	-	1100	107	113		
XWCON	-	800	245	286		
XWC2	-	1100				
XWMLW	-	2700				
XXICON	-	800				
XXJCON	-	800				
XZICON	-	2000	521=	527		
YAEFF	-	2400	281=	353=		
YAEPLW	-					

Figure G.6. (Continued)

5000 JTIME RTFAST

I N D E X

YAERN	-	2300	254=	527	513	517			
YAERNL	-	2300	254=	250	264				
YAERNP	-	2300	256=	258	264				
YAERD	-	2700	277=	671					
YAERRW	-	2400	282=	357=	267				
YAERT	-	2600	511=	527					
YAERAG	-	2400	362=	527					
YARFP	-	2900	521						
YARHT	-	2600	498=	500	512	511			
YARVT	-	2600	505=	507	509	511			
YN	-	1100	32	34	85	37	531	537	
YPA	-	1100							
YMAC	-	1100	106	108	112	114			
YYICON	-	RCO							
YYJCON	-	RCO							
ZAERE	-	2700	522=	529	287	351=	354	364	574
ZAERLW	-	2300	283=	285	534				
ZAERN	-	2300	255=	528	534				
ZAERL	-	2300	282=	285	531	528	575		
ZAERNR	-	2300	257=	265	531	555	571		
ZAEPD	-	2700	533=	545	551	564			
ZAERW	-	2400	254=	266	287	350=	350	555	571
ZAERT	-	2400	512=	520					
ZAFOJG	-	2400	463=	350	523				
ZARFP	-	2300	522		512				
ZARHT	-	2600	489=	521					
ZAPRG	-	520=	523	523					
ZAPVJ	-	528=	530	533					
ZARVT	-	2400	524=	528	512				
ZCG	-	1700	79	81	512	500	537	538	535
ZDICG	-	1700	52=	91	267				
ZETHL	-	2300	134=	135AC					
ZETH2	-	2300	137=	137=					
ZETR1	-	2400							
ZETR2	-	2400							
ZETR3	-	2400							
ZETR4	-	2400							
ZF	-	2700							
ZFAC	-	1100							
ZFCON	-	RCO							
ZFMEHF	-	2700							
ZMT	-	1100	126	500	501				
ZL	-	2700							
ZLONS	-	2700	518						
ZLSIN	-	2700							
ZPA	-	1100							
ZR	-	2700							
ZRCOS	-	2700							
ZRLCON	-	RCO							
ZRSIN	-	2700	516						
ZVT	-	1100	128	129	537	538			
ZW	-	2700							
ZMAC	-	1100	106	107	112	113	354	355	
ZMCIN	-	RCO							
ZMMH4W	-	2700							

Figure G.6. (Continued)

I N D E X

ZZICON - ACO
 ZZJCON - BCO

Figure G.6. (Continued)

SUBROUTINE RTSLOW

INDEX

```

*SK44 ,SK47 ,SK48 ,SK49 ,SK50 ,SL ,SLF ,SLPA ,SLW , 99 TO 97
*SM ,SMF ,SMN ,SMW ,SPAN ,TAUHT ,TAUTV ,XFAC ,XHT , 98 TO 106
*SMC ,XVT ,YN ,YPA ,YMAC ,ZFAC ,ZHT ,ZPA ,ZMAC ,
*ZVT ,CLOAL ,PHIPH ,SK37H1 ,EN2REF ,XMC2 ,BT1 ,BT2 ,BT3 ,
*SKDIT ,RKDIT ,RKDIT ,BKMT ,BKMT ,BKMT ,BKMT ,SK31H1 ,
*FEU ,CLMAX ,ALARK ,BKLSW ,BKNSW ,SQPRM ,DEG20 ,DGTORD ,HTVTKT , 133 TO 141
*IND2 ,RDTOG ,ROTEFS ,SKFDS ,ALNCBK ,TAURT1 ,TAURT2
COMMON/SPIN/ RCBL(19),ISTRBL,IADC3(32)
COMMON/XLINTP/ AKFY(16),AMEY(2),BKEY(16),BMEY(2),CKEY(10),CHEM
COMMON/XFUNC / VSTARG(33),TAUG(9),SVSTAB(33,9),SOFARG(35),
1 GAATAR(35),GBATAR(35),ALFTAB(35)
COMMON/INITVR/
1 AVEIN ,CILAML,CILAMR,COSINL,COSINR,COSPSI,CZINL ,CZINR ,DLFPSQ, 1 - 9
2 HSD ,SILAML,SILAMR,SININL,SININR,SINPSI,SSQINL,SSQINR,SZINL , 10 - 18
3 SZINR 19
COMMON/CGGTVR/
1 VEAST ,VWORTH,XCG ,XDTG ,ZCG ,ZDTG 1 - 6
COMMON/ZENGVAR/
1 AMACH ,AMACSQ,DEL ,EMAXY1,EMAXN2,EMXADT,ENZSTR,FSMACH,OMEGEL, 1 - 9
2 OMGER,ONOVTC,OVFSM,OVSOH,OVTHOL,ROE ,ROENV2,SHPPRL,SHPPRR, 10 - 18
3 S4A ,SQNIMX,SQTHIC,SQDIX,TJEGF ,TEAL ,TEAR ,TMODEL,THETC 19 - 27
4,PTQL,PTQR 28 TO 29
COMMON/VELVAR/
1 AMUL ,AMULSQ,AMUR ,AMJRSQ,AROTL ,OMDIL ,OMDTR ,OMEGAL,OMEGAR, 1 - 9
2 OMSQ ,OMSQR ,LHT ,UL4 ,ULMPR ,ULMSQ ,UP ,JRL ,URLPR , 10 - 18
3 URLURL,URP ,URPR ,URRURR,URW ,URMPR ,JRSQ ,USQ ,UVT , 19 - 27
4 VALFLM,VALFRM,VALFS ,VALNCL,VALNCR,VBEVT,VLM ,VLMPR ,VLMSQ , 28 - 36
5 VP ,VRL ,VRLPR ,VRLVRL,VRR ,VRRPR ,VRRVR,VVM ,VRMPR , 37 - 45
6 VRSQ ,VSO ,VTIPL ,VTIPR ,VTOTAL,VTOTLR,VTOTR,VVT ,VZETL , 46 - 54
7 VZETR ,WHT ,WLV ,WLPDR ,WLSQ ,WP ,WRL ,WRLPR ,WRLVRL, 55 - 53
8 WRW ,WRWPR ,WRWSQ ,WR3 ,WRRPR ,WRRRRR,WSQ ,WVT 64 - 71
COMMON/FUSVAR/
1 ALARF ,ALAREP,ALFSD ,ALPHF ,AMARF ,AMAREP,ANARF ,ANAREP,REAF , 1 - 9
2 RTFSQ,CRCHF ,CDF ,CLF ,CMF ,CMF ,COSALF,COSBTF,CYF , 10 - 18
3 DILG ,DMLG ,DNLG ,DYL3 ,DYL3 ,DYL3 ,DYL3 ,DYL3 ,DYL3 ,DYL3 , 19 - 27
4 SINLAF,SINRTF,SOF ,XAEPE ,XAEPE ,XAEPE ,XAEPE ,XAEPE ,XAEPE , 28 - 36
* ,SINTHE,COSTHF,SINPHI,COSPHI
COMMON/GFEVAR/
1 AGVAT,AGVAM,RIGX ,RK39 ,RMVTL,BHOVTR,COPCOR,CLTCOR,CLMCR, 1 - 9
2 DOVTL ,DOVTR ,EPPRM ,GEF ,HGEFLR,HGEFRR,HLEHUB ,HRHUB ,HTC4 , 10 - 18
3 HWC4 ,PR11 ,PR12 ,SRI ,TISEL ,TIGER 19 - 24
COMMON/NACVAR/
1 ALLNSQ,ALPHLN,ALPHRN,ALPNSQ,BETALN,BETARN,BILNSQ,BTRNSQ,CALLV , 1 - 9
2 CALPN ,CBFTLN,CBETRN,COLN ,COLN ,COLN ,COLN ,COLN ,COLN , 10 - 18
3 CLN ,CMRN ,CNLN ,CMRN ,CYLN ,CYRN ,CYLN ,CYLN ,CYLN ,CYLN , 19 - 27
4 DMZNC ,DNLNC ,DNPNC ,DXLNC ,DXLNC ,DXLNC ,DXLNC ,DXLNC ,DXLNC , 27 - 36
5 SALN ,SALN ,SBFTLN,SBETRN,SQLNC ,SQRCN ,THACI ,TNAC2 36 - 44
COMMON/ROTVAR/
1 ATCL ,ATCLDP,ATCR ,ATCROP,ALARNC,ALLRH ,ALARNL,ALARNR,ALRRH , 1 - 9
2 ALPHR ,ALPHRR,AMARNC ,AMARNL,AMARNR,ANLRH ,ANRNL,ANRRP,ANROTL , 10 - 18
3 AMROTR,AMRRH ,ANARNC ,ANARNL,ANARNR,ANLRH ,ANROTL,ANROTR,ANRRH , 19 - 27
4 RCL ,RCLDP,BICR ,BICRDP,CNFAIL,CNFAIR,CNFBIL,CNFBIR,CNFI , 28 - 36
5 CNFR ,COSZHL,COSZHR,CPMAIL,CPMAIL,CPMAIL,CPMAIL ,CPMR , 37 - 45
6 CSFAIL,CSEAIR,CSEBIL,CSEFIR,CSEF ,CSEF ,CTR ,CYMAIL , 46 - 54
7 CYMAIL,CYMAIL,CYMBIL,CYMBIR,CYML ,CYMR ,FIPOML,FIPOMR,FNORML,FNORR, 55 - 63

```

Figure G.6. (Continued)

MUTUAL INTELLIGENCE

Figure G.6. (Continued)

SUBROUTINE RTSLOW

INDEX

```

C      XP= COS(INR-LAMDA)
C      ZLSIN = ZI* SIN(INL-LAMDA)
C      ZLCS = ZI* COS(INL-LAMDA)
C      XLSIN = XI* SIN(INL-LAMDA)
C      XLCS = XI* COS(INL-LAMDA)
C      ZPHF= SMF* SHW * ZF
C      ZPHF= SMF* SHW * ZF
C      XF4LF= SMF* SLF * XF
C      XW4LW= SMF* SLW * XW
C      TERM1 = (IXPR-172PI)*(SSQINR + SSQINL)
C      TERM2 = (IX7PR)*(S2INR +S2INL)
C      TERM3 = (SL*SMI)*(ZRSIN +ZLSIN)
C      TERM4 = (IXXP-172PI)*(S2INR +S2INL) * 0.5
C      TERM5 = IX2PR *(C2INR+C2INL)
C      TERM6 = (SL*SMI) *IXRCOS + XLCOS)
C      DOVIXX= 1./E1XX
C      DOVIVV= 1./E1VY
C      DOVIZZ= 1./E1ZZ
C      RQ = P*Q
C      PQ = P*Q
C      RR = P*R
C      PR = P*R
C      PP = P*P
C      FOR PT CALC USE FOLLOWING TRIG IDENTITIES WHERE
C      A= INCIDENCE ANGLE INR,INL A= LAMDA
C      COS(A-R) = COS(A)*COS(-R) -SIN(A)*SIN(-R)
C      = COS(A)*COS(R) +SIN(A)*SIN(R)
C      SIN(A-R) = SIN(A)*COS(-R) +COS(A)*SIN(-R)
C      = SIN(A)*COS(R) -COS(A)*SIN(R)
C      SIN(2A) = 2.*SIN(A)*COS(A)
C      COS(2A) = 1. - 2.*SIN(A)*SIN(A)
C
C      DISCRETE LINE ALLOCATION:
C      CONSOLF 1
C
C      PT NUMBER    DSS NUMBER    FUNCTION
C      31            17            PANIC
C      33            16            TRIM
C      29            15            CONSOLE OPERATE
C
C      HORIZONTAL TAIL
C
C      1. IF HWC/4 GT 50 FT.    GFF = 0.
C      2. IF V LE 30 FT.    TAIL AERO = 0.
C      3. IF DEL FLAP GT 75 DEG    EPSILON TAIL = 0.
C      4. IF CTS LT 0.5    EPSILON P = 0.
C      5. LIMIT RANGE OF ABS(ALPHAT) TO (ALHTSTALL - 2. DEG) AND
C      PRINT WARNING
C
C      VERTICAL TAIL
C      1. LIMIT THE RANGE OF ABS(ALPHAT) TO (ALVTSTALL -2 DEG) AND
C      PRINT WARNING
C      DEAD DISCRETES FROM ANALOGS

```

Figure G.6. (Continued)

SURROUTINE RTSLOW

LINE 15

```

161 TRMNC3= SAL*CALPN
162 TRMNC3= SBETLN*CBETLN
163 TRMNC4= SBETPN*CBETPN

C
C      WIND AXES
164 IF (ABS(ALPHEN).GT.ALNCRK) GO TO 723
165 COMN= COMHLO
166 SK30L= SK30LO
167 SK31L= SK31LO
168 GO TO 740
169 COMN= COMH1
170 SK31L= SK30HI
171 SK31L= SK31HI
172 CONTINUE
173 COMN= COMH1+SK31L*AP5(ALPHEN)+SK31L*ALPHEN*ALPHN
174 CLIN= SK32+TRMNC1
175 COMN= COMH1+TRMNC1*(SK34+SK35*ATS(TRMNC1))
176 COMN= TRMNC3*(SK43+SK44*ABS(TRMNC3))
177 COMN= COMH1+TRMNC3*(SK47+SK48*ABS(TRMNC3))

C
C      IF (ABS(ALPHEN).GT.ALNCRK) GO TO 740
178 COMN= COMHLO
179 SK30L= SK31LO
180 SK31L= SK31LO
181 GO TO 773
182 COMN= COMH1
183 SK30L= SK30HI
184 SK31L= SK31HI
185 CONTINUE
186 COMN= COMH1+SK31L*AP5(ALPHEN)+SK31L*ALPHEN*ALPHN
187 CLPN= SK32+TRMNC2
188 COMN= COMH1+TRMNC2*(SK34+SK35*ABS(TRMNC2))
189 COMN= TRMNC4*(SK36+SK37*ABS(TRMNC4))
190 COMN= COMH1+TRMNC4*(SK39+SK40*ABS(TRMNC4))

C
C      RIGHT NACELLE APPROXIMATES - BODY AXES
191
192 COMN= COMH2*(HFLHRL*VOLV1+HFLHRL)
193 COMN= COMH2*(HFLHRL*VOLV2+HFLHRL)
194 TRAC1= SBPNC*COEFF1
195 TRAC2= SOLN*COEFF1

C
196 TRMNC= -TRAC1*(CLPN*CALPN+SALRN*(CBRN*CBETPN+CBRN*SBETPN))
197 TRMNC= TRAC1*(CLPN*CALPN-CALRN*(CBRN*CBETPN+CBRN*SBETPN))
198 TRMNC= TRAC1*(CBRN*CBETPN-CBRN*SBETPN)
199 TRMNC= TRAC1*COMN+CBRN*CBETPN
200 TRMNC= TRAC1*COMN+CBRN*CBETPN-COEFL7*CBRN*SBETPN
201 TRMNC= -TRAC1*SPAN*(COEFF7*COMN*SBETPN*CALPN+CBRN*SALRN)

C
C      LEFT NACELLE AERO FORCES - BODY AXES
202
203 TRMNC= -TRAC1*(CLPN*CALPN+SALRN*(CBRN*CBETPN+CBRN*SBETPN))
204 TRMNC= TRAC1*(CLPN*CALPN-CALRN*(CBRN*CBETPN+CBRN*SBETPN))

```

Figure G.6. (Continued)

```

SUBROUTINE RTSLOW
C
      CMLN = TNAC2*(CYLN*SBEFLN - COLN * SBEFLN )
      CMNC = TNAC2*CHORD * CMLN * SBEFLN
      CNLNC = TNAC2*SPAN * CALLN*(CNLN -COFFI7*CMLN* SBEFLN )
      CLNLC = -TNAC2*SPAN *( COFFI7*CMLN*SBEFLN*CALLN +CNLN*SALLN )
C
      ( R L A N K   C A R D )
      ( R L A N K   C A R D )
      ( R L A N K   C A R D )
      ( R L A N K   C A R D )
      ( R L A N K   C A R D )
      ( R L A N K   C A R D )
      ( R L A N K   C A R D )
      ( R L A N K   C A R D )
      ( R L A N K   C A R D )
      ( R L A N K   C A R D )
      ( R L A N K   C A R D )
      ( R L A N K   C A R D )
      ***** S Y N T A X E R R O R *****
C
      WING AERODYNAMICS
C
      PRELIMINARY CALCULATIONS
      RIGHT ROTOR
C
      TAURR = ALPHRR + ATAN2(FNORMR,TR)
      RESRR= FSORT((TR+FNORMR*FNDRMR+FSIDER*FSDIR,WORK)
      TRWG1= COEF25 / ROE
      SORESR= FSORT((RESRR+LG.)*TRWGI,WOKP)
      VSTAR = VNTRR/SORES
C
      ATAURR = ABS(ATAURR)
      CALL LINT (AKEY, AMEM,AMEN ,ISTA,VSTAR ,ATAURR,SVSTAB ,SVSTAR )
      KPAN = 32
      IWAPNI(11)= .FALSE.
      IF(ISTA.EQ.2) IWAPNI(11)= .TRUE.
C
      CALL SINCS(TAUHR,TSTAURP,CTAURD)
C
      TWG1J= SVSTAR*STAURR
      TWG1I= VSTAR+SVSTAR*CTAUPR
      FPRR= ATAN2(TWGL0,TWGL1)
      CTSPR= 4./14.* VSTAR*VSTAR
C
      LEFT ROTOR
      TA'LR = ALPHA'R + ATAN2(FNORM'L,TL)
      RESLP= FSORT((TL+FNORM'L*FNOPML+FSIDEL*FSDIL,WOKK)
      SORESL= FSORT((RESLR+LG.)*TRWGI,WOKK)
      VSTARL= VTOTLR/SORESL
C
      CALL SINCS(TAULR,STAULR,CTAULR)

```

Figure G.6. (Continued)

SUBROUTINE RTSLOW

I N D E X

```

220 ATAU1 = A*STAU1P)
221 CALL LINT (HKEY, HMEM, HMEM, IST1, VSTAR1, ATAU1R, SVSTAB, SVSTPL )
222 IWARN(112) = .FALSE.
223 KPAN = 321
224 IF (IST1.EQ.2) IWARN(112) = .TRUE.
225
226 C
227 C
228 TRMNG4= SVSTPL*STAU1R
229 YPMNG9= VSTAR1*SVSTPL*CTAU1R
230 FPDLP= ATAN2(TRMNG4, YPMNG9)
231 CTSLR= 4.7/(4.+ VSTAR1*SVSTAR1)
232
233 C
234 C
235 C
236 C
237 C
238 C
239 C
240 C
241 C
242 C
243 C
244 C
245 C
246 C
247 C
248 C
249 C
250 C
251 C
252 C
253 C
254 C
255 C
256 C
257 C
258 C
259 C
260 C
261 C
262 C
263 C
264 C
265 C
266 C
267 C
268 C
269 C
270 C
271 C
272 C
273 C
274 C
275 C
276 C
277 C
278 C
279 C
280 C
281 C
282 C
283 C
284 C
285 C
286 C
287 C
288 C
289 C
290 C
291 C
292 C
293 C
294 C
295 C
296 C
297 C
298 C
299 C
300 C
301 C
302 C
303 C
304 C
305 C
306 C
307 C
308 C
309 C
310 C
311 C
312 C
313 C
314 C
315 C
316 C
317 C
318 C
319 C
320 C
321 C
322 C
323 C
324 C
325 C
326 C
327 C
328 C
329 C
330 C
331 C
332 C
333 C
334 C
335 C
336 C
337 C
338 C
339 C
340 C
341 C
342 C
343 C
344 C
345 C
346 C
347 C
348 C
349 C
350 C
351 C
352 C
353 C
354 C
355 C
356 C
357 C
358 C
359 C
360 C
361 C
362 C
363 C
364 C
365 C
366 C
367 C
368 C
369 C
370 C
371 C
372 C
373 C
374 C
375 C
376 C
377 C
378 C
379 C
380 C
381 C
382 C
383 C
384 C
385 C
386 C
387 C
388 C
389 C
390 C
391 C
392 C
393 C
394 C
395 C
396 C
397 C
398 C
399 C
400 C
401 C
402 C
403 C
404 C
405 C
406 C
407 C
408 C
409 C
410 C
411 C
412 C
413 C
414 C
415 C
416 C
417 C
418 C
419 C
420 C
421 C
422 C
423 C
424 C
425 C
426 C
427 C
428 C
429 C
430 C
431 C
432 C
433 C
434 C
435 C
436 C
437 C
438 C
439 C
440 C
441 C
442 C
443 C
444 C
445 C
446 C
447 C
448 C
449 C
450 C
451 C
452 C
453 C
454 C
455 C
456 C
457 C
458 C
459 C
460 C
461 C
462 C
463 C
464 C
465 C
466 C
467 C
468 C
469 C
470 C
471 C
472 C
473 C
474 C
475 C
476 C
477 C
478 C
479 C
480 C
481 C
482 C
483 C
484 C
485 C
486 C
487 C
488 C
489 C
490 C
491 C
492 C
493 C
494 C
495 C
496 C
497 C
498 C
499 C
500 C
501 C
502 C
503 C
504 C
505 C
506 C
507 C
508 C
509 C
510 C
511 C
512 C
513 C
514 C
515 C
516 C
517 C
518 C
519 C
520 C
521 C
522 C
523 C
524 C
525 C
526 C
527 C
528 C
529 C
530 C
531 C
532 C
533 C
534 C
535 C
536 C
537 C
538 C
539 C
540 C
541 C
542 C
543 C
544 C
545 C
546 C
547 C
548 C
549 C
550 C
551 C
552 C
553 C
554 C
555 C
556 C
557 C
558 C
559 C
560 C
561 C
562 C
563 C
564 C
565 C
566 C
567 C
568 C
569 C
570 C
571 C
572 C
573 C
574 C
575 C
576 C
577 C
578 C
579 C
580 C
581 C
582 C
583 C
584 C
585 C
586 C
587 C
588 C
589 C
590 C
591 C
592 C
593 C
594 C
595 C
596 C
597 C
598 C
599 C
600 C
601 C
602 C
603 C
604 C
605 C
606 C
607 C
608 C
609 C
610 C
611 C
612 C
613 C
614 C
615 C
616 C
617 C
618 C
619 C
620 C
621 C
622 C
623 C
624 C
625 C
626 C
627 C
628 C
629 C
630 C
631 C
632 C
633 C
634 C
635 C
636 C
637 C
638 C
639 C
640 C
641 C
642 C
643 C
644 C
645 C
646 C
647 C
648 C
649 C
650 C
651 C
652 C
653 C
654 C
655 C
656 C
657 C
658 C
659 C
660 C
661 C
662 C
663 C
664 C
665 C
666 C
667 C
668 C
669 C
670 C
671 C
672 C
673 C
674 C
675 C
676 C
677 C
678 C
679 C
680 C
681 C
682 C
683 C
684 C
685 C
686 C
687 C
688 C
689 C
690 C
691 C
692 C
693 C
694 C
695 C
696 C
697 C
698 C
699 C
700 C
701 C
702 C
703 C
704 C
705 C
706 C
707 C
708 C
709 C
710 C
711 C
712 C
713 C
714 C
715 C
716 C
717 C
718 C
719 C
720 C
721 C
722 C
723 C
724 C
725 C
726 C
727 C
728 C
729 C
730 C
731 C
732 C
733 C
734 C
735 C
736 C
737 C
738 C
739 C
740 C
741 C
742 C
743 C
744 C
745 C
746 C
747 C
748 C
749 C
750 C
751 C
752 C
753 C
754 C
755 C
756 C
757 C
758 C
759 C
760 C
761 C
762 C
763 C
764 C
765 C
766 C
767 C
768 C
769 C
770 C
771 C
772 C
773 C
774 C
775 C
776 C
777 C
778 C
779 C
780 C
781 C
782 C
783 C
784 C
785 C
786 C
787 C
788 C
789 C
790 C
791 C
792 C
793 C
794 C
795 C
796 C
797 C
798 C
799 C
800 C
801 C
802 C
803 C
804 C
805 C
806 C
807 C
808 C
809 C
810 C
811 C
812 C
813 C
814 C
815 C
816 C
817 C
818 C
819 C
820 C
821 C
822 C
823 C
824 C
825 C
826 C
827 C
828 C
829 C
830 C
831 C
832 C
833 C
834 C
835 C
836 C
837 C
838 C
839 C
840 C
841 C
842 C
843 C
844 C
845 C
846 C
847 C
848 C
849 C
850 C
851 C
852 C
853 C
854 C
855 C
856 C
857 C
858 C
859 C
860 C
861 C
862 C
863 C
864 C
865 C
866 C
867 C
868 C
869 C
870 C
871 C
872 C
873 C
874 C
875 C
876 C
877 C
878 C
879 C
880 C
881 C
882 C
883 C
884 C
885 C
886 C
887 C
888 C
889 C
890 C
891 C
892 C
893 C
894 C
895 C
896 C
897 C
898 C
899 C
900 C
901 C
902 C
903 C
904 C
905 C
906 C
907 C
908 C
909 C
910 C
911 C
912 C
913 C
914 C
915 C
916 C
917 C
918 C
919 C
920 C
921 C
922 C
923 C
924 C
925 C
926 C
927 C
928 C
929 C
930 C
931 C
932 C
933 C
934 C
935 C
936 C
937 C
938 C
939 C
940 C
941 C
942 C
943 C
944 C
945 C
946 C
947 C
948 C
949 C
950 C
951 C
952 C
953 C
954 C
955 C
956 C
957 C
958 C
959 C
960 C
961 C
962 C
963 C
964 C
965 C
966 C
967 C
968 C
969 C
970 C
971 C
972 C
973 C
974 C
975 C
976 C
977 C
978 C
979 C
980 C
981 C
982 C
983 C
984 C
985 C
986 C
987 C
988 C
989 C
990 C
991 C
992 C
993 C
994 C
995 C
996 C
997 C
998 C
999 C
1000 C

```

Figure G.6. (Continued)

SUBROUTINE RTSLOW

INDEX

```

331 DOVIXX= 1./FIXX
332 DOVIYY= 1./FIYY
333 DOVIZZ= 1./FIZZ
334 ISLOW= 0
335 CALL TRACK('RTSLOW',2)
336 RETURN
337 DO 510 J=1,32
338 510 CALL DISABLI(J-1)
339 IPAN = KPAN
340 RETURN
341 END

```

Figure G.6. (Continued)

SUBROUTINE RISLOW

I N D E X

ALAFNR	-	2100			
ALART	-	2400			
ALART	-	2400			
ALARMG	-	2200			
ALPRK	-	1000			
ALFSQ	-	1800			
ALFTAB	-	1300			
ALHTE	-	2400			
ALHTM	-	2400			
ALHTP	-	2400			
ALHTPR	-	2400			
ALHTST	-	1000			
ALLNSQ	-	2000			
ALLRM	-	2100			
ALLAPP	-	2200			
ALNCBK	-	1000			
ALPHF	-	1800			
ALPHFP	-	86 =	154	178	91
ALPHHT	-	2400			
ALPHLN	-	2000			
ALPHLR	-	2100	152 =	156AG	164
ALPHLW	-	2200	224	239	173
ALPHPN	-	2000			
ALPHRR	-	2100	153 =	157AG	170
ALPHRW	-	2200	29	230	137
ALPHVT	-	2400			
ALRGLW	-	2200			
ALRGRW	-	2200			
ALRNSQ	-	2200			
ALRRH	-	2100			
ALRWPP	-	2200			
ALVTE	-	2400			
ALVTM	-	2400			
ALVTP	-	2400			
ALVTPR	-	2400			
ALVTST	-	1000			
ALWSSQ	-	2200			
AMACH	-	1600	45 =	46	
AMACLP	-	900			
AMACRP	-	900			
AMACSQ	-	1600	45 =	47	
AMACTL	-	2300			
AMACTR	-	2300			
AMAFSO	-	2500			
AMARE	-	1800			
AMAREP	-	1800	39 =		
AMARHT	-	2400			
AMARLW	-	2200			
AMARNC	-	2100			
AMARNL	-	2100			
AMARNR	-	2100			
AMARNW	-	2200			
AMART	-	2400			
AMARVT	-	2400			
AMARWG	-	2200			

Figure G.6. (Continued)

SUPERJUMP RTSLW

I N D E X

CMOF	-	100	91		
CMON	-	100	175	189	
CMOW	-	250			
CMRN	-	200	190	200	201
CMRMAO	-	220			
CMRWSS	-	220			
CMSLW	-	220			
CMRW	-	220			
CNE	-	180	92	100	101
CNFAIL	-	210			
CNFAIR	-	210			
CNFBIL	-	210			
CNFAIR	-	210			
CNFL	-	210			
CNFPL	-	90			
CNPR	-	90			
CNFR	-	210			
CNLN	-	200	177	206	207
CNOF	-	100	92		
CNOLN	-	100	177		
CNORN	-	100	191		
CMRN	-	200	191	200	201
CNSW	-	220			
COEF1	-	80	52		
COEF1C	-	80			
COEF11	-	80			
COEF12	-	80			
COEF13	-	80			
COEF14	-	80			
COEF15	-	80			
COEF16	-	80			
COEF17	-	80			
COEF18	-	80	95	200	201
COEF19	-	80	194	195	
COEF2	-	80			
COEF20	-	80			
COEF21	-	80			
COEF22	-	80			
COEF23	-	80			
COEF24	-	80			
COEF25	-	80	211		
COEF26	-	80	265		
COEF27	-	80	270	271	
COEF28	-	80	266	269	
COEF29	-	80	272	273	
COEF3	-	80	316	319	
COEF30	-	80	125		
COEF31	-	80			
COEF32	-	80			
COEF33	-	80			
COEF34	-	80	294		
COEF35	-	80			
COEF36	-	80			
COEF37	-	80			
COEF38	-	80			

Figure G.6. (Continued)

SUBROUTINE RTSLOW

I N D E X

COEF39	-	800			
COEF4	-	907	318	321	323
COEF40	-	807			
COEF41	-	907			
COEF42	-	900			
COEF5	-	800	312		
COEF6	-	800	313		
COEF7	-	907	314	323	
COEF8	-	800	315	323	
COEF9	-	800			
CONS1	-	2600			
CONS10	-	2600			
CONS11	-	2600			
CONS12	-	2600			
CONS13	-	2600			
CONS14	-	2600			
CONS15	-	2600			
CONS16	-	2600			
CONS17	-	2600			
CONS18	-	2600			
CONS19	-	2600			
CONS2	-	2600			
CONS20	-	2600			
CONS21	-	2600			
CONS22	-	2600			
CONS23	-	2600			
CONS24	-	2600			
CONS25	-	2600			
CONS26	-	2600			
CONS27	-	2600			
CONS28	-	2600			
CONS29	-	2600			
CONS3	-	2600			
CONS30	-	2600			
CONS31	-	2600			
CONS32	-	2600			
CONS33	-	2600			
CONS34	-	2600			
CONS35	-	2600			
CONS36	-	2600			
CONS37	-	2600			
CONS38	-	2600			
CONS39	-	2600			
CONS4	-	2600			
CONS40	-	2600			
CONS41	-	2600			
CONS42	-	2600			
CONS43	-	2600			
CONS44	-	2600	117		
CONS45	-	2600	117		
CONS46	-	2600	117		
CONS47	-	2600	121		
CONS48	-	2600	121		
CONS49	-	2600	121		
CONS5	-	2600	121		

Figure G.6. (Continued)

SUBROUTINE RTSLOW

I N D E X

CONS50	-	26C0	128	141			
CONS51	-	26C0	131	144			
CONS52	-	26C0	131	144			
CONS53	-	26C0	131	144			
CONS54	-	26C0	131	144			
CONS55	-	26C0	131	144			
CONS56	-	26C0	131	144			
CONS57	-	26C0	277	284			
CONS58	-	26C0	282	288			
CONS59	-	26C0	107				
CONS60	-	26C0	197				
CONS61	-	26C0	107				
CONS62	-	26C0	110				
CONS63	-	26C0	110				
CONS64	-	26C0	110				
CONS65	-	26C0					
CONS66	-	26C0					
CONS67	-	26C0					
CONS68	-	26C0					
CONS69	-	26C0					
CONS70	-	26C0					
CONS71	-	26C0					
CONS72	-	26C0					
CONS73	-	26C0					
CONS74	-	26C0					
CONS75	-	26C0					
CONS76	-	26C0					
CONS77	-	26C0					
CONS78	-	26C0					
CONS79	-	26C0					
CONS80	-	26C0					
CONS81	-	26C0					
CONS82	-	26C0					
CONS83	-	26C0					
CONS84	-	26C0					
CONS85	-	26C0					
CONS86	-	26C0					
CONS87	-	26C0					
CONS88	-	26C0					
CONS89	-	26C0					
CONS90	-	26C0					
CONS91	-	26C0					
CONS92	-	26C0					
CONS93	-	26C0					
CONS94	-	26C0					
CONS95	-	26C0					
CONS96	-	26C0					
CONS97	-	26C0					
CONS98	-	26C0					
CONS99	-	26C0					
CONS100	-	26C0					
CONS101	-	26C0					
CONS102	-	26C0					
CONS103	-	26C0					
CONS104	-	26C0					
CONS105	-	26C0					
CONS106	-	26C0					
CONS107	-	26C0					
CONS108	-	26C0					
CONS109	-	26C0					
CONS110	-	26C0					
CONS111	-	26C0					
CONS112	-	26C0					
CONS113	-	26C0					
CONS114	-	26C0					
CONS115	-	26C0					
CONS116	-	26C0					
CONS117	-	26C0					
CONS118	-	26C0					
CONS119	-	26C0					
CONS120	-	26C0					
CONS121	-	26C0					
CONS122	-	26C0					
CONS123	-	26C0					
CONS124	-	26C0					
CONS125	-	26C0					
CONS126	-	26C0					
CONS127	-	26C0					
CONS128	-	26C0					
CONS129	-	26C0					
CONS130	-	26C0					
CONS131	-	26C0					
CONS132	-	26C0					
CONS133	-	26C0					
CONS134	-	26C0					
CONS135	-	26C0					
CONS136	-	26C0					
CONS137	-	26C0					
CONS138	-	26C0					
CONS139	-	26C0					
CONS140	-	26C0					
CONS141	-	26C0					
CONS142	-	26C0					
CONS143	-	26C0					
CONS144	-	26C0					
CONS145	-	26C0					
CONS146	-	26C0					
CONS147	-	26C0					
CONS148	-	26C0					
CONS149	-	26C0					
CONS150	-	26C0					
CONS151	-	26C0					
CONS152	-	26C0					
CONS153	-	26C0					
CONS154	-	26C0					
CONS155	-	26C0					
CONS156	-	26C0					
CONS157	-	26C0					
CONS158	-	26C0					
CONS159	-	26C0					
CONS160	-	26C0					
CONS161	-	26C0					
CONS162	-	26C0					
CONS163	-	26C0					
CONS164	-	26C0					
CONS165	-	26C0					
CONS166	-	26C0					
CONS167	-	26C0					
CONS168	-	26C0					
CONS169	-	26C0					
CONS170	-	26C0					
CONS171	-	26C0					
CONS172	-	26C0					
CONS173	-	26C0					
CONS174	-	26C0					
CONS175	-	26C0					
CONS176	-	26C0					
CONS177	-	26C0					
CONS178	-	26C0					
CONS179	-	26C0					
CONS180	-	26C0					
CONS181	-	26C0					
CONS182	-	26C0					
CONS183	-	26C0					
CONS184	-	26C0					
CONS185	-	26C0					
CONS186	-	26C0					
CONS187	-	26C0					
CONS188	-	26C0					
CONS189	-	26C0					
CONS190	-	26C0					
CONS191	-	26C0					
CONS192	-	26C0					
CONS193	-	26C0					
CONS194	-	26C0					
CONS195	-	26C0					
CONS196	-	26C0					
CONS197	-	26C0					
CONS198	-	26C0					
CONS199	-	26C0					
CONS200	-	26C0					
CONS201	-	26C0					
CONS202	-	26C0					
CONS203	-	26C0					
CONS204	-	26C0					
CONS205	-	26C0					
CONS206	-	26C0					
CONS207	-	26C0					
CONS208	-	26C0					
CONS209	-	26C0					
CONS210	-	26C0					
CONS211	-	26C0					
CONS212	-	26C0					
CONS213	-	26C0					
CONS214	-	26C0					
CONS215	-	26C0					
CONS216	-	26C0					
CONS217	-	26C0					
CONS218	-	26C0					
CONS219	-	26C0					
CONS220	-	26C0					
CONS221	-	26C0					
CONS222	-	26C0					
CONS223	-	26C0					
CONS224	-	26C0					
CONS225	-	26C0					
CONS226	-	26C0					
CONS227	-	26C0					
CONS228	-	26C0					
CONS229	-	26C0					
CONS230	-	26C0					
CONS231	-	26C0					
CONS232	-	26C0					
CONS233	-	26C0					
CONS234	-	26C0					
CONS235	-	26C0					
CONS236	-	26C0					
CONS237	-	26C0					
CONS238	-	26C0					
CONS239	-	26C0					
CONS240	-	26C0					
CONS241	-	26C0					
CONS242	-	26C0					
CONS243	-	26C0					
CONS244	-	26C0					
CONS245	-	26C0					
CONS246	-	26C0					
CONS247	-	26C0					
CONS248	-	26C0					
CONS249	-	26C0					
CONS250	-	26C0					
CONS251	-	26C0					
CONS252	-	26C0					
CONS253	-	26C0					
CONS254	-	26C0					
CONS255	-	26C0					
CONS256	-	26C0					
CONS257	-	26C0					
CONS258	-	26C0					
CONS259	-	26C0					
CONS260	-	26C0					
CONS261	-	26C0					
CONS262	-	26C0					
CONS263	-	26C0					
CONS264	-	26C0					
CONS265	-	26C0					
CONS266	-	26C0					
CONS267	-	26C0					
CONS268	-	26C0					
CONS269	-	26C0					
CONS270	-	26C0					
CONS271	-	26C0					
CONS272	-	26C0					
CONS273	-	26C0					
CONS274	-	26C0					
CONS275	-	26C0					
CONS276	-	26C0					
CONS277	-	26C0					
CONS278	-	26C0					
CONS279	-	26C0					
CONS280	-	26C0					
CONS281	-	26C0					
CONS282	-	26C0					
CONS283	-	26C0					
CONS284	-	26C0					
CONS285	-	26C0					
CONS286	-	26C0					
CONS287	-	26C0					
CONS288	-	26C0					
CONS289	-	26C0					
CONS290	-	26C0					
CONS291	-	26C0					
CONS292	-	26C0					
CONS293	-	26C0					
CONS294	-	26C0					
CONS295	-	26C0					
CONS296	-	26C0					
CONS297	-	26C0					
CONS298	-	26C0					
CONS299	-	26C0					
CONS300	-	26C0					
CONS301	-	26C0					
CONS302	-	26C0					
CONS303	-	26C0					
CONS304	-						

SUBROUTINE RTSLOH

I N D E X

DBRK7	-	26C7	
DBRK8	-	26C3	
DBRK9	-	26C3	
DCDDF	-	22C7	
DCDLDA	-	22C0	99
DCDLG	-	10C3	
DCMLSP	-	22C0	
DCORDA	-	22C3	
DCDRSP	-	22C0	
DCLDF	-	22C3	
ECLLDA	-	22C0	
ECLLSP	-	22C0	
ECLROA	-	22C0	
ECLRSP	-	22C0	
ECLSPW	-	22C0	
DCMDF	-	22C3	
DCMLDA	-	22C0	31
DCMLG	-	10C0	
DCMLSP	-	22C3	
DCMRDA	-	22C3	
DCMRSP	-	22C0	
DCNSPW	-	22C0	
DEG20	-	10C0	
DEL	-	16C3	57=
DELAS	-	9C0	62
DELAT	-	9C0	
DELEV	-	9C0	
DEFLP	-	9C0	
DELS	-	9C3	
DELRT	-	9C0	
DELRTD	-	9C0	
DELSPL	-	9C3	
DELSPR	-	9C0	
DELS	-	9C0	
DELST	-	9C0	
DELTH	-	9C0	
DFLATL	-	9C3	
DFLAIR	-	9C0	
DGTORD	-	10C0	
DIGAN	-	3C0	
DIGAN2	-	3C0	
DISABL	-	338*	
DLFPSQ	-	14C0	
DLG	-	18C0	237=
LLNC	-	20C0	231=
DLRNC	-	20C0	
DMLG	-	18C0	
CMLNC	-	20C0	235=
CMRNC	-	20C3	199=
DMLG	-	18C0	
CMLNC	-	20C0	236=
CMRNC	-	20C0	230=
COVT	-	13C0	149
COVTL	-	19C0	145
DOVTR	-	19C3	132

Figure G.6. (Continued)

SUBROUTINE RTSLOW

I N D E X

TAURR	-	2200	214	219AG
TAURT1	-	1000		
TAURT2	-	1000		
TAUVT	-	1000		
TAVSEP	-	2200	245	252
TCEFF	-	500		
TDEFF	-	1600	59	
TEAL	-	1600		
TEAR	-	1600	72=	79AG
TERMP1	-	2500		
TERMQ1	-	2500		
TERMR1	-	2500		
TERM1	-	2500	316=	326
TERM1L	-	2500		
TERM1R	-	2500		
TERM2	-	2500	317=	326
TERM2L	-	2500		
TERM2P	-	2500		
TERM3	-	2500	319=	324
TERM3L	-	2500		
TERM3R	-	2500		
TERM4	-	2500	319=	323
TERM5	-	2500	321=	323
TERM6	-	2500	321=	324
THCDEL	-	1600	50=	70
THE	-	900	60AG	
THETC	-	1600	50=	61
THILAC	-	2300		
THIRAC	-	2300		
TH75L	-	900		
TH75R	-	900		
TIGEL	-	1900	144=	148=
TIGER	-	1900	131=	135=
TL	-	2100	224	225
TMG1C	-	2300	221=	222
TMG11	-	2300	221=	222
TNAC1	-	2000	194=	196
TNAC2	-	2000	195=	202
TOROL	-	2100		
TORQR	-	2100		
TPSP	-	900	72	
TR	-	2100	210	
TRACK	-	270	315=	
TRIM	-	300		
TRIM2	-	300		
TRVAR1	-	2100		
TRVAR2	-	2100		
TRNAP1	-	2100		
TRNAP4	-	2100		
TRNHR1	-	2100		
TRNHR2	-	2100		
TRNHT	-	2400		
TRNHT2	-	2400		
TRNHT3	-	2400		
TRNNC1	-	174	175	

Figure G.6. (Continued)

INDEX

SUBROUTINE AILSPIDEL,SPDIL,DCLA,DCOA,DCMA,DCLS,DCDS,DCMS

```

1  SUPROUTINE AILSPIDEL,SPDIL,DCLA,DCOA,DCMA,DCLS,DCDS,DCMS
2  CLASH=0
3  *PIV2,ROTDGG,ROTPPS,SKPS,ALNCBK,TAUTL1,TAUTL2
4  COMMON/XPAB37/CONS1,CONS7,CONS10,CONS11,CONS12,CONS13,CONS14,
5  CONS15,CONS16,CONS17,CONS18,CONS19,CONS20,CONS21,
6  CONS22,CONS23,CONS24,CONS25,CONS26,CONS27,CONS28,
7  CONS29,CONS30,CONS31,CONS32,CONS33,CONS34,CONS35,
8  CONS36,CONS37,CONS38,CONS39,CONS40,CONS41,CONS42,
9  CONS43,CONS44,CONS45,CONS46,CONS47,CONS48,CONS49,
10 CONS50,CONS51,CONS52,CONS53,CONS54,CONS55,CONS56,
11 CONS57,CONS58,CONS59,CONS60,CONS61,CONS62,CONS63,
12 CONS64,CONS65,CONS66,CONS67,CONS68,CONS69,CONS70,
13 CONS71,CONS72,CONS73,CONS74,CONS75,CONS76,CONS77,
14 CONS78,CONS79,CONS80,CONS81
15 133TOL1
16 1 TO 7
17 8 TO 14
18 15 TO 21
19 22 TO 28
20 29 TO 35
21 36 TO 42
22 43 TO 49
23 50 TO 56
24 57 TO 63
25 64 TO 70
26 71 TO 77
27 78 TO 84
28 85 TO 91
29 104TOL1
30 114TOL1
31
32
33
34
35
36
37
38
39
40
41
42
43
44
45
46
47
48
49
50
51
52
53
54
55
56
57
58
59
60
61
62
63
64
65
66
67
68
69
70
71
72
73
74
75
76
77
78
79
80
81
82
83
84
85
86
87
88
89
90
91
92
93
94
95
96
97
98
99
100

```

Figure G.6. (Continued)

SUBROUTINE ATLSP(DEL,SP0IL,DCLA,DCJA,DYMA,DCLS,DCDS,DMS)

DCDS= CONSG9+SP0IL*(CCNSTC+CONST1*SP0IL)

DCMS= r.

RETURN

END

END

32 C

33 C

34

35

Figure G.6. (Continued)

SUBROUTINE	DEL	<POIL	DCLA	DCDA	DCMA	DCLS	DCON	DMS	REFERENCES
5	-	5	-	-	-	-	-	-	18*
30	-	9	-	-	-	-	-	-	12*
40	-	12	-	-	-	-	-	-	15*
45	-	11	-	-	-	-	-	-	14
48	-	17	-	-	-	-	-	-	20*
50	-	22	-	-	-	-	-	-	25*
55	-	24	-	-	-	-	-	-	26*
60	-	27	-	-	-	-	-	-	30*
65	-	29	-	-	-	-	-	-	31*
AILSP	-	1*	-	-	-	-	-	-	
AILRK	-	200	-	-	-	-	-	-	
ALNCRK	-	200	-	-	-	-	-	-	
ARKLSW	-	200	-	-	-	-	-	-	
ARKLSW	-	200	-	-	-	-	-	-	
CLF1	-	6*	-	-	-	-	-	-	
CLMAX	-	200	-	-	-	-	-	-	
CLZ	-	445	-	-	-	-	-	-	18=
INS1	-	300	-	-	-	-	-	-	
CONS10	-	300	-	-	-	-	-	-	
CONS11	-	300	-	-	-	-	-	-	
CONS12	-	300	-	-	-	-	-	-	
CONS13	-	300	-	-	-	-	-	-	
CONS14	-	300	-	-	-	-	-	-	
CONS15	-	300	-	-	-	-	-	-	
CONS16	-	300	-	-	-	-	-	-	
CONS17	-	300	-	-	-	-	-	-	
CONS18	-	300	-	-	-	-	-	-	
CONS19	-	300	-	-	-	-	-	-	
CONS20	-	300	-	-	-	-	-	-	
CONS21	-	300	-	-	-	-	-	-	
CONS22	-	300	-	-	-	-	-	-	
CONS23	-	300	-	-	-	-	-	-	
CONS24	-	300	-	-	-	-	-	-	
CONS25	-	300	-	-	-	-	-	-	
CONS26	-	300	-	-	-	-	-	-	
CONS27	-	300	-	-	-	-	-	-	10
CONS28	-	300	-	-	-	-	-	-	13
CONS29	-	300	-	-	-	-	-	-	13
CONS30	-	300	-	-	-	-	-	-	13
CONS31	-	300	-	-	-	-	-	-	15
CONS32	-	300	-	-	-	-	-	-	15
CONS33	-	300	-	-	-	-	-	-	15
CONS34	-	300	-	-	-	-	-	-	23
CONS35	-	300	-	-	-	-	-	-	23
CONS36	-	300	-	-	-	-	-	-	25
CONS37	-	300	-	-	-	-	-	-	25
CONS38	-	300	-	-	-	-	-	-	25
CONS39	-	300	-	-	-	-	-	-	28
CONS40	-	300	-	-	-	-	-	-	30
CONS41	-	300	-	-	-	-	-	-	

Figure G.6. (Continued)

SUBROUTINE ATLSPIDEL, SPOIL, DCLA, DCDA, DCMA, DCLS, DCDS, DCMS)

I N D E X

CONS42	-	3C0	
CONS43	-	3C0	
CONS44	-	3C0	
CONS45	-	3C0	
CONS46	-	3C0	
CONS47	-	3C0	
CONS48	-	3C0	
CONS49	-	3C0	
CONS5	-	3C0	
CONS50	-	3C0	
CONS51	-	3C0	
CONS52	-	3C0	
CONS53	-	3C0	
CONS54	-	3C0	
CONS55	-	3C0	
CONS56	-	3C0	
CONS57	-	3C0	
CONS58	-	3C0	
CONS59	-	3C0	
CONS6	-	3C0	
CONS60	-	3C0	
CONS61	-	3C0	
CONS62	-	3C0	
CONS63	-	3C0	
CONS64	-	3C0	
CONS65	-	3C0	
CONS66	-	3C0	
CONS67	-	3C0	
CONS68	-	3C0	
CONS69	-	3C0	
CONS7	-	3C0	
CONS70	-	3C0	
CONS71	-	3C0	
CONS72	-	3C0	
CONS73	-	3C0	
CONS74	-	3C0	
CONS75	-	3C0	
CONS76	-	3C0	
CONS77	-	3C0	
CONS78	-	3C0	
CONS79	-	3C0	
CONS8	-	3C0	
CONS80	-	3C0	
CONS81	-	3C0	
CONS9	-	3C0	
DBRK1	-	3C0	
DBRK10	-	3C0	
DBRK11	-	3C0	
DBRK12	-	3C0	
DBRK13	-	3C0	
DBRK14	-	3C0	
DBRK15	-	3C0	
DBRK16	-	3C0	
DBRK17	-	3C0	
DBRK18	-	3C0	

30
31
32
32

Figure G.6. (Continued)

SUBROUTINE CLCOCM(ALPHA,DEL,CLDEL,CLSP,CDASP,CMEASP,CL,CD,CM,

I N D E X

```

1  SUBROUTINE CLCOCM(ALPHA,DEL,CLDEL,CLSP,CDASP,CMEASP,CL,CD,CM,
2  CLP,CDPI)
3  COMMON/XACDEF/ ACOWO,ACOW1,ACOW2,ACOW3,ACOW4,
4  ACOW5,ACOW6,ACOW7,ACOW8,ACOW9,
5  ACOW10,ACOW11,ACOW12,ACOW13,ACOW14,
6  ACOW15,ACOW16,ACOW17,ACOW18,ACOW19,
7  ACOW20,ACOW21,ACOW22,ACOW23,ACOW24
8  COMMON/XPAR1/ AINHT,AINW,ALAMDA,ALHTST,ALVTST,AREAMT,AREAM,
9  AREAVT,ARHT,ARVT,AVEYAC,AVECS,BLS,COOF,COOHT,COOVT,
10 CHORD,CLALHT,CLALPH,CMOF,CMON,CMOF,CNOLN,CNORN,CYALVT,
11 3DCOLG,DCMLG,FINPR,DOVT,DSOBT,EFFHT,EFFVT,FIE,FINDEG,
12  *CIP,FIIXF,FIIXPR,FIIXW,FIIXZ,FIIXPR,FIIXW,FIIXZ,FIIXW,FIIXZ,
13  *FIYVM,FIIZF,FIIZPR,FIIZW, *P,OMREF,PC,PI,ROTRAD,
14  *SBFPR,SBWPP,SG,SHF,SHW,SKJ,SKL,SK2,SK3,
15  *SK4,SK5,SK6,SK7,SK8,SK9,SK10,SK20,SK21,
16  *SK22,CDONLO,SK30LO,SK31LO,SK32,CDONHI,SK34,SK35,SK36,
17  *SK37,SK38,SK39,SK40,SK41,SK42,SK43,SK44,SK45,
18  *SK46,SK47,SK48,SK49,SK50,SL,SLF,SLPA,SLW,
19  *SM,SMF,SMN,SMW,SPAN,TAUHT,TAUVT,XFAC,XMT,
20  *XMAC,XVT,YN,YPA,YMAC,ZFAC,ZMT,ZPA,ZMAC,
21  *ZVT,CLOAL,PHIPH,SK30HI,ENREF,XWC2,BY1,BT2,BT3,
22  *RKD1T,RKD2T,RKD3T,RKMT,RKM2T,RKM3T,BK44T,SK31HI,
23  *FFU,CLMAX,ALROK,PKLSM,RKNSM,SQFPRM,DEG25,OGTORD,MTVTKT,
24  *PIQV2,ROTORQ,ROTEPS,SKEPS,ALNCRK,TAURTI,TAURT2
25  COMMON/GEFVAR/
26  1 ACVAT,AGOVAM,RIGX, *RK99, *BMDVTL,BMDVTS,CONCOR,CLICOR,CLWCJR,
27  2 DQVTL,DOVTR,EPRM,GEF, *HGEFLR,HGEFR,HLHUB,HRHUB,HTC4,
28  3 HNC4,RR11,RR12, *SBI, *TIGEL, *TIGER
29  COMMON/FLAGS/ IWARN1(16),IWARN2(16),ISENCE(2),IMREVT(2),ICOND,
30  1 ITA,ISTB,NCEF,NWB,NTWST
31  LOGICAL *1 IWARN1,IWARN2
32  COMMON/XPAR3/ CONS1,CONS2,CONS3,CONS4,CONS5,CONS6,CONS7,
33  1 CONS8,CONS9,CONS10,CONS11,CONS12,CONS13,CONS14,
34  2 CONS15,CONS16,CONS17,CONS18,CONS19,CONS20,CONS21,
35  3 CONS22,CONS23,CONS24,CONS25,CONS26,CONS27,CONS28,
36  4 CONS29,CONS30,CONS31,CONS32,CONS33,CONS34,CONS35,
37  5 CONS36,CONS37,CONS38,CONS39,CONS40,CONS41,CONS42,
38  6 CONS43,CONS44,CONS45,CONS46,CONS47,CONS48,CONS49,
39  7 CONS50,CONS51,CONS52,CONS53,CONS54,CONS55,CONS56,
40  8 CONS57,CONS58,CONS59,CONS60,CONS61,CONS62,CONS63,
41  9 CONS64,CONS65,CONS66,CONS67,CONS68,CONS69,CONS70,
42  10 DRAK1,DRAK2,DRAK3,DRAK4,DRAK5,DRAK6,DRAK7,
43  11 DRAK8,DRAK9,DRAK10,DRAK11,DRAK12,DRAK13,DRAK14,
44  12 DRAK15,DRAK16,DRAK17,DRAK18,DRAK19,DRAK20,DRAK21,
45  13 SFLL,SFNL,SFSL,SFPHL,SFPHL,SFPHL,SFPHL,SFPL,
46  14 SFTR,SFTR,SFTR,SFTR,SFTR,SFTR,SFTR,SFTR,SFTR,
47  15 *CONS71,CONS72,CONS73,CONS74,CONS75,CONS76,CONS77,
48  16 *CONS78,CONS79,CONS80,CONS81
49  NOPT= 0
50  GO TO 5
51  ENTRY CLF2IALPHA,CLDEL,CLSP,CLZ1
52  NOPT= 1
53  CONTINUE
54  5 C

```

Figure G.6. (Continued)

```

13 ALDEG = ALPHA * BXTDQ
14 CLALDG = CLALDG + DGTDQ
15
16 IF (DEL.GT.DARK2) GO TO 11
17 ALNLP = CONST + CONS2*DEL
18 ALNLN = CONS3 + CONS4*DEL
19 GO TO 20
20 ALNLP = CONS5
21 ALNLN = CONS6
22 CONTINUE
23 ALARK1 = ALNLP + DARK3
24 ALARK2 = ALNLN - DARK3
25
26 IF (DEL.GT.DARK3) GO TO 112
27 F = CONS21*DEL + (CONS22 + (CONS23*DEL))
28 GO TO 114
29 F = (CONS24*DEL + (CONS25 + (CONS26*DEL))
30 CONTINUE
31 CLI = CLAL + CLDEL + CLSP*F
32 IMAPN1(4) = .FALSE.
33 IF (ALDEG.GE.ALARK2) GO TO 100
34 CLNLP = CLI + CLALDG + ALNLN
35 CLP = CLNLP + (CONST + ALDEG) / (CONST + ALARK2)
36 IMAPN1(4) = .TRUE.
37 GO TO 140
38
39 IF (ALDEG.GE.ALNLN) GO TO 110
40 CLMP = CLI + CLALDG + ALNLN
41 ALDUM = ALNLN - ALDEG + CONST1
42 DCNLN = ALDUM + (CONS8*ALDUM + CONS9) + CONS10
43 CLP = CLNLP - DCNLN
44 IMAPN1(4) = .TRUE.
45 GO TO 140
46
47 IF (ALDEG.GT.ALNLP) GO TO 120
48 CLP = CLALDG + ALDEG + CLI
49 GO TO 140
50
51 IF (ALDEG.GT.ALARK1) GO TO 130
52 CLNLP = CLI + CLALDG + ALNLP
53 ALDUM = ALDEG - ALNLP + CONST1
54 DCNLN = ALDUM + (CONS8*ALDUM + CONS9) + CONS10
55 CLP = CLNLP + DCNLN
56 IMAPN1(4) = .TRUE.
57 GO TO 140
58
59 CONTINUE
60 CLNLP = CLI + CLALDG + ALNLP
61 CLP = CLNLP + (CONST - ALDEG) / (CONST - ALARK1)
62 CONTINUE
63 IF (IMAPN1(4) = 1) GO TO 150
64 CL7 = CLP + CLWCR
65 RETURN
66 CONTINUE
67
68 CLPMX = CLMAX + CLDEL + CLSP
69 CLICE = CLP + CLWCR
70 IF (CLICE.LT.CLPMX) GO TO 160
71 DOIOE = 0

```

Figure G.6. (Continued)

```

INDEX
65      SUM=0;IF CLDGM(ALPHA+DEL+CLDEL+CLSP+CDFASP+CMFASP+CL+CD+CM+
66      CLICE= CLPMX
67      GO TO 170
68      YCNICE= CDWCDP*(CLIGE-CLP)*(CLIGE-CLP)
69      CONTINUE
70      ALDUM= DRK5
71      IF(ALDEG+LT+DRPK4) ALDUM=DRK4
72      IF(ALDEG+GE+DRPK4) AND(ALDEG+LE+DRK5) ALDUM= ALDEG
73      COT= ACDW0+DEL*(ACDW1+DEL*(ACDW2+DEL*(ACDW3+DEL*(ACDW4)))) +
74      1ALDUM*(ACDW5+DEL*(ACDW6+DEL*(ACDW7+DEL*(ACDW8+DEL*(ACDW9)))) +
75      2ALDUM*(ACDW10+DEL*(ACDW11+DEL*(ACDW12+DEL*(ACDW13+DEL*(ACDW14)))) +
76      3ALDUM*(ACDW15+DEL*(ACDW16+DEL*(ACDW17+DEL*(ACDW18+DEL*(ACDW19)))) +
77      4ALDUM*(ACDW20+DEL*(ACDW21+DEL*(ACDW22+DEL*(ACDW23+DEL*(ACDW24))))))
78      5)
79      IF(ALDEG+GE+DRPK4) GO TO 180
80      CM= CONS11+CD1+CMFASP
81      CDE= CM-(1-COM)*(ALDEG-DRPK4)*CONS12
82      CDP= (CONS17+CMFASP)*(CONS7+ALDEG)*CONS12
83      GO TO 200
84      IF(ALDEG+GT+DRPK5) GO TO 190
85      CDP= ALDEG*(CONS13+ALDEG*(CONS14) +CONS15+CD1)+CDFASP
86      CDE= CONS18+CONS19*ALDEG+CMFASP
87      GO TO 200
88      CDEPLUS= CONS10+CD1+CDFASP
89      CDP= CDEPLUS+(1-CDEPLUS)*(ALDEG-DRPK5)*CONS12
90      CDE= (CONS20+CMFASP)*(CONS7-ALDEG)*CONS12
91      CONTINUE
92      CL= CLIGE
93      CD= CDP+CDIGE
94      CM= CDE
95      GETUPN
96      END

```

Figure G.6. (Continued)

SUBROUTINE CLC3CMIALP4A,DEL,CLDEL,CLSP,CD,ASP,CMEASP,CL,CD,CM,

I N D E X

CONS48	-	TCO			
CONS49	-	TCO			
CONS5	-	TCO	19		
CONS5C	-	TCO			
CONS51	-	TCO			
CONS52	-	TCO			
CONS53	-	TCO			
CONS54	-	TCO			
CONS55	-	TCO			
CONS56	-	TCO			
CONS57	-	TCO			
CONS58	-	TCO			
CONS59	-	TCO	20		
CONS6	-	TCO			
CONS60	-	TCO			
CONS61	-	TCO			
CONS62	-	TCO			
CONS63	-	TCO			
CONS64	-	TCO			
CONS65	-	TCO			
CONS66	-	TCO			
CONS67	-	TCO			
CONS68	-	TCO			
CONS69	-	TCO	33	55	74
CONS7	-	TCO			
CONS70	-	TCO			
CONS71	-	TCO			
CONS72	-	TCO			
CONS73	-	TCO			
CONS74	-	TCO			
CONS75	-	TCO			
CONS76	-	TCO			
CONS77	-	TCO			
CONS78	-	TCO			
CONS79	-	TCO			
CONS8	-	TCO	39	49	
CONS80	-	TCO			
CONS81	-	TCO			
CONS8	-	TCO	39	47	
CYALVT	-	3CO			
DBRK1	-	TCO			
DBRK10	-	TCO			
DBRK11	-	TCO			
DBRK12	-	TCO			
DBRK13	-	TCO			
DBRK14	-	TCO			
DBRK15	-	TCO			
DBRK16	-	TCO			
DBRK17	-	TCO			
DBRK18	-	TCO			
DBRK19	-	TCO			
DBRK2	-	TCO	15		
DBRK2C	-	TCO			
DBRK21	-	TCO	22	23	
DBRK3	-	TCO			

Figure G.6. (Continued)

SURONITINE C1C0CM(1PHA,DEL,C1CDEL,C1SP,CDFASP,CNFASP,CL,CD,CM,

I N D E X

CBRK4	-	70	71	73	75
CBRK5	-	69	71	78	83
CBRK6	-	24			
CBRK7	-				
CBRK8	-				
CBRK9	-				
DCDIGE	-	67=	87		
DCDLG	-	40	49=	50	
DCMLG	-				
DEG20	-				
DEL	-	15	16	17	24
DGTORD	-	14		25	27
DOWT	-				72
DOWTL	-				
DOWTR	-				
DSDBET	-				
EFFMT	-				
EFFVT	-				
EN2REF	-				
ENPRM	-				
F	-	27=	29		
FEU	-				
FTE	-				
FINDEG	-				
FIMPR	-				
FIP	-				
FIXKF	-				
FIXPR	-				
FIXXW	-				
FIXZF	-				
FIXZPR	-				
FIXZW	-				
FIVVF	-				
FIVPR	-				
FIVW	-				
FIZZF	-				
FIZZPR	-				
FIZZW	-				
FLAGS	-				
GMUTOM	-				
GEF	-				
GEFVAR	-				
MGFLR	-				
MGEFRR	-				
MLMJB	-				
MP	-				
MRMJB	-				
HTC4	-				
HTVTKT	-				
HMC4	-				
ICONOP	-				
IPHA5E	-				
ISENCE	-				
ISLOW	-				

Figure 6. (Continued)

SUBROUTINE CLCOCMIALPHA,DEL,CLOEL,CLSP,CDFASP,CMFASP,CL,CD,CM,

I N D E X

ISTA	-	500
ISTR	-	500
ITRM	-	500
IWARN1	-	500
IWARN2	-	500
IWREV	-	500
JTPIM	-	500
KTRIM	-	500
NGEF	-	500
NOPT	-	8=
NPLT	-	500
NPLT2	-	500
NTWST	-	500
NV8	-	500
OMREF	-	300
PC	-	300
PI	-	300
PIOV2	-	300
ROTODG	-	300
RETURN	-	59*
ROTEPS	-	300
ROTRAG	-	300
RR11	-	400
RR12	-	400
SBFPR	-	300
SBNPR	-	300
SBI	-	400
SFNL	-	700
SFNER	-	700
SFPL	-	700
SFPHL	-	700
SFPHR	-	700
SFPR	-	700
SFQL	-	700
SFOR	-	700
SFSEL	-	700
SFSFR	-	700
SFTL	-	700
SFTR	-	700
SFVHL	-	700
SFYMR	-	700
SG	-	300
SHF	-	300
SHW	-	300
SKFPS	-	300
SKO	-	300
SK1	-	300
SK10	-	300
SK2	-	300
SK20	-	300
SK21	-	300
SK22	-	300
SK3	-	300
SK30HI	-	300

*

Figure G.6. (Continued)

I N D E X

SK3CLD	-	3CO
SK3IMI	-	3CO
SK3ILD	-	3CO
SK32	-	3CO
SK34	-	3CO
SK35	-	3CO
SK36	-	3CO
SK37	-	3CO
SK38	-	3CO
SK39	-	3CO
SK4	-	3CO
SK40	-	3CO
SK41	-	3CO
SK42	-	3CO
SK43	-	3CO
SK44	-	3CO
SK45	-	3CO
SK46	-	3CO
SK47	-	3CO
SK48	-	3CO
SK49	-	3CO
SK5	-	3CO
SK50	-	3CO
SK6	-	3CO
SK7	-	3CO
SK8	-	3CO
SK9	-	3CO
SL	-	3CO
SLF	-	3CO
SLPA	-	3CO
SLW	-	3CO
SM	-	3CO
SMF	-	3CO
SMN	-	3CO
SMW	-	3CO
SPAN	-	3CO
SQPRM	-	3CO
SMG	-	5CO
TAUNT	-	3CO
TAUNT1	-	3CO
TAUNT2	-	3CO
TAUNT	-	3CO
TIGEL	-	4CO
TIGER	-	4CO
XACDEF	-	2*
XFAC	-	3CO
XMT	-	3CO
XPAR1	-	3*
XPAR3	-	7*
XVT	-	3CO
XMAC	-	3CO
XMC2	-	3CO
YN	-	3CO
YPA	-	3CO
YMAC	-	3CO

* * *

Figure G.6. (Continued)

SUBROUTINE CUCOCH(ALPHA, DEL, CLOFL, CLSP, CDFASP, CMFASP, CL, CO, CM,

I N D E X

ZFAC - 3CO
 ZHT - 3CN
 ZPA - 3CO
 ZVT - 3CN
 ZWAC - 3CO

Figure G.6. (Continued)

IN	DFX	1	2	3	4	5	6	7	8	9	10	11	12	13	14	15	16	17	18	19	
		SUBROUTINE ENGINE(TFA, SHPOUT, CMENG, PCTORQ)																			
		SURROJTIME ENGINE(TFA, SHPOUT, CMENG, PCTORQ)																			
		COMMON/ENG/ NWDITD, N1ND, N1THID, N2IND, NOIND, MRNDID,																			
		FWDTHX, ENIMX, ENLTHX, EN2MX, FQMX, SHPSTR																			
		, EWDTPR, EN1STR, ROE2, TZERO, TCDEF																			
		COMMON/ENGVAR/																			
		1 AMACH, AMACSO, DEL, FMAXN1, EMAXN2, EMXWDI, EN2STR, FSNACH, OMEGEL,																			
		2 OMEGER, OMVTC, OVFSM, OVSO, TH, OVTHDL, ROE, ROEDV2, SHPRL, SHPPRR,																			
		3 SMA, SON1MX, SQTHC, SQWDTX, TDEGF, TEAL, TEAR, TMCDEL, TMETC																			
		4, PCTOR, PCTOR																			
		COMMON/FLAGS/ IWARN1(16), IWARN2(16), ISENCE(2), IMREVT(2), ICONOP,																			
		1 ITRIM, JTRIM, KTRIM, NPLOT, NPLT2, IPHASE, ISLOW, SMLG, GBDTON,																			
		2 ISTR, NGEF, NVB, NTWST																			
		LOGICAL*1 IWARN1, IWARN2																			
		ENGINE CHARACTERISTICS USED																			
		VWDITD = 1 FUEL FLOW CUTOFF																			
		N1IND = 1 N1 CUTOFF																			
		N1THID = 0 NO REFERRED N1 CUTOFF																			
		N2IND = 2 N2 CUTOFF - NON-OPTIMUM N2 VARIATION																			
		N3IND = 1 TORQUE CUTOFF																			
		MRNDID = 0 NO REYNOLDS NUMBER CORRECTIONS																			
		TEASQ = TEA * TEA																			
		TEACUR = TEASQ * TEA																			
		TEA4TH = TEACUR * TEA																			
		NOTE TEA = TPS / TMETC																			
		IF(NWDITD.EQ.0) GO TO 1000																			
		FIND (NWDITD/SHPI) AT TEA,M																			
		W TOT = F(TFA) EQUATION FROM CURVE FIT PROGRAM																			
		4TH ORDER IN TEA																			
		EMDWT = -2.0503260368*3531349133E-32*TEA-.2594440658E-05*TEASQ																			
		* *.1014275181E-08*TEACUR-.144138415E-12*TEA4TH																			
		IWARN1(1) = .FALSE.																			
		IF(EMDWT.LT.EMXWDI) GO TO 1000																			
		IWARN1(1) = .TRUE.																			
		FIND TEA AT MAX WDT, M																			
		TEA = F(W DOTHX) FROM CURVE FIT PROGRAM																			
		4TH ORDER IN W DOTHX																			
		TEA = 1587.5824254398-1375.3423740741*EMXWDI+12872.89968281*																			
		* SQWDTX-22742.78987105*SQWDTX*EMX4DI+13929.828136*31*SQWDTX *																			
		* SQWDTX																			
		TEASQ = TEA * TEA																			
		TEACUR = TEASQ * TEA																			
		TEA4TH = TEACUR * TEA																			
		IF(N1IND.EQ.0) GO TO 2000																			
		FIND N1/N1STAR AT TEA,M																			
		N1 = F(TEA,M) EQUATION FROM CURVE FIT PROGRAM																			
		3RD ORDER IN TEA, 2ND ORDER IN M																			
		EN1 = -2.262254343 +1.2-12886559*AMACH+.9621240231*AMACSO																			

Figure G.6. (Continued)

```

20 * (+.351958E+42*-02-.1539742133E-02*AMACH+-.1308445977E-02*AMACSQ)*
21 * TEA +
22 * (-.13116093319E-05+.6259888594E-06*AMACH+.6664941537E-06*AMACSQ)*
23 * TEASQ +
24 * (-.1765915983E-09-.8357285710E-10*AMACH-.9302102725E-10*AMACSQ)*
25 * TEACUB
26
27 IWARN(2) = .FALSE.
28 IF (EN1.LT.FMAXN1) GO TO 2000
29 IWARN(2) = .TRUE.
30 FEND TEA AT MAX N1,M
31
32 TEA = F(N1MAX,M) EQUATION FROM CURVE FIT PROGRAM
33 3RD ORDER IN N1MAX , 2ND ORDER IN M
34 TEA = 4555.7525996C75+4266.63519C7663*AMACH-10962.24966689*AMACSQ
35 * (+-10591.376223561-14(06.747644625*AMACH+34472.653759217*AMACSQ)*
36 * FMAXN1 +
37 * (1.0876.684523467+151(0.9688113C98*AMACH-36112.607870716*AMACSQ)*
38 * SQN1MX +
39 * (-2601.662341542-5379.983822401*AMACH+12502.173136418*AMACSQ)*
40 * SQN1MX*FMAXN1
41 TEASQ = TEA * TEA
42 TEACUB = TEASQ * TEA
43 TEA4TH = TEACUB * TEA
44 EN1 = FMAXN1
45 IF (N1HID.F3.0) GO TO 3000
46 THIS OPTION WILL BE LEFT BLANK UNTIL NEEDED
47
48 2000 CONTINUE
49
50 THIS SECTION CORRESPONDS TO THE ENG 1 SUBR BLOCK IN FLOW DIAG
51 SKPN= 1.
52 IF (N2IND.NE.2) GO TO 4000
53 FEND N2/N2STAR AT TEA,M
54
55 N2 = F(TEA,M) EQUATION FROM CURVE FIT PROGRAM
56 3RD ORDER IN TEA , 2ND ORDER IN M
57 EN2 = -5.5804780552-2.6637228923*AMACH+1.1263419372*AMACSQ
58 * (+(-.7055C66994E-02+.3351714914E-02*AMACH-.1239191608E-03*AMACSQ)*
59 * TEA +
60 * (-.2593416699E-05-.1287559251E-05*AMACH-.4369359301E-06*AMACSQ)*
61 * TEASQ +
62 * (-.3395936162E-09+.1505373934E-09*AMACH+.1178189720E-09*AMACSQ)*
63 * TEACUB
64
65 EN2OPT= EN2STR/EN2* OVSQTH
66 SKPN= 1.-11.-EN2OPT)*11.-EN2OPT)
67 CONTINUE
68
69 SKPN= 1.
70 IF (N2HID.EQ.0) GO TO 5000
71 THIS OPTION WILL BE LEFT BLANK UNTIL NEEDED
72
73 4000 CONTINUE
74 FEND SHP/SHPTAR
75
76 5000 CONTINUE
77
78 SHP = F(TEA,M) EQUATION FROM CURVE FIT PROGRAM
79 3RD ORDER IN TEA , 2ND ORDER IN M

```

Figure G.6. (Continued)

I N D E X

SUBROUTINE ENGINE(TEA, SHPDT, OMENG, PCTORQ)

```

30  ESNP = 2.943431215-.2571992619*AMACH+.13604785868*AMACSQ
    *+(-.6857620248E-02+.7364751077E-03*AMACH-.1979318276E-02*AMACSQ)*
    * TEA +
    * (-.4348718891E-05-.3926992714E-06*AMACH+.1001305662E-05*AMACSQ)*
    * TEASO +
    * (-.7488074668E-09+.696958120E-10*AMACH+.1674167095E-09*AMACSQ)*
    * TEACUB
C
40  ENGSHP= SHPDT*SNPRESHP
C    END OF ENG 1 SUBR BLOCK
41  IF(IN2IND.EQ.1) GO TO 6000
42  IF(IN2IND.NE.1) GO TO 8000
C    THIS OPTION WILL BE LEFT BLANK UNTIL NEEDED
43  GO TO 8000
44  IF(IN2IND.EQ.2) GO TO 7000
C    THIS OPTION WILL BE LEFT BLANK UNTIL NEEDED
45  SHPMAX= FOMX*EN2STR*OUTHDI
46  IWARN1(3)=.FALSE.
47  IF(ENGSHP.LT.SHPMAX) GO TO 9000
48  IWARN1(3)=.TRUE.
49  ENGSHP= SHPMAX
C
C    FIND TEA AT MAX SHP * M
C
C    TEA = F(SHP,M) EQUATION FROM CURVE FIT PROGRAM
C    3RD ORDER IN SHPMAX * 2ND ORDER IN M
C
50  TEA= 1550.0865704333-170.14330746603*AMACH-242.7678229176*AMACSQ
    *+(-1145.2371955474+149.9327819876*AMACH+706.56693216443*AMACSQ)*
    * SHPMAX +
    * (-1125.4640744348+74.2324453353*AMACH-792.57223629916*AMACSQ)*
    * SHPMAX * SHPMAX +
    * (456.38766443477-226.4415181202*AMACH+311.0686620534*AMACSQ)*
    * SHPMAX*SHPMAX*SHPMAX
    TFASO = TEA * TEA
    TEACUB = TEASO * TEA
    TEA4TH = TEACUB * TEA
C
C    SINCE TORQUE LIMIT HIT CAUSING A LOWER TEA TO BE REQ. THE
C    M1 CALCULATION MUST BE RE-CALCULATED
51  EN1 = -2.242254353 +1.2512986559*AMACH+.9621240231*AMACSQ
52  *+(-.3519585479E-07-.1539742133E-02*AMACH-.1308445977E-02*AMACSQ)*
53  * TEA +
    * (-.13116093310E-05+.6259888594E-06*AMACH+.6764941537E-06*AMACSQ)*
    * TEASO +
    * (-.1745905983E-09-.8357285710E-10*AMACH+.9302102725E-10*AMACSQ)*
    * TEACUB
C
54  IF(IN2IND.NE.1) GO TO 9000
C    THIS OPTION WILL BE LEFT BLANK UNTIL NEEDED
55  SHPDT= ENGSHP*SHPSTR*THCDEL
56  OMENG= EN1*SQTHTC * EN1STR*0.10471356
57  PCTORQ = 100. *THCDEL *ENGSHP /EN2STR
58  RETURN
59  END
60

```

Figure G.6. (Continued)

SUBROUTINE	ENGINE	TEA	SHOOT	ORNG	PCTORQ
1000	9	12	18*		
2000	19	21	28*		
3000	29*				
4000	31	35*			
5000	37	38*			
6000	41	44*			
7000	44	45*			
8000	42	47	55*		
9000	55				
AMACH	300	19	23	30	54
AMACSO	300	19	23	39	54
DEL	300				
EMAXN1	300	21	23	27	
EMAXN2	300				
ENXNDT	300	17	14		
ENG	2*				
ENGINE	1*				
ENGSHIP	47*	47	49=	56	58
ENGVAR	3*				
ENI	19=	21	27=	54=	57
ENIMX	200				
FNISTR	200	57			
ENITMX	200				
ENZ	32=	33			
EN2MX	200				
EN2DPT	33=	34			
FN2STD	300	33	45	54	
EQMX	200	45			
ESHP	39=	4*			
EWDDT	10=	12			
EWOTMX	200				
EWOTPP	200				
FLGS	4*				
FSWACH	300				
GRUTCH	400				
ICONGP	400				
IPHASE	400				
ISFACE	400				
ISLOW	400				
ISTA	400				
ISTB	400				
ITRIM	400				
IWARN1	400	SLG	11=	13=	22=
IWARN2	400	SLG			46=
IMREVT	400				48=
JTRIM	400				
KTRIM	400				
NCEF	400				
NPLDT	400				
NPLDT2	400				
NOIND	200	41			
NMOLD	200	37			
NTWST	400				

Figure G.6. (Continued)

SURF TUBE GEAR

I N D E X

```

30  HCPHIN= COS(PI*(YN*SIN(PI*(ZN+RAD(N)))+(COS(PI-1.1))
31  DNVCTP= 1./((COS(PI-1.1))
32  HTN= (H+HGTEN-HCPHIN)*DNVCTP
33  IF (HTN-1.0) GO TO 100
34  DX(N)= 0.
35  DY(N)= 0.
36  DZ(N)= 0.
37  DL(N)= 0.
38  DM(N)= 0.
39  DN(N)= 0.
40  GO TO 200
41  RATE OF STRUT DEFLECTION
42  HTDYN= HDOT+DNVCTP*OPRIME*HN-PPRIME*YN
43  C
44  C
45  C
46  C
47  C
48  C
49  C
50  C
51  C
52  C
53  C
54  C
55  C
56  C
57  C
58  C
59  C
60  C

```

VERTICAL FORCE

FGZ= SKST(N)*HTN +SDST(N)*HTDYN

LONGITUDINAL FORCE

FHN= (FRICTO+FRICT1*RG(N))*C57*SIGNU

SINCE FGZ IS ALWAYS NEGATIVE

IF U GT 0. FHN IS NEGATIVE

IF U LT 0. FHN IS POSITIVE

IF U EQ 0. FHN IS ZERO

SIDE FORCE

FSN= FRICTS*FGZ*SIGNV

SINCE FSN IS ALWAYS NEGATIVE

IF V GT 0. FSN IS NEGATIVE

IF V LT 0. FSN IS POSITIVE

IF V EQ 0. FSN IS ZERO

FORCE AND MOMENT CONTRIBUTION

DX(N)= FHN - FGZ * THE

DY(N)= FSN+FGZ*PHI

DZ(N)= FHN*THE-FSN*PHI+FGZ

DM(N)= -DZ(N)*YN+DX(N)*(ZN+RAD(N)+HTN)

DL(N)= DZ(N)*YN -DY(N)*(ZN+RAD(N)+HTN)

DN(N)= -DX(N)*YN +XN*DY(N)

N= N+1

IF (N-1.3) GO TO 50

DXLG= DX(1)+DX(2)+DX(3)

DYLG= DY(1)+DY(2)+DY(3)

DZLG= DZ(1)+DZ(2)+DZ(3)

DLG= DL(1)+DL(2)+DL(3)

DMG= DM(1)+DM(2)+DM(3)

DNLG= DN(1)+DN(2)+DN(3)

RETURN

END

Figure G.6. (Continued)

SYMBOL	REFERENCES	REFERENCES	REFERENCES
SC	74*	52	
75	12	13*	
1	31	51*	
11	12	15*	
12	12	17*	
12*	14	14	19*
13	19	20*	
14	19	22*	
15	19	24*	
15*	21	23	25*
20	4	51*	
ADC	20		
ADC3	200		
ALARE	500		
ALAREP	500		
ALFSD	500		
ALPHE	500		
AMARE	500		
AMAREP	500		
ANARE	500		
ANAREP	500		
AREAE	500		
BETESC	500		
BG	43		
BRKQUM	100		
BRK1	100		
BRK2	100		
BRK3	100		
CRCAR	500		
CDI	500		
CGTVP	4*		
CIF	500		
CMF	500		
CAF	500		
CNEPL	200		
CNEPD	200		
COSALF	500		
COSBTF	500		
COSPHI	500		
COSTHC	500		
CPL	200		
CPMPL	200		
CPMPR	200		
CPP	200		
CSFPL	200		
CSFPR	200		
CTLPRM	200		
CTPRM	200		
CVF	500		
CVMPL	200		
CVMPR	200		
DELSPL	200		
DELSPR	200		

Figure G.6. (Continued)

SUBROUTINE SEAP

I N D E X

SCDAC3	-	200			
SCDAC4	-	200			
SDT	-	701	42		
SDSTOM	-	300			
SDST1	-	300			
SDST2	-	300			
SDST3	-	300			
SDST4	-	300			
SDST5	-	300			
SDST6	-	300			
SDST7	-	300			
SDST8	-	300			
SDST9	-	300			
SDST10	-	300			
SDST11	-	300			
SDST12	-	300			
SDST13	-	300			
SDST14	-	300			
SDST15	-	300			
SDST16	-	300			
SDST17	-	300			
SDST18	-	300			
SDST19	-	300			
SDST20	-	300			
SDST21	-	300			
SDST22	-	300			
SDST23	-	300			
SDST24	-	300			
SDST25	-	300			
SDST26	-	300			
SDST27	-	300			
SDST28	-	300			
SDST29	-	300			
SDST30	-	300			
SDST31	-	300			
SDST32	-	300			
SDST33	-	300			
SDST34	-	300			
SDST35	-	300			
SDST36	-	300			
SDST37	-	300			
SDST38	-	300			
SDST39	-	300			
SDST40	-	300			
SDST41	-	300			
SDST42	-	300			
SDST43	-	300			
SDST44	-	300			
SDST45	-	300			
SDST46	-	300			
SDST47	-	300			
SDST48	-	300			
SDST49	-	300			
SDST50	-	300			
SDST51	-	300			
SDST52	-	300			
SDST53	-	300			
SDST54	-	300			
SDST55	-	300			
SDST56	-	300			
SDST57	-	300			
SDST58	-	300			
SDST59	-	300			
SDST60	-	300			
SDST61	-	300			
SDST62	-	300			
SDST63	-	300			
SDST64	-	300			
SDST65	-	300			
SDST66	-	300			
SDST67	-	300			
SDST68	-	300			
SDST69	-	300			
SDST70	-	300			
SDST71	-	300			
SDST72	-	300			
SDST73	-	300			
SDST74	-	300			
SDST75	-	300			
SDST76	-	300			
SDST77	-	300			
SDST78	-	300			
SDST79	-	300			
SDST80	-	300			
SDST81	-	300			
SDST82	-	300			
SDST83	-	300			
SDST84	-	300			
SDST85	-	300			
SDST86	-	300			
SDST87	-	300			
SDST88	-	300			
SDST89	-	300			
SDST90	-	300			
SDST91	-	300			
SDST92	-	300			
SDST93	-	300			
SDST94	-	300			
SDST95	-	300			
SDST96	-	300			
SDST97	-	300			
SDST98	-	300			
SDST99	-	300			
SDST100	-	300			

Figure G.6. (Continued)

I N D E X		S U B R O U T I N E G E A R				PAGE 120
ZN	-	28=	29	30	40	
----- ROUTINES IN WHICH THE SYMBOL IS USED ----- SYMPT - -----						

Figure G.6. (Continued)

***** SUPER INDEX *****

T	A	D	F	X
ASS	-			RTSLOW
ACDW	-			CLCOCM
ACDW1	-			CLCOCM
ACDW1C	-			CLCOCM
ACDW11	-			CLCOCM
ACDW12	-			CLCOCM
ACDW13	-			CLCOCM
ACDW14	-			CLCOCM
ACDW15	-			CLCOCM
ACDW16	-			CLCOCM
ACDW17	-			CLCOCM
ACDW18	-			CLCOCM
ACDW19	-			CLCOCM
ACDW2	-			CLCOCM
ACDW2C	-			CLCOCM
ACDW21	-			CLCOCM
ACDW22	-			CLCOCM
ACDW23	-			CLCOCM
ACDW24	-			CLCOCM
ACDW3	-			CLCOCM
ACDW4	-			CLCOCM
ACDW5	-			CLCOCM
ACDW6	-			CLCOCM
ACDW7	-			CLCOCM
ACDW8	-			CLCOCM
ACDW9	-			CLCOCM
ADC	-			RTFAST
ADCFLT	-			RTFAST
AGDVAT	-			RTSLOW
AGDVAT	-			RTSLOW
ATCL	-			RTFAST
ATCLP	-			RTFAST
ATCLPS	-			RTFAST
ATCLP	-			RTFAST
ATC2	-			RTFAST
ATCPN	-			RTFAST
ATCPGS	-			RTFAST
ATCPPP	-			RTFAST
ATLSP	-			RTFAST
ATNOTL	-			RTFAST
ATNOTR	-			RTFAST
AINHT	-			RTFAST
AINL	-			RTFAST
AINR	-			RTFAST
AINW	-			RTFAST
ATRIIP	-			RTFAST
AKY	-			RTSLOW
ALARP	-			RTFAST
ALARP	-			RTFAST
ALARHT	-			RTFAST
ALARNC	-			RTFAST
ALAFNL	-			RTFAST
ALARNP	-			RTFAST
ALARPC	-			RTFAST

RTSLOW
RTSLOW
RTSLOW
RTSLOW

RTSLOW

Figure G.6. (Continued)

***** SUPER INDEX *****

I N D E X		
ALART	-	RTFAST
ALARVB	-	RTFAST
ALARVT	-	RTFAST
ALARWG	-	RTFAST
ALBRK1	-	CLCDDC4
ALBRK2	-	CLCDDC4
ALDEG	-	CLCDDC4
ALDUM	-	CLCDDC4
ALFGLS	-	RTFAST
ALFREF	-	RTFAST
ALFTAB	-	RTFAST
ALHTE	-	RTFAST
ALHTM	-	RTFAST
ALHTP	-	RTFAST
ALHTPR	-	RTFAST
ALLRH	-	RTFAST
ALLVPP	-	RTFAST
ALNCRK	-	RTSLOW
ALNLA	-	CLCDDC4
ALNLP	-	CLCDDC4
ALPHA	-	CLCDDC4
ALPHF	-	RTFAST
ALPHFP	-	RTSLOW
ALPHHT	-	PTFAST
ALPHEN	-	RTSLOW
ALPHLP	-	RTFAST
ALPHLM	-	RTFAST
ALPHRN	-	RTSLOW
ALPHRP	-	RTFAST
ALPHRW	-	RTFAST
ALPHVT	-	RTFAST
ALRGLW	-	RTFAST
ALRGRW	-	RTFAST
ALRRH	-	RTFAST
ALRHPF	-	RTFAST
ALYTE	-	RTFAST
ALVTM	-	RTFAST
ALVTP	-	RTFAST
ALVTPP	-	RTFAST
ALWSSD	-	RTFAST
AMACH	-	ENGINE
AMACLP	-	RTFAST
AMACRP	-	RTFAST
AMACSC	-	ENGINE
AMACTL	-	RTFAST
AMACTR	-	RTFAST
AMAEPO	-	RTFAST
AMARF	-	RTFAST
AMAREP	-	RTFAST
AMARHT	-	RTFAST
AMARLW	-	RTFAST
AMARNC	-	RTFAST
AMARNL	-	RTFAST
AMARNP	-	RTFAST
AMARRG	-	RTFAST
		RTSLOW
		RTSLOW
		RTSLOW
		RTSLOW
		RTSLOW

Figure G.6. (Continued)

***** SUPER INDEX *****

I N D E X	
RG	GEAP
RIGGLS	RTFAST
BICL	RTFAST
BICLDP	RTFAST
BICLPP	RTFAST
BICR	RTFAST
BICRDP	RTFAST
BICRPR	RTFAST
BICK	RTSLOW
BKALPR	RTFAST
BKARPP	RTFAST
BKDI1	RTSLOW
BKDZT	RTSLOW
BKD3T	RTSLOW
BKEY	RTSLOW
BKR1T	RTSLOW
BKR2T	RTSLOW
BKR3T	RTSLOW
BK44T	RTSLOW
BK99	RTSLOW
BLS	RTFAST
BMEH	RTSLOW
BMOVTL	RTFAST
BMOVTR	RTFAST
BRK1	GEAR
BT1	RTSLOW
BT2	RTSLOW
BT3	RTSLOW
CALINT	RTFAST
CALLN	RTSLOW
CALLW	RTFAST
CALRN	RTSLOW
CALRW	RTFAST
CAVINW	RTSLOW
CAVZET	RTSLOW
CBCHF	RTSLOW
CBETLN	RTFAST
CBETLN	RTFAST
CBETRN	RTFAST
CBETRW	RTFAST
CBETSC	RTFAST
CD	CLCOC4
CDCN1L	RTFAST
CDCNTR	RTFAST
CDDOH	RTFAST
CDF	RTSLOW
CDFASP	CLCOC4
CDHT	RTFAST
CDHTST	RTFAST
CDLN	RTSLOW
CDLWAD	RTFAST
CDLWPR	RTFAST
CDLWSS	RTFAST
CDM	CLCOC4
CDOF	RTSLOW

Figure G.6. (Continued)

***** SUPER INDEX *****

T N D F X	-	RTFAST	
CDHNT	-	RTSLOW	
CDOLN	-	RTSLOW	
CDQHP	-	RTSLOW	
CDMLC	-	RTSLOW	
CDORN	-	RTFAST	
CDQVT	-	CLDCM	
CDP	-	CLDCM	
CDPLUS	-	RTSLOW	
CDRN	-	RTFAST	
CDRWAO	-	RTFAST	
CDRMPR	-	RTFAST	
CDRWSS	-	RTFAST	
CDSLW	-	RTFAST	
CDSRW	-	RTFAST	
CDVT	-	RTFAST	
CDVTST	-	RTFAST	
CDWGOR	-	CLDCM	
CDI	-	CLDCM	
CEPLN	-	RTFAST	
CEPRW	-	RTFAST	
CGGTVR	-	GEAR	
CHORD	-	RTFAST	
CILAM	-	RTFAST	
CILAMF	-	RTFAST	
CL	-	CLDCM	
CLALDG	-	CLDCM	
CLALHT	-	RTFAST	
CLALPH	-	CLDCM	
CLAT	-	RTFAST	
CLAVE	-	RTFAST	
CLDCM	-	RTFAST	
CLDEL	-	CLDCM	
CLDUP	-	RTFAST	
CLF	-	RTSLOW	
CLF1	-	RTSLOW	
CLF2	-	CLDCM	
CLHT	-	RTFAST	
CLHTST	-	RTFAST	
CLIGE	-	CLDCM	
CLILW	-	RTSLOW	
CLIRW	-	RTSLOW	
CLLN	-	RTSLOW	
CLLWAO	-	RTFAST	
CLLWPP	-	RTFAST	
CLLWSS	-	RTFAST	
CLMAX	-	CLDCM	
CLMLP	-	CLDCM	
CLOAL	-	CLDCM	
CLP	-	CLDCM	
CLPMX	-	CLDCM	
CLRN	-	RTSLOW	
CLRWAO	-	RTFAST	
CLRWPR	-	RTFAST	
CLRWSS	-	RTFAST	
CLSLW	-	RTFAST	

Figure G.6. (Continued)

***** SUPER INDEX *****

I N D E X		
CLSP	-	CLCOCM
CLSRW	-	RTFAST
CLSW	-	RTFAST
CLTCOR	-	RTFAST
CLWOPR	-	CLCOCM
CLZ	-	AILSP
CLZERO	-	RTFAST
CL1	-	CLCOCM
CM	-	CLCOCM
CMCNLT	-	RTFAST
CMCNTR	-	RTFAST
CMF	-	RTSLOW
CMFASP	-	CLCOCM
CMNLN	-	RTSLOW
CMNLWAD	-	RTFAST
CMNLWSS	-	RTFAST
CMOF	-	RTSLOW
CMON	-	RTSLOW
CMOW	-	RTFAST
CMF	-	CLCOCM
CMRN	-	RTSLOW
CMRWAD	-	RTFAST
CMRWSS	-	RTFAST
CMSLW	-	RTFAST
CMSRW	-	RTFAST
CMF	-	RTSLOW
CMFAIL	-	RTFAST
CMFAIR	-	RTFAST
CMFBI	-	RTFAST
CMFBIR	-	RTFAST
CMFL	-	RTFAST
CMFPL	-	RTFAST
CMFPR	-	RTFAST
CMFR	-	RTFAST
CMNLN	-	RTSLOW
CMOF	-	RTSLOW
CMOLN	-	RTSLOW
CMORN	-	RTSLOW
CMRN	-	RTSLOW
CMNW	-	RTFAST
COEF1	-	RTSLOW
COEF1C	-	RTFAST
COEF11	-	RTFAST
COEF12	-	RTFAST
COEF13	-	RTFAST
COEF16	-	RTFAST
COEF17	-	RTSLOW
COEF18	-	RTFAST
COEF19	-	RTFAST
COEF2	-	RTFAST
COEF20	-	RTFAST
COEF21	-	RTFAST
COEF22	-	RTFAST
COEF23	-	RTFAST
COEF24	-	RTFAST

Figure G.6. (Continued)

***** SUPER INDEX *****

I N D E X	
COEF25	- RTSLOW
COEF26	- RTSLOW
COEF27	- RTSLOW
COEF28	- RTSLOW
COEF29	- RTSLOW
COEF3	- RTSLOW
COEF30	- RTSLOW
COEF31	- RTEAST
COEF32	- RTEAST
COEF33	- RTEAST
COEF34	- RTEAST
COEF35	- RTSLOW
COEF4	- RTEAST
COEF5	- RTSLOW
COEF6	- RTSLOW
COEF7	- RTSLOW
COEF8	- RTSLOW
COEF9	- RTEAST
CONS1	- CLCDCM
CONS10	- CLCDCM
CONS11	- CLCDCM
CONS12	- CLCDCM
CONS13	- CLCDCM
CONS14	- CLCDCM
CONS15	- CLCDCM
CONS16	- CLCDCM
CONS17	- CLCDCM
CONS18	- CLCDCM
CONS19	- CLCDCM
CONS2	- CLCDCM
CONS20	- CLCDCM
CONS21	- CLCDCM
CONS22	- CLCDCM
CONS23	- CLCDCM
CONS24	- CLCDCM
CONS25	- CLCDCM
CONS26	- CLCDCM
CONS27	- AILSP
CONS28	- AILSP
CONS29	- AILSP
CONS3	- CLCDCM
CONS30	- AILSP
CONS31	- AILSP
CONS32	- AILSP
CONS33	- AILSP
CONS34	- AILSP
CONS35	- AILSP
CONS36	- AILSP
CONS37	- AILSP
CONS38	- AILSP
CONS39	- AILSP
CONS4	- CLCDCM
CONS40	- AILSP
CONS41	- RTEAST
CONS42	- RTEAST

RTSLOW

Figure G.6. (Continued)

***** SUPER INDEX *****

I	N	D	E	X	
CONS43	-	RTFAST			
CONS44	-	RTSLOW			
CONS45	-	RTSLOW			
CONS46	-	RTSLOW			
CONS47	-	RTSLOW			
CONS48	-	RTSLOW			
CONS49	-	RTSLOW			
CONS50	-	CLCDCM			
CONS51	-	RTSLOW			
CONS52	-	RTSLOW			
CONS53	-	RTSLOW			
CONS54	-	RTSLOW			
CONS55	-	RTSLOW			
CONS56	-	RTSLOW			
CONS57	-	RTSLOW			
CONS58	-	RTSLOW			
CONS59	-	RTSLOW			
CONS60	-	CLCDCM			
CONS61	-	RTSLOW			
CONS62	-	RTSLOW			
CONS63	-	RTSLOW			
CONS64	-	RTSLOW			
CONS65	-	RTFAST			
CONS66	-	RTFAST			
CONS67	-	RTFAST			
CONS68	-	RTFAST			
CONS69	-	RTFAST			
CONS70	-	RTFAST			
CONS71	-	RTFAST			
CONS72	-	RTFAST			
CONS73	-	RTFAST			
CONS74	-	RTFAST			
CONS75	-	RTFAST			
CONS76	-	RTFAST			
CONS77	-	RTFAST			
CONS78	-	RTFAST			
CONS79	-	RTFAST			
CONS80	-	RTFAST			
CONS81	-	RTFAST			
CONS82	-	RTFAST			
CONS83	-	RTFAST			
CONS84	-	RTFAST			
CONS85	-	RTFAST			
CONS86	-	RTFAST			
CONS87	-	RTFAST			
CONS88	-	RTFAST			
CONS89	-	RTFAST			
CONS90	-	RTFAST			
CONS91	-	RTFAST			
CONS92	-	RTFAST			
CONS93	-	RTFAST			
CONS94	-	RTFAST			
CONS95	-	RTFAST			
CONS96	-	RTFAST			
CONS97	-	RTFAST			
CONS98	-	RTFAST			
CONS99	-	RTFAST			
CONS100	-	RTFAST			

Figure G.6. (Continued)

***** SUPER INDEX *****

T	N	D	F	X
COSZHR	-			RTFAST
CPHIP	-			RTFAST
CPL	-			RTFAST
CPMAIL	-			RTFAST
CPMAIP	-			RTFAST
CPMAIL	-			RTFAST
CPMAIL	-			RTFAST
CPML	-			RTFAST
CPMPL	-			RTFAST
CPMPR	-			RTFAST
CPMR	-			RTFAST
CPR	-			RTFAST
CSPAIL	-			RTFAST
CSEAIR	-			RTFAST
CSEBIL	-			RTFAST
CSEBIR	-			RTFAST
CSEL	-			RTFAST
CSEPL	-			RTFAST
CSEPR	-			RTFAST
CSEPR	-			RTFAST
CSEPR	-			RTFAST
CTAULF	-			RTSLOW
CTAURR	-			RTSLOW
CTL	-			RTFAST
CTLPPM	-			RTFAST
CTR	-			RTFAST
CTRPPM	-			RTFAST
CTSLP	-			RTFAST
CTSRP	-			RTFAST
CYALVT	-			RTFAST
CYAT	-			RTFAST
CYF	-			RTSLOW
CYLY	-			RTSLOW
CYMAIL	-			RTFAST
CYMAIP	-			RTFAST
CYMBIL	-			RTFAST
CYMBIR	-			RTFAST
CYML	-			RTFAST
CYML	-			RTFAST
CYMP	-			RTFAST
CYMPR	-			RTFAST
CYMR	-			RTFAST
CYRN	-			RTSLOW
CYVT	-			RTFAST
CYVTST	-			RTFAST
C2INL	-			RTSLOW
C2INP	-			RTSLOW
CACFLT	-			RTFAST
CACFLT	-			RTFAST
CACIO	-			RTFAST
CAC1	-			RTFAST
CAC2	-			RTFAST
DBRK1	-			RTFAST
DBRK1C	-			RTSLOW
DBRK11	-			RTSLOW
DBRK12	-			RTSLOW
DBRK13	-			RTSLOW
DBRK14	-			RTSLOW

Figure G.6. (Continued)

***** SUPER INDEX *****

I N D E X

DBRK 15	-	RTSLOW
DBRK 16	-	RTSLOW
DBRK 17	-	RTFAST
DBRK 18	-	RTFAST
DBRK 19	-	RTFAST
DBRK 2	-	CLCOCM
DBRK 20	-	AIL SP
DBRK 21	-	AIL SP
DBRK 22	-	CLCOCM
DBRK 23	-	CLCOCM
DBRK 3	-	CLCOCM
DBRK 4	-	CLCOCM
DBRK 5	-	CLCOCM
DBRK 6	-	CLCOCM
DBRK 7	-	AIL SP
DBRK 8	-	AIL SP
DBRK 9	-	RTFAST
DBRK 9	-	AIL SP
DCCA	-	AIL SP
DCDI GE	-	CLCOCM
DCDL DA	-	RTFAST
DCDL 6	-	RTSLOW
DCDL SP	-	RTFAST
DCDR DA	-	RTFAST
DCDR SP	-	RTFAST
DCDS	-	AIL SP
DCLA	-	AIL SP
DCLL CA	-	RTFAST
DCLL SP	-	RTFAST
DCLM	-	CLCOCM
DCLR DA	-	RTFAST
DCLR SP	-	RTFAST
DCLS	-	AIL SP
DCLSPH	-	RTFAST
DCHA	-	AIL SP
DCML DA	-	RTFAST
DCML G	-	RTSLOW
DCML SP	-	RTFAST
DCMR DA	-	RTFAST
DCMR SP	-	RTFAST
DCMS	-	AIL SP
DCNSPM	-	RTFAST
DEGZO	-	RTFAST
DEL	-	AIL SP
DELEV	-	RTFAST
DELEPZ	-	RTFAST
DELEPZ	-	RTFAST
DELFLP	-	RTFAST
DELKUN	-	RTFAST
DELSPL	-	RTFAST
DELSPR	-	RTFAST
DEPCAL	-	RTFAST
DEPLAL	-	RTFAST
DELATR	-	RTFAST
DGTORD	-	CLCOCM
DIGAN	-	RTFAST
DISAB	-	RTFAST
DL	-	RTSLOW
DL FPSQ	-	GEAR
	-	RTFAST

CLCOCM RTFAST RTSLOW

RTFAST

RTSLOW

***** SUPER INDEX *****

I N P X	-	RTFAST		
ENF2	-	RTFAST		
ENF3	-	RTFAST		
ENF4	-	RTFAST		
ENG	-	ENGINE	RTSLOW	
ENGINE	-	RTSLOW		
ENGSH	-	ENGINE		
ENGVAR	-	ENGINE		
EN1	-	ENGINE	RTFAST	RTSLOW
EN1X	-	ENGINE		
EN1STR	-	RTSLOW		
EN2	-	ENGINE		
EN2X	-	ENGINE		
EN2DPT	-	ENGINE		
EN2REF	-	RTSLOW		
EN2STR	-	ENGINE		
EN2VAR	-	RTFAST	RTSLOW	
EP1LR	-	RTFAST	RTSLOW	
EP1RL	-	RTFAST	RTSLOW	
EP1	-	RTFAST		
EP2	-	RTFAST		
EP3	-	RTFAST		
EP4	-	RTFAST		
EP5	-	RTFAST		
EP6	-	RTFAST		
EP7	-	RTFAST		
EPPLR	-	RTFAST	RTSLOW	
EPPLM	-	RTSLOW		
EPPLR	-	RTFAST		
EPTAIL	-	RTFAST		
EPTL1	-	RTFAST		
EPURL	-	RTFAST		
EPURL	-	RTFAST		
EPURL	-	RTFAST		
EP7ER	-	RTFAST		
EQM	-	ENGINE		
ESF1	-	RTFAST		
ESF2	-	RTFAST		
ESF3	-	RTFAST		
ESF4	-	RTFAST		
ESMP	-	ENGINE		
ENDOT	-	ENGINE		
ENDT4X	-	RTSLOW		
ENDT4R	-	RTSLOW		
EYN1	-	RTFAST		
EYN2	-	RTFAST		
EYN3	-	RTFAST		
EYN4	-	RTFAST		
EYN5	-	RTFAST		
EYN6	-	RTFAST		
EYN7	-	RTFAST		
F	-	CLCOC		
FEU	-	RTFAST		
FGZN	-	GEAR		
FIE	-	RTFAST		
FINDEF	-	RTFAST		
FINPR	-	RTFAST		

Figure G.6. (Continued)

***** SUPER INDEX *****

INDEX		
CMOTR	-	RTFAST
OMEGA	-	RTFAST
OMEGAL	-	RTFAST
OMEGAR	-	RTFAST
OMEGEL	-	RTFAST
OMEGEP	-	RTFAST
CMENG	-	ENGINE
OMREF	-	RTSLOW
OMSQL	-	RTFAST
OMSOR	-	RTFAST
OMOVTC	-	RTSLOW
OMOVCTP	-	GEAR
OMVDSK	-	RTFAST
OMVFSM	-	RTSLOW
OMVIXX	-	RTFAST
OMVIVY	-	RTFAST
OMVIZZ	-	RTFAST
OMVDTIM	-	RTFAST
OMVSOIH	-	ENGINE
OMVTHDL	-	ENGINE
PC	-	RTSLOW
PCTORO	-	ENGINE
PCVQR	-	RTFAST
PGUST	-	RTFAST
PHI	-	GEAR
PI	-	RTFAST
PIOV2	-	RTFAST
PNLN	-	RTFAST
PNLR	-	RTFAST
PNRN	-	RTFAST
PNRR	-	RTFAST
PP	-	RTFAST
PPRIME	-	GEAR
PQ	-	RTFAST
PR	-	RTFAST
PSI	-	RTSLOW
O	-	RTFAST
QFSW	-	RTSLOW
QGUST	-	RTFAST
QNLN	-	RTFAST
QNL	-	RTFAST
QNRN	-	RTFAST
QNR	-	RTFAST
QPRIME	-	GEAR
R	-	RTFAST
RAD	-	GEAR
RAOI	-	GEAR
RCBI	-	RTSLOW
RODODG	-	CLDCDM
RESLR	-	RTSLOW
RESRR	-	RTSLOW
RETURN	-	RTSLOW
REVTN	-	RTSLOW
RGUST	-	RTFAST

Figure G.6. (Continued)

***** SUPER INDEX *****

SILAMP	-	RFEAST	RTSLOW
SILW	-	RFEAST	RTSLOW
SINALF	-	RTSLOW	
SINATF	-	RTSLOW	
SINCOS	-	RFEAST	RTSLOW
SININL	-	RFEAST	RTSLOW
SININP	-	RFEAST	RTSLOW
SINIW	-	RFEAST	
SINLAM	-	RFEAST	
SINPHI	-	GEAR	RTSLOW
SINPSI	-	RTSLOW	
SINTHE	-	GEAR	RTSLOW
SINZHL	-	RFEAST	
SINZHP	-	RFEAST	
SIR	-	RTSLOW	
SIRW	-	RFEAST	
SIT	-	RTSLOW	
SKPN	-	ENGINE	
SKPR	-	ENGINE	
SKST	-	GEAR	
SKST1	-	GEAR	
SKW1	-	RFEAST	
SKW1C	-	RFEAST	
SKW2	-	RFEAST	
SKW3	-	RFEAST	
SKW4	-	RFEAST	
SKW5	-	RFEAST	
SKW6	-	RFEAST	
SKW7	-	RFEAST	
SKW8	-	RFEAST	
SKW9	-	RFEAST	
SKO	-	RTSLOW	
SK1	-	RTSLOW	
SK10	-	RTSLOW	
SK2	-	RTSLOW	
SK2C	-	RFEAST	
SK21	-	RFEAST	
SK22	-	RFEAST	
SK3	-	RTSLOW	
SK3CH1	-	RTSLOW	
SK3CL	-	RTSLOW	
SK3OLD	-	RTSLOW	
SK3CP	-	RTSLOW	
SK31H1	-	RTSLOW	
SK31L	-	RTSLOW	
SK31N	-	RTSLOW	
SK31R	-	RTSLOW	
SK32	-	RTSLOW	
SK34	-	RTSLOW	
SK35	-	RTSLOW	
SK36	-	RTSLOW	
SK37	-	RTSLOW	
SK3R	-	RTSLOW	
SK39	-	RTSLOW	
SK4	-	RTSLOW	

Figure G.6. (Continued)

***** SUPER INDEX *****

I N D E X		
TEASQ	-	ENGINE
TEATH	-	ENGINE
TERMP1	-	PTFAST
TERMQ1	-	PTFAST
TERMP1	-	PTFAST
TERM1	-	RTSLOW
TERM1L	-	RTFAST
TERM1R	-	PTFAST
TERM2	-	RTSLOW
TERM2L	-	RTFAST
TERM2R	-	RTFAST
TERM3	-	RTSLOW
TERM3L	-	RTFAST
TERM3R	-	RTFAST
TERM4	-	RTSLOW
TERM5	-	RTSLOW
TERM6	-	RTSLOW
THCODEL	-	ENGINE
THE	-	GEAR
THETC	-	RTSLOW
THTLAC	-	RTFAST
THTRAC	-	RTFAST
THTRIP	-	RTFAST
TIGEL	-	RTFAST
TIGER	-	RTFAST
TL	-	RTFAST
TMHRIC	-	RTFAST
TMHR11	-	RTFAST
TMHR12	-	RTFAST
TMHGIC	-	RTSLOW
TMHG11	-	RTSLOW
TNAC1	-	RTSLOW
TNAC2	-	RTSLOW
TOROL	-	RTFAST
TOROP	-	RTFAST
TPSR	-	RTSLOW
TP	-	RTFAST
TRACK	-	RTFAST
TRMAR1	-	RTFAST
TRMAR2	-	PTFAST
TRMAR3	-	PTFAST
TRMAP4	-	PTFAST
TPMCKN	-	RTFAST
TPMHB1	-	RTFAST
TPMHR2	-	RTFAST
TPMHR3	-	RTFAST
TPMHR4	-	RTFAST
TPMHPK	-	PTFAST
TPMHR6	-	RTFAST
TPMHR7	-	RTFAST
TPMHR8	-	RTFAST
TPMHR9	-	RTFAST
TPMHT	-	RTFAST
TPMHT2	-	RTFAST
TPMHT3	-	PTFAST

RTSLOW
RTSLOW

RTSLOW
RTSLOW
RTSLOW

RTSLOW
RTSLOW

Figure G.6. (Continued)

***** SUPER INDEX *****

WVT	-	RFAST		
XACDEF	-	CLCDM		
XABF	-	RFAST		
XABRLW	-	RFAST		
XABRNC	-	RFAST		
XABRNL	-	RFAST		
XABNR	-	RFAST		
XABRD	-	RFAST		
XABRDJ	-	RFAST		
XABRT	-	RFAST		
XABRG	-	RFAST		
XATO	-	GEAR	RTSLOW	
XARFP	-	RFAST	RTSLOW	
XARHT	-	RFAST		
XARVT	-	RFAST		
XCG	-	GEAR	RTFAST	RTSLOW
XCNRL	-	RFAST		
XDTG	-	RFAST		
XF	-	RTSLOW		
XFAC	-	RTSLOW		
XFHFLF	-	RTSLOW		
XFUMC	-	RFAST		
XG	-	GEAR	RTSLOW	
XGEAR	-	GEAR		
XG1	-	GEAR		
XHT	-	RFAST	RTSLOW	
XL	-	RTSLOW		
XLCD	-	RFAST	RTSLOW	
XLINTP	-	RFAST	RTSLOW	
XLSTN	-	RTSLOW		
XMAP	-	RFAST		
XN	-	GEAR		
XPAR1	-	AILSP	RTFAST	RTSLOW
XPAR3	-	AILSP	RTFAST	RTSLOW
XR	-	RTSLOW		
XCDS	-	RFAST		
XRLCON	-	RTSLOW		
XRSIN	-	RTSLOW		
XVT	-	RFAST		
XW	-	RTSLOW		
XWAC	-	RFAST		
XWC2	-	RFAST		
XWNLW	-	RTSLOW		
XXICOM	-	RTSLOW		
XZICOM	-	RTSLOW		
YAEF	-	RFAST		
YAEFLW	-	RFAST		
YABRNC	-	RFAST		
YABRNL	-	RFAST		
YABNR	-	RFAST		
YABRO	-	RFAST		
YABRW	-	RFAST		
YABT	-	RFAST		
YABRG	-	RFAST		
YARFP	-	RTSLOW		

Figure G.6. (Continued)

***** SUPER INDEX *****

I N D E X

YARHT	-	RTFAST	
YARVT	-	RTFAST	
YG	-	GEAR	
YG1	-	GEAR	
YN	-	GEAR	RTSLOW
YNAC	-	RTFAST	
YVICON	-	RTSLOW	
ZAERF	-	RTFAST	
ZARLW	-	RTFAST	
ZARNC	-	RTFAST	
ZARNL	-	RTFAST	
ZARNR	-	RTFAST	
ZARRO	-	RTFAST	
ZARRW	-	RTFAST	
ZART	-	RTFAST	
ZARWG	-	RTFAST	
ZARFP	-	RTFAST	RTSLOW
ZARHT	-	RTFAST	
ZARRG	-	RTFAST	
ZARVB	-	RTFAST	
ZARVT	-	RTFAST	
ZCG	-	GEAR	RTSLOW
ZDTGG	-	RTFAST	
ZFTHL	-	RTFAST	RTSLOW
ZETHR	-	RTFAST	RTSLOW
ZETR1	-	RTSLOW	
ZETR2	-	RTSLOW	
ZETR3	-	RTSLOW	
ZETR4	-	RTSLOW	
ZF	-	RTSLOW	
ZFAC	-	RTSLOW	
ZFMFH	-	RTSLOW	
ZG	-	GEAR	
ZG1	-	GEAR	
ZHT	-	RTFAST	RTSLOW
ZL	-	RTSLOW	
ZLCOS	-	RTSLOW	
ZLSIN	-	RTFAST	RTSLOW
ZN	-	GEAR	
ZR	-	RTSLOW	
ZRCOS	-	RTSLOW	
ZPLCON	-	RTSLOW	
ZRSIN	-	RTFAST	RTSLOW
ZVT	-	RTFAST	
ZW	-	RTSLOW	
ZWAC	-	RTFAST	RTSLOW
ZMMHM	-	RTSLOW	
ZZTCN	-	RTSLOW	

Figure G.6. (Continued)

***** TABLE OF CONTENTS *****

I N D E X

ATLSP	94
CLCDCM	99
CLF1	-94
CLF2	-99
ENGINE	110
GEAR	115
RTFAST	1
RTSLOW	55
TSTRF	-1
TSTRS	-55
SUPER INDEX	120

Figure G.6. (Continued)

time tasks (RTFAST and RTSLOW), the aileron-spoiler subroutine (AILSP), the total lift, drag and moment subroutine (CLCDCM), the engine power subroutine (ENGINE), and the landing gear subroutine (GEAR) . The aileron spoiler subroutine calculates the lift, drag and pitching moment increments. The total wing lift, drag, and moment characteristics are computed in subroutine CLCDCM. Engine performance is computed in the engine subroutine and landing gear forces and moments in the gear subroutine. This listing contains an index of all the variables immediately following each subroutine. The index specifies by location number where the particular variable is defined and used in the subroutine. A master index is provided at the end which specifies the subroutine in which a particular variable is located.

In programming the analog portion of the simulation, size also was of prime concern, where in this case size implies an equipment limitation. From the beginning, equipment was allocated with maximum efficiency, but due to the complexity of the engine/governor, the phasing of the controls, the number of second order representations of actuators, and the number of functions needed to program these sections, the result was 1) three analogs used with a minimum of spare equipment and 2) 31 out of 32 BCA channels needed to program functions (includes

rotor). When the capability of using the nudge-base simulator is added, the simulation uses every piece of hardware available in the hybrid laboratory. Figure G.7 shows the definition of the symbols used on the analog diagrams for the Model 222 simulation presented in Figure G.8.

The scale factors for any of the elements shown in the analog diagrams may be determined by referring to Figure G.9, which is the subroutine used to static check the analog boards. The subroutine shows all the equations on the analogs and all of the scale factors. This program is used for static check only, in the operate mode the real time task continuously updates the analog. As an example, if the scale factor (and value) for potentiometer 240, which is used in the pitch equation of motion on board 1E console 1 is required the following steps are taken. Refer to the potentiometer calculation section of Figure G.9. This lies between statement numbers 0416 and 0518. Look up the definition of pot 240 [P1(240)]. This appears in statement number 0444 and is $P1(240) = P1C/PMX$. P1C is contained in common |X1C|, statement number 0008 and PMX is contained in common |XMAX|, statement number 0013. Substituting numerical values and dividing would yield the scale factor for pot 240.

G.2 TRIM LOOPS

The Model 222 trim loops are on the analog. The aircraft accelerations are used in feedback loops to drive the aircraft into

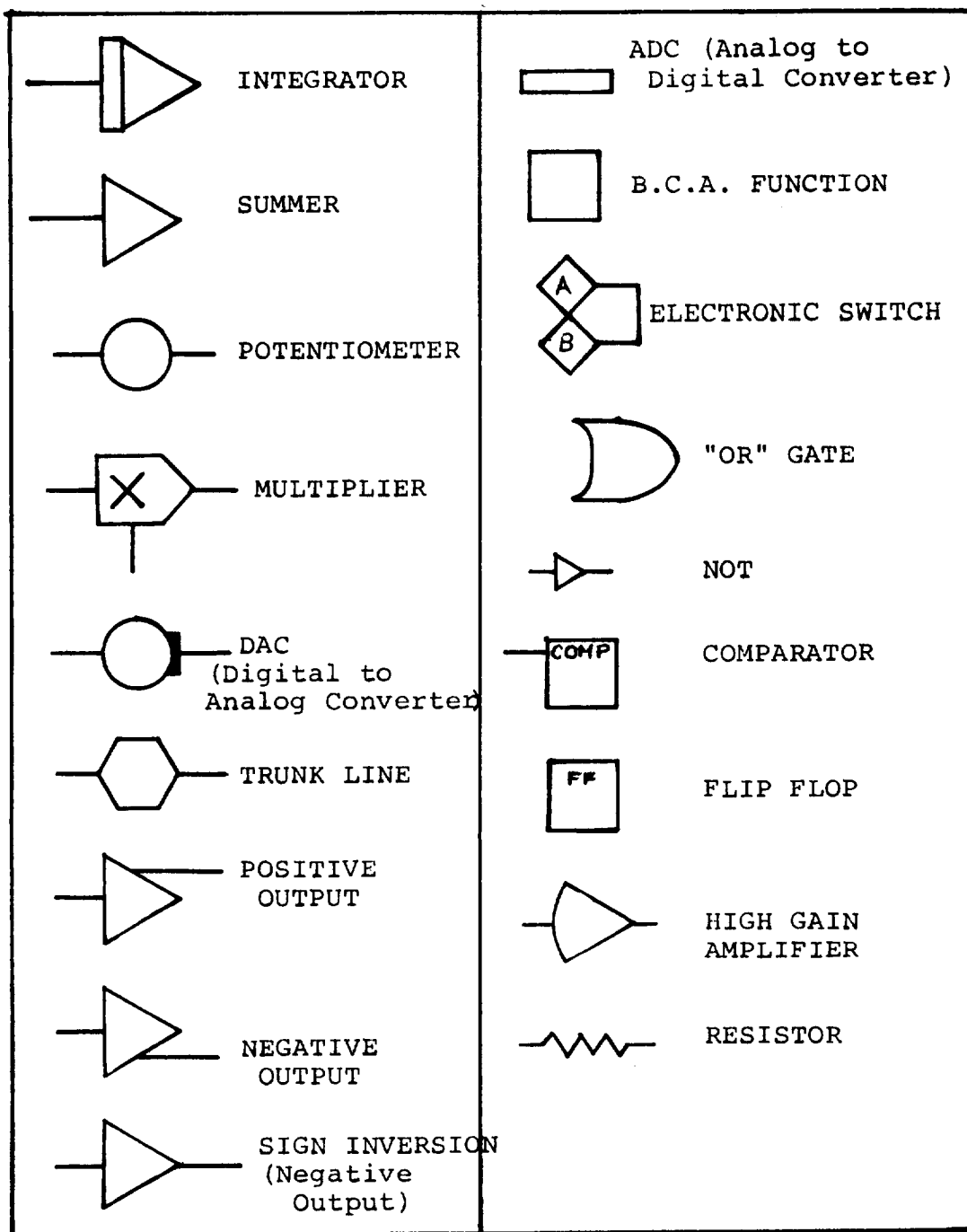


Figure G.7. Analog Symbols

TRIM LOOPS

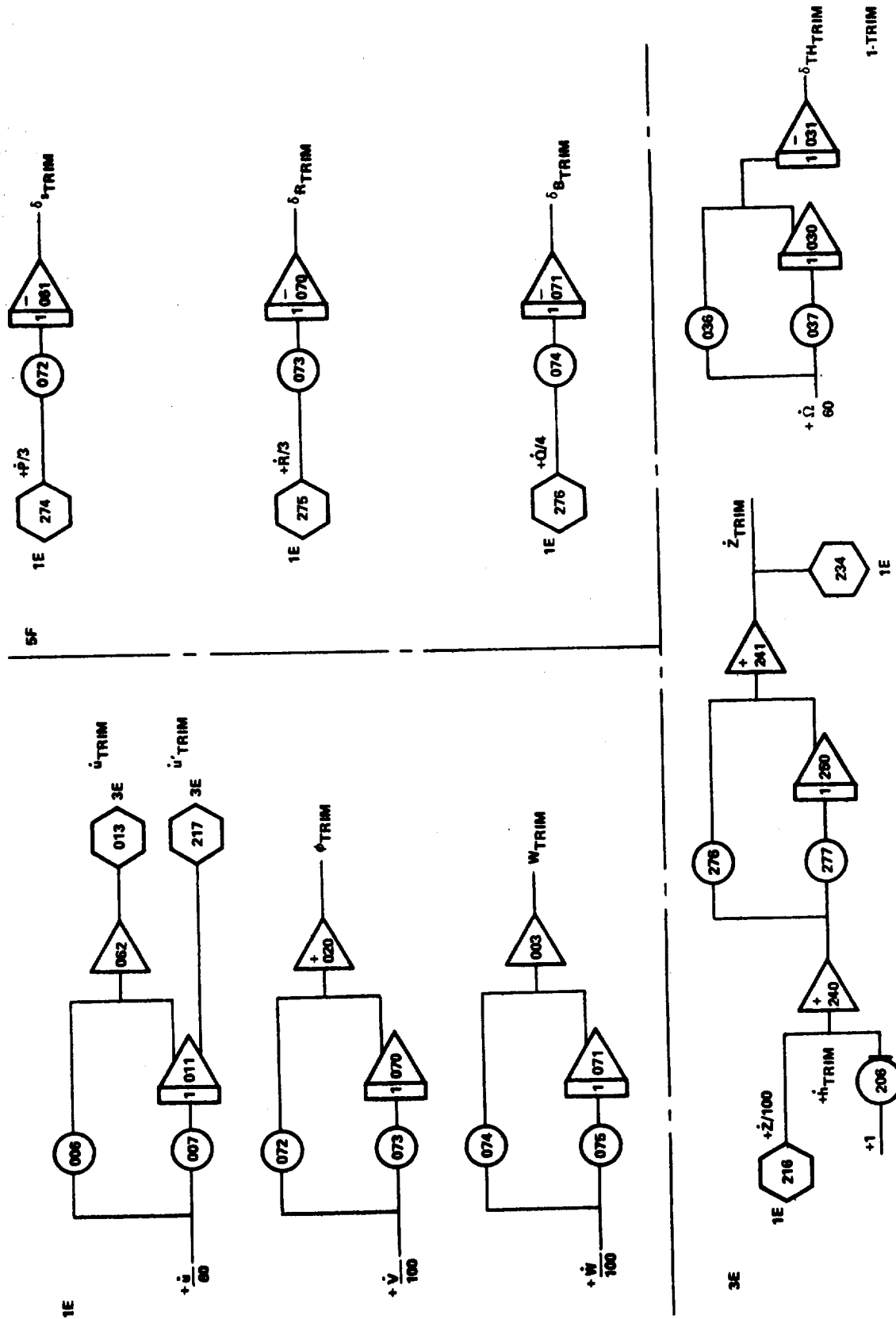


Figure G.8. Analog Diagrams for Model 222 Simulation

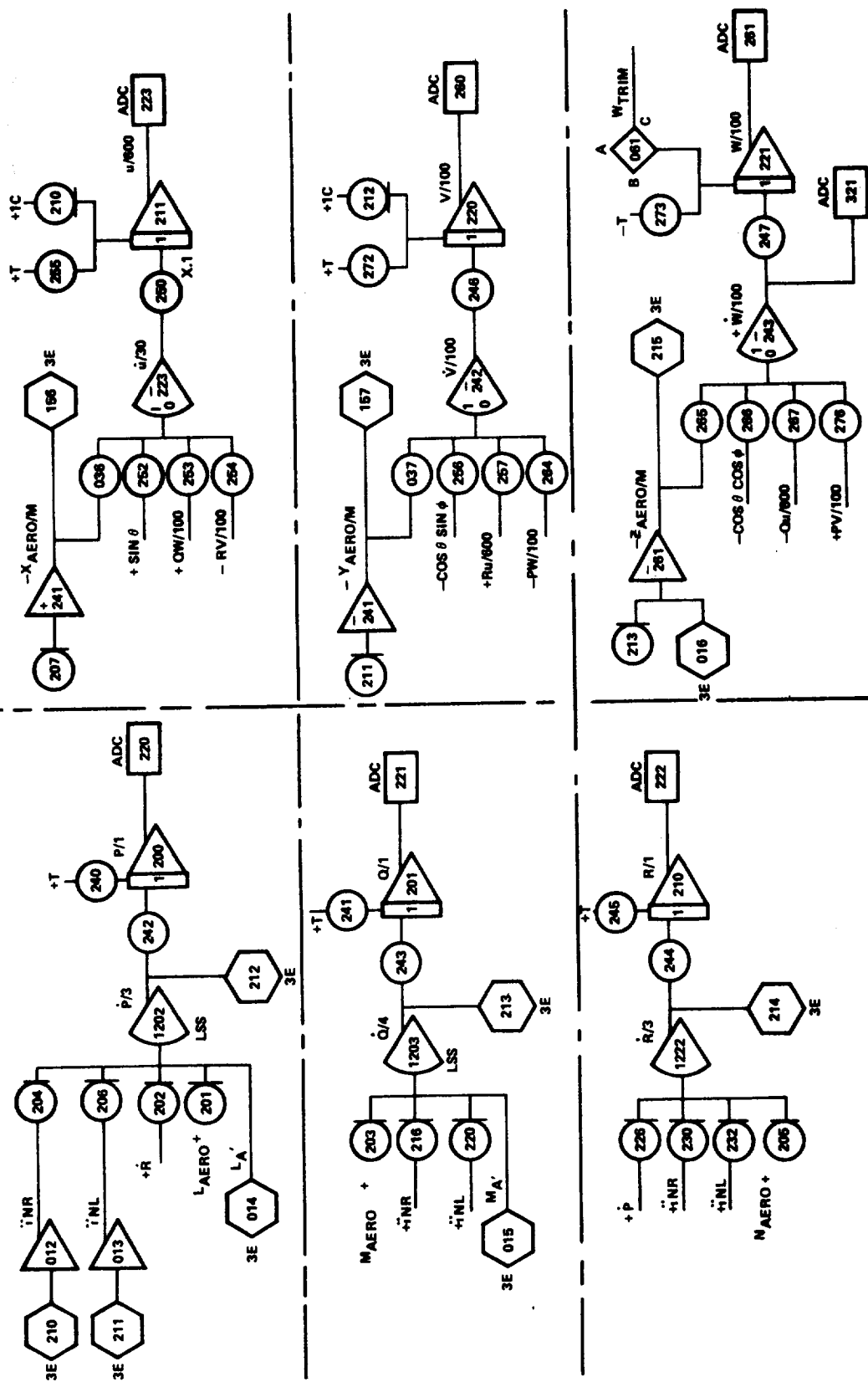
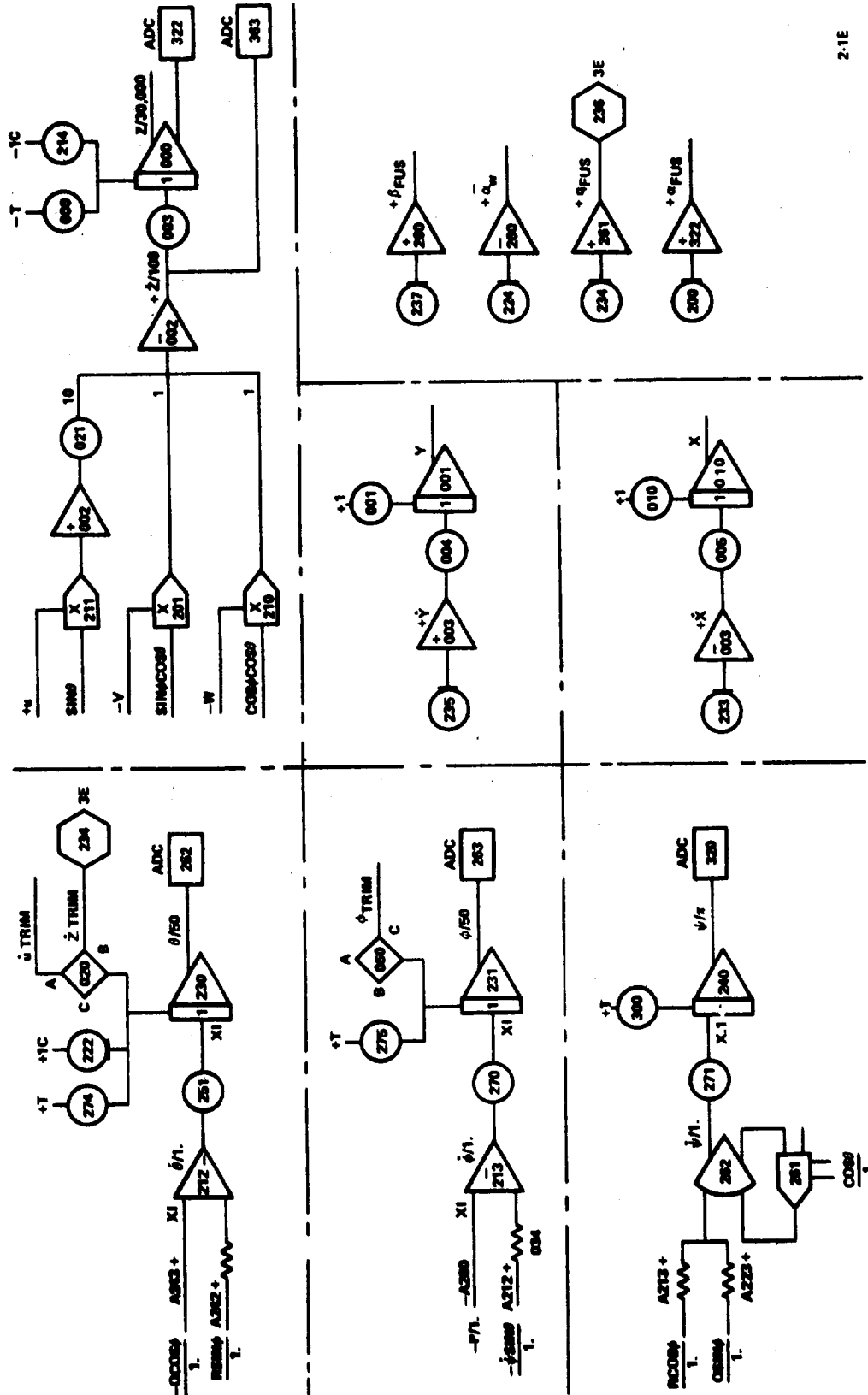


Figure G.8. (Continued)

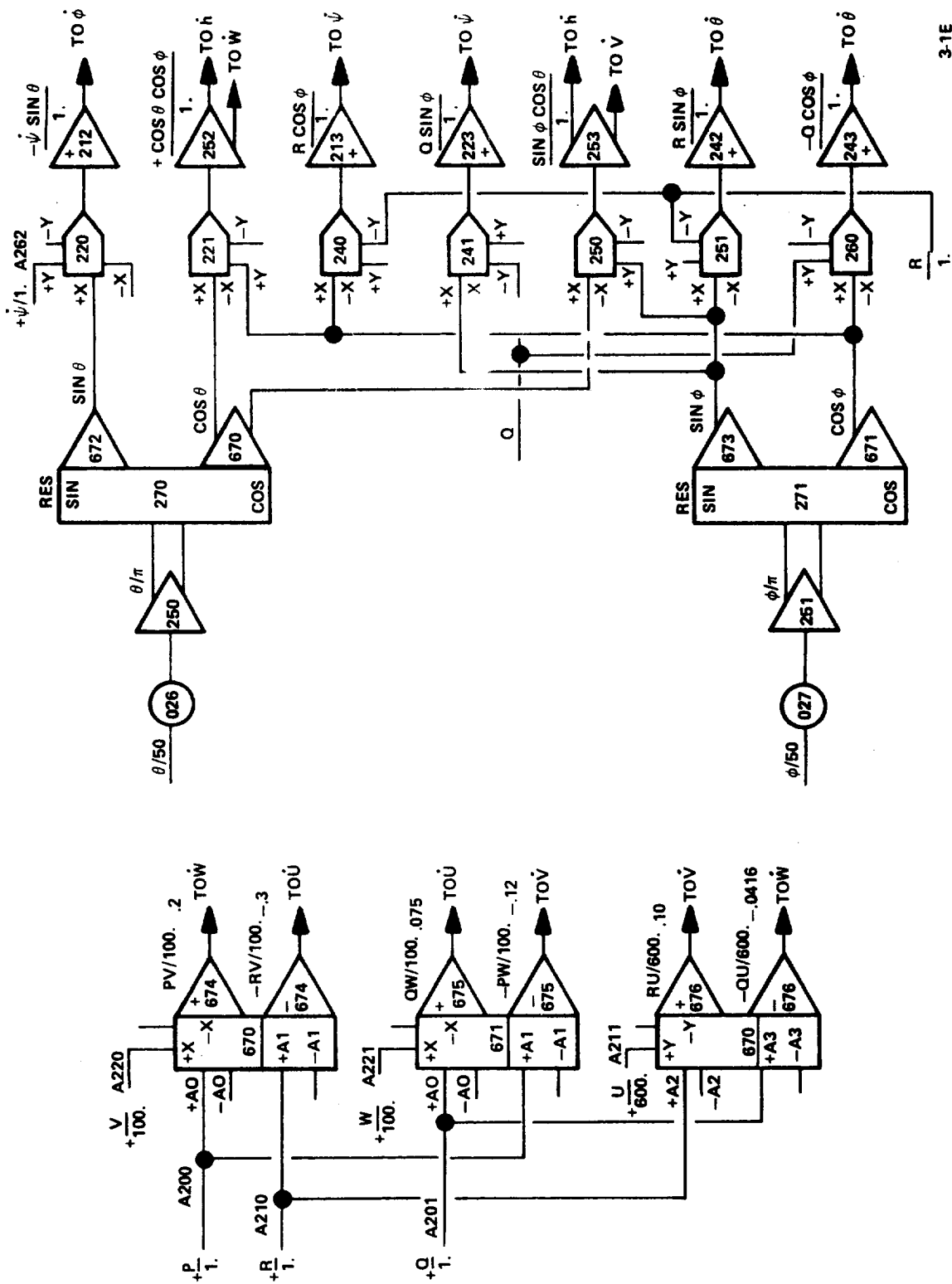
EQUATIONS OF MOTION: $\theta, \phi, \psi, X, Y, Z$



2-1E

Figure G.8. (Continued)

EQUATIONS OF MOTION MULTIPLICATIONS



3-1E

Figure G.8. (Continued)

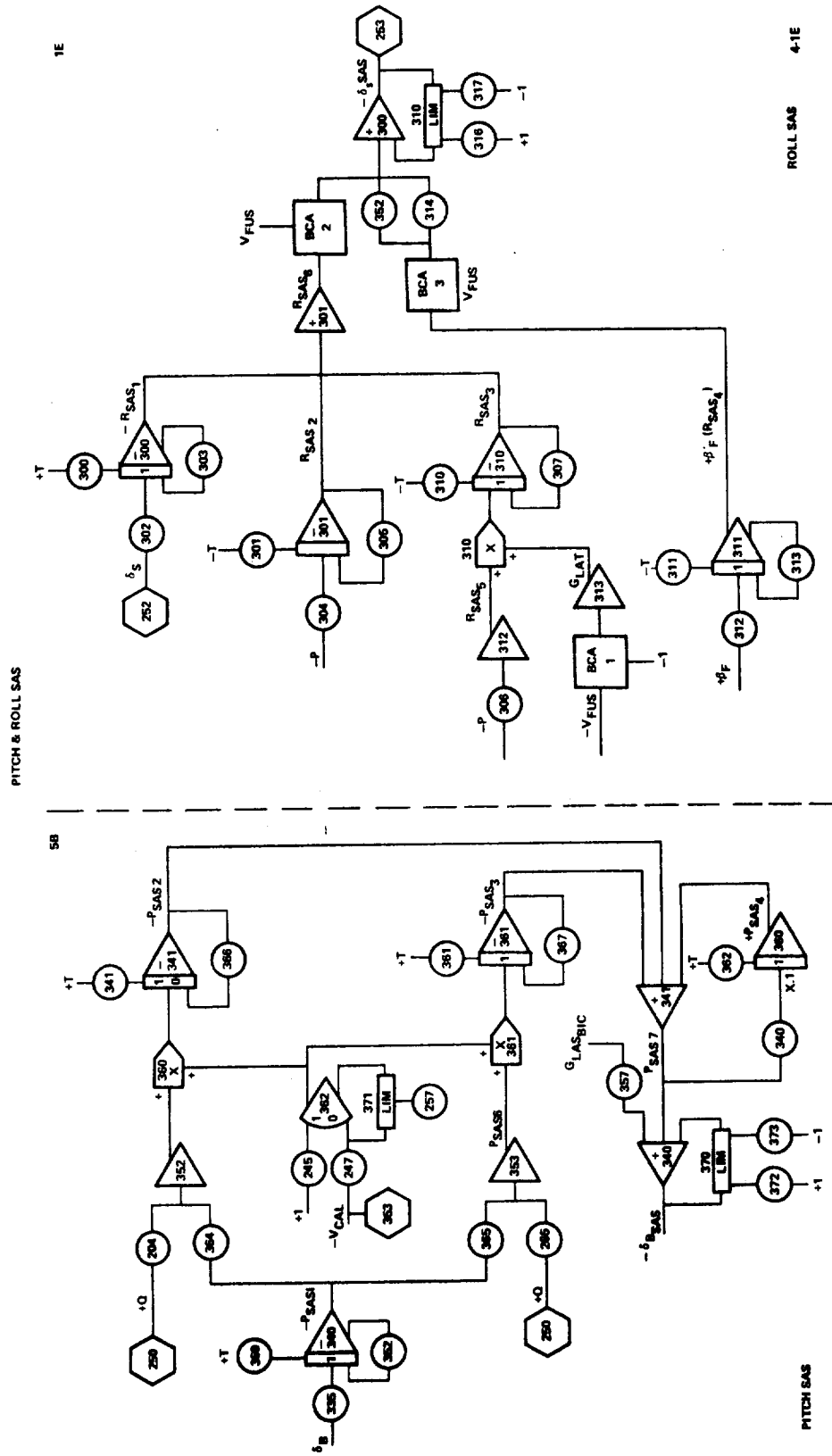


Figure G.8. (Continued)

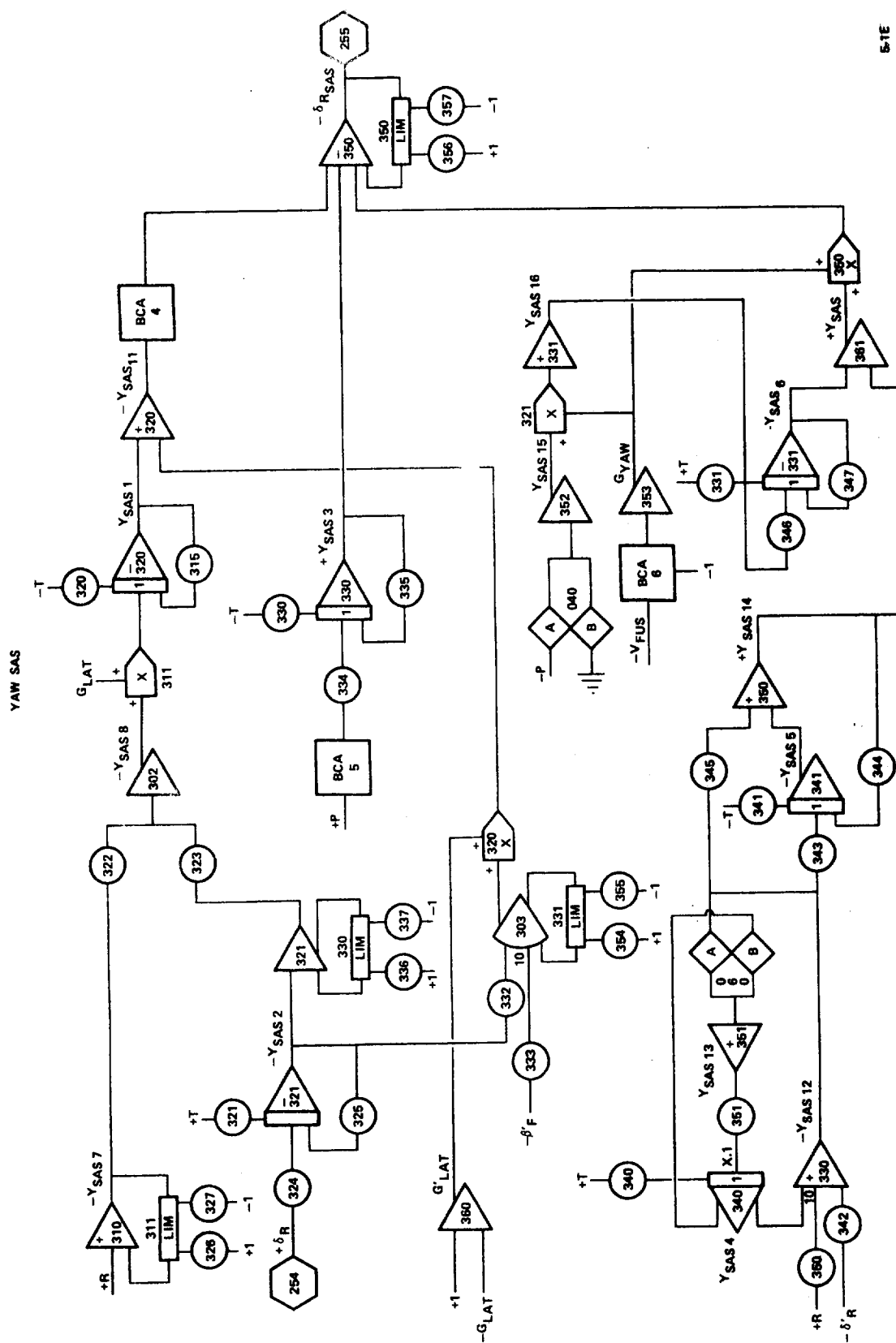


Figure G.8. (Continued)

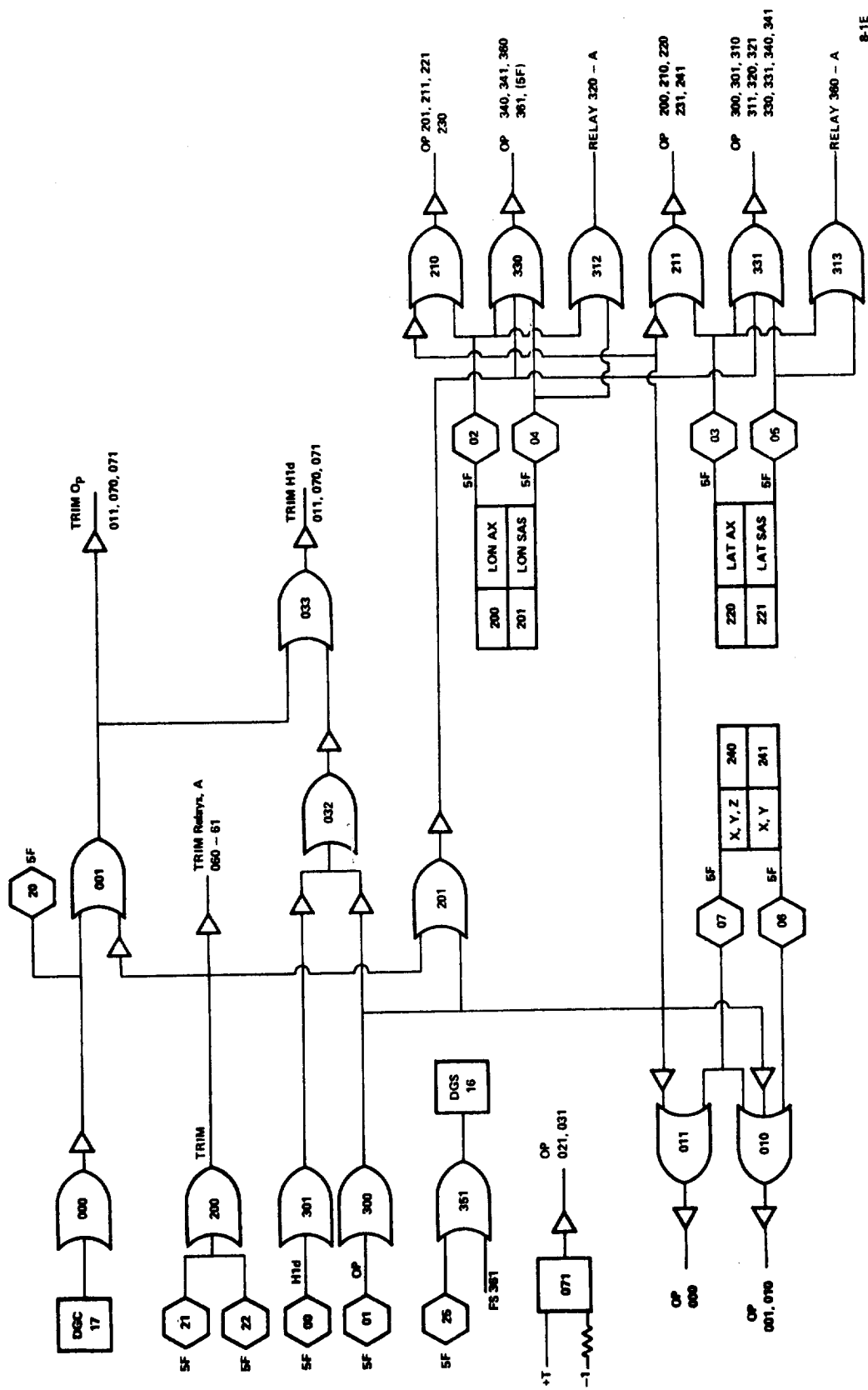


Figure G.8. (Continued)

TRIM LOGIC

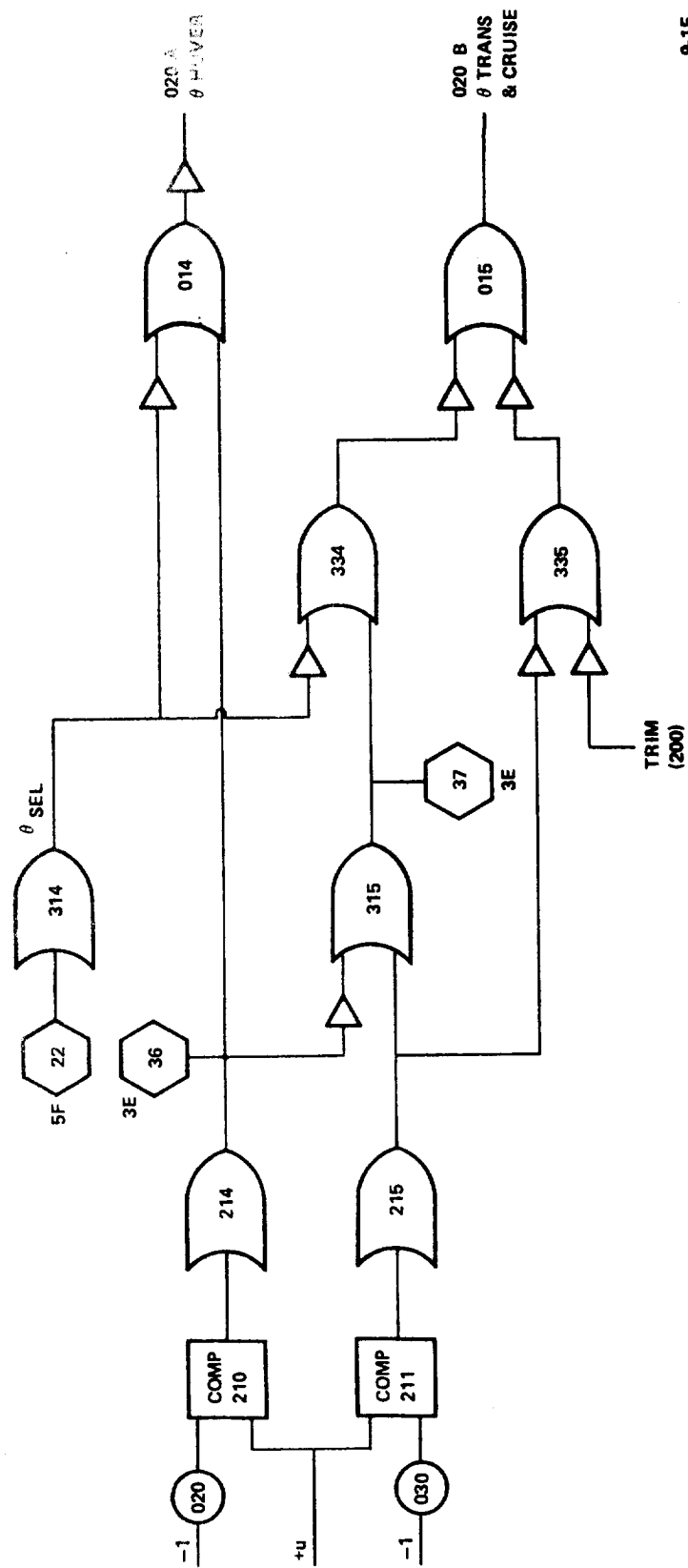
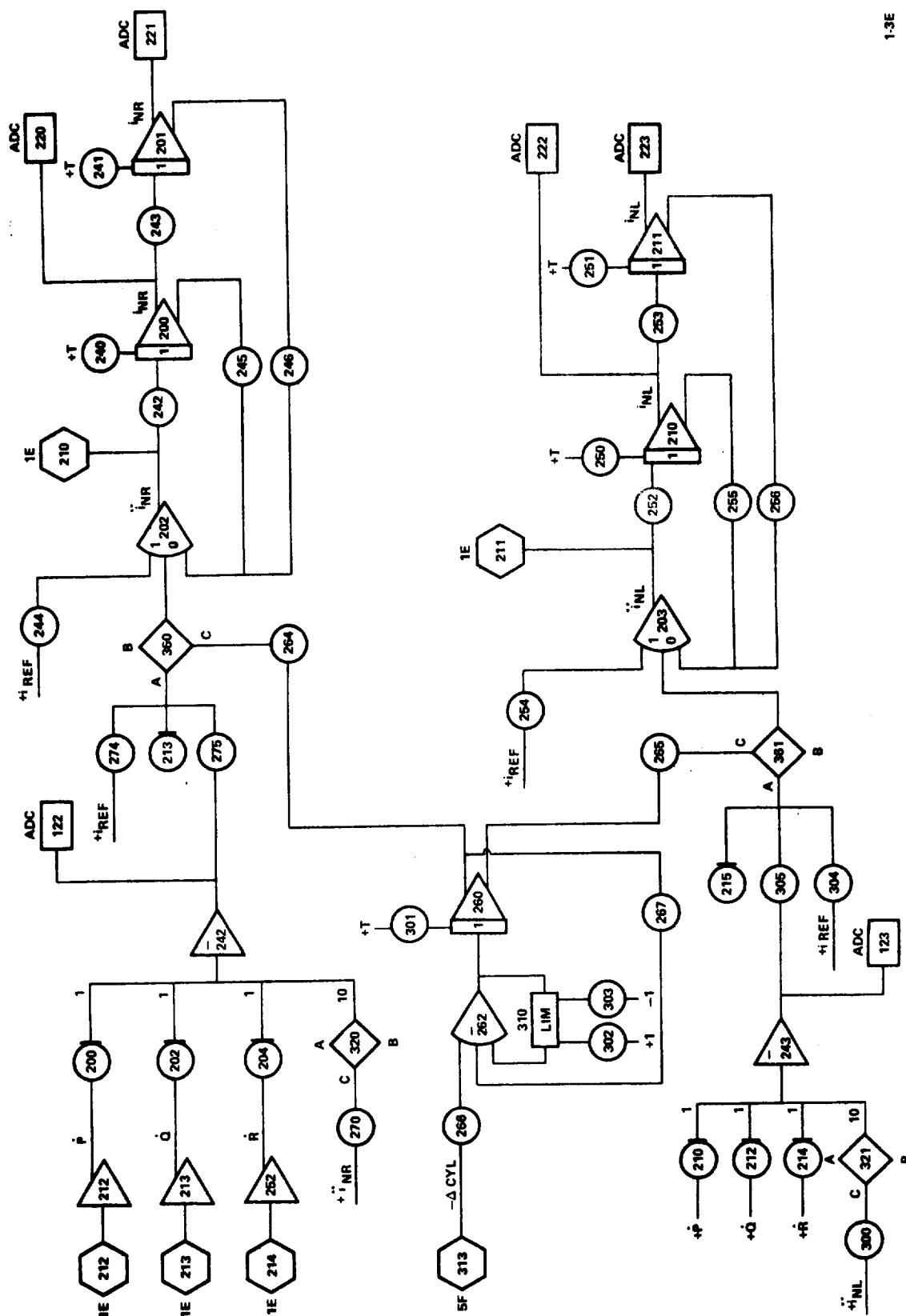


Figure G.8. (Continued)

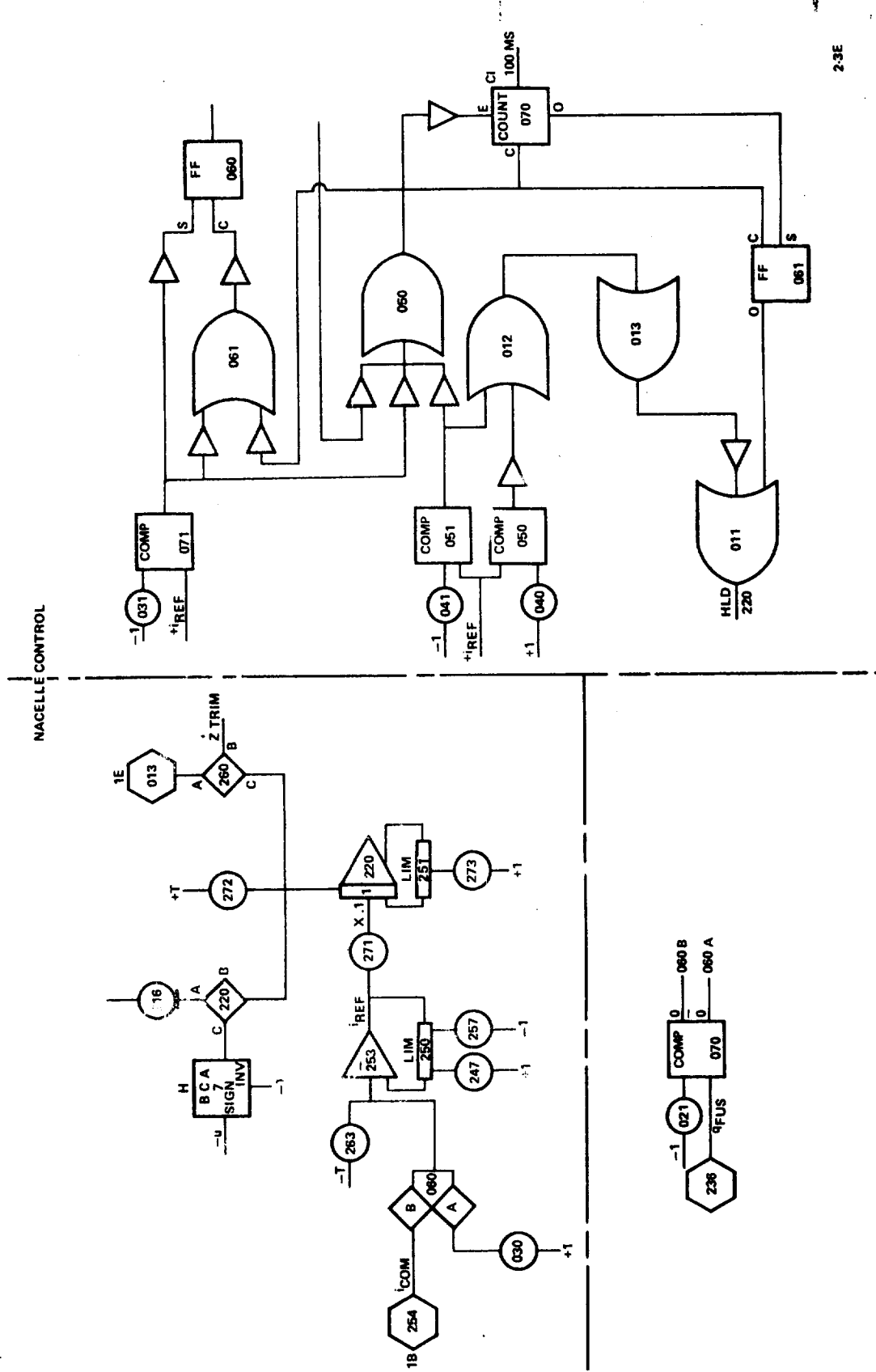
9-1E

NACELLES



1-3E

Figure G.8. (Continued)



23E

Figure G.8. (Continued)

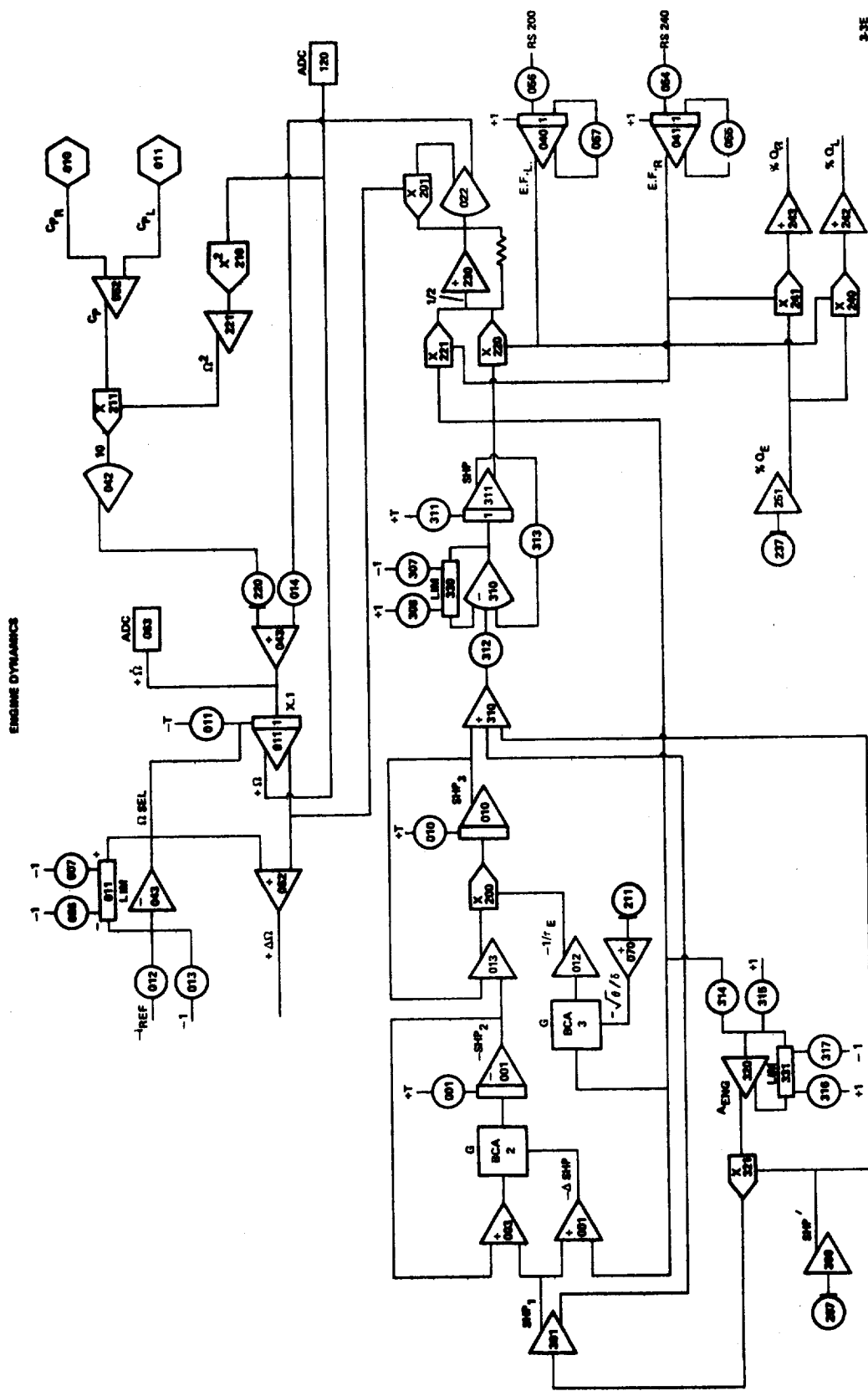


Figure G.8. (Continued)



Figure G.8. (Continued)

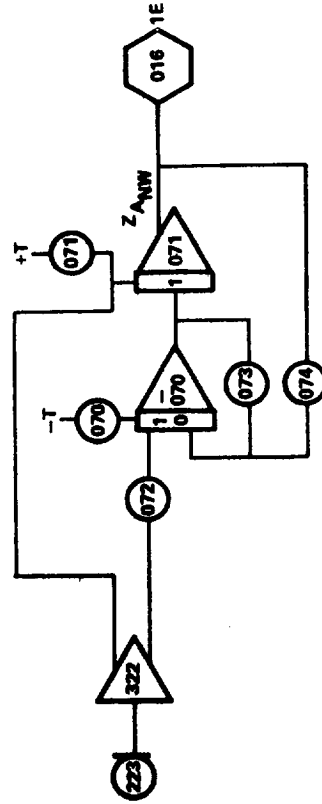
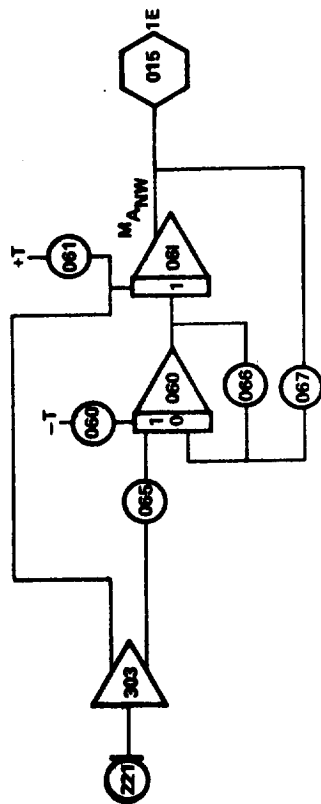
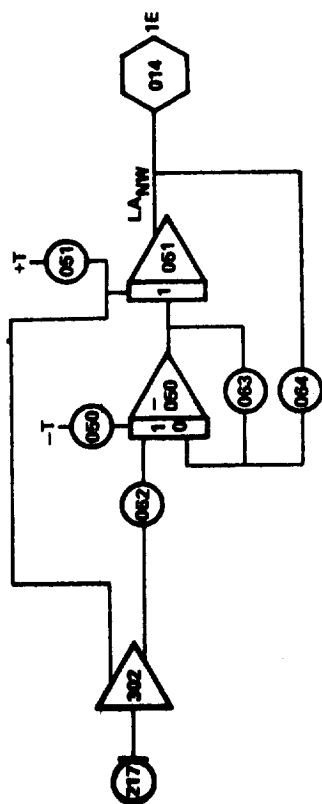
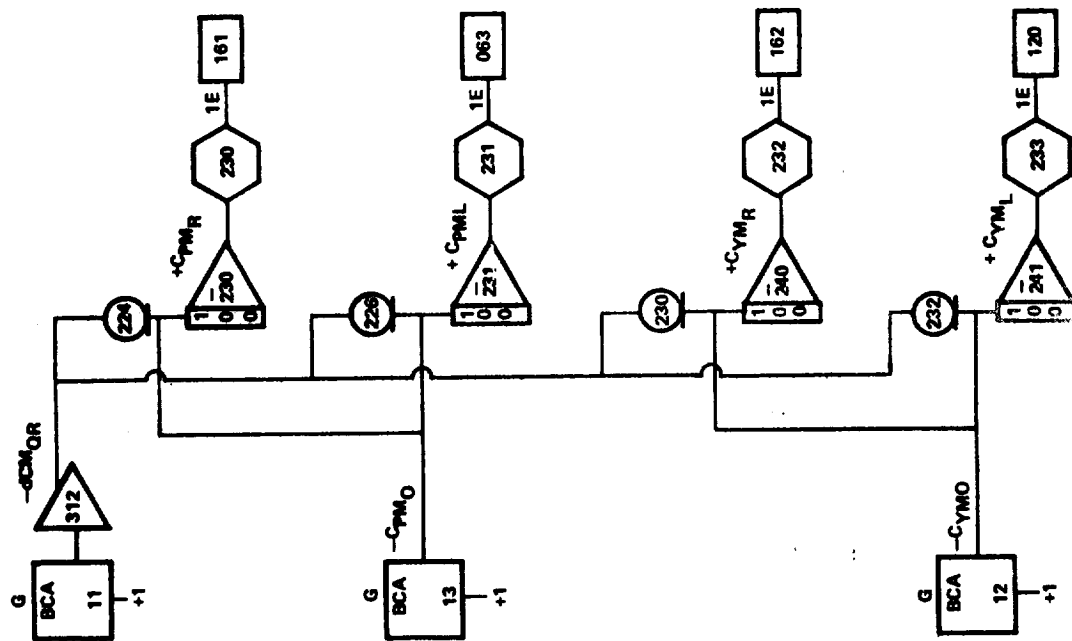


Figure G.8. (Continued)

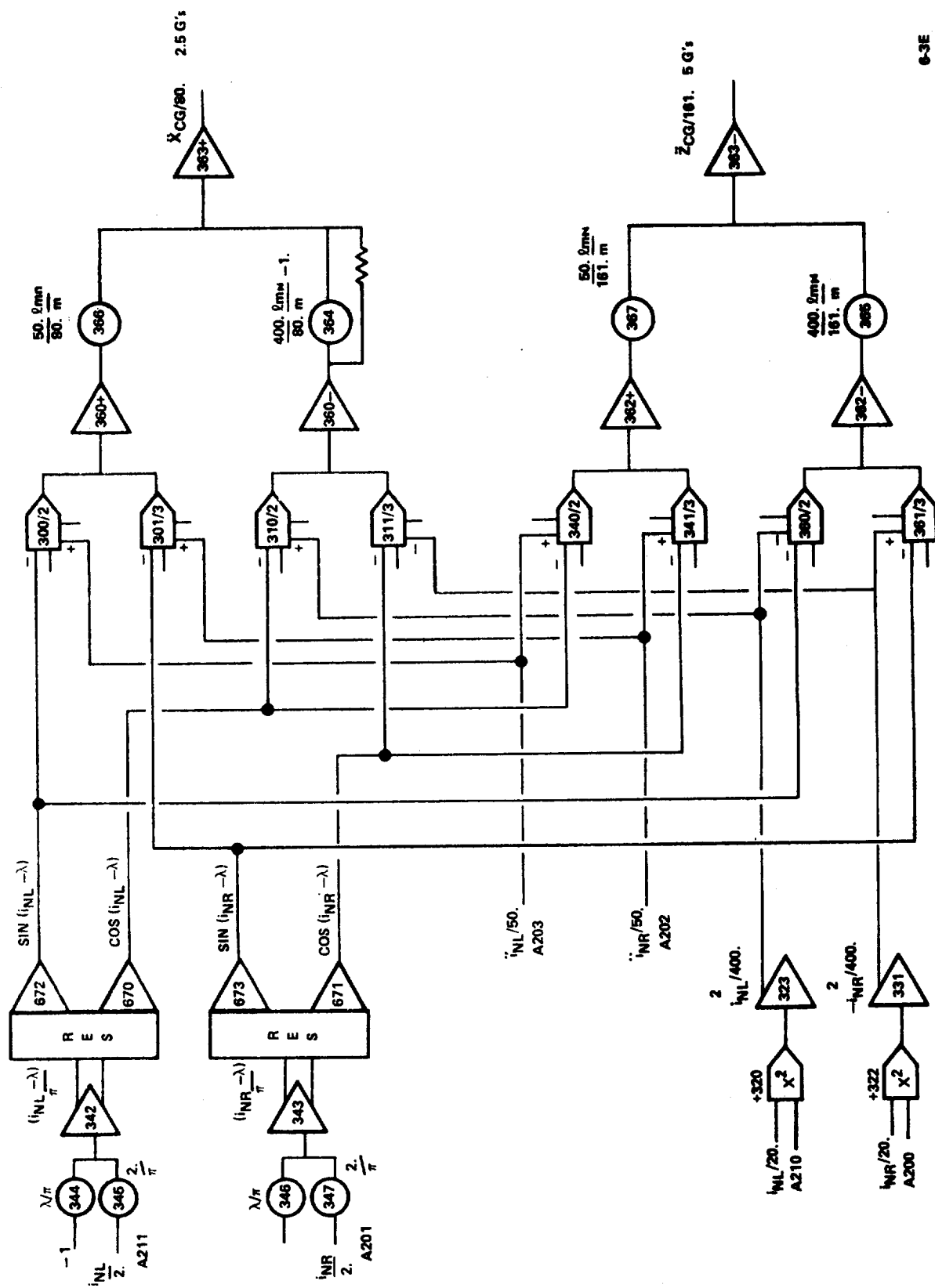


Figure G.8. (Continued)

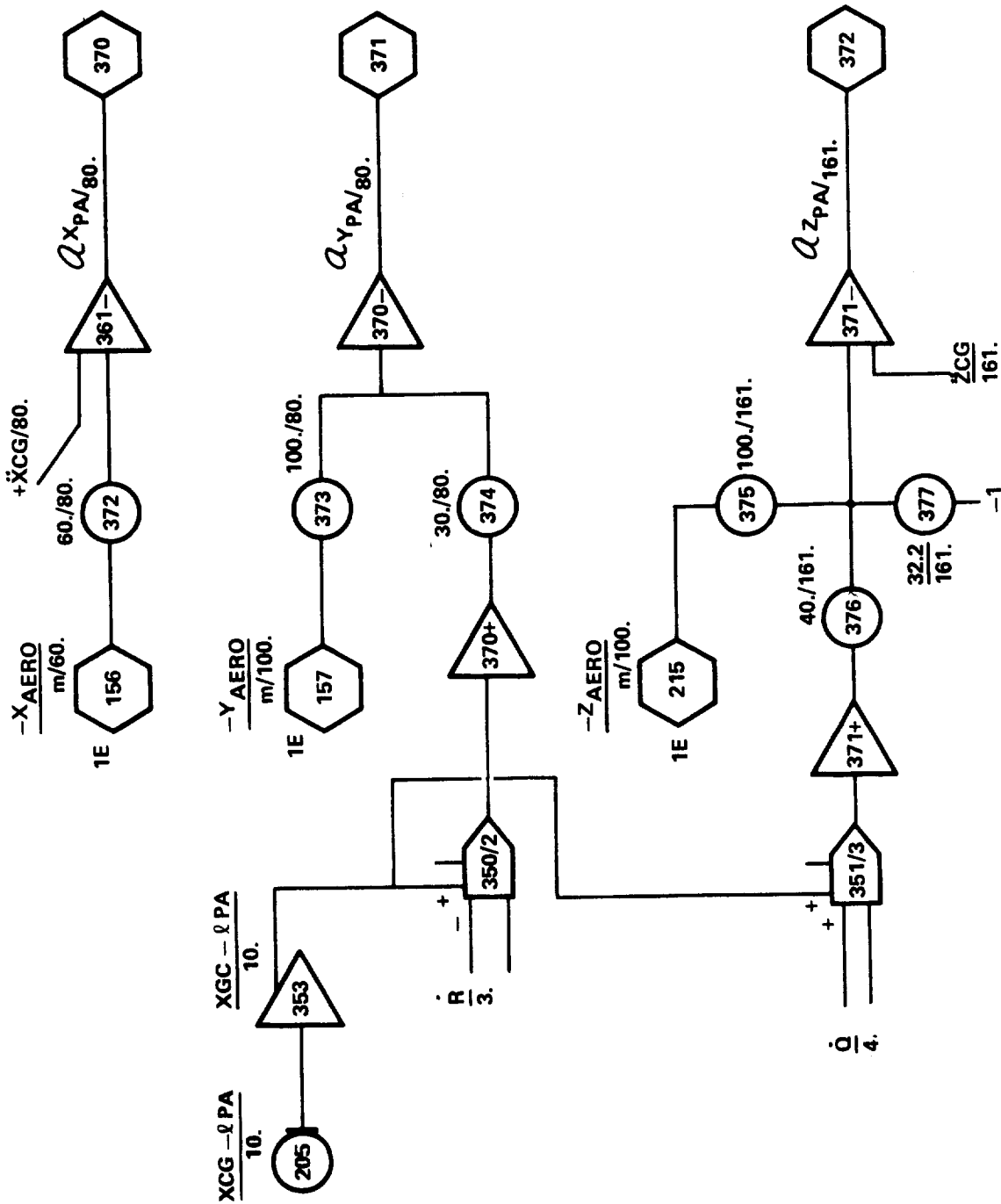


Figure G.8. (Continued)

7-3E





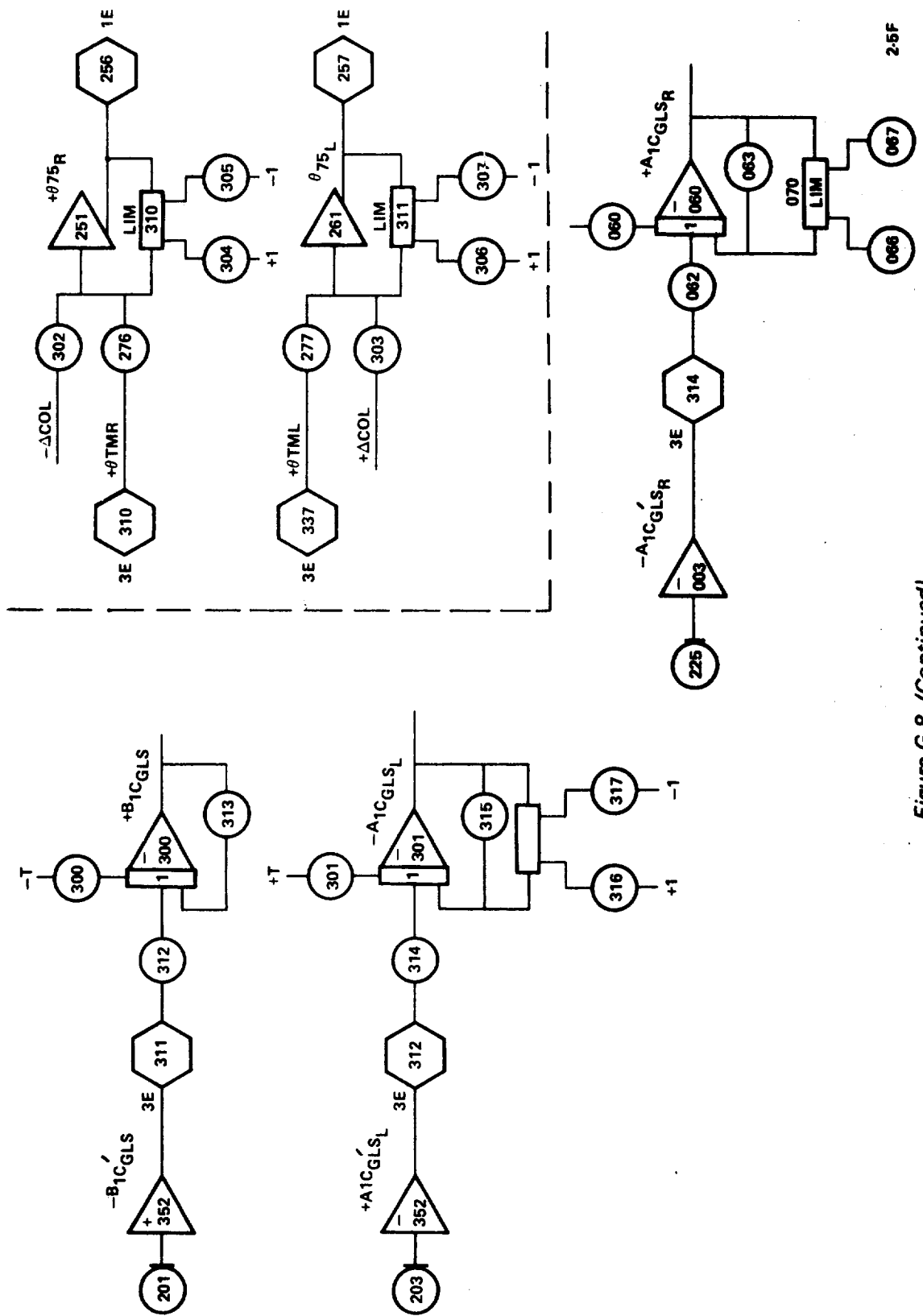
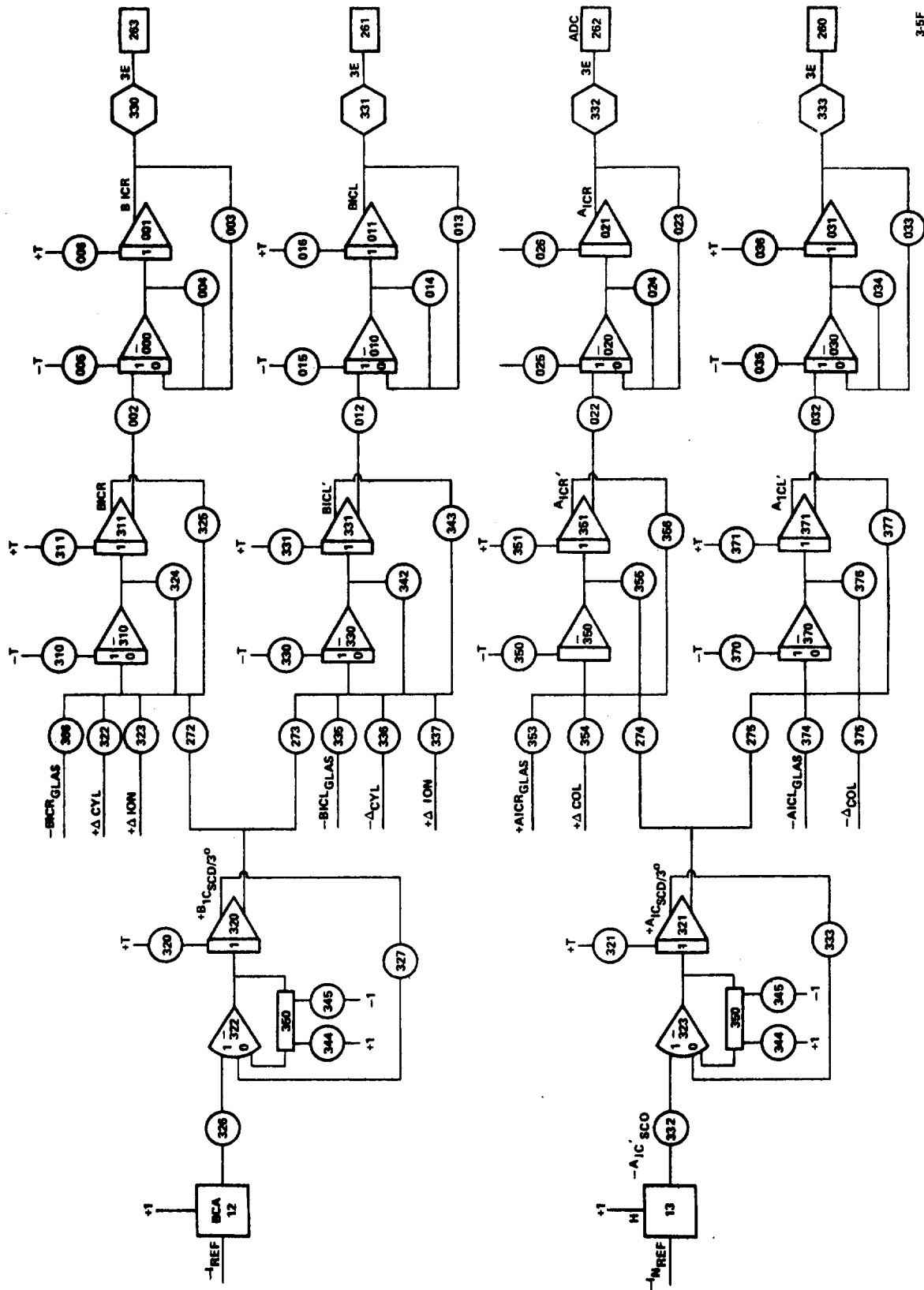
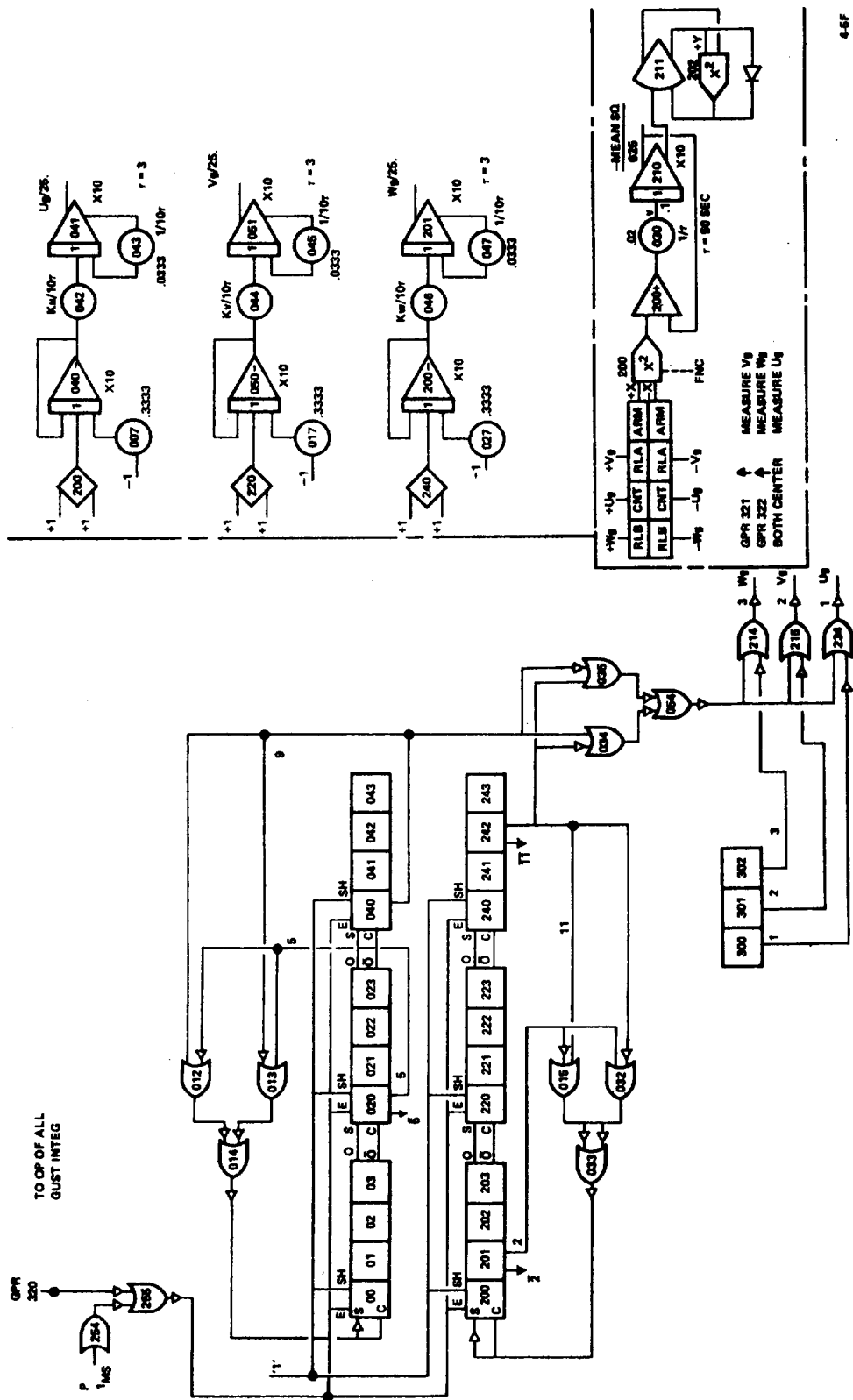


Figure G.8. (Continued)



3-5F



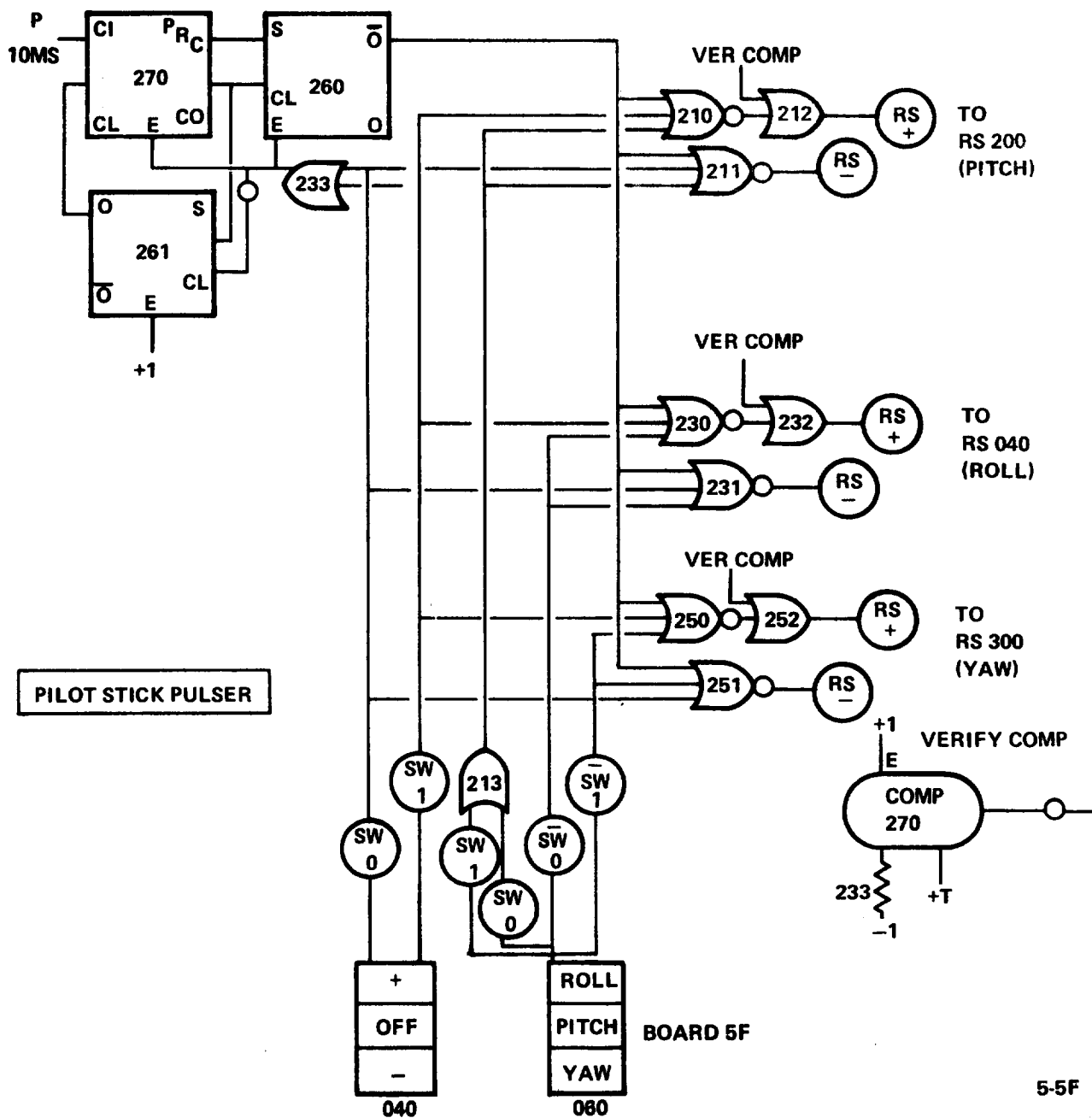


Figure G.8. (Continued)

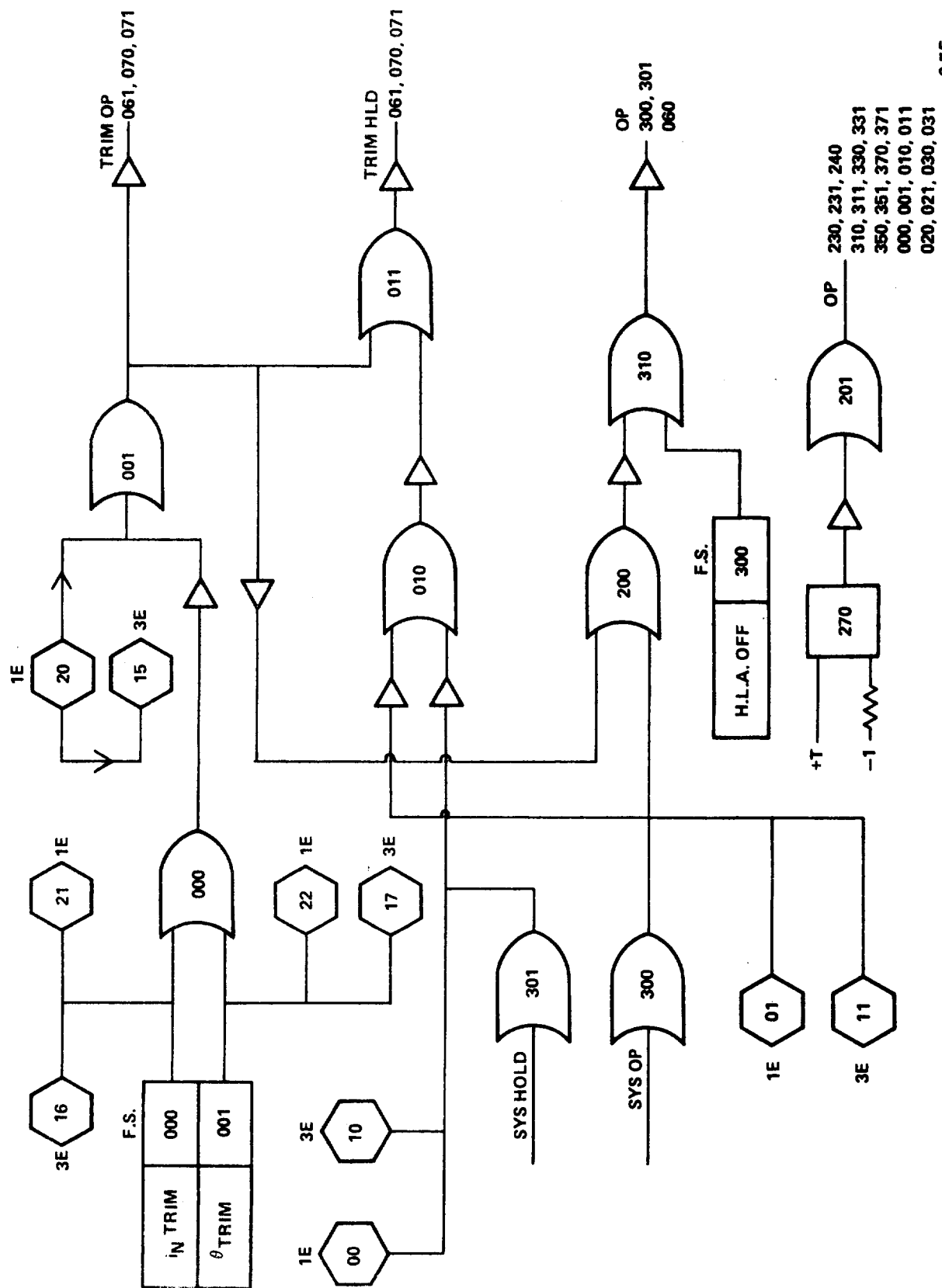
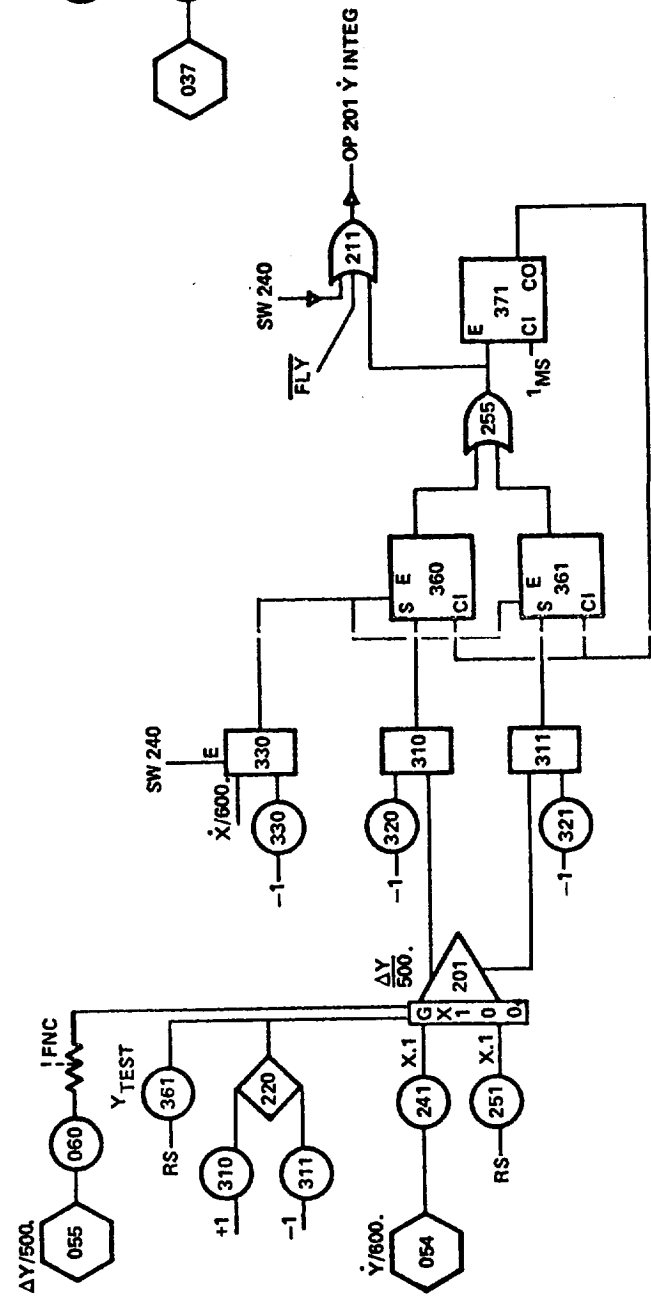
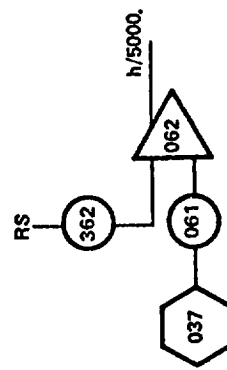


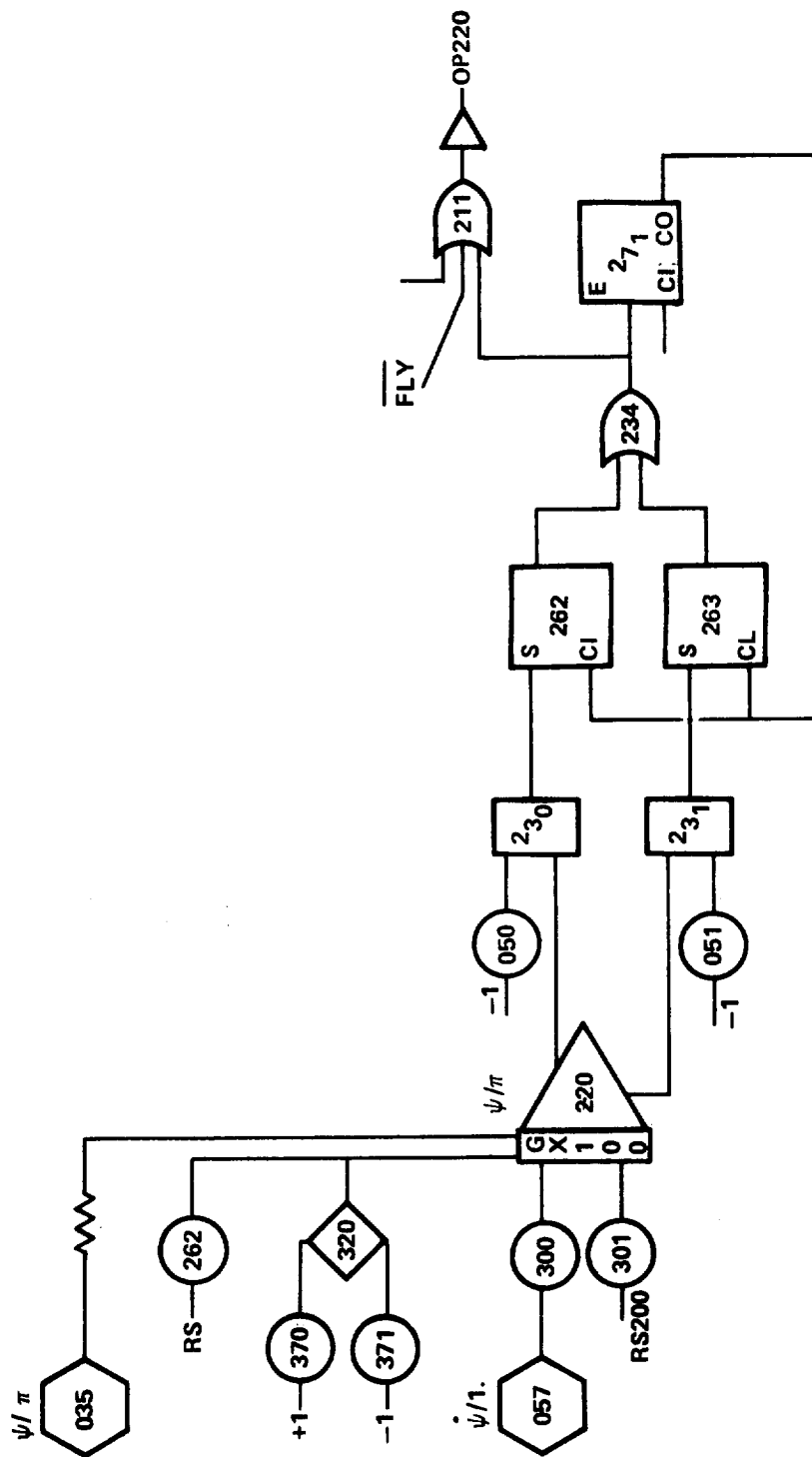
Figure G.8. (Continued)



Figure G.8. (Continued)



2-1B



3-1B

Figure G.8. (Continued)

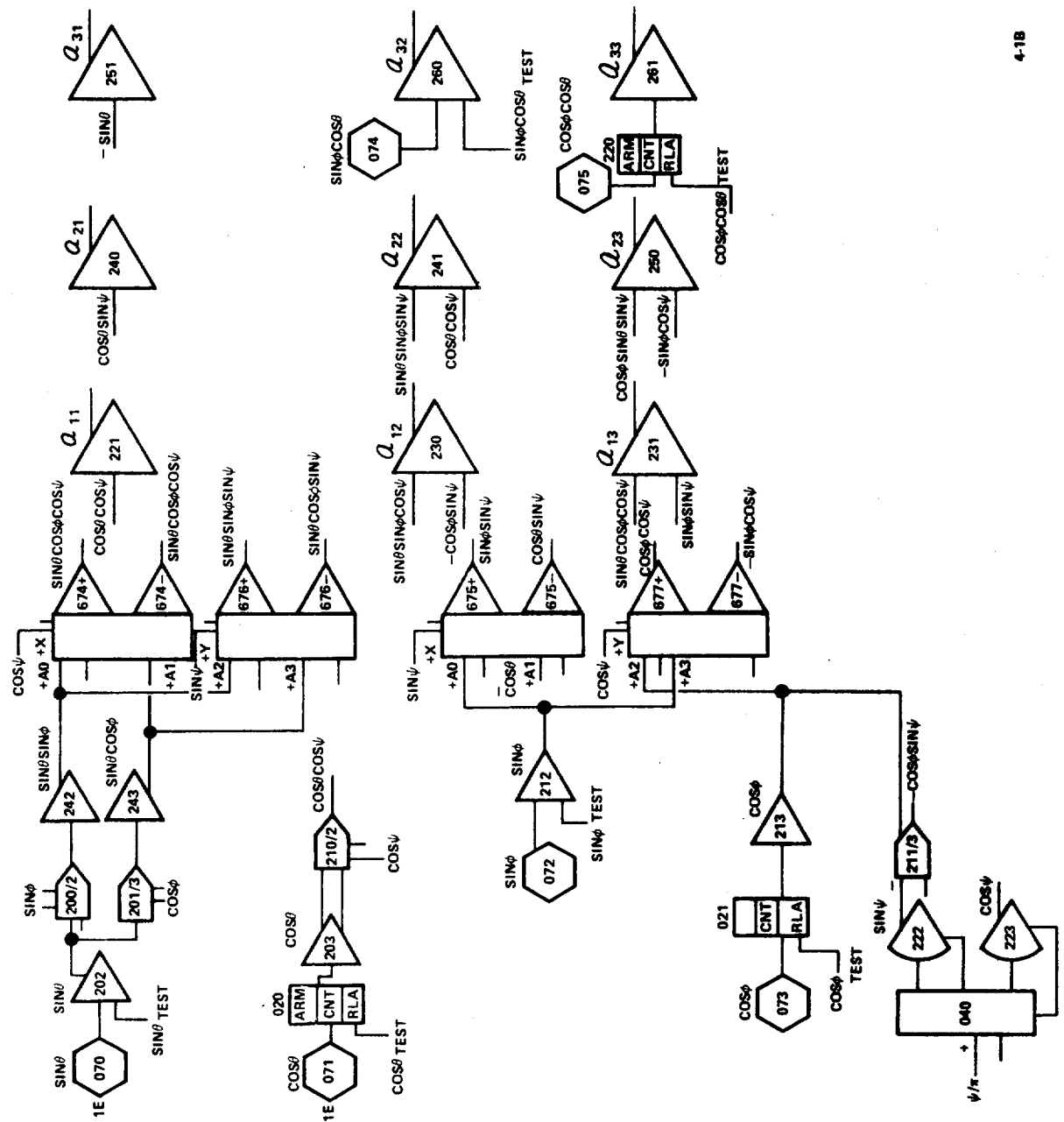
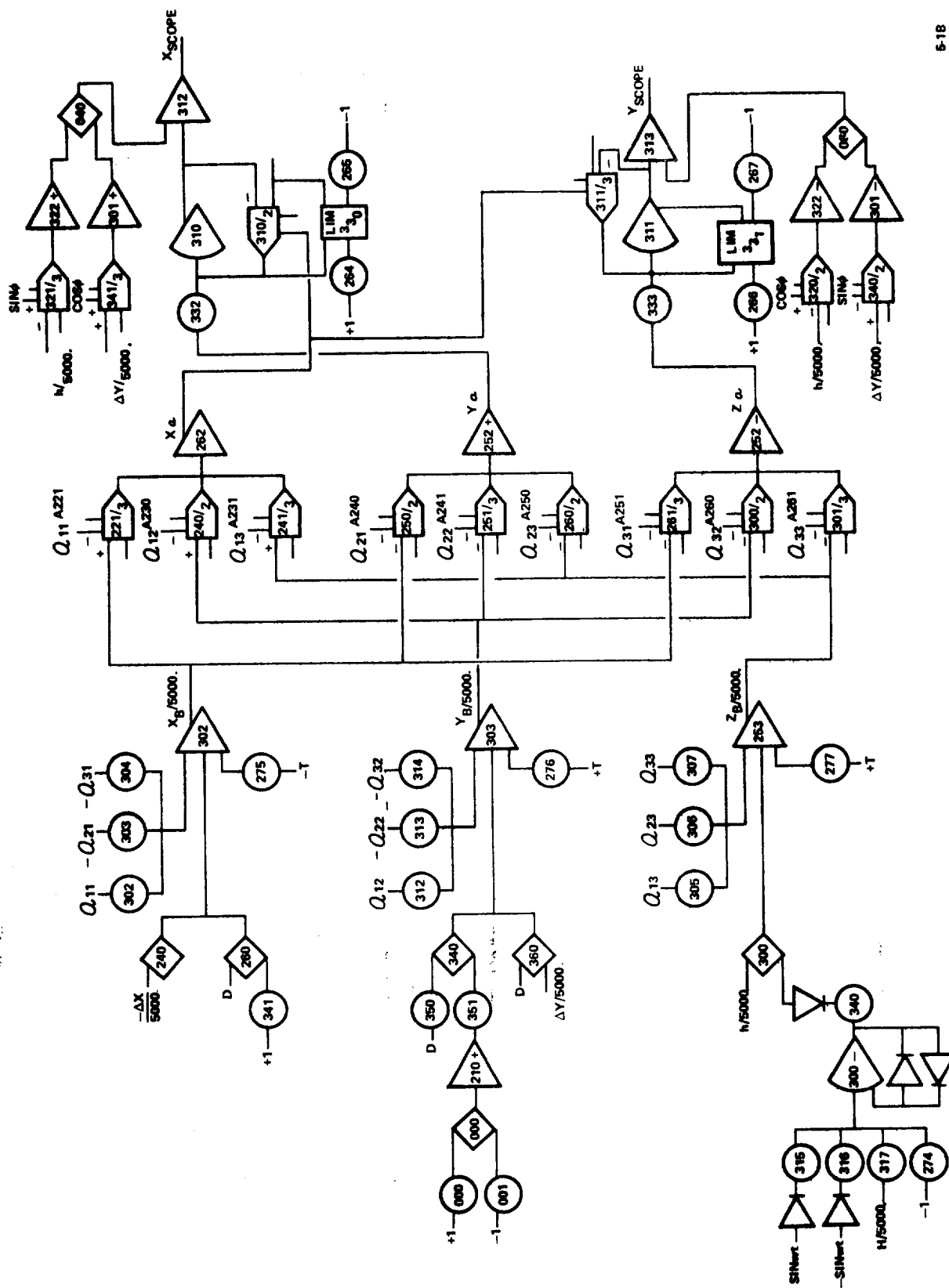


Figure G.8. (Continued)

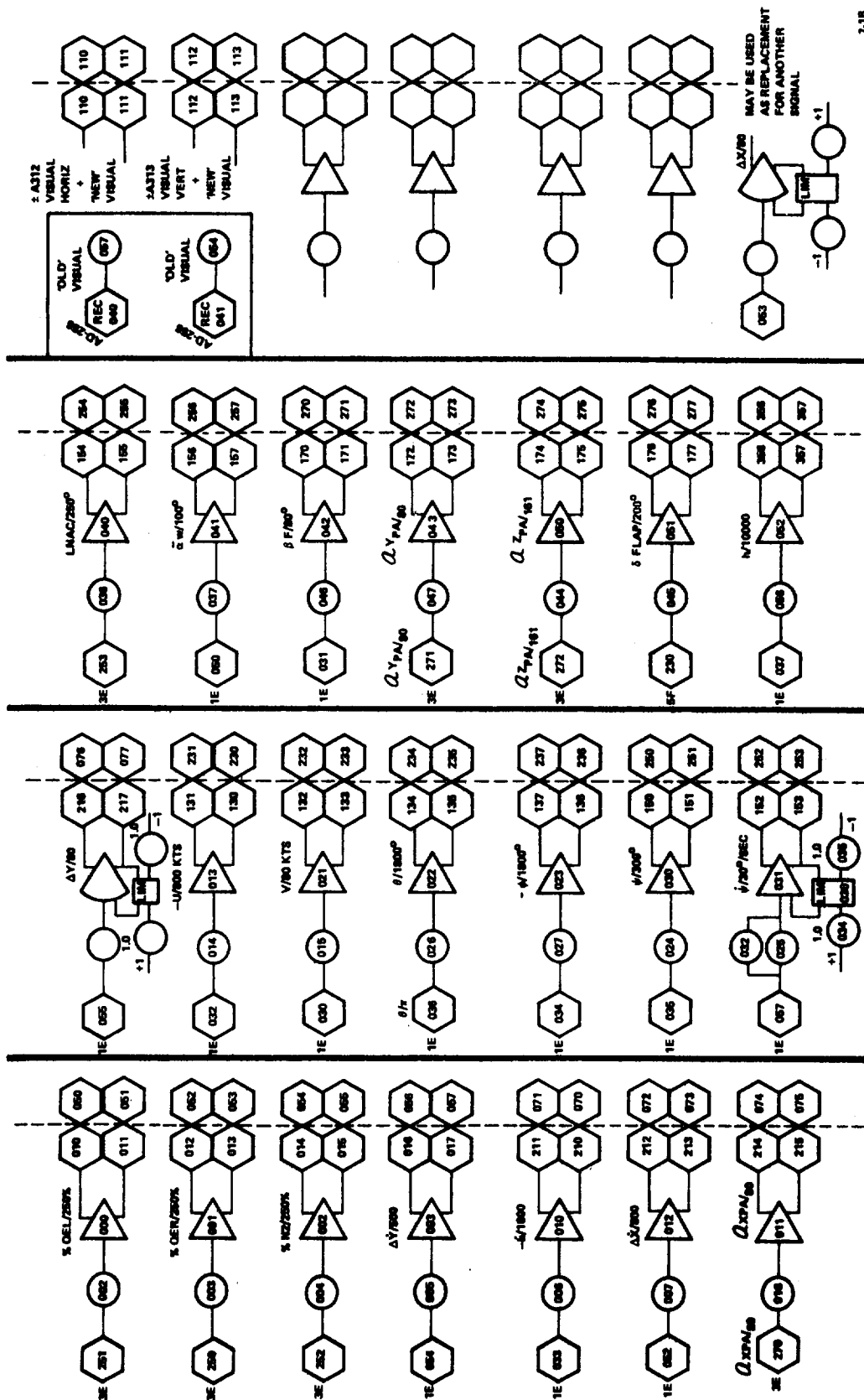


6-18

Figure G.8. (Continued)



G-191



7-18

Figure G.8. (Continued)

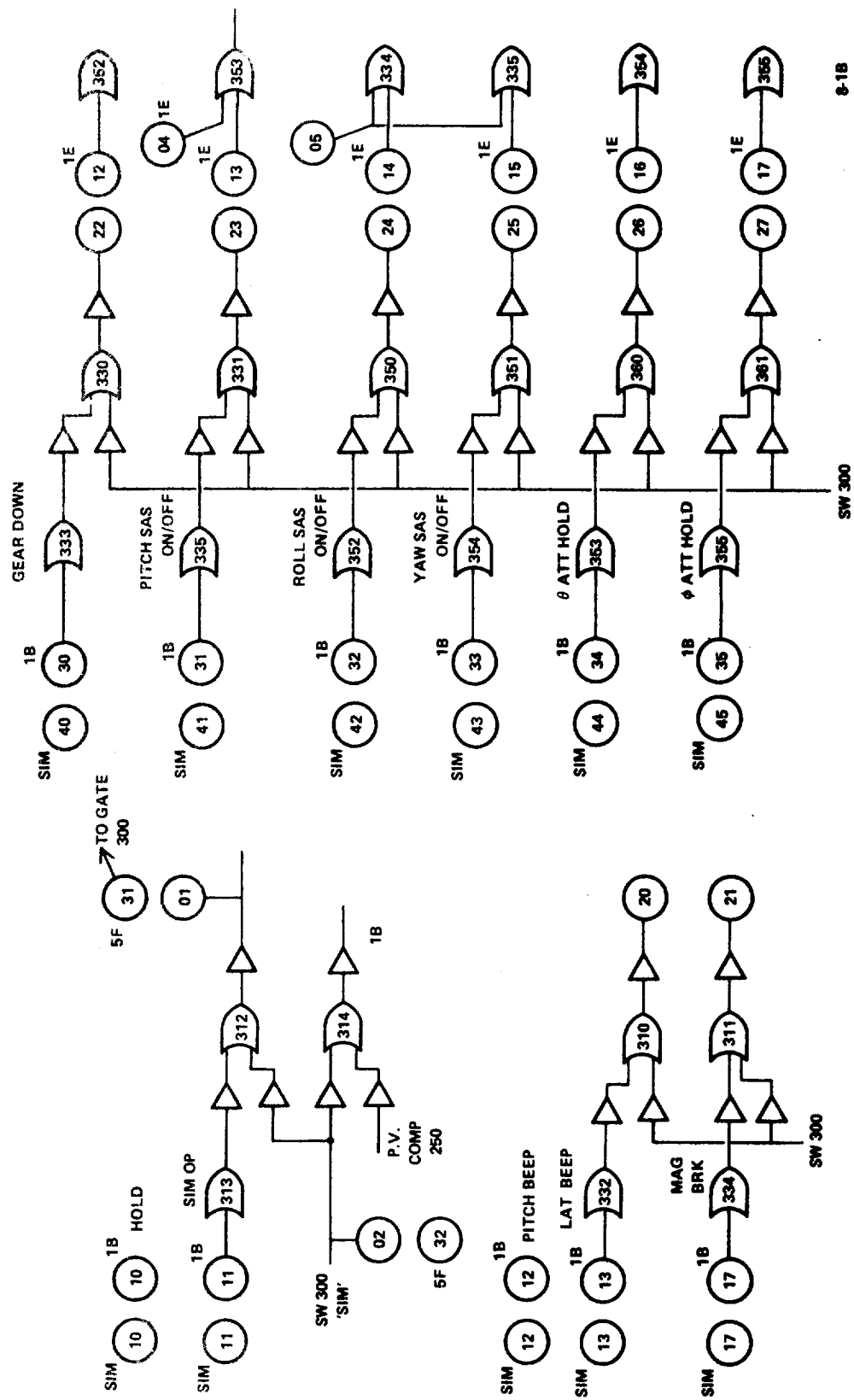


Figure G.8. (Continued)


```

3 SHPMX,THOMMX,THOMMX,OMERMX,ITMSMX,DCVLYX,DCOLMX,DLGNMX,
4 XMXCL,ALCMX,BICMX,TH7MX,ALPOMX,AWPOMX,CTMX,CPMX,CNFMX,
5 CSEMX,COMMX,CVPMX,CPOMX,CYPMX,ATSMX,ALDOMX,ALIDMX,
6 AINMX,AINOMX,AMACMX,THEMX,PIIMX,PSIMX,BSLYMX,GE CYMX,
7 GSCOMX,GECCMX,TAUFMX,BICMX,ALGCMX,SOFCMX,XCOMX,POTCMX,
8 DLELFX,GUSTMX,
9 PMX,CMX,RMX,THOMX,PHOMX,PSDMX

```

```

0014 COMMON/XPART/ AINM,ALAMDA,ALHST,ALVIST,AREAPT,AREA,
*AREAVT,APRT,APVT,AVEYAC,AVEYCS,BLS,COOF,COUHT,COUVT,
*CHORD,CLALHT,CLALPH,CMOF,CMON,CMOF,CMOLN,CMORN,CYALVT,
3CDLG,DCMLG,FINPR,DOVT,DSDBET,EFFHT,EFFVT,FIE,FINDEG,
*FIP,FIIXE,FIIXPR,FIIXH,FIIXE,FIIXPR,FIIXH,FIIXE,FIIXPR,
*FIYH,FIZZ,FIZZPR,FIZZH,FIZZPR,FIZZH,FIZZPR,FIZZH,FIZZPR,
*SFPR,SPVPR,SG,SHF,SHW,SK1,SK2,SK3,SK4,SK5,SK6,SK7,SK8,
*SK9,SK10,SK11,SK12,SK13,SK14,SK15,SK16,SK17,SK18,SK19,
*SK20,SK21,SK22,SK23,SK24,SK25,SK26,SK27,SK28,SK29,SK30,
*SK31,SK32,SK33,SK34,SK35,SK36,SK37,SK38,SK39,SK40,SK41,
*SK42,SK43,SK44,SK45,SK46,SK47,SK48,SK49,SK50,SK51,SK52,
*SK53,SK54,SK55,SK56,SK57,SK58,SK59,SK60,SK61,SK62,SK63,
*SK64,SK65,SK66,SK67,SK68,SK69,SK70,SK71,SK72,SK73,SK74,
*SK75,SK76,SK77,SK78,SK79,SK80,SK81,SK82,SK83,SK84,SK85,
*SK86,SK87,SK88,SK89,SK90,SK91,SK92,SK93,SK94,SK95,SK96,
*SK97,SK98,SK99,SK100,SK101,SK102,SK103,SK104,SK105,SK106,
*SK107,SK108,SK109,SK110,SK111,SK112,SK113,SK114,SK115,
*SK116,SK117,SK118,SK119,SK120,SK121,SK122,SK123,SK124,
*SK125,SK126,SK127,SK128,SK129,SK130,SK131,SK132,SK133,
*SK134,SK135,SK136,SK137,SK138,SK139,SK140,SK141,SK142,
*SK143,SK144,SK145,SK146,SK147,SK148,SK149,SK150,SK151,
*SK152,SK153,SK154,SK155,SK156,SK157,SK158,SK159,SK160,
*SK161,SK162,SK163,SK164,SK165,SK166,SK167,SK168,SK169,
*SK170,SK171,SK172,SK173,SK174,SK175,SK176,SK177,SK178,
*SK179,SK180,SK181,SK182,SK183,SK184,SK185,SK186,SK187,
*SK188,SK189,SK190,SK191,SK192,SK193,SK194,SK195,SK196,
*SK197,SK198,SK199,SK200,SK201,SK202,SK203,SK204,SK205,
*SK206,SK207,SK208,SK209,SK210,SK211,SK212,SK213,SK214,
*SK215,SK216,SK217,SK218,SK219,SK220,SK221,SK222,SK223,
*SK224,SK225,SK226,SK227,SK228,SK229,SK230,SK231,SK232,
*SK233,SK234,SK235,SK236,SK237,SK238,SK239,SK240,SK241,
*SK242,SK243,SK244,SK245,SK246,SK247,SK248,SK249,SK250,
*SK251,SK252,SK253,SK254,SK255,SK256,SK257,SK258,SK259,
*SK260,SK261,SK262,SK263,SK264,SK265,SK266,SK267,SK268,
*SK269,SK270,SK271,SK272,SK273,SK274,SK275,SK276,SK277,
*SK278,SK279,SK280,SK281,SK282,SK283,SK284,SK285,SK286,
*SK287,SK288,SK289,SK290,SK291,SK292,SK293,SK294,SK295,
*SK296,SK297,SK298,SK299,SK300,SK301,SK302,SK303,SK304,
*SK305,SK306,SK307,SK308,SK309,SK310,SK311,SK312,SK313,
*SK314,SK315,SK316,SK317,SK318,SK319,SK320,SK321,SK322,
*SK323,SK324,SK325,SK326,SK327,SK328,SK329,SK330,SK331,
*SK332,SK333,SK334,SK335,SK336,SK337,SK338,SK339,SK340,
*SK341,SK342,SK343,SK344,SK345,SK346,SK347,SK348,SK349,
*SK350,SK351,SK352,SK353,SK354,SK355,SK356,SK357,SK358,
*SK359,SK360,SK361,SK362,SK363,SK364,SK365,SK366,SK367,
*SK368,SK369,SK370,SK371,SK372,SK373,SK374,SK375,SK376,
*SK377,SK378,SK379,SK380,SK381,SK382,SK383,SK384,SK385,
*SK386,SK387,SK388,SK389,SK390,SK391,SK392,SK393,SK394,
*SK395,SK396,SK397,SK398,SK399,SK400,SK401,SK402,SK403,
*SK404,SK405,SK406,SK407,SK408,SK409,SK410,SK411,SK412,
*SK413,SK414,SK415,SK416,SK417,SK418,SK419,SK420,SK421,
*SK422,SK423,SK424,SK425,SK426,SK427,SK428,SK429,SK430,
*SK431,SK432,SK433,SK434,SK435,SK436,SK437,SK438,SK439,
*SK440,SK441,SK442,SK443,SK444,SK445,SK446,SK447,SK448,
*SK449,SK450,SK451,SK452,SK453,SK454,SK455,SK456,SK457,
*SK458,SK459,SK460,SK461,SK462,SK463,SK464,SK465,SK466,
*SK467,SK468,SK469,SK470,SK471,SK472,SK473,SK474,SK475,
*SK476,SK477,SK478,SK479,SK480,SK481,SK482,SK483,SK484,
*SK485,SK486,SK487,SK488,SK489,SK490,SK491,SK492,SK493,
*SK494,SK495,SK496,SK497,SK498,SK499,SK500,SK501,SK502,
*SK503,SK504,SK505,SK506,SK507,SK508,SK509,SK510,SK511,
*SK512,SK513,SK514,SK515,SK516,SK517,SK518,SK519,SK520,
*SK521,SK522,SK523,SK524,SK525,SK526,SK527,SK528,SK529,
*SK530,SK531,SK532,SK533,SK534,SK535,SK536,SK537,SK538,
*SK539,SK540,SK541,SK542,SK543,SK544,SK545,SK546,SK547,
*SK548,SK549,SK550,SK551,SK552,SK553,SK554,SK555,SK556,
*SK557,SK558,SK559,SK560,SK561,SK562,SK563,SK564,SK565,
*SK566,SK567,SK568,SK569,SK570,SK571,SK572,SK573,SK574,
*SK575,SK576,SK577,SK578,SK579,SK580,SK581,SK582,SK583,
*SK584,SK585,SK586,SK587,SK588,SK589,SK590,SK591,SK592,
*SK593,SK594,SK595,SK596,SK597,SK598,SK599,SK600,SK601,
*SK602,SK603,SK604,SK605,SK606,SK607,SK608,SK609,SK610,
*SK611,SK612,SK613,SK614,SK615,SK616,SK617,SK618,SK619,
*SK620,SK621,SK622,SK623,SK624,SK625,SK626,SK627,SK628,
*SK629,SK630,SK631,SK632,SK633,SK634,SK635,SK636,SK637,
*SK638,SK639,SK640,SK641,SK642,SK643,SK644,SK645,SK646,
*SK647,SK648,SK649,SK650,SK651,SK652,SK653,SK654,SK655,
*SK656,SK657,SK658,SK659,SK660,SK661,SK662,SK663,SK664,
*SK665,SK666,SK667,SK668,SK669,SK670,SK671,SK672,SK673,
*SK674,SK675,SK676,SK677,SK678,SK679,SK680,SK681,SK682,
*SK683,SK684,SK685,SK686,SK687,SK688,SK689,SK690,SK691,
*SK692,SK693,SK694,SK695,SK696,SK697,SK698,SK699,SK700,
*SK701,SK702,SK703,SK704,SK705,SK706,SK707,SK708,SK709,
*SK710,SK711,SK712,SK713,SK714,SK715,SK716,SK717,SK718,
*SK719,SK720,SK721,SK722,SK723,SK724,SK725,SK726,SK727,
*SK728,SK729,SK730,SK731,SK732,SK733,SK734,SK735,SK736,
*SK737,SK738,SK739,SK740,SK741,SK742,SK743,SK744,SK745,
*SK746,SK747,SK748,SK749,SK750,SK751,SK752,SK753,SK754,
*SK755,SK756,SK757,SK758,SK759,SK760,SK761,SK762,SK763,
*SK764,SK765,SK766,SK767,SK768,SK769,SK770,SK771,SK772,
*SK773,SK774,SK775,SK776,SK777,SK778,SK779,SK780,SK781,
*SK782,SK783,SK784,SK785,SK786,SK787,SK788,SK789,SK790,
*SK791,SK792,SK793,SK794,SK795,SK796,SK797,SK798,SK799,
*SK800,SK801,SK802,SK803,SK804,SK805,SK806,SK807,SK808,
*SK809,SK810,SK811,SK812,SK813,SK814,SK815,SK816,SK817,
*SK818,SK819,SK820,SK821,SK822,SK823,SK824,SK825,SK826,
*SK827,SK828,SK829,SK830,SK831,SK832,SK833,SK834,SK835,
*SK836,SK837,SK838,SK839,SK840,SK841,SK842,SK843,SK844,
*SK845,SK846,SK847,SK848,SK849,SK850,SK851,SK852,SK853,
*SK854,SK855,SK856,SK857,SK858,SK859,SK860,SK861,SK862,
*SK863,SK864,SK865,SK866,SK867,SK868,SK869,SK870,SK871,
*SK872,SK873,SK874,SK875,SK876,SK877,SK878,SK879,SK880,
*SK881,SK882,SK883,SK884,SK885,SK886,SK887,SK888,SK889,
*SK890,SK891,SK892,SK893,SK894,SK895,SK896,SK897,SK898,
*SK899,SK900,SK901,SK902,SK903,SK904,SK905,SK906,SK907,
*SK908,SK909,SK910,SK911,SK912,SK913,SK914,SK915,SK916,
*SK917,SK918,SK919,SK920,SK921,SK922,SK923,SK924,SK925,
*SK926,SK927,SK928,SK929,SK930,SK931,SK932,SK933,SK934,
*SK935,SK936,SK937,SK938,SK939,SK940,SK941,SK942,SK943,
*SK944,SK945,SK946,SK947,SK948,SK949,SK950,SK951,SK952,
*SK953,SK954,SK955,SK956,SK957,SK958,SK959,SK960,SK961,
*SK962,SK963,SK964,SK965,SK966,SK967,SK968,SK969,SK970,
*SK971,SK972,SK973,SK974,SK975,SK976,SK977,SK978,SK979,
*SK980,SK981,SK982,SK983,SK984,SK985,SK986,SK987,SK988,
*SK989,SK990,SK991,SK992,SK993,SK994,SK995,SK996,SK997,
*SK998,SK999,SK1000,SK1001,SK1002,SK1003,SK1004,SK1005,
*SK1006,SK1007,SK1008,SK1009,SK1010,SK1011,SK1012,SK1013,
*SK1014,SK1015,SK1016,SK1017,SK1018,SK1019,SK1020,SK1021,
*SK1022,SK1023,SK1024,SK1025,SK1026,SK1027,SK1028,SK1029,
*SK1030,SK1031,SK1032,SK1033,SK1034,SK1035,SK1036,SK1037,
*SK1038,SK1039,SK1040,SK1041,SK1042,SK1043,SK1044,SK1045,
*SK1046,SK1047,SK1048,SK1049,SK1050,SK1051,SK1052,SK1053,
*SK1054,SK1055,SK1056,SK1057,SK1058,SK1059,SK1060,SK1061,
*SK1062,SK1063,SK1064,SK1065,SK1066,SK1067,SK1068,SK1069,
*SK1070,SK1071,SK1072,SK1073,SK1074,SK1075,SK1076,SK1077,
*SK1078,SK1079,SK1080,SK1081,SK1082,SK1083,SK1084,SK1085,
*SK1086,SK1087,SK1088,SK1089,SK1090,SK1091,SK1092,SK1093,
*SK1094,SK1095,SK1096,SK1097,SK1098,SK1099,SK1100,SK1101,
*SK1102,SK1103,SK1104,SK1105,SK1106,SK1107,SK1108,SK1109,
*SK1110,SK1111,SK1112,SK1113,SK1114,SK1115,SK1116,SK1117,
*SK1118,SK1119,SK1120,SK1121,SK1122,SK1123,SK1124,SK1125,
*SK1126,SK1127,SK1128,SK1129,SK1130,SK1131,SK1132,SK1133,
*SK1134,SK1135,SK1136,SK1137,SK1138,SK1139,SK1140,SK1141,
*SK1142,SK1143,SK1144,SK1145,SK1146,SK1147,SK1148,SK1149,
*SK1150,SK1151,SK1152,SK1153,SK1154,SK1155,SK1156,SK1157,
*SK1158,SK1159,SK1160,SK1161,SK1162,SK1163,SK1164,SK1165,
*SK1166,SK1167,SK1168,SK1169,SK1170,SK1171,SK1172,SK1173,
*SK1174,SK1175,SK1176,SK1177,SK1178,SK1179,SK1180,SK1181,
*SK1182,SK1183,SK1184,SK1185,SK1186,SK1187,SK1188,SK1189,
*SK1190,SK1191,SK1192,SK1193,SK1194,SK1195,SK1196,SK1197,
*SK1198,SK1199,SK1200,SK1201,SK1202,SK1203,SK1204,SK1205,
*SK1206,SK1207,SK1208,SK1209,SK1210,SK1211,SK1212,SK1213,
*SK1214,SK1215,SK1216,SK1217,SK1218,SK1219,SK1220,SK1221,
*SK1222,SK1223,SK1224,SK1225,SK1226,SK1227,SK1228,SK1229,
*SK1230,SK1231,SK1232,SK1233,SK1234,SK1235,SK1236,SK1237,
*SK1238,SK1239,SK1240,SK1241,SK1242,SK1243,SK1244,SK1245,
*SK1246,SK1247,SK1248,SK1249,SK1250,SK1251,SK1252,SK1253,
*SK1254,SK1255,SK1256,SK1257,SK1258,SK1259,SK1260,SK1261,
*SK1262,SK1263,SK1264,SK1265,SK1266,SK1267,SK1268,SK1269,
*SK1270,SK1271,SK1272,SK1273,SK1274,SK1275,SK1276,SK1277,
*SK1278,SK1279,SK1280,SK1281,SK1282,SK1283,SK1284,SK1285,
*SK1286,SK1287,SK1288,SK1289,SK1290,SK1291,SK1292,SK1293,
*SK1294,SK1295,SK1296,SK1297,SK1298,SK1299,SK1300,SK1301,
*SK1302,SK1303,SK1304,SK1305,SK1306,SK1307,SK1308,SK1309,
*SK1310,SK1311,SK1312,SK1313,SK1314,SK1315,SK1316,SK1317,
*SK1318,SK1319,SK1320,SK1321,SK1322,SK1323,SK1324,SK1325,
*SK1326,SK1327,SK1328,SK1329,SK1330,SK1331,SK1332,SK1333,
*SK1334,SK1335,SK1336,SK1337,SK1338,SK1339,SK1340,SK1341,
*SK1342,SK1343,SK1344,SK1345,SK1346,SK1347,SK1348,SK1349,
*SK1350,SK1351,SK1352,SK1353,SK1354,SK1355,SK1356,SK1357,
*SK1358,SK1359,SK1360,SK1361,SK1362,SK1363,SK1364,SK1365,
*SK1366,SK1367,SK1368,SK1369,SK1370,SK1371,SK1372,SK1373,
*SK1374,SK1375,SK1376,SK1377,SK1378,SK1379,SK1380,SK1381,
*SK1382,SK1383,SK1384,SK1385,SK1386,SK1387,SK1388,SK1389,
*SK1390,SK1391,SK1392,SK1393,SK1394,SK1395,SK1396,SK1397,
*SK1398,SK1399,SK1400,SK1401,SK1402,SK1403,SK1404,SK1405,
*SK1406,SK1407,SK1408,SK1409,SK1410,SK1411,SK1412,SK1413,
*SK1414,SK1415,SK1416,SK1417,SK1418,SK1419,SK1420,SK1421,
*SK1422,SK1423,SK1424,SK1425,SK1426,SK1427,SK1428,SK1429,
*SK1430,SK1431,SK1432,SK1433,SK1434,SK1435,SK1436,SK1437,
*SK1438,SK1439,SK1440,SK1441,SK1442,SK1443,SK1444,SK1445,
*SK1446,SK1447,SK1448,SK1449,SK1450,SK1451,SK1452,SK1453,
*SK1454,SK1455,SK1456,SK1457,SK1458,SK1459,SK1460,SK1461,
*SK1462,SK1463,SK1464,SK1465,SK1466,SK1467,SK1468,SK1469,
*SK1470,SK1471,SK1472,SK1473,SK1474,SK1475,SK1476,SK1477,
*SK1478,SK1479,SK1480,SK1481,SK1482,SK1483,SK1484,SK1485,
*SK1486,SK1487,SK1488,SK1489,SK1490,SK1491,SK1492,SK1493,
*SK1494,SK1495,SK1496,SK1497,SK1498,SK1499,SK1500,SK1501,
*SK1502,SK1503,SK1504,SK1505,SK1506,SK1507,SK1508,SK1509,
*SK1510,SK1511,SK1512,SK1513,SK1514,SK1515,SK1516,SK1517,
*SK1518,SK1519,SK1520,SK1521,SK1522,SK1523,SK1524,SK1525,
*SK1526,SK1527,SK1528,SK1529,SK1530,SK1531,SK1532,SK1533,
*SK1534,SK1535,SK1536,SK1537,SK1538,SK1539,SK1540,SK1541,
*SK1542,SK1543,SK1544,SK1545,SK1546,SK1547,SK1548,SK1549,
*SK1550,SK1551,SK1552,SK1553,SK1554,SK1555,SK1556,SK1557,
*SK1558,SK1559,SK1560,SK1561,SK1562,SK1563,SK1564,SK1565,
*SK1566,SK1567,SK1568,SK1569,SK1570,SK1571,SK1572,SK1573,
*SK1574,SK1575,SK1576,SK1577,SK1578,SK1579,SK1580,SK1581,
*SK1582,SK1583,SK1584,SK1585,SK1586,SK1587,SK1588,SK1589,
*SK1590,SK1591,SK1592,SK1593,SK1594,SK1595,SK1596,SK1597,
*SK1598,SK1599,SK1600,SK1601,SK1602,SK1603,SK1604,SK1605,
*SK1606,SK1607,SK1608,SK1609,SK1610,SK1611,SK1612,SK1613,
*SK1614,SK1615,SK1616,SK1617,SK1618,SK1619,SK1620,SK1621,
*SK1622,SK1623,SK1624,SK1625,SK1626,SK1627,SK1628,SK1629,
*SK1630,SK1631,SK1632,SK1633,SK1634,SK1635,SK1636,SK1637,
*SK1638,SK1639,SK1640,SK1641,SK1642,SK1643,SK1644,SK1645,
*SK1646,SK1647,SK1648,SK1649,SK1650,SK1651,SK1652,SK1653,
*SK1654,SK1655,SK1656,SK1657,SK1658,SK1659,SK1660,SK1661,
*SK1662,SK1663,SK1664,SK1665,SK1666,SK1667,SK1668,SK1669,
*SK1670,SK1671,SK1672,SK1673,SK1674,SK1675,SK1676,SK1677,
*SK1678,SK1679,SK1680,SK1681,SK1682,SK1683,SK1684,SK1685,
*SK1686,SK1687,SK1688,SK1689,SK1690,SK1691,SK1692,SK1693,
*SK1694,SK1695,SK1696,SK1697,SK1698,SK1699,SK1700,SK1701,
*SK1702,SK1703,SK1704,SK1705,SK1706,SK1707,SK1708,SK1709,
*SK1710,SK1711,SK1712,SK1713,SK1714,SK1715,SK1716,SK1717,
*SK1718,SK1719,SK1720,SK1721,SK1722,SK1723,SK1724,SK1725,
*SK1726,SK1727,SK1728,SK1729,SK1730,SK1731,SK1732,SK1733,
*SK1734,SK1735,SK1736,SK1737,SK1738,SK1739,SK1740,SK1741,
*SK1742,SK1743,SK1744,SK1745,SK1746,SK1747,SK1748,SK1749,
*SK1750,SK1751,SK1752,SK1753,SK1754,SK1755,SK1756,SK1757,
*SK1758,SK1759,SK1760,SK1761,SK1762,SK1763,SK1764,SK1765,
*SK1766,SK1767,SK1768,SK1769,SK1770,SK1771,SK1772,SK1773,
*SK1774,SK1775,SK1776,SK1777,SK1778,SK1779,SK1780,SK1781,
*SK1782,SK1783,SK1784,SK1785,SK1786,SK1787,SK1788,SK1789,
*SK1790,SK1791,SK1792,SK1793,SK1794,SK1795,SK1796,SK1797,
*SK1798,SK1799,SK1800,SK1801,SK1802,SK1803,SK1804,SK1805,
*SK1806,SK1807,SK1808,SK1809,SK1810,SK1811,SK1812,SK1813,
*SK1814,SK1815,SK1816,SK1817,SK1818,SK1819,SK1820,SK1821,
*SK1822,SK1823,SK1824,SK1825,SK1826,SK1827,SK1828,SK1829,
*SK1830,SK1831,SK1832,SK1833,SK1834,SK1835,SK1836,SK1837,
*SK1838,SK1839,SK1840,SK1841,SK1842,SK1843,SK1844,SK1845,
*SK1846,SK1847,SK1848,SK1849,SK1850,SK1851,SK1852,SK1853,
*SK1854,SK1855,SK1856,SK1857,SK1858,SK1859,SK1860,SK1861,
*SK1862,SK1863,SK1864,SK1865,SK1866,SK1867,SK1868,SK1869,
*SK1870,SK1871,SK1872,SK1873,SK1874,SK1875,SK1876,SK1877,
*SK1878,SK1879,SK1880,SK1881,SK1882,SK1883,SK1884,SK1885,
*SK1886,SK1887,SK1888,SK1889,SK1890,SK1891,SK1892,SK1893,
*SK1894,SK1895,SK1896,SK1897,SK1898,SK1899,SK1900,SK1901,
*SK1902,SK1903,SK1904,SK1905,SK1906,SK1907,SK1908,SK1909,
*SK1910,SK1911,SK1912,SK1913,SK1914,SK1915,SK1916,SK1917,
*SK1918,SK1919,SK1920,SK1921,SK1922,SK1923,SK1924,SK1925,
*SK1926,SK1927,SK1928,SK1929,SK1930,SK1931,SK1932,SK1933,
*SK1934,SK1935,SK1936,SK1937,SK1938,SK1939,SK1940,SK1941,
*SK1942,SK1943,SK1944,SK1945,SK1946,SK1947,SK1948,SK1949,
*SK1950,SK1951,SK1952,SK1953,SK1954,SK1955,SK1956,SK1957,
*SK1958,SK1959,SK1960,SK1961,SK1962,SK1963,SK1964,SK1965,
*SK1966,SK1967,SK1968,SK1969,SK1970,SK1971,SK1972,SK1973,
*SK1974,SK1975,SK1976,SK1977,SK1978,SK1979,SK1980,SK1981,
*SK1982,SK1983,SK1984,SK1985,SK1986,SK1987,SK1988,SK1989,
*SK1990,SK1991,SK1992,SK1993,SK1994,SK1995,SK1996,SK1997,
*SK1998,SK1999,SK2000,SK2001,SK2002,SK2003,SK2004,SK2005,
*SK2006,SK2007,SK2008,SK2009,SK2010,SK2011,SK2012,SK2013,
*SK2014,SK2015,SK2016,SK2017,SK2018,SK2019,SK2020,SK2021,
*SK2022,SK2023,SK2024,SK2025,SK2026,SK2027,SK2028,SK2029,
*SK2030,SK2031,SK2032,SK2033,SK2034,SK2035,SK2036,SK2037,
*SK2038,SK2039,SK2040,SK2041,SK2042,SK2043,SK2044,SK2045,
*SK2046,SK2047,SK2048,SK2049,SK2050,SK2051,SK2052,SK2053,
*SK2054,SK2055,SK2056,SK2057,SK2058,SK2059,SK2060,SK2061,
*SK2062,SK2063,SK2064,SK2065,SK2066,SK2067,SK2068,SK206
```



```

0045      AINOTL = AINLDI
0046      AINOTR = AINRDI
0047      SMOGJM = XLIM(DMLM,DNGC,DMSI*(DMSSEL+DMSLP*AINRPF)
0048      IMEGA = IMEGIC+GMOGJM
0049      THOM = THOMIC+UIC*THOMMX/UMX*THOCITJ-GDTHRT*DLTH*GDLTH
0050      CPMOJ = CMOOR
0051      CVMOR = CMOOR
0052      CPL = CP
0053      CPP = CP
0054      CNEPL = CNE
0055      CNFPP = CNF
0056      CSFPL = CSF
0057      CSFPR = CSF
0058      CPMOL = CPM
0059      CPMOR = CPM
0060      CPMOL = CPMO
0061      CPMOR = CPMO
0062      CVMOL = CVM
0063      CVMOR = CVM
0064      CVMRL = CVMR
0065      CVMR = CVMR
0066      PCTO = PCTO
0067      PCTOL = PCTO

0068      CONI = SMJ*SL*SL*(1.-SMN/SM)+ETVDP
0069      CALL SINCOS(PHLS*SGTORO,SPGLS,CPHGLS)
0070      CALL SINCOS(THF,SINTHE,COSTHE)
0071      CALL SINCOS(PHI,SINPHI,COSPHI)
0072      CALL SINCOS(PSI,SINPSI,COSPSI)
0073      CALL SINCOS(AINR,SININR,COSINR)
0074      CALL SINCOS(AINL,SININL,COSINL)
0075      CALL SINCOS(AINR-ALAMDA,SILAMP,CILAMP)
0076      CALL SINCOS(AINL-ALAMDA,SILAML,CILAML)
0077      CALL SINCOS(2.*AINR,S2INR,C2INR)
0078      CALL SINCOS(2.*AINL,S2INL,C2INL)
0079      CALL SINCOS(2.*(AINR-ALAMDA),SNDJIM,C2LAMR)
0080      CALL SINCOS(2.*(AINL-ALAMDA),SNDJIV2,C2LAVL)
0081      SSQINR = SININR * SININR
0082      SSQINL = SININL * SININL
0083      CALL SINCOS(AINW,SINIW,COSIW)
0084      AVETA = 0.5*(AINR+AINL)
0085      CALL SINCOS(PHIPH1,SPHIP,CPHIP)

C
C      GROUND TRACK
C
C      NORTHWARD VELOCITY
0086      VNORTHE = U*COSTHE*COSPSI+V*((SINPAI*SINTHE+COSPSI-COSPHI*(SINPSI)
      * +*(COSPHI*SINTHE+COSPSI+SINPHI*SINPSI))

```

Figure G.9. (Continued)


```

C      EASTWARD VELOCITY
0047  VEAST= U*COSTHE+V*SINPT+V*(SINPHI*SINTHE+STOPS)+COSPHI*(COSPT)
      = V*(COSPHI*STPTHE+ST*PT-SINPHI*(COSPSI))
C      NORTHWARD VELOCITY
0048  VNMW= -U*SINTHE+V*SINPHI*(COSTHE+W*COSPHI*(COSTHE
C      XDOT= VNMWTH
0049  YDOT= VFAST
0050  ZDOT= VDMW
0051  HDOT= -VDMW
0052  HSO= H*H
C      CENTER OF GRAVITY CALCULATION
C      CG LOCATION W.P.T. PIVOT
0054  XCG= (SME*SLF+S*W*SLW)/S4+SL*S*W/S4*(CILAM*U+CILAMP)
0055  ZCG= (SME*SHF+S*W*SHW)/S4-SL*S*W/S4*(SILAM*U+SILAMP)
C      CG VELOCITY W.P.T. PIVOT (NON-ROTATING AXES)
0056  XTCG= -SL*SMW/S4*(A1*DTL+SILAM*AT*DOT+SILAMP)
0057  ZTCG= -SL*SMW/S4*(A1*DTL+CILAM*AT*DOT+CILAMP)
C      DENSITY CALCULATIONS
C      EQUATION FOR DEL FROM CURVE FIT PROGRAM
0058  DEL= .049584347 - .362343204E-7*H
      + .567995171E-09*H50 - .372741304E-14*H50*H
C      TDEGE= TZERO - TDEFF*H
0059  THETC= .11927933*(TDEGE+459.69)
0100  SQTHC= SQRT(THETC)
0101  UNQVTC= 1. / THETC
0102  RPF= RPF0*DEL*UNQVTC
0103  RPI45= RPF*PI*ROTAN**5
0104  VTOTAL= SQRT(U*U+V*V+W*W)
0105  VCALTR= VTOTAL*SQRT(RPF/RPF0)
C      CHSELAGF= PIVOT VELOCITY
C      UP= U - Q*ZCG - XDOTCG
0107  VP= V + Q*ZCG - YDOTCG
0108  WP= W + Q*XCG - ZDOTCG
C      FUSELAGF AERODYNAMICS
C      INPUT EQUATIONS
0110  VALFS= SQRT(U*U+W*W)

```

5771415

Figure G.9. (Continued)

FORTRAN IV MODEL 44 PS VERSION 3, LEVEL 3 DATE 73092

```

0111 ALPHF= ATAN2(W*U)
0112 3TAF= ATAN2(V,VALES)
0113 SDF= (.5*ONE*VTOTAL*VTOTAL
C LEFT ROTOR HUB VELOCITY - BODY AXES
0114 URLP2 = UP + R*YA -ALS*SININL*(Q+AINDTL) + Q*HIL
0115 URLP2 = VP + RLS*(Q+COSINL+P*SININL) -P*HIL
0116 URLP2 = WP -P*YN -ALS*(Q+AINDTL)*COSINL + HIDL
C RIGHT ROTOR HUB VELOCITY - BODY AXES
0117 URLP2 = UP - R*YN -ALS*SININR*(Q+AINDTL) + Q*HIL
0118 URLP2 = VP + RLS*(Q+COSINR+P*SININR) -P*HIL
0119 URLP2 = WP +P*YN -ALS*(Q+AINDTL)*COSINR + HIDL
C LEFT ROTOR HUB VELOCITY - SHAFT AXES
0120 URL = URLP2*COSINL -WRLP2*SININL
0121 VRL = VRLP2
0122 URL = URLP2*SININL +WRLP2*COSINL
C RIGHT ROTOR HUB VELOCITY - SHAFT AXES
0123 URL = URLP2*COSINR -WRLP2*SININR
0124 VRL = VRLP2
0125 URL = URLP2*SININR +WRLP2*COSINR
C ROTOR INPUT EQUATIONS (AF20)
C
C FREE STREAM VELOCITY
0126 VTOTR = SQRT(U**2+V**2+W**2)
0127 VTOTL = SQRT(URL**2+VRL**2+WRL**2)
0128 WOTL = WRL+P*WRL*HIL
0129 WOTR = WRL + EPWRQ*UPP
0130 VZFTL = SQRT(VRL**2+WOTL**2)
0131 VZETR = SQRT(VPR**2+WOTR**2)
C ANGLE OF ATTACK
C
C NOTE ALPHA0 AND ALPHA1 ARE DEFINED BETWEEN 0 AND 180 DEGREES
C I.E. 90 +DP- 90 DEGREES
0132 ALPHR= ATAN2(VZFTL,URL) + EPTRL
0133 ZETHL= ATAN2(VRL,WOTL)
0134 CALL SINCOS(ZETHL,SINZHL,COSZHL)
0135 ALPHR= ATAN2(VZETR,URR) + EPILR
0136 ZETHR= ATAN2(VRR,WOTR)
0137 CALL SINCOS(ZETHR,SINZHR,COSZHR)
C
C ROTOR ANGULAR RATE TRANSFORMS
C
C LEFT ROTOR - VACELLE AXES
0138 PNLN = P*COSINL - P*SININL
0139 QNLN = Q + AINOTL
0140 RNLN = P*SININL + R*COSINL
C LEFT ROTOR - WIND AXES
0141 PNLR = PNLN

```

Figure G.9. (Continued)

```

0142 QNLQ = QNLN*COSZHL - RNLN*SINZHL
0143 QNLF = QNLN*COSZHL + QNLN*SINZHL
C   QNLT = ROTPR - NACELLE AXES
0144 PNPQ = -P*COSIPR + R*SINIPR
0145 QPNQ = Q + A*INDO
0146 RPNQ = -P*SINIPR - Q*COSIPR
C   RQNT = ROTPR - WIND AXES
0147 PNPQ = PNPQ
0148 QPNQ = QPNQ*COSZHR + RPNQ*SINZHR
0149 RPNQ = RPNQ*COSZHR - QPNQ*SINZHR
C
0150 QMEGAL = OMEGA + PNLQ
0151 QMEGAN = OMEGA + PNLQ
0152 VTIPL = ROTRAD * OMEGAL
0153 VTIPR = ROTRAD * OMEGAR
0154 AMUL = VTOTLR/VTIPL
0155 AMUR = VTOTRR/VTIPR
0156 CMQR = CMQR - CMQR*QNRQ
0157 CMQR = CMQR + CMQR*QNRQ
0158 CMQL = CMQL - CMQL*QNLQ
0159 CMPL = CMQL + CMQL*QNLQ
C
C   BASIC EQUATIONS OF MOTION -- PRELIMINARY CALCULATIONS
C   CHSELAGE
C   XF = SLF - XCG
C   YF = SHF - ZCG
C
C   WING
C   XW = SLW - XCG
C   YW = SHW - ZCG
C
C   NACELLES
C   QR = SL * CILQK - XCG
C   YQ = -SL * SILQK - ZCG
C
C   XL = SL * CILXL - XCG
C   YL = -SL * SILXL - ZCG
C   IMEDTIA TERMS
0168 SUMIXX = FIXX + FIXX + 2.*FIXXR
0169 SUMIYY = FIYY + FIYY + 2.*FIYYR
0170 SUMIZZ = FIZZ + FIZZ + 2.*FIZZR
0171 SUMIXZ = FIXZ + FIXZ + 2.*FIXZR
C
0172 FIXX = SUMIXX + (FIZZR - FIXXR)*(SSOIVP + SSOIUL) - FIXZR*(S2INR + S2IUL)
      + 2.*SMN*YN*YV + S*F*SHF*ZF + SMW*SHW*ZW - SL*SMN*(ZR*SILAMR +

```

Figure G.9. (Continued)

```

0173      C      ZL* SILAML )
      FIXX = (SUMI77-SUMIYY)+(FIXXPP-FI7ZPP)*(SS2INR+SS2INL)-FIX7PP*(
      S2INR+S2INL)+2.*SMN*YN*YI-(34F*SHF*ZF+SMN*SL*70*CI*LA*Z) +
      SL*SMN*(ZR* SILAMR+ZL*SILAML)

0174      C      FIXZP = FIXZF+FIXZWP+.5*(FIXXPP-FI7ZPP)*(S2INR+S2INL)+FIXZPP*(
      C2INR+C2INL)+(SMF*SLF*ZF+SMN*SL*70*CI*LA*Z)+
      ZL* SILAML )

0175      C      FIYY = SUMIYY+SMF*(SLF*XF+SHF*ZF)+SMN*(SLW*XM+SHW*Z4) +SMN* SL*
      (XP*GILAMR-ZR*SILAMR)+SMN*SL*(XL*GILAML-ZL*SILAML)

0176      C      FIYY = (FIXXF-FI7ZF)+(FIXXW-FI7Z4)+(FIXXPP-FI7ZPP)*(C2INR+C2INL)
      -2.*FIXZPP*(S2INR+S2INL)+S4F*(-SLF*XF+SHF*ZF) +SMN*(-CI*W*
      XM+SHW*Z4)-SMN*SL*(XR*GILAMR+ZR*SILAMR +XL*GILAML+ZL*SILAML)

0177      C      FIXZQ = FIXZF+FIXZWP+.5*(FIXXPP-FI7ZPP)*(S2INR+S2INL) +FIXZPP*
      (C2INR+C2INL)-SMN*SL*(XP*GILAMR+XL* SILAML )

0179      C      FI7Z = SUMI77+FIXXPP-FI7ZPP*(SS2INR+SS2INL)+FIXZPP*(S2INR+
      S2INL)+2.*SMN* YN*YI+SMF*SLF*ZF+SMN*SLW*XM+SMN*SL*(XP*
      GILAMR +XL*GILAML)

0179      C      FI77 = SUMIYY-SUMIXX +(FIXXPP-FI7ZPP)*(SS01UP+SS214L)+FIX7PP*(
      S2INR+S2INL) -2.*SMN* YN*YI+SHF*SLF*XF+S21*SL*W*XM +SMN*SL*
      (XP*GILAMR +XL*GILAML)

0180      C      FIXZ4 = FIXZF+FIXZWP+.5*(FIXXPP-FI7ZPP)*(S2INR+S2INL)+FIXZPP*
      (C2INR+C2INL) +SMF*SLF*XF +SMN*SLW*XM -SL*SMN*(XR*GILAMR+
      XL*SILAML )

0181      C      ALARMN = ALARP+ALARIC*FIXX
0182      C      AMAPIN = AMARP+AMARIC*FIYY
0183      C      ZARMN = ZARP+ZARIC*SM
0184      C      ALAERN = ALAERP+ALARWI
0185      C      AMAERN = AMAFRP+AMARWN
0186      C      ZAERN = ZARPD+ZARWN

0187      C      ROOT EQUATION CROSS TERMS
      TERMP1 = -FJXX*RR*O*P*O*FI7ZP

0188      C      ROOT EQUATION CROSS TERMS
      TERMO1 = -FJYY*O*P*O -FIXZQ*(P*P -R*P)

0189      C      ROOT EQUATION CROSS TERMS
      TERMR1 = -FJZZ*P*P*Q -FIXZRR*Q

```

Figure G.9. (Continued)

```

C
C      ROOT EQUATION  ROOT COEFFICIENT
0190  C      MATAC(1,1) = C1XX
C      ROOT EQUATION  ROOT COEFFICIENT
0191  C      MATAC(1,2) = C1
C      ROOT EQUATION  ROOT COEFFICIENT
0192  C      MATAC(1,3) = -FIXZP
C      ROOT EQUATION  AINDOR COEFFICIENT
0193  C      MATAC(1,4) = -SL*SMN*YN * CILAMR
C      ROOT EQUATION  AINDOL COEFFICIENT
0194  C      MATAC(1,5) = SL*SMN*YN * CILAML
C      ROOT EQUATION  FORCING FUNCTION
0195  C      MATB(1,1) = TERMP1 + ALAERO
C
C
C      ROOT EQUATION  ROOT COEFFICIENT
0196  C      MATAC(2,1) = C1
C      ROOT EQUATION  ROOT COEFFICIENT
0197  C      MATAC(2,2) = C1VV
C      ROOT EQUATION  ROOT COEFFICIENT
0198  C      MATAC(2,3) = C1
C      ROOT EQUATION  AINDOR COEFFICIENT
0199  C      MATAC(2,4) = FIVVDB+SL*SMN*(-ZR*SLAMR +XZ*CILAMR )
C      ROOT EQUATION  AINDOL COEFFICIENT
0200  C      MATAC(2,5) = FIVVDB+SL*SMN*(-ZL*SLAML +XL*CILAML )
C      ROOT EQUATION  FORCING FUNCTION
0201  C      MATB(2,1) = TERMP1 + ANAERO
C
C
C      ROOT EQUATION  ROOT COEFFICIENT
0202  C      MATAC(3,1) = -FIXZP
C      ROOT EQUATION  ROOT COEFFICIENT
0203  C      MATAC(3,2) = C1
C      ROOT EQUATION  ROOT COEFFICIENT
0204  C      MATAC(3,3) = F1Z7
C      ROOT EQUATION  AINDOR COEFFICIENT
0205  C      MATAC(3,4) = SMN*SL*YN*SLAMR
C      ROOT EQUATION  AINDOL COEFFICIENT
0206  C      MATAC(3,5) = -SMN*SL*YN*SLAML
C      ROOT EQUATION  FORCING FUNCTION
0207  C      MATB(3,1) = TERMP1 + ANAERO
C
C
C      AINDOR EQUATION ROOT COEFFICIENT
0208  C      MATAC(4,1) = C1
C      AINDOR EQUATION ROOT COEFFICIENT
0209  C      MATAC(4,2) = C1
C      AINDOR EQUATION ROOT COEFFICIENT
0210  C      MATAC(4,3) = C1
C      AINDOR EQUATION AINDOR COEFFICIENT

```

Figure G.9. (Continued)

```

0211      MATA(4,4)= 1.0
           AINDOL EQUATION AINDOL COEFFICIENT
0212      MATA(4,5) = 0.
           AINDOL EQUATION FORCING FUNCTION
0213      MATR(4)= 0MIRF**2*(AIRF+GINF**OCVIC-AIRL)-2.*CTAIRF*UMTIC*AINDT
           C
           AINDOL EQUATION POUT COEFFICIENT
0214      MATA(5,1) = 0.
           AINDOL EQUATION QOUT COEFFICIENT
0215      MATA(5,2) = 0.
           AINDOL EQUATION POUT COEFFICIENT
0216      MATA(5,3) = 0.
           AINDOL EQUATION AINDOL COEFFICIENT
0217      MATA(5,4) = 0.
           AINDOL EQUATION AINDOL COEFFICIENT
0218      MATA(5,5)= 1.0
           AINDOL EQUATION FORCING FUNCTION
0219      MATR(5)= 0MIRF**2*(AIRF+GINF**OCVIC-AIRL)-2.*CTAIRF*UMTIC*AINDT
           C
           SAVE MATR APPAY
           DO 10 JJ=1,5
0220      MATRSV(JJ)= MATR(JJ)
           DO 20 KK=1,5
0221      MATSAV(JJ,KK)= MATR(JJ,KK)
           CONTINUE
0222      CONTINUE
           CALL MATINV(MATA,5,5,MATR,1,DET)
           C
           POUT = MATR(1)
           QOUT = MATR(2)
           ROUT = MATR(3)
           AINDOL= MATR(4)
           AINDOL= MATR(5)
           C
           RESTORE MATR APPAY
           DO 30 JJ=1,5
0223      MATR(JJ)= MATRSV(JJ)
           DO 40 KK=1,5
0224      MATA(JJ,KK)= MATSAV(JJ,KK)
           CONTINUE
0225      CONTINUE
           C
           C
           C
           AIRCRAFT CONDITION CALCULATIONS
           C
           C
           C
           LINEAR EQUATIONS OF MOTION (PSI,THETA,PHI FULER SYSTEM)
           UDOT = XAERO /SM -SG*SINPHI -Q*V + R*V
           VDOT = YAERO /SM +SG*CSINPHI*SINPHI -R*U + P*V
           WDOT = ZAERO /SM +SG*CSINPHI*COSPHI -Q*U - P*V
           C
           FULER ANGLE CALCULATION PSI,THETA,PHI SYSTEM
           THEDOT = Q*CSINPHI - R*SINPHI

```

Figure G.9. (Continued)

FORTRAN IV MODEL 44 PS VERSION 3, LEVEL 3 DATE 73-92

```

0242 PHIDOT = P + (C*SINPHI + P*CDSPHI) * SINTH / CUSTHE
0243 PSIDOT = (C* SINPHI + P* CDSPHI) / CUSTHE

C
C C.G. ACCELERATION F.R.T. PIVOT (NON-ROTATING AXES)
0244 XDCG = -SL*SMN/SM*(AINDL*SLAML + AINDL*AINDL*SLAML + AINDL*P*
      * SLAML + AINDL*AINDL*SLAML)
0245 ZDCG = -SL*SMN/SM*(AINDL*SLAML + AINDL*AINDL*SLAML + AINDL*P*
      * SLAML + AINDL*AINDL*SLAML)

C
C PILOT STATION ACCELERATIONS (BODY AXES)
0246 AVAIL = 12345678.
0247 ACCXPA = XAERQ/SM - YDDCG
0248 ACCYPA = YAERQ/SM - PDOT*(XCG-SIPA)
0249 ACCZPA = ZAERQ/SM + PDOT*(XCG-SIPA) - ZDDCG + SG

C
C PILOT STATION VELOCITIES (BODY AXES)
0250 VPA = UP + P*ZPA - R*YPA
0251 VPA = VP + R*SLPA - P*ZPA
0252 VPA = WP + P*VPA - Q*SLPA

C
0253 AMACDP = ( SMN*SL*Y*ACILAMR*PDOT - (SMN*SL*SL*(1.-SMN/SM)*FIVYD*
      * (PDOT+AINDDP) - SM*SL*Y*SLAML*PDOT)
0254 AMACDP = (-SMN*SL*Y*ACILAML*PDOT - (SMN*SL*SL*(1.-SMN/SM)*FIVYD*
      * (PDOT+AINDDL) + SMN*SL*Y*SLAML*PDOT)
0255 AIRPD = XLIM(AMACDP, -ATNPLM, ATNCPH)

C
C THRUST MANAGEMENT SYSTEM
0256 DLTRPD = GTH/TAUTH*DELTH - DLTHP/TAUTH
0257 AEHG = XLIM(ALIM, -1.0, AO-ASLP*SHPIC)
0258 SHP1 = SHPRP*AEHG
0259 DSHP = SHP1-SHPIC
0260 DSHP = SHP1-SHP2IC
0261 SHP2 = CVTAD*DSHP
0262 DSHP = SHP2IC-SHP3IC
0263 SHP3 = CVTAE*SQTHC/DEL*DSHP
0264 SHP4 = SHPRP+SHP3IC-SHP1
0265 SHPD = XLIM(SHPLM, -SHPLM, (SHP4-SHPIC)/TAUSHP)
0266 JAVL = SHPIC/OMEGA
0267 CPO = 0.5*(CPL+CPE)
0268 PRD = CPO*OMEGA**2
0269 PDOT = (50.*QAVL-R)*PRD/ELP
0270 DLTH = CMEGA - OAGC
0271 THOM = XLIM(THOMLM, -THMLM, COM*DLTH)
0272 THOM = XLIM(THOMLM, -THMLM, COM*DLTH)
0273 TMS2 = THOM + DTHOM*COM*DLTH*GDTHPT*DLTH*DLTH
0274 TMS1 = XLIM(THRLM, -THPLM, 1./1*(TMS2-TMS1-TTHM-GDTHPT*DLTH*
      * DLTH))

```

Figure G.9. (Continued)

FORTRAN IV MODEL 44 PS VERSION 3, LEVEL 3 DATE 73002

0275 TMS3= XLIM(THATL4,-THATLM,TMS2-TMS1-T43M-GDTURT*DLTHP*GDLTH)
 0276 THMS = XLIM(TTMSLP,TTMSLN,TMS1+THCM+TMS3+GDTURT*DLTHP*GDLTH)
 0277 THMSR = THMS+GT4G,OV*THGVR
 0278 THMSI = THMS+GTHGOV*THGOVL

C
 C
 C
 C

RTOR THRUST

0279 CTRCM = RDT1 + CTC*TAURO1/TAURQ2*SFTR
 0280 RDT10 = CTC/TAURQ2*SFTR-CTRPCM/TAURQ2
 0281 CILPRM = RDT2+CTC*TAURO1/TAURQ2*SFTR
 0282 RDT20 = CTC/TAURQ2*SFTR-CILPRM/TAURQ2

C
 C
 C
 C

SAS (LATERAL, LONGITUDINAL)

PITCH SAS

0283 PSAS10 = (DELR-PSAS1)/TAURR
 0284 PSAS5 = (GJ*Q-GDB2*PSAS1)/TAUC1
 0285 PSAS6 = (GTHE*Q-GDB1*PSAS1)*TAUT4F/TAUT4E
 0286 GLONPH = XLIM(1.0,0.9GLP-GLPSLP*VCALTR)
 0287 PSAS20 = PSAS5*GLONPH-PSAS2/TAUC1
 0288 PSAS30 = PSAS6*GLONPH-PSAS3/TAUTHE
 0289 PSAS7 = PSAS2+PSAS3-PSAS4
 0290 PSAS40 = PSAS7/TAU2
 0291 DELR5 = XLIM(DELRM,-OLRLM,PSAS7+OLSLIC)

C

ROLL SAS

0292 RSAS10 = (GPOS*DEL6-R*PSAS1)/TAUPDS
 0293 PSAS20 = (GP*P-PSAS2)/TAUP
 0294 RSAS40 = (RETAF-R*PSAS4)/TAURET
 0295 RSAS55=GRPHI*P*TAUPHI/TAUPHI
 0296 RSAS30 = PSAS5*GLATPH-R*PSAS3/TAUPHI
 0297 RSAS6 = PSAS2+PSAS3-R*PSAS1
 0298 DELS5 = XLIM(OLSLM,-OLSLM,PSAS6+GROLL-PSAS4*GRFETP*30ETOH)

C

YAW SAS

0299 YSAS20 = (DELR-YSAS2)/TAURR
 0300 YSAS7 = XLIM(RLM,-PLM,R)
 0301 YSAS9 = XLIM(DRLM,-DRLM,YSAS7)
 0302 YSAS3 = (GPSI*YSAS7-GPSI0K*YSAS9)*TAJPS1/TAJPS1
 0303 YSAS10 = YSAS8*GLATPH4-YSAS1/TAUPSI
 0304 YSAS10 = XLIM(DELRMX,-DELRMX,-G3ETP*YSAS4-GRFETR*YSAS2)
 0305 GLATPR = 1.-GLATPH4
 0306 YSAS11 = YSAS1+YSAS10*GLATPR
 0307 YSAS40 = (P*GPPPH-YSAS3)/TAUPR
 0308 YSAS12 = GP*R-GPDR*YSAS2-YSAS6
 0309 YSAS13 = YSAS12
 0310 IF(VCALTR-17.00FT1*SKFPS) YSAS13 = -YSAS4
 0311 YSAS40 = YSAS13/TAURI
 0312 YSAS14 = YSAS12*TAUP2/TAUP3+YSAS5
 0313 YSAS50 = (YSAS12-YSAS14)/TAUP3

Figure G.9. (Continued)


```

0314 YSAS15 = P
0315 IF (VICALIP.LT.WPCTI*SKRPS) YSAS15 = .
0316 YSAS16 = YSAS15*GYAW
0317 YSAS17 = (CPH1*YSAS16*TAUPR1-YSAS6)/TAUPR1
0318 YSAS17 = YSAS16-YSAS6
0319 DELR5 = XLIM(DCLP1)*DELPL1,YSAS11*GDSIPR1+YSAS3+YSAS17*GYAW)

C
C
C      CONTROL EQUATIONS
C
0320 DELRT = DELR
0321 DELST = DELS - DELSS
0322 DELRT = DELR - DELRS
0323 DELRJD = -SKDLR0*DELRT
0324 DELFLV = -SKDLF*DELRT + GDF*DELTR0
0325 DELFLP = GDFLP
0326 DELA12 = -XLIM(D1)*DELAMX,SKDA*DELST)
0327 DELA12 = XLIM(DELAMX*,*,SKDA*DELST)
0328 DELA12 = XLIM(DELAT14,0.,DELAR0*DELST)
0329 DELA11 = XLIM(DELAL4,0.,DELAL2*DELFLP)
0330 DELAR = DELA11 + DELFLP
0331 DELAL = DELA11 + DELFLP
0332 DELSPR = XLIM(DLSPM,*,0,GDSPI)
0333 DELSPL = -XLIM(D1)*DLSPLM,GDSPI)
0334 DELRT*SKDLR*GDSCYL-DELST*SKDLR*GDSCYL
0335 DELST*SKDLR*GDSCYL
0336 DELRT*SKDLR*GDSCYL-DELST*SKDLR*GDSCYL
0337 DELRT*SKDLR*GDSCYL-DELST*SKDLR*GDSCYL
0338 DELRT*SKDLR*GDSCYL-DELST*SKDLR*GDSCYL
0339 DELRT*SKDLR*GDSCYL-DELST*SKDLR*GDSCYL
0340 GLSR0 = GLSB/TAUGLS-GLSHIC/TAUGLS
0341 GLSAP0 = GLSAR/TAUGLS-GLSAT/TAUGLS
0342 GLSAL0 = GLSAL/TAUGLS-GLSAIL/TAUGLS
C
0343 BIRP00 = GMA**2*(GRICP-DCYL-DLON)-2.*ETA*GMA*BIC000
1 - GMA**2*BIC00
0344 YILP00 = GMA**2*(GALCP+DCYL-DCYL)-2.*ETA*GMA*BILCP0
1 - GMA**2*BILCP0
0345 AIRP00 = GMA**2*(-GLSAP0-SKDCOL*DCYL+GALCP)-2.*ETA*GMA*AIC000
1 - GMA**2*AIC00
0346 AILP00 = GMA**2*(GLSAIL+SKDCOL*DCYL+GALCP)-2.*ETA*GMA*AIC000
1 - GMA**2*AIC00
0347 BIC000 = G4P0**2*BICRP-2.*ETA*GMA*BRD*BICR01-BIR0**2*BICR1C
0348 BICL00 = G4P0**2*BICLP-2.*ETA*GMA*BRD*BICL01-BIR0**2*BICL1C
0349 AICR00 = G4P0**2*AICRP-2.*ETA*GMA*BRD*AICR01-BIR0**2*AICR1C
0350 AICL00 = G4P0**2*AICLP-2.*ETA*GMA*BRD*AICL01-BIR0**2*AICL1C
0351 TH751 = XLIM(TH751,2,TH75LN,TH75R-DCOL)
0352 TH75L = XLIM(TH751,2,TH75LN,TH75L+DCOL)
C

```

Figure G.9. (Continued)

```

C
C      WING VERTICAL BENDING
C
C353      ALA2(0) = DMH*2*(ALARP-ALARP)/FIXX-2.*ETAW*DMH*ALARP
C354      ALA3(0) = DMH*2*(AMARP-AMARP)/FIYY-2.*ETAW*DMH*AMARP
C355      ZAP(0) = (DMH*2*(ZARP-ZARP)/SM-2.*ETAF*DMH*ZARP)
C
C356      CALL ANDAIN(PROJ, RNDOS(1), LETP(1), FPC(1), ACOUN(1), P1, 3, 3)
C357      CALL ANDAIN(PROJ, RNDOS(2), LETP(2), FPC(2), ACOUN(2), P2, 3, 3)
C358      CALL ANDAIN(PROJ, RNDOS(3), LETP(3), FPC(3), ACOUN(3), P3, 3, 3)
C359      CALL ANDAIN(PROJ, RNDOS(4), LETP(4), FPC(4), ACOUN(4), P4, 3, 3)
C
C      DAC CALCULATION SECTION
C
C360      P1(2,0) = -ALPH/ARFSMX
C361      P1(2,1) = (ALARP+TERMP1)/FIXX/RODTMX
C362      P1(2,2) = -MATA(1,3)/FIXX*RODTMX/RODTMX
C363      P1(2,3) = (AMARP+TERMP1)/FIYY/RODTMX
C364      P1(2,4) = -MATA(1,4)/FIXX*ATODMX/RODTMX
C365      P1(2,5) = MATA(3,4)/FI77 / RODTMX
C366      P1(2,6) = -MATA(1,5)/FIXX*ATODMX/RODTMX
C367      P1(2,7) = XAFR1/ SW /LODTMX
C368      P1(2,8) = JTFIM*SKRPS/U4X
C369      P1(2,9) = YAFR1/ SW /VRODTMX
C370      P1(2,10) = VTRIM*SKRPS/VW4X
C371      P1(2,11) = ZAFR1 / SM / ZAROMX
C372      P1(2,12) = -HTRIM/ZMX
C373      P1(2,13) = VCALIP/ZMX
C374      P1(2,14) = -MATA(2,4)/FIYY*ALODMX/RODTMX
C375      P1(2,15) = VTOTLR/SOTRAD/AMJPMX/ARFSMX
C376      P1(2,16) = -MATA(2,5)/FIYY*ALODMX/RODTMX
C377      P1(2,17) = -ALPHLR / ALFRMX
C378      P1(2,18) = THTRIM/THFMX/RODTMX
C379      P1(2,19) = VTOTPR/PGTRAD/AMJRMX/ME5MX
C380      P1(2,20) = -AVEALW / ALWGMX
C381      P1(2,21) = -ALPHRR / ALFRMX
C382      P1(2,22) = -MATA(3,1)/FI7Z*RODTMX/RODTMX
C383      P1(2,23) = PNLN/DMFGMX
C384      P1(2,24) = -MATA(3,4)/FI7Z*ATODMX/RODTMX
C385      P1(2,25) = PNRN/DMFGMX
C386      P1(2,26) = -MATA(3,5)/FI7Z*ATODMX/RODTMX
C387      P1(2,27) = -VNDTH/XRODTMX
C388      SGNOSQF = 1.0
C389      IF(U.LT.C.) SGNOSQF = -1.0
C390      P1(2,28) = -SQF*SGNOSQF/SQF*MX
C391      P1(2,29) = -VEAST/VRODTMX
C392      P1(2,30) = -BETAF / ARFS*MX
C393      P2(2,0) = -SMN*SL*VN*CLAMR*RODTMX/AMACMX
C394      P2(2,1) = GLSR/GLSMX
C395      P2(2,2) = (SMN*SL*SL*1.-SMN/SM)+FIYPRI*RODTMX/AMACMX
C396      P2(2,3) = -GLSAL/GLSMX
C397      P2(2,4) = SMN*SL*VN*SLAMR*RODTMX/AMACMX

```

Figure G.9. (Continued)

```

0398 P2(125) = (XCG-SLPA)/XCG1X
0399 P2(126) = WDTOT14/VW1X/AC
0400 P2(127) = SHDPP/SUDMX
0401 P2(128) = SMN*SLAYN*CLLAL*DOT1X/AVAG1X
0402 P2(129) = -SQTATC/NFL*TAUFMX/GUTON
0403 P2(130) = (SMN*SL*SL*U1-SM/SW)+E1YDPI*DOT1X/AVAG1X
0404 P2(131) = -SMN*SL*YV*CLLAL*DOT1X/AVAG1X
0405 P2(132) = ATT14/AT1MX /DOT1DG
0406 P2(133) = ALAPP/F1XX/DOT1MX
0407 P2(134) = WDRIP5/FIP*MEG1X*CMX /2. /17.
0408 P2(135) = AWARP/F1YV/DOT1MX
0409 P2(136) = ZARP/SW/ZARMX
0410 P2(137) = -QNR / QMX * CPMQ1X / CPM1X
0411 P2(138) = GLSAR/GLSMX
0412 P2(139) = -QNL / QMX * CUM1X / CPM1X
0413 P2(140) = RNR / RMX * CYP1X / CPM1X
0414 P2(141) = RNL / RMX * CYP2X / CPM1X
0415 P2(142) = PCTOR / PCT1X

```

87AP5 IF (CONSOLE 1) POT. CALCULATION SECTION

```

0416 P1(130) = -ZIC/ZMX
0417 P1(131) = VIC/VMX
0418 P1(132) = VW1X/Z1X/GUTON
0419 P1(133) = YDOT1X/VMX/GUTON
0420 P1(134) = XDOT1X/X1X/GUTON
0421 P1(135) = SKTRIM(1)
0422 P1(136) = SKTRIM(2)
0423 P1(137) = XIC/XMX
0424 P1(138) = 1./TAUR02/GUTON*SFTR
0425 P1(139) = TAUR01/TAUR02*SFTR
0426 P1(140) = 1./TAUR02/GUTON
0427 P1(141) = 1./TAUR02/GUTON*SFTR
0428 P1(142) = TAUR01/TAUR02*SFTR
0429 P1(143) = 1./TAUR02/GUTON
0430 P1(144) = R7.*SKEPS/UMX
0431 P1(145) = UMX/VW1X/17.
0432 P1(146) = THEMX/PI
0433 P1(147) = PH1MX/PI
0434 P1(148) = 141.*SKEPS/UMX
0435 P1(149) = ROT1 / CTMX
0436 P1(150) = ROT2 / CTMX
0437 P1(151) = 1./17.
0438 P1(152) = 1./17.
0439 P1(153) = WDT1 *SKEPS / IMX
0440 P1(154) = SKTRIM(3)
0441 P1(155) = SKTRIM(4)
0442 P1(156) = SKTRIM(5)
0443 P1(157) = SKTRIM(6)

```

Figure G.9. (Continued)

```

0444      P1(240) = PIC/PMX
0445      P1(241) = QIC/PMX
0446      P1(242) = PDOTMX/PMX/GRUTON
0447      P1(243) = PDOTMX/PMX/GRUTON
0448      P1(244) = RDOTMX/PMX/GRUTON
0449      P1(245) = RIC/RMX
0450      P1(246) = VDOTMX/VMMX/GRUTON
0451      P1(247) = WDOTMX/VMMX/GRUTON
0452      P1(250) = UDOTMX/UMX/GRUTON*10.
0453      P1(251) = THOMX/THMX/GRUTON
0454      P1(252) = SG*1.0/UDOTMX/10.
0455      P1(253) = QMX*VMMX/UDOTMX/10.
0456      P1(254) = PMX*VMMX/UDOTMX/10.
0457      P1(255) = UIC/UMX
0458      P1(256) = SG*1.0/VDOTMX/10.
0459      P1(257) = PMX*UMX/VDOTMX/10.
0460      P1(264) = PMX*VMMX/VDOTMX/10.
0461      P1(265) = ZAPMX/WDOTMX/10.
0462      P1(266) = SG*1.0/VDOTMX/10.
0463      P1(267) = QMX*UMX/VDOTMX/10.
0464      P1(270) = PHOMX/PHIMX/GRUTON
0465      P1(271) = PSDMX/PSIMX/GRUTON*10.
0466      P1(272) = VIC/VMMX
0467      P1(273) = WIC/VMMX
0468      P1(274) = THEIC/THMX
0469      P1(275) = PHIIC/PHIMX
0470      P1(276) = PMX*VMMX/WDOTMX/10.
0471      P1(277) = PSIC/PSIMX
0472      P1(300) = RSAS1/DELSMX
0473      P1(301) = PSAS2/DELSMX
0474      P1(302) = GPDS/TAUPDS*DELSMX/DELSMX/GRUTON
0475      P1(303) = 1.0/TAUPDS/GRUTON
0476      P1(304) = GP/TAUP*PMX/DELSMX/GRUTON
0477      P1(305) = 1.0/TAUP/GRUTON
0478      P1(306) = GPHI*PMX/DELSMX/GRUTON
0479      P1(307) = 1.0/TAUPHI/GRUTON
0480      P1(310) = RSAS3/DELSMX
0481      P1(311) = RSAS4/ARFSMX
0482      P1(312) = 1.0/TAURET/GRUTON
0483      P1(313) = 1.0/TAURET/GRUTON
0484      P1(314) = GBETO*ARFSMX/DELSMX-1.0
0485      P1(315) = 1.0/TAUPSI/GRUTON
0486      P1(316) = DLSLM/DELSMX
0487      P1(317) = DLSLM/DELSMX
0488      P1(320) = YSAS1/DELRMX
0489      P1(321) = YSAS2/DELRMX
0490      P1(322) = GPSI*RMX/DELRMX/GRUTON
0491      P1(323) = GPSIOR/GRUTON
0492      P1(324) = 1.0/TAUDP*DELRMX/DELRMX/GRUTON

```

Figure G.9. (Continued)

```

0493 P1(325) = 1./TAURK/GRUTON
0494 P1(326) = PLW/RMX
0495 P1(327) = PLW/RMX
0496 P1(331) = VSAS2/DELFMX
0497 P1(331) = VSAS6/DELFMX
0498 P1(332) = GRETDP/1.
0499 P1(333) = GRETDP*AGFSMX/DELFMX/1.
0500 P1(334) = 2./TAURK*DMX/DELFMX/GRUTON
0501 P1(335) = 1./TAURK/GRUTON
0502 P1(336) = DRLM/DELFMX
0503 P1(337) = DRLM/DELFMX
0504 P1(340) = VSAS4/DELFMX
0505 P1(341) = VSAS5/DELFMX
0506 P1(342) = GROR
0507 P1(343) = 1./TAUR3/GRUTON
0508 P1(344) = 1./TAUR3/GRUTON
0509 P1(345) = TAUP2/TAUR3
0510 P1(346) = GR21DMX/DELFMX/GRUTON
0511 P1(347) = 1./TAURP1/GRUTON
0512 P1(353) = (R*SMX/DELFMX/1.
0513 P1(351) = 1./TAUR1/GRUTON/0.1
0514 P1(352) = GRETDP*0.1
0515 P1(354) = 1.0
0516 P1(355) = 1.0
0517 P1(356) = DRLM/DELFMX
0518 P1(357) = DRLM/DELFMX

      3ARD 34      (C) (S) (L) (F) (2)      POT. CALCULATION SECTION

0519 P2(031) = DLTHP/DLTHMX
0520 P2(031) = SHP2IC/SHPMX
0521 P2(032) = GTH/TAUTH/GRUTON
0522 P2(033) = 1.0/TAUTH/GRUTON
0523 P2(034) = OMLM/OMEGMX
0524 P2(037) = OMG0/OMEGMX
0525 P2(031) = SHP3IC/SHPMX
0526 P2(031) = -OMEGIC/OMEGMX
0527 P2(031) = OMSL*AINMX /OMEGMX
0528 P2(031) = OMG0/OMEGMX
0529 P2(034) = 550./FID*SHPMX/OMEGMX/145MX
0530 P2(035) = GTHG0V/TTW5MX
0531 P2(035) = THW1IC/THW1MX
0532 P2(037) = TW51/THW1MX
0533 P2(032) = THGCTU
0534 P2(031) = QTHPE/SOEMX
0535 P2(032) = THQVLP/THQV1MX
0536 P2(033) = -THQV1N/THQV1MX
0537 P2(034) = THRTL1/THQV1MX
0538 P2(035) = THRTL1/THQV1MX

```

Figure G.9. (Continued)

```

0539      P2(076) = THATMX/THOMMX
0540      P2(077) = THATMY/THOMMY
0541      P2(078) = AFRATE/ATAPRX*DGTD03
0542      P2(079) = P4.5*LOG(D03)/AINMX
0543      P2(080) = GTHGVV/TIMMX
0544      P2(081) = THOMMY/TIMMX
0545      P2(082) = THOMMX/TIMMX
0546      P2(083) = GDLTH*GDLTHX/THOMMX
0547      P2(084) = SKTRP(12)
0548      P2(085) = SKTRM(13)
0549      P2(086) = AINDEF*DGTD03/AINRMX
0550      P2(087) = AINDEF*DGTD03/AINRMX
0551      P2(088) = GDLTH*GDLTHX/THOMMX
0552      P2(089) = GONG*OMEGMX/THOMMX
0553      P2(090) = TOWOLM/TOMMX
0554      P2(091) = TOWOLM/TOMMX
0555      P2(092) = GDLTH*GDLTHX/THOMMX
0556      P2(093) = TOWOLM/TOMMX
0557      P2(094) = ALARPI/POOTMX/10.
0558      P2(095) = ALARPI/POOTMX
0559      P2(096) = TIMSLD/TIMSMX
0560      P2(097) = TIMSLD/TIMSMX
0561      P2(098) = 1./TAUFE/GRUTON
0562      P2(099) = 1./TAUFE/GRUTON
0563      P2(100) = 1./TAUFE/GRUTON
0564      P2(101) = 1./TAUFE/GRUTON
0565      P2(102) = AMARDI/POOTMX/10.
0566      P2(103) = AMARDI/POOTMX
0567      P2(104) = OMWB**2/10./GRUTON/10.
0568      P2(105) = 2.*E*TA*OMWB/GRUTON/10.
0569      P2(106) = OMWB**2/10./GRUTON/10.
0570      P2(107) = OMWB**2/10./GRUTON/10.
0571      P2(108) = 2.*E*TA*OMWB/GRUTON/10.
0572      P2(109) = OMWB**2/10./GRUTON/10.
0573      P2(110) = ZARDIC/ZAPMX/10.
0574      P2(111) = ZARDIC/ZAPMX
0575      P2(112) = OMWB**2/10./GRUTON/10.
0576      P2(113) = 2.*E*TA*OMWB/GRUTON/10.
0577      P2(114) = OMWB**2/10./GRUTON/10.
0578      P2(115) = AINROI/AINOMX
0579      P2(116) = AINROI/AINOMX
0580      P2(117) = AIDOMX/AINOMX/GRUTON
0581      P2(118) = AIDOMX/AINOMX/GRUTON
0582      P2(119) = OMIRE**2*AINMX/AINOMX/10.
0583      P2(120) = 2.*E*TA*OMWB/GRUTON/10.
0584      P2(121) = OMIRE**2*AINMX/AINOMX/10.
0585      P2(122) = AINRLM/AINPMX
0586      P2(123) = AINRLM/AINPMX
0587      P2(124) = AINRLM/AINPMX

```

Figure G.9. (Continued)

```

C588      P2(252) = AIDOMX/AINDMX /GRUTON
C589      P2(241) = AINDMX/AINDMX/GRUTON
C590      P2(254) = (MIREF**2*AINMX/AIDOMX/L.
C591      P2(235) = 2.*ETAIDP**2*AIPE*AIPE*AIPE*AIPE/L.
C592      P2(256) = (MIREF**2*AINMX/AIDOMX/L.
C593      P2(237) = AINDMX/AINDMX
C594      P2(253) = DELTA /DLTHX
C595      P2(261) = C.
C596      P2(262) = C.
C597      P2(263) = AINDMX/AINDMX
C598      P2(264) = GIMREF*MIREF**2*OCVLMX/AIDOMX/L.
C599      P2(265) = GIMREF*MIREF**2*OCVLMX/AIDOMX/L.
C600      P2(266) = 1./TAUCYR/L. /GRUTON
C601      P2(267) = 1./TAUCYR/L. /GRUTON
C602      P2(270) = CONI*AIDOMX/AMACMX /L.
C603      P2(271) = AINDMX/AINDMX
C604      P2(272) = AIRFC/AINDMX
C605      P2(273) = 105.*OGTOPD/AINDMX
C606      P2(274) = 2.*ETAIDP**2*AIPE*AIPE*AIPE*AIPE/L.
C607      P2(275) = AMACMX/CONI/AIDOMX/L.
C608      P2(274) = SKTEIM*7)
C609      P2(277) = SKTEIM* 3)
C610      P2(270) = CONI*AIDOMX/AMACMX /L.
C611      P2(271) = OCYIC/OCVLMX
C612      P2(272) = OCYIC/OCVLMX/GRUTON
C613      P2(273) = OCYIC/OCVLMX/GRUTON
C614      P2(274) = 2.*ETAIDP**2*AIPE*AIPE*AIPE*AIPE/L.
C615      P2(275) = AMACMX/CONI/AIDOMX/L.
C616      P2(276) = SHPLN/SHPMX/GRUTON
C617      P2(277) = SHPLN/SHPMX/GRUTON
C618      P2(311) = SHPIC/SHPMX
C619      P2(312) = 1./TAUSHO/GRUTON/L.
C620      P2(313) = 1./TAUSHO/GRUTON/L.
C621      P2(314) = ASLP*SHPMX
C622      P2(315) = AC
C623      P2(316) = ALIM
C624      P2(317) = 1.C
C625      P2(320) = ATOM*OCVLMX/TTSMX/L.
C626      P2(322) = TOM/L.
C627      P2(323) = TOM*OCVLMX/L.
C628      P2(324) = TOM/L.
C629      P2(344) = ALAND*PI
C630      P2(345) = AINDMX/PI
C631      P2(346) = ALAND*PI
C632      P2(347) = AINDMX/PI
C633      P2(344) = AINDMX**2/OCVLMX*SL*SMN/SM -1.
C634      P2(365) = AINDMX**2/OCVLMX*SL*SMN/SM
C635      P2(366) = AIDOMX/OCVLMX*SL*SMN/SM
C636      P2(377) = AIDOMX/OCVLMX*SL*SMN/SM

```

Figure G.9. (Continued)

```

0637      P2(372)= UDOTMX/AXPAMY
0638      P2(373)= VDOTMX/AYPAMY
0639      P2(374)= P2(372)*XCCMX/AYPAMY
0640      P2(375)= WDOTMX/AYPAMY
0641      P2(376)= UDOTMX*XCCMX/AYPAMY
0642      P2(377)= SG/AYPAMY

C
C      RGRD SF      (C/VSQ/F 3)      POT. CALCULATION SECTION
C
0643      P3(02) = QW00**2/10./GRUTON/10.
0644      P3(03) = QWR0**2/10./GRUTON/10.
0645      P3(04) = 2.0*FTARD*QWRD/GRUTON/10.
0646      P3(05) = RIGR01/RICMX/10.
0647      P3(06) = RIGR1C/RICMX
0648      P3(07) = GRATS
0649      P3(08) = QWR0**2/10./GRUTON/10.
0650      P3(09) = QWR0**2/10./GRUTON/10.
0651      P3(10) = 2.0*FTARD*QWRD/GRUTON/10.
0652      P3(11) = RIGR01/RICMX/10.
0653      P3(12) = RIGR1C/RICMX
0654      P3(13) = GRATS
0655      P3(14) = QWR0**2/10./GRUTON/10.
0656      P3(15) = QWR0**2/10./GRUTON/10.
0657      P3(16) = 2.0*FTARD*QWRD/GRUTON/10.
0658      P3(17) = RIGR01/RICMX/10.
0659      P3(18) = RIGR1C/RICMX
0660      P3(19) = GRATS
0661      P3(20) = 1./TAUGMN
0662      P3(21) = QWR0**2/10./GRUTON/10.
0663      P3(22) = QWR0**2/10./GRUTON/10.
0664      P3(23) = 2.0*FTARD*QWRD/GRUTON/10.
0665      P3(24) = RIGR01/RICMX/10.
0666      P3(25) = RIGR1C/RICMX
0667      P3(26) = GRATS
0668      P3(27) = QWR0**2/10./GRUTON/GRUSTMX
0669      P3(28) = 1./TAUGST/GRUTON
0670      P3(29) = GRUST/TAUGST/GRUTON/GRUSTMX
0671      P3(30) = 1./TAUGST/GRUTON
0672      P3(31) = GRUST/TAUGST/GRUTON/GRUSTMX
0673      P3(32) = 1./TAUGST/GRUTON
0674      P3(33) = GLSAR/GLSMX
0675      P3(34) = 1./TAUGLS/GRUTON
0676      P3(35) = GLSLW/GLSMX
0677      P3(36) = GLSLW/GLSMX
0678      P3(37) = SKTRIM(C9)
0679      P3(38) = SKTRIM(10)
0680      P3(39) = SKTRIM(11)
0681      P3(40) = SKDLRD*DELPMX/PLRDMX
0682      P3(41) = SKDLRD*DELPMX/DCVLMX*GRCYMX

```

Figure G.9. (Continued)

FORTRAN IV MODEL 44 PS VERSION 3, LEVEL 2 DATE 7-7-72

```

0683 P3(244) = SKDLS*DELSMX/DCVLMY*GSCVMX
0684 P3(245) = GLCP/1.
0685 P3(246) = SKDLS*DELSMX/DCVLMY*GSCVMX
0686 P3(247) = GLCP*UMX/10.
0687 P3(252) = SKDLS*DEFLRMX/DLONMX
0688 P3(253) = SKDLS*DEFLRMX/DELEMX
0689 P3(254) = DELALM/DELAMX
0690 P3(255) = DELALM/DELAMX
0691 P3(257) = 1.
0692 P3(260) = DFLR /DELRMX
0693 P3(261) = DELS /DELSMX
0694 P3(262) = DELR /DEFLRMX
0695 P3(264) = GQ/TAUQ1*QMX/DLONMX/GRUTON/10.
0696 P3(265) = GTHE*QMX/DLONMX/GRUTON
0697 P3(266) = SKDA*DELSMX/DELAMX
0698 P3(267) = SKDA*DELSMX/DELAMX
0699 P3(272) = OMA**2*GICMX/AICMX/10./GRUTON/10.
0700 P3(273) = OMA**2*GICMX/BICMX/10./GRUTON/10.
0701 P3(274) = OMA**2*GICMX/AICMX/10./GRUTON/10.
0702 P3(275) = OMA**2*GICMX/AICMX/10./GRUTON/10.
0703 P3(276) = THSMX/TH75MX
0704 P3(277) = THSMX/TH75MX
0705 P3(300) = GLSHIC/GLSMX
0706 P3(301) = GLSAIL/GLSMX
0707 P3(302) = DCOLMX/TH75MX
0708 P3(303) = DCOLMX/TH75MX
0709 P3(304) = TH75LP/TH75MX
0710 P3(305) = TH75LN/TH75MX
0711 P3(306) = TH75LP/TH75MX
0712 P3(307) = TH75LN/TH75MX
0713 P3(310) = RICRPO/AICMX/10.
0714 P3(311) = RICRP /AICMX
0715 P3(312) = 1./TAUGLS/GRUTON
0716 P3(313) = 1./TAUGLS/GRUTON
0717 P3(314) = 1./TAUGLS/GRUTON
0718 P3(315) = 1./TAUGLS/GRUTON
0719 P3(316) = GLSLM/GLSMX
0720 P3(317) = GLSLM/GLSMX
0721 P3(320) = -GBICP/GICMX
0722 P3(321) = -GAICP/GICMX
0723 P3(322) = OMA**2*DCVLMX/BICMX/10./GRUTON/10.
0724 P3(323) = OMA**2*DCVLMX/BICMX/10./GRUTON/10.
0725 P3(324) = 2.*EIA*QMA/GRUTON/10.
0726 P3(325) = OMA**2/10./GRUTON/10.
0727 P3(326) = 1./TAUGIC/GRUTON/10.
0728 P3(327) = 1./TAUGIC/GRUTON/10.
0729 P3(330) = PICLPO/BICMX/10.
0730 P3(331) = AICLP /BICMX
0731 P3(332) = 1./TAUGIC/GRUTON/10.

```

Figure G.9. (Continued)

```

0732 P(333) = 1./TAUCIC/GRUTON/10.
0733 P(334) = DLFLPC/DLFLMX
0734 P(335) = 1./TAUDH*DELPMX/DLQNMX/GRUTON
0735 P(336) = DMA**2*GCLMX/ALCMX/10./GRUTON/10.
0736 P(337) = DMA**2*DLQNMX/ALCMX/10./GRUTON/10.
0737 P(338) = 1./TAUD2/GRUTON/10.
0738 P(339) = PSAS2/DLQNMX
0739 P(340) = 2.*DELTA*DMA/GRUTON/10.
0740 P(341) = DMA**2/10./GRUTON/10.
0741 P(342) = GICLM/GICMX/GRUTON
0742 P(343) = GICLM/GICMX/GRUTON
0743 P(344) = GICLM/GICMX/GRUTON
0744 P(345) = GICLM/GICMX/GRUTON
0745 P(346) = GICLM/GICMX/GRUTON
0746 P(347) = GICLM/GICMX/GRUTON
0747 P(348) = AICRPO/ALCMX/10.
0748 P(349) = AICRPO/ALCMX
0749 P(350) = 1./TAUDR/GRUTON
0750 P(351) = DMA**2*GLSMX/ALCMX/GRUTON/10./10.
0751 P(352) = SKDCOL*DMA**2*DCCLMX/ALCMX/10./GRUTON/10.
0752 P(353) = 2.*DELTA*DMA/GRUTON/10.
0753 P(354) = DMA**2/10./GRUTON/10.
0754 P(355) = GLSMX/DLQNMX
0755 P(356) = PSAS1/DLQNMX
0756 P(357) = PSAS3/DLQNMX
0757 P(358) = PSAS4/DLQNMX
0758 P(359) = GDB2/TAUD2/GRUTON/10.
0759 P(360) = GDB1/GRUTON
0760 P(361) = 1./TAUD1/GRUTON/10.
0761 P(362) = AICLPO/ALCMX/10.
0762 P(363) = AICLIP/ALCMX
0763 P(364) = DLRLM/DLQNMX
0764 P(365) = DMA**2*GLSMX/ALCMX/GRUTON/10./10.
0765 P(366) = SKDCOL*DMA**2*DCCLMX/ALCMX/10./GRUTON/10.
0766 P(367) = 2.*DELTA*DMA/GRUTON/10.
0767 P(368) = DMA**2/10./GRUTON/10.
C
C
XDDY= -XIC+VISIC+XHOPIZ+XBIC
YDDY= YPOAD+YPOAD+VISIC+VIC+YVIC
ZDDY= H+ZBIC
C
S11 = COSTHE * COSPSI
S12 = SINPHI *SINTHE *COSPSI - COSPHI * SINPSI
S13 = COSPHI *SINTHE *COSPSI + SINPHI * SINPSI
C
S21 = COSTHE * SINPSI
S22 = SINPHI *SINTHE*SINPSI + COSPHI * COSPSI
S23 = COSPHI *SINTHE *SINPSI -SINPHI * COSPSI

```

Figure G.9.1(Continued).

```

C
0777 SA31 = - SIN(THC)
0778 SA32 = SIN(PI * COS(THC)
0779 SA33 = COS(PI * COS(THC)
C
0780 XACVIS = -(SA11*XBDY + SA12*YBDY + SA13*ZBDY)
0781 YACVIS = -(SA21*XBDY + SA22*YBDY + SA23*ZBDY)
0782 ZACVIS = -(SA31*XBDY + SA32*YBDY + SA33*ZBDY)
C
0783 YSCOPE = ZACVIS/XACVIS*VCAL1*XVIS-X/ZVISMX
0784 XSCOPE = YACVIS/XACVIS*VCAL2*XVISMX/YVISMX
C
0785 EFDR = XLIM(EFBMX,FFMLD,BLSLOPE*SQF/QSTAR + BDB)
0786 FEUS = XLIM(EFSMX,FFMLD,SSLOPE*SQF/QSTAR + BDB)
0787 FEOK = XLIM(EFBMX,FFMLD,BLSLOPE*SQF/QSTAR + BDB)
0788 PCAP = MIN(EA/CMPEF*100,
0789 DRK10 = COMDLR-DELR
0790 DRK11 = COMDLR-DELR
0791 DRK12 = COMDLR-DELR
0792 THAKR = -SKTRIM(12)*COMDOT/CMFGAX*DELTHY
0793 PSOSIM = XL14(PDTSX,-PDTSX,PSIDT*DELTHY)
0794 XSIM = XLIM(DXSIMX,-DXSIMX,XIC)
0795 YSIM = XLIM(DYSIMX,-DYSIMX,YIC)
0796 IF(DELTHY.GT.2) GO TO 975
0797 COMDLR = 0.0
0798 COMDLR = 0.0
0799 COMDLR = 0.0
0800 COMDLR = 0.0
0801 BRAKE = 0.0
0802 CONTINUE
C
0803 P4(00) = 1.0000
0804 P4(01) = 1.0000
0805 P4(02) = PC10MX/TQSIMX
0806 P4(03) = PC10MX/TQSIMX
0807 P4(04) = CACGMK/CMPEF*100./PDMSX
0808 P4(05) = YDPMX/YDTSMX
0809 P4(06) = VMXX/HQTSMX
0810 P4(07) = XDPMX/XDTSMX
0811 P4(08) = UMXX/SKEPS/LSIMX
0812 P4(09) = VMXX/SKEPS/VSIMX
0813 P4(10) = AXPMX/AXPA/4X
0814 P4(11) = PSIMX*PDTCOG/PSISMX
0815 P4(12) = PSOMX*PDTCOG/PSDTSX/2.0
0816 P4(13) = PDTCOG/THESMX
0817 P4(14) = PDTCOG/PHISMX
0818 P4(15) = PSOMX*PDTCOG/PSDTSX/2.0
0819 P4(16) = PSDTSX/PSDTSX
0820 P4(17) = PSDTSX/PSDTSX

```

Figure G.9. (Continued)

```

0821      AINMX=RTOTCG/AINSMX
0822      ALGMMX=CTODG/ALWSMX
0823      AZPAMX/AZPAMX
0824      DLFIMX/DLFPSMX
0825      ABFSMX=RTOTCG/RTSIMX
0826      AYPAMX/AYPAMX
0827      C.1475
0828      C.1475
0829      DXSIMX/DXSIMX
0830      DXSIMX/DXSIMX
0831      1.0000
0832      XMX/DXSIMX/10.
0833      ZMX/HSIMX
0834      1.0000
0835      VMX/YVISMX
0836      ZMX/YVISMX
0837      XDOTMX / XVISMX /10.
0838      YDOTMX / YVISMX / 10.
0839      XOTEST/XVISMX/10.
0840      YOTEST/YVISMX/1.
0841      THF / PI
0842      OHF / PI
0843      PSI / PI
0844      FREQMT / 100.
0845      SCOPLM
0846      SCOPLM
0847      SCOPLM
0848      SCOPLM
0849      1.0000
0850      .0132
0851      XHOKTZ / XVISMX
0852      ZMX / ZVISMX
0853      PIASMT/ZVISMX
0854      YBIC / XVISMX
0855      YBIC / YVISMX
0856      ZBIC / ZVISMX
0857      PSDMX/PI/10.
0858      C.1500/PI/10.
0859      SLX / XVISMX
0860      SLV / YVISMX
0861      SLZ / XVISMX
0862      SLX / ZVISMX
0863      SLV / ZVISMX
0864      SLZ / ZVISMX
0865      C.6200
0866      C.6200
0867      SLX / YVISMX
0868      SLV / YVISMX
0869      SLZ / YVISMX

```

Figure G.9. (Continued)

```

0870      P4(315) = PMT1 / ZVISMX
0871      P4(316) = PMT2 / ZVISMX
0872      P4(317) = GZMTSI
0873      P4(320) = 0.6500
0874      P4(331) = 0.6500
0875      P4(322) = DRPSMX/DRDPMX
0876      P4(323) = DELPMX/DRHDMX
0877      P4(324) = DRPSMX/DRDPMX
0878      P4(325) = DELPMX/DRDPMX
0879      P4(326) = DRPSMX/DRDPMX
0880      P4(327) = DELSMX/DRSDMX
0881      P4(330) = 1C * SKFPS / XDGTMX
0882      P4(332) = VCALL * XVISMX / YVISMX
0883      P4(333) = VCALL2 * XVISMX / ZVISMX
0884      P4(334) = 2.0*RRKMX/RRKSMX
0885      P4(335) = DLTHMX/THRDPMX
0886      P4(336) = FFRMX/FFRSMX
0887      P4(337) = FFLMLQ/FFRSMX
0888      P4(340) = GZMTS2
0889      P4(341) = XHGP12 / XVISMX
0890      P4(342) = -RDS/FFRSMX
0891      P4(343) = -RDS/FFRSMX
0892      P4(344) = DSLOPE/STARRH*SQF4X/FFR4X
0893      P4(345) = SSLOPE/OSTARS*SQF4X/FFR4X
0894      P4(346) = PSLOPE/STARRH*SQF4X/FFR4X
0895      P4(347) = -HQR/FFRSMX
0896      P4(350) = YHQR / YVISMX
0897      P4(351) = YHQR2 / YVISMX
0898      P4(354) = FFSMX/FFRSMX
0899      P4(355) = FFRMX/FFRSMX
0900      P4(356) = FFLML / FFSMX
0901      P4(357) = FFLMLQ/FFRSMX
0902      P4(360) = XIC / XVISMX
0903      P4(361) = YIC / YVISMX
0904      P4(362) = H/ZMX
0905      P4(364) = 2.0*DELPMX/DRPSMX
0906      P4(365) = 2.0*DELPMX/DRPSMX
0907      P4(367) = 2.0*DELPMX/DRPSMX
0908      P4(370) = 0.1400
0909      P4(371) = 0.1400
0910      P4(374) = 2.0*DELPMX/DRPSMX
0911      P4(375) = 2.0*DELPMX/DRPSMX
C
0912      RETURN
0913      STOP
0914      CALL ANDAIN(PROJ, RNDOS(1), LUTR(1), IFC(1), NCIN(1), A10, 5, A11, 1, 5,
*          SJ1, 4, 5, TR1, 6, 5)
C
0915      AIP(380) = 7IC/Z4X

```

BOARD IE (CONSOLE II) AMPLIFIER SCALE FACTOR CALCULATION: P DENOTES POSITIVE OUTPUT,
 N DENOTES NEGATIVE OUTPUT.

Figure G.9. (Continued)

```

0916 AIP(071) = YIC/YMX
0917 AIP(072) = UIC*STATH/UMX
0918 AIP(073) = ZOOT/VIMY
0919 AIP(081) = YDOT/YDOTMX
0920 AIP(083) = XDOT/XDOTMX
0921 AIP(090) = XIC/XMX
0922 AIP(111) = D.C
0923 AIP(120) = AINGER/AIDOMX
0924 AIP(131) = AINDDL/AIDOMX
0925 AIP(020) = -SKTRIM(03)*VDDT/VDDTAX
0926 AIP(020) = CTO/CTMX
0927 AIP(021) = ROT1/CTMX
0928 AIP(030) = -CIRPRM/CTMX
0929 AIP(030) = CTC/CTMX
0930 AIP(031) = ROT2/CTMX
0931 AIP(040) = TH75R/TH75MX
0932 AIP(040) = CPR/CPMX
0933 AIP(041) = TH75L/TH75MX
0934 AIP(041) = CPL/CPMX
0935 AIP(050) = -TH75R/TH75MX
0936 AIP(050) = CNFPL/CNFMX
0937 AIP(051) = -ALPHA/ALFMX
0938 AIP(051) = C4PR/CNFMX
0939 AIP(052) = CIRPRM/CTMX
0940 AIP(053) = CYLPRM/CTMX
0941 AIP(060) = -AMID/AMPMY
0942 AIP(060) = CSPR/CPMX
0943 AIP(061) = -L
0944 AIP(061) = CSEPL/CSFMX
0945 AIP(062) = SKTRIM(01)*UDDT/UDDTAX
0946 AIP(063) = SKTRIM(05)*UDDT/UDDTAX
0947 AIP(070) = D.C
0948 AIP(071) = D.C
0949 AIP(072) = PIC/PMY
0950 AIP(081) = QIC/QMX
0951 AIP(082) = PDDT/PDDTMX
0952 AIP(083) = QDDT/QDDTAX
0953 AIP(090) = RIC/RMX
0954 AIP(091) = UIC/UIMX
0955 AIP(092) = -PSIDT*STATH/PSIMX
0956 AIP(092) = THDOT/THOMX
0957 AIP(093) = *COSPHI/RMX
0958 AIP(093) = CHIDDT/CHDMX
0959 AIP(095) = VIC/VIMX
0960 AIP(091) = AIC/VIMX
0961 AIP(092) = ROT/ROTAX
0962 AIP(093) = Q*STNPHI/OMX
0963 AIP(093) = UDDT/UDDTAX
0964 AIP(093) = THIC/THMX

```

Figure G.9. (Continued)

```

0965 AIP(231) = PHIC/PHIMX
0966 AIP(241) = PSIC/PSIMX
0967 AIP(241) = -XAFRO / SM / UOFTAX
0968 AIP(241) = -YAFRO / SM / UOFTAX
0969 AIP(242) = R*SINPHI/RMX
0970 AIP(242) = VORT/VORTMX
0971 AIP(243) = -Q*COSPHI/QMX
0972 AIP(243) = WORT/WORTMX
0973 AIP(250) = THE/PI
0974 AIP(251) = PHI/PI
0975 AIP(252) = COSTHE*COSPHI
0976 AIP(253) = COSTHE*SINPHI
0977 AIP(260) = BETAF / ABFSMX
0978 AIP(260) = AVEALW / ALWGMX
0979 AIP(261) = SOF / SOFMAX
0980 AIP(261) = -7AEP0/SM/ZAPMX
0981 AIP(262) = PSIDOT/PSDMX
0982 AIP(300) = -DELSS/DELSMX
0983 AIP(300) = -R*SAS1/DELSMX
0984 AIP(301) = -R*SAS4/DELSMX
0985 AIP(301) = -R*SAS2/DELSMX
0986 AIP(302) = -Y*SAS3/DELPWX/GRU10
0987 AIP(303) = Y*SAS1/DELPWX
0988 AIP(310) = -Y*SAS7/RMX
0989 AIP(310) = R*SAS3/DELSMX
0990 AIP(311) = R*SAS4/ABFSMX
0991 AIP(312) = -R*SAS5/DELSMX/GRU10
0992 AIP(313) = GLATPH/L
0993 AIP(320) = -Y*SAS11/DELRMX
0994 AIP(320) = Y*SAS1/DELPWX
0995 AIP(321) = Y*SAS9/DELPWX
0996 AIP(321) = -Y*SAS2/DELRMX
0997 AIP(322) = ALPHF/AFPSMX
0998 AIP(322) = -VCAL12/UMX
0999 AIP(323) = ALPHK3/ALFRMX
1000 AIP(323) = ALPHL2/ALFRMX
1001 AIP(330) = -Y*SAS12/DELRMX
1002 AIP(330) = Y*SAS3/DELRMX
1003 AIP(331) = Y*SAS16/PMX
1004 AIP(331) = -Y*SAS6/DELRMX
1005 AIP(340) = Y*SAS4/DELPWX
1006 AIP(341) = -Y*SAS5/DELRMX
1007 AIP(342) = AMUP/AMURMX
1008 AIP(343) = AMUL/AMJPMX
1009 AIP(350) = Y*SAS14/DELPWX
1010 AIP(350) = -DEIKS/DELPWX
1011 AIP(351) = Y*SAS13/DELPWX
1012 AIP(352) = -Y*SAS15/PMX
1013 AIP(353) = GYAW/L

```

Figure G.9. (Continued)

```

1014 A10(442) = Q1AT04/1.
1015 A10(441) = YSA517/DEL2MX
1016 A10(442) = OMEGAR/DEL2MX
1017 A10(443) = OMEGAL/DEL2MX
C
VALUES AT SUMMING JUNCTIONS OF AMPLIFIERS: BOARD 1E (CONSOLE 1)
1018 SJ1(341) = ZOUT/ZMX/GPUTON
1019 SJ1(341) = YSA517/DEL2MX
1020 SJ1(341) = XOUT/VMX/GPUTON
1021 SJ1(341) = SKRT14(0.2)*XOUT/DEL2MX
1022 SJ1(341) = 0.0
1023 SJ1(321) = ROT10/CTMX/GPUTON
1024 SJ1(331) = 0.0
1025 SJ1(331) = ROT20/CTMX/GPUTON
1026 SJ1(341) = 0.0
1027 SJ1(341) = 0.0
1028 SJ1(351) = 0.0
1029 SJ1(351) = 0.0
1030 SJ1(361) = 0.0
1031 SJ1(361) = 0.0
1032 SJ1(371) = SKRT14(0.2)*VOUT/DEL2MX
1033 SJ1(371) = SKRT14(0.2)*VOUT/DEL2MX
1034 SJ1(371) = POUT/PMX/GPUTON
1035 SJ1(381) = QOUT/QMX/GPUTON
1036 SJ1(391) = UOUT/UMX/GPUTON
1037 SJ1(391) = VOUT/VMX/GPUTON
1038 SJ1(401) = ROT/VMX/GPUTON
1039 SJ1(401) = THEOUT/THMX/GPUTON
1040 SJ1(411) = PHOUT/PHMX/GPUTON
1041 SJ1(421) = PS1001/PS1MX/GPUTON
1042 SJ1(431) = PSA510/DELSMX/GPUTON
1043 SJ1(441) = RSA520/DELSMX/GPUTON
1044 SJ1(451) = RSA530/DELSMX/GPUTON
1045 SJ1(461) = RSA540/DELSMX/GPUTON
1046 SJ1(471) = YSA510/DELSMX/GPUTON
1047 SJ1(481) = YSA520/DELSMX/GPUTON
1048 SJ1(491) = YSA530/DELSMX/GPUTON
1049 SJ1(501) = YSA540/DELSMX/GPUTON
1050 SJ1(511) = YSA550/DELSMX/GPUTON
1051 SJ1(521) = YSA560/DELSMX/GPUTON
1052 SJ1(531) = YSA570/DELSMX/GPUTON
C
BOARD 1E (CONSOLE 1) VALUES OF TRUNK LINES AND ADCS (FIRST 32 TRS ARE ADCS)
1053 TR1(221) = P/PMX
1054 TR1(221) = Q/QMX
1055 TR1(221) = R/RMX
1056 TR1(221) = U/UMX
1057 TR1(261) = V/VMX
1058 TR1(261) = W/WMX
1059 TR1(261) = THE/THMX
1060 TR1(261) = PH/PHMX

```

Figure G.9. (Continued)


```

1061      TR1(130) = PSI/PSI**Y
1062      TR1(121) = WOOT/WOOT**X
1063      TR1(122) = -TIC/T**X
1064      TR1(143) = ZDOT/VN**X
1065      TR1(120) = -DELAL/DELAL**X
1066      TR1(121) = DELAR/DELAR**X
1067      TR1(122) = -DELSPL/DELSPL**X
1068      TR1(123) = DELSPL/DELSPL**X
1069      TR1(160) = CLEPM/C**X
1070      TR1(161) = CNEPL/CNEF**X
1071      TR1(162) = CSEPL/CSEF**X
1072      TR1(163) = CMPL/CPM**X
1073      TR1(170) = SINTE
1074      TR1(171) = COSTHE
1075      TR1(172) = SINPHI
1076      TR1(173) = COSPHI
1077      TR1(174) = SINPHI*COSTHE
1078      TR1(175) = COSPHI*COSTHE
1079      TR1(120) = CYNPL/CY**X
1080      TR1(121) = CPL/C**X
1081      TR1(122) = CTRDRV/C**X
1082      TR1(123) = CNEPR/CNEF**X
1083      TR1(160) = CSEPR/CSEF**X
1084      TR1(161) = CPMPR/CPM**X
1085      TR1(162) = CYMPO/CY**X
1086      TR1(163) = CPE/C**X

1087      TR1(110) = COP/CP**X
1088      TR1(111) = COL/CP**X
1089      TR1(112) = OMEGA/OMEG**X
1090      TR1(113) = SKTOT/MTOT*DELDT/UMOT**X
1091      TR1(114) = ALAPW/ET**X/DM**X
1092      TR1(115) = AMEPM/ET**X/DM**X
1093      TR1(116) = ZAPW/SW/TAZ**X
1094      TR1(117) = DELTH/DELTH**X
1095      TR1(111) = -DSUP/SHPM**X
1096      TR1(112) = -SHPIC/SHPM**X
1097      TR1(113) = -ATPRF/AT**X
1098      TR1(114) = -TPS/TPS**X
1099      TR1(115) = SHPPD/SHPM**X/GUT**X
1100      TR1(116) = -DSHPP/SHPM**X
1101      TR1(117) = -DVTAUF*SOITIC/DEL/GRIT**X
1102      TR1(118) = SOITIC/DEL*TAUPW/GRIT**X
1103      TR1(113) = THATL**X/TA**X
1104      TR1(113) = GTHRT/DELTH**X
1105      TR1(113) = -GTHRT/DELTH**X
1106      TR1(114) = DTHDMMPL/CMC/THC**X/1.0
1107      TR1(115) = DLONG/OMEG**X
1108      TR1(116) = -THGOVL/1.0

```

Figure G.9. (Continued)

Figure G.9. (Continued)

```

1203 A2P(23) = THUMB/TCMXX
1204 A2P(24) = 0.
1205 A2P(25) = -GDTH/THUMB*ODTH/TCMXX
1206 A2P(26) = -SVTH/THUMB*ODTH/TCMXX
1207 A2P(27) = 1.0
1208 A2P(28) = 1.0
1209 A2P(29) = 0.05/ODTH/TCMXX*2.0
1210 A2P(30) = 0.05/ODTH/TCMXX
1211 A2P(31) = 0.05/ODTH/TCMXX
1212 A2P(32) = -THUMB/TCMXX
1213 A2P(33) = ALARDI/POCTMX/1.0
1214 A2P(34) = ALARMN/FIXX/POCTMX
1215 A2P(35) = CPRQ/CPMX *2.0
1216 A2P(36) = THATLM/THATMX
1217 A2P(37) = AMARDI/POCTMX/1.0
1218 A2P(38) = AMARMN/FIXX/POCTMX
1219 A2P(39) = 0.05/ODTH/TCMXX
1220 A2P(40) = -THUMB/TCMXX
1221 A2P(41) = THUMB/TCMXX
1222 A2P(42) = 0.05/ODTH/TCMXX
1223 A2P(43) = 0.05/ODTH/TCMXX
1224 A2P(44) = 0.05/ODTH/TCMXX
1225 A2P(45) = 0.05/ODTH/TCMXX
1226 A2P(46) = 0.05/ODTH/TCMXX
1227 A2P(47) = 0.05/ODTH/TCMXX
1228 A2P(48) = 0.05/ODTH/TCMXX
1229 A2P(49) = 0.05/ODTH/TCMXX
1230 A2P(50) = 0.05/ODTH/TCMXX
1231 A2P(51) = 0.05/ODTH/TCMXX
1232 A2P(52) = 0.05/ODTH/TCMXX
1233 A2P(53) = 0.05/ODTH/TCMXX
1234 A2P(54) = 0.05/ODTH/TCMXX
1235 A2P(55) = 0.05/ODTH/TCMXX
1236 A2P(56) = 0.05/ODTH/TCMXX
1237 A2P(57) = 0.05/ODTH/TCMXX
1238 A2P(58) = 0.05/ODTH/TCMXX
1239 A2P(59) = 0.05/ODTH/TCMXX
1240 A2P(60) = 0.05/ODTH/TCMXX
1241 A2P(61) = 0.05/ODTH/TCMXX
1242 A2P(62) = 0.05/ODTH/TCMXX
1243 A2P(63) = 0.05/ODTH/TCMXX
1244 A2P(64) = 0.05/ODTH/TCMXX
1245 A2P(65) = 0.05/ODTH/TCMXX
1246 A2P(66) = 0.05/ODTH/TCMXX
1247 A2P(67) = 0.05/ODTH/TCMXX
1248 A2P(68) = 0.05/ODTH/TCMXX
1249 A2P(69) = 0.05/ODTH/TCMXX
1250 A2P(70) = 0.05/ODTH/TCMXX
1251 A2P(71) = 0.05/ODTH/TCMXX

```

STK2391

Figure G.9. (Continued)

```

1252 A2N(262) = DCYPO/DCYLX/GBUTON
1253 A2P(263) = THT*SP/TTXSMX
1254 A2N(263) = THTMSL/TTXSMX
1255 A2P(300) = SHPPRR/SHPPX
1256 A2P(301) = SHP1/SHPMX
1257 A2P(302) = ALARP/FIYX/PDGTIX
1258 A2P(303) = A*ARP/FIYV/QDGTIX
1259 A2P(310) = SHP4/SHPMX
1260 A2N(310) = SHPO/SHPMX/GRUTON
1261 A2P(311) = SHPIC/SHPMX
1262 A2P(312) = -CMDQR/CPMCX
1263 A2P(320) = AENG
1264 A2P(321) = DTHDM/L
1265 A2P(322) = ZARP/SM/TAPMX
1266 A2P(323) = AINLOI**2/AINDMX**2
1267 A2P(330) = DLOWG/CMGCMX
1268 A2P(331) = -AINRDI**2/AINDMX**2
1269 A2P(340) = DTHDM*ULCMG/CMGCMX
1270 A2P(342) = (AINL-ALAMD)/PI
1271 A2P(343) = (AINR-ALAMD)/PI
1272 A2P(352) = -CLSR/GLSMX
1273 A2P(352) = GLSAL/GLSMX
1274 A2P(353) = (XCG-SLPA)/XCGMX
1275 A2P(360) = (AINLOL*SLAML+AINDR*SLAML)/AINDMX
1276 A2P(360) = (AINLOI**2*CLAML+AINRDI**2*CLAML)/AINDMX**2
1277 A2P(361) = ACCXPA/AXPAMX
1278 A2P(362) = (AINLOL*CLAML+AINRDI*CLAML)/AINDMX
1279 A2P(362) = (AINLOI**2*SLAML+AINRDI**2*SLAML)/AINDMX**2
1280 A2P(363) = XDCG/XDGMX
1281 A2P(363) = ZDCG/ZDGMX
1282 A2P(370) = RDT*(XCG-SLPA)/(RDTMX*XCGMX)
1283 A2P(370) = ACCYPA/AYPAMX
1284 A2P(371) = -QDGT*(XCG-SLPA)/(QDGTMX*XCGMX)
1285 A2P(371) = ACCZPA/AZPAMX

C BOARD 3E (CONSOLE 2) VALUES AT SUMMING JUNCTIONS OF AMPLIFIERS
1286 SJ2(107) = DLTHP/OLTHMX/GBUTON
1287 SJ2(107) = SHPPG/SHPPMX/GBUTON
1288 SJ2(110) = SHP30/SHPPMX/GBUTON
1289 SJ2(111) = CMQNT/CMQCMX/GBUTON
1290 SJ2(120) = THDMG/THDMMX/GBUTON
1291 SJ2(121) = THS10/THDMMX/GBUTON
1292 SJ2(130) = SKTRI*(13)*CMQNT/CMQCMX
1293 SJ2(131) = 0.
1294 SJ2(140) = 0.
1295 SJ2(141) = 0.
1296 SJ2(150) = -ALARP/PDGTIX/10./GBUTON/10.
1297 SJ2(151) = ALARPDI/PDGTIX/GBUTON
1298 SJ2(160) = -A*ARP/QDGTIX/10./GBUTON/10.
1299 SJ2(161) = A*ARPDI/QDGTIX/GBUTON

```

Figure G.9. (Continued)

FORTRAN IV MODEL 44 OS VERSION 3.4 LEVEL 3 DATE 73092

```

1302 SJ2(170) = ZARND/ARNDX/1.0/GBUTN/10.
1301 SJ2(71) = ZARND/ARNDX/GBUTN.
1302 SJ2(121) = ARND/ARNDX/GBUTN.
1303 SJ2(11) = ARND/ARNDX/GBUTN.
1304 SJ2(10) = ARND/ARNDX/GBUTN.
1305 SJ2(11) = ARND/ARNDX/GBUTN.
1306 SJ2(12) = ARND/ARNDX/GBUTN.
1307 SJ2(13) = 0.
1308 SJ2(14) = 0.
1309 SJ2(15) = 0.
1310 SJ2(16) = 0.
1311 SJ2(17) = -(700+400000)*SKTR1*(A)/VMAX
1312 SJ2(18) = SHD/SHDXX/GBUTN
1313 SJ2(19) = SHD/SHDXX/GBUTN

C BOARD 3E (CONSOLE 2) VALUES OF TRUNK LINES AND ADCS (FIRST 32 TR'S ARE ADCS)
1314 TR2(121) = ARND/ARNDX
1315 TR2(122) = ARND/ARNDX
1316 TR2(123) = ARND/ARNDX
1317 TR2(124) = ARND/ARNDX
1318 TR2(125) = ARND/ARNDX
1319 TR2(126) = ARND/ARNDX
1320 TR2(127) = ARND/ARNDX
1321 TR2(128) = ARND/ARNDX
1322 TR2(129) = ARND/ARNDX
1323 TR2(130) = ARND/ARNDX
1324 TR2(131) = 0.
1325 TR2(132) = 0.
1326 TR2(133) = 0.
1327 TR2(134) = 0.
1328 TR2(135) = 0.
1329 TR2(136) = 0.
1330 TR2(137) = DMORT/DMORTX
1331 TR2(138) = DMORT/DMORTX
1332 TR2(139) = DMORT/DMORTX
1333 TR2(140) = DMORT/DMORTX
1334 TR2(141) = DMORT/DMORTX
1335 TR2(142) = 1.0
1336 TR2(143) = 1.0
1337 TR2(144) = DMORT/DMORTX
1338 TR2(145) = DMORT/DMORTX

1339 TR2(146) = DMORT/DMORTX
1340 TR2(147) = DMORT/DMORTX
1341 TR2(148) = DMORT/DMORTX
1342 TR2(149) = DMORT/DMORTX
1343 TR2(150) = DMORT/DMORTX
1344 TR2(151) = DMORT/DMORTX
1345 TR2(152) = DMORT/DMORTX
1346 TR2(153) = 0.

```

Figure G.9. (Continued)

```

1347 TR2(131) = 0.
1348 TR2(132) = 0.
1349 TR2(110) = DELTH/DLTHMX
1350 TR2(111) = -DSHP/SHPMX
1351 TR2(112) = -SHTC/SHPMX
1352 TR2(113) = -AINRF/AINMX
1353 TR2(114) = -TPS/TPSMX
1354 TR2(115) = SHPPD/SHPPMX/GRUTIN
1355 TR2(116) = -DSHP/SHPMX
1356 TR2(117) = -QVTAUE*SQTHTC/DEL/GRUTIN
1357 TR2(130) = SQTHTC/DEL*TAUEMX/GRUTIN
1358 TR2(131) = THATLM/THATMX
1359 TR2(132) = GDIHRT*DLTHP/DLTHMX
1360 TR2(133) = DLTHP/DLTHMX
1361 TR2(134) = DTHDOM*DLCMG/THOMMX/LC.
1362 TR2(135) = DLDMG/CHESMX
1363 TR2(136) = -THGOL/L.
1364 TR2(150) = -CWDOR/CPMCMX
1365 TR2(151) = -CYMO/CYMPMX
1366 TR2(152) = -CPMT/CPMPMX
1367 TR2(153) = AINSEF/AINMX
1368 TR2(154) = ACC/PA/AZPAMX
1369 TR2(155) = ACCYPA/AYPAMX
1370 TR2(156) = -XAEPO/SV/UDOTMX
1371 TR2(157) = -YAEFJ/SM/VDOTMX
1372 TR2(170) = -AINP/AINMX
1373 TR2(171) = -AINL/AINMX
1374 TR2(172) = -THGOL/L.
1375 TR2(210) = AINDOR/AIDOMMX
1376 TR2(211) = AINDOL/AIDOMMX
1377 TR2(212) = PDOT/PDOUTMX
1378 TR2(213) = QDOT/QDOTMX
1379 TR2(214) = PDOT/RDOUTMX
1380 TR2(215) = -ZAEPO/SM/VDOTMX
1381 TR2(216) = ZDOT/VMMX
1382 TR2(217) = 0.
1383 TR2(230) = CPMPR/CPMPMX
1384 TR2(231) = CPMFL/CPMPMX
1385 TR2(232) = CPMPR/CYMPMX
1386 TR2(233) = CPMPL/CYMPMX
1387 TR2(234) = -SKTRIM(7)*(INDOT-HDTP1")/VMMX
1388 TR2(235) = UIC/UMX
1389 TR2(310) = TIMSR/TMSPMX
1390 TR2(311) = GLSR/GLSPMX
1391 TR2(312) = GLSAL/GLSPMX
1392 TR2(313) = -DCYL/DCYLMX
1393 TR2(314) = -GLSAR/GLSPMX
1394 TR2(315) = -DELQUD/DLPDMX
1395 TR2(316) = -DEFLV/DELEPMX

```

Figure G.9. (Continued)

FORTRAN IV MODEL 44 OS VERSION 3, LEVEL 3 DATE 73092

```

1396 TR2(317) = DELFLV/ALFLMX
1397 TR2(331) = RICLIC/ALFLMX
1398 TR2(331) = RICLIC/ALFLMX
1399 TR2(332) = RICLIC/ALFLMX
1400 TR2(333) = RICLIC/ALFLMX
1401 TR2(334) = DELFLV/ALFLMX
1402 TR2(337) = TOTXSL/ALFLMX

1403 TR2(352) = POTOL/PCINMX
1404 TR2(351) = POTOL/PCINMX
1405 TR2(252) = OMEGA/CMGCMX
1406 TR2(253) = AINOF / ALFLMX
1407 TR2(254) = COMIDT/ALFLMX
1408 TR2(255) = COMDTH/ALFLMX
1409 TR2(256) = -SKTPTM(12)CMQOT/OMEGMX
1410 TR2(257) = AVAIL
1411 TR2(370) = ACCXPA/AYXMX
1412 TR2(371) = ACCYPA/AYDMMY
1413 TR2(372) = ACCZPA/AYDMMY

```

BOARD 5F (CONSOLE 3): AMPLIFIER SCALE FACTOR CALCULATION. P DENOTES POSITIVE OUTPUT
N DENOTES NEGATIVE OUTPUT

```

GETIN
ENTRY SIGM3
CALL ANDAIN(1000J,200M(SIG),LEFT(3),LEFT(3),NCCN(3),NCCN(3),5,430,1,5,430,1,5,
      SJ3,4,5,123,4,5)

```

```

1417 AB(340) = RICOL/RICOMY/I
1418 AB(341) = RICOL/RICOMY/I
1419 AB(341) = RICOL/RICOMY/I
1420 AB(311) = RICLIC/ALFLMX
1421 AB(322) = RICOL/RICOMY/I
1422 AB(321) = RICLIC/ALFLMX
1423 AB(331) = RICOL/RICOMY/I
1424 AB(331) = RICLIC/ALFLMX
1425 AB(347) = 0
1426 AB(341) = 0
1427 AB(350) = 0
1428 AB(351) = 0
1429 AB(362) = CLSAT/ALFLMX
1430 AB(361) = 0
1431 AB(377) = 0
1432 AB(371) = 0
1433 AB(383) = 0
1434 AB(387) = 0
1435 AB(381) = 0
1436 AB(382) = DELST/ALFLMX
1437 AB(383) = DELST/ALFLMX
1438 AB(383) = DELFLV/ALFLMX
1439 AB(381) = 0
1440 AB(381) = 0

```

Figure G.9. (Continued)


```

1441 A3P(212) = -DELAR/DELMX
1442 A3N(212) = DELAP2/DELMX
1443 A3P(213) = DELAL/DELMX
1444 A3N(213) = -DELAL2/DELMX
1445 A3P(222) = DELVL/DELVMX
1446 A3P(223) = DELVL/DELVMX
1447 A3P(242) = DELR/DELMX
1448 A3P(243) = DELS/DELSMX
1449 A3P(251) = TH75R/TH75X
1450 A3P(252) = -DELQUD/OLQOMX
1451 A3N(252) = -DELSR/OLSPMX
1452 A3P(253) = -DELRT/DELRMX
1453 A3N(253) = DELSPL/OLSPMX
1454 A3P(261) = TH75L/TH75X
1455 A3P(262) = DELR/DELMX
1456 A3P(263) = DELFLP/DEFLMX
1457 A3N(300) = GLSALC/GLSMX
1458 A3N(301) = GLSAIL/GLSMX
1459 A3P(302) = OLON/OLONMX
1460 A3P(303) = DELFPP/DEFLMX
1461 A3N(310) = BICPP/BICMX/1.
1462 A3P(311) = BICRP/BICMX
1463 A3P(312) = DELAR/DELMX
1464 A3N(312) = -DELAL/DELMX
1465 A3P(313) = -VCLALH/VMX
1466 A3P(320) = GATCP/GICMX
1467 A3P(321) = GATCP/GICMX
1468 A3N(322) = GICD/GICMX/GRUTON
1469 A3N(323) = GATCP/GICMX/GRUTON
1470 A3N(330) = BICLPD/BICMX/1.
1471 A3P(331) = BICLP/BICMX
1472 A3P(340) = -DELS/OLONMX
1473 A3N(340) = -PSAS1/OLONMX
1474 A3N(341) = PSAS7/OLONMX
1475 A3N(341) = -PSAS2/OLONMX
1476 A3P(342) = DLSPLW/OLSPMX
1477 A3N(350) = AICRP/AICMX/1.
1478 A3P(351) = AICRP/AICMX
1479 A3P(352) = PSAS5/OLONMX/GRUTON/1.
1480 A3P(353) = PSAS6/OLONMX/GRUTON
1481 A3P(360) = PSAS4/OLONMX
1482 A3N(361) = -PSAS3/OLONMX
1483 A3P(362) = GLONPH/1.
1484 A3N(370) = AICLPD/AICMX/1.
1485 A3P(371) = AICLP/AICMX
C BOARD SE (CONSOLE 3) VALUES AT SUMMING JUNCTIONS OF AMPLIFIERS
S13(330) = -BICRPD/BICMX/1. /GRUTON/1.
S13(301) = BICRDT/BICMX/GRUTON
S13(310) = -BICLDN/AICMX/1. /GRUTON/1.

```

Figure G.9. (Continued)

```

1489 SJ3(11) = AICD1/GICMX/GAUTN
1490 SJ3(20) = AICD2/AICMX/1./GAUTN/1.
1491 SJ3(21) = AICD1/AICMX/GAUTN
1492 SJ3(30) = AICD3/AICMX/1./GAUTN/1.
1493 SJ3(31) = AICD1/AICMX/GAUTN
1494 SJ3(40) = GLSAD2/SLSMX/GAUTN
1495 SJ3(51) = B7775 TH75L/TH75MX
1496 SJ3(70) = B7775 TH75L/TH75MX
1497 SJ3(71) = B7775 TH75L/TH75MX
1498 SJ3(80) = GLSAD1/SLSMX/GAUTN
1499 SJ3(81) = GLSAD2/SLSMX/GAUTN
1500 SJ3(810) = B7775 TH75L/TH75MX
1501 SJ3(811) = B7775 TH75L/TH75MX
1502 SJ3(820) = GICD/GICMX/GAUTN
1503 SJ3(821) = GICD/GICMX/GAUTN
1504 SJ3(830) = B7775 TH75L/TH75MX
1505 SJ3(831) = GICD/GICMX/GAUTN
1506 SJ3(840) = PSAS10/DLSMX/GAUTN
1507 SJ3(841) = PSAS20/DLSMX/GAUTN/1.
1508 SJ3(850) = AICD2/AICMX/1./GAUTN/1.
1509 SJ3(851) = AICD3/AICMX/GAUTN
1510 SJ3(860) = PSAS40/DLSMX/GAUTN
1511 SJ3(861) = PSAS50/DLSMX/GAUTN
1512 SJ3(870) = AICD1/AICMX/1./GAUTN/1.
1513 SJ3(871) = AICD2/AICMX/GAUTN

```

BOARD 5F (CONSOLE 3) VALUES OF TRUNK LINES AND ADC'S (FIRST 32 TR'S ARE ADC'S)

```

1514 TR3(121) = DELT/DELPMX
1515 TR3(121) = DELT/DELPMX
1516 TR3(221) = DELT/DELPMX
1517 TR3(221) = DELT/DELPMX
1518 TR3(251) = DELT/DELPMX
1519 TR3(261) = DELT/DELPMX
1520 TR3(262) = DELT/DELPMX
1521 TR3(263) = TH75L/TH75MX
1522 TR3(320) = TH75L/TH75MX

1523 TR3(320) = 0.
1524 TR3(31) = 0.
1525 TR3(32) = 0.
1526 TR3(250) = 0/0MX
1527 TR3(251) = DELT/DELPMX
1528 TR3(252) = DELT/DELPMX
1529 TR3(253) = DELT/DELPMX
1530 TR3(254) = DELT/DELPMX
1531 TR3(255) = DELT/DELPMX
1532 TR3(256) = TH75L/TH75MX
1533 TR3(257) = TH75L/TH75MX
1534 TR3(270) = DELT/DELPMX
1535 TR3(271) = DELT/DELPMX

```

Figure G.9. (Continued)

```

1536 TR3(272) = -DELSPR/DLSPMX
1537 TR3(273) = DELSPL/DLSOMX
1538 TR3(274) = DDOT/PODTMX
1539 TR3(275) = DDUT/PODTMX
1540 TR3(276) = DDUT/QDDTMX
1541 TR3(317) = THHSG/TTTSMX
1542 TR3(311) = -GLSB/GLSMX
1543 TR3(312) = GLSAL/GLSMX
1544 TR3(313) = -DCYL/DCYLMX
1545 TR3(314) = -GLSAR/GLSMX
1546 TR3(315) = -DELRUD/DLRDMX
1547 TR3(316) = -DEFLV/DELEMX
1548 TR3(317) = DELFLP/DLFMLX
1549 TR3(330) = AICRIG/RICMX
1550 TR3(331) = AICLIC/RICMX
1551 TR3(332) = AICPIC/AICMX
1552 TR3(333) = AICLIC/AICMX
1553 TR3(334) = DFLTH/DLTHMX
1554 TR3(337) = THHSL/TTTSMX
1555 TR3(350) = -DELST/DELSMX
1556 TR3(351) = GORLON*DELRT/DLFOMX
1557 TR3(352) = -DELST/DELSMX
1558 TR3(353) = -VCALTR/UMX
1559 TR3(354) = -DELRT/DELRMX
1560 TR3(355) = GOSCOL*DELST/GSCOMX/DELSMX
1561 TR3(356) = GORCYL*DELRT/GFCYMX/DEFLMX
1562 TR3(357) = -GOSCYL*DELST/GSCYMX/DELSMX
1563 TR3(370) = DELST/DELSMX
1564 TR3(371) = -GATC/GICMX
1565 TR3(372) = -GBTC/GICMX
1566 TR3(373) = GDFLP/DLFMLX
1567 TR3(374) = GDE/DLEFMX*DGTRD
1568 TR3(375) = GOSP/DLSPMX

C
1569 TR3(230) = DELFLP/DLFMLX
1570 TR3(231) = DELR / DELBMX
1571 TR3(232) = DELS / DELSMX
1572 TR3(233) = DFLR / DELPMX
1573 TR3(234) = COMDLR / DELRMX
1574 TR3(235) = COMDLS / DELSMX
1575 TR3(236) = COMDLP / DELPMX
1576 TR3(237) = AVAIL

C BOARD 18 (CONSOLE 4) AMPLIFIER SCALE FACTOR CALCULATION: P DENOTES POSITIVE OUTPUT
RETURN N DENOTES NEGATIVE OUTPUT
ENTRY STCON4
PDNOS(4) = HD4
LETR(4) = LT4
CALL ANDAIN(PROJ,'1R','4',JEC(1),3,44P,5,5,44N,1,5,5,44,5,5,1R4,5,
*5)

```

Figure G.9. (Continued)

C

```

1582 A4P(1307) = PCTOL/TQSI*MX
1583 A4P(1311) = PCTOR/TQSI*MX
1584 A4P(1321) = PCA2/RPM*MX
1585 A4P(1331) = VDOT/VOT*MX
1586 A4P(1341) = -HDOT/HOTS*MX
1587 A4P(1351) = ACCXPA/AXPA*MX
1588 A4P(1361) = XDOT/XOTS*MX
1589 A4P(1371) = -VCALTR/SKFPS/LSI*MX
1590 A4P(1381) = VZSKFPS/VSI*MX
1591 A4P(1391) = THE*ROTUDG/THE*MX
1592 A4P(1401) = -PHI*ROTUDG/PHI*MX
1593 A4P(1411) = PSI*ROTUDG/PSI*MX
1594 A4P(1421) = P*OSI*W/P*SDT*MX
1595 A4P(1431) = AINRF*ROTUDG/AI*MX
1596 A4P(1441) = AVEAL*ROTUDG/AL*MX
1597 A4P(1451) = RCTAF*ROTUDG/RT*MX
1598 A4P(1461) = ACCYPA/AYPA*MX
1599 A4P(1471) = ACCZPA/AZPA*MX
1600 A4P(1481) = DELCLP/DLPC*MX
1601 A4P(1491) = H/H*SI*MX
1602 A4P(1501) = 0.
1603 A4P(1511) = 0.
1604 A4P(1521) = 1.0000
1605 A4P(1531) = H/7*MX
1606 A4P(1541) = 0.
1607 A4P(1551) = 0.
1608 A4P(1561) = 1.0000
1609 A4P(1571) = XIC / XVIS*MX
1610 A4P(1581) = VIC / YVIS*MX
1611 A4P(1591) = SINTHE
1612 A4P(1601) = COSTHE
1613 A4P(1611) = 1.0000
1614 A4P(1621) = VSIC / XVIS*MX
1615 A4P(1631) = SINDPHI
1616 A4P(1641) = COSPHI
1617 A4P(1651) = PSI / PI
1618 A4P(1661) = SA11
1619 A4P(1671) = SINDPSI
1620 A4P(1681) = COSPSI
1621 A4P(1691) = SA12
1622 A4P(1701) = SA13
1623 A4P(1711) = SA21
1624 A4P(1721) = SA22
1625 A4P(1731) = SINTRIE *SINDPHI
1626 A4P(1741) = SINTRIE *COSPHI
1627 A4P(1751) = SA23
1628 A4P(1761) = SA31
1629 A4P(1771) = YACVIS / YVIS*MX

```

Figure G.9. (Continued)

```

1630      A4N(252) = ZACVIS / ZVISMX
1631      A4P(253) = ZADDDY / ZVISMX
1632      A4P(260) = SA32
1633      A4P(261) = SA33
1634      A4P(262) = XACVIS / XVISMX
1635      A4P(263) = FREQMT / LDD
1636      A4P(300) = (XHPH17-H)/XVISMX
1637      A4P(305) = (QIASMT-H*GZMTSL) / ZVISMX
1638      A4P(307) = XADDDY / XVISMX
1639      A4P(303) = YADDDY / YVISMX
1640      A4P(310) = XSCOPE/SCOPMX
1641      A4P(311) = YSCOPE/SCOPMX
1642      A4P(312) = -XSCOPE/SCOPMX-YIC*CDSPH1/XVISMX+H*SINPH1/XVISMX
1643      A4P(313) = YSCOPE/SCOPMX+H*CDSPH1/YVISMX+X*YIC*SINPH1/YVISMX
1644      A4P(325) = C3000
1645      A4P(321) = C3000
1646      A4P(321) = -DRKOP/DRDPMX
1647      A4P(330) = C3000
1648      A4P(331) = C3000
1649      A4P(341) = FEFS / FEFSX
1650      A4P(342) = -BRAKE/BRKSMX
1651      A4N(342) = BRAKE/BRKMX
1652      A4P(343) = THRKOR/THRDPMX
1653      A4P(350) = FEFS / FEFSX
1654      A4P(351) = C3
1655      A4P(352) = -STKOR/CSRPMX
1656      A4P(353) = -DRKOR/DRDPMX
1657      A4P(362) = -COMPL3/DRPSMX
1658      A4N(360) = COMPL3/DELSMX
1659      A4P(361) = -COMPLS/DRPSMX
1660      A4N(361) = COMPLS/DELSMX
1661      A4P(362) = -COMDT/ATDSMX
1662      A4N(362) = COMDT/AINPMX
1663      A4P(363) = FEFR/FEFRMX
1664      A4P(370) = -COMPLR/DRPSMX
1665      A4N(373) = COMPLR/DELSMX
1666      A4P(371) = -COMDTH/DTPSMX
1667      A4N(371) = COMDTH/DLTHMX

C
C BOARD 1B (CONSOLE 4) VALUES OF TRUNK LINES (NO ADC'S ON THIS BOARD)
TR4(010) = PCTOL / TQSI*MX
TP4(011) = -TR4(010)
TR4(012) = PCTOR/TQSI*MX
TP4(013) = -TR4(012)
TR4(014) = PCN2/RPMSMX
TP4(015) = -TR4(014)
TR4(016) = YDPT/YDTPSMX
TP4(017) = -TR4(016)
TR4(030) = V / VMMX

```

Figure G.9. (Continued)

FORTRAN IV MODEL 44 PS VERSION 3, LEVEL 3 DATE 73092

```

1677 TR4(131) = RETAF / ARESMX
1678 TR4(132) = -VCALIR / LMX
1679 TR4(133) = -HOUT / VMX
1680 TR4(134) = -PHI / PI
1681 TR4(135) = PSI / PSIMX
1682 TR4(136) = THE / PI
1683 TR4(137) = H / ZMX
1684 TR4(138) = AVEALW / ALWGMX
1685 TR4(139) = SQE / SQEMX
1686 TR4(140) = XOUT / XDUTMX
1687 TR4(141) = XIC / XMX
1688 TR4(142) = YDOT / YDOTMX
1689 TR4(143) = YIC / YMX
1690 TR4(144) = PSIDOT / PSDMX
1691 TR4(145) = SIN THE
1692 TR4(146) = COS THE
1693 TR4(147) = SIN PHI
1694 TR4(148) = COS PHI
1695 TR4(149) = SIN PHI * COS THE
1696 TR4(150) = COS PHI * COS THE
1697 TR4(151) = VISHOR
1698 TR4(152) = -TR4(111)
1699 TR4(153) = VISVEP
1700 TR4(154) = -TR4(112)
1701 TR4(155) = VCALIR / SKFPS / LSTMX
1702 TR4(156) = -TR4(140)
1703 TR4(157) = V / SKFPS / VSTMX
1704 TR4(158) = -TR4(132)
1705 TR4(159) = THE * RDTODG / THE SMX
1706 TR4(160) = -TR4(134)
1707 TR4(161) = PHI * RDTODG / PHISMX
1708 TR4(162) = -TR4(136)
1709 TR4(163) = PSI * RDTODG / PSISMX
1710 TR4(164) = -TR4(150)
1711 TR4(165) = PSDSTW / PSDSTX
1712 TR4(166) = -TR4(152)
1713 TR4(167) = AINDF * RDTODG / AINFSMX
1714 TR4(168) = -TR4(154)
1715 TR4(169) = AVEALW * RDTODG / ALWFSMX
1716 TR4(170) = -TR4(156)
1717 TR4(171) = 3 * RETAF * RDTODG / ATSTIMX
1718 TR4(172) = -TR4(171)
1719 TR4(173) = ACCYPA / AYPAMX
1720 TR4(174) = -TR4(172)
1721 TR4(175) = ACCZPA / AZPAMX
1722 TR4(176) = -TR4(174)
1723 TR4(177) = DELELP / DELEPSMX
1724 TR4(178) = -TR4(176)
1725 TR4(179) = HOUT / HOUTSMX

```

Figure G.9. (Continued)

```

1726 TR4(211) = -TR4(210)
1727 TR4(212) = XDOT/XOTSMX
1728 TR4(213) = -TR4(212)
1729 TR4(214) = ACCXPA/AYPAMX
1730 TR4(215) = -TR4(214)
1731 TR4(230) = DEFLD/DLFLMX
1732 TR4(231) = DELB / DELRMX
1733 TR4(232) = DELS / DELSMX
1734 TR4(233) = DELR / DELRMX
1735 TR4(234) = COMDLR / DELBMX
1736 TR4(235) = COMDLS / DELSMX
1737 TR4(236) = COMDLR / DELRMX
1738 TR4(237) = AVAIL
1739 TR4(250) = PCTOL/PCTOMX
1740 TR4(251) = PCTOR/PCTOMX
1741 TR4(252) = OMEGA / CMEGMX
1742 TR4(253) = AINRF/AINMX
1743 TR4(254) = COMIDT/AINRMX
1744 TR4(255) = COMDTH / DLTHMX
1745 TR4(256) = -SKTRIM(12)*COMDT/CMEGMX
1746 TR4(257) = AVAIL
1747 TR4(270) = ACCXPA/AYPAMX
1748 TR4(271) = ACCYPA/AYPAMX
1749 TR4(272) = ACCZPA/AZPAMX
1750 TR4(310) = -COMIDT/ATDSMX
1751 TR4(311) = -TR4(310)
1752 TR4(312) = -BRAKE/BRKSMX
1753 TR4(313) = -TR4(312)
1754 TR4(330) = DRBKDR/DRBDMX
1755 TR4(331) = -TR4(330)
1756 TR4(332) = DRBKDR/DRPHDMX
1757 TR4(333) = -TR4(332)
1758 TR4(334) = DSAKDR/DSADMX
1759 TR4(335) = -TR4(334)
1760 TR4(336) = THBKDR/THBDMX
1761 TR4(337) = -TR4(336)
1762 TR4(350) = FFOR/FFRMX
1763 TR4(351) = -TR4(350)
1764 TR4(352) = FFDS/FFSMX
1765 TR4(353) = -TR4(352)
1766 TR4(354) = FFDR/FFRMX
1767 TR4(355) = -TR4(354)
1768 TR4(356) = H/HSIMX
1769 TR4(357) = -TR4(356)
1770 TR4(370) = -COMDLR/DRPSMX
1771 TR4(371) = -TR4(370)
1772 TR4(372) = -COMDLS/DRSPSMX
1773 TR4(373) = -TR4(372)
1774 TR4(374) = -COMDLR/DRPSMX

```

Figure G.9. (Continued)

DATE 73092

LEVEL 3

VERSION 3

PS

MODEL 44

FORTRAN IV

```

1775      TP4(375)= -TP4(374)
1776      TO4(376)= -CUMMTH/TP4(374)
1777      TR4(377)= -TP4(374)
      C
1778      RETURN
1779      END
    
```

Figure G.9. (Continued)

equilibrium. The equations for these feedback loops are shown in Appendix E. Several trim options are available: for a given initial condition of altitude, u and v components of velocity, rotor RPM and initial rates (p,q,r) the aircraft can be trimmed with attitude for specified nacelle angle or with nacelle angle for specified attitude. In addition, the aircraft can be trimmed in backwards or sideways flight. The trim gains used vary with the flight condition. Trim is generally attained in 5-10 seconds for any flight condition using this technique.

G.3 SIMULATION PROGRAM OUTPUT

The primary output of the mathematical model are:

- Trim sheet information
- Dynamic time histories of aircraft response

Figure G.10 shows a typical trim sheet with 180 aircraft parameters printed out and Figure G.11 contains the definitions of all the parameters. Four brush recorders with eight channels of output each are available for recording of the aircraft real time response. Figure G.12 shows a typical example of the output from one recorder. These data are extremely useful in analyzing aircraft responses and in optimizing stability augmentation and control systems.

TILT ROTOR TRIM DATA

DATE	03/23/73	TIME	11 HR	2 MIN	40 SEC	FLIGHT NO.=	RUN NO.=	TAPE SEQ. NO.=	0		
VTOT= 250.0 KT U = 250.0 KT V = -0.0 KT W = -2.0 KT G.W.= 12320.5 LBS RP4= 385.8 H = 51.5 FT XC3= 9.2 IN ZCG= 21.9 IN											
THETA	-C.44000E 00	PHI	C.24500E 00	PSI	-C.22918E-01	IN REF	THWST LM	THWST RM	RCE	TH75 L	TH75 R
DELR TOT	-C.12590E 01	DELS TOT	-C.11000E-01	DELR TOT	C.20350E 01	THROTTL	DELB SAS	DELS SAS	DEL R SAS	AICL	AICR
ELEVATOR	0.23835E 01	RUNNER	0.0	DEL L	C.63000E-01	DEL R	DELSPL	DELSPR	FLAP	BICL	BICR
TPS	C.18870E 04	OM ENG	C.23582E 04	SHP AV	C.82417E 03	SHP RQL	SHP RQR	IXX	IYY	IZZ	D.PRES F
MU L	0.80349E 00	THRUST L	C.79523E 03	NORMAL L	C.62197E 02	SIDE L	M ROT L	M ROT R	L HUB L	M HUB L	N HUB L
MU R	0.80389E 00	THRUST R	C.82572E 03	NORMAL R	C.13206E 03	SIDE R	M ROT R	M ROT R	L HUB R	M HUB R	N HUB R
X FUSE	-C.32474E 03	X TAIL	-C.16235E 03	X WING L	-C.54787E 03	X WING R	X NAC L	X NAC R	X TIP L	X TIP R	X/M
Y FUSE	0.19445E 01	Y TAIL	C.78296E 00	Y WING L	C.30284E-01	Y WING R	Y NAC L	Y NAC R	Y TIP L	Y TIP R	Y/M
Z FUSE	-C.19685E 04	Z TAIL	0.52210E 03	Z WING L	-C.55187E 04	Z WING R	Z NAC L	Z NAC R	Z TIP L	Z TIP R	Z/M
L FUSE	-0.35475E 01	L TAIL	0.22225E 01	L WING	0.58618E 03	M ACT L	L NAC L	L NAC R	L TIP L	L TIP R	L/IXX
M FUSE	-C.17206E 04	M TAIL	0.10696E 05	M WING	-C.56448E 04	M ACT R	M NAC L	M NAC R	M TIP L	M TIP R	M/IYY
N FUSE	0.17683E 02	N TAIL	-C.14728E 02	N WING	0.20164E 02	Z WING	N NAC LM	NAC R	N TIP L	N TIP R	N/IZZ
ALPH FUS	-0.44233E 00	ALPH HT	-0.18752E 01	ALPHLWSS	0.15366E 01	ALPHRWSS	AL NAC L	AL NAC R	AL ROT L	AL ROT R	H1 L
BETA FUS	-0.54272E-02	ALPH VT	0.14400E-02	ALPHA LW	0.15458E 01	ALPHA RW	CY NAC L	CY NAC R	ZETA L	ZETA R	H1 R
CL FUSF	0.48603E-01	CL HT	-0.41885E-01	CL WNG L	0.25928E 00	CL WNG R	CL NAC L	CL NAC R	CP L	CT L	CMF L
CD FUSE	0.73200E-02	CD HT	0.86827E-02	CD WNG L	0.23336E-01	CD WNG R	CD NAC L	CD NAC R	CSF L	CPM L	CYM L
CM FUSF	-0.56233E-02	CY VT	0.84995E-04	CM WNG L	-0.31167E-01	CM WNG R	CM NAC L	CM NAC R	CP R	CT R	CMF R
CN FUSE	0.12411E-04	CD VT	0.78915E-02	CL(ROLL)	-C.41168E-03	CN WING	CN NAC L	CN NAC R	CSF R	CPM R	CYM R
EP ZERO	0.71116E 00	EP TAIL	0.14595E 01	EP PRR	0.14267E-01	EP PLR	EP ILR	EP IRL	EP MRR	EP MRL	OMDOT
									0.0	0.0	-0.11160E 01

Figure G.10. Typical Model 222 Trim Sheet

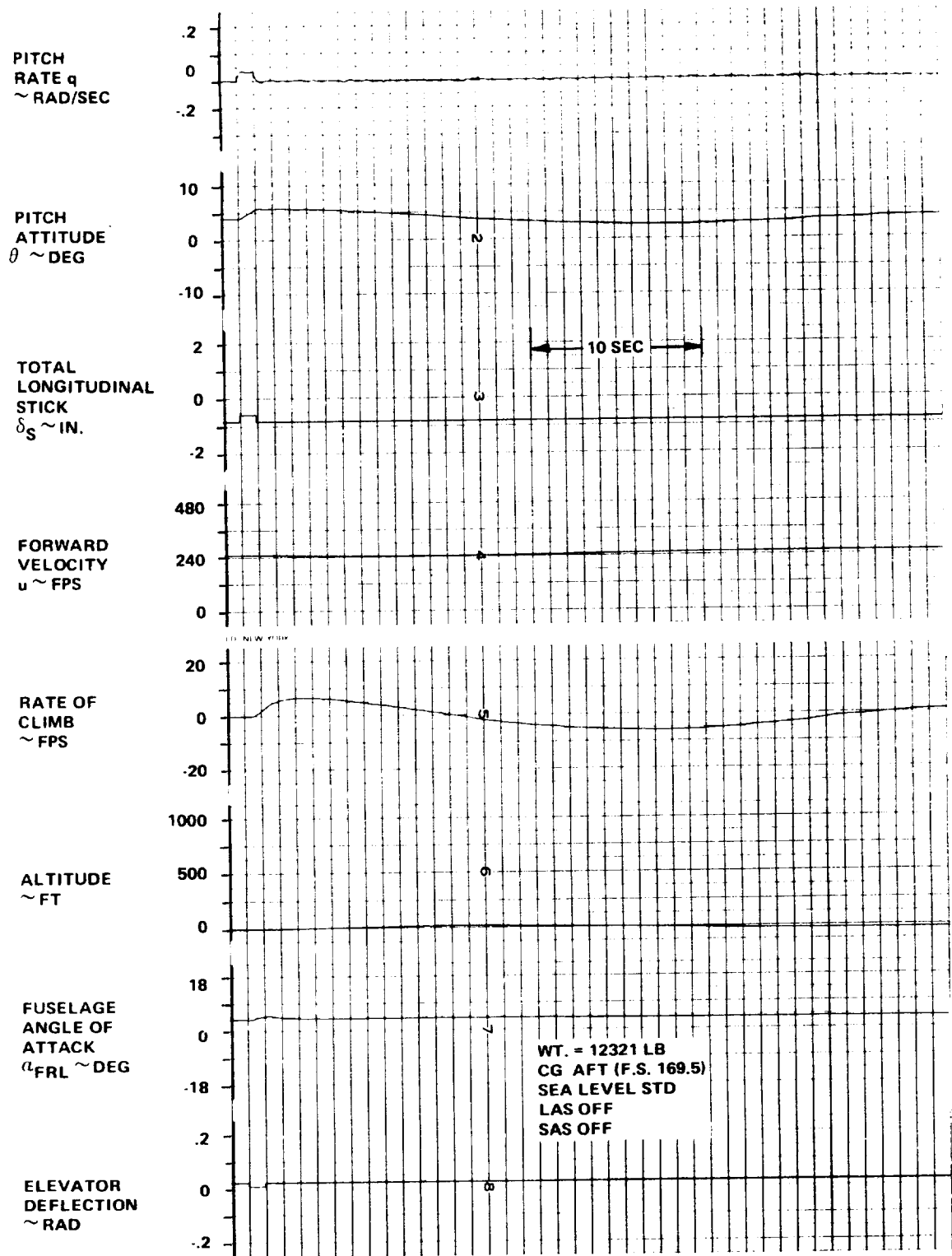


Figure G.12. Typical Time History Response to A .25 Inch Longitudinal Stick Pulse at 150 Knots

APPENDIX H VALIDATION OF THE MODEL 222 SIMULATION AT
AMES RESEARCH CENTER

This section presents the validation plan which was submitted to NASA prior to the checkout and validation period at the Ames Research Center, and the simulation acceptance and pilot operating instructions and limitations submitted after the checkout period.

H.1 VALIDATION PLAN AND CRITERIA

Validation of large scale hybrid math model is an extremely time consuming and difficult process. The validation plan and criteria to be used by Boeing Vertol personnel in checking out and validating the NASA Model 222 simulation is developed in the following section. The following items will be considered in this validation:

● Trim Checks

- Range of data: 25 kt increments from minimum to maximum speed. (including backward and sideward flight).
- Accuracy (when compared against Boeing Vertol check cases)

<u>Trim Data</u>	<u>Tolerance</u>
Pilot control position	<u>+0.25 in.</u>
Stick and pedal position slope with speed	<u>+10%</u>
Thrust or wing lift	<u>+2 1/2%</u>
Pitch, roll, yaw angles	<u>+1.0°</u>
Collective pitch	<u>+0.5°</u>

These requirements are subject to change pending a detailed selection of the trim conditions.

- Dynamic Responses (Response to control pulses)

- Range of data: An axis by axis check with SAS and LAS systems on and off. Same speeds as for trim data.

- Accuracy (when compared against Boeing Vertol check cases)

Period	$\pm 10\%$
Time to double (or half) amplitude	$\pm 10\%$

- Stability Derivative Checks

- Range of data: Selected stability and control derivatives will be obtained at no more than five conditions.

- Accuracy when compared against Boeing Vertol check cases)

Selected major stability and control derivatives

($L_V, N_V, L_P, N_P, L_R, N_R, X_U, M_W, M_Q, Z_W,$
 $L_{\delta_S}, N_{\delta_S}, L_{\delta_R}, N_{\delta_R}, M_{\delta_B}, M_{i_N}, Z_{\delta_{TH}}$) $\pm 10\%$

- Validation of Time Frame

Run selected dynamic response checks at hover and cruise in real time and 1/10 real time i.e. reduced interval of integration. Damping of predominant modes shall not change by more than $\pm 10\%$.

- Transport Lag Checks

The transport lag i.e. aircraft response following control input shall not be greater than one to two time frames (average 1 1/2 time frames)

- Pilot acceptance will be based on a subjective comparison between the results obtained in the Boeing nudge base simulator and those obtained on the FSAA.

H.2 SIMULATION ACCEPTANCE

Following the checkout period at Ames, the following simulation acceptance document was submitted.

The math model, as programmed, is considered acceptable for initial evaluations.

The following differences exist between the math model and the aircraft described in Boeing's proposal for Phase II.

1. The data bank in the math model gives very conservative values of power around the autorotation region. The math model uses data from computer program D-88. Boeing's proposal uses data from wind tunnel model tests which were compared with D-88 predictions. The wind tunnel data showed consistently lower power required in and near autorotation. Revision of the rotor data bank to incorporate the wind tunnel data was not practicable within the time available. The extent of the difference is indicated by a minimum rate of descent at 80 knots from the math model of 2600 feet per minute compared to about 2000 feet per minute from the wind tunnel model data as reported in Volume I, Appendix G.
2. There is no autopilot in the math model. This was not required by the contract Statement of Work.
3. The landing gear dynamics in the model are an existing CSC program and do not represent the Model 222. There is some

indication that the CSC gear causes lateral instability on the ground at less than 25% power.

4. The wing bending and torsion modes were not checked out due to lack of time. Data obtained at Vertol indicate that these have no measurable effect on performance or flying qualities.
5. The representation of the SAS gives proper dynamic characteristics in the SAS on and SAS off modes. Individual component failures are not represented because of mechanization differences between the aircraft and the math model.
6. The actuator dynamics, which were included in the math model used on Boeing's nudge base simulator, were removed from the FSAA simulation in order to keep the time frame to a minimum. Evaluation on the Sigma 8 Computer at NASA showed no measurable difference as a result of removing the actuator dynamics. (The actuators have time constants less than the 50 millisecond time frame of the FSAA simulation.)
7. Boeing's proposed aircraft provides a pilot override for flap position and for rpm selection. These are not included in the math model. The checkout and validation of the tilt rotor math model was accomplished in two phases. These were the math model acceptance and the simulator acceptance.
 - A. Math Model Acceptance:
 1. Trim checks were calculated for a range of speeds from hover to 250 knots in 25 knot intervals. These were checked against previously computed trim conditions.

The results agreed within the tolerances specified in the reference.

2. Due to the limited time available for validation, dynamic responses were not checked over the full range of condition noted in the reference. However, dynamic responses were computed for a representative sample of condition. These compared favorably with those generated at Boeing and were generally within the specified tolerances. Differences could be explained by the different methods which were used to mechanize the equations; e.g., ---in the Boeing hybrid mechanization, rotor data were interpolated parabolically for angle of attack and linearly for advance ratio. In the NASA mechanization, curve fit equations were solved at each angle of attack and linearly interpolated for advance ratio. This tends to produce differences in areas where the data is highly non-linear such as in transition.
3. Stability derivative checks were made at four speeds; 0, 75, 150 and 250 knots. These were generally within the +10% accuracy specified by Boeing. Differences between the results are explainable and primarily due to the different ways the equations were mechanized.
4. Time frame studies and transport lag checks were made. Neither proved to be problem areas even though the NASA

simulation has a frame time in excess of 50 milliseconds. No lags were apparent in the simulation cab due to transport lag.

B. Boeing Pilot Acceptance:

The simulation is considered acceptable for initial evaluation however, Boeing's evaluation pilot made the following comments:

1. Controls:

- . Power lever location not optimum but acceptable for evaluation using seat arm rest for support.
- . Nacelle tilt switch - spring gradient slightly weak, 5° detents appear to be not in center of available travel. Switch occasionally sticks producing uncommanded nacelle actuation. Suitable for evaluation.
- . Stick forces - breakout and damping poor- difficult to achieve positive trim detent. Occasional shift in stick trim from one run to the next. (Simulator equipment problem)

2. Motion:

- . B V pilot considered motion cues unsatisfactory.
- . Lateral motion washouts and/or recentering produced spurious jerks and pulses which were disorienting.

- . Roll angular acceleration cues weak.
- . Pitch, yaw and heave satisfactory.
- . Longitudinal acceleration cues - long period cab tilt ok, short period were jerky and disconcerting with recentering reversals apparent.
- . Summary: There was enough spurious motion that overall the tilt/motion cues were detrimental and the pilot preferred fixed base.

3. Model Flying Qualities:

Generally similar to B V in-house simulation except for:

- . Vertical response slightly overdamped.
- . Unable to cut engine(s) until last day. As a result, not able to properly check out power lever governor override.
- . Pedal fixed turns in prop mode not as well coordinated - 30° banked turns show 1/2 to 3/4 ball slip to T & S indicator, with S/S ind. reading 1° - 2°.

4. Boeing was not able to evaluate the Model 222's response to gusts, since the gust model has not been defined. Response to random turbulence was evaluated.

C. General:

The original time allotted for the checkout and validation of this model was extremely short, particularly in view of the computer software problems and the difficulties encountered in establishing the gains for the FSAA motion drive equations. As a result, the checkout period had to be extended by NASA for two weeks.

H.3 OPERATING INSTRUCTIONS AND LIMITATIONS

As part of the simulation checkout, a set of operating instructions and limitations were prepared. For the most part these refer to the piloted simulation and the mathematical model and do not imply limitations on the Model 222 aircraft.

General:

1. I.C. - Set power lever trim to "0". (suggest using left-hand arm rest)
2. Stick grip has both Mag. brake and vernier "beep" force retrim. If Mag. braking is desired, use only in hover -- advise beep retrimming for transition and prop mode. (In real A/C, Mag. brake will deactivate above 150 KIAS)
3. Flaps and RPM are programmed automatically as a function of nacelle angle. In the Model 222 there will be manual flap and RPM override controls.

4. Nacelle angle has "q" interlock. Nacelles cannot be programmed "up" above 160 KIAS. IF 160 KIAS is exceeded with nacelle angle greater than 0°, they will automatically program to 0° at a rate of 2°/sec.
5. Nacelle angle switch gives nacelle rate proportional to displacement. Switch is spring loaded to center off position and has a detent either side of center, corresponding to approximately $\pm 5^\circ/\text{sec}$ rate. Full displacement will give approximately $\pm 10^\circ/\text{sec}$. For smoothest nacelle operation, use proportional feature; avoid "flick" type beep inputs.
6. Wing leading edge umbrellas automatically open or close at 50 KIAS.
7. Normal power lever travel is 8". This range represents flight idle to maximum power. There is a soft detent at 8 inches of travel which, when exceeded, overrides the governor. In this condition, the power lever controls collective pitch directly. This is provided for use as desired in autorotation and single engine landings.
8. The Model 222 is designed to go through transition at speeds between zero and 160 knots. Typical trimmed nacelle incidences at various speeds are:

iN - DEG	90	75	60	30	0
Speed - KEAS	0	52	71	95	150

In investigating handling characteristics in the transition mode, it is recommended that these values be used as initial conditions.

In performing normal transitions to and from hover, it is recommended that the nacelle tilt be used as the primary speed control rather than flying at fixed tilt and using the stick for speed control.

Limitations:

1. Observe torque limits:

75% twin engine
100% single engine

2. Autorotation:

Engines must be failed from console to achieve zero torque. Transitions can be made from airplane to helo mode with power lever full back, but some residual torque remains (10% total) and N_R trims out nominally at 70%.

. Autorotative sink rate at $i_N=90^\circ$ approximately 3500 ft/min. Minimum rate of sink is about 2600 ft/min at 80 knots at $i_N=60^\circ$ (70% RPM). Model gives higher descent rates than airplane.

. Power lever has detent at approximately 8". Pushing through detent will override governor (single engine failure or auto collective) and give direct control of collective pitch.

. Technique on engine cut in hover - advance power lever to detent, remaining engine will go to 100% torque. Use override as required, but once into direct C.P. control N_R will bleed off in same manner as turbine helo with one engine over-pitched. At topping power, model gross weight is too high for single engine hover. At max single engine power, vertical speed is -300 FPM.

3. At speeds above the normal flight envelope with nacelles tilted, the math model data bank is extrapolated from a curve fit and is not representative of the full scale aircraft. Speed and nacelle incidence limits for valid simulation are shown in the following table:

i_N - DEG	90	60	45	30
Speed - KEAS	100	125	125	140

These speeds should not be exceeded.

4. Aircraft oscillates if power is reduced below approximately 25% on the ground.
5. The math model is not set up to readily perform SAS or governor hardover studies. These may be approximated by setting the appropriate authority limits.
6. The Model 222 autopilot has not been incorporated into the simulation.